TECHNISCHE UNIVERSITÄT MÜNCHEN

Lehrstuhl für Entwicklungsgenetik

Genetic dissection of CRH-controlled neurocircuitries of stress

Nina Dedic

Vollständiger Abdruck der von der Fakultät Wissenschaftszentrum Weihenstephan für Ernährung, Landnutzung und Umwelt der Technischen Universität München zur Erlangung des akademischen Grades eines

Doktors der Naturwissenschaften

genehmigten Dissertation.

Vorsitzender:	Univ.-Prof. Dr. Alfons Gierl
Prüfer der Dissertation:	1. Univ.-Prof. Dr. Wolfgang Wurst
	2. Univ.-Prof. Angelika E. Schnieke, Ph.D.
	3. Priv.-Doz. Dr. Mathias V. Schmidt

Die Dissertation wurde am 06.08.2014 bei der Technischen Universität München eingereicht und durch die Fakultät Wissenschaftszentrum Weihenstephan für Ernährung, Landnutzung und Umwelt am 07.12.2014 angenommen.

TABLE OF CONTENTS

SUMMARY

Prolonged exposure to stressful life events represents an overlapping risk factor for various neuropsychiatric disorders. Accordingly, there is growing interest in neuroscience to better understand neuronal stress-circuitries in health and disease. The neuropeptide corticotropin-releasing hormone (CRH) is the key regulator of the endocrine stress response given its ability to drive hypothalamic-pituitary-adrenal (HPA) axis activity and consequently influence the release of glucocorticoids in the periphery. Importantly, CRH and its high affinity type 1 receptor (CRHR1) are also involved in modulating behavioral adaptations to stress, which is owed to their wide distribution within the mammalian brain. However, little is known about the underlying CRH-controlled neurocircuitries that regulate emotional responses to stress. This study aimed to functionally dissect stress-modulating CRH pathways and provide a close assessment of CRH-neurotransmitter interactions.

Hypersecretion of central CRH and increased glucocorticoid levels have been shown to accompany mood and anxiety disorders. Employing different CRH overexpressing mouse models, we initially established that central CRH hyperdrive can modulate behavioral responses independent of, or in synergism with elevated glucocorticoids. In addition, the study effectively demonstrated the ability of central nervous system (CNS)-specific CRH overexpressing mice ($Crh^{CNS\text{-}COE}$) to model endophenotypes of stress-related neuropsychiatric disorders. $Crh^{CNS\text{-}COE}$ mice displayed a wide range of behavioral abnormalities related to mania, anxiety and depression, which was linked to enhanced noradrenergic function. Importantly, this model displayed strong predictive validity given that many of the behavioral alterations could be reversed by chronic application of lithium, a commonly prescribed mood stabilizer.

In order to avoid the uncertainties associated with ectopic gene expression in CRH ovrerxpressing mice, loss-of-function approaches were subsequently applied to further unravel the underlying neurotransmitter circuits controlled by CRH/CRHR1 that modulate stress-related behavior. Using conditional mutagenesis, CRHR1 was specifically deleted in forebrain glutamatergic and GABAergic neurons as well as in midbrain dopaminergic and serotonergic neurons, all of which were previously identified to express the receptor. Selective deletion of CRHR1 in forebrain glutamatergic circuits reduced anxiety, which is in agreement with the previously established phenotype of forebrain-specific CRHR1 knockout mice, and the anxiolytic properties of CRHR1-antagonists. Remarkably, specific deletion from midbrain dopaminergic neurons enhanced anxiety, highlighting a previously unidentified negative effect of CRHR1-deletion on emotional behavior. Importantly, this anxiety-inducing effect was

associated with reduced dopamine release in the prefrontal cortex. These results defined a bidirectional role of CRHR1 in anxiety, suggesting that CRH/CRHR1-controlled glutamatergic and dopaminergic systems might function in a concerted but antagonist manner to keep emotional responses to stressful situations in balance. In order to characterize the responsible CRH-producing neurons, neurochemical, morphological, and viral-mediated tracing analyses were performed. Cortical and limbic CRH was primarily expressed in GABAergic neurons, which exhibited distinct morphologies depending on the brain region. Anterograde tracing studies of forebrain limbic CRH neurons revealed long-range projecting axons, which innervated distant brain regions including the ventral tegmental area (VTA), which harbors the majority of CRHR1-expressing dopaminergic neurons. Furthermore, a subpopulation of limbic CRH neurons is characterized by the expression of CAMK2α. Many of these exhibited dendritic spines and long-range axons, giving rise to the hypothesis that CAMK2α-positive CRH neurons represent a subpopulation of spiny GABAergic long-range projection neurons. In order to address the involvement of different CRH subpopulations in emotional behavior, conditional *Crh* knockout mice were generated via homologous recombination in embryonic stem cells. Deletion of *Crh* from *Camk2α*-positive neurons enhanced anxiety and fear memory expression, implicating that this specific CRH pathway is required under physiological conditions to maintain a positive emotional state. Considering that deletion of *Crhr1* from dopaminergic neurons produces similar effects, suggests that limbic, triple-positive, CAMK2α-CRH-expressing GABAergic projection neurons target dopaminergic CRH type 1 receptors to modulate emotional behavior by influencing dopamine release. The ability of CRH to positively regulate dopamine release and reduce anxiety was demonstrated upon overexpression of CRH in forebrain GABAergic neurons, and is probably caused by enhanced CRH drive in the Camk2α-positive GABAergic subpopulation. Remarkably, the ability of CRH/CRHR1 to modulate emotional responses in a bidirectional manner is lost upon prolonged exposure to severe stress. This was demonstrated by the fact that deletion of *Crh* from most cortical and limbic structures diminished stress-induced neuronal activation and the susceptibility to chronic social defeat stress. The switch to an “all-aversive” effect of CRH during chronic stress is likely caused by overactivation of both anxiogenic and anxiolytic CRH receptors, resulting in a persistent dysregulation of positive CRH-neurotransmitter interactions as well as the initiation of HPA axis hyperfunction.

Overall, this study unraveled novel insights into the CRH-system, which will help to expand our knowledge of adaptive and maladaptive stress-circuitries.

ZUSAMMENFASSUNG

Chronischer Stress stellt einen bedeutenden Risikofaktor für zahlreiche neuropsychiatrischen Erkrankungen, wie z. B. Depressionen, Schizophrenie, Bipolare Störung oder Angststörungen dar. Demzufolge widmen sich immer mehr Studien der Aufklärung von neuronalen Stress-Schaltkreisen und Netzwerken. Eines der wichtigsten Effektormoleküle innerhalb der physiologischen Stressantwort des Körpers ist das Neuropeptid Corticotropin-Releasing Hormon (CRH), welches die Freisetzung von Glucocorticoiden durch Aktivierung der Hypothalamus-Hypophysen-Nebennieren (HHN)-Achse steuert. Darüber hinaus koordinieren CRH und dessen hoch affiner Typ 1 Rezeptor (CRHR1) komplexe stressassoziierte Verhaltensweisen wie Lernen, Gedächtnisprozesse, Aufmerksamkeit und Emotionalität. Allerdings sind die CRH/CRHR1-kontrollierten neuronalen Netzwerke, welche ursächlich für die emotionale Stressantwort sind, noch weitgehend unerforscht. Ziel dieser Arbeit war es spezifische CRH-Neurotransmitter Interaktionen zu untersuchen, um somit die Funktion des Stress-modulierenden CRH/CRHR1-System weiter zu entschlüsseln.

Eine Hyperaktivität des zentralen CRH/CRHR1-Systems und ein erhöhter Glucocorticoid-Spiegel sind häufige Begleiterscheinungen von stressabhängigen Erkrankungen wie z.B. Depressionen und Angststörungen. Mit Hilfe verschiedener konditionaler CRH-überexprimierender Mauslinien konnte hier gezeigt werden, dass eine CRH-Hypersekretion Verhaltensweisen sowohl unabhängig von der HHN-Achse, als auch im Synergismus mit selbiger beeinflusst. Des Weiteren wurde verdeutlicht, dass Mäuse mit einer spezifischen Überexpression von CRH im zentralen Nervensystem (*Crh*$^{CNS\text{-}COE}$) bestimmte Endophenotypen stressbedingter neuropsychiatrischer Erkrankungen aufweisen. *Crh*$^{CNS\text{-}COE}$ Mäuse zeigten zahlreiche Verhaltensstörungen, ähnlich den Symptomen in manischen und depressiven Patienten, die höchstwahrscheinlich durch eine CRH-bedingte erhöhte Aktivierung des Noradrenergen Systems verursacht werden. In Anbetracht der Tatsache, dass einige dieser Verhaltensanomalien durch die chronische Gabe von Lithium aufgehoben werden konnten, erfüllt dieses Mausmodell nicht nur das Kriterium der Inhaltsvalidität sondern auch der Vorhersagevalidität.

Um die Limitation der ektopischen Genexpression in CRH-überexprimierenden Mauslinien zu umgehen, wurden zusätzlich konditionale *Crhr1*-Knockout Mäuse in Bezug auf CRH/CRHR1-Neurotransmitter-Interaktionen untersucht. Die bislang weitgehend ungeklärte Identität von CRHR1-produzierenden Neuronen konnte im Vorfeld in der Arbeitsgruppe entschlüsselt werden. Es wurde gezeigt, dass der *Crhr1* in glutamatergen, GABAergen, dopaminergen und

vereinzelten serotonergen Neuronen exprimiert wird. Ein weiteres Ziel dieser Arbeit war es die Funktion des CRHR1 in diesen Neuronenpopulationen zu untersuchen. Die selektive Inaktivierung des *Crhr1* in Glutamat-produzierenden Neuronen des Vorderhirns (*Crhr1*$^{Glu\text{-}CKO}$) verminderte das Angstverhalten in verschiedenen Tests. Im Gegensatz dazu zeigten Mäuse, denen der *Crhr1* in Dopamin-produzierenden Neuronen des Mittelhirnes (*Crhr1*$^{iDA\text{-}CKO}$) fehlt, ein erhöhtes Angstverhalten und eine geringere Freisetzung von Dopamin im präfrontalen Cortex nach akutem Stress. Diese Daten deuten auf einen bislang unentdeckten, negativen emotionalen Effekt einer *Crhr1*-Inaktivierung hin. Die gegensätzliche Modulation des Angstverhaltens durch den CRHR1 legt nahe, dass eine Störung des Gleichgewichts von CRHR1-kontrollierten glutamatergen und dopaminergen neuronalen Netzwerken für die Entstehung neuropsychiatrischer Erkrankungen verantwortlich sein könnte. Um die verantwortlichen CRH-produzierenden Neuronen weiter zu charakterisieren, wurden neurochemische, morphologische und virusvermittelte Tracertechniken angewandt. Dadurch konnte gezeigt werden, dass *Crh* in kortikalen und limbischen Gehirnregionen primär in GABAergen Neuronen synthetisiert wird, die unter anderem verschiedene morphologische Eigenschaften aufweisen. Anterograde Tracing-Experimente legten nahe, dass limbische CRH Neuronen über Axone verfügen die über lange Strecken projizieren (Langstreckenaxone). Diese innervieren Mittelhirnstrukturen, darunter das ventrale Tegmentum (Area tegmentalis ventralis), welches die höchste Anzahl an CRHR1-produzierenden dopaminergen Neuronen enthält. Des Weiteren wurde eine spezifische CRH-Subpopulation beschrieben, die durch den Marker CAMK2α charakterisiert werden kann, dendritsche Dornfortsätze (Spines) besitzt und über Langstreckenaxone verfügt. Daraus ergab sich die Hypothese, dass CAMK2α-positive CRH Neuronen eine Subgruppe von GABAergen Langstrecken-projizierenden Neuronen umfassen. Zu einer detaillierten Analyse der Funktion von CRH in verschiedenen Neuronenpopulationen, wurde mittels homologer Rekombination in embryonalen Stammzellen eine konditionale *Crh*-Knockout Mauslinie generiert. Die gezielte Inaktivierung von *Crh* in *Camk2α*-positiven Neuronen führte zu erhöhtem Angstverhalten und stärker ausgeprägtem Furchtgedächtnis, was darauf hindeutet, dass unter physiologischen Bedingungen spezifische CRH-Schaltkreise für die Äußerung positiver emotionaler Reaktionen erforderlich sind. In Anbetracht der Tatsache, dass die Inaktivierung von *Crhr1* in dopaminergen Neuronen einen ähnlichen Phänotyp verursacht, wird postuliert, dass limbische, dreifach-positive CAMK2α-CRH-produzierende GABAerge Langstreckenneuronen den CRHR1 auf dopaminergen Neuronen aktivieren, um die Freisetzung von Dopamin und letztendlich emotionales Verhalten zu

modulieren. Die Fähigkeit des CRH-Systems, die Dopamin Ausschüttung zu erhöhen und Angstverhalten zu reduzieren, wurde in Mäusen mit einer spezifischen Überexpression von CRH in GABAergen Neuronen gezeigt. Dieser Effekt ist wahrscheinlich durch die CRH-Hyperfunktion in der CAMK2α-positiven GABAergen Neuronensubpopulation bedingt. Erstaunlicherweise verliert CRH unter chronischen Stressbedingungen die Fähigkeit emotionale Verhaltensweisen in gegensätzliche Richtungen zu modulieren. Dies wird durch Experimente verdeutlicht, die zeigen, dass eine Inaktivierung von *Crh* in den meisten kortikalen und limbischen Strukturen sowohl mit einer geringeren chronischen Stressanfälligkeit, als auch mit einer reduzierten Stressbedingten neuronalen Aktivierung einhergeht. Die Umschaltung zu einem allgemeinen CRH-induzierten aversiven Effekt während andauernder Stressbelastung ist vermutlich durch die Aktivierung angstverursachender und angstlösender CRH Rezeptoren, sowie der Hyperaktivierung der HHN-Achse bedingt. Dies führt letztendlich zu einer permanenten Dysregulation positiver CRH-Neurotransmitterinteraktionen die unentbehrlich für eine gesunde Stressantwort sind.

Insgesamt gewährt diese Arbeit neue und bislang unbekannte Einblicke in das CRH/CRHR1-System und bereichert somit den aktuellen Wissensstand über adaptive und pathologische Stress-Netzwerke.

1. INTRODUCTION

1.1. How stress gets under our skin

"It's not Stress that kills us, it is our reaction to it"
Hans Selye (1907-1982)

Over the past decades, growing evidence has linked life stress to various pathalogies, including cardiovascular disease, inflammation, metabolic dysfunctions, and most prominently neurodegenerative and psychiatric disorders. Especially conditions of severe prolonged stress are considered most devastating because they tend to induce long-term or permanent changes in the physiological, emotional and behavioral responses that influence susceptibility to disease. Persistent stress, such as prolonged exposure to war, physical abuse, devastating socioeconomic status and social/psychological surroundings has been shown to enhance the likelihood to develop depression and anxiety disorders, cognitive dysfunctions, metabolic conditions such as obesity and diabetes, as well as sleep and cardiovascular disorders, just to name a few (Adler and Ostrove, 1999; de Kloet et al., 2005a; Cohen et al., 2007; McEwen, 2007; Chrousos, 2009; McEwen and Gianaros, 2010; Steptoe and Kivimaki, 2012). Ironically, a clear cut definition of the term "stress" is still missing, which is largely owed to the subjective nature of stress-perception. Although the word has long been (and still is) in everyday use, its significance in biology was initially recognized by the pioneering work of Walter Cannon and Hans Selye during the early-mid 20th century. Selye defined stress as the "*nonspecific deviation from the normal resting state*" based on the concept of homeostasis proposed by Cannon (Cannon, 1932; Selye, 1936). The term homeostasis refers to the ability of all organisms to maintain a complex equilibrium, which is constantly challenged by internal or external adverse effects (Cannon, 1932). Later on, the term *stressor* was defined as a stimulus that threatens homeostasis. The *stress-response* in turn, constitutes reactions performed by the organism to restore homeostasis. However, we tend to forget that stress *per se* is not a bad thing, but that it is rather the reaction and/or inability to adapt to it that constitutes health or disease. Importantly, acute stress can exert a wide range of positive effects, as it primes the brain towards optimal alertness, behavioral and cognitive performance (Roozendaal et al., 2006; Joels et al., 2006; Sandi and Pinelo-Nava, 2007; Smeets et al., 2009; Kirby et al., 2013). The reaction to stress represents an adaptive mechanism, triggering the so-called "fight-or-flight" response in order to cope with a dangerous situation, be it a predator, an accident, or a natural

disaster. The organism needs the normal stress response to adapt to changes in the environment, and survive these threatening conditions. The promotion of such short-term adaptation has also been termed allostasis (McEwen, 1998; McEwen, 2004; McEwen, 2007). However, prolonged activation of stress-circuitries can have deleterious effects on health and survival. In general, we are not equipped to withstand chronic activation of specific stress-pathways, which occurs more frequently in today's social environments. The concept of "time" with regards to stress exposure was initially addresses by Selye who defined three explicit stages of the General Adaption Syndrome: *"1) the alarm reaction, in which adaptation has not yet been acquired; 2) the stage of resistance, in which adaptation reaches its optimum; and 3) the stage of exhaustion, in which the acquired adaptation is lost again*" (Selye, 1955). Today we know that the brain represents the key stress-integrating system. In this regard, a large body of work has demonstrated dysregulated neurocircuits in response to severe chronic stress exposure across many species, including rodents, primates and humans (de Kloet et al., 2005b; Joels and Baram, 2009; Chrousos, 2009; Stevens et al., 2009; Lupien et al., 2009; McEwen and Gianaros, 2010; Parker and Maestripieri, 2011; Popoli et al., 2012; Russo et al., 2012; Russo and Nestler, 2013). Moreover, such changes often result in inappropriate responses to non-specific stressors, which can eventually lead to disease. But when does stress, or more precisely the stress-response, cross the line from being adaptive to maladaptive? This question is extremely difficult to answer, considering that the threshold of stress-resistance is different for every single individual and may be influenced by genetic predisposition. Thus, the concept of gene-environment interactions further complicates the assessment of stress-related disorders. Various substances are released in response to stress, which are then orchestrated into a coordinated physiological and behavioral response (Joels and Baram, 2009). These so-called stress-mediators are generally classified into three classes; the monoamines, neuropeptides and steroids. Non-specific effects of stress are mirrored by the rapid activation of the monoaminergic system and the hypothalamic-pituitary-adrenal (HPA) axis, which in turn regulates the secretion and release of glucocorticoids from the adrenal glands (Joels and Baram, 2009). The complex interaction between these different stress-mediators has gained substantial interest in the past years. However, some play more important roles than others and are especially relevant in dysfunctional stress-circuits, which can result in various neuropsychopathologies. Already in 1955, Hans Selye postulated that "*through some unknown pathway the first mediator travels directly from the injured target area to the anterior pituitary. It notifies the latter that a condition of stress exists and thus induces it to discharge*

adrenocorticotropic hormone (ACTH)" (Selye, 1955). It took another 26 years until Wylie Vale and colleagues discovered this central stress mediator - the neuropeptide corticotropin-releasing hormone/factor (CRH/CRF) (Vale et al., 1981).

1.2. Neuroendocrine stress-responses are modulated by CRH-mediated regulation of the hypothalamic-pituitary-adrenal (HPA) axis

Perception of physical or psychological stress by an organism is followed by a series of events, including the release of CRH from parvocellular neuroendocrine neurons of the paraventricuar nucleus of the hypothalamus (PVN). These neurons project via the external zone of the median eminence and release CRH into the hypophysial portal vasculature, which transports the neuropeptide to CRH receptor 1 containing secretory corticotroph cells of the anterior pituitary (Figure 1). The activation of CRHR1 stimulates the synthesis of adrenocorticotropic hormone (ACTH) and other proopiomelanocortin (POMC) derived peptides (Vale et al., 1983). About 50% of the medial-dorsal parvocellular CRH secreting neurons also express arginine vasopressin (AVP) (Sawchenko et al., 1984a; Sawchenko et al., 1984b). AVP, also known as antidiuretic hormone, primarily regulates water retention in the kidneys, and blood vessel constriction. However, AVP can also synergizes with CRH to potentiate the latter's effects on the release of ACTH from the anterior pituitary (DeBold et al., 1984; Whitnall, 1993). ACTH, in turn, reaches the adrenal glands via the blood circulation where it binds to its specific receptors in the zona fasciculata of the adrenal cortex. This leads to the synthesis and release of glucocorticoids into the blood stream; cortisol in humans and corticosterone in rodents, which mediate numerous physiological and metabolic reactions such as cardiovascular activation, energy mobilization, anti-inflammatory effects and suppression of reproductive and digestive functions (Munck et al., 1984; Sapolsky et al., 2000; de Kloet, 2004; Stahn and Buttgereit, 2008; Buttgereit et al., 2009; Quax et al., 2013; Picard et al., 2014). In order to restore the HPA axis to its normal state and to protect it from overshooting, glucocorticoids signal back via negative feedback mechanisms, thereby inhibiting the secretion of CRH and consequently ACTH (Figure 1). This effect is mediated by the glucocorticoid (GR) and the mineralcorticoid receptor (MR) at various feedback sites, such as the hippocampus, PVN and the pituitary (Reul and de Kloet, 1985; Sapolsky et al., 2000; Furay et al., 2008; Groeneweg et al., 2012). Consequently, HPA axis activation and enhanced cortisol levels are generally believed to indicate a state of stress. But is this really the case? This issue was recently revitalized by Koolhaas and colleagues, who reached the conclusion that the mere presence of

a neuroendocrine response is not sufficient to label it as stress, nor is it indicative of the presence of a stressor due to its general role in the metabolic support of behavior (Koolhaas et al., 2011). The researchers emphasized that the physiological stress-response to appetitive, rewarding stimuli (which are generally not considered as stressors) can be as large as the response to a negative stimuli.

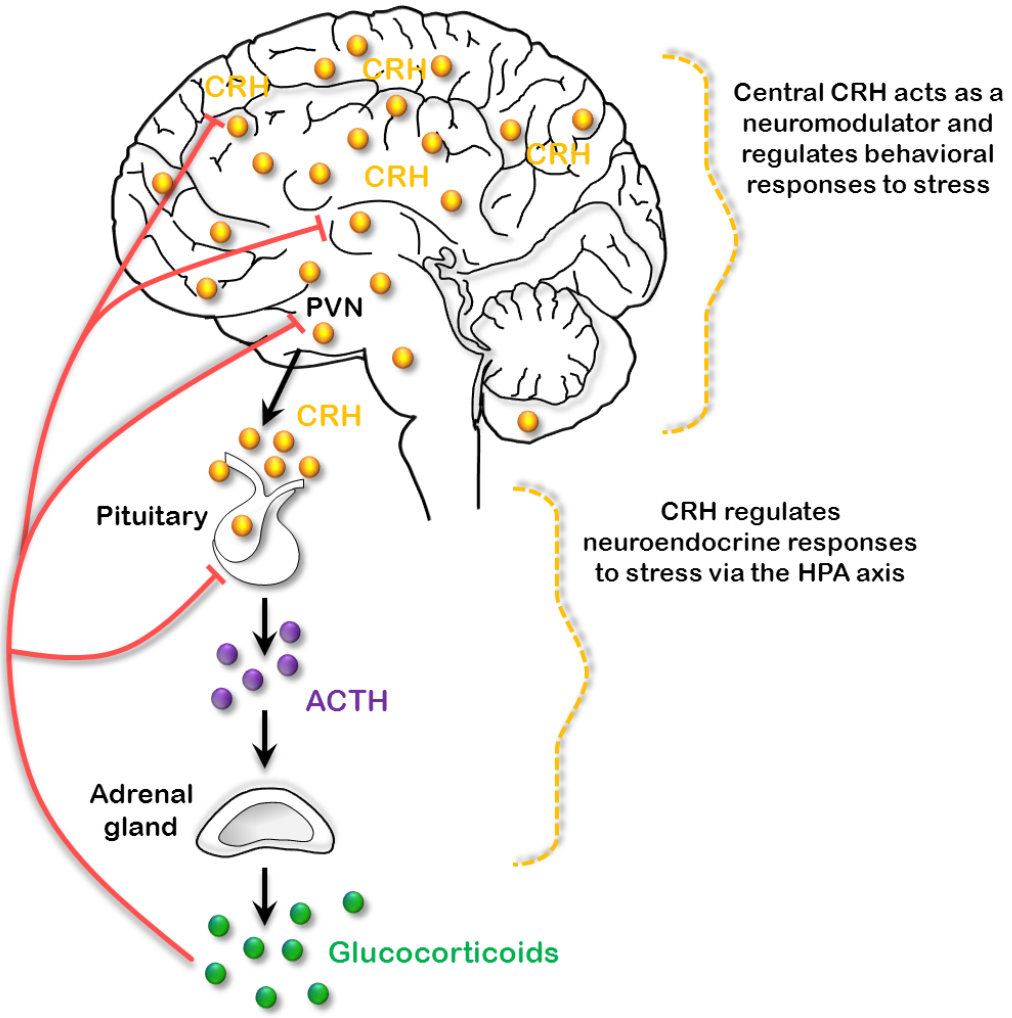

Figure 1: CRH mediates neuroendocrine responses to stress via the HPA axis.
CRH integrates the neuroendocrine and higher order behavioral responses to stress by acting as a secretagogue within the line of the HPA axis an as a modulator of synaptic transmission in the CNS. Adrenocorticotropic hormone (ACTH), corticotropin-releasing hormone (CRH), hypothalamic-pituitary-adrenal (HPA) axis, hypothalamic paraventricular nucleus (PVN). Modified from Deussing and Wurst, 2005.

Thus, positive experiences such as sexual encounter, wheel running and social victory in rats induce a similar degree of HPA axis activation as an aversive footshock, social defeat and restraint stress (Koolhaas et al., 1997; Koolhaas et al., 2011). Koolhaas and colleagues propose that the term "stress" *should be restricted to conditions where an environmental demand exceeds the natural regulatory capacity of an organism, in particular situations that include*

unpredictability and uncontrollability. Physiologically, stress seems to be characterized by either the absence of an anticipatory response (unpredictable) or a reduced recovery (uncontrollable) of the neuroendocrine reaction" (Koolhaas et al., 2011). But do certain stressors affect brain circuitries independent of HPA axis function? An increasing number of studies support the notion that different types of stressors require different responses. In other words, not all stressors initiate the same non-specific physiological stress-response. For example, fast recruitment of the brainstem and hypothalamic regions occurs in response to physical stressors such as blood loss, cold or trauma (Fenoglio et al., 2006; Joels and Baram, 2009; Ulrich-Lai and Herman, 2009). On the other hand, psychological stressors such as social discomfort, loss of loved ones, examinations or deadlines predominantly engage stress mediators in brain regions responsible for regulating emotion, learning and memory, and decision making (Joels and Baram, 2009). These include the amygdala, bed nucleus of the stria terminalis (BNST), hippocampus, and prefrontal cortex (de Kloet et al., 2005a; McEwen, 2007; McEwen and Gianaros, 2010). Importantly, different stress-pathways often act in a synergistic manner to modulate physiology and behavior. The specific involvement of CRH in stress-related neurocircuitries will be explored in this thesis.

1.3. The CRH peptide family and their receptors

It becomes evident that CRH represents the major physiological mediator of the HPA axis, and thereby coordinates the neuroendocrine response to stress. Consequently, a number of studies have implicated altered HPA axis function in the pathogenesis of psychiatric disorders including anxiety and depression. In 1966, McClure and co-workers detected increased cortisol levels in the urine of depressed patients (McClure, 1966), which was confirmed by follow-up studies. Later on, elevated cortisol concentrations were also detected in the blood and cerebrospinal fluid (CSF) of patients with major depressive disorder (MDD) (Gillespie and Nemeroff, 2005). This can reflect hyperactive CRH signaling, or changes at the glucocorticoid and mineralcorticoid receptor level, leading to alterations in negative feedback control. However, nowadays hypercortisolemia is regarded as a state rather than a trait marker for depression, and is consequently not considered specific enough to function as a biomarker for mood disorders (Ozbolt and Nemeroff, 2013). Importantly, in 1984 Nemeroff and colleagues initially showed increased CRH levels in the CSF of depressed patients, which was confirmed by other studies (Nemeroff et al., 1984; Fossey et al., 1996; Carpenter et al., 2004). However, the actions of CRH are not confined to the neuroendocrine, HPA-system. The anatomical

distribution of CRH in the brain suggests that this peptide not only acts as a key neuroendocrine stress mediator, but is also able to regulate neuronal activity in a neuromodulatory fashion. In fact, CRH is expressed throughout the central nervous system (CNS) including most limbic and cortical structures (Figure 3). Alterations in *CRH* and *CRHR1* mRNA expression were thus not only found in the PVN of post mortem tissue of depressed patients, but also in extrahypothalamic nuclei including the prefrontal cortex (Nemeroff et al., 1988; Merali et al., 2004). In rodents, CRH-expressing neurons are located in the olfactory bulb, PVN, cerebral cortex, piriform cortex, central nucleus of the amygdala, BNST, nucleus accumbens, hippocampus, medial preoptic area, periaqueductal grey, medial geniculate nucleus, anterior pretectal nucleus, raphe magnus, lateral tegmental nucleus, parabrachial nucleus, Barrington's nucleus, medial vestibular nucleus and the inferior olive (Olschowka et al., 1982a; Olschowka et al., 1982b; Swanson et al., 1983; Cummings et al., 1983; Sakanaka et al., 1987; Keegan et al., 1994; Alon et al., 2009) (Figure 3). Activation of central CRH circuits in rodents elicits behavioral responses similar to those observed following stress. These include increased anxiety-related behavior, arousal, decreased food-consumption, alterations in locomotion, and diminished sexual behavior and sleep disturbances (Sutton et al., 1982; Sirinathsinghji et al., 1983; Tazi et al., 1987; Dunn and File, 1987; Butler et al., 1990; Koob et al., 1993; Stenzel-Poore et al., 1994; Heinrichs et al., 1997; Lu et al., 2008; Pitts et al., 2009; Kimura et al., 2010; Sztainberg and Chen, 2012; Chen et al., 2012b). The emotional components of stress are believed to be mediated by CRH in limbic regions, including the CeA, BNST and hippocampus, and will be discussed in more detail later on.

The biologically active form of CRH is represented by a 41-amino acid long peptide, which is identical with regards to size and amino-acid sequence in humans, rats and mice. It is generated by cleavage of the C-terminus of pre-pro CRH, the 196-amino-acid precursor. To date, the mammalian CRH-family comprises three additional peptides (Figure 2). Urocortin (UCN) 1 was initially described in 1995 by Vaughan and colleagues (Vaughan et al., 1995). The discovery of UCN2 (or stresscopin-related peptide) and UCN3 (or stresscopin) followed shortly afterwards (Hsu and Hsueh, 2001; Lewis et al., 2001; Reyes et al., 2001)(Figure 2). The primary structure of CRH is more closely related to UCN1 than to the other two family members. CRH and UCN1 share 43% amino-acid homology, in contrast to CRH and UCN2 or UCN3 which display 34% and 26% sequence identity respectively (Dautzenberg and Hauger, 2002). In contrast to CRH, urocortin-expressing neurons are found in more discrete regions of the CNS (Figure 3). UCN1 is mainly expressed in the Edinger-Westphal nucleus and weakly distributed in

the lateral superior olive and supraoptic nucleus (Vaughan et al., 1995). UCN2 is found in the PVN, supraoptic nucleus, arcuate nucleus, locus coeruleus and brainstem, whereas UCN3 is mainly expressed in the medial amygdala, rostral perifornical area of the hypothalamus, BNST, superior paraolivary nucleus, nucleus parabrachialis and the premammillary nucleus (Hsu and Hsueh, 2001; Lewis et al., 2001; Reyes et al., 2001; Deussing et al., 2010). All four peptides have also been detected in the periphery, although this is most strongly pronounced for UCN2 and UCN3, which have recently been recognized as novel modulators of centrally- and peripherally-controlled metabolic function (Li et al., 2003; Chen et al., 2004a; Kuperman and Chen, 2008). The expression sites of the CRH-peptide family in the rodent brain are illustrated in figure 3. CRH and the urocortins signal through activation of two class B1 membrane-bound G-protein-coupled receptors, CRHR1 and CRHR2, which share 70 % amino acid identity (Chen et al., 1993; Perrin et al., 1993; Chang et al., 1993; Vita et al., 1993; Perrin et al., 1995). The lowest degree of homology exsists in their extracellular domains, particularly the N-termini (40% identity). In contrast, the transmembrane domains of CRHR1 and CRHR2 are highly homologous (80-85% amino acid identity) (Dautzenberg and Hauger, 2002). CRHR1 has one known functional splice variant in the CNS, whereas CRHR2 is expressed in three functional membrane splice variants in humans (α, β, and γ) and two in rodents (α and β) (Lovenberg et al., 1995). CRH shows a much higher affinity for CRHR1 than for CRHR2 while UCN1 displays equal affinities for both receptors (Figure 2). UCN2 and UCN3, on the other hand, appear to be selective ligands for CRHR2 (Perrin et al., 1995; Hsu and Hsueh, 2001; Dautzenberg and Hauger, 2002). Similarly to its main ligand CRH, CRHR1 mRNA is found throughout the CNS including the olfactory bulb, cerebral cortex, BNST, basolateral amygdala, hippocampus, globus pallidus, reticular thalamic nucleus, caudate putamen, ventral tegmental area and the cerebellum (Figure 3). It is also highly expressed in the anterior pituitary where it initiates HPA axis activity in response to CRH binding (Van Pett et al., 2000; Kuhne et al., 2012). In contrast, CRHR2α (the major splice variant in rodents and from here on referred to as CRHR2), displays a more confined expression, with high densities in the olfactory bulb, BNST, lateral septum, ventromedial hypothalamic nucleus, and the dorsal raphe nucleus (Lovenberg et al., 1995; Van Pett et al., 2000). CRHR2β is primarily expressed in peripheral tissue and in the choroid plexus of the brain (Perrin et al., 1995). In addition, the activity of CRH and UCN1 can be regulated by the CRH binding protein (CRH-BP), which is not capable of binding UCN2 or UCN3 (Seasholtz et al., 2001; Dautzenberg and Hauger, 2002).

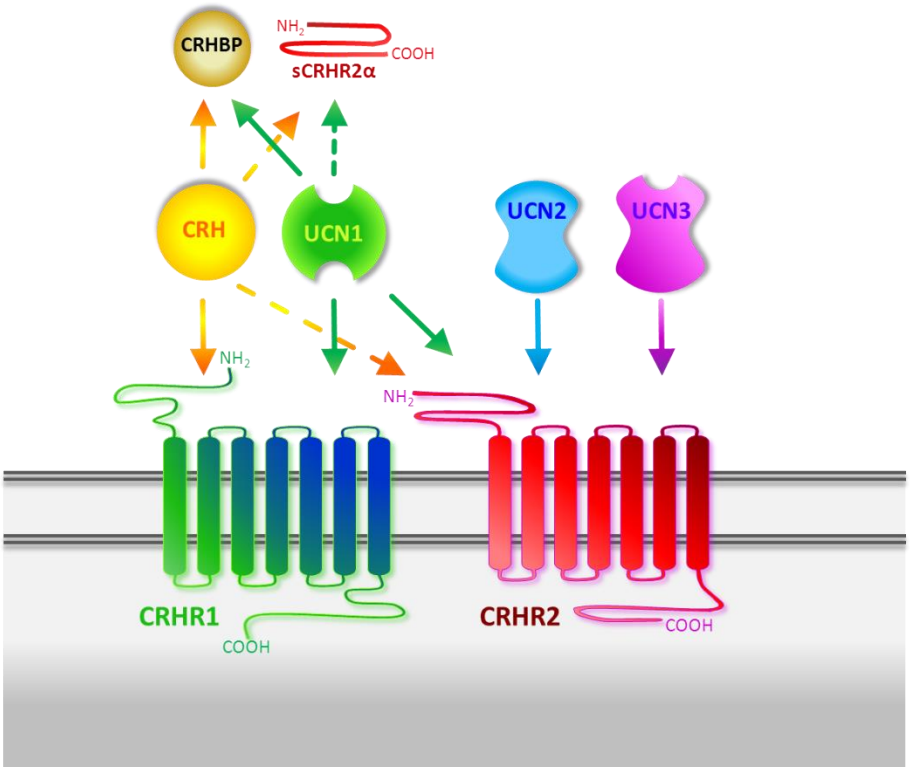

Figure 2: CRH-family members, their receptors and binding proteins.
The arrows represent ligand-receptor or ligand-binding protein interactions. Dashed arrows indicate relatively low binding affinities, compared to unbroken arrow-lines. CRH displays a relatively high affinity for CRHR1 and low affinity for CRHR2. UCN1 binds to both receptors with equal affinity. UCN2 and UCN3 are selective ligands for CRHR2. CRHBP is able to sequester both CRH and UCN1. The same is also proposed for the recently discovered sCRHR2α, but not yet proven. Abbreviations: corticotropin-releasing hormone (CRH), urocortin 1 (UCN1), urocortin 2 (UCN2), urocortin 3 (UCN3), CRH receptor 1 (CRHR1), CRH receptor 2 (CRHR2), CRH binding protein (CRHBP), soluble variant of CRHR2 (sCRHR2α).

Past research has largely ignored the presence of the CRH-BP, which is suggested to act as an endogenous buffer, possibly by regulating neuroendocrine and synaptic release of CRH and UCN1 (Behan et al., 1995; Seasholtz et al., 2001; Seasholtz et al., 2002). The complexity of the CRH-system is further increased by the recently discovered soluble splice variant of CRHR2 (sCRHRα), which encodes the extracellular receptor ligand-binding domain, but terminates before the transmembrane domains (Chen et al., 2005). Although its function is still largely unknown, sCRHR2α was originally proposed to act as a decoy receptor, mimicking the ability of the CRH-BP to sequester free CRH. However, Evens and colleagues have disclaimed this, favoring the idea that the unproductive splicing of *Crhr2* pre-mRNA to *sCrhr2* may selectively alter the cellular levels of full-length *Crhr2* mRNA and consequently affect the number of functional CRHR2 receptors (Evans and Seasholtz, 2009).

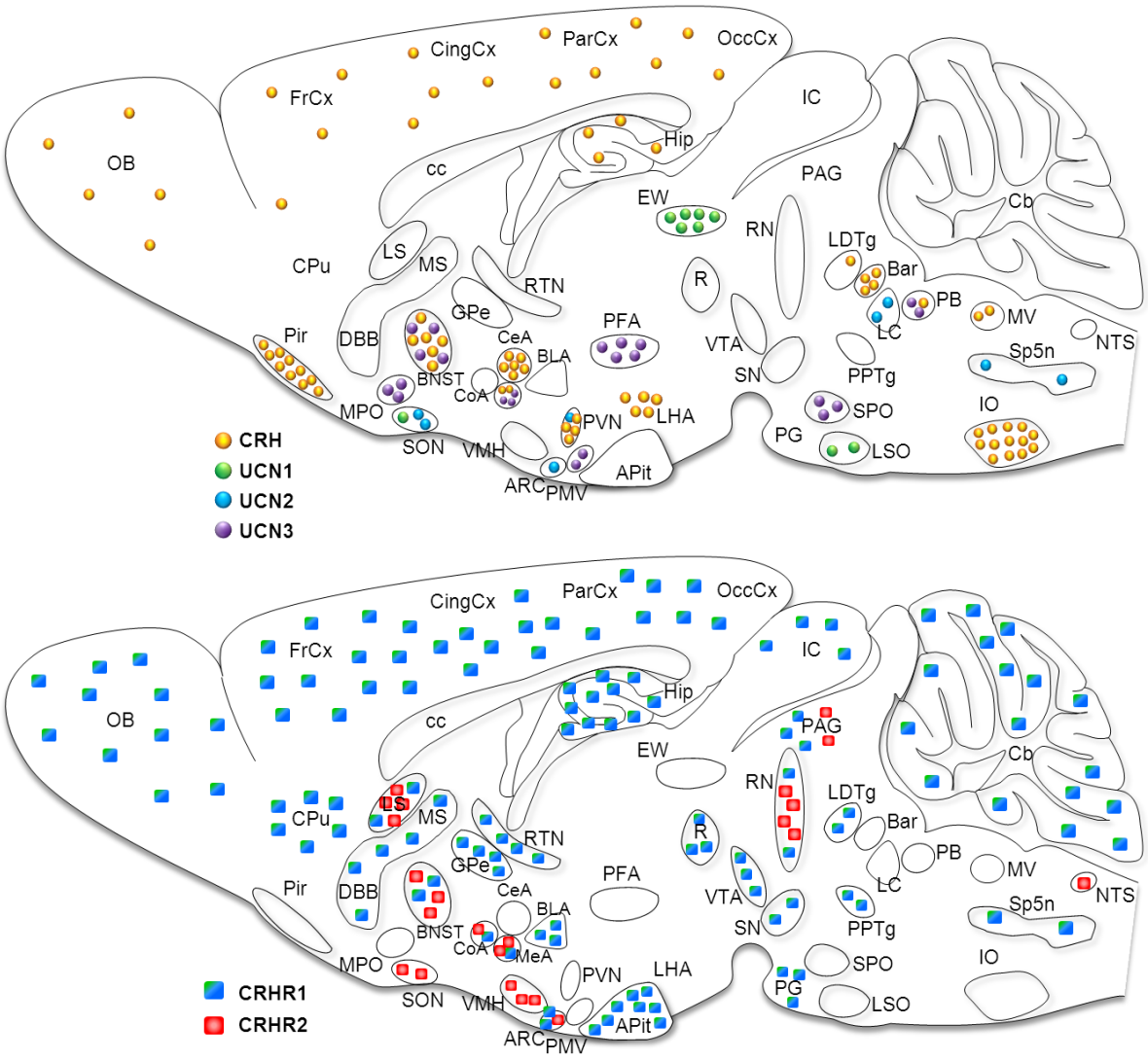

Figure 3: Schematic illustration of the spatial distribution and relative expression of CRH-family peptides and their receptors in the mouse brain.

Abbreviations: Anterior pituitary (APit), arcuate nucleus (ARC), basolateral nucleus of the amygdala (BLA), bed nucleus of the stria terminalis (BNST), corpus callosum (cc), central nucleus of the amygdala (CeA), cerebellum (Cb), cingulate cortex (CingCx), cortical nucleus of the amygdala (CoA), caudate putamen (CPu), Barrington's nucleus (Bar), diagonal band of Broca (DBB), Edinger Westphal nucleus (EW), frontal cortex (FrCx), globus pallidus (GPe), inferior colliculi (IC), inferior olive (IO), locus coeruleus (LC), lateral septum (LS), laterodorsal tegmental nucleus (LDTg), lateral hypothalamic area (LHA), lateral superior olive (LSO), medial nucleus of the amygdala (MeA), medial preoptic area (MPO), medial septum (MS), medial vestibular nucleus (MV), nucleus tractus solitarii (NTS), olfactory bulb (OB), occipital cortex (OccCx), periaquaductal gray (PAG), parietal cortex (ParCx), parabrachial nucleus (PB), perifornical area (PFA), pontine gray (PG), piriform cortex (Pir), pedunculopontine tegmental nucleus (PPTg), premammillary nucleus (PMV), paraventricular nucleus of the hypothalamus (PVN), red nucleus (R), raphe nuclei (RN), reticular thalamic nucleus (RTN), superior colliculi (SC), substantia nigra (SN), supraoptic nucleus (SON), spinal trigeminal nucleus (Sp5n), superior paraolivary nucleus (SPO), ventral medial hypothalamus (VMH), ventral tegmental area (VTA). Modified from Reul and Holsboer, 2002

The diverse and broad expression patterns of CRH peptides and receptors, as well as the high level of signaling complexity, allow this circuitry to effectively integrate neuroendocrine, autonomic and behavioral responses of stress. The thought comes to mind that CRH might even regulate specific behaviors independent of stress.

1.4. Stress - an overlapping cause of mental disorders

Mental disorders including schizophrenia, depression, anxiety-disorders, dementia, alcohol and substance abuse, epilepsy and Parkinson's disease constitute roughly 13% of the global disease burden (World Health Organisation, 2008; Collins et al., 2011), surpassing both cardiovascular disease and cancer. In Europe, the financial burden associated with brain disorders adds up to 800 billion euros a year, more than cancer, cardiovascular disease and diabetes combined (Smith, 2011). Depression tops the estimated costs, representing the most prevalent mental illness and third leading contributor to the global disease burden (Collins et al., 2011; Lepine and Briley, 2011). The lack of effective treatments or preventive interventions for most mental disorders partially reflects our limited understanding of the underlying brain-circuitries. Perhaps this is not surprising considering that clinicians and scientists have not yet agreed on how to best define and diagnose mental illnesses (Adam, 2013). At present diagnosis is still based soley on phenomenology, that is, on symptoms, signs and course of illness according to the guidelines proposed by the fourth Diagnostic and Statistical Manual of Mental Disorders (DSM-IV) (Nestler and Hyman, 2010). Hence, DSM-IV places mental illnesses in discrete categories such as major-depressive disorder, bipolar disorder, schizophrenia, autism and obsessive-compulsive disorder, which is complicated by the fact that many patients suffering from these illnesses display a substantial amount of overlapping symptoms (Adam, 2013). For example, positive symptoms in schizophrenia, including delusions and disordered thoughts, are commonly observed in bipolar patients during the manic phase (Berrettini, 2000; Benabarre et al., 2001; Buckley et al., 2009). Consequently, psychiatrists have come to use the term schizoaffective disorder in patients with overlapping symptoms of schizophrenia and bipolar disorder. Similarly, the inability to enjoy pleasurable activities (anhedonia) is found in many illnesses including schizophrenia and depression (Pelizza and Ferrari, 2009; Adam, 2013). Most patients with mixed symptoms are frequently diagnosed with several disorders, so called comorbidities. This is also illustrated by the fact that one-fifth of individuals who fulfill criteria for one DSM-IV disorder meet the criteria for at least two more (Kessler et al., 2005; Maj, 2005; Kessler et al., 2012; Adam, 2013). Consequently, a number of scientists are proposing

the so called "dimensional approach" with regards to the classification and assessment of psychiatric disorders (Figure 4). An example is given by Craddock and Owen, where mental-health conditions lie on a spectrum that has partially overlapping causes and symptoms (Craddock and Owen, 2010a; Craddock and Owen, 2010b; Adam, 2013).

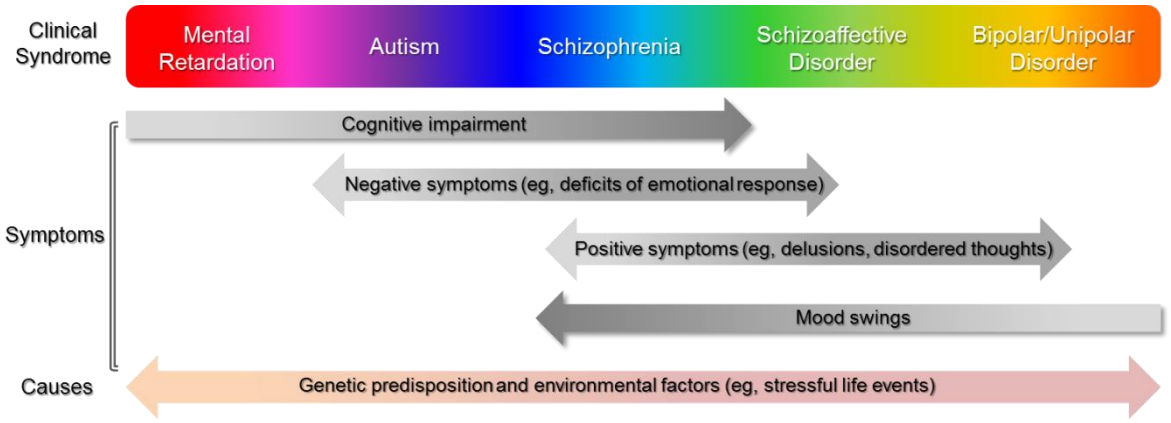

Figure 4: Ovlerapping causes and symptoms of mental illnesses.
The "dimensional approach to psychiatry" proposes that mental disorders lie on a spectrum that has partially overlapping causes and symptoms. Besides genetic predisposition, life stress represents a major risk factor for psychiatric disorders. Together, genetic predisposition and environmental exposure interact to shape brain circuitries, and ultimately determine disease susceptibility or resilience. Modified from David Adam, 2013.

This overlap also exists at the genetic level, as recently demonstrated by the Cross-Disorder Group of the Psychiatric Genomic Consortium led by Jordan Smoller, Kenneth Kendler and Naomi Wray (Lee et al., 2013). The group demonstrated evidence for shared genetic etiology in five psychiatric disorders including schizophrenia, major depressive disorder, autism spectrum disorder and attention-deficit/hyperactivity disorder. Some of these relationships are supported by previously conducted genetic and genome-wide association studies (GWAS), which have frequently reported shared genetic risk factors for a number of psychiatric disorders. For example, *NRG1*, *DISC1* and *ANK3* have been associated with both schizophrenia and bipolar disorder (Craddock et al., 2006; Ferreira et al., 2008; Ripke et al., 2011; Wirgenes et al., 2014). *CACNA1C*, which encodes the L-type calcium channel $Ca_v1.2$, has been repeatedly associated with schizophrenia, BPD and depression (Ferreira et al., 2008; Bigos et al., 2010; Green et al., 2010; Bhat et al., 2012). These data clearly support an overlapping genetic etiology across many mental illnesses, which are likely to underlie genetic alterations in key neuronal circuits relevant to emotion, motivation and cognition. Prominent examples include the serotonergic, noradrenergic and dopaminergic circuits, which are targeted by many antipsychotic and antidepressive drugs. However, it is highly unlikely that a single risk-gene

exclusively contributes to a given mental illness. Although a vast number of family and twin studies suggest a high degree of heritability of psychiatric disorders, many of the recent GWAS studies were not able to identify robust and replicable findings especially for major depressive disorder (MDD). Hence, single-nucleotide-polymorphism (SNP)-based heritabilities suggest a significantly lower genetic contribution to psychiatric disorders than previously estimated (Maher, 2008). Although this "case of missing heritability" is not fully understood, it underscores that genetic predisposition is not the sole cause of psychiatric illness, and hints towards the involvement of additional factors such as the environment. In fact, stress represents a key predisposing factor for most psychiatric disorders, and is also able to aggravate established symptoms (Dunner et al., 1979; Brown et al., 1987; Holsboer, 2001; de Kloet et al., 2005a). For example, chronic stress represents a strong proximal predictor of MDD onset and can also induce recurrence of depressive symptoms (Kendler, 1995; Kendler et al., 1999; Hammen, 2006; Burcusa and Iacono, 2007). Similarly, stressful life events are associated with substance and drug abuse and were frequently reported to trigger relapse (Le and Koob, 2007; Koob, 2008; Russo and Nestler, 2013). Even adverse experiences *in utero* or during early childhood are increasingly asscociated with lifelong health disparities (Maher, 2008; Buss et al., 2012). Adverse environmental insults during gestation or the perinatal period are postulated to increase the risk of developing schizophrenia (Lewis and Levitt, 2002; Jones et al., 2011). In addition, severe stress seems to be associated with the worsening or relapse of psychotic symptoms in schizophrenic individuals (Nuechterlein and Dawson, 1984; Corcoran et al., 2003; Tessner et al., 2011). But why does stress cause disease in some individuals but not in others? A common perception is that adverse environments might trigger disease onset in genetically predisposed individuals. Evidence for such gene-environment interactions have been provided by a number of studies. The influence of stressful life events on depression was shown to be moderated by a functional SNP in the promoter region of the serotonin transporter gene (Caspi et al., 2003). Along these lines, a functional polymorphism in the *FKBP5* gene, an important regulator of stress-induced glucocorticoid receptor action, increased the likelihood to develop post-traumatic stress disorder (PTSD) in individuals that have experienced childhood abuse (Klengel et al., 2013). Persistent physiological, molecular and behavioral alterations caused by stress are believed to underlie long-lasting epigenetic changes. In cases of genetic predisposition, certain risk-SNPs might enable differential epigenetic regulations in response to specific environmental demands. The matter is further complicated by more recent studies reporting transgenerational inheritance of epigenetic marks (Dias and Ressler,

2014; Heard and Martienssen, 2014). However, the idea that the parents' environment could affect future generations is still highly controversial and not fully understood. Nevertheless, altered stress-neurocircuitries, either caused by genetic, and/or environmental changes, might constitute a common domain of many mental disorders.

1.5. Modeling neuropsychiatric disorders in animals

An important step towards the dissection of complex genetic and environmental factors in neuropsychiatric disorders is the development of appropriate animal models. In the past decades the mouse has evolved as the organism of choice in biomedical research. In addition to a number of practical and economic advantages compared with other mammalian species, the ability to efficiently and precisely "engineer" the mouse genome has mainly contributed to its wide use (Deussing, 2013). However, mimicking any human behavioral trait in rodents is extremely difficult, which makes the undertaking to try and model multifactorial mental diseases nearly impossible. For example, how do we recapitulate all aspects of depression in an animal, when the criteria used to classify MDD are of extreme heterogeneous and sometimes even opposite nature (e.g., substantial weight gain or loss, insomnia or hypersomnia)? On top of that, animals not only lack consciousness of self, self-reflection and consideration of others but also aspects of the disorder such as depressed mood, low self-esteem or suicidality (Deussing, 2006). Similarly, most available mouse models of schizophrenia are not able to accurately reflect the positive-symptoms, which include hallucinations and delusion, and the characteristic cycles between manic and depressive episodes in bipolar disorder patients have also not been successfully mirrored in animals. Moreover, the difficulty in generating mouse models of specific mental disorders is further emphasized by the fact that we cannot even clearly define many neuropathologies in humans. This does not mean that it is impossible to develop useful animal models, but rather highlights the unlikelihood of generating a model that will mirror the full extent of a given human neuropsychiatric disorder (Nestler and Hyman, 2010). Nonetheless, certain endophenotypes of a given disorder can be reproduced independently and evaluated in mice (Table 1) including physiological, endocrinological, molecular, neuroanatomical and behavioral alterations. So far a variety of different mouse models has been established to improve our understanding of the pathophysiology of a wide spectrum of psychiatric diseases. However, a full consensus regarding the prerequisites of a valid animal model is still lacking in the scientific community. Up to now, the three criteria set up by McKinney and Bunney (McKinney, Jr. and Bunney, Jr.,

1969) are still widely accepted; they include construct validity, face validity, and predictive validity.

Construct (or etiologic) validity, the most complex of the three terms, requires that the symptoms produced in the animal model are based on the same underlying neurobiological mechanisms as in humans. Thus, one tries to recreate mechanisms/processes in the animal which would also initiate the disease in humans. The ideal way would be to introduce a known human disease-causing gene variant into a mouse and thereby alter intracellular mechanisms, which in the end lead to the disease (Chadman et al., 2009; Nestler and Hyman, 2010). Unfortunately this is currently far from being realistic, since most disease-causing genetic alterations have not been established with certainty and the probability that a single gene is solely responsible for a given disease is highly unlikely. In addition, an animal model does not have to be based on a genetic change, but can also be subjected to an environmental challenge or a combination of both. *Face validity* is achieved when the animal exhibits specific symptoms of the disease which are similar in the human condition. These can be of biochemical, anatomical, neuropathological or behavioral nature. Thus the concept of face validity can also be regarded as the attempt to reproduce certain endophenotypes which can be accurately measured in the animal. Finally, *predictive validity* refers to the ability of the animal to correctly respond to pharmacological treatment, which should correlate with results from clinical trials. In this context, it is important to note that the more criteria the proposed model meets, the more compelling it will be (Malkesman et al., 2009). Simply put, researchers are faced with the challenge of 1) constructing a model with similarity in disease progression and symptomatology to humans, 2) detecting these phenotypes with the appropriate behavioral tests and 3) reverting them with treatment modalities that are also effective in humans.

It is important to point out that that animal models and behavioral tests represent two very separate entities. Animal models are expected to show sufficient construct, face and predictive validity. Behavioural tests on the other hand are used to assess phenotypic alterations relevant to the disease and should be regarded as a technical tool and not as a model. Similarly, antidepressant screening paradigms, such as the forced swim test (FST), do not represent a model of depression but should rather be regarded as drug-screening assays.

1.5.1. Behavioral tests - tools used to assess phenotypic alterations in animal models

Mental illnesses in humans are highly complex and constitute an enormous heterogeneity of symptoms. However, the number of related behaviors which can be observed in mice is fairly limited. These include anxiety-, reward-, social-, despair-, and active versus passive stress-coping behavior, cognitive dysfunction, startle reactivity and prepulse inhibition, as well as alterations in general locomotion, sleep, food and liquid intake. Alterations in these specific behavioral domains are observed across a variety of animal models of psychiatric disorders (Table 2). These are believed to underlie alterations in neurocircuits responsible for autonomic, emotional and cognitive processes, which are likely to be affected in all mental disorders. The most common behavioral tests used to assess phenotypic alterations in animals are summarized below. Many of these were also used in this study.

Anxiety-based tests

Anxiety is a normal state of cognitive and behavioral preparedness that an organism mobilizes in response to a future or distant potential threat (Leonardo and Hen, 2008). Although anxiety is often necessary and even protective, excessive anxiety can trigger disabling responses that, in time, lead to anxiety disorders (e.g., generalized anxiety disorder, social phobia, simple phobia, panic disorder, posttraumatic stress disorder (PTSD), and obsessive compulsive disorder) (Bienvenu et al., 2009). Anxiety can often emerge as part of other psychiatric syndrome such as depression, but this does not hold true for all patients (Krishnan et al., 2007; Kessler et al., 2012). In animal models anxiety is considered a core endophenotype of many psychiatric disorders, which mainly results from the availability of a wide range of standardized tests, all of which assess anxiety-like behavior. Most of these assays are based on approach-avoidance conflicts and were developed and validated using classical benzodiazepine-like anxiolytic compounds. Mice generally display high levels of exploration of a novel environment but also have an innate aversion to enter exposed, well-lit areas. The elevated plus-maze (EPM) and elevated zero-maze present the subject mouse with the choice of spending time exploring the aversive open areas of a plus-shaped or circular runway, versus spending time exploring the enclosed arms and arcs (Handley and Mithani, 1984; Chadman et al., 2009). Other exploration-based tasks, founded on similar conflicting tendencies to approach versus avoid a potentially dangerous area are the dark- light box (DaLi) and open field (OF) test. The novel object exploration test makes use of similar principles, the only difference being that

mice are first habituated to an environment and then exposed to novelty (novel object). Thus the latter is proposed to reflect trait anxiety in contrast to the EPM, DaLi and OF which are measures of state anxiety (Griebel et al., 1993; Belzung et al., 1994; van Gaalen and Steckler, 2000). However, approach-avoidance conflicts have to be interpreted with caution since increased time spent in an aversive area can be interpreted as both, decreased anxiety or increased motivation or arousal.

Reward-related and anhedonic behavior

Anhedonia, a hallmark of depression is defined as the inability to experience pleasure from activities formally perceived enjoyable. Decreased intake of palatable solutions, such as sucrose is regarded as a behavioral measure of hedonic deficit/depressive-like state in rodents (Willner, 2005; Nestler and Hyman, 2010). Consequently, the most widely accepted approach to assess reward- seeking behavior is via the sucrose consumption and preference tests. One drawback, however, is that one cannot rule out appetitive, metabolic or sensorial influences, which may be altered in genetically modified animals. In addition, enhanced hedonic drive and motivation, which are hallmarks of manic symptoms in bipolar disorder, may often be misinterpreted as decreased depression-like behavior (Hasler et al., 2004). Operant paradigms, such as the conditioned place-preference (CPP), are also widely applied to assess anhedonic behavior. Even though methodological details differ among laboratories, a typical CPP experiment includes differential pairing of two distinct sets of environmental (contextual) cues with a stimulus (e.g., drug, food, copulatory opportunity) (Bardo and Bevins, 2000). When tested later on in the absence of the stimulus, the approaches and the amount of time spent in the compartments previously associated with the positive stimulus serve as an indicator of preference and a measure of reward learning.

Cognition-based tests

The majority of psychiatric disorders are characterized by cognitive deficits typically consisting of memory impairments, poor attention, and executive dysfunction (Deussing, 2006; Nestler and Hyman, 2010; Adam, 2013). The fact that the rodent cortex is much more primitive than the human, makes it extremely difficult to address many aspects of cognitive processing in mice (Cryan and Holmes, 2005). Therefore, many of the applied cognition tasks, such as the the Y-maze or different versions of the Morris water maze (MWM) focus on general cognitive function mediated by the hippocampal region. Developed by Morris in 1984, the MWM test assesses spatial learning in mice and rats and is strongly reflective of hippocampal synaptic

plasticity and N-Methyl-D-aspartic acid (NMDA) receptor function (Morris, 1984). The test relies on distal, visual cues that can help the animal to locate and navigate to a submerged escape platform from different starting locations within an open swimming arena. Spatial learning is evaluated across repeated trials and reference memory is assessed by preference for the platform area once the platform is absent (Morris, 1984; D'Hooge and De Deyn, 2001). The water-cross maze (WCM), which consists of four intersecting arms, employs similar principles. The main adavantage of the WCM is that it offers the possibility to assess different learning strategies and hence discriminate between place and response learning (Kleinknecht et al., 2012). The Y-maze, Barn's maze and Radial arm maze also assesse spatial memory and hippocampal integrity, but do not utilize the strong aversive stimulus induced by swimming. They are based on the animal's natural curiosity to discover novel environments (Olton and Samuelson, 1976; Barnes, 1979; Conrad et al., 1996; Dellu et al., 2000). Novel object recognition tasks are also commonly applied, and believed to relay on hippocampal and perirhinal cortex function. In most cases, mice/rats have to discriminate between a familiar and novel object. This is demonstrated by an enhanced interaction time with the unfamiliar object. Alterations in fear memory formation are observed in a subset of psychiatric conditions including post-traumatic-stress disorder, and are commonly assessed by Pavlovian fear-conditioning paradigms. Such contextual and cued fear conditioning tasks represent methodologies to investigate memory, as they require that the animals learn the association of a non-aversive context or cue with an aversive stimulus (Davis, 1990; Fendt and Fanselow, 1999; Maren, 2001). The ability to learn this association is measured by the amount of freezing exhibited in response to the cue or context alone. Many variations of the paradigm exist, including altering the type of cue and stimulus, and, once learned, testing the rate at which learning is extinguished (Fanselow, 1980).

Tests assessing despair-based / stress-coping behavior

In earlier days, the Porsolt forced swim test (FST) and the tail suspension test (TST) were regarded as typical depression-like paradigms, given the fact that both are responsive to monoamine-based antidepressant drugs. However, this view has been rejected by man scientists in the field which regard both tests as simple antidepressant screening paradigms (Nestler and Hyman, 2010; Krishnan and Nestler, 2011). The FST makes use of the fact that rodents eventually develop immobility when being placed in a cylinder of water after they have stopped active escape behaviors, such as climbing or swimming (Cryan and Holmes, 2005; Slattery and Cryan, 2012). A related task is the TST, which relies on similar assumptions and

interpretations as the FST. Given that water is not required to perform the task, the TST is not confounded by changes in thermoregulation (Cryan et al., 2005). Here the mice are hung upside down by their tails and the time spent immobile is assessed. In either case the underlying principles measuring active versus passive coping behavior are identical. Acute (but also chronic) administration of antidepressants decreases overall immobility in the FST and TST, shifting passive stress-coping toward active coping. Importantly, both tests assess the response to an acute inescapable stressor, provoking despair-based behavior/immobility or passive stress-coping behavior and not depression-like behavior. Moreover, passive-stress coping can also reflect the attempt to conserve energy and should thus be interpreted with caution. A disadvantage is that neither test reflects the slow onset of antidepressant action, which is commonly observed in depressed patients. In addition to the FST and TST, the learned helplessness paradigm also makes use of stressor uncontrollability and passive vs. active coping responses (Cryan and Holmes, 2005; Krishnan and Nestler, 2011). The paradigm is based on the observation that animals exposed to uncontrolled or unpredictable aversive events (e.g. electrical shocks) for a sufficient period of time will develop long-lasting deficits in escape performance. Short-term treatment with antidepressants as well as anxiolytics has shown to reverse the enforced behavioral phenotype, which does not make the paradigm particularly selective (Cryan and Mombereau, 2004). Similar to the FST and TST, the learned helplessness paradigm does not parallel clinical settings with regards to the slow onset of antidepressant action, but remains a good tool for the assessment of stress-coping behavior (Deussing, 2006).

Tests assessing social behavior

Social behavior can be defined as any behavior that influences, or is influenced by, other members of the same species. A number of neuropsychiatric disorders, are characterized by disruptions of social behavior, including schizophrenia, depression, bipolar disorder and autism (Nestler and Hyman, 2010; Fernando and Robbins, 2011). In rodents, the classical social interaction paradigm encompasses the free exploration of an unfamiliar conspecific by the experimental mouse. Social interaction is measured by the time spent in close proximity to the unfamiliar mouse as well as the amount and duration of additional behavior including sniffing, following, grooming, biting, mounting and the like. The social avoidance paradigm represents a similar but faster and more systematic approach to assess social behavior. In contrast to the standard tests, social approach towards an unfamiliar mouse enclosed in a wire mesh cage is measured (Berton et al., 2006; Golden et al., 2011). This excludes subject bias from the

observer, since only the time spent in close proximity to the target is assessed. In addition, aggressive behaviors such as biting and fighting can be excluded. Other paradigms, including the sociability test can be used to assess the social preference between a stranger/conspecific and an object (Moy et al., 2004; Nadler et al., 2004). In addition, social novelty can be evaluated by introducing a second unfamiliar mouse. Most social tasks in mice are employed after repeated exposure to a stressor, given that this can induce profound social deficits. However, an increasing number of studies are staring to employ social tests also under basal conditions especially when evaluating transgenic mouse lines.

Prepulse inhibition (PPI) of the acoustic startle reflex

PPI represent a cross-species measure where a response to a startling stimulus (such as loud noise) is inhibited by previous presentation of a low intensity prepulse (Braff et al., 1978; Swerdlow et al., 2002). Deficits in prepulse inhibition (PPI) are commonly observed in schizophrenic individuals and can also be measured in mice (Swerdlow et al., 2008). Importantly, alterations in PPI can also occur in several other neuropsychiatric disorders including bipolar disorder, and are believed to reflect impairments in sensorimotor gating.

1.5.2. Outline of existing mouse models of neuropsychiatric disorders

Considering the comprehensive literature on currently available animal models of neuropsychiatric disorders (Cryan and Mombereau, 2004; Cryan and Holmes, 2005; Deussing, 2006; Gould and Gottesman, 2006; Chadman et al., 2009; Nestler and Hyman, 2010; Arguello et al., 2010; Chen et al., 2010a; Krishnan and Nestler, 2011; Jones et al., 2011; Fernando and Robbins, 2011; Young et al., 2011; Russo et al., 2012; Berton et al., 2012; Koob, 2012; Tye and Deisseroth, 2012), the next section is meant to outline a few examples with particular focus on major stress-related disorders including depression, bipolar disorder (BPD) and schizophrenia (SCZ). A number of different methods have been applied in the past to generate animal models of neuropsychiatric disorders including selective breeding, genetic engineering, brain lesions and environmental manipulations (Table 1). However, most animal models are either based on genetic manipulations, environmental challenges or a combination of both. Assessment of specific circuits via optogenetic manipulation is currently on the rise of becoming a powerful asset (Nestler and Hyman, 2010; Tye and Deisseroth, 2012). In fact, applying projection-defined activity control, a number of optogentic studies have repeatedly demonstrated the ability to induce specific behaviors related to reward, motivation, depression, social interaction, compulsion and cognition (Witten et al., 2010; Kravitz et al., 2010; Goshen et al.,

2011; Yizhar et al., 2011a; Yizhar et al., 2011b; Tye and Deisseroth, 2012; Kim et al., 2013; Tye et al., 2013; Chaudhury et al., 2013; Deisseroth, 2014). The strengths and weaknesses of most prominent animal models of neuropsychiatric disorders are described in Table 1. Moreover, overlapping symptoms between SCZ, BPD and MDD and the corresponding endophenotypes in mice are summarized in Table 2, which also points out the most common behavioral tests used to assess face validity in these models.

Animal models of schizophrenia

Schizophrenia represents a highly complex mental disorders characterized by three symptom clusters: positive (including hallucinations, delusion, conceptual disorganization and though disorder), negative (emotional blunting, anhedonia, diminished motivation, social withdrawal and impoverished speech), and cognitive dysfunction (including deficits in working memory, attention and impaired executive function)(Andreasen and Olsen, 1982; Andreasen, 1995; Tandon et al., 2013; APA, 2013). However, patients often display extremely heterogeneous symptoms, which make diagnosis difficult. Most available antipsychotic drugs are efficient in targeting positive symptoms, but are largely ineffective in treating negative and cognitive symptoms (Keefe et al., 2007). A large body of evidence has linked the manifestation of positive symptoms to alterations in dopaminergic circuitries, predominately excessive mesolimbic dopamine release (Cohen and Servan-Schreiber, 1992; Goto et al., 2007; Goto and Grace, 2007). Cognitive impairments are believed to arise from the thinning of the cerebral cortex due to reduced dendritic aborization. Decreased synthesis of the inhibitory neurotransmitter GABA in cortical neurons has also been observed (Cannon et al., 2002; Lewis and Sweet, 2009). The observation that NMDA glutamate receptor antagonists, such as phencyclidine (PCP) and ketamine produce psychotic symptoms and cognitive disturbances in healthy individuals gave rise to the glutamate hypothesis of schizophrenia (Olney and Farber, 1995; Nestler and Hyman, 2010). Hence a number of pharmacological and genetic mouse models were developed based on dopamine and glutamate dysfunction, but none were able to reflect a combination of positive, negative and cognitive symptoms. For example, both PCP- and amphetamine-induced hyperlocomotion and sensitization is proposed to mirror psychotic-like changes in mice. Amphetamine induces synaptic dopamine release by directly acting on the presynaptic terminals of dopamine neurons (Nestler et al., 2009). PCP can indirectly also cause dopamine release (Nestler et al., 2009). Importantly, excessive striatal dopamine release in response to acute amphetamine administration was also observed in individuals with schizophrenia compared to healthy controls (Kegeles et al., 2010).

General approach	Specific method	Strengths	Weaknesses
Genetics	Selective breeding	Focus on phenotypes of interest	May produce a phenocopy of human disorder
	Random mutation & screening	Focus on phenotypes of interest	May produce a phenocopy of human disorder
	Transgenic animals (e.g. knockouts, knockins, overexpression)	Recapitulates genetic abnormality in human disorder; focus on gene of interest	Variable penetrance of genetic abnormality in rodents Human relevance of phenotype may be difficult to establish
	Virally mediated gene delivery	Spatial and temporal control over genetic change; focus on gene of interest	Does not recapitulate genetic cause of human disorder
Environmental	Chronic social stress (adult or during development)	May recapitulate risk factors in humans	Lack of specificity for a given human disorder
	Chronic physical stress	Easy to administer	Lack of construct validity for most human disorders
Pharmacological	Administration of neurotransmitter agonists or antagonists	Temporal and some spatial control (with intracranial delivery); focus on neurotransmitter system of interest	Lack of evidence that common mental disorders involve selective lesions of a single neurotransmitter system
Brain lesions	Anatomical lesions	May produce behavioral abnormalities reminiscent of human disorder	Lack of evidence for anatomical lesions as cause of human disorder
Optogenetic stimulation / inhibition	Modulation of neuronal activity in neurons genetically sensitized to light	Spatial and temporal control over neural circuit function; may recapitulate some findings in humans with DBS	Current limitations in knowledge of neural circuit abnormalities in human disorder

Table 1: Animal models of neuropsychiatric disorders. Adapted from Nestler and Hyman 2010.

Moreover, deficits in PPI can be induced in rodents upon amphetamine or NMDA receptor blockade, and can be alleviated following dopamine receptor 2 (D_2) antagonist treatment (Swerdlow et al., 2008). However, locomotor activation does not really reflect any of the key symptoms of schizophrenia and is also used to model mania-like behavior in animals (Table 2). In addition, these pharmacological models largely failed to induce negative or cognitive symptoms, although some studies have reported social withdrawal and memory impairments after acute PCP administration in rodents (Jones et al., 2011).

The majority of genetic models have been developed on the basis of replicating changes in mRNA and protein levels believed to be altered in schizophrenia. Most of the associated genes are involved in neuronal plasticity, synaptogenesis, glutamatergic or dopaminergic function.

Prominent members include disrupted-in-schizophrenia (DISC1), neuregulin 1 (NGR1) and its receptor ERBB4, dysbindin (DTNBP1) and reelin (RELN), although DISC1 and reelin have also been associated with bipolar disorder (Guidotti et al., 2000; Hodgkinson et al., 2004; Jaaro-Peled, 2009; Jaaro-Peled et al., 2009; Jones et al., 2011). Different knockout mice have been generated for all of the mentioned candidate genes, some of which display alterations in PPI, drug-induced hyperlocomotion, mild impairments in cognitive performance and social interaction (Nestler and Hyman, 2010; Jones et al., 2011; Koob, 2012). Brain structural and neurochemical changes were also observed, but these were often specific for the given knockout line. In some cases, the observed alterations could be reversed upon treatment with antipsychotic-drugs. However, deficits in PPI, cognition and social function are not very specific and can occur in other conditions such as bipolar disorder, Alzheimer's disease and depression. Consequently, these readouts are also commonly used in depression and bipolar disorder models (Table 2).

Human epidemiological studies strongly suggest that adverse environments during gestation or the prenatal period can enhance the risk to develop schizophrenia. Maternal stress, malnutrition, infection or enhanced immune activation during birth can result in neurodevelopmental defects which enhance the likelihood to develop disease later on in life (Lewis and Levitt, 2002). Consequently prenatal-stress, maternal deprivation and/or post-weaning social isolation have been used to model schizophrenia-like behavior in rodents. For instance, post-weaning social isolation was shown to induce spontaneous hyperactivity, PPI deficits, cognitive impairments, enhanced anxiety and aggression, and enhanced responses to novelty (Lapiz et al., 2003; Fone and Porkess, 2008; Jones et al., 2011). Again, the matter of specificity becomes an issue, as developmental and adult stress models are commonly used to induce a variety of endophenoytes of neuropsychiatric disorders. Importantly, maladaptive stress exposures are known to integrate different CRH-circuitries although this has hardly been investigated in connection to schizophrenia.

Animal models of depression

Similarly to schizophrenia, depression comprises a heterogeneous constellation of symptoms including depressed mood, anhedonia, feelings of guilt and worthlessness, disturbed sleep or appetite, psychomotor agitation or retardation, and suicidality (APA, 2013). Currently, three main theories try to conceptualize the molecular mechanisms underlying depression. These include the monoamine, neurotrophic, and HPA-axis hypothesis. The monoamine hypothesis postulates that depression is caused by an impairment of serotonergic, noradrenergic and/or

dopaminergic neurotransmission. It evolved from the observation that most common antidepressants inhibit the reuptake or degradation of monoamines, thereby increasing their concentrations in the synaptic cleft. Monoaminergic deficiency can be caused by several factors including decreased synthesis or early degradation of neurotransmitters, altered expression or function of neurotransmitter receptors and impairment of signal transduction systems activated by post-synaptic neurotransmitter receptors (Owens, 2004; Berton and Nestler, 2006; Krishnan and Nestler, 2008). Thus, earlier genetic approaches aimed to alter the expression of genes that are involved in these neurotransmitter systems and thereby analyze their respective role in animal behavior, neuroendocrine and molecular parameters. Several knockout mice of candidate genes related to the monoamine hypothesis were generated in the past (Urani et al., 2005; Krishnan and Nestler, 2008; Krishnan and Nestler, 2011). The main ones included the serotonin-(SERT), noradrenaline (NET)-, and dopamine (DAT) transporters, which represent major targets of antidepressants and psychostimulants such as cocaine and 3,4-methylendioxy N-methylamphetamine (MDMA/ecstasy). Many of these, including NET and DAT knockouts, displayed reduced immobility in the FST and TST, which fits the profile of antidepressant efficacy (Giros et al., 1996; Spielewoy et al., 2000; Xu et al., 2000). However, the behavioral readouts of immobility in these tests have to be interpreted with caution as they do not reflect depressive-symptoms. Alterations in sucrose-consumption, anxiety-related and social behavior were observed in some of the models, but the results were rather inconclusive (Perona et al., 2008; Haenisch et al., 2009; Haenisch and Bonisch, 2011). Hence, monoamine receptor KOs represent valuable pharmacological tools, but they are limited in their value as an animal model of depression. This is likely due to the fact that deletion of a single receptor is not sufficient to induce reliable depression-like phenotypes, and is further supported by family, twin and GWAS studies, which have failed to identify highly penetrant genetic variants that might be associated with depression (Maher, 2008). Consequently, much work in animal modeling has relied on the observation that chronic stress represents a major risk factor for depression (McEwen, 1998; de Kloet et al., 2005a; de Kloet et al., 2005b; Ising and Holsboer, 2006; Rice et al., 2008; Lupien et al., 2009). Several stress models have been developed with the aim to fulfill criteria of construct validity (Kudryavtseva et al., 1991; Koolhaas et al., 1997; Willner, 2005; Krishnan and Nestler, 2008; Nestler and Hyman, 2010; Koolhaas et al., 2011; Golden et al., 2011; Russo et al., 2012). The most common include early life stress, chronic mild and unpredictable stress, and the chronic social defeat stress (CSDS) paradigm. During chronic mild and unpredictable stress animals are primarily exposed to a

number of physical stressors, such as restraint, wet bedding, isolation, reversal of dark-light cycle etc. On the other hand CSDS involves subjecting rodents to repeated bouts of social subordination, which is more likely to mimic a natural situation. In many cases, these stress procedures induce signs of anhedonia, social withdrawal and cognitive impairments, many of which can be reversed with chronic antidepressant treatment, which suggests that severe stress can alter monoamine circuitries (Meaney, 2001; Berton et al., 2006; Nestler and Hyman, 2010; Krishnan and Nestler, 2011). Interestingly, most of the stress-based models also induce enhanced anxiety-related behavior in a range of tests including the EPM, DaLi and OF. Hence the assessment of anxiety-related behavior has become a major endophenotype of depression. This is also supported by the fact that many individuals with major depression also exhibit anxiety (Buckley et al., 2009; Nestler and Hyman, 2010), although one has to keep in mind that anxiety disorders constitute a syndrome-class of their own. Importantly, chronic stress models are also used to model other psychiatric conditions such as schizophrenia, bipolar disorder, obsessive-compulsive disorder and various forms of cognitive dysfunction. Rodent stress models were also largely responsible for the development of the neurotrophic hypothesis of depression. The latter assumes that the cAMP responsive element-binding protein (CREB) - brain derived neurotrophic factor (BDNF) - tyrosine kinase B receptor (TRKB) pathway is involved in the pathophysiology of depression and action of antidepressants. A number of groups could demonstrate that acute or chronic stress decreases BDNF expression in the hippocampus and that diverse classes of antidepressants produce the opposite effect and can prevent the actions of stress (Smith et al., 1995; Nestler et al., 2002; Duman, 2005; Berton et al., 2006; Berton and Nestler, 2006; Groves, 2007; Krishnan and Nestler, 2008). Many of the stress models also result in altered glucocorticoid homeostasis, which is ultimately linked to the HPA-axis hypothesis of depression. Hyperactivity of the HPA axis is observed in a number of patients with depression, as manifested by reduced feedback inhibition by CRH and glucocorticoids, increased expression of CRH in the hypothalamus and increased levels of CRH in the CSF (Nemeroff et al., 1984; Nemeroff et al., 1988; Arborelius et al., 1999; Holsboer, 2000; Sapolsky et al., 2000; Holsboer, 2001; Deussing and Wurst, 2005; de Kloet et al., 2005a; Muller and Holsboer, 2006; Ozbolt and Nemeroff, 2013). In addition, chronic stress can result in altered CRH/CRHR expression in extrahypothalamic sites such as the amygdala, BNST and hippocampus. The generation and analysis of numerous constitutive and conditional mouse mutants affecting different parts of the HPA axis has confirmed the role of the CRH and glucocorticoid system in the pathogenesis of affective disorders including depression (Table 2).

CRH overexpressing mice model some endophenotypes of depression including enhanced HPA axis function, and anxiety-like behavior (Stenzel-Poore et al., 1992; Stenzel-Poore et al., 1994; van Gaalen et al., 2002; Kolber et al., 2010). Accordingly, CRHR1 knockout mice display the opposite phenotype (Timpl et al., 1998; Smith et al., 1998; Muller et al., 2003). Glucocorticoid receptor knockout mice exhibit disrupted HPA feedback inhibition, which has also been observed in depressed individuals (Holsboer, 2000; Muller and Holsboer, 2006; Arnett et al., 2011). However, HPA axis abnormalities are not universally observed in depression and are not considered specific enough to provide diagnostic criteria. Nevertheless, the generated knockout and overexpressing mice are useful in modeling specific endophenotypes associated with depression.

Animal models of bipolar disorder

Bipolar disorder (BPD) is characterized by alternating manic (elevated mood) and depressive (depressed mood) states, although mania is the defining feature of the disorder (APA, 2013). The most effective treatment modality is lithium, although sodium valproate, lamotrigine and certain antipsychotics are also used to ameliorate specific symptoms (Bourin et al., 2005; Smith et al., 2007; Grandjean and Aubry, 2009). As previously mentioned, many psychotic features associated with manic episodes are also observed in individuals with schizophrenia (Table 2). Hence, the term schizoaffective disorder refers to individuals with symptoms of both schizophrenia and BPD (either mania, depression or both). Considering the simplistic behavioral readouts in mice, one might assume that BPD models combine features of depression- and schizophrenia models. However, none of them have yet successfully mimicked the fluctuations between these complex mood conditions in rodents, and it is questionable whether this can be achieved. Consequently, most effort in BPD research has been devoted to developing animal models of mania. Similarly as in schizophrenia, the most common model involves psychostimulant-induced hyperlocomotion in rodents, which is sensitized upon repeated administration of these drugs (most frequently amphetamine and cocaine) (Einat and Manji, 2006; Malkesman et al., 2009; Chen et al., 2010a; Young et al., 2011). Administration of amphetamine can also induce mania-like symptoms in healthy controls and aggravate symptoms in patients (Meyendorff et al., 1985; Peet and Peters, 1995; Hasler et al., 2006). Decreased immobility in the FST is generally regarded as an endophenotype of mania-like behavior given the ability of lithium to reverse the effects (Roybal et al., 2007). In addition, enhanced exploration of aversive areas in common anxiety tests (decreased anxiety-related behavior), is observed in a number of mania models (Roybal et al., 2007; Shaltiel et al., 2008;

Maeng et al., 2008; Kirshenbaum et al., 2011). This is believed to reflect enhanced risk-taking behavior and/or impulsivity, which is characteristic of BPD individuals in the manic phase. Prominent genetic models of mania include glycogen synthase kinase-3β (GSK3β) overexpressing mice, which were generated based on the hypothesis that lithium exerts its therapeutic effect via inhibition of GSK3β (Prickaerts et al., 2006). These animals displayed hyperlocomotion, reduced immobility in the FST, enhanced risk taking and hypophagia. Additional models include *Clock* mutants (knockout mice), which also display a range of mania-like endophenotypes, suggesting that circadian abnormalities play a prominent role in BPD (Roybal et al., 2007). Alterations in in glutamatergic function are also proposed in BPD, and deletion of the ionotropic glutamate receptor 6 (*Glur6* or *Gluk2*) in mice induces behavioral alterations related to symptoms of mania including hyperactivity, aggressiveness, risk-taking and sensitivity to psychostimulants (Shaltiel et al., 2008). More recent studies are starting to implicate altered synaptic function with neuropsychiatric disorders including BPD. For example, SHANK3 (a core scaffolding proteins of the postsynaptic density) overexpressing mice were recently shown to display a range of mania-like symptoms (Han et al., 2013). Importantly, in most of the studies, mania-like endophenotypes could be reversed by lithium and/or valproate treatment. Accordingly, these genetic models meet some criteria for face and predictive validity, but not construct validity. Interestingly, cognitive parameters are seldom assessed in mania models, which is surprising considering the wide body of research indicating neurocognitive impairments in BPD (Young et al., 2011). Prominent environmental models shown to induce manic-like features in rodents are the sleep deprivation model, resident-intruder stress and footsock stress (Malkesman et al., 2009; Chen et al., 2010a; Young et al., 2011). Again, most of these are not specific, as they induce a variety of symptoms observed in many neuropsychiatric disorders, including sleep disturbances, anxiety, and aggression. However, they further highlight the involvement of stress-circuits in prominent neuropathologies such as BPD.

Symptoms in humans	Associated psychiatric disorder	Endophentoypes in mice	Appropriate tests / analysis in mice
Cognitive impairments	SCZ, BPD, MDD	Deficits in spatial, working and fear memory, and object recognition memory	Morris water maze, water cross maze, Y-maze, T-maze, fear conditioning, operant learning paradigms
Anxiety	MDD, PBD	Increased anxiety-related behavior	EPM, 0-Maze, DaLi, OF, novelty-induced hypophagia, novel object exploration and modified hole board
Increased risk-taking/impulsivity	BPD	Decreased anxiety-related behavior (often referred to as increased risk-taking)	EPM, 0-Maze, DaLi, OF, novelty-induced hypophagia, novel object exploration and modified hole board
Social dysfunction	SCZ, BPD, MDD	Alterations in social behavior	Social interaction/avoidance paradigms, sociability and social novelty tests
Decreased interest or loss of pleasure (anhedonia)	SCZ, BPD, MDD	Decreased preference for rewarding stimuli	Sucrose preference, conditioned place preference, intracranial self-stimulation
Excessive involvement in pleasurable activities	BPD	Increased preference for rewarding stimuli	Sucrose preference, conditioned place preference, intracranial self-stimulation
Insomnia or hypersomnia	SCZ, BPD, MDD	Altered sleep architecture	Electroencephalogram recordings
Psychotic symptoms	SCZ, BPD	Psychostimulant-induced locomotion	Acute/chronic psychostimulant administration (ex, amphetamine, cocaine, PCP)
Psychomotor retardation or agitation	BPD, MDD	General alterations in locomotion, psychostimulant-induced locomotion, enhanced novel object exploration	OF, home cage-activity, treadmill running, nest building, psychostimulant administration
Hyperactivity	BPD	Hyperlocomotion in the OF and FST and TST	OF, FST, TST, Home cage activity
HPA axis hyperactivity	MDD, BPD	HPA axis hyperactivity	Assessment of basal and stress-induced plasma ACTH and corticosterone levels
Sensorimotor gating deficits (PPI deficits)	SCZ, BPD	Altered PPI	PPI
Depressed or irritable mood	SCZ, BPD, MDD	Cannot be modeled	
Recurrent thoughts of death and suicide	SCZ, BPD, MDD	Cannot be modeled	

Table 2: Overlapping symptoms of schizophrenia (SCZ), bipolar disorder (BPD) and major depressive disorder (MDD), the corresponding endophenotypes in mice and the behavioral tests used to assess them. Abbreviations: adrenocorticotropic hormone (ACTH), forced-swim test (FST), hypothalamic-pituitary-adrenal (HPA) axis, open field test (OF), prepulse inhibition (PPI), phencyclidine (PCP) and tail suspension test (TST).

It becomes quite clear that no single rodent model fulfills all the criteria necessary to be coined schizophrenia-, depression-, or bipolar-model. This is largely due to the complex and multi-factorial nature of most neuropsychiatric disorders, which cannot be accurately mimicked in

animals. Difficulties arise due to the fact that multiple susceptibility genes act synergistically and in conjunction with epigenetic processes and adverse environments to shape the individual risk to develop any given neuropsychiatric disorder. A major step towards more appropriate animal models is a more precise dissection of brain circuits associated with these disorders. For example, unraveling the interaction of stress-pathways with different neurotransmitter systems might elucidate some common domains observed throughout many mental illnesses. It will be necessary to implement and combine all recent advances in genetics, optogenetics, epigenetics, molecular biology and pharmacology with environmental challenges. This will hopefully initiate the development of new treatment modalities which are based on knowledge and not serendipity.

1.6. Genetic approaches to study neuronal function *in vivo*

The human brain is one of the most complex organs in the body and commonly assessed by non-invasive imaging techniques such as electroencephalography, functional magnetic resonance imaging, transcranial magnetic stimulation etc. However, these methods are limited in the ability to accurately assess circuit function and provide little information about the genetic basis of neuronal circuits. The limited accessibility of the human brain represents the biggest hurdle, however studies of invertebrates and lower vertebrate nervous systems have provided the basis for analysis of complex mammalian brains. As previously mentioned, mice and rats are the most commonly used model organisms to study neuronal development, brain structure and circuits, and ultimately behavior. The availability of genetic mouse models has revolutionized our understanding of single gene function in the context of a complex network such as the brain. Different methods and tools have been designed in the past to dissect and analyse gene function *in vivo* including conditional mouse mutants, viral-mediated genetic manipulations and most recently optogenetic techniques.

1.6.1. Gene targeting procedures in mice

Gene targeting refers to the precise modification of a specific location within the genome via homologous recombination, which takes places between a specifically designed targeting vector and a locus of interest (Deussing, 2013). To date, gene targeting in embryonic stem (ES) cells is the most commonly used method to generate genetically engineered mice (Smithies et al., 1984; Thomas and Capecchi, 1987). This approach is frequently referred to as “reverse genetics” and can be used to obtain either loss- or gain-of-function mutants. These include

classical transgenic mice that have additional copies of certain genes in their genome, which results in a gain-of-function. Similarly, knock-in techniques are frequently applied to generate gain-of-function animals. However, transgenes can also be used to induce a loss-of-function if the inserted transgene produces an antisense mRNA of the target gene. Similarly, short hairpin RNAs directed against the gene of interest have also been widely used (Kleinhammer et al., 2010). Disruption of specific target genes is most commonly achieved via generation of knockout mice. In that case, the targeting vector is constructed to allow the precise disruption of a gene resulting in the complete ablation of protein and/or mRNA production within every cell. Targeting vectors are then introduced into ES cells by electroporation. Correctly targeted ES cells (determined by positive and negative marker selection and subsequent Southern blot or PCR methods) are injected into blastocysts of donor mice. Ultimately, this results in chimeric animals which can then transmit the targeted allele to their offspring. Conventional/constitutive knockout mice were of immense importance in identifying candidate genes involved in more general and specific brain functions. However, they were limited in their ability to further uncover specific brain regions and neural circuitries involved in disease etiology. In many cases, homozygous knockouts were not viable or induced developmental and peripheral changes such as reduced body seize and organ dysfunction. Accordingly, the role of many genes could not be investigated in adulthood. Since then, technologies in this field have expanded rapidly, introducing sophisticated conditional strategies (Kilby et al., 1993; Branda and Dymecki, 2004; Kühn and Wurst, 2008; Deussing, 2013). This progress has allowed an increasingly refined control of spatial and temporal gene expression. The Cre/loxP system from the bacteriophage P1 has been most widely used in the mouse (Hoess et al., 1982). In this case, *loxP* (locus of crossover [x] of P1) sites are inserted into the gene of interest via homology-based gene targeting. The Cre (cyclization recombination) DNA recombinase recognizes and efficiently catalyzes the recombination between two pairs of *loxP* sites (floxed fragments) (Argos et al., 1986). The relative orientation of *loxP* sites with respect to each other determines whether the DNA fragment will be excised or inverted. Importantly, the Cre/loxP system can also be used to induce gene expression via removal of a floxed transcriptional terminator sequence. Similarly, Cre/loxP-mediated inversion of floxed transgenes, which are inverted in relation to the promoter, can also induce gene expression. This progress of site-specific recombination has allowed an increasingly refined control of spatial and temporal gene expression.

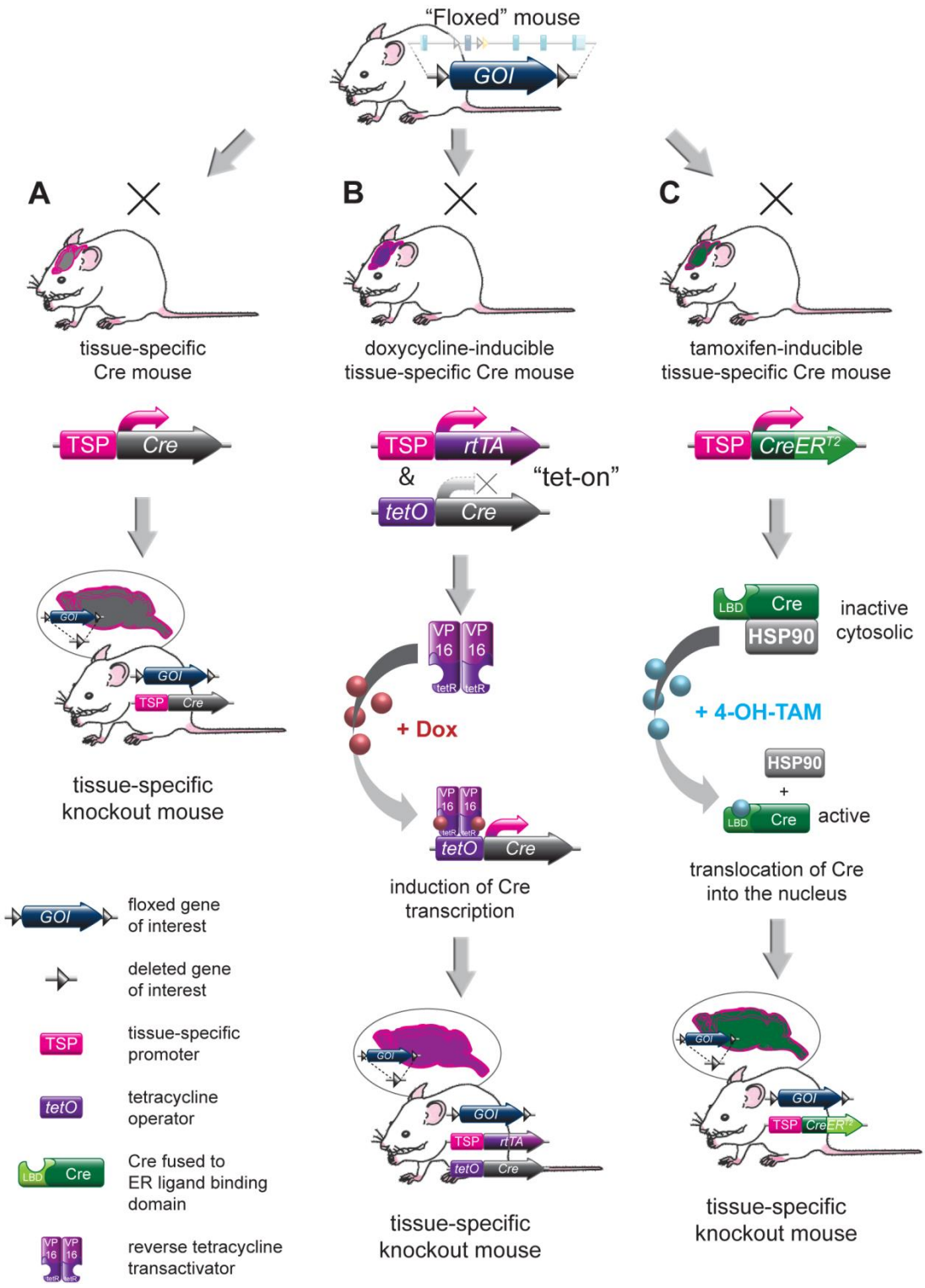

Figure 5: Cre recombinase-mediated spatial and temporal control of gene inactivation.
(A) Tissue-/cell-type-specific inactivation of a gene of interest (*GOI*). Breeding floxed GOI mice to site-specifc Cre mice results in inactivation of GOI in a specifc region/tisssue (in this case the brain). The spatial and temporal deletion pattern is soley dependent on the properties of the tissue-specific promoter (*TSP*) driving Cre expression. **(B)** Transcriptional control of Cre activity. Temporal control over gene inactivation is obtained upon combination of a floxed GOI with a Cre recombinase regulated by the tetracycline system (here illustrated by the reverse "*tet-on*" system). Application of doxycycline (Dox) enables the reverse transactivator (*rtTA*) to bind to the tetracycline operator (*tetO*) and activate Cre expression, which is spatially restricted by the TSP driving rtTA expression. **(C)** Posttranslational control of Cre activity. The Cre

recombinase fused to the ligand-binding domain of the estrogen receptor (*CreERT2*) is sequestered by the heat shock protein 90 (*HSP90*) within the cytoplasm. Cre translocation into the nucleus and inactivation of the GOI occurs only upon binding of 4-hydroxy tamoxifen (*4-OH-TAM*), and is spatial restricted by the TSP. With permission from Dr. Jan M. Deussing, adapted from Deussing et al., 2013.

In particular, the propagation of site-specific recombinases makes it possible to address gene function in a spatially and temporally restricted manner (Gaveriaux-Ruff and Kieffer, 2007; Deussing, 2013). For example, mouse lines expressing Cre recombinases selectively in neurons of a specific neurotransmitter type enable gene targeting in distinct neuronal populations (Figure 5). The *Escherichia coli*-derived tetracycline (*tet*) system (either *tet-off* or *tet-on*) has also been widely applied given that it provides temporal control over gene activation (Gossen and Bujard, 1992). The *tet-off* system makes use of the tetracycline transactivator (*tTA*), which represents a fusion protein of the tetracycline repressor and the acidic C-terminal domain of the HSV transcription factor VP16. The *tTA* protein is able to bind to a specific tetracycline operator (*tetO*) sequence, which is fused to the minimal promoter of the human cytomegalovirus (*CMV*) immediate early gene. The Cre recombinase can be placed under the control of the *tetO* sequence. In the presence of tetracycline, or its derivative doxycycline, Cre expression is prevented. Absence of tetracycline/doxycycline enables the transactivator to bind to the minimal promoter and activated Cre expression (St-Onge et al., 1996). However, the slow responsiveness of the system (due to slow clearance of the inducer), has favored the use of the *tet-on* system, which is similarly engineered but works in an opposite fashion (Kistner et al., 1996; Hasan et al., 2001; Schonig et al., 2002). Here, the induction of Cre expression follows administration of doxycycline (Figure 5). However, the *tet-on/tet-off* systems are reltively laborious procedures that require the stimoutanous presence of a tissue-specifc *tTA* or *rtTA*, a *tetO*-driven Cre and a floxed gene of interest. Consequently, the increasing availability of tamoxifen-inducible Cre lines represents a more suitable approach for temporal-spatial gene control (Feil et al., 1996; Danielian et al., 1998; Deussing, 2013). This system is based on posttranslational control of Cre-mediated recombination. A ligand-binding-domain (LBD) is fused to the Cre recombinase and is sequestered by the heat shock protein 90 within the cytoplasm. Nuclear translocation and subsequent Cre activation only occurs in the presence of 4-hydroxy tamoxifen (Figure 5). In addition to temporal control, spatial control is provided by the specific promoter utilized to drive Cre expression. Commonly used LBDs are the mutated versions of the human or mouse estrogen receptor (*CreER^{T}* and *CreER^{TM}* respectively)(Feil et al., 1996; Danielian et al., 1998; Wunderlich et al., 2001). The use of tissue-specific and tamoxifen-inducible tissue-specific Cre mice was employed throughout this study.

More recently developed techniques for genome engineering include the Zinc Finger nucleases, transcription activator-like effector nucleases (TALENs) and RNA-guided endonucleases (RGNs) used in the CRISPR/Cas system (clustered regulatory interspaced short palindromic repeats/CRISPR-associated protein)(Sun et al., 2012; Deussing, 2013; Gaj et al., 2013). These nucleases are able to introduce site-specific double strand breaks (DSBs) into any mammalian genome. This leads to the activation of one of two DNA repair mechanisms: 1) non-homologous end joining (NHEJ), and -homology directed repair (HDR). Importantly, these nucleases are designed to recognize and bind specific DNA motifs, and thereby induce DSBs at a desired location (Marcaida et al., 2010; Gaj et al., 2013). NHEJ is error-prone leading to insertions or deletions within the given site. This mechanism can be exploited to generate mutant alleles in a random manner. The high-fidelity HDR enables targeted and specific modifications such as single nucleotide alterations or large insertions (Deussing, 2013). Single-stranded oligonucleotides or larger targeting vectors can serve as templates for HDR. Importantly, all of the described nucleases directly target the genome of one-cell stage embryos. Consequently, these technologies hold great potential to achieve site-specific mutagenesis and transgenesis not only in mice, but also in rats, pigs, rabbits, cattle and other higher order mammalian organisms.

1.6.2. Viral-mediated genetic analyses

Viral-mediated gene transfer is another popular method used to study neuronal function in the mouse brain. Adeno-associated viruses (AAVs) and lentiviruses (LVs) are the most commonly used viral vectors to infect adult neurons *in vivo*, which can be achieved via stereotactic injections in any given brain-region. These can be genetically modified to express a variety of DNA or RNA fragments encoding fluorescent markers, genes of interest, fusion proteins, Cre recombinases or short-hairpin RNAs (shRNAs) (Davidson and Breakefield, 2003; Hommel et al., 2003; Tenenbaum et al., 2004; Wong et al., 2006; Atasoy et al., 2008; Regev et al., 2010; Osakada et al., 2011; Betley and Sternson, 2011; Bartel et al., 2012; Lentz et al., 2012). Spatial restriction can be achieved by utilizing cell-type specific promoters to drive gene expression. Consequently, AAVs or LVs can be used for gain-of-function or loss-of-function approaches or simply to label neurons. For example, delivery of AAVs, expressing the Cre recombinase, into a specific brain region of mice with a floxed gene of interest results in Cre-mediated deletion of the floxed gene. Another possibility is to generate floxed viral constructs (Cre-dependent viral vectors), which are only active upon the presence of Cre recombinase, for example in region-

or site-specific Cre-mice. Tracing and mapping studies of neuronal circuits have also heavily relied on viral-mediated delivery of fluorescent proteins (Grinevich et al., 2005; Li et al., 2010; Ugolini, 2010; Lo and Anderson, 2011; Harris et al., 2012). For instance, AAVs can be designed to harbor synaptic proteins fused to fluorescent markers, which will be actively transported to the synapses enabling the visualization of axonal projections. Specific neuronal circuits can be targeted by expressing these "tracers" in a Cre-dependent manner. One important issue is given by differences in transduction efficiencies between different viral serotypes (Baekelandt et al., 2002; Baekelandt et al., 2003; Burger et al., 2004; Cearley et al., 2008). In addition, serotypical variations are also observed with respect to toxicity and immune responses triggered by the viral capsule (Thomas et al., 2003; Bessis et al., 2004; Mingozzi and High, 2013). Nonetheless, the combination of mouse genetics and recombinant AAVs has greatly improved our ability to map, monitor and manipulate neurons. One method in neuroscience which has greatly benefitted from this is optogenetics.

1.6.3. Optogenetics in neuronal circuits

Optogenetics refers to the integration of optics and genetics to achieve gain or loss-of-function of well-defined events within specific cells of living tissue (Deisseroth, 2010; Deisseroth, 2011; Yizhar et al., 2011a; Deisseroth, 2014). In the past 10 years this method has advanced our understanding of complex brain circuitries and is further paving the way to establish causal relationships between brain activity and behavior in health and disease (Deisseroth, 2011; Tye and Deisseroth, 2012). Optogenetics makes use of microbial opsins or related effectors that can be activated by illumination to manipulate cells with high specificity and temporal precision even within intact tissue or behaving animals (Deisseroth, 2010; Deisseroth, 2011; Zhang et al., 2011; Tye and Deisseroth, 2012). The most commonly used optogenetic effectors are genetically engineered variants of natural opsins, light-sensitive ion channels that can be stimulated in response to specific wavelengths of light leading either to membrane depolarization, hyperpolarization or change in intracellular signaling (Deisseroth et al., 2006; Deisseroth, 2010; Carter and de, 2011; Deisseroth, 2011; Rein and Deussing, 2012). Viral-mediated delivery of opsins is the method of choice in optogenetic research, and the propagation of transgenic Cre-driver mice in combination with viral systems is increasing with every day. The first class of opsins includes channelrhodopsin-2 (ChR2), isolated from the green algae *Chlamydomonas reinhardtii* which is sensitive to blue light and has already successfully been used in transgenic mice (Deisseroth et al., 2006; Arenkiel et al., 2007; Deisseroth, 2011;

Zhang et al., 2011). Photons are absorbed by the all-trans-retinal cofactor of ChR2 that is endogenously expressed at sufficient levels in the central nervous system of vertebrates (Li et al., 2005; Boyden et al., 2005; Zhang et al., 2006; Bi et al., 2006; Ishizuka et al., 2006; Deisseroth, 2011). ChR2 can be activated and closed very rapidly upon light on- and offset, respectively, allowing stimulation of neurons within milliseconds. The inhibitory counterpart of ChR2, the chloride pump halorhodopsin (NpHR), was isolated from the bacterium *Natronomonas pharaoni* and possesses an activation spectrum in the yellow range, complementary to that of channelrhodopsin (Zhang et al., 2007; Deisseroth, 2010; Zhang et al., 2011). Similarly to ChR2, NpHR uses all-trans retinal as chromophore and can therefore be applied in vertebrate organisms without exogenous cofactors. By expressing both proteins in the same neuron, one can either activate or silence the cell by illumination with different wavelengths. However, the optogenetic toolbox has greatly expanded in the last few years to include a diverse number of new opsin variants including the ChETA family and ChIEF (Lin et al., 2009; Gunaydin et al., 2010; Mattis et al., 2012). These effectors provide greater flexibility in experimental design and enable more powerful and refined manipulations. For example, newly engineered ChRs, termed step-function opsins (SFO), enable bistable, step-like control of neuronal membrane potential. Hence, many of the designed SFOs can depolarize neurons for prolonged periods, up to 30 min (Yizhar et al., 2011a; Yizhar et al., 2011b).

Optogenetic approaches are increasingly applied to investigate neural circuitries and molecular mechanisms underlying mammalian behavior and the etiology of neurological disorders. A number of studies have examined whether optogenetic activation or inhibition of defined brain areas and neuronal circuits can trigger specific behavioral responses, such as anxiety, despair, impulsivity, reward-seeking etcetera. For example, a specific population of amygdala synapses was identified that can rapidly and reversibly modulate baseline anxiety levels in mice (Tye et al., 2011). This was achieved via optogenetic-mediated stimulation and inhibition of basolateral amygdala (BLA)-central amygdala (CeA) projections. Simillarly, a bidirectional mode of anxiety regulation was illustrated for the bed nucleus of the stria terminalis (Kim et al., 2013). Another study, looking at the circuitry of addiction, employed a conditional strategy to target ChR2 to dopamine neurons in the ventral tegmental area (VTA) (Tsai et al., 2009). Phasic, but not tonic, stimulation of VTA dopamine neurons was sufficient to support conditioned place preference, a paradigm commonly applied to assess drug-related behaviors. Another group investigated noradrenergic function via optogenetic manipulation of the locus coeruleus (LC). Stimulation of the LC lead to an immediate shift from sleep to wakefulness

whereas optogenetic inhibition causes a decrease in wakefulness (Carter and de, 2011). Many other studies have used optogenetic methods to investigate fundamental research questions in a variety of neurological and neuropsychological disorders such as schizophrenia, autism, Parkinson's disease, epilepsy and depression (Tye and Deisseroth, 2012). Accordingly, optogenetics is developing into a state-of-the-art technology and will likely represent the future method of choice in neuroscience.

1.7. The CRH system - what have we learned so far?

The ability of CRH to coordinate the physiological/neuroendocrine responses to stress via the HPA axis was previously introduced. In addition, CRH and its high affinity receptor CRHR1 are widely distributed throughout the brain, which allows them to orchestrate autonomic and behavioral stress responses. Consequently, hyperfucntion of the CRH/CRHR1 system has been linked to stress-associated psychiatric disorders that involve a strong emotional component such as depression and anxiety (Nemeroff et al., 1984; Holsboer, 1999; Arborelius et al., 1999; Holsboer, 2000; Gillespie and Nemeroff, 2005; de Kloet et al., 2005a; Binder and Nemeroff, 2010). Shortly after its isolation in 1981, a number of studies demonstrated that i.c.v. administration of CRH results in behavioral responses that are similar to those observed in stressed animals. These include increased arousal and anxiety-related behavior, altered locomotor activity and social behavior, diminished sexual behavior and food consumption as well as sleep disturbances (Sutton et al., 1982; Sirinathsinghji et al., 1983; Koob et al., 1984; Eaves et al., 1985; Krahn et al., 1986; Dunn and File, 1987; Dunn and Berridge, 1990; Heinrichs et al., 1992; Heinrichs and Koob, 2004; Sztainberg and Chen, 2012). Importantly, many of these effects were independent of downstream HPA axis alterations. This defined the ability of central CRH to coordinate behavioral responses independent of, or in synergism with peripheral HPA axis function. A more recent study showed that adult overexpression of CRH in the cerebrospinal fluid (CSF) via viral-mediated delivery of the neuropeptide to the choroid plexus, results in increased anxiety-related behavior (Regev et al., 2010). This is in accordance with previous findings in depressed individuals that displayed enhanced CRH levels in the CSF (Nemeroff et al., 1984; Fossey et al., 1996; Carpenter et al., 2004). Evidently, all of these studies support a role of CRH hyperactivity in stress-related neuropathophysiologies. In order to further elucidate the brain regions responsible for mediating the effects of CRH on behavior, a large body of research focused on site-specific CRH administration (Sztainberg and Chen, 2012). Naturally the involvement of the limbic system was investigated given that it modulates

a variety of functions including emotion, motivation and cognition. The major structural components include the amygdalar complex, bed nucleus of the stria terminalis (BNST), hippocampus and prefrontal cortex, all of which express CRH and/or CRHR1 (Swanson et al., 1983; Alon et al., 2009; Kuhne et al., 2012).

The effects of CRH on hippocampal function and integrity with respect to memory function were repeatedly investigated in the past. The hippocampus contains numerous scattered CRH-expressing interneurons and a more dense population of CRHR1-expressing excitatory pyramidal neurons (Swanson et al., 1983; Yan et al., 1998; Chen et al., 2004c; Justice et al., 2008; Kuhne et al., 2012). It is generally proposed that a short-lived increase in CRH facilitates hippocampus-dependent learning and memory (similarly to acute stress), whereas prolonged exposure to elevated CRH impairs cognitive performance (Heinrichs et al., 1996; Radulovic et al., 1999b; Chen et al., 2012b). Importantly, CRH exerts its effect by potentiating excitatory neurotransmission in the hippocampus, providing direct evidence for an interaction with the glutamatergic system (Aldenhoff et al., 1983; von Wolff et al., 2011). The adverse effects of chronic CRH release (as they occur during persistent stress) are proposed to result from CRH-induced dendritic spine loss on CRHR1-expressing neurons (Chen et al., 2008; Chen et al., 2012b; Chen et al., 2013a). Accordingly, CRHR1-antagonsits were shown to reduce hippocampus-dependent deficits in memory and synaptic long-term-potentiation (LTP) (Ivy et al., 2010). At the same time, CRH is required for fear memory formation given that acute injections into the dorsal hippocampus enhance contextual and auditory fear memory (Radulovic et al., 1999a). This is supported by previous experiments with CRH receptor antagonists, which have resulted in fear memory impairments (Hikichi et al., 2000; Thoeringer et al., 2012). In addition, CRH injections into the ventral hippocampus were shown to increase anxiety-related behavior (Pentkowski et al., 2009).

CRH is also viewed as a potential mediator of stress-elicited locus coeruleus (LC) activation, the brain's major noradrenergic nuclei (Valentino et al., 1983; Valentino and Van Bockstaele, 2008). The LC sends noradrenergic projections throughout the brain, including brain-stem, cortical, limbic and hypothalamic structures, and is consequently able to modulate various behavioral endocrine and autonomic responses (Swanson and Hartman, 1975; Foote et al., 1980; Valentino and Van Bockstaele, 2008; Chamberlain and Robbins, 2013). Dysregulated noradrenergic circuits via excessive CRH have been proposed to underlie pathological hyperarousal observed in numerous stress-related psychiatric disorders (Wong et al., 2000; Gold and Chrousos, 2002; Bissette et al., 2003). CRH is able to induce LC neuronal firing, which

is believed to modulate behavioral arousal and attention during stressful situations (Valentino et al., 1983; Valentino and Wehby, 1988; Valentino and Van Bockstaele, 2008). Hence, CRH not only facilitates activation of glutamatergic neurotransmission in the hippocampus but also noradrenergic firing in the LC. In addition, CRH can indirectly regulate endocrine responses via activation of the noradrenergic system, which in turn regulates components of the HPA axis (Herman and Cullinan, 1997; Hwang et al., 1998; Valentino and Van Bockstaele, 2008). CRH-immunoreactive fibers innervate the LC (Valentino et al., 1992), although convincing evidence for the presence of CRHR1 or CRHR2 in the LC is still lacking (Van Pett et al., 2000; Valentino and Van Bockstaele, 2008). Moreover, the source of CRH afferents to the LC which modulate specific behavioral effects have not been clearly identified.

The amygdala plays a prominent role in fear memory acquisition and expression, and modulates aspect of anxiety-related behavior. CRH is highly expressed in the central nucleus of the amygdala (CeA), whereas CRHR1 is primarily located in the basolateral amygdala (BLA) (Swanson et al., 1983; Keegan et al., 1994; Justice et al., 2008; Alon et al., 2009; Kuhne et al., 2012). CRH application into the BLA enhances anxiety-related behavior and reduces social interaction (Sajdyk et al., 1999). CeA-infusions of CRH receptor antagonists ameliorate stress-induced anxiety and freezing behavior (Heinrichs et al., 1992; Swiergiel et al., 1993), which is likely due to blockage of BLA-receptors caused by spreading of the antagonists. Simillarly, intra-BLA administration of antalarmin, a CRHR1-antagonist, counteracts social defeat-induced defensive behavior in mice (Robison et al., 2004). Along these lines, viral-mediated knockdown of *Crhr1* in the BLA mimicked the anxiolytic effect of environmental enrichment (Sztainberg et al., 2010). Another CRH-expressing brain region which has gained increasing attention in the last years is the BNST. Often referred to as the extended amygdala, the BNST is heavily innervated by the amygdala and is known to project to the PVN and monoaminergic nuclei including the LC and VTA (Mulders et al., 1997; Van Bockstaele et al., 1999; Dong et al., 2001; Georges and Aston-Jones, 2002; Dong and Swanson, 2004; Kudo et al., 2012). Recent optogenetic studies have clearly implicated the BNST in the modulation of anxiety (Kim et al., 2013; Jennings et al., 2013). Consequently, some of these effects might be modulated via CRH, but so far only a few studies have investigated the role of BNST-CRH neurons in emotional behavior. Microinfusions of CRH into the BNST enhanced startle amplitude, and retention in an inhibitory avoidance task (Lee and Davis, 1997; Liang et al., 2001). Similarly, intra-BNST administration of CRH elicited a dose-dependent increase in anxiety-related behavior, which could be reversed upon CRHR1 antagonist treatment (Sahuque et al., 2006). A more prominent

role of CRH in the BNST is linked to addiction, more specifically stress-induced relapse (George et al., 2012; Haass-Koffler and Bartlett, 2012). This is interesting considering that 30-40% of individuals suffering from addictive disorders have a comorbid mood or anxiety disorder (Russo and Nestler, 2013). Intra-BNST injection of CRH can induce reinstatement, whereas injections of CRH antagonists were shown to block stress-induced reinstatement (Erb and Stewart, 1999; Wang et al., 2006). A number of studies have consequently linked the CRH-pathway to dopaminergic signaling, which is primarily involved in addiction-processes (Le and Koob, 2007; Koob and Zorrilla, 2010; George et al., 2012; Haass-Koffler and Bartlett, 2012; Silberman and Winder, 2013; Silberman et al., 2013). Direct and indirect mechanism were proposed by which CRH is able to enhance dopaminergic firing in order to drive stress- or cue-induced drug- and alcohol seeking behaviors. However, CRH-dopamine interactions in the context of anxiety, social behavior and/or cognition have only scarcely been investigated.

1.7.1. Transgenic mice targeting CRH system components

A limitation of most of the above mentioned studies is that they assessed the effects of acute administration of exogenous CRH, which might not necessarily mimic normal patterns of endogenous CRH signaling. Moreover, these experiments provide little insight into the outcomes of long-lasting CRH-system dysregulations as they might occur in stress-related mood and anxiety disorders. In many cases it is not clear whether the effects of CRH were mediated by CRHR1 or CRHR2. Although some studies applied CRHR1 and CRHR2 antagonists to answer this question, the selectivity of these compunds is still not entirely established. The generation of transgenic mice, overexpressing or lacking different CRH-family members, has provided crucial insights into the involvement of the CRH-system in stress-related behavior.

CRH overexpressing mice

In order to study the role of chronic CRH hyperdrive in the context of mood and anxiety-disorders, independent models of CRH excess were generated in the past (Table 3). The first CRH overexpressing mouse line was generated via a classical transgenic approach applying the broadly active metallothionine 1 promoter (Stenzel-Poore et al., 1992). These mice (CRF-OE^{Mt1}) showed strong CRH overexpression in the brain and peripheral organs including lung, adrenal, heart, and testis. CRH overproduction resulted in elevated plasma corticosterone levels and Cushing-like symptoms. CRF-OE^{Mt1} showed increased anxiety-related behavior, which was reversible by the CRH receptor antagonist α-helical CRH (Stenzel-Poore et al., 1994). Moreover, these mice displayed deficiets in learning, decreased immobility in the FST and reduced

attention (Heinrichs et al., 1996; van Gaalen et al., 2002). Another CRH overexpressing mouse line was developed using the Thy1.2 promoter driving CRH expression in postnatal and adult neurons of the brain (Dirks et al., 2001). However, CRH-OE$^{Thy1.2}$ did not show an altered stress response or phenotype indicative of changes in anxiety behavior (Dirks et al., 2001; Groenink et al., 2002). Instead, CRH-OE$^{Thy1.2}$ mice displayed reduced startle reactivity as well as reduced freezing following fear conditioning (Dirks et al. 2002b; Groenink et al. 2003). With some delay CRH-OE$^{Thy1.2}$ also developed a mild cushingoid phenotype (Dirks et al., 2002a). Finally, different conditional CRH-overexpressing mouse lines have been established in recent years. Two studies applied the ''*tet-on/tet-off*'' system, which allows for reversible and inducible overexpression of CRH (Vicentini et al., 2009; Kolber et al., 2010). Although both made use of the forebrain-specifc CAMK2α promoter combined with a tet-operator driven CRH-construct, the behavioral and neuroendocrine consequences of CRH excess were rather specific for each mouse line. Taken together, these examples illustrate the difficulties to compare results from different transgenic mouse lines even if they are based on similar constructs. To circumvent these problems, our group has recently developed a mouse model which permits conditional CRH overexpression avoiding common uncertainties of classical transgenesis such as unpredictable influences of the site of transgene insertion and the number of inserted transgene copies (Lu et al., 2008). This was achieved by introducing a CRH expression unit into the ubiquitously expressed ROSA26 (*R26*) locus. Undesired ubiquitous expression of CRH driven by the *R26* promoter is prevented unless a *loxP* flanked transcriptional terminator is deleted via a site-specific Cre recombinase. Using this novel mouse model of CRH overexpression it was demonstrated that CNS-restricted CRH overexpression in *Crh*$^{CNS\text{-}COE}$ mice, achieved by breeding with *Nestin-Cre* mice, leads to HPA axis hyperdrive and increased active stress-coping behavior and altered sleep regulation (Lu et al., 2008; Kimura et al., 2010). Importantly, reduced immobility in the FST was not observed in mice overexpressing CRH specifically in forebrain-CAMK2α-positive or forebrain GABAergic neurons, suggesting an involvement of hindbrain-regions in CRH-induced active-stress coping behavior. However, additional behavioral and cognitive parameters were not investigated in these mice and will be addressed in this study.

***Crhr1* knockout mice**

The contribution of CRHR1 to the modulation of stress-related behaviors was addressed by conventional and conditional *Crhr1* knockout mice (Table 3). Expectedly, *Crhr1* null mice exhibited a glucocorticoid deficiency due to disrupted HPA axis activity (observed in two

independently generated *Crhr1* deficient mouse lines; *Crhr1-KO* and *Crfr1-KO*) (Timpl et al., 1998; Smith et al., 1998). In both cases enhanced anxiety-related behavior was observed (Smith et al., 1998; Timpl et al., 1998; Contarino et al., 1999). In order to exclude the possibility that decreased glucocorticoid levels are mediating the observed behavioral effects, conditional forebrain-specific *Crhr1* knockout mice (*Crhr1*$^{FB\text{-}CKO}$) were generated in 2002 by Müller and colleagues (Muller et al., 2003). In this mouse lines, Cre mediated deletion of *Crhr1* is initiated in the second week of postnatal life, and is primarily restricted to cortical and limbic forebrain regions including the amygdala, hippocampus, BNST, but not the anterior pituitary. *Crhr1*$^{FB\text{-}CKO}$ mice displayed reduced anxiety-related behavior and normal glucocorticoid levels under basal conditions, supporting the notion that limbic CRHR1 can regulate emotional behavior independent of HPA axis alterations (Muller et al., 2003). However, corticostereone levels were slightly enhanced in *Crhr1*$^{FB\text{-}CKO}$ mice following 30 and 90 min of restraint stress, suggesting that limbic CRHR1 is partially required in HPA axis feedback regulation (Muller et al., 2003). Both *Crhr1-KO* and *Crhr1*$^{FB\text{-}CKO}$ mice displayed Impairments in remote fear memory consolidation, suggesting that cognitive processes are also mediated by CRHR1 in forebrain cortical and limbic structures (Thoeringer et al., 2012). In addition, more recent work demonstrated that forebrain *Crhr1* deficiency prevents cognitive deficits induced by early-life, and chronic adult-stress (Wang et al., 2011a; Wang et al., 2011b; Wang et al., 2013). Moreover, chronic-stress-induced dendritic remodeling and spine loss was attenuated in *Crhr1*$^{FB\text{-}CKO}$ mice (Wang et al., 2011a; Wang et al., 2013). All these studies have clearly implicated a role of CRHR1 in the modulation of emotional and cognitive responses.

***Crhr2* knockout mice**

In contrast to the reliable and reproducible phenotype of *Crhr1* knockout mice, a number of discrepancies have been observed in *Crhr2* kockout mice (Table 3). Until now three conventional *Crhr2* knockout mouse models have been generated (Coste et al., 2000; Bale et al., 2000; Kishimoto et al., 2000). Two studies reported enhanced ACTH and corticosterone release in response to stress, but an early termination of ACTH release, suggesting that CRHR2 is involved in maintaining HPA drive (Coste et al., 2000; Bale et al., 2000). In addition, Coste and colleagues observed an overall blunted corticosterone recovery in *Crhr2-KO* mice, implying an involvement in HPA feedback function. The effects of *Crhr2* deficieny on anxiety-related behavior are less clear. Coste and colleagues reported no changes in anxiety-related behavior. However, Bale et al., and Kishimoto et al., demonstrated increased anxiety-related behavior. Importantly, Bale and colleagues reported compensatory upregulation of CRH in the central

amygdala of *Crhr2-KO* mice, which might have influenced the anxiogenic phenotype. Two of the studies also reported increased floating time in the FST (Bale et al., 2000; Kishimoto et al., 2000). In addition, enhanced social discrimination was observed in *Crhr2-KO* mice (Deussing et al., 2010). Based on the above studies, CRHR2 was initially proposed to exert opposite functions compared to CRHR1, but this simplistic view has been rejected by more recent research. Double *Crhr1/Crhr2* knockout mice have also been generated, but only mild behavioral alterations were observed in one of the lines, which were specific for the females (Preil et al., 2001; Bale et al., 2002). However, both lines displayed impaired stress-induced HPA axis activation. In addition, CRHR2 and its major ligands, UCN1 and UCN2 have been repeatedly implicated in centrally controlled metabolic functions (Kuperman and Chen, 2008). The generation of conditional *Crhr2* knockout mice will be mandatory in order to uncover the precise role of CRHR2 on behavior, HPA axis and metabolic function.

Crh knockout mice

Although CRH overexpressing mice represent valuable disease models with respect to chronic CRH and HPA axis hyperdrive, they are confounded by ectopic peptide expression in non-endogenous brain regions and peripheral organs. Consequently a loss of function approach is more likely to reveal physiologically relevant effects of CRH on behavior. The development of constitutive *Crh* knockout mice (*Crh-KO*) by Muglia et al, has been important in addressing this issue (Muglia et al., 1995). *Crh-KO* mice displayed severely blunted corticosterone levels indicative of diminished HPA axis function. Importantly, this study revealed fetal glucocorticoid requirement for lung maturation, which was severely impaired in CRH deficient mice obtained from homozygous breedings (Muglia et al., 1995). Surprisingly, *Crh-KO* mice displayed no gross alterations in emotional behavior and CRHR1 antagonists were still able to exert an anxiolytic effect in these animals (Weninger et al., 1999). The discrepancy between constitutive CRH and CRHR1 mouse mutants with respect to behavioral outcomes could be due to a number of reasons: 1) UCN1, the only other CRHR1 ligand, might compensate for the loss of CRH; 2) early deletion of CRH might trigger compensatory processes; 3) corticosterone deficiency might mask potential phenotpyes; 4) CRH might exert its action primarily under conditions of chronic or severe stress; 5) the CRHR1 might comprise ligand-independent activity, e.g. due to constitutive activity or heteromerization with other receptors; 6) and last but not least, it might suggest the presence of a yet unidentified CRHR1-ligand. The generation of conditional *Crh* knockout mice would significantly help to shed light on some of these issues.

Transgenic mice targeting the urocortins

Three different *Ucn1* kockout lines have been independently generated in the past, however their phenotype remains controversial (Vetter et al., 2002; Wang et al., 2002; Zalutskaya et al., 2007). Vetter and colleagues reported increased anxiety-related behavior in their mouse model, which was not confirmed by the study of Wang et al., and so far not investigated in *Ucn1*$^{-/-}$ mice generated by Zalutskaya and colleagues. Consequently, UCN1 seems an unlikely candidate to compensate for CRH deficiency in *Crh-KO* mice. This is also supported by the restricted expression pattern of UCN1 compared to CRH (Figure 3). Importantly, all *Ucn1* knockout lines exhibited normal basal and stress-induced glucocorticoid levels, supporting the notion that UCN1 plays a minor role in HPA axis function. However, Zalutskaya and colleagues observed that corticosterone levels in male *Ucn1*$^{-/-}$ mice do not adapt to repeated restraint stress. The role of the other two urocortin members has been assessed in *Ucn2* and *Ucn3* knockout mice. Female *Ucn2* knockout mice display mild alterations in basal circadian rhythm of ACTH and corticosterone secretion (Chen et al., 2006); whereas no differences were observed in basal and stress-induced corticosterone levels im male mice (Chen et al., 2006; Breu et al., 2012). Male and female *Ucn2-KO* mice generated by Chen et al., exhibited no alterations in locomotion, anxiety and contextual fear conditioning. However, only female *Ucn2-KO* mice displayed reduced immobility in the FST (Chen et al., 2006). Male *Ucn2* deficient mice developed by Deussing and colleagues (*Ucn2*$^{tz/tz}$) displayed reduced aggressiveness, but showed no changes in anxiety, immobility in the FST and social discrimination (Deussing et al., 2010; Breu et al., 2012). Differences in HPA axis activity and anxiety were also not observed in *Ucn3-KO* mice (Deussing et al., 2010). However, male and female *Ucn3-KO* mice showed enhanced social discrimination abilities, which was also observed in *Crhr2-KO* mice, and attributed to UCN3 expression in the olfactory bulb, BNST and medial amygdala. These data suggest an involvement of the UCN3/CRHR2-system in social memory. Interpretations of these results are further complicated by recently generated *Ucn1/Ucn2* double and *Ucn1/Ucn2/Ucn3* (*tKO*) triple knockout mice. *Ucn1/Ucn2-KO* mice displayed no changes in basal HPA axis activity, but exhibited elevated levels following acute stress exposure (Neufeld-Cohen et al., 2010a). On the other hand, HPA axis function was indistinguishable in *tKO* mice compared to controls (Neufeld-Cohen et al., 2010b). *Ucn1/Ucn2-KO* mice demonstrated decreased anxiety under basal and acute-stress conditions, which was linked to elevated serotonin concentrations in a number of brain regions including the raphe nucleus, hippocampus, basolateral amygdala and subiculum (Neufeld-Cohen et al., 2010a). In contrast, *tKO* mice exhibited increased anxiety-like

behavior, but only 24 h following restraint-stress. Moreover, *tKO* mice displayed an incresed stress-induced startle response (Neufeld-Cohen et al., 2010b). As opposed to *Ucn1/Ucn2-KO* mice, the behavioral phenotype in *tKO* mice was associated with decreased serotonergic metabolism in regions such as the septum, central and basolateral amygdala (Neufeld-Cohen et al., 2010b). Again, the effect of compensatory changes in CRH expression on emotional behavior cannot be excluded in many of the urocortin mouse models, as shown in *Ucn1/Ucn2-KO* mice. Overall the majority of the data suggests that the Ucrocortins and CRHR2 are able to regulate aspects of stress-related emotional behavior, but not to the same extent as CRH and CRHR1. As previously mentioned, more recent studies are starting to implicate UCN2 and UCN3 in the modulation of glucose homesostasis and metabolic function. The generation of conditional urocortin knockout and overexpressing mice will be mandatory to further dissect the role of these neuropeptides in diverse physiological and behavioral functions.

Taken together, the above cited studies clearly support a role for the CRH/CRHR-system in stress-related neuroendocrine, autonomic and behavioral alterations, which is of relevance to a number of psychiatric disorders. Especially the involvement of CRH/CRHR1 in the regulation of HPA axis function and emotional behavior is well established. On the other hand, the role of the central urocortin/CRHR2-system is less clearly defined. Pharmacological and genetic studies have repeatedly implicated CRH hyperfunction with anxiety and mood-related behavior. Importantly, CNS-specific infusions of CRH have demonstrated the ability of this stress-system to modulate noradrenergic and dopaminergic neurotransmission (Valentino et al., 1983; Muramatsu et al., 2006; Valentino and Van Bockstaele, 2008; Wanat et al., 2008; George et al., 2012). However, little is known about these specific CRH-neurotransmitter interactions during normal and pathological conditions. Moreover, they have scarcely been investigated in any of the described transgenic mouse models. In addition, the neurochemical identity of CRH and CRHR1 neurons remains largely unknown as well as their projection profiles. The generation of more specific transgenic mouse models and viral tools will enable the assessment of CRH/CRHR1 function during development and adulthood in specific brain regions and neurotransmitter circuits, and will help to further dissect the brains' most prominent stress-system.

Table 3: Summary of genetic mouse models targeting the CRH system

Transgenic Line	Construct	Phenotype	Reference
CRH overexpression			
CRF-OE^{Mt} Developmental	non-selective OE of rat CRH under murine metallothionein promoter	Cushing-like phenotype (↑ ACTH & corticosterone levels, = stress response), Adrenal hypertrophy, ↓ general locomotion, ↑ anxiety, ↓ immobility FST, deficits in learning and spatial memory	*Stenzel-Poore et al., 1992* Stenzel-Poore et al., 1994 Heinrichs et al., 1997 Van Gaalen et al., 2002
CRH-OE$^{Thy1.2}$ Developmental	OE of rat CRH under *Thy-1* promoter / developmental	Cushing-like phenotype at 6 months (↑ corticosterone levels, marginal increase in ACTH, = stress response), adrenal hypertrophy, nonsupression of dextamethasone, ↓locomotion, ↓startle reactivity & habituation, ↓PPI, = anxiety	*Dirks et al., 2002a* Groenink et al., 2002 Groenink et al., 2002
Crh$^{CNS\text{-}COE}$ Developmental / CNS-restricted	Conditional *Nestin*-Cre induced COE of murine CRH driven by the *Rosa26*-promoter	Stress-induced hypersecretion of corticosterone (no changes in basal corticosterone levels), ↓ immobility FST/TST, ↑ REM sleep and slightly suppressed non-REM sleep	*Lu et al., 2008* Kimura et al., 2010
Crh$^{FB\text{-}COE}$ Postnatal / forebrain-restricted	Conditional *Camk2α*-Cre induced COE of murine CRH driven by the *Rosa26*-promoter	= basal HPA axis and stress response, = immobility FST, ↑ REM sleep	*Lu et al., 2008* Kimura et al., 2010
Crh$^{GABA\text{-}COE}$ developmental / restricted to GABAergic neurons	Conditional *Dlx5/6-Cre* induced COE of murine CRH driven by the *Rosa26*-promoter	= immobility FST	*Lu et al., 2008* Kimura et al., 2010
Camk2α-rtTA/tetO-Crf / Inducible forebrain restricted	*Camk2α*-Cre induced COE of rat CRH driven by the CMV promoter (*tet*-on system; Dox induces expression)	Dox administration at P56 for 3 weeks, ↑ corticosterone at circadian nadir, = ACTH levels & stress response, ↓thymus size, = dextamethason suppression	*Vicentini et al., 2009*
FBCRHOE *(Camk2α-rtTA/tetop-CRH)* Inducible forebrain restricted	*Camk2α*-Cre induced COE of CRH driven by the CMV promoter (*tet*-off system; Dox represses expression)	Early life forebrain CRH OE (off Dox E15-P21) causes ↑ corticosterone levels only during development and long-lasting anxiogenic and despair-like alterations; Lifetime CRH OE induces Cushing-like phenotype at 8 weeks and ↑ corticosterone and ACTH levels only at circadian nadir	*Kolber at la., 2010*
CRH knockout			
Crh-KO Developmental	Replacement CRH coding region with neomycin cassette	Blunted HPA axis activity (↓ basal and stress-induced corticosterone levels), = basal & acute stress-induced anxiety, = locomotion, exploration, startle response and learning	*Muglia et al., 1995* Weninger et al., 1999

Table 3 continued

Transgenic Line	Construct	Phenotype	Reference
CRHR1 knockout			
Crhr1-KO Developmental	Replacement of exons 8-13 with a neomycin cassette	Blunted HPA axis activity (↓ basal and stress-induced corticosterone levels), ↓ anxiety, ↑ locomotion; ↑ and deleyed stress-induced alcohol intake, ↓ remote fear memory consolidation	*Timpl et al., 1998* Sillaber et al., 2002 Thoeringer et al., 2012
Crfr1-KO Developmental	Replacement of exons 5-8 with a neomycin cassette	Blunted HPA axis activity (↓ basal and stress-induced corticosterone levels), ↓ anxiety; ↓ spatial memory performance	*Smith et al., 1998* Contarino et al., 1999
Crhr1$^{FB\text{-}CKO}$ Postnatal / forebrain-specific inactivation	Conditional *Camk2α*-Cre mediated *Crhr1* inactivation (floxed exons 9-13)	= basal HPA axis activity, slightly enhanced corticosterone after acute stress, ↓ anxiety, ↓ chronic-stress induced cognitive deficits , dendritic atrophy and spine loss , ↓ remote fear memory consolidation	*Müller et al., 2003* Wang et al., 2011a Wang et al., 2011b Wang et al., 2011c Thoeringer et al., 2012
CRHR2 knockout			
Crhr2-KO Developmental	Replacement of transmembrane domains 3-5 with a neomycin cassette	↓ ACTH and corticosterone response to stress and early termination of ACTH release, = anxiety, ↑ social discrimination	*Coste et al., 2000* Deussing et al., 2010
Crfr2-KO Developmental	Replacement of exons 10-12 with a neomycin cassette	↓ ACTH and corticosterone response to stress and early termination of ACTH release, ↑ anxiety & immobility FST	*Bale et al., 2000*
Crhr2-null Development	Replacement of 3rd cytoplasmic region with a neomycin cassette	= HPA axis activity, = locomotion, ↑ anxiety & immobility FST	*Kishimoto et al., 2000*
CRHR1/CRHR2 double knockout			
Crhr1/Crhr2 dKO Developmental	Crossbreeding	↓HPA stress response	*Preil et al., 2001*
Crfr1/Crfr2 dKO Developmental	Crossbreeding	↓HPA stress response, ↓ anxiety only in females	*Bale et al., 2002*
UCN1 knockout			
Ucn1-KO Developmental	Replacement of coding region with neomycin cassette	= HPA axis and feeding, ↑ anxiety, impaired hearing	*Vetter et al., 2002*
Ucn1-null developmental	Replacement of exon 2 with eGFP-LacZ reporter cassette	= HPA axis, locomotion & anxiety, ↓ impaired acoustic startle response	*Wang et al., 2002*
Ucn1$^{-/-}$ Developmental	Replacement of exon 2 with a neomycin cassette	= HPA axis, but ↓ HPA adaptation to repeated restraint stress	*Zalutskaya et al., 2007*

Table 3 continued

Transgenic Line	Construct	Phenotype	Reference
UCN2 knockout			
Ucn2$^{tz/tz}$ Developmental	Replacement of open reading frame with *tau-LacZ* reporter cassette	= HPA axis, anxiety, immobility FST, & social discrimination, ↓ aggressiveness	*Deussing et al., 2010* Breu et al., 2012
Ucn2-KO Developmental	Replacement of exon 2 with a neomycin cassette	↑ nocturnal ACTH & cortisocterone levels & ↓ FST immobility only in females, = anxiety,locomotion & fear conditioning in males and females	*Chen et al., 2006*
UCN3 knockout			
Ucn3$^{tz/tz}$	Replacement of open reading frame with *tau-LacZ* reporter cassette	= HPA axis, anxiety and immobility FST, ↑ social discrimination	*Deussing et al., 2010*
UCN1/UCN2 double knockout			
Ucn1-KO/Ucn2-KO	Crossbreeding	↑ stress-induced HPA response only in males, ↓ anxiety	*Neufeld-Cohen et al., 2010*
UCN1/UCN2/UCN3 triple knockout			
Ucn1-KO/Ucn2-KO/Ucn3-KO	Crossbreeding	= HPA activity, ↓ locomotion, ↑ anxiety 24h after acute stress but not under basal conditions	*Neufeld-Cohen et al., 2010*

All knockout lines were generated by means of targeted deletion via homologous recombination in embryonic stem cells. ↑ indicates an increase, ↓ indicates a decrease, = indicates no difference compared to control animals. Abbreviations: adrenocorticotropic hormone (ACTH), overexpression (OE), conditional overexpression (COE), doxycycline (Dox), forced swim test (FST), hypothalamic-pituitary-adrenal (HPA) axis. Modified from Janssen and Kozicz 2013, and Sztainberg and Chen 2010.

2. AIMS OF THE THESIS

Chronic stress exposure during life represents a major risk factor for the development of psychiatric disorders including depression, anxiety, bipolar disorder and schizophrenia. CRH represents a key effector of physical and psychological stressors and modulates the necessary physiological and behavioral responses. However, the CRH-system does not act on its own. Other brain circuits such as the noradrenergic, dopaminergic and serotonergic system are heavily involved in the modulation of emotional response under physiological and pathological conditions. In order to further dissect CRH-controlled neurocircuitries of stress this study aimed to answer the following question: How does the CRH-system interact with other neurotransmitter circuits to modulate emotional behavior. This question was addressed using a variety of genetic mouse models, stress-paradigms, molecular analyses and imaging techniques.

1) **Do CRH overexpressing mice model endophenotypes of stress-related disorders? How does CRH overexpression modulate stress-related behavior when restricted to specific neurotransmitter circuits?**

The first aim of this study was to differentiate between the CRH/CRHR1 pathways that control stress induced behaviors from those regulating the HPA axis. To achieve this we applied conditional mutagenesis to generate two mouse lines of HPA axis hyperdrive with and without direct alteration of central CRH expression: $Crh^{Del\text{-}COE}$ mice overexpress CRH throughout the body, while $Crh^{Apit\text{-}COE}$ mice selectively overexpress CRH in the anterior and intermediate pituitary. Both mouse lines were investigated with regards to physiological, neuroendocrine and behavioral parameters.

Next we aimed to assess whether CNS-specific CRH overexpressing mice ($Crh^{CNS\text{-}COE}$) represent sufficient face and predictive validity to model features of stress-related neurophatologies. A number of behavioral, cognitive, neuroendocrine, pharmacological and electrophysiological parameters were evaluated in $Crh^{CNS\text{-}COE}$ mice under basal and chronic-stress condtions. In addition, molecular and microarray analyses were applied to uncover possible alterations in downstream signaling.

In order to specify the brain regions and circuits involved in the regulation of emotional behavior via CRH, conditional CRH overexpressing mice were bred to different region- and

neurotransmitter-specific Cre recombinase lines. All mouse models were investigated with regards to physiological, neuroendocrine and behavioral alterations. *In vivo* microdialysis was utilized to investigate possible alterations in serotonergic, noradrenergic and dopaminergic neurotransmission caused by cell-type specific CRH overexpression.

2) **Which are the underlying neurotransmitter circuits controlled by CRHR1 that modulate stress-related behavior?**

Although conditional CRH overexpressing mice represent an indispensable genetic tool in the dissection of stress-induced neuropsychiatric disorders, they are hampered by lack of construct validity and uncertainties that arise due to ectopic CRH expression. Importantly, they provide little information about the location and type of receptors that modulate emotional behavior. Consequently our group identified that CRHR1 is expressed in forebrain glutamatergic and GABAergic neurons, dopaminergic neurons of the ventral tegmental area and a few serotonergic neurons of the raphe nucleus. An additional aim of this study was to assess the behavioral effects of *Crhr1*-deletion in these different neuronal subpopulations.

3) **What is the neurochemical identity and morphology of CRH neurons? Which are the CRH-projection targets, and which CRH-subpopulation modulates stress-related emotional responses?**

CRH is expressed throughout the mammalian brain including cortical, limbic and hindbrain structures. However, the identity, location and projection sites of CRH neurons responsible for regulating stress-induced emotional behavior are largely unknown. Using a sensitive double *in situ* method we set out to characterize the neurochemical identity of CRH-expressing neurons. Moreover, the morphology of cortical and limbic CRH neurons was analyzed in recently generated *Crh-IRES-Cre* mice bred to different reporter mice using light and confocal microscopy. Injections of Cre-dependent anterograde viral tracers into limbic regions of *Crh-IRES-Cre* mice enabled the identification specific CRH projection sites.

With the intention to unravel the role of endogenous CRH function our group generated the first conditional *Crh* knockout mice based on the Cre/loxP system using homologous recombination in ES cells. In order to gain more insight into the neurocircuitry level and specifically dissect the involvement of CRH in distinct neuronal subpopulations, conditional *Crh* knockout mice were crossed with different cell type-specific Cre recombinase lines.

Physiological, neuroendocrine, behavioral and molecular alterations were investigated under basal and chronic-stress conditions.

This thesis provides a comprehensive assessment of the body's major stress-integrating system in the context of neuropsychiatric disorders. Importantly, it is one of the first studies to investigate CRH-neurotransmitter interactions in genetic mouse models of CRH hyperdrive as well as CRH and CRHR1 deficiency. The obtained results will aid in identifying distinct and overlapping stress-circuits in different neuropsychiatric disorders.

3. MATERIALS AND METHODS

3.1. Reagents, buffers and solutions

Unless stated otherwise, all chemicals and reagents were obtained from Roche applied science, Sigma-Aldrich and Roth or Merck.

1 x PBS

137 mM NaCl

2.7 mM KCl

20 mM Na_2HPO_4

2 mM KH_2PO_4

Adjust to pH 7.4

1 x TRIS acetate EDTA (TAE) buffer

4.84 g tris(hydroxylmethyl)-aminomethane (TRIS, Sigma-Aldrich, Munich, Germany)

1.142 ml acetic acid (Karl Roth, Karlsruhe, Germany)

20 ml 0.5 M ethylendiaminetetraacetate (EDTA, Sigma-Aldrich), pH 8.0

800 ml H_2O_{bidest}

adjust pH to 8.3 with acetic acid

adjust volume to 1 liter with H_2O_{bidest}

6 x DNA loading buffer (orange)

1 g orange G (Sigma-Aldrich)

10 ml 2 M TRIS/HCl, pH 7.5

150 ml glycerol

adjust volume to 1 liter with H_2O_{bidest}

20 x Saline-sodium citrate (SSC)

3 M NaCl (Karl Roth)

300 mM sodium citrate (Sigma-Aldrich)

adjust to pH 7.4

ad. H_2O_{bidest}, add 1 ml diethylpyrocarbonate (DEPC)/liter

incubate over night

2 x autoclave

10 x phosphate buffered saline (PBS)-DEPC

1.37 M NaCl

27 mM KCl (Karl Roth)

200 mM Na_2HPO_4 x 12 H_2O (Merck, Darmstadt, Germany)

20 mM KH_2PO_4 (Merck)

adjust to pH 7.4

ad. H_2O_{bidest}, add 1 ml DEPC/liter

incubate over night

2 x autoclave

20% paraformaldehyde (PFA)-DEPC

20% w/v paraformaldehyde (Sigma-Aldrich)

in 1x PBS-DEPC

adjust to pH 7.4

10 x triethanolamine (TEA)

1 M TEA (Sigma-Aldrich)

pH 8.0

ad. H_2O_{bidest}, add 1 ml DEPC/liter

incubate over night

2 x autoclave

H_2O-DEPC

2 ml DEPC (Sigma-Aldrich)

ad. 2l H_2O_{bidest}

2 x autoclave

5 M DTT/DEPC

7.715 g DTT

4 ml H_2O-DEPC

shake the falcon tube until the powder is nearly disolved

adjust volume to 10 ml with H_2O-DEPC

5 x NTE

146.1 g NaCl

50 ml 1 M TRIS/HCl, pH 8.0

50 ml 0.5 M EDTA, pH 8.0

adjust volume to 1 liter with H_2O_{bidest}, add 1 ml DEPC

incubate o.n., autoclave

3 M NH_4OAc

3 M NH_4OAc (Sigma)

adjust volume with H_2O_{bidest}

autoclave

0.2M HCl-DEPC (500 ml)

8 ml 37% HCl (Roth) in 492 ml DEPC-H_2O

1x TNT

0.1 M Tris-HCl

0.15 M NaCl 0.05% (500 µl) Tween 20 (Sigma-Aldrich)

add 800 ml H_2O bidest.

adjust pH to 7.6 adjust volume with H_2O bidest.

NEN-TNB blocking buffer

dissolve 0.5% blocking reagent (NEL700A kit Perkin Elmer)

in 1 × TNT buffer

Hybridization-mix (hybmix)

(50%) 50 ml formamide

(20 mM) 1 ml 2 M TRIS/HCl, pH 8.0

(300mM) 1.775 g NaCl

(5mM) 1 ml 0.5 M EDTA, pH 8.0

(10%) 10 g dextran sulphate (Sigma-Aldrich)

(0.02%) 0.02 g ficoll 400 (Sigma-Aldrich)

(0.02%) 0.02 g polyvinylpyrrolidone 40 (PVP40, Sigma-Aldrich)

(0.02%) 0.02 g BSA (Sigma-Aldrich)

5 ml tRNA (10 mg/ml, Roche Diagnostics GmbH, Mannheim, Germany)

1 ml carrier DNA (salmon sperm, 10 mg/ml, Sigma-Aldrich)

(200 mM) 4 ml 5 M dithiothreitol (DTT, Roche)

store as 1 to 5 ml aliquots at - 80°C

Hybridization chamber fluid

250 ml formamide

50 ml 20 x SSC

200 ml H_2O_{bidest}

Lysogeny broth (LB) medium

1% (w/v) bacto-tryptone (BD, Heidelberg, Germany)

0.5% (w/v) bacto-yeast-extract (BD)

1.5% (w/v) NaCl

pH 7.4 with NaOH (Karl Roth)

autoclave

LB agar plates

1% (w/v) bacto-tryptone

0.5% (w/v) bacto-yeast-extract

1.5% (w/v) NaCl

1.5% (w/v) bacto-agars (BD)

pH 7.4 with NaOH

autoclave

NBT/BCIP

200 µl NBT/BCIP stock solution (Roche)

10 µl levamisole (1 M) (Sigma-Aldrich)

10 ml buffer 2 (DIG Wash and Block Buffer Set, Roche)

TBFI solution

30 nM KAc

50 nM $MnCl_2$

100 nM RbCl

10 nM $CaCl_2$

15 % glycerol

adjust pH with acetic acid, filter sterile

TBFII solution

10nM NaMOPS, pH 7.0

10 nM $RbCl_2$

15 nM $CaCl_2$

10 nM $CaCl_2$

15 % glycerol

filter sterile

3.2. Consumables, antibodies, primers and probes

Table 4: Kits used throughout this study

Kit	Company
RNeasy Mini Kit	Quiagen (Hilden, Germany)
QIAquick Spin Miniprep Kit	Quiagen (Hilden, Germany)
QIAGEN Plasmid Midi Kit	Quiagen (Hilden, Germany)
QIAGEN Plasmid Maxi Kit	Quiagen (Hilden, Germany)
DIG Nucleic Acid Detection Kit	Roche (Mannheim, Germany)
DIG RNA Labeling Kit (SP6/T7)	Roche (Mannheim, Germany)
DIG Wash and Block Buffer Set	Roche (Mannheim, Germany)
Radioimmunoassay (RIA) Kit	MP Biomedicals (Eschwege, Germany)
TOPO TA Cloning Kit pCRII TOPO	Invitrogen (Darmstadt, Germany)
TSA™ Biotin System	PerkinElmer (Groningen, Netherlands)
Vector® Red Alkaline Phospatase Substrate Kit	Vector Laboratories (Lörrach, Germany)
NBT/BCIP Stock solution	Roche (Mannheim, Germany)

Table 5: Enzymes, nucleotides and nucleic acids

Enzyme/Nucleotide/Nucleic Acid	Company
Proteinase K	Sigma-Aldrich (Taufkirchen, Germany)
RNAse H	Sigma (Taufkirchen, Germany)
T4 DNA Polymerase	Roche (Mannheim, Germany)
T4 DNA Ligase	Roche (Mannheim, Germany)
T3-, T7-, SP6-plymerase (20U/µl)	Roche (Mannheim, Germany)
Taq DNA -polymerase	ABgene (Hamburg, Germany)
DNase I, RNAse free	Roche (Mannheim, Germany)
RNasin	Roche (Mannheim, Germany)
Restriction enzymes with 10x buffer	Fermentas (St. Leon-Rot, Germany)
[α-thio-^{35}S]-UTP	PerkinElmer (Groningen, Netherlands)
Desoxynucleotides	Roche (Mannheim, Germany)
DIG RNA labeling mix	Roche (Mannheim, Germany)
Oligo(dT)$_{15}$ Primer	Roche (Mannheim, Germany)

Table 6: Genotyping primers

Name	Sequence 5´ → 3´	Amplicon (bp)	Detection of
ROSA-1	AAAGTCGCTCTGAGTTGTTAT	398	Wild-type product
ROSA-5	TAGAGCTGGTTCGTGGTGTG	646	Mutant product
ROSA-6	GCTGCATAAAACCCCAGATG	505	Premature deletion of floxed
ROSA-7	GGGGAACTTCCTGACTAGGG		terminator sequence
R1-GT1	TCACCTAAGTCCAGCTGAGGA	697	Wild-type *Crhr1* product
R1-GT3B	GGGGCCCTGGTAGATGTA-GT	790	Floxed *Crhr1* product
R1-CK1	GAGCGGATCTCAAACTCTCC	500	Premature deletion of floxed allele
CCK1-fw	AAGAATGGCTCCCCTATTGC	213	Wild-type *Crh* product
CCK2-rev	TAAAGCCACAGCAACCTTTG	399	Floxed *Crh* product
CCK3-rev	CCCTGGCTCCTCTTCCTAAG	611	Premature deletion of floxed allele
Tau-rev	TCTGCAGGGGAGACTCTTTC	479	*LacZ* product
Neo-fwd	CGATCCCATGGTTTAGTTCC	890	Neomycin product
CRE-F	GATCGCTGCCAGGATATACG	574	Cre recombinase
CRE-R	AATCGCCATCTTCCAGCAG	372	*Thy1* control product
Thy1-fw	TCTGAGTGGCAAAGGACCTTAGG		
Thy1-rev	CCACTGGTGAGGTTGAGG		
DatCre-fw	GGCTGGTGTGTCCATCCCTGA A	1098	Cathepsin (*Ctsq*) wild-type product
DatCre-rev	GGTCAAATCCACAAAGCCTGGCA	405	*Dat-CreERT2* product
CTSQ-fw	ACAAGGTCTGTGAATCATGC		
CTSQ-rev	TTACAATGTGGATTTTGTGGG		
i-Cre 1	GGTTCTCCGTTTGCACTCAGGA	375	*Camk2α-CreERT2*
i-Cre 2	CTGCATGCACGGGACAGCTCT	290	Control product (endogenous
i-Cre 3	GCTTGCAGGTACAGGAGGTAGT		*Camk2α*)

Table 7: Primers for qRT-PCR

Name	Sequence 5´ → 3´	Amplicon (bp)
Aqp4_fw	GCACACGAAAGATCAGCA	200
Aqp4_rev	GAACACCAACTGGAAAGTGA	
Dock10_fw	TGCTGGATGACGGCTCAGTTAG	186
Dock10_rev	AAGCATCCAACGAAACCATAATCTC	
Gapdh_fw	CCATCACCATCTTCCAGGAGCGAG	362
Gapdh_rev	GATGGCATGGACTGTGGTCATGAG	
Hprt_fw	ACCTCTCGAAGTGTTGGATACAGG	167
Hprt_rev	CTTGCGCTCATCTTAGGCTTTG	
Ifitm1_fw	GCCTACTCCGTGAAGTCTA	200
Ifitm1_rev	GCCCCAGAATCTGTTATCTAC	
Nfib_fw	GATGAAATCCTTGCTTCTGGA	200
Nfib_rev	GCCTCAATAAATGGGTGGAAT	

Table 8: Additional primers

Name	Sequence 5´ → 3´	Amplicon (bp)
Camk2α_fw	ACGCGTTTAACATTATGGCCTTAGG	1299
Camk2α_rev	GTCGACGCTGCCCCCAGAACTAGGG	
T7 pCRII TOPO	GAATTGTAATACGACTCACTATAGGGCGAATTG	depending on
Sp6 pCRII TOPO	CCAAGCTATTTAGGTGACACTATAGAATACT	insert size
Aqp4_fw	AGCAATTGGATTTTCCGTTG	718
Aqp4_rev	CCAGGTATTCCGGGATGA	

Table 9: mRNA probes, antibodies and peptides

Probe	Antisense	Vector	Accession Nr.	Location/Size (bp)
Aqp4	Sp6	pCRII-TOPO	AI115947	627-1371
CRH (3'-UTR)	Sp6	pCRII-TOPO	AY128673	2108-2370
CRH	Sp6	pCRII-TOPO	AY128673	1306-1661
LacZ	Sp6	pCRII-TOPO	X65335	2649-3281
Gad65	T3	pBluescript	NH_008078	1000
Gad67	T3	pBluescript	NM_008077	984-1940
VGlutI	Sp6	pCRII-TOPO	NM_010484	1716-2332
c-fos	Sp6	pCRII-TOPO	NM_010234	608-978
Zif268	Sp6	pCRII-TOPO	NM_007913	245-786
Camk2α	Sp6	pCRII-TOPO	NM_177407.4	2034-2903
Tomato	T7	pCRII-TOPO	EU855182.1	689

Table 10: Antibodies and Peptides

Antibodies and Peptides	Supplier
anti-DIG-alkaline phosphatase (FAB fragments)	Roche
anti-DIG(Fab)-peroxidase	Roche
Streptavidin-alkaline phosphatase	Roche
α-GFP (polyclonal, chicken, dilution 1:2000)	Abcam, #ab13970
α-tyrosine hydroxylase (polyclonal, rabbit, dilution 1 :3000)	Pel Freez, #P40101
Alexa Fluor 488 goat α-chicken IgG	Invitrogen, #A11039
Alexa Fluor 488 goat α-rabbit IgG	Invitrogen, #A11034
Alexa Fluor 594 goat α-chicken IgG	Invitrogen, #A11042

3.3. Animals and animal housing

All animal experiments were conducted in accordance with the Guide of the Care and Use of Laboratory Animals of the Government of Bavaria, Germany. Mice were group housed under standard laboratory conditions (22 ± 1°C, 55 ± 5% humidity) and were maintained on a 12 h light-dark cycle (lights on between 7:00 a.m. and 7:00 p.m.) with food and water ad libitum. At weaning mice were numbered by ear-punching, and a small tail biopsy was taken for genotyping. Mice were single housed two weeks prior behavioral testing or hormone assessment.

3.4. Microbiological methods

Preparation of chemically competent bacteria

Initially, 5 ml of DH5α or XL1-Blue *E. coli* culture was grown overnight in LB medium. On the following day, 100 ml LB medium was inoculated with the overnight culture and grown on a shaker at 37°C until an optical density (OD) of OD 550nm < 500 was obtained. Subsequently, the bacteria were centrifuged for 15 min at 5000 rpm at 4°C. The supernatant was decanted

and the pellet was gently resuspended on ice in 30 ml cold TBFI. After incubation on ice for 20 min bacteria were centrifuged for 5 min at 4000 rpm at 4°C. The pellet was gently resuspended in 3.6 ml TBFII and 100 µl aliquots were prepared. Competent bacteria were frozen and stored at -80°C.

Transformation

Chemically competent DH5α or XL1-Blue *E. coli* bacteria were shortly thawed on ice. The DNA was added to the bacteria and mixed by gently tapping the tube. Bacteria were incubated for 20-30min min on ice. Competent cells were then heat-shocked at 42°C for 30-90 sec and subsequently put on ice. This enabled the uptake of the plasmid DNA. 1 ml SOC or LB medium was added, and the cells were incubated on a shaker at 37°C for 1-2 h. Subsequently, cells were plated on LB plates containing the appropriate antibiotic for selection (100 µg/ml ampicillin or 50 µg/ml kanamycin) and incubated overnight at 37°C. Single colonies were picked and inoculated in 5 ml LB medium containing the appropriate selection marker (100 µg/ml ampicillin or 50 µg/ml kanamycin) and grown overnight at 37°C on a shaker at 250 rpm for subsequent DNA preparation.

Glycerol stocks

For long-term storage, 750 µl of an overnight bacteria culture was mixed with 250 µl 80% glycerol and frozen at -80°C.

3.5. Preparation and analysis of plasmid DNA

Preparation of plasmid DNA

Plasmid DNA was prepared using DNA isolation Kits from Qiagen (Mini-, Midi- and Plasmid Maxi-Kit) according to the manufacturer's instructions. For MiniPreps, a single colony was inoculated in 3-5 ml LB medium with a selective antibiotic o.n. on a shaker at 37°C. For MidiPreps, a single colony was inoculated in 100 ml LB medium with a selective antibiotic o.n. on a shaker at 37°C. For MaxiPreps, 500 µl of an o.n. MiniPrep, or the approprioate glycerol-stock of bacteria was added to 250 ml LB medium with the appropriate antibiotic and incubated o.n. on a shaker at 37°C.

Polymerase Chain Reaction (PCR)

In order to amplify desired DNA sequences for further cloning procedures, PCRs were carried out using genomic DNA, cDNA or plasmid DNA as templates. For a regular 50 µl PCR reaction 0.5-5 µg genomic DNA, 0.1-1 µg cDNA or 20-200 ng plasmid DNA were used. The reaction was prepared as follows:

x template (as stated above)
5 µl 10 x reaction buffer IV (ABgene)
3 µl 25 mM $MgCl_2$ (ABgene)
1 µl 10 mM dNTPs (Roche)
3 µl 10 µM primer forward
3 µl 10 µM primer reverse
0.5 µl Thermoprime Plus DNA polymerase (5 U/µl, ABgene)
adjust to 50 µl with H_2O_{bidest}

In general, the following standard PCR reaction was carried out: 95°C 5 min, 35 cycles of 95°C for 30 sec, 58-60°C for 30 sec, 72°C for 1 min per 1 kb of DNA, followed by 72°C for 10 min and subsequent hold at 4°C. If required, the annealing and elongation temperatures were adjusted for a specific DNA product. PCR products were analyzed via gel electrophoresis in a 1-2% agarose gel (1 x TAE), containing ethidium bromide. For this, a small aliquot of the PCR (1-5µl) was mixed with 6x Orange loading dye and loaded onto the gel, which was subsequently analysed with a UV-transilluminator and a BioDoc II gel documentation system from Biometra or the Quantum gel documentation system 1100 from Vilber Lourmat.

Genotyping

For genotyping PCRs of transgenic mice, tail tissue was digested in 100 µl 50 mM NaOH for 30 min at 95°C followed by a neutralization step using 30 µl 1 M Tris-HCl (pH 7.0) and stored at 4°C. 1-2 µl of the tail lysates were used as template for PCRs. For genotyping, 1 µl of the lysed genomic DNA was used in a 25 µl-PCR reaction, containing 2.5 µl 10x PCR buffer (Abgene), 1.5 µl 25 mM $MgCl_2$, 0.5 µl dNTPs (10 mM each, Roche), 0.5 µl of each primer and 0.5 µl Taq DNA polymerase (5 U/µl, Abgene). A standard PCR program was carried out: 95°C 5 min, 35 cycles of 95°C for 30 sec, 58-60°C for 30 sec, 72°C for 1 min per 1 kb of DNA, followed by 72°C for 10 min and subsequent hold at 4°C.

Assessment of DNA/RNA concentrations

DNA or RNA concentrations were measured in a UV photometer (Gene Quant II, Pharmacia Biotech). An optical density (OD) of 1 at a wavelength of 260 nm and a cuvette thickness of 1 cm corresponded the following concentrations: 50 µg/ml double stranded DNA, 33 µg/ml single stranded DNA and 40 µg/ml RNA. Consequently, concentrations can be determined by the following equation: X µg/ml = OD260 x n x f, with f being the dilution factor and n the default 50 µg/ml double stranded DNA, 33 µg/ml single stranded DNA and 40 µg/ml RNA.

3.6. Cloning procedures

DNA restriction digests

For analytical purposes only, restriction digestion of DNA samples was performed using restriction enzymes and working buffers from Fermentas Life Science or New England Biolabs (NEB). Plasmid-DNA was digested for 1-2 h at 37°C with 10 units/µg of the restriction enzyme in corresponding buffers. Fragment sizes were analyzed by agarose gel electrophoresis.

DNA gel extraction

The QIAquick Gel Extraction Kit (Qiagen) was used according to manufacturer´s instructions to purify DNA fragments out of an agarose gel. DNA was eluted in 30-50 µl of H_2O bidest. The DNA concentration was determined by spectrophotometry and the DNA quality was assessed by gel electrophoresis.

Ligation of DNA fragments

For ligations of linearized vectors and the insert the Rapid DNA Ligation Kit (Fermentas) was used. 50 ng of vector backbone was ligated to 3x molar excess of insert. The appropriate amount of insert was calculated as following: m insert (ng) = 3 x 50 ng x (bp of insert / bp of backbone vector). T4 DNA ligase buffer and 5 U of T4 DNA ligase (Fermentas) were added in a total volume of 10-15 µl, and incubated o.n. at 16°C. On the next day, a heat shock transformation using 1-2 µl of the ligation product was performed in chemocompetent bacteria.

TOPO TA Cloning

For ligation of products obtained from PCR reactions, inserts were cloned into the pCRII-TOPO vector (TOPO TA cloning Dual promoter Kit, Invitrogen), containing Sp6 and T7 promoters for efficient in vitro transcription. PCR products with 3'-A-overhangs were inserted into a

linearized pCRII-TOPO vector with single 3'-T-overhangs. The reaction was set up as follows: 4 µl PCR product, 1 µl salt solution and 1 µl pCR®II-TOPO® vector. After 10 min of incubation at room temperature 1-4 µl of the mixture was transformed into chemically competent bacteria as described above. For blue-white selection of the colonies, 40 µl of 40 mg/ml X-Gal in dimethylformamide (DMF) solution were added to the LB-agar plates.

Sequencing

All sequencing reactions were carried out by Sequiserve (www.sequiserve.de).

3.7. RNA isolation and quantitative real-time PCR (qRT-PCR)

RNA was isolated either from mammalian cells or from murine tissue using the TRIzol protocol (Invitrogen). cDNA was generated from the RNA using Reverse Trancriptase Superscript II from Invitrogen and oligo-dT primers according to the manufacture's protocol. Aliquotes of the prepared cDNA were utilized as templates for quantitative real time PCR, which was carried out in the Lightcycler 2.0 System (Roche) using the QuantiFast SYBR Kit (Quiagen). The mastermix was prepared as follows (volume/sample): 5 µl 5x PCR mix (QuantiFast SYBR Green PCR Mix), 1 µl 10 µM primer fwd , 1 µl 10 µM primer rev and 1 µl H_2O (Quiagen, Hilden). 8 µl of the mastermix were pipetted into each capillary, which was fixed in the Lightcycler carousel (Roche). Subsequently, 2 µl of diluted cDNA (1/10) were added and the capillaries were closed. Samples were centrifuged before they were placed into the LightCycler. The same PCR settings were chosen for all runs. At the end of every run a melting curve was measured to ensure the quality of the PCR product. Crossing points (Cp) were determined using the absolute quantification fit points´ method. The calculations were conducted by the LightCycler®Software 4.05 (Roche). Threshold and noise band values were set to the same level in all compared runs. Relative gene expression was determined with the 2-ΔΔCT method (Livak and Schmittgen, 2001), using the real PCR efficiency calculated from an external standard curve, normalized to the housekeeping genes *Hprt* and *Gapdh* and related to the data of control experiments.

3.8. Gene expression analysis using microarray technology

The microarray experiments were performed by Torsten Klengel, Claudia Kühne and Peter Weber at the Max Planck Institute of Psychiatry. Hippocampal RNA was isolated using the TRIzol protocol (Invitrogen) and the quality was verified by agarose gel electrophoresis. RNA

was amplified using the Illumina® TotalPrep RNA Amplification Kit (Ambion) according to the manufacture's protocol. For the analysis of differential expression patterns of control and CNS-specific CRH overexpressing animals ($Crh^{CNS\text{-}COE}$), the Illumina Sentrix® BeadChip Array for Gene Expression Mouse-6 (Illumina, San Diego, USA) was used, containing 45200 transcripts covering more than 19100 unique, curated genes in the NCBI RefSeq database (Build 36, Release 22). On average every probe is represented by 10 beads. The data was normalized with the BeadStudio software version 1.5.1.3. (Illumina) using the cubic spline parameter for balancing non-linear effects. Illumina custom settings were chosen for statistical analysis, which are based on a moderate t-test adjusted with empirical factors.

3.9. Preparation of brain slices and immunohistochemistry

Mice were killed with an overdose of isoflurane (Floren®, Abbott) and transcardially perfused with a peristaltic pump for 1 min with PBS, 5 min with 4% PFA (w/v) in PBS, pH 7.4, and 1 min with PBS at a flow rate of 10 ml/min. The brains were removed and post-fixed o.n. in 4% PFA at 4°C and subsequently cryoprotected in 15% (w/v) saccharose in PBS, pH 7.6 o.n. at 4°C. Brains were washed with PBS and embedded in warm 4% (w/v) agarose (Invitrogen) in PBS for vibratome-sectioning (MICROM HM 650V, ThermoScientific). 40-50 µm thick vibratome sections were prepared and stored in cryopreservation solution (25 % (v/v) glycerol, 25% (v/v) ethylenglycol, 50% (v/v) PBS, pH 7.4) until further use. Slices were washed 3 x with PBS and permeabilized with PBS-TritonX-100 0.1% 3 x 5 min. Blocking was performed at RT for 1 h in 5% BSA (w/v) in PBS-TritonX-100 0.1%. Brain slices were then incubated o.n. at 4°C with the primary antibody, which was previously diluted in 5% BSA (w/v) in PBS-TritonX-100 0.1%. After a 3 x 10 min washing step with PBS, an Alexa Fluor secondary antibody (Invitrogen), diluted in PBS-Triton 0.01%, was added and incubated for 2 h at RT. Brain sections were washed 3 x with PBS, stained with DAPI and mounted with anti-fading fluorescence VectaShield medium (Vector Labs).

3.10. *In situ* hybridization (*ISH*)

ISH was performed as previously described (Lu et al., 2008; Refojo et al., 2011). Male mice (age 2-4 months) were anaesthetized with isoflurane and sacrificed by decapitation. Brains were immediately dissected, and shock frozen on dry ice. Frozen brains were cut on a cryostat in 20-µm thick sections and mounted on SuperFrost Plus slides and shortly dried on a 37°C warming plate. Slides were stored at -20°C until further processing. Before pretreatment, slides were

thawn approximately for 30 min at 37°C. Fixation and pretreatment of slides were performed at room temperature according to Table 11.

Table 11: Pretreatment of slides during *ISH*

Step	Duration (min)	Solutions	Comment
1. Fix	10	4% PFA in 1x PBS / DEPC	On ice
2. Wash	2 x 5	1x PBS / DEPC	
3. Acetylate	10	0,1M triethanolamine-HCl in 1 TEA, pH 8,0	Add freshly 600 µl acetic anhydride per 200 ml TEA and stir
4. Wash	2 x 5	2x SSC / DEPC	
9. Dehydrate	1 1 1 1 1 1	60% Ethanol/DEPC 70% Ethanol/DEPC 96% Ethanol/DEPC 100% Ethanol $CHCl_3$ 100 % Ethanol	
Air dry slides in a dust free, RNase-free area			

Specific riboprobes were generated by PCR applying T7 and SP6 primers using plasmids containing the required template cDNA (Table 9). Radiolabeled sense and antisense cRNA probes were generated from the respective PCR products by in vitro transcription with 35S-UTP (PerkinElmer) using T7 and SP6 RNA polymerase. After 20 min of DNase I (Roche) treatment, the probes were purified using the RNeasy-Mini Kit protocol (Qiagen) and measured in a scintillation counter. The sections were hybridized overnight at 57°C with a probe concentration of $7x10^6$ counts per minute (cpm)/µl. Subsequently they were washed at 64°C in 0.1 x saline sodium citrate (SSC) and 0.1 mM dithiothreitol. The stringency washing steps are described in Table 12.

Table 12: Stringency washing procedure during *ISH*

Step	Temp. (°C)	Duration (min)	Solutions	Comment
1. Wash	RT	4 x 5	4x SSC	
2. RNase	37	20	1x NTE / 500 µl RNaseA (20 µg / ml)	Add RNase freshly
3. Wash	RT	2 x 5	2x SSC / 1mM DTT	Add DTT freshly
4. Wash	RT	10	1x SSC / 1mM DTT	Add DTT freshly
5. Wash	RT	10	0.5x SSC / 1mM DTT	Add DTT freshly
6. Wash	64	2 x 30	0.1x SSC / 1mM DTT	Add DTT freshly
7. Wash	RT	2 x 10	0.1x SSC	
8. Dehydrate	RT	1 1 1 1 2 x 1	30% Ethanol / 300mM NH_4OA_c 50% Ethanol / 300mM NH_4OA_c 70% Ethanol / 300mM NH_4OA_c 95% Ethanol 100% Ethanol	
Air dry slides in a dust free area				

In order to visualize hybridization signals, dried slides were exposed to a special high performance X-ray film (Kodak, BioMax) for different time intervals. For quantification, autoradiographs were digitized and relative levels of mRNA were determined by computer-assisted optical densitometry (ImageJ). To obtain cellular signal-resolution hybridized slides were dipped in autoradiographic emulsion (type NTB2), developed after 3-6 weeks and counterstained with cresyl violet. Dark-field photomicrographs were captured with digital cameras adapted to an imaging microscope and a stereomicroscope (Leica, Wetzlar, Germany). Images were digitalized using Axio Vision 4.5, and afterwards photomicrographs were integrated into plates using image-editing software. Only sharpness, brightness and contrast were adjusted. For an adequate comparative analysis in corresponding mutant and control sections the same adjustments were performed. Brain slices were digitally cut out and set onto an artificial black or white background using Adobe Photoshop CS2.

3.11. Double *in situ* hybridization

In order to perform co-expression studies in brain slices, double *ISH* was applied, which enables the simultaneous detection of two different mRNA markers. The protocol was adapted from Refojo et al. (2011). The same riboprobes used for single *ISH* were also applied here (Table 9). Antisense and sense cRNA probes were synthesized and labeled with 35S-UTP or with dioxygenin (DIG) by in vitro transcription from 200 ng of respective PCR product used as templates. For purification of riboprobes the RNeasy Mini Kit (Qiagen) was used following the manufacturer's protocol. Frozen brains were cut on a cryostat in 20-µm thick sections and mounted on SuperFrost Plus slides. During pretreatment the slides were fixed for 15 min in 4% PFA and dehydrated in H_2O_2. The exact pretreatment steps which were all performed at RT are shown in Table 13. For hybridisation an appropriate amount of hybridisation mix with the riboprobe, containing 6 to 7 Million counts per slide and/or ~0.2 ng/µl DIG was prepared. The concentration of the DIG-labeled riboprobe was determined by making several dilutions and spotting these onto a nylon membrane, and subsequently staining and comparing them to the intensity of standards with known concentrations. The sections were hybridized overnight at 57°C. A series of washing steps were performed after hybridization to remove unspecific probe-binding (Table 14).

Table 13: Pretreatment of slides during double *ISH*

Step	Duration (min)	Solutions	Comment
1. Fix	15	4% PFA in 1x PBS / DEPC	On ice
2. Wash	2 x 5	1x PBS / DEPC	
3. Quench endogenous peroxidase	15	1% H_2O_2 in 100 % MeOH	
4. Wash	2 x 5	1x PBS/DEPC	
5. Reduce background	8	0.2M HCl / DEPC	Can be used 3x
6. Wash	2 x 5	1x PBS / DEPC	
7. Acetylate	10	0,1M triethanolamine-HCl in 1 x TEA, pH 8,0	Add freshly 600 µl acetic anhydride per 200ml TEA and stir
8. Wash	5	1x PBS / DEPC	
9. Dehydrate	1 1 1 1	60% Ethanol / DEPC 70% Ethanol / DEPC 96% Ethanol / DEPC 100% Ethanol	
Air dry slides in a dust free, RNase-free area			

Table 14: Stringency washing procedure and primary antibody treatment during double *ISH*

Step	Temp. (°C)	Duration (min)	Solutions	Comment
1. Wash	42	20-25	4x SSC / 0.05% Tween20 / 1mM DTT	Add Tween20 & DTT freshly
2. Wash	42	20-25	2x SSC / 50% formamide / 0.05% Tween20 / 1mM DTT	Add Tween20 & DTT freshly
3. Wash	42	20-25	1x SSC / 50% formamide / 0.05% Tween20 / 1mM DTT	Add Tween20 & DTT freshly
4. Wash	62	30	0.1x SSC / 0.05% Tween20 / 1mM DTT	Add Tween20 & DTT freshly
5. RNase	37	30	1x NTE / 0.05 % Tween/ 500 µl RNaseA	Add RNase freshly
6.	30	15	15 mM Iodoacetamide	
7. Wash	30	3 x 2-5	1x NTE / 0.05% Tween20	
8. Block	30	60	4% BSA / TNT	
9. Wash	30	60	TNT	
10. Block	30	30	NEN-TNB	400 µl / slide
11. AB	4	over night	Roche anti-DIG(Fab)-POD in NEN-TNB	1:400 dilution (400 µl /slide)

For DIG detection anti-DIG-POD (Fab) antibody was dilution 1/400 and pipetted onto the slides, which were incubated o.n. at 4°C. On the next day, the secondary antibody was applied and the signal was enhanced by performing tyramide-biotin signal amplification (TSA) using the NEL700A Kit (PerkinElmer), according to the manufacturer's instructions. The substrate for the secondary antibody was pipetted onto the slides (Vector Red) and the staining reaction was monitored to avoid high background staining. The appropriate signal intensity is usually observed 1-30 min after Vector®Red application, depending on the mRNA probe. The reaction was terminated by placing the slides in 1x PBS. Slices were eventually fixed with 2.5% glutaraldehyd (Sigma) and dehydrated using a degrading ethanol series. The exact steps are

shown in Table 15. Dipping, development and acquisition of the autoradiograms were performed as described for the single *ISH* before.

Table 15: Washing procedure, secondary antibody treatment and amplification during double *ISH*

Step	Temp. (°C)	Duration (min)	Solutions	Comment
1. Wash	30	3 x 5	TNT	
2. Amp.	30	15	TSA in 0.3 ml DMSO	dilute TSA mix 1:50 with amplification diluent, 300µl/slide, KEEP IN DARK
3. Wash	30	3 x 5	1x Roche washing buffer	
4. 2nd AB	30	60	Roche streptavidin-AP	Dilute 1:400 in 1x Roche blocking buffer
5. Wash	30	3 x 5	1x Roche washing buffer	
6.	RT	5	100 mM Tris/HCl	pH 8.2-8.5 very critical!
7. Staining	RT	1-30	Vector® Red	5ml 1xTris-HCl pH 8.2-8.5 +5µl 1M levamisole Add 2 drops reagent 1 → vortex Add 2 drops reagent 2 → vortex Add 2 drops reagent 3 → vortex Pipet onto slides (300µl/slide) Check staining intensity under stereomicroscope, but avoid movement when possible
8. Stop Reaction	RT	10	1x PBS	
9. Fix	RT	20	2.5% glutaraldehyd / 1 x PBS	Prepare fresh
10. Wash	RT	3 x 5	0.1x SSC	400 µ / slide
11. Dehydrate	RT	30 sec 30 sec 30 sec 10 sec	30% Ethanol 50% Ethanol 70% Ethanol 96% Ethanol	1:400 dilution (400 µl /slide)
Air dry slides in a dust free area				

3.12. Generation of transgenic mice

3.12.1. Conditional CRH overexpressing mice

Mice conditionally overexpressing (COE) CRH were generated by breeding *R26*$^{flopCrh/flopCrh}$ mice (here referred to as *Crh*$^{COE\text{-}Ctrl}$) (Lu et al., 2008) to different transgenic Cre recombinase driver lines. In the F2 generation homozygous over-expressing mice and control littermates were obtained (for detailed description see results section 4.1.1 and 4.1.3). The following Cre recombinase driver lines were used: Ubiquitously targeting *Deleter-Cre* (expresses a single copy of the Cre recombinase transgene under the control of the *Rosa26* locus; purchased from TaconicArtemis, Cologne, Germany), anterior-pituitary specific *Pomc-Cre* (Akagi et al., 1997), central nervous specific *Nestin-Cre* (Tronche et al., 1999), principal forebrain neuron-specific *Camk2α-Cre* (Minichiello et al., 1999), tamoxifen inducible principal forebrain neuron-specific *Camk2α-CreERT2* (Erdmann et al., 2007), and mid-hindbrain-specific *En1-Cre* (Kimmel et al., 2000). In addition the *Nex-Cre* was used to target glutamatergic neurons (Goebbels et al., 2006), *Dlx5/6-Cre* for GABAergic neurons (Monory et al., 2006), *D1-Cre* (Mantamadiotis et al., 2002; Lemberger et al., 2007) and tamoxifen inducible *D1-CreERT2* (Mantamadiotis et al., 2002; Lemberger et al., 2007) for dopaminoceptive neurons, inducible *Dat-CreERT2* for dopaminergic neurons (Engblom et al., 2008), and the *Slc6a2-Cre* for noradrenergic neurons (Gong et al., 2007). Inducible CRH overexpression was initiated via two weeks of oral tamoxifen administration starting between postnatal weeks 8-10.

Genotyping of conditional CRH overexpressing mice was performed by PCR using the following primers: ROSA-1, 5´-AAA-GTC-GCT-CTG-AGT-TGT-TAT-3´; ROSA-5, 5´-TAG-AGC-TGG-TTC-GTG-GTG-TG-3´, ROSA-6 5´-GCT-GCA-TAA-AAC-CCC-AGA-TG-3´ and ROSA-7, 5´-GGG-GAA-CTT-CCT-GAC-TAG-GG-3´. Standard PCR conditions resulted in a 398-bp wild-type and a 646-bp mutant PCR product. Animals with a premature deletion of the floxed transcriptional terminator sequence were identified by the occurrence of a 505-bp PCR product. The presence of Cre was evaluated using primers CRE-F, 5'-GAT-CGC-TGCC-AGG-ATA-TAC-G-3', CRE-R, 5'-AAT-CGC-CATC-TTC-CAG-CAG-3', Thy1-fw, 5´-TCT-GAG-TGG-CAA-AGG-ACC-TTA-GG-3´ and Thy1-rev, 5´-CCA-CTG-GTG-AGG-TTG-AGG-3´, resulting in a Cre-specific PCR product of 574 bp and a control PCR product of *Thy1* of 372 bp. The presence of the inducible *Camk2α-CreERT2* was evaluated using primers i-Cre 1, 5´-GGT-TCT-CCG-TTT-GCA-CTC-AGG-A-3´, i-Cre 2, 5´-CTG-CAT-GCA-CGG-GAC-AGC-TCT-3´ and i-Cre 3, 5´-GCT-TGC-AGG-TAC-AGG-AGG-TAG-T-3´ resulting in a Cre-specific PCR product of 375 bp and a control PCR product of 290 bp. The presence of the

inducible *Dat-CreERT2* was evaluated using primers Dat-fw, 5´- GGC-TGG-TGT-GTC-CAT-CCC-TGA-A´, Dat-rev, 5´-GGT-CAA-ATC-CAC-AAA-GCC-TGG-CA-3´, CTSQ-fwd, 5´-ACA-AGG-TCT-GTG-AAT-CAT-GC-3´, and CTSQ-rev, 5´-TTA-CAA-TGT-GGA-TTT-TGT-GGG-3´, resulting in a *Dat-CreERT2*-specific PCR product of 405 bp and a control cathepsin (*Ctsq*) PCR product of 1098 bp. Mice were on a mixed 129S2/Sv×C57BL/6J genetic background.

3.12.2. Conditional *Crhr1* knockout mice

The generation of *Crhr1-floxed* mice was previously described (Muller et al., 2003). Conditional *Crhr1* mutant mice were obtained by breeding $Crhr1^{flox/flox}$ mice to the respective Cre-driver mouse lines described in the results section 4.2. For selective disruption of *Crhr1* in forebrain glutamatergic and dopaminergic neurons, $Crhr1^{flox/flox}$ mice were bred to *Nex-Cre* (Goebbels et al., 2006) and *Dat-CreERT2* (Engblom et al., 2008) mice respectively, using a three generation breeding scheme. The inducible *Dat-CreERT2* was activated in 8 week-old mice by the administration of tamoxifen (25 mg/kg i.p.) twice a day for a total of five days. Genotyping of conditional *Crhr1* knockout mice mice was performed by PCR using the following primers: R1-GT1, 5´-TCA-CCT-AAG-TCC-AGC-TGA-GGA-3´, R1-GT3B, 5´-GGG-GCC-CTG-GTA-GAT-GTA-GT-3´ and R1-CK1, 5´-GAG-CGG-ATC-TCA-AAC-TCT-CC-3´. Standard PCR conditions resulted in a 697-bp wild-type and a 790-bp floxed PCR product. A premature deletion of the floxed allele would have been identified by the occurrence of a 500-bp PCR product. The presence of *Cre* and the inducible *Dat-CreERT2* was determined as described above. Mice were on a mixed 129S2/Sv×C57BL/6J genetic background.

3.12.3. Conditional *Crh* knockout mice

Crh-floxed mice (Crh^{flox}) were generated by Claudia Kühne based on the previously described strategy used to generate *Crhr1*-reporter mice, and conditional *Crhr1* knockout mice (Kuhne et al., 2012). The targeting vector was based on a universal shuttle vector with an inverted diphtheria toxin A (DTA) expression cassette for negative selection. The shuttle vector comprises the following components, which were flanked by *attP* sites, thereby enabling cassette exchange in ES cells subsequent to homologous recombination (from 5' to 3'): *Crh*-exon 1, *loxP* site, first *frt* site, adenovirus splice acceptor (*SA*), *tZ* reporter gene equipped at its C-terminus with a flag tag, second *frt* site, and a reverse-oriented *EM7-neo* positive selection cassette, including a bovine growth hormone polyadenylation signal. Finally, a reverse-oriented *PGK* promoter, a third *frt* site and the floxed *Crh exon 2* were placed downstream of

the second *attP* site. The linearized (*ScaI*) targeting vector was introduced into intron 1 of the murin *Crh* gene via homolgous recombination in TBV2 ES cells (129S2) (for detailed description see results section 4.3.3). Mutant ES cells were identified by southern blot analysis of genomic ES cell DNA digested with *EcoRI* (5'-probe) and *BamHI* (3'-probe), respectively. External southern blot probes, used for identification of homologous recombination events in ES cells, were amplified by PCR from genomic mouse DNA and subcloned into pCRII-TOPO: 5'-probe forward 5'-AAC-TGG-CCT-ACC-ACA-ACA-GG-3' and reverse 5'-CTG-GCA-CAG-CAT-AGA-CTG-GA-3': 3'-probe forward 5'-TGC-TAC-ATG-CCA-GCT-TTC-AC-3' and reverse 5'-TTA-AGA-TGC-CCC-CAA-GTG-AG-3'. Mutant ES cells were used to generate chimeric mice by blastocyst injection. Male chimeras were bred to wildtype C57BL/6J mice and germline transmission of the modified *Crh* allele (Crh^{tz} - which is a null allele harboring the reporter-selection cassette insertion in intron 1, and the floxed *Crh* exon 2) was confirmed by PCR in F1 offspring. Breeding the Crh^{tz} reporter mice with transgenic *Flpe-deleter* mice (Rodriguez et al., 2000) led to deletion of the *tZ-neo* cassette and resulted in a conditional *Crh* allele (Crh^{flox}) leaving exon 2 flanked by *loxP* sites. Subsequent breeding to transgenic Cre mouse lines resulted in conditional deletion of the *loxP* flanked *Crh*-exon 2 (Crh^{CKO}). Region and neurotransmitter-specific *Crh* knockout lines were generated by breeding to the following Cre recombinase lines: *Cre-deleter* (expresses a single copy of the Cre recombinase transgene under the control of the *Rosa26* locus; purchased from TaconicArtemis, Cologne, Germany), *Camk2α-CreERT2* (Erdmann et al., 2007), *Dlx5/6-Cre* (Monory et al., 2006), *Nex-Cre* (Goebbels et al., 2006), and *En1-Cre* (Kimmel et al., 2000).

Genotyping of conditional *Crh* knockout mice mice was performed by PCR using the following primers: CCK1-fwd, 5´-AAG-AAT-GGC-TCC-CCT-ATT-GC-3´, CCK2-rev, 5´-TAA-AGC-CAC-AGC-AAC-CTT-TG-3´, CCK3-rev, 5´-CCC-TGG-CTC-CTC-TTC-CTA-AG-3´, Tau-rev, 5´-TCT-GCA-GGG-GAG-ACT-CTT-TC-3´, Neo-fwd, 5´-CGA-TCC-CAT-GGT-TTA-GTT-CC-3´. Standard PCR conditions resulted in a 213 bp wild-type and a 399 bp floxed PCR product. A premature deletion of the floxed *Crh* allele would have been identified by the occurrence of a 611 PCR product. The presence of *tauLacz* and *Neo* resulted in a 479 bp and 890 bp product respectively. The presence of *Flp* recombinase was evaluated using the primers Flipase forward, 5'-TTC-GAA-TCA-TCG- GAA-GAA-GC-3' and Flipase reverse, 5'-TTG-CCG-GTC-CTA-TTT-ACT-CG-3', resulting in a PCR product of 413 bp. The presence of Cre and the inducible *Camk2α-CreERT2* was determined as described above. Mice were on a mixed 129S2/Sv×C57BL/6J genetic background.

3.12.4. Conditional urocortin 2 (UCN2) overexpressing mice

Conditional UCN2 overexpressing mice were generated by Ailing Lu (unpublished data). The targeting procedure is based on the strategy used to generate conditional CRH overexpressing mice (Lu et al., 2008), the only difference being that a *tauLacZ* was employed as a reporter. The fusion of β-galactosidase to the microtubule-associated TAU targets β-galactosidase to the axons. Thus, the Rosa26 (*R26*) locus was engineered to harbor a transcriptional terminator sequence flanked by *loxP* sites, followed by a *Ucn2-IRES-tauLacZ* expression unit ($R26^{flopUcn2}$, flop: floxed stop). Cre-mediated excision of the transcriptional terminator leads to the expression of UCN2 and β-galactosidase driven by the endogenous *R26* promoter. To obtain UCN2 overexpression selectively in GABAergic neurons, $R26^{flopUcn2/flopUcn2}$ mice were bred to *Dlx5/6-Cre mice* (Monory et al., 2006). In the F2 generation homozygous UCN2 overexpressing mice ($Ucn2^{GABA\text{-}COE}$) and control littermates ($Ucn2^{GABA\text{-}Ctrl}$) were obtained. Genotyping of conditional CRH overexpressing mice was performed by PCR using the following primers: ROSA-1, 5′-AAA-GTC-GCT-CTG-AGT-TGT-TAT-3′; ROSA-5, 5′-TAG-AGC-TGG-TTC-GTG-GTG-TG-3′, ROSA-6 5′-GCT-GCA-TAA-AAC-CCC-AGA-TG-3′ and ROSA-7, 5′-GGG-GAA-CTT-CCT-GAC-TAG-GG-3′. Standard PCR conditions resulted in a 398-bp wild-type and a 646-bp mutant PCR product. Animals with a premature deletion of the floxed transcriptional terminator sequence were identified by the occurrence of a 505-bp PCR product. The presence of Cre was determined as described above. Mice were on a mixed 129S2/Sv×C57BL/6J genetic background.

3.12.5. Additional transgenic lines

In order to investigate the morphology and projection sites of CRH-neurons, recently generated *Crh-IRES-Cre* knockin driver mice (Taniguchi et al., 2011) were bred to Cre-inducible *Ai9* mice which harbor a *loxP-STOP-lox-tdTomato* allele, located in the *Rosa26* locus, driven by the CAG promotor (Madisen et al., 2010). The visualization of dendritic spines in a subgroup of *CRH* neurons was achieved by breeding *Crh-IRES-Cre* mice to Cre-inducible *Ai32* mice which harbor a CAG promotor driven *channelrhodopsin2-eYF*P fusion-protein allele, located in the *Rosa26* locus (Madisen et al., 2012).

3.13. Chronic social defeat stress (CSDS) paradigm

The CSDS paradigm is commonly applied to induce anxiety- and depression-related endophenotypes in mice (Berton et al., 2006; Wagner et al., 2011; Golden et al., 2011; Hartmann et al., 2012a; Wang et al., 2013). Experimental mice (9-13 male mice per group between 11-13 weeks of age) were submitted to chronic social defeat stress for 21 consecutive days. They were introduced into the home cage (45 cm x 25 cm) of a dominant CD1 resident for no longer than 5 min, and were subsequently defeated. Following defeat, animals spent 24 hours in the same cage, which was separated via a holed steel partition, enabling sensory but not physical contact. Every day experimental mice were exposed to a new unfamiliar resident. Defeat encounters were randomized, with variations in starting time in order to decrease the predictability to the stressor and minimize habituation effects. Control animals were housed in their home cages throughout the course of the experiment. All animals were handled daily; weight and fur status were assessed every 3-4 days; fur was evaluated as previously described (Mineur et al., 2003). Behavioral testing took place during the last week of the paradigm. In order to minimize possible carry-over effects of the different behavioral tests, the sequence of tests was arranged from least to most stressful (McIlwain et al., 2001; Kalueff and Murphy, 2007). Genotype and condition groups were randomly distributed in order to exclude apparatus bias.

In order to assess the neuroendocrine profile of basal and chronically stressed animals, blood samples were collected by tail cut, 15 and 90 min after the start of the forced swim test (FST), respectively. A small incision with a razorblade into the tail vein of the mouse allowed for the collection of blood samples necessary for corticosterone measurements (10µl). These were collected in 1.5 ml EDTA-coated microcentrifuge tubes (Kabe Labortechnik). Blood samples were immediately centrifuged for 15 min at 4°C and 8000 rpm. The supernatant (blood plasma) was then transferred to a new collection tube and stored at -20°C until further processing.

Animal sacrifice was performed by decapitation on day 21 of the experiment. In order to obtain basal corticosterone levels, trunk blood was collected and processed as described. Brains were removed, flash-frozen on dry-ice and then stored at -80°C until further use. Additionally, thymus and adrenal glands were removed and stored in Ringer's solution. In order to determine the organ weight, additional surrounding tissue was removed from the thymus and adrenal glands.

3.14. Endocrine analysis

Retrobulbar blood was taken using glass capillaries under isoflurane anesthesia for all transgenic mice, apart from those that were exposed to the CSDS paradigm. To determine basal plasma hormone levels, mice were left undisturbed for at least two days prior to the experiment. Blood sampling was performed in the early morning (08:00–09:00 a.m.) and afternoon (04:30–05:30 p.m.). For evaluation of the endocrine response to stress, blood samples were collected immediately after 10 min of acute restraint stress, for which animals were placed in a 50-ml conical tube with the bottom removed. Stress recovery levels were assessed 90 min following 10 min of acute restraint stress. All stress experiments were performed in the morning (08:00–10:00 a.m.). Plasma corticosterone concentrations were measured in duplicate by commercially available RIA kits (MP Biomedicals, Eschwege, Germany) according to the manufactures manual.

3.15. Behavioral assessment

All behavioral experiments were carried out in adult male mice (age 9-15 weeks), which were habituated to single housing and test room conditions one week before testing. All behavioral tests were performed during the light phase, starting at 8:30 a.m., with the exception of fear conditioning, prepulse inhibition and acoustic startle response measures. Fear conditioning experiments were assessed in ENV-307A conditioning chambers from MED Associates. The acoustic startle reflex and prepulse inhibiton were investigated in chambers from SR-LAB, San Diego Instruments SDI, San Diego, USA. All other experiments were analyzed using the automated video-tracking system ANYmaze (Stoelting, Wood Dale, IL). In order to minimize possible carryover effects of the different behavioral tests, the sequence of tests was arranged from least to most stressful (McIlwain et al., 2001; Kalueff and Murphy, 2007).

Open field (OF) test

The open field test was originally designed to characterize explorative behavior and general locomotor activity in a novel environment. Open field boxes (50 x 50 x 60 cm) were made up of grey polyvinyl chloride (PVC) and evenly illuminated (<15 Lux). The apparatus was virtually divided into an outer an inner zone (15 cm x 15 cm). All mice were placed into a corner of the apparatus at the beginning of the trial. The test duration varied between 5-30 min depending on the experimental setup. Parameters assessed included the total distance travelled, immobility time, number of inner zone entries and inner zone time.

Novel object exploration test (NOET)

The novel object exploration task was used to investigate avoidance of a novel object in a familiar environment, which is considered to reflect aspects of trait anxiety. In an initial open field trial, mice were first allowed to habituate to an OF arena (50 x 50 x 60 cm high, 30 lux) for 15 min. Subsequently a novel square object was introduced into the center of the arena and the animals were allowed to explore the object for an additional 15 min (object trial). The distance travelled as well as the time spent in the center zone were measured in both trials. Additionally, the time spent interacting with the object was assessed. In order to exclude locomotion bias or preference for a particular quadrant, the time spent in the central object zone relative to baseline (time spent in the central zone during the OF trial) was calculated.

Home Cage Activity

To investigate baseline activity in a familiar environment that is not compromised by novelty, home cage activity was monitored by an automated infrared tracking system (Mouse-E-Motion 2.3.6, Infra-E-Motion, Hagendeel, Germany). Each mouse was tracked for three days to obtain an accurate average activity score during the light and dark cycle.

Elevated plus-maze (EPM) test

The elevated plus-maze is used to assess anxiety-related behavior in mice. It is based on a conflict between the mice's exploratory drive and its innate fear of illuminated, unprotected and heightened areas (Lister, 1987). The EPM consisted of a plus-shaped platform which is elevated 50 cm above the floor, with four intersecting arms. Two opposing open (30 x 5 x 15 cm) and closed arms (30 x 5 x 15 cm) are connected by a central zone (5 x 5 cm). The maze was made of grey PVC. The illumination was 25 lux in the open arms and < 10 lux in the closed arms. Animals were placed in the center of the apparatus facing the closed arm and allowed to freely explore the maze for 10 min. Parameters measured included time spent in the open arms, open arm entries, latency to first open arm entry, immobility time, lit distance and total distance travelled.

Elevated 0-Maze

The elevated 0-Maze represents a modification of the classical EPM and is also used to assess anxiety-related behavior (Shepherd et al., 1994). It consists of a circular platform with two open and two closed runways without a central zone (width 12 cm, diameter 110 cm, height of side walls 50 cm). This excludes any ambiguity in the interpretation of the time spent in the

central zone of the traditional EPM. The maze was made of grey PCV and elevated 50 cm above the floor. For testing, animals were placed on one of the closed zones facing the closed part of the apparatus for 10 min. Parameters measured included time spent in the open zone, open zone entries, latency to first open zone entry, immobility time, open distance and total distance travelled.

Dark-light box (DaLi) test

The dark-ligh box test was additionally applied to investigate anxiety-related behavior. It is based on the innate aversion of rodents to brightly illuminated areas and on their spontaneous exploratory behavior, including novel environment and light (Hascoet et al., 2001). The apparatus is made up of PVC and consists of a secure black compartment (15 x 28 x 27 cm) and an aversive, illuminated white compartment (48 x 28 x 27 cm), which are connected by an small tunnel (5 x 7 cm). The illumination in the dark compartment was < 5 lux and 700 lux in the lit compartment. Animals were placed into a corner of the dark compartment and allowed to freely explore the test arena for 5 min. Parameters assessed included time spent in the lit compartment, latency to first lit- compartment entry, number of lit compartment entries, lit compartment distance and total distance travelled.

Forced swim test (FST)

The forced swim test represents a well-established antidepressant-screening paradigm (Porsolt et al., 1977; Porsolt et al., 1978), but is also used to assess active versus passive stress-coping or despair-like behavior in mice (Slattery and Cryan, 2012). On top of that, the FST represents a strong stressor for mice considering that the animals are facing a psychological and physiological challenge. Each animal was placed into a two liter glass beaker (radius: 11 cm, height; 23.5 cm) filled up to a height of 15 cm (1.6 l) with 21°C tap water. Three behavioral parameters were assessed for 6 min including time struggling, swimming and floating. A mouse was judged floating once it stopped any movements expect those that were necessary to keep its head above water. Vigorous swimming movements involving all four limbs of the mouse, with the front paws breaking the surface of the water, usually at the walls of the beaker, were regarded as struggling. Behavior which could not be assigned to either floating or struggling, such as the movement of only two limbs, was termed swimming.

Modified hole board (mHB) Test

The mHB test was conducted by Martin Schweizer as previously described (Refojo et al., 2011). Prior to testing, all animals were acutely stressed using a restraint challenge. For this, the mice were placed in a 50-ml conical tube with a hole in the middle to enable ventilation. After 60 min animals were removed and returned to their home cages. 180 min later mice were placed in a corner of the mHB box (grey PVC, 100x50x40 cm, illumination 60 lux) with the board (grey PVC, 70x20x1cm; 12 cylinders with a diameter of 3 cm and height of 2 cm were staggered in two lines) located in the middle of the box. The test duration was 5 min, during which a trained observed, blind to genotype assessed a number of behavioral parameters (e.g. board visits, stretched attends).

Object recognition task

Object recognition memory was assessed in the OF arena under low illumination (10 lux) and consisted of two trials. During the acquisition trial mice were presented with two identical objects (cubes) for 10 minutes. Following a 30 min intertrial interval, one of the familiar objects was exchanged for a novel one (salt shaker), and the mice were allowed to explore the apparatus for another 10 min. The percentage of time exploring the novel objects was calculated as follows: [novel object time (s) / (novel object time (s) + familiar object time (s))] x 100. A higher preference for the novel object indicates an intact object recognition memory.

Y-Maze test

Spatial memory was investigated in the Y-Maze, which consisted of three evenly illuminated arms (15 lux), each marked by a distinct intra-maze cue (triangle, bar or plus sign). The test included an acquisition and retrieval stage, separated by a 30-minute inter trial interval. During the acquisition stage, one of the arms was blocked, and the mice were allowed to freely explore the other two arms for 10 min. During the retrieval stage, the mice were allowed to freely explore all three arms for another 10 min. Learning performance was successful, if the time spent in the novel arm compared to the known arms, was significantly higher than chance level (> 33.3%).

Operant conditioning

Five days before the training sessions, food consumption was restricted to 75% of the average daily diet in order to increase the motivation for reward. Mice were subsequently introduced to the operant conditioning chamber (Bioseb, France) for 5 days. 30 min trials were performed

in which mice received a sucrose reward (Bio-serv, NJ, USA) every 45s, which was always paired with a 3s light and sound (5000 Hz) stimulus. The commercially available software (Packwin V2.0.01; Panlab, Spain) was used to operate stimuli and reward delivery. During the training stage, a fixed ratio/variable ratio (FR/VR) protocol was applied. Thus, animals received a reward after a single lever press for the first 10 presses (FR1) followed by 1-3 lever presses to receive a reward (VR1-3). The 30 min training trial was conducted in bouts of 5 consecutive daily trials per weeks, until 75% of mice in the control group received at least 60 rewards. Considering that CNS-specific CRH overexpressing mice did not pass the training stage (in contrast to controls), animals were not further tested in a progressive ratio task.

Auditory and contextual fear conditioning

Contextual and auditory fear memories were assessed in conditioning chambers (ENV-307A, MED Associates) as previously described (Kamprath and Wotjak, 2004). Two different contexts were used for the experiments. Foot shock delivery and context-dependent fear memory were assessed in a cubic-shaped chamber with metal grid floors, which was thoroughly cleaned and sprayed with 70% Ethanol before the animals were introduced. A neutral context consisting of a plexiglas cylinder with bedding was used to investigate auditory (tone-dependent) fear memory, which was cleaned and sprayed with 1% acetic acid. For foot shock application (day 0) mice were placed into the conditioning chamber for 3 min. After 180 sec, a sine wave tone (80 dB, 9 kHz) was presented for 20 sec, which co-terminated with a 2 sec scrambled electric foot shock of 1.5 mA. The mice remained in the conditioning chamber for another 60 sec. In order to measure freezing responses to the tone, mice were placed into the neutral environment (cylinder) on the following day (day 1). Three minutes later, a 3 min tone was presented (80 dB, 9 kHz). The animals were returned to their home cages 60 sec after the end of tone presentation. Contextual (associative) fear was tested by re-exposing the animals to the conditioning grid chamber for 3 min on day 2. As a measure of fear, freezing behavior was recorded and analyzed by an observer blind to genotype.

Acoustic startle response and prepulse inhibition (PPI)

The acoustice startle response (ASR) was analyzed as previously described (Golub et al., 2009). Mice were introduced into a non-restrictive plexiglas cylinder, which was mounted to a plastic platform located in a sound attenuated chamber (SR-LAB, San Diego Instruments SDI, San Diego, CA, USA). This set-up quantified changes in the conductance as a response to varying acoustic stimuli, which are then detected by a piezoelectric sensor located underneath each

cylinder. The background noise was set to 50 dB. After an acclimatization period of five minutes, the mice were subjected to white noise bursts of varying intensities (75, 90, 105, and 115 dB) in a random order. The data are represented as mean peak startle amplitude in mV ± SEM in response to 136 randomized trials of the mentioned intensities including background noise measurements.

PPI was measured within the same set-up but using a different protocol. Mice were presented with a brief pre-pulse white noise burst at 2, 4, 8 and 16 dB above background 25 ms before they were exposed to a 115 dB acoustic stimulus. The protocol consisted of 270 pseudo randomized trials. ASR was also elicited 22 times at 115 dB without a prepulse in order to determine the baseline response and assess habituation effects. The mean startle-amplitude per prepulse intensity was calculated by subtracting the startle amplitude at the 115 dB pulse from the startle amplitude after prepulse presentation and dividing this by the startle amplitude at 115 dB x 100.

Social avoidance test

The two-trial social avoidance test was modified from (Berton et al., 2006; Golden et al., 2011). In the first trial, each experimental mouse was introduced into the open field arena for 2.5 min containing an empty wire mash cage, placed at one side of the apparatus (marked as the interaction zone). During the second 2.5 min trial, test animals were confronted with an unfamiliar male C57/bL6 mouse, which had previously been introduced into the wire mash cage. The ratio between the time in the interaction zone of the non-target trial and the time in the interaction zone of the target trial was calculated.

3.16. Lithium treatment

Lithium chloride was mixed into the drinking water of $Crh^{CNS\text{-}Ctrl}$ and $Crh^{CNS\text{-}COE}$ mice at 600 mg/liter for 10 days according to (Dehpour et al., 2002; Roybal et al., 2007). Behavioral testing stated on day 11 and lasted for an additional 10 days throughout which LiCl was continuously administered. Vehicle treated mice recived normal water. 24 h after the last behavioral tests animals were decapitated and trunk blood was collected for assessment of plasma lithium concentrations. Lithium levels were measured in the laboratory of Manfred Uhr at the Max Planck Institute of Psychiatry using an atomic absorption spectrophotometer at a wavelength of 670 nm. Measurements were compared with values for standards of known concentrations. The applied lithium dosage produced stable lithium serum concentrations of 0.3 - 0.4

nmol/liter, which is within the lower therapeutic range for humans and does not significantly impact the animals health.

3.17. Food and water intake

Absolute food and water intake were measured over 40 hours in automated metabolic cages from TSE systems Inc., Germany. Liquid and food consumption were recorded every 5 min. The animals were initially allowed to habituate to the cages for 24h before recordings started. To assess stress-induced feeding behavior, animals were food-deprived for 24h, after which feeding behavior was assessed for and additional 40 hours.

3.18. *In vivo* microdialysis

Surgery, probe implantation and experimental procedure

Monoaminergic neurotransmission was assessed in the prefrontal cortex (PFC) by *in vivo* microdialysis as described elsewhere (Refojo et al., 2011; Anderzhanova et al., 2013). Male adult mice (age 10-12 weeks) were anesthetized with isoflurane and placed in a stereotaxic apparatus (TSE systems Inc., Germany) with adapted components to allow mouse inhalation anaesthesia. The fur of the skull was cleaned with 70% ethanol and the scalp was opened with a sterile scalpel along the midline. A hole was drilled and a microdialysis probe guide cannula (MAB 4.15.IC, Microbiotech AB, Sweden) was implanted into the right PFC so that the tip was 2 mm above the targeted area. The coordinates for the PFC were determined based on the stereotactic atlas (Paxinos and Franklin, 2001): Anterior/posterior +1.9 mm, medial/lateral +0.4 mm, and dorsal/ventral -2.0 mm. The guide cannula was fixed to the skull with dental cement. To connect a liquid swivel and counterbalancing arm during the microdialysis experiments, a small peg was additionally attached to the skull. Animals were allowed to recover in the experimental square plexiglas home cage for one week. Metacam® was added to the drinking water at 0.25 mg/100 ml for three consecutive days after surgery. One day prior to the experiment, mice were shortly anesthetized and microdialysis probes (0.d. 0.2 mm, cuprophane membrane 2 mm of length, MAB 4.15.2.Cu, Microbiotech/se AB, Sweden) were inserted into the PFC through the pre-implanted guide cannula and connected to the perfusion lines which consisted of FEP tubing (i.d. 0.15 0.05 mm). In addition, mice were connected to a liquid swivel and counterbalancing system (Instech Laboratories, Plymouth Meeting, PA, USA). The probes were continuously perfused with sterile, pyrogen-free Ringer solution at a flow rate of 0.5 µl/min. Two hours before the experiment, the flow rate was increased to 1 µl/min. After

a 2 h equilibration period, 20 min microdialysis fractions were collected in plastic vials positioned in a refrigerated microsampler (Univentor, Malta).

In *Crhr1*$^{iDA\text{-}CKO}$ mice three consecutive samples (20 min intervals) were collected under basal conditions. Thereafter, mice were placed into a custom-made cubic shock chamber for 1 min. After receiving a foot-shock (2 sec, 1.5 mA), the animals remained and additional 30 sec in the chamber and were then placed back in their microdialysis home cage. The chamber was cleaned with 70% ethanol after each procedure. In total, 6 consecutive samples were collected to determine foot shock-induced dopamine release. In *Crh*$^{GABA\text{-}COE}$ were, five consecutive samples (20 min intervals) were collected under basal conditions. To obtain stress-induced neurotransmitter release, *Crh*$^{GABA\text{-}COE}$ mice and controls were placed onto a small circular elevated platform (diameter 10 cm) for 20 min, and then returned to their microdialysis home cage. Eight additional samples were collected following elevated platform-stress.

Monoamine measurements

Monoamine measurements were performed in collaboration with Carsten Wotjak's laboratory at the Max Planck Institute of Psychiatry. Dopamine, noradrenaline, 5-hydroxytryptophan (5-HT), 3,4-Dihydroxyphenylacetic acid (DOPAC), and homovanilic acid (HVA) contents were determined by reverse-phase high-performance liquid chromatography (HPLC) with an electrochemical detection system which consisted of the SunFlow100 isocratic pump (SunChrom, Germany) coupled with the Decade amperometric detector (ANTEC Leyden, the Netherlands) (Anderz). The injection volume was 10 µl. The mobile phase contained 0.09 M Na_2HPO_4, 0.05M Na citrate, 1.7 mM OSA, 0.05mM Na_2-EDTA and 10% acetonitrile (v/v) and pH was adjusted to 3.0 with 10M NaOH. Monoamines were separated on an analytical column (C18, 150 mm x 3.2 mm, 3 µm, YMC-PackProC18, YMC Europe GMBH, Germany). The chromatograms were analyzed, and monoamine identification and peak quantification were determined by comparison with known standards.

Histology

After completion of the microdialysis experiments, animals were decapitated under isoflurane anaesthesia, and brains were extracted and stored at -80°C. Brains were further sectioned with a cryostat, and sections were stained with cresyl violet for histological verification of the probe's localization. In case of non-correctly placed microdialysis probes, mice were excluded from the experiment.

3.19. Viral-mediated neuronal imaging and tracing experiments

Adeno-associated viruses (AAV) serotype 1/2, were used as vectors to deliver synpatophysin-eGFP (*AAV-DIO-Syn-eGFP*) fusion proteins into the bed nucleus of the stria terminalis (BNST) of *Crh-IRES-Cre* mice. The original synaptophysin-eGFP containing construct was kindly provided by Dr. Valery Grinevich (Knobloch et al., 2012). *Syn-eGFP* was then cloned into a Cre-inducible flip-excision (*FLEX*) vector. Synaptophysin is a major synaptic vesicle protein. Consequently fusion of synaptophysin to a fluorescent marker targets the latter to the synapse enabling the visualization of axonal projections. In this case, *Syn-eGFP* is expressed from a Cre-inducible *FLEX* vector under the control of the human *EF1α* promoter, specifically in CRH neurons. Male adult mice (age 10-12 weeks) were anesthetized with isoflurane and placed in a stereotaxic apparatus (TSE systems Inc., Germany) with adapted components to allow mouse inhalation anesthesia. The fur of the skull was cleaned with 70% ethanol and the scalp was opened with a sterile scalpel along the midline. Mice were stereotactically injected with 500 nl of *AAV-DIO-Syn-eGFP* into the right dorsal BNST (coordinates from bregma: anterior/posterior +0.14 mm, medial/lateral +0.5 mm, and dorsal/ventral -4.25 mm) and an additional 500 nl were injected into the right ventral BNST (coordinates from bregma: anterior/posterior +0.14 mm, medial/lateral +0.5 mm, and dorsal/ventral -4.75 mm). For this, a small hole was drilled and a micropipette containing the virus was positioned at the appropriate anterior/posterior and medial/lateral coordinates, and then slowly lowered to the desired dorsal/ventral position. The virus was injected using an automated microinjection pump (World Precision Instruments) at a rate of 100 nl /min. Following injection, the micropipette was left undisturbed for an additional 10 min in order to enable an efficient spread of the virus. The skull was subsequently cleaned and the scalp was sewn up using an absorbable thread. The animals were placed on a 37°C heating plate to recover from anesthesia. Metacam® was added to the drinking water at 0.25 mg/100 ml for three consecutive days after surgery.

In order to visualize and morphologically characterize CAMK2α-positive CRH neurons, an AAV containing a Cre-inducible *FLEX* vector, expressing *eYFP* driven by the *Camk2α* promoter, was stereotactically delivered into the PFC, central amygdala (CeA) and BNST of *Crh-IRES-Cre* mice. The original construct, containing an *EF1α-eYFP*, was commercially obtained from the Deisseroth laboratory (http://stanford.edu/group/dlab/optogenetics/index.html). The *EF1α* promoter was exchanged for the *Camk2α* promoter using *MluI* and *SalI* restriction sites (the cloning procedure is described in the methods section above). Viral preparations were performed in the group of Valery Grinevich at the Max Planck Institute for Medical Research in

Heidelberg. Stereotactic injections into the BNST were performed as described above and were carried out in the same manner for the PFC and CeA. The coordinates from bregma for the CeA were: anterior/posterior -0.82 mm, medial/lateral +2.5 mm, and dorsal/ventral -4.75 mm. The coordinates from bregma for the PFC were: anterior/posterior +1.9 mm, medial/lateral +0.4 mm, and dorsal/ventral -2.0 mm.

3.20. Image acquisition and morphological analyses

For overview images in *Crh-IRES-Cre:Ai9* mice, *Crh-IRES-Cre:Ai32* mice, *AAV-DIO-Syn-eGFP* and *AAV-Camk2α-floxed-eYFP* injected mice as well as immunohistochemical analysis, fluorescent microscopy was used. Images were taken using a Zeiss Axioplan2 microscope (Göttingen, Germany) and digitalized using AxioVision Rel. 4.5, Adobe Photoshop CS2, and Adobe Illustrator CS2 image editing software (San Jose, CA). In order to analyses dendritic spine morphology, images of individual neurons were obtained using an Olympus IX81 inverted laser scanning confocal microscope and the Fluoview 1000 software. The images were captured with a 10x UPlanSApo, 0.40 numerical aperture (NA), 20x UPlanSApo, 0.75 NA, 40x PlanApo, 0.9 NA WLSM or 60x UPlanSApo, 1.2 NA W Olympus objective. Fluorescently labeled neurons were excited at 405 nm (DAPI, Alexa-405), 488 nm (GFP and eYFP, Alexa-488), and 559 nm (RFP, tomato, Alexa-594), and emission was collected at 425-475 nm, 500-545 nm, and 575-675 nm respectively. Depending on the area of interest, a Z-stack of pictures was obtained with 0.4-1.2 µm step size and 800x800 to 1024x1024 pixel picture size. The acquired images were exported and processed with the open access software ImageJ (http://rsweb.nih.gov/ij/). Pictures were adjusted to obtain optimized signals using Adobe Photoshop CS2.

3.21. Electrophysiology

Electrophysiological analysis was carried out as previously described (Schmidt et al., 2011; Dine et al., 2013). Field excitatory postsynaptic potential (fEPSP) recordings were performed in horizontal brain slices (350 mm-thick) containing the hippocampal formation. Hippocampal slices were continuously perfused (4–5 ml/min flow rate) at room temperature (23–25uC) in a submerged chamber with carbogenated (95% O_2/5% CO_2) ACSF containing: NaCl, 125 mM, KCl, 2.5 mM, NaH_2PO_4, 1.25 mM, $NaHCO_3$, 25 mM, $MgCl_2$, 1 mM, $CaCl_2$, 2 mM, and glucose, 25 mM (pH 7.4). Square pulse electrical stimuli (0.066 Hz, 50 ms) were delivered to the stratum radiatum of the CA1 subfield and evoked fEPSPs were recorded. For all experiments the stimulation intensity was set to the half maximum intensity at which population spikes

appeared in order to enable comparisons between control and CNS-specific overexpressing mice. The paired-pulse ratio was calculated as fEPSP2 amplitude/fEPSP1 amplitude. Long-term-potentiation (LTP) was induced by high-frequency stimulation (HFS, 100 stimuli at 100 Hz).

3.22. Statistical analysis

All results are presented as mean ± standard error of the mean (SEM) and were analysed by the commercially available software SPSS 16.0 and GraphPad Prism 5 software. Behavioral phenotypic differences were evaluated with Students T-test or Mann-Whitney U test in case of non-Gaussian distribution. Time-dependent measures including the startle response, neurotransmitter release, segmented distance travelled and fur state progressions were assessed with multi-factorial analysis of variance (ANOVA) with repeated measures (RM-ANOVA). The effects of treatment, genotype and/or condition on behavioral and neuroendocrine parameters were assessed by two factorial analysis of variance (two-way ANOVA). Whenever significant main or interaction effects were found by the ANOVAs, Bonferroni post hoc tests were carried out to locate simple effects. Statistical significance was defined as $p < 0.05$.

4. RESULTS

4.1. Conditional CRH overexpressing mice model endophenotypes of stress-related neuropsychopathologies

CRH and its cognate receptors have been implicated in the pathophysiology of stress-related disorders. Hypersecretion of central CRH and elevated glucocorticoid levels, as a consequence of impaired feedback control, have been shown to accompany mood and anxiety disorders. However, a clear discrimination of direct effects of centrally hypersecreted CRH from those resulting from HPA axis activation has been difficult. To shed light on this we initially generated two conditional CRH overexpressing mouse lines: $Crh^{Del\text{-}COE}$ mice overexpress CRH throughout the body, while $Crh^{APit\text{-}COE}$ mice selectively overexpress CRH in the anterior and intermediate lobe of the pituitary. Both mouse lines were investigated with regards to neuroendocrine parameters and behavioral endophenotypes of psychiatric disorders.

Next we aimed to specifically assess the effects of central CRH hyperdrive on various neuroendocrine, behavioral and cognitive parameters under basal and chronic stress conditions using $Crh^{Nes\text{-}COE}$ mice, which were previously reported to display enhanced stress-coping behavior in the FST (Lu et al., 2008). In addition, molecular analyses were applied to uncover possible downstream targets and/or effector genes.

To substantiate the results observed in $Crh^{Nes\text{-}COE}$ mice we aimed to further specify the brain regions and neurotransmitter circuits involved in the regulation of emotional behavior via CRH. Once again a genetic strategy was applied by breeding the conditional CRH overexpressing mice to a diverse set of brain-region and cell-type specific Cre recombinase driver mouse lines. Subsequent neuroendocrine and behavioral analyses were performed for all mouse lines.

4.1.1. Assessing behavioral effects of chronic HPA axis activation

To discriminate between central effects of chronic CRH hyperdrive and effects mediated via the HPA axis and its final effector - glucocorticoids, we used the recently generated conditional mouse model of CRH excess (Lu et al., 2008). Initially $R26^{flopCrh/flopCrh}$ mice were bred to *Pomc-Cre* mice (Akagi et al., 1997). Subsequently, mice ubiquitously overexpressing CRH ($Crh^{Del\text{-}COE}$) were obtained by breeding female $R26^{+/flopCrh}$ *Pomc-Cre* mice to male $R26^{flopCrh/flopCrh}$ mice. In this combination *Pomc-Cre* is transiently expressed during oogenesis and thus acts as a deleter. Early deletion of the floxed stop (flop) cassette results in ubiquitous expression of CRH.

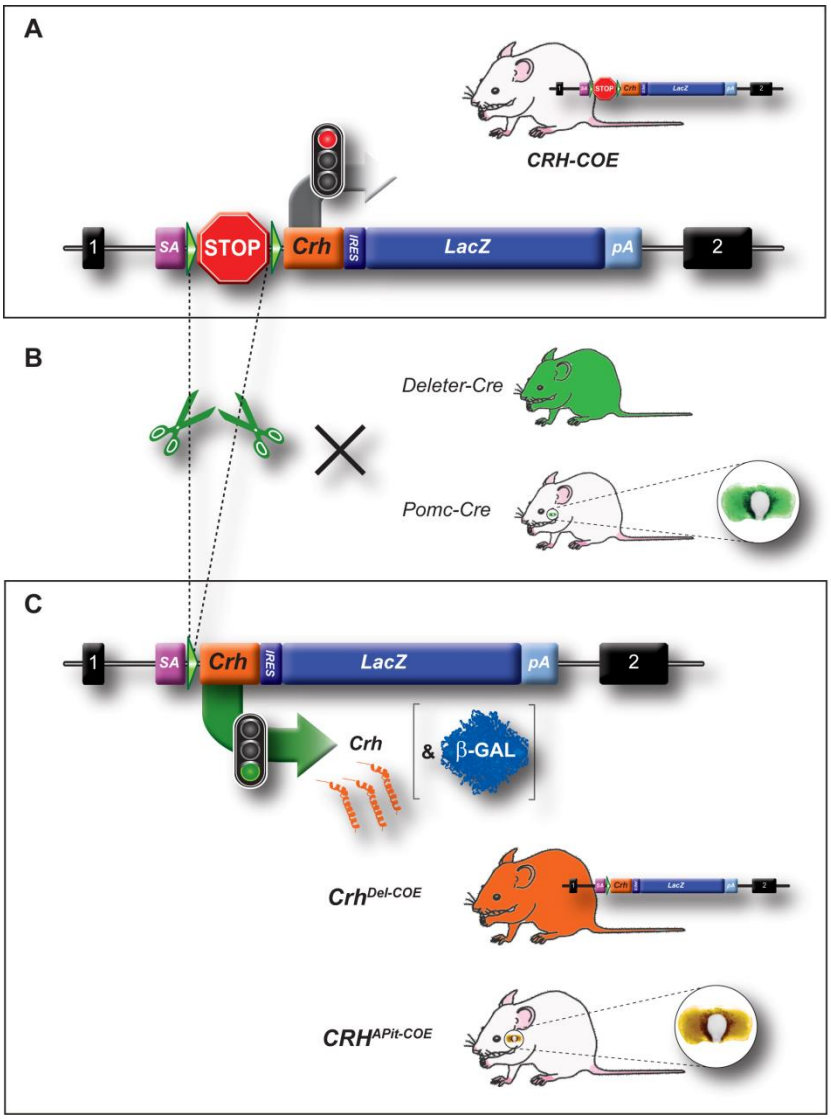

Figure 6: Strategy for conditional overexpression of CRH.
(A) Schematic representation of the *ROSA26* (*R26*) locus, which was engineered to harbour a Cre-inducible *Crh-LacZ* expression unit ($R26^{flopCRH}$, flop: floxed stop). **(B)** Breeding to *Deleter-Cre* or *Pomc-Cre* mice to remove the transcriptional terminator sequence (Cre recombinase expression pattern depicted in green). **(C)** Cre recombinase-induced expression of CRH (depicted in orange) and β-galactosidase throughout the body ($CRH\text{-}COE^{Del}$) or within the anterior pituitary ($CRH\text{-}COE^{APit}$). *R26* exons are indicated as black boxes, the transcriptional terminator as a STOP sign and *loxP* sites as green arrowheads. Abbreviations: conditional CRH overexpression (COE), internal ribosomal entry side (IRES), splice acceptor (SA), poly A signal (pA).

$R26^{Crh/flopCrh}$ mice were intercrossed, however, no viable homozygous $R26^{Crh/Crh}$ were obtained. Therefore, only $R26^{flopCrh/flopCrh}$ ($Crh^{Del\text{-}Ctrl}$) and heterozygous ubiquitously overexpressing $R26^{Crh/flopCrh}$ ($Crh^{Del\text{-}COE}$) mice were used. Anterior pituitary specific overexpressing mice ($Crh^{Apit\text{-}COE}$) were obtained by breeding male $R26^{+/flopCrh}$ *Pomc-Cre* mice to female $R26^{flopCrh/flopCrh}$ mice. The following genotypes were used for further analyses: $R26^{flopCrh/flopCrh}$ ($Crh^{APit\text{-}Ctrl}$), $R26^{+/flopCrh}$ *Pomc-Cre* ($Crh^{APit\text{-}COE\text{-}het}$), and $R26^{flopCrh/flopCrh}$ *Pomc-Cre* ($Crh^{APit\text{-}COE\text{-}hom}$) mice. Breeding of Crh^{COE} mice (Figure 6A) to *Deleter-* and *Pomc-Cre* mice (Figure 6B) resulted in the excision of

the transcriptional terminator and expression of exogenous CRH throughout the body or in the pituitary, respectively (Figure 6C). Cre-mediated deletion of the transcriptional terminator and concomitant expression of CRH mRNA and β-galactosidase was observed in all tissues of $Crh^{Del\text{-}COE}$ mice and is shown for the brain in Figure 7A-B. In $Crh^{APit\text{-}COE}$ mice *Crh* mRNA and β-galactosidase expression was selectively observed in the anterior and intermediate lobe of the pituitary (data not shown).

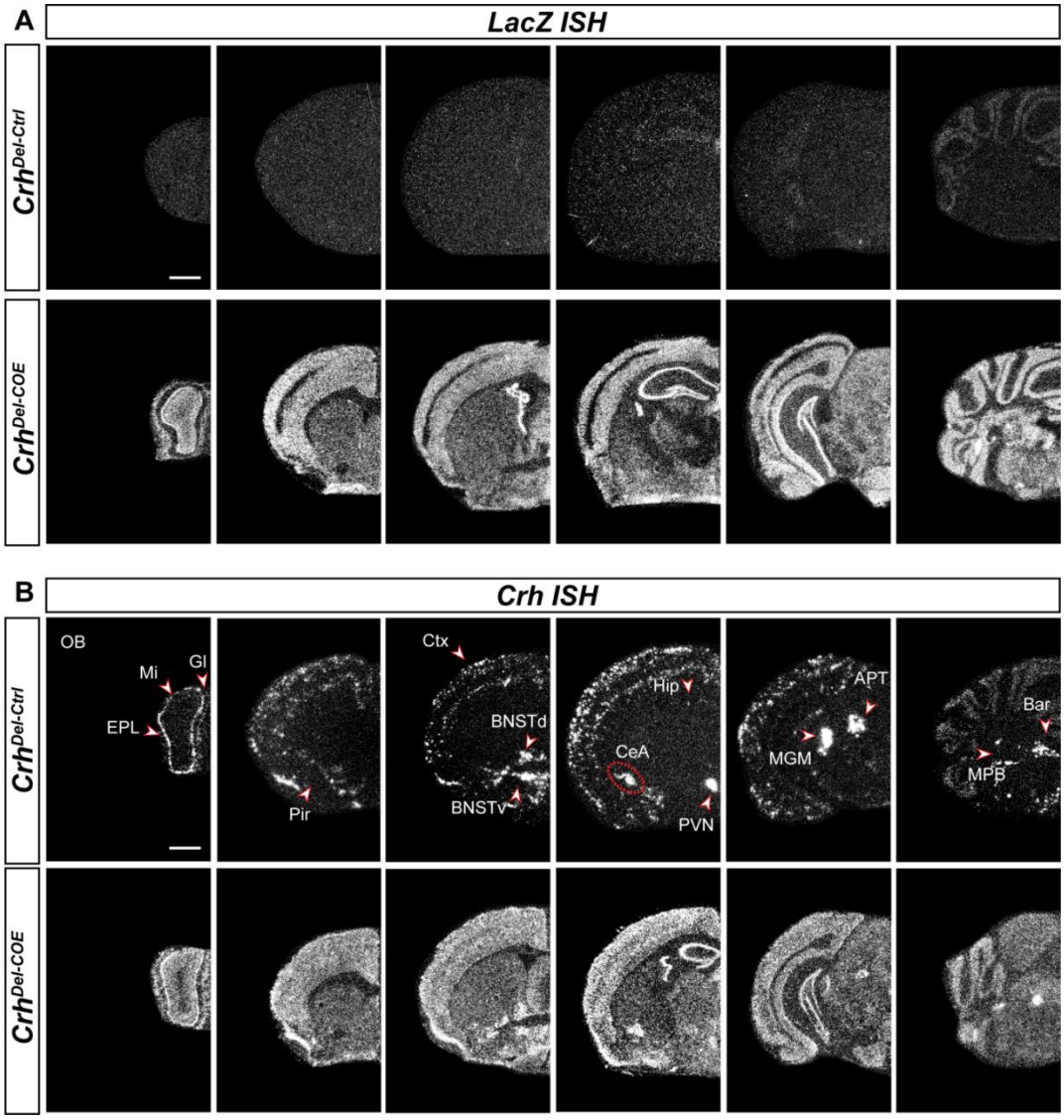

Figure 7: Verification of *LacZ* (A) and *Crh* (B) mRNA expression in $Crh^{Del\text{-}COE}$ mice assessed by *ISH*.
Representative dark-field photomicrographs of coronal brain sections are depicted. *LacZ* and exogenous *Crh* mRNA expression were detected throughout the brain. $Crh^{Del\text{-}Ctrl}$ mice display characteristic *Crh* expression throughout the entire brain with strong expression in the mitral (Mi), glomerular (Gl) and external plexiform layer (EPL) of the olfactory bulb (OB), piriform cortex (Pir), paraventricular nucleus of the hypothalamus (PVN), central nucleus of the amygdala (CeA), dorsal and ventral bed nucleus of the stria terminalis (BNST), medial geniculate nucleus (MGM), anterior pretectal nucleus (APT), medial parabrachial nucleus (MPB) and Barrington's nucleus (Bar). Scattered *Crh* expression was also observed in the cortex (Ctx) and hippocampus (Hip). Scale bar represents 1 mm.

4.1.1.1. $Crh^{Del\text{-}COE}$ mice exhibit endocrine abnormalities and increased anxiety-related behavior

Already at the age of three weeks male and female *$Crh^{Del\text{-}COE}$* mice showed physical changes reminiscent of Cushing's syndrome such as hair loss and thin skin (data not shown). Adult mice showed excess fat accumulation and overall increased body weight (*males*: Ctrl = 30.73 ± 0.53 g vs. COE = 35.73 ± 2.02 g, U =37.0, $p < 0.05$ / fema*l*es: Ctrl = 25.00 ± 0.59 g vs. COE = 31.50 ± 1.57 g, U = 15.0, $p < 0.01$) (Figure 8A-B). Adrenal weights were also significantly increased in male and female *$Crh^{Del\text{-}COE}$* mice compared to *$Crh^{Del\text{-}Ctrl}$* littermates (*males*: U = 13.0, $p < 0.01$ / *females*: U = 9, $p < 0.05$). In addition, a reduction in thymus weight was observed in male *$Crh^{Del\text{-}COE}$* mice (U = 8.0, p = 0.1) (Figure 8A-B). In order to evaluate HPA axis rhythmicity, we measured corticosterone levels at circadian nadir (a.m.) and peak (p.m.). Chronic CRH overproduction resulted in drastically elevated levels of circulating plasma corticosterone, in male and female mice compared to control littermates at both times of the day (*males*: 2-way ANOVA; time $F_{(1,32)} = 13.60$, $p < 0.0005$; genotype $F_{(1,32)} = 49.47$, $p < 0.0001$; Bonferroni post-test, $p < 0.05$ \ *females*: 2-way ANOVA, time $F_{(1,31)} = 21.3$; genotype $F_{(1,31)} = 8.89$; Bonferroni post-test, $p < 0.005$) (Figure 8A-B). Thus, regular circadian rhythmicity of corticosterone secretion was virtually absent in male *$Crh^{Del\text{-}COE}$* mice, as illustrated by similarly elevated corticosterone levels during the diurnal trough and diurnal peak. Interestingly, this effect was less pronounced in female *$Crh^{Del\text{-}COE}$* mice, which displayed elevated corticosterone levels in the afternoon compared to those measured at circadian nadir. However, 10 min of acute restraint stress failed to induce a neuroendocrine stress response in *$Crh^{Del\text{-}COE}$* mice compared to littermate controls, independent of gender (Figure 8). Generally, plasma corticosterone concentrations were higher in control females compared to control males (*am*: m = 9.35 ± 2.45 ng/ml vs. f = 60.97 ± 14.20 ng/ml, U = 3.0, $p < 0.001$ / *pm*: m = 102.7 ± 14.07 ng/ml vs. f = 179.6 ± 29.09 ng/ml, U = 23.0, p = 0.059 / *restraint stress*: m = 174.3 ± 13.59 ng/ml vs. f = 301.0 ± 23.44 ng/ml, U = 4.0, $p < 0.001$) (Figure 8). In the case of CRH overexpressing mice, gender-specific differences in corticosterone levels were only observed at circadian peak, although this did not reach statistical significance, and after acute restraint stress (*pm*: m = 198.5 ± 23.54 ng/ml vs. f = 283.9 ± 34.01 ng/ml, U = 10.0, p = 0.075 / *stress*: m = 144.3 ± 24.22 ng/ml vs. f = 284.4 ± 20.94 ng/ml, U = 5.0, $p < 0.001$).

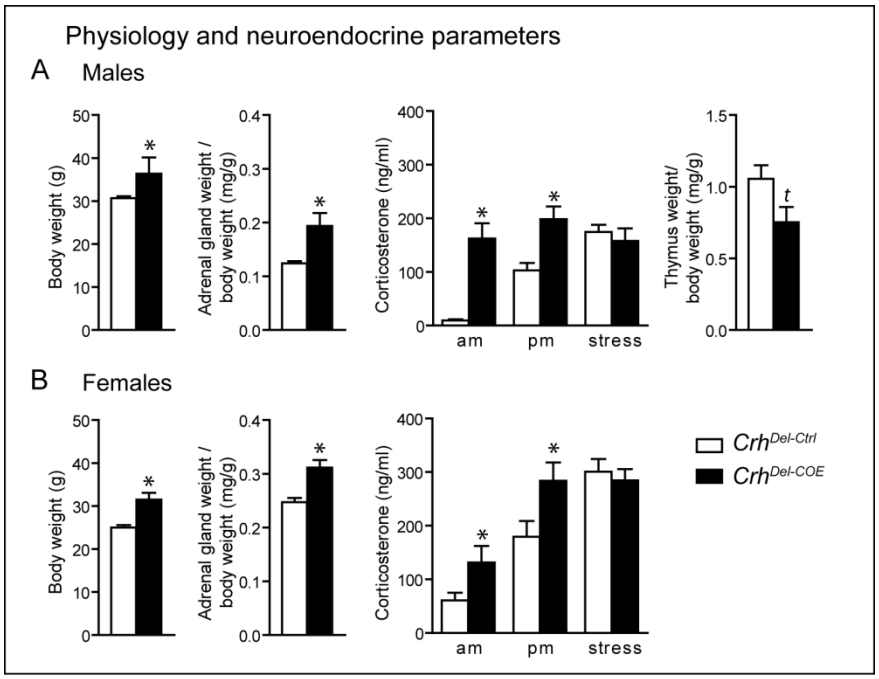

Figure 8: Physiological and neuroendocrine alterations in male (A) and female (B) *Crh*$^{Del\text{-}COE}$ mice.
Both male and female *Crh*$^{Del\text{-}COE}$ mice showed significantly increased body and adrenal gland weights as well as increased corticosterone levels measured in the morning (a.m.) and evening (p.m.) compared to control littermates. *Significant from control mice; Mann-Whitney U test, $p < 0.05$; *t* trend, $p \leq 0.1$; n = 11-12.

The open field test (OF) was employed to assess novelty-induced locomotion and exploratory behavior. *Crh*$^{Del\text{-}COE}$ mice showed no significant differences in locomotion and inner zone time compared to control littermates; however, they made significantly fewer entries into the center zone ($U = 33.0$, $p < 0.05$)(Figure 9A). In the elevated plus-maze (EPM) *Crh*$^{Del\text{-}COE}$ mice revealed an increase in anxiety-related behavior, by making fewer entries ($U = 13.0$, $p < 0.05$) and spending less time ($U = 14$, $p < 0.05$) in the open arms compared to control littermates (Figure 9C). Again, general locomotion was not altered. An increase in anxiety-like related behavior was also detected in the dark-light box test (DaLi), indicated by decreased lit compartment time ($U = 24.0$, $p < 0.05$) and entries ($U = 18.5$, $p < 0.05$) as well as an increased latency to enter the lit compartment ($U = 29.0$, $p < 0.05$) (Figure 9D). To examine stress-coping behavior, *Crh*$^{Del\text{-}COE}$ mice were subjected to the forced swim test (FST). Ubiquitous CRH overexpression resulted in significantly increased struggling time ($p = 0.05$) and a trend towards decreased floating time ($p = 0.1$) (Figure 9B).

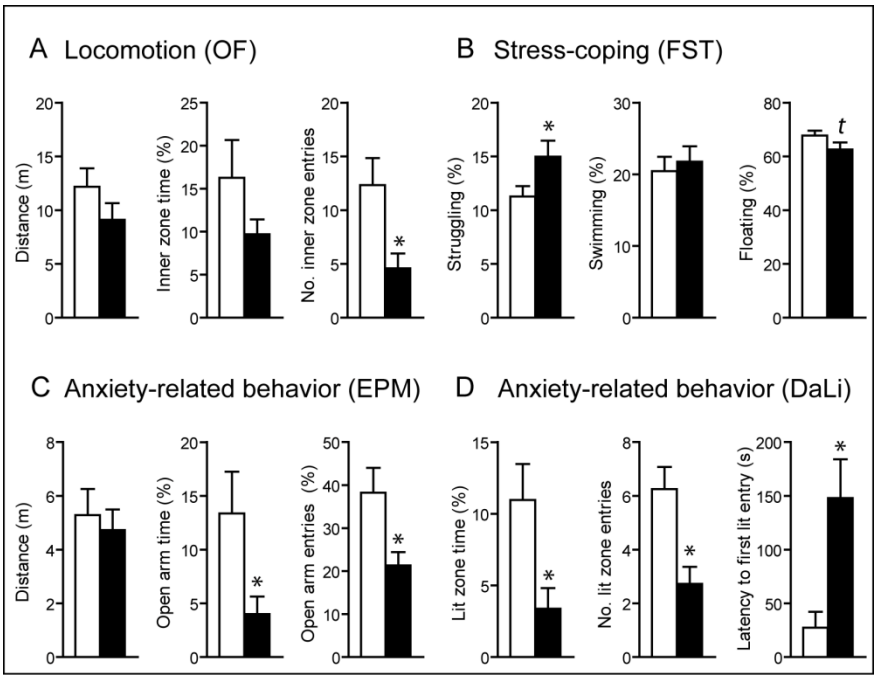

Figure 9: Behavioral characterization of male *Crh*$^{Del\text{-}COE}$ mice.
(A) Locomotor activity in the OF was not altered in *Crh*$^{Del\text{-}COE}$ mice compared to control littermates. Anxiety-related behavior, assessed in the EPM **(C)** and DaLi **(D)** was significantly increased in *Crh*$^{Del\text{-}COE}$ mice. **(B)** A mild increase in active stress-coping behavior was observed in *Crh*$^{Del\text{-}COE}$ mice in the FST. * Significant from control; Mann-Whitney U test, $p < 0.05$; *t* trend, $p \leq 0.1$; n = 10-12.

4.1.1.2. Crh$^{APit\text{-}COE}$ *mice exhibit endocrine abnormalities and mild behavioral alterations*

In contrast to *Crh*$^{Del\text{-}COE}$ mice, pituitary-specific CRH overexpression led to a mild Cushing-like phenotype, which was mainly associated with hair loss and thinning of skin, starting at 5-6 months of age (data not shown). Animals used for the assessment of the neuroendocrine profile and behavioral analysis were between 10-12 weeks of age, and at that time not distinguishable from controls. We analyzed heterozygous as well as homozygous male CRH-*Crh*$^{APit\text{-}COE}$ mice in order to assess the dosage-dependent effect of CRH overexpression. Interestingly, heterozygous and homozygous *Crh*$^{APit\text{-}COE}$ mice weight significantly less than control littermates (*males*: Ctrl = 31.61 ± 0.43 g vs. COE_{het} = 27.94 ± 0.39 g vs. COE_{hom} 28.99 ± 0.73 g; Kruskal Wallis test (KW), H = 13.37, $p < 0.05$; Dunn's post-test, $p < 0.05$ / *females*: Ctrl = 23.0 ± 0.22 g vs. COE_{hom} = 21.58 ± 0.74 g; U = 31.5, $p < 0.05$) (Figure 10A-B). Furthermore, CRH overexpression in the pituitary resulted in a dose-dependent increase in relative adrenal gland weight of male mice (KW, H = 20.65, $p < 0.0001$; Dunn's post-test, $p < 0.05$) (Figure 10A).

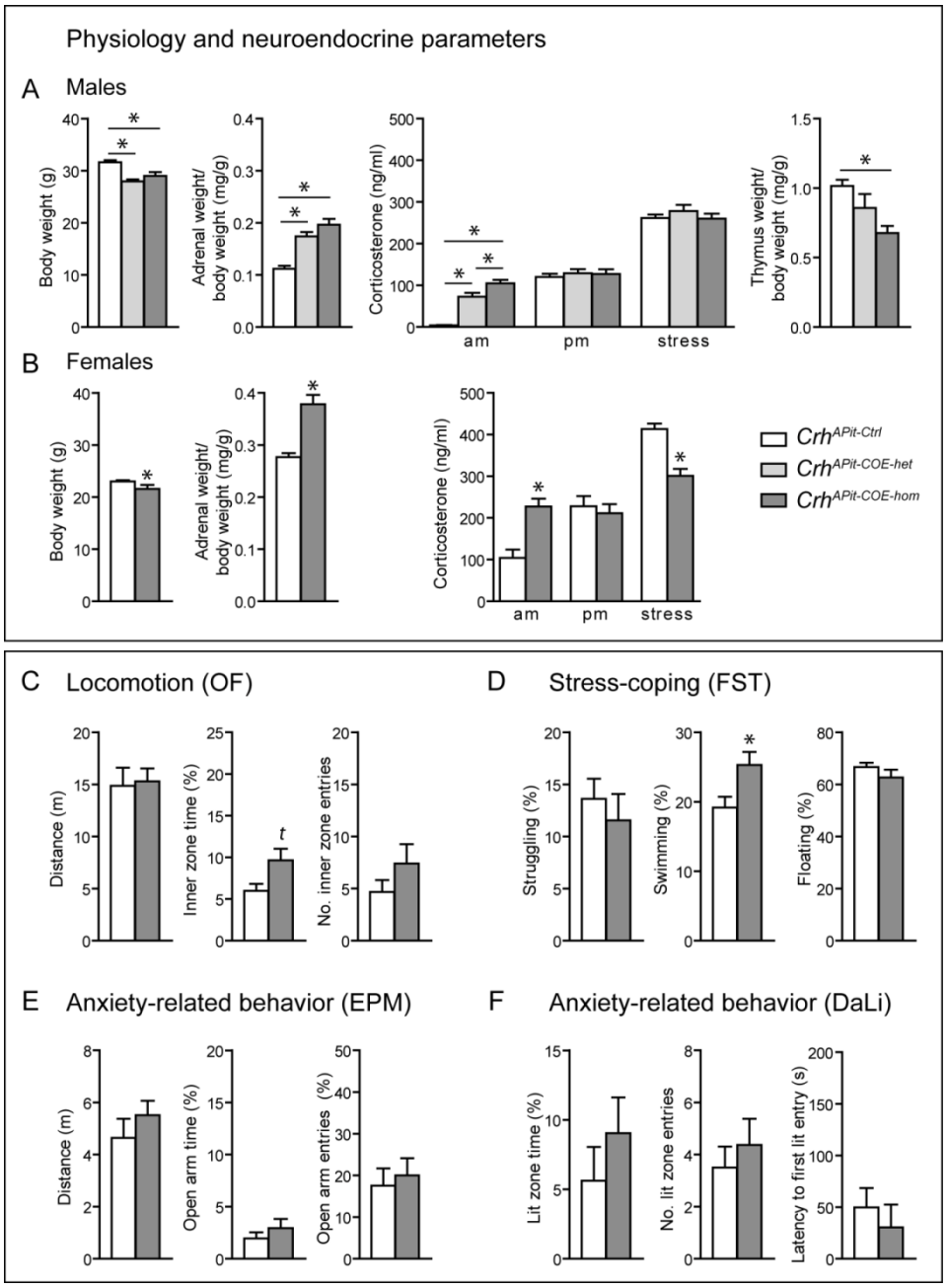

Figure 10: Physiological, neuroendocrine and behavioral alterations in male and female *Crh*$^{APit\text{-}COE}$ mice.
(A) Similar to *Crh*$^{Del\text{-}COE}$ mice, adrenal gland weight and morning corticosterone levels were increased in homozygous *Crh*$^{APit\text{-}COE}$ mice, while thymus size was reduced. In contrast, body weight was reduced in male and female *Crh*$^{APit\text{-}COE}$ mice compared to control littermates **(A, B)**. A dosage-dependent increase in morning corticosterone levels was observed in heterozygous and homozygous mice compared to controls **(A)**. Locomotion **(C)** and anxiety-related behavior **(E, F)** were not altered in male *Crh*$^{APit\text{-}COE}$ mice. A mild increase in stress-coping behavior, depicted by increased swimming time was observed in *Crh*$^{APit\text{-}COE}$ mice in the FST **(D)**. *Significant from control; Kruskal Wallis test + Dunn's post-test, $p < 0.05$; Mann-Whitney U test, $p < 0.05$; *t* trend, $p \leq 0.1$; n = 12.

Similarly, female homozygous *Crh*$^{APit\text{-}COE}$ mice also showed enlarged adrenal glands ($U = 7$, $p < 0.05$) (Figure 10B). As was the case in *Crh*$^{Del\text{-}COE}$ mice, circulating corticosterone levels were significantly elevated in heterozygous and homozygous *Crh*$^{APit\text{-}COE}$ mice compared to littermate controls at circadian nadir (*males*: 2-way ANOVA, time $F_{(1,94)} = 75.44$, $p < 0.0001$; genotype $F_{(2,94)}$

= 21.68, p < 0.0001; time x genotype $F_{(2,94)}$ = 16.09, p < 0.000; Bonferroni post-test, p <0.05 / *female*: 2-way ANOVA, time $F_{(1,39)}$ = 6.39, p < 0.05; genotype $F_{(1,39)}$ = 6.16, p < 0.05; time x genotype $F_{(1,39)}$ = 10.57, p < 0.05) (Figure 10). Again, a dose-dependent increase in corticosterone could be observed between heterozygous and homozygous $Crh^{APit\text{-}COE}$ mice. Female animals showed essentially the same phenotype (Figure 10B). However, differences in circulating corticosterone were not observed at circadian peak, neither in male nor in female $Crh^{APit\text{-}COE}$ mice compared to control littermates. Thus, similarly to male $Crh^{Del\text{-}COE}$ animals, homozygous male and female $Crh^{APit\text{-}COE}$ mice exhibit marked alterations in circadian corticosterone rhythmicity, showing only minimal diurnal changes between morning and afternoon levels. However, morning and afternoon plasma corticosterone levels were generally much lower in male $Crh^{APit\text{-}COE}$ compared to male $Crh^{Del\text{-}COE}$ mice. Along these lines, HPA axis reactivity is not inhibited in $Crh^{APit\text{-}COE}$ mice. Additionally, male heterozygous and homozygous $Crh^{APit\text{-}COE}$ mice showed the same corticosterone response as control littermates following 10 min of restraint stress (Figure 10A). In case of the $Crh^{APit\text{-}COE}$ line, corticosterone plasma concentrations were not only higher in control but also in CRH-overexpressing females compared to males (Figure 10A-B).

Locomotion as well as the number of entries into the inner zone of the OF were not altered in $Crh^{APit\text{-}COE}$ mice (Figure 10C). Homozygous $Crh^{APit\text{-}COE}$ mice however, tended to spent more time in the inner zone (U = 28, p = 0.062). Anxiety-related behavior, assessed in the EPM and DaLi test, was not changed in homozygous $Crh^{APit\text{-}COE}$ mice (Figure 10E-F). In the FST, homozygous $Crh^{APit\text{-}COE}$ mice spent more time swimming than control littermates (U = 35.5, p < 0.05). However, struggling and floating behavior, which are considered the main readout parameters of activity, were not significantly altered (Figure 10D).

The results obtained so far suggest that hypercorticosteroidism alone is not sufficient to alter anxiety-related behavior but rather that central CRH hyperdrive on its own or in combination with elevated glucocorticoids is responsible for the increase in anxiety-related behavior.

4.1.2. CNS-specific overexpression of CRH induces behavioral alterations reminiscent of bipolar disorder

As shown above, ubiquitous overexpression of CRH enhances anxiety-related behavior, which is considered a core endophenotype of many psychiatry disorders (Nestler and Hyman, 2010). In contrast, enhanced HPA axis activation on its own failed to produce similar effects. However, we cannot fully exclude a synergistic effect of central CRH hyperdrive and elevated glucocorticoid levels on the behavioral outcomes. In order to specifically address the role of central CRH in the pathophysiology of psychiatric disorders, we bred conditional CRH overexpressing mice to the CNS-specific *Nestin-Cre* driver ($Crh^{CNS\text{-}COE}$). The *Nestin* promoter and neural enhancer regulate and drive Cre expression in neuronal and glial precursors as early as embryonic day 10.5 (Tronche et al., 1999; Dubois et al., 2006). $Crh^{CNS\text{-}COE}$ mice were previously reported to elicit enhanced active stress-coping behavior in the FST and TST, mediated by enhanced noradrenergic activation (Lu et al., 2008). In addition, central CRH overexpression increased HPA axis sensitivity to acute stress, which is additionally depicted in Figure 11B. While dysregulated HPA axis activity has been observed in rodent models of various psychiatry disorders (Dedic et al., 2011; Bonfiglio et al., 2011; Arnett et al., 2011), endogenously enhanced FST activity (not caused by application of antidepressant-like drugs) is commonly associated with mouse models of mania (Nestler and Hyman, 2010; Young et al., 2011). In order to assess whether this mouse line can serve as an animal model for stress-elicited pathologies and treatments, we decided to extend the physiological, molecular and behavioral characterization of $Crh^{CNS\text{-}COE}$ mice.

4.1.2.1. $Crh^{CNS\text{-}COE}$ mice display mania-like behavior

The pattern of *LacZ* expression and *Crh* mRNA overexpression in $Crh^{CNS\text{-}COE}$ mice strongly resembled that of ubiquitously overexpressing animals (Figure 7 and Figure 11). Plasma corticosterone levels are indistinguishable between control and $Crh^{CNS\text{-}COE}$ mice over the circadian cycle, both at the diurnal through and the diurnal peak (Lu et al., 2008). However, corticosterone levels measured after acute restraint stresses were significantly elevated in $Crh^{CNS\text{-}COE}$ mice. This effect was further intensified with increasing restraint durations (Figure 11B). Interestingly, $Crh^{CNS\text{-}COE}$ mice displayed reduced body weight compared to littermate controls (Figure 11B).

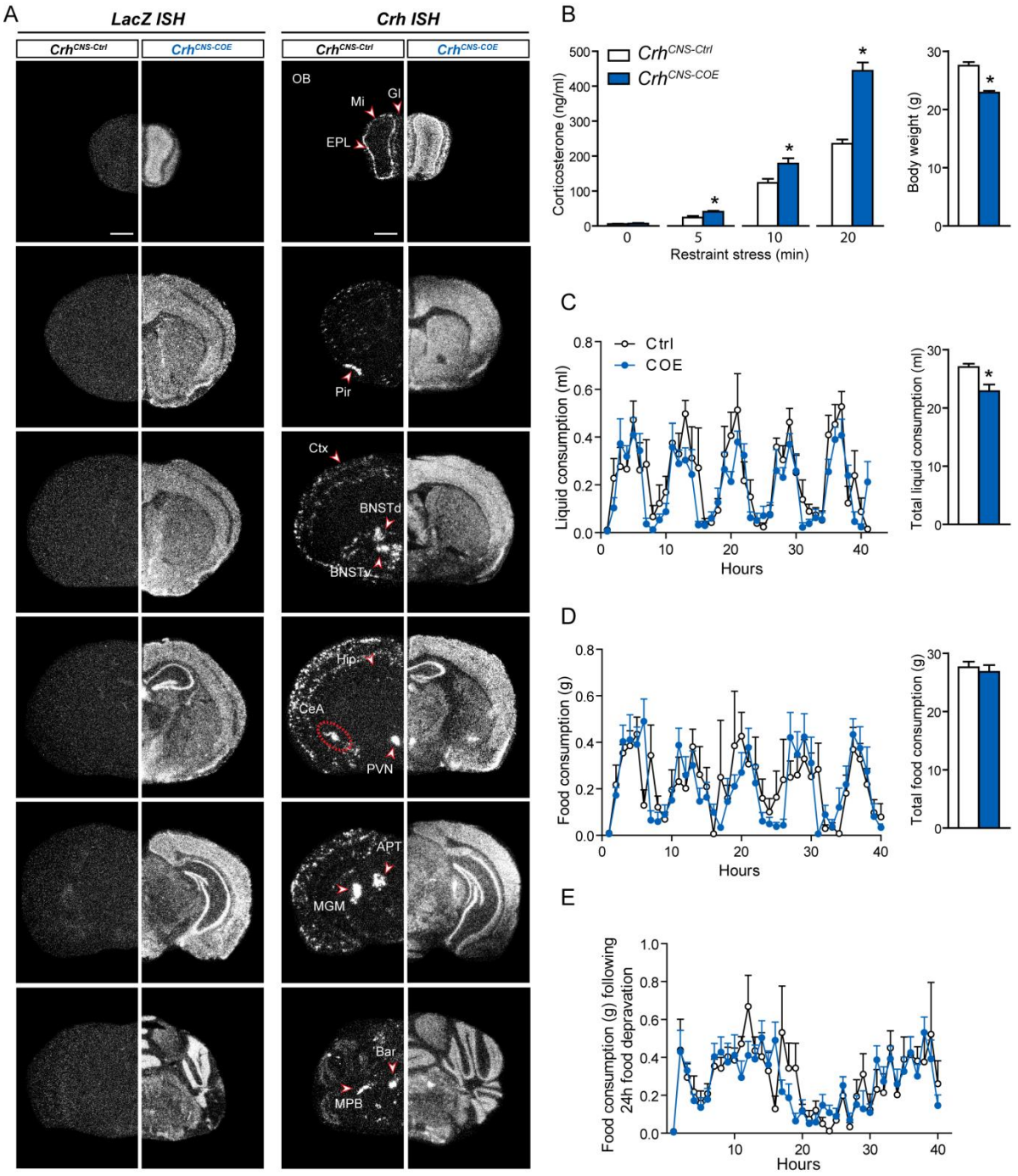

Figure 11: *Crh*$^{CNS\text{-}COE}$ mice display enhanced stress-reactivity and reduced body weight.
(A) Verification of of *LacZ* and *Crh* mRNA overexpression in *Crh*$^{CNS\text{-}COE}$ mice assessed by *ISH*. *Crh*$^{CNS\text{-}Ctrl}$ mice display the characteristic *Crh* pattern throughout the entire brain with strong expression in the mitral (Mi), glomerular (Gl) and external plexiform layer (EPL) of the olfactory bulb (OB), piriform cortex (Pir), paraventricular nucleus of the hypothalamus (PVN), central nucleus of the amygdala (CeA), bed nucleus of the stria terminalis (BNST), medial geniculate nucleus (MGM), anterior pretectal nucleus (APT), medial parabrachial nucleus (MPB) and Barrington's nucleus (Bar). Scattered CRH-expression was also observed in the cortex (Ctx) and hippocampus (Hip). **(B)** Whereas basal morning cortiocsterone levels did not differ between genotypes, 5 min of acute restraint stress significantly enhanced glucocorticoid levels *Crh*$^{CNS\text{-}COE}$ mice, which was further aggravated by prolonged restraint durations. *Crh*$^{CNS\text{-}COE}$ mice displayed reduced body weight and overall liquid consumption, but showed no difference in food intake under basal conditions **(C-D)** and following 24h of food deprivation **(E)**. Scale bar represents 1 mm. *Significant from control; Student's t-test, $p < 0.05$; *t* trend; $p \leq 0.1$; n = 12.

Keeping in mind that CRH has anorexic properties, we investigated feeding behavior over 40 hours and observed diminished overall water, but not food intake in *Crh*$^{CNS\text{-}COE}$ mice (Figure 11C-D). However, it remains to be elucidated whether decreased liquid consumption is the cause of, or a consequence of decreased body weight. In order to assess whether HPA axis hyperactivity might induce alterations in feeding behavior after stress exposure, we assessed food intake following 24 hours of food deprivation. However, circadian rhythmicity of food intake was altered to a similar degree in *Crh*$^{CNS\text{-}COE}$ and *Crh*$^{CNS\text{-}Ctrl}$ mice following 24 hours of food depravation (Figure 11E).

Next we investigated mood-related behaviors by measuring general locomotion and anxiety. In the OF test, *Crh*$^{CNS\text{-}COE}$ mice exhibited pronounced hyperlocomotion throughout the entire 15 min test duration (RM-ANOVA, genotype $F_{(1,44)} = 5.7$, $p < 0.05$), decreased immobility ($t = 2.7$, $p < 0.05$) and an increased number of entries into the inner zone ($t = 2.2$, $p < 0.05$) (Figure 12A). In addition, anxiety-related behavior, analyzed with the EPM and DaLi, was significantly reduced in *Crh*$^{CNS\text{-}COE}$ mice compared to control littermates (Figure 12C). However, increased locomotor activity can often obscure the interpretation of anxiety-related behavior. To control for the possible effects of enhanced locomotion on these tests, we investigated home cage activity. To our initial surprise, activity in the home cage was slightly reduced in *Crh*$^{CNS\text{-}COE}$ compared to *Crh*$^{CNS\text{-}Ctrl}$ mice (RM-ANOVA, time x genotype $F_{(11,209)} = 1.8$, $p = 0.052$) (Figure 12B). This suggests that *Crh*$^{CNS\text{-}COE}$ mice display novelty-induced hyperlocomotion and overall enhanced risk-assessment. Interestingly, low levels of anxiety, greater risk-taking and impulsivity are often observed in bipolar patients experiencing a manic phase (Steiner, 1972). In addition, many rodent models of mania, such as mice carrying a mutation in the *Clock* gene or SHANK3 and GSK3β overexpressing mice, display a similar behavioral profile including hyperactivity, decreased anxiety, decreased sleep and enhanced stress-coping behavior in the FST (Prickaerts et al., 2006; Roybal et al., 2007; Han et al., 2013). Importantly, our group previously reported enhanced active stress-coping behavior in the FST (which is additionally confirmed in Figure 13F) and sleep disturbances caused by enhanced rapid eye movement sleep (REM) in *Crh*$^{CNS\text{-}COE}$ mice (Lu et al., 2008; Kimura et al., 2010). To further unravel the behavioral phenotype, novel object exploration in a familiar environment was assessed in *Crh*$^{CNS\text{-}COE}$ mice given that bipolar patients in the manic phase were shown to explore unfamiliar objects more frequently (Young et al., 2007). In support of this, mania-like behavior induced by genetic dysfunction of the neuron-specific Na^+, K^+-ATPase a3 sodium pump results in enhanced novel object exploration in mice (Kirshenbaum et al., 2011).

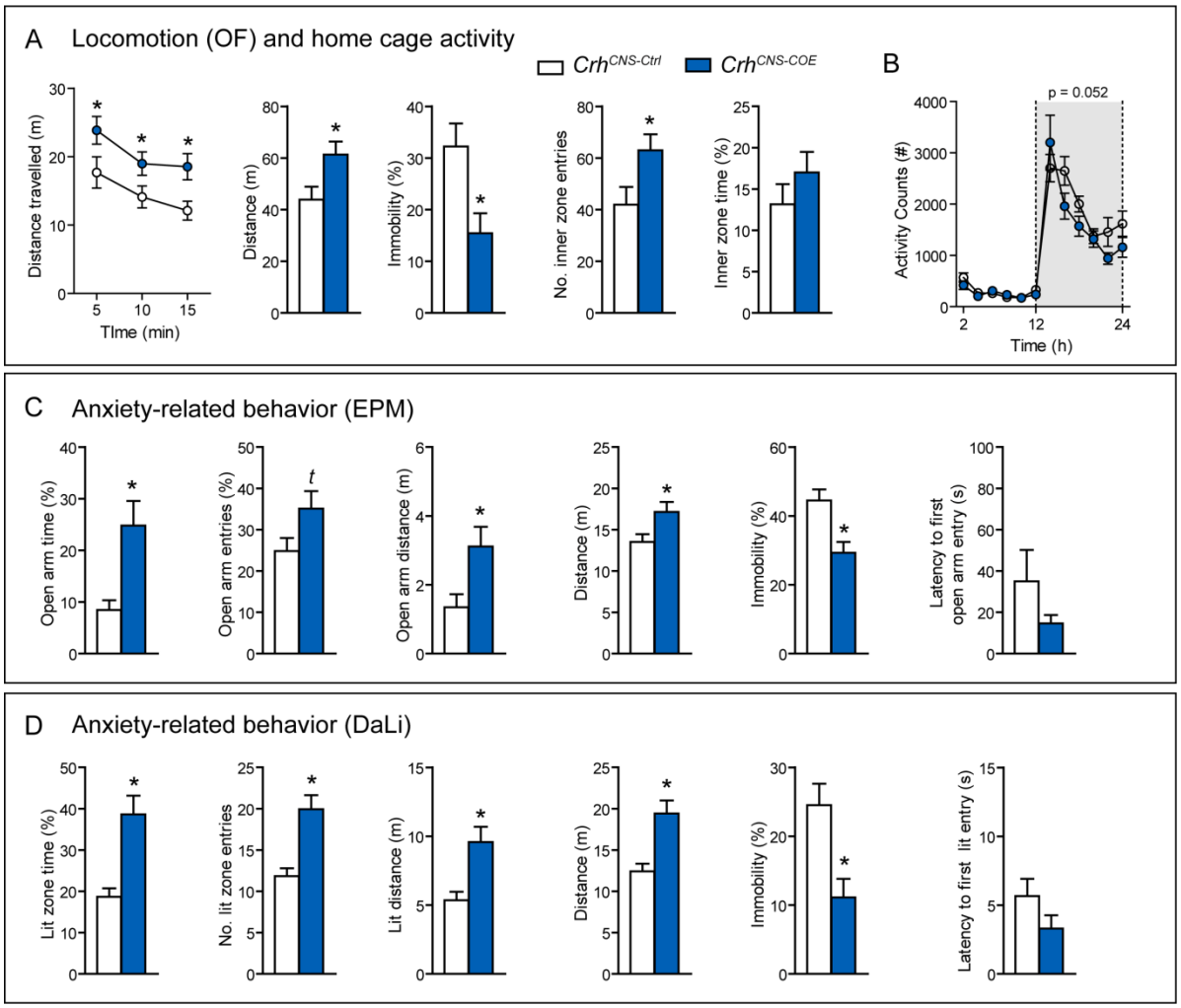

Figure 12: *Crh*$^{CNS\text{-}COE}$ mice display behavioral responses associated with mania.
These include hyperactivity in the OF **(A)** depicted by a significant increase in total distance travelled. This is further supported by decreased immobility and an increased number of inner zone entries. **(B)** In contrast, home cage activity was reduced in *Crh*$^{CNS\text{-}COE}$ mice. **(C)** *Crh*$^{CNS\text{-}COE}$ mice demonstrated decreased anxiety-related behavior in the EPM, by spending more time in the open arms ($t = 3.0$, $p < 0.01$) and entering these more frequently ($t = 1.9$, $p = 0.07$). Both, total distance travelled ($t = 2.3$, $p < 0.05$) as well as open arm distance ($t = 2.5$, $p < 0.05$) were significantly increased in *Crh*$^{CNS\text{-}COE}$ mice, which additionally displayed reduced immobility throughout the test ($t = 3.4$, $p < 0.005$). **(D)** Similarly, in the DaLi *Crh*$^{CNS\text{-}COE}$ mice spent more time and made more entries into the aversive lit compartment ($t = 3.9$, $p < 0.001$; $t = 4.0$, $p < 0.001$) and displayed reduced immobility ($t = 3.2$, $p < 0.005$) compared to controls. In addition, lit zone distance as well as overall distance travelled was significantly increased in *Crh*$^{CNS\text{-}COE}$ mice ($t = 3.8$, $p < 0.005$; $t = 3.2$, $p < 0.005$). *Significant from control; RM-ANOVA for time-dependent analysis, $p < 0.05$; Student's t-test, $p < 0.05$; *t* trend $p \leq 0.1$; n = 10-12.

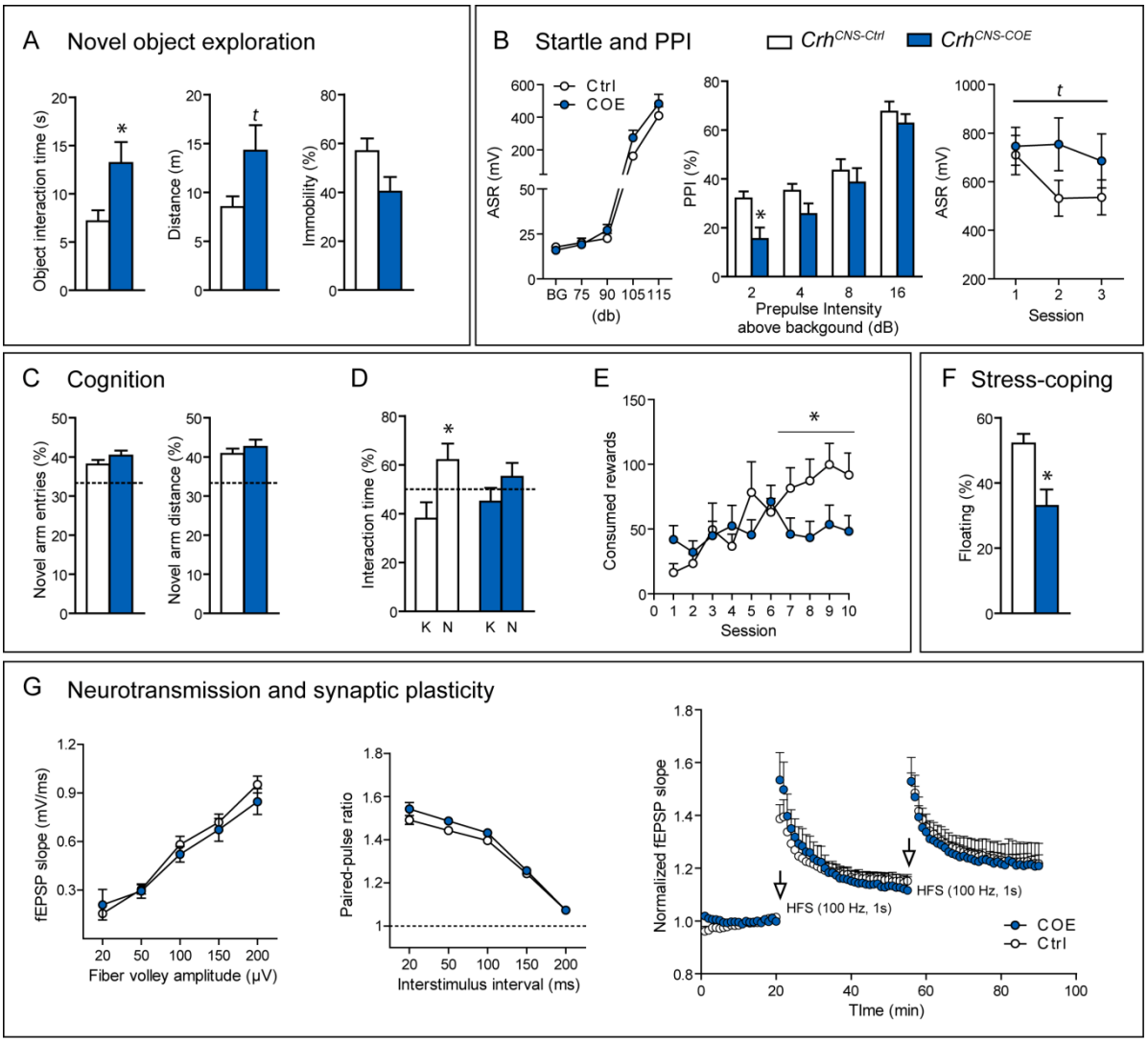

Figure 13: *Crh*$^{CNS\text{-}COE}$ mice exhibit increased novel object exploration, and mild changes in PPI and cognition. **(A)** *Crh*$^{CNS\text{-}COE}$ mice interacted significantly more with the novel object. **(B)** The acoustic startle response was not altered in *Crh*$^{CNS\text{-}COE}$ mice, but a slight overall decrease in PPI was observed, which was more strongly pronounced at lower prepulse intensities. *Crh*$^{CNS\text{-}COE}$ mice failed to show a habituation of the acoustic startle response during the PPI sessions. **(C)** Hippocampal-dependent spatial memory was not affected in *Crh*$^{CNS\text{-}COE}$ mice performing the Y-Maze task. **(D)** Contrary, object recognition memory was impaired in *Crh*$^{CNS\text{-}COE}$ mice, which barely discriminated between the known (K) and novel (N) object. **(E)** Similarly, in an operant conditioning task, *Crh*$^{CNS\text{-}COE}$ mice were not able to properly associate lever presses with the reception of a reward, which is depicted by the decreased numbered consumed rewards. **(F)** Confirmation of the previously reported FST-phenotype in *Crh*$^{CNS\text{-}COE}$ mice (Lu et al., 2008), showing enhanced active stress-coping behavior ($t = 3.5$, $p < 0.005$). **(G)** Glutamatergic neurotransmission assessed with input-output measurements and paired-pulse facilitation, and synaptic plasticity analyzed with LTP recordings at hippocampal CA3-CA1 synapses, was not affected by central CRH overexpression. *Significant from control; RM-ANOVA for time-dependent analysis, $p < 0.05$; Student's t-test, $p < 0.05$; *t* trend $p \leq 0.1$; n = 10-12 for behavior, n = 7-8 slices from 6 animals for electrophysiological recordings.

We observed a similar effect in *Crh*$^{CNS\text{-}COE}$ mice which spent significantly more time interacting with the unfamiliar object than control animals ($t = 2.5$, $p < 0.05$) (Figure 13A). An elevated startle response, as well as reduced prepulse inhibition (PPI) is additionally observed in bipolar

patients, but also in individuals with schizophrenia (Perry et al., 2001; Geyer et al., 2001; Belmaker, 2004; Jones et al., 2011). The acoustic startle response measured at different decibels was not altered *Crh*$^{CNS\text{-}COE}$ mice (Figure 13B). However overexpressing animals displayed a slight decrease in PPI (RM-ANOVA, time x genotype $F_{(3, 66)} = 1.7$, $p = 0.17$; genotype $F_{(1, 66)} = 3.5$; $p = 0.07$, Bonferroni $p < 0.05$) and exhibited no habituation to of the acoustic startle reflex during PPI compared to controls (RM-ANOVA, time x genotype $F_{(2, 34)} = 2.2$, $p = 0.12$) (Figure 13B). Cognitive performance, which is impaired in a wide range of psychiatric disorders, was only mildly affected in *Crh*$^{CNS\text{-}COE}$ mice. Although hippocampal-dependent spatial memory in the Y-maze remained intact (Figure 13C), *Crh*$^{CNS\text{-}COE}$ mice were barely able to discriminate the novel from the familiar object during the object recognition task ($t = 2.5$, $p < 0.05$) (Figure 13D). In addition, *Crh*$^{CNS\text{-}COE}$ mice did not learn to associate lever presses with reception of a reward in an operant conditioning task (RM-ANOVA, time x genotype $F_{(9, 117)} = 2.7$, $p = 0.006$) (Figure 13E). Memory impairments often result from alterations in synaptic transmission and plasticity. Thus, we analyzed whether central CRH overexpression impacts paired-pulse facilitation and long term potentiation (LTP) at CA3-CA1 synapses. Field potential recordings were performed in hippocampal slices of *Crh*$^{CNS\text{-}COE}$ mice but no differences in paired-pulse facilitation, input-output curves and LTP were observed between *Crh*$^{CNS\text{-}COE}$ and control mice (Figure 13G). Thus, central CRH overexpression does not alter basal glutamatergic neurotransmission and plasticity at hippocampal CA3-CA1 synapses, suggesting that other mechanisms and/or brain regions might be responsible for the observed behavioral alterations in *Crh*$^{CNS\text{-}COE}$ mice. This is also in agreement with the behavioral data, which showed that hippocampal-dependent spatial memory was not altered by central CRH overexpression (Figure 13C). In addition, previous experiments in our group revealed enhanced stress-dependent activation of the locus coeruleus (LC) in *Crh*$^{CNS\text{-}COE}$ mice (Lu et al., 2008), and increased noradrenaline-release in the hippocampus following an acute FST challenge (unpublished data). This supports the notion that CRH modulates emotional behavior via activation of the endogenous catecholaminergic system, which has also been postulated by others (Valentino et al., 1983; Butler et al., 1990; Lu et al., 2008; Refojo et al., 2011). In conclusion, the behavioral phenotype of *Crh*$^{CNS\text{-}COE}$ mice is largely in line with other mouse models of mania and similar to many characteristics of human bipolar patients in the manic state (Table 16).

Table 16: *Crh*$^{CNS\text{-}COE}$ mice exhibit a behavioral profile similar to prominent mouse models of mania and human bipolar patients in the manic phase.

Symptoms of mania	Prominent genetic models of mania	Indications in mice	*Crh*$^{CNS\text{-}COE}$ mice
Hyperactivity	mCLOCK, Glur6$^{-/-}$, tgSHANK, tgGSK3β, Myk/$^{+}$	Hyperactivity in the OF	Hyperactivity in the OF
	mCLOCK, Glur6$^{-/-}$, tgSHANK, tgGSK3β, Myk/$^{+}$	Hyperactivity in the FST/TST	Hyperactivity in the FST and TST (Lu et al., 2008)
Increased risk-taking / impulsivity	mCLOCK, Glur6$^{-/-}$, tgBAG1, Myk/$^{+}$	Reduced anxiety	Reduced anxiety
Psychomotor agitation / increased object exploration	Myk/$^{+}$	Increased novel object exploration	Increased novel object exploration
Decreased sleep/abnormal circadian rhythm	mCLOCK, Glur6$^{-/-}$, Myk/$^{+}$ tgSHANK,	Decreased sleep/abnormal circadian rhythm	Decreased sleep (enhanced REM, Kimura et al., 2010)
Psychotic features / propensity toward drug abuse	mCLOCK, Glur6$^{-/-}$, Myk/$^{+}$ tgSHANK, tgBAG1	Psychostimulant-induced locomotion and sensitization	n.d.
	mCLOCK, Glur6$^{-/-}$, Myk/$^{+}$		n.d.
Excessive involvement in pleasurable activities		Increased sucrose preference	
	tgSHANK, tgGSK3β, Myk/$^{+}$		Slightly decreased PPI
Enhanced ASR and/or diminished PPI		Enhanced ASR and diminished PPI	
Impaired executive function and working memory	not reported for the above	Cognitive dysfunction	Impaired object recognition and operant learning

References: mCKOCK (Roybal et al., 2007), Glur6$^{-/-}$ (Shaltiel et al., 2008) tgSHANK3 (Han et al., 2013), tgBAG1 and BAG1$^{+/-}$ (Maeng et al., 2008), tgGSK3β (Prickaerts et al., 2006), Myk/$^{+}$ (Kirshenbaum et al., 2011). Not determined (n.d.), forced swim test (FST), tail suspension test (TST). Table modified from Roybal et al., 2007.

4.1.2.2. Gene expression analysis in Crh$^{CNS\text{-}COE}$ mice reveals Aqp4 as a possible new target gene for mania

To identify possible new target genes altered by central CRH hyperdrive, we previously assessed hippocampal gene expression profiles in *Crh*$^{CNS\text{-}Ctrl}$ and *Crh*$^{CNS\text{-}COE}$ mice using microarray technology (unpublished data). The hippocampus was chosen due to the fact that stress-induced noradrenaline release was enhanced in in this brain region of *Crh*$^{CNS\text{-}COE}$ mice. Total RNA isolated out of hippocampi from 4-6 independent biological samples from control and *Crh*$^{CNS\text{-}COE}$ mice was reverse transcribed. The amplified RNA (rRNA) was subsequently analyzed using the Illumina® Sentrix Mouse-6 v1.1 expression bead chip, covering 46657 gene probes from 10 samples. The main candidate genes differently regulated by central CRH

overexpression are depicted in Table 17, and were selected based on the fold change in regulation (FC) and whether they were previously reported to be involved in specific brain functions. The upregulation of *LacZ* and the downregulation of *NeoR* served as an internal control confirming the efficient performance of the microarray. Their differential regulation further confirmed the ability of the microarray to detect robust effects. However, only a few genes, including *Dock10* and *Zfp367*, remained significantly regulated after correction for multiple testing (Adj. p value < 0.05).

Table 17: Differentially regulated genes in *Crh*$^{CNS\text{-}COE}$ mice revealed by microarray analysis.

Symbol	Accession	Description	FC	P value	Adj. p value
LacZ		LacOperon-S	10.2	5.7E-10	8.8E-06
NeoR		Neomycin resitance	-9.0	1.0E-08	8.1E-05
Dock10	AA267455	Dedicator of cytokinesis protein 10	-2.2	9.9E-08	0.0005
Zfp367	AI853766	Zinc finger protein 367	4.2	2.6E-06	0.010
Ifitm1	AI464509	Interferon induced transmembrane protein 1	2.0	4.1E-08	0.1
Casp8	NM009812	Caspase 8	1.8	0.0002	0.2
Aqp4	AI115947	Aquaporin 4	1.4	0.00028	0.30
Mtap2	AI849758	Microtubule-associated protein 2	-6.3	0.0003	0.32
Srd5a1	NM175283	Steroid 5 alpha-reductase 1	2.7	0.0003	0.33
Nfib	AI836780	Nuclear factor I/B	-1.9	0.0008	0.5
Sstr1	NM009216	Somatostatin receptor type 1	-2.1	0.0242	0.7

Nevertheless, further qRT-PCR validation in the same samples (2nd half of the hippocampus) confirmed the microarray results for most candidates as illustrated for *Aqp4*, *Ifitm1*, *Nfib* and *Dock10* (Figure 14A). Interestingly, only *Aqp4* was also shown to be upregulated in brain regions other than the hippocampus as demonstrated by *ISH* in *Crh*$^{CNS\text{-}COE}$ mice (Figure 14B). These included the cortex, thalamus, mid/hind-brain regions and the cerebellum. *ISH* further revealed a broad expression of *Aqp4* throughout the brain, most prominently in the stratum lacunosum moleculare and moleculare layer of the dentate gyrus of the hippocampal formation, as well as the thalamus and cerebellum. AQP4 belongs to the aquaporine family of water channel proteins that facilitate bidirectional transport of water across the plasma membrane (King et al., 2004), and is primarily expressed in astrocytes and ependymocytes (Nagelhus and Ottersen, 2013). This is supported by the absence of mRNA expression in the pyramidal layers of the hippocampus which mainly harbor neuronal cell bodies.

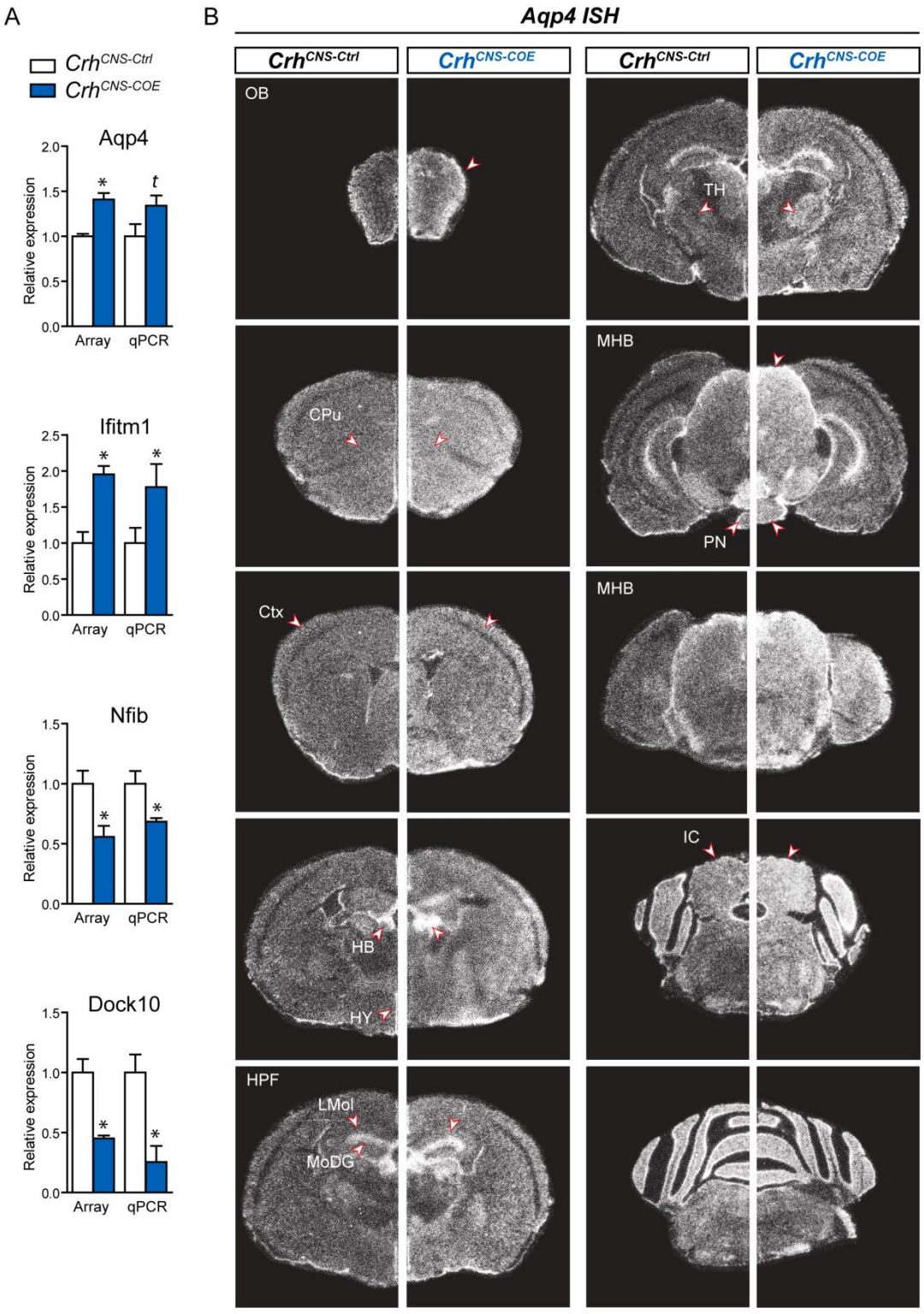

Figure 14: Independent validation of selected candidate genes using qRT-PCR and *ISH*.
(A) qRT-PCR validation of the microarray results is shown for four representative genes; *Aqp4*, *Ifitm1*, *Nfib* and *Dock10*. **(B)** Apart from the hippocampus, *Aqp4* was the only candidate found to be upregulated throughout the brain of $Crh^{CNS\text{-}COE}$ mice. Regions of interest are depicted by arrows. CPu (caudate putamen), HB (habenula nucleus), HPF (hippocampal formation), HY (hypothalamus), IC (inferior colliculus), Lmol (stratum lacunosum moleculare), MHB (mid-hindbrain), MoDG (moleculare layer of the dentate gyrus), OB (olfactory bulb), PN (pontine nuclei), TH (thalamus). *Significant from control; Student's t-test, $p < 0.05$; *t* trend $p \leq 0.1$; n = 4-6, Scale bar represents 1 mm.

4.1.2.3. Chronic lithium treatment reverses mania-like behavior in $Crh^{CNS\text{-}COE}$ mice

Lithium is a commonly prescribed mood stabilizer for the treatment of mania (Shastry, 1997), and is able to reverse many of the behavioral abnormalities observed in genetic models of mania (Roybal et al., 2007; Shaltiel et al., 2008; Kirshenbaum et al., 2011). To assess whether the manic-like state in $Crh^{CNS\text{-}COE}$ mice can be reversed with chronic lithium treatment, we added LiCl to the drinking water at 600 mg/liter as described by others (Dehpour et al., 2002; Roybal et al., 2007). Behavioral assessment started 10 days after the onset of lithium treatment and lasted for 11 days during which LiCl was continuously administered. This produced stable serum Li^+ concentrations of 0.3 - 0.4 mmol/liter in both control and $Crh^{CNS\text{-}COE}$ mice (Figure 15A), which is within the lower therapeutic range for humans, and does not significantly impact the animals health which commonly includes dehydration and decreased body weight (Roybal et al., 2007). Consequently, body weight progression was indistinguishable between lithium and vehicle treated mice (Figure 15A). However, we observed a mild genotype effect which revealed increased body weight progression in $Crh^{CNS\text{-}COE}$ compared to $Crh^{CNS\text{-}Ctrl}$ mice independent of treatment (RM-ANOVA, genotype $F_{(1,42)} = 3.5$, $p < 0.05$). Decreased floating time in the FST was normalized to control levels in $Crh^{CNS\text{-}COE}$ mice following lithium treatment (2-Way ANOVA, genotype $F_{(1,45)} = 8.5$, $p < 0.01$; genotype x treatment $F_{(1,45)} = 2.8$, $p < 0.1$; Bonferroni $p < 0.05$) which is additionally illustrated by the significant increase in delta floating time (in which each lithium treated group was normalized to the corresponding vehicle treated group)(Figure 15B). Similarly, hyperlocomotion in the OF was no longer observed in $Crh^{CNS\text{-}COE}$ mice following chronic lithium treatment (2-Way ANOVA, genotype x treatment $F_{(1,42)} = 2.2$, $p = 0.07$; Bonferroni post-test, $p < 0.05$) (Figure 15C). This effect was most strongly pronounced during the first 5 min of the OF, where also immobility was nearly restored to control levels following lithium application (2-Way ANOVA, genotype $F_{(1,42)} = 7.5$, $p < 0.01$; genotype x treatment $F_{(1,42)} = 2.2$, $p = 0.14$; Bonferroni post-test, $p < 0.05$). For all parameters, the changes in delta demonstrate nicely the opposing effects Li^+ on behavior in control and $Crh^{CNS\text{-}COE}$ mice. This was also observed in the EPM where lithium treatment reduced the duration on the open arms of $Crh^{CNS\text{-}COE}$ but not control mice (2-Way ANOVA, genotype x treatment $F_{(1,43)} = 6.5$, $p < 0.05$) (Figure 16A).

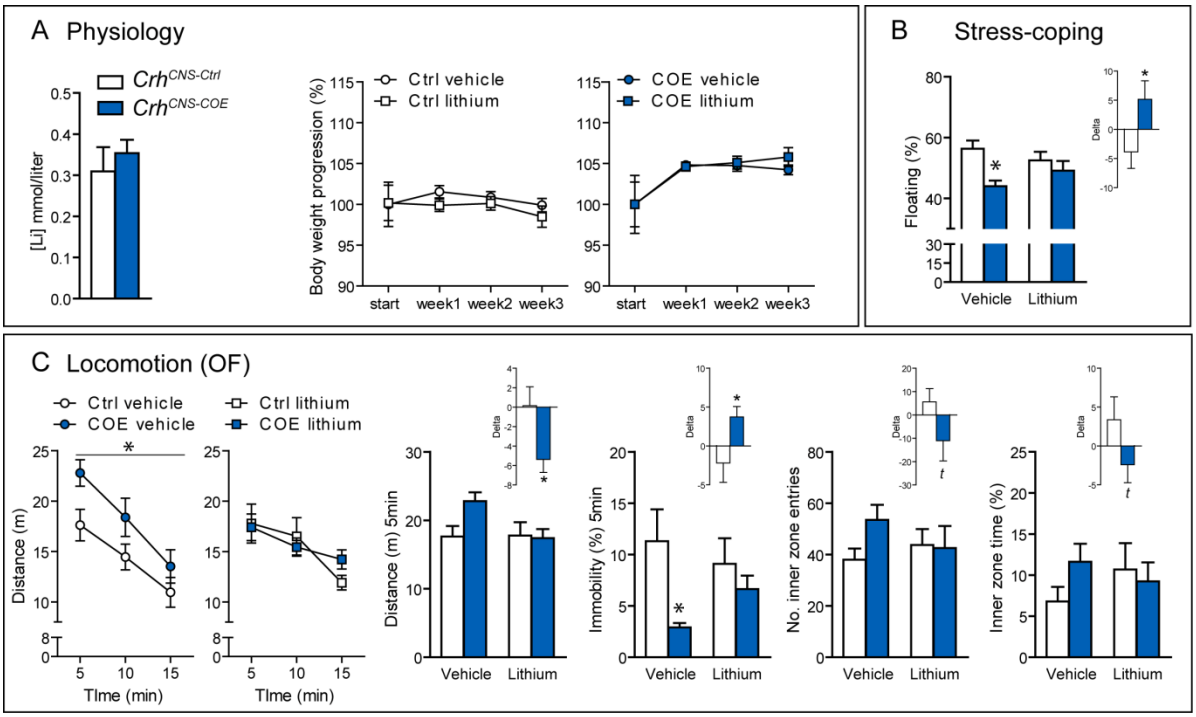

Figure 15: Manic-like behavior in *Crh*$^{CNS-COE}$ mice is reversed upon chronic lithium treatment.
(A) Li^+ serum concentrations were indistinguishable between control and overexpressing mice after three weeks of treatment. Body weight progression was not affected by chronic lithium treatment. **(B)** Lithium treatment restored floating time in the FST to control levels (Delta, $t = 2.1$, $p < 0.05$). **(C)** Hyperlocomotion and reduced immobility in the OF were reversed to control levels following lithium treatment (Delta distance, $t = 2.4$, $p < 0.05$; Delta immobility (%), $t = 2.2$, $p < 0.05$). A similar trend was observed for the time and number of inner zone entries. *Significant from control of the same treatment group; RM-ANOVA or 2-Way ANOVA, $p < 0.05$; Bonferroni post-test, $p < 0.05$; Delta = each lithium-group normalized to the corresponding vehicle group, Student's t-test, $p < 0.05$, *t* trend $p \leq 0.1$; n = 10-12.

A similar trend was observed for the number of open arm entries, total and open arm distance. The applied lithium dosage did not significantly affect control mice in the OF and FST, however it induced an increase in all parameters of the EPM, especially open arm time (Figure 16A). Such Li^+ effects have also been observed in wild-type mice by a previous study using similar concentrations (Roybal et al., 2007). Lithium also restored novel object exploration to control levels in *Crh*$^{CNS-COE}$ mice (2-Way ANOVA, genotype x treatment $F_{(1,46)} = 5.6$, $p < 0.05$; Bonferroni post-test, $p < 0.05$). Again, lithium produced opposing effects in controls, leading to an increase in object exploration time, which was however not significant (Figure 16B). Similarly, additional parameters assessed during the test such as the number of inner zone entries, distance travelled and immobility were differentially affected by lithium in controls than *Crh*$^{CNS-COE}$ mice. As shown in Figure 13, hippocampal-dependent spatial memory measured in the Y-maze was not altered by central CRH overexpression. Importantly, the applied concentrations of lithium did not affect cognitive performance in both, control and *Crh*$^{CNS-COE}$ mice (Figure 16C).

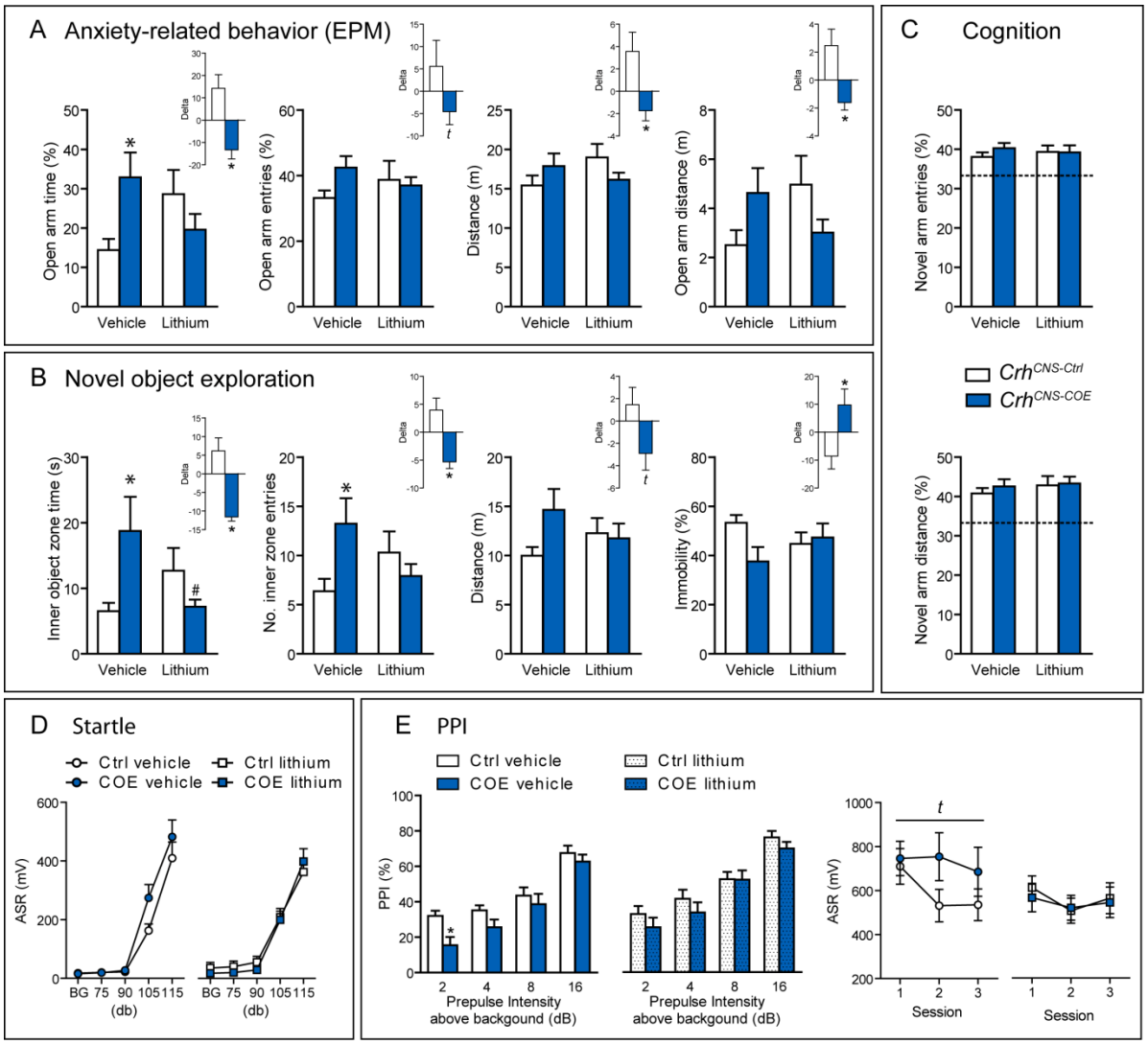

Figure 16: Additional evidence for lithium-induced reversal of mania-like behavior in *Crh*$^{CNS\text{-}COE}$ mice.
(A) Open arm time in the EPM was significantly reduced in lithium treated *Crh*$^{CNS\text{-}COE}$ mice (Delta, t = 3.6, p < 0.005). A similar trend was observed for the other parameters. **(B)** Novel object exploration was restored to control levels in lithium treated overexpressing mice (Delta, t = 4.9, p < 0.0001). The number of entries into the object-containing inner zone were also reduced in *Crh*$^{CNS\text{-}COE}$ mice following lithium treatment (Delta, t = 7.8, p < 0.005). A differential effect of lithium in control and overexpressing mice was additionally observed for the distance travelled and immobility (Delta, t = 1.9, p = 0.08; t = 2.5, p < 0.05). **(C)** Cognitive performance in the Y-maze and the ASR **(D)** were not affected by 600 mg/liter lithium treatment. **(E)** Lithium treatment increased PPI at low prepulse intensities in *Crh*$^{CNS\text{-}COE}$ mice and reinstated habituation of the ASR during the PPI sessions. Conditional overexpression (COE); *Significant from control of the same treatment group, # significant from the vehicle treated group of the same genotype; RM-ANOVA or 2-Way ANOVA, p < 0.05; Bonferroni post-test, p < 0.05; Delta = each lithium-group normalized to the corresponding vehicle group, Student's t-test, p < 0.05, *t* trend p ≤ 0.1; n = 10-12.

Similarly, we observed no significant changes in the acoustic startle repose following lithium treatment (Figure 16D). However, PPI at lower prepulse intensities was slightly enhanced in lithium treated *Crh*$^{CNS\text{-}COE}$ mice but not in controls (*vehicle*: 2-Way ANOVA, genotype $F_{(1,66)} = 1.7$, p = 0.07; Bonferroni post-test, p < 0.05 / *lithium*: 2-Way ANOVA, genotype $F_{(1,66)} = 0.9$, p = 0.6)

(Figure 16E). The inability to show a proper habituation of the acoustic startle reflex during the PPI sessions was also ameliorated by lithium in *Crh*$^{CNS\text{-}COE}$ mice (*vehicle*: 2-Way ANOVA, genotype x treatment $F_{(2.34)} = 2.2$, $p = 0.12$ / *lithium*: 2-Way ANOVA, genotype x treatment $F_{(2,46)} = 0.3$, $p = 0.7$) (Figure 16E). Overall chronic lithium treatment was able to reverse many of the altered behavioral responses to control levels, establishing *Crh*$^{CNS\text{-}COE}$ mice as a potential model of mania.

4.1.2.4. Chronic social defeat stress (CSDS) induces a switch from a manic to a depressive state in Crh$^{CNS\text{-}COE}$ mice

The difficulty in modeling bipolar disorder is given by the alternating manic (elevated mood) and depressive (depressed mood) mood states which are experienced by patients (Belmaker and Bersudsky, 2004). Thus far researches have failed to mimic the fluctuation between these complex human mood conditions in mice or rats, and it is debatable whether this can be achieved. However, it has become possible to model endophenotypes of both manic and depressive-like behavior in mice, as shown in the previous section for the *Crh*$^{CNS\text{-}COE}$ line. Chronic social defeat stress (CSDS) represents a well-established paradigm used to induce endophenotypes of psychiatric disorders in rodents (Nestler and Hyman, 2010; Dedic et al., 2011; Berton et al., 2012). The most common include enhanced anxiety-related behavior, anhedonia, impaired cognitive performance and novel object exploration as well as alterations in social behavior. Thus, we aimed to investigate the extent to which CSDS would affect the mania-like phenotype of *Crh*$^{CNS\text{-}COE}$ mice. For this, we subjected control and *Crh*$^{CNS\text{-}COE}$ mice to three weeks of CSDS as previously described (Hartmann et al., 2012b; Wang et al., 2013). Chronically stressed mice exhibited elevated morning plasma corticosterone levels (2-Way ANOVA, genotype $F_{(1,40)} = 6.4$, $p < 0.05$), increased adrenal gland weights (2-Way ANOVA, genotype $F_{(1,42)} = 215$, $p < 0.0001$) and decreased thymus weights (2-Way ANOVA, genotype $F_{(1,39)} = 16.1$, $p < 0.0005$) independent of genotype (Figure 17A). These robust stress markers demonstrate the effectiveness of the paradigm as reported by earlier studies (Wagner et al., 2011; Hartmann et al., 2012a; Hartmann et al., 2012b; Wang et al., 2013). In addition, *Crh*$^{CNS\text{-}COE}$ mice displayed an enhanced corticosterone response, and a slightly diminished recovery following forced swim stress independent of condition, which is in line with the previously presented results (Section 4.1.2.1) (*acute stress*: 2-Way ANOVA, genotype $F_{(1,39)} = 10.7$, $p < 0.005$; Bonferroni post-test, $p < 0.05$ / *recovery*: 2-Way ANOVA, genotype $F_{(1,38)} = 5.7$, $p < 0.05$;

stress $F_{(1,38)} = 3.7$, $p = 0.06$). However, CSDS had no significant effect on the acute stress response, and only mildly enhanced recovery levels independent of genotype (Figure 17A). Locomotion in the OF test was significantly reduced in control and *Crh*$^{CNS\text{-}COE}$ mice following CSDS (2-Way ANOVA, genotype x stress $F_{(1,72)} = 2.9$, $p = 0.09$; genotype $F_{(1,72)} = 26.1$, $p < 0.0001$; stress $F_{(1,72)} = 36.5$, $p < 0.0001$; Bonferroni $p < 0.05$)(Figure 17B). Although chronically stressed *Crh*$^{CNS\text{-}COE}$ mice still remained hyperactive compared to stressed controls, the delta decrease in locomotion following CSDS was significantly greater in *Crh*$^{CNS\text{-}COE}$ mice (Delta, $t = 2.3$, $p < 0.05$). Similarly, chronic-stress induced immobility in the OF test was enhanced to a greater extent in *Crh*$^{CNS\text{-}COE}$ than control mice (2-Way ANOVA, genotype $F_{(1,72)} = 16.6$, $p < 0.0005$; stress $F_{(1,72)} = 25.3$, $p < 0.0001$; Bonferroni post-test, $p < 0.05$). On the other hand, inner zone time and number of entries were reduced in an equal manner following CSDS (*time*: 2-Way ANOVA, stress $F_{(1,71)} = 4.7$, $p < 0.05$ / *entries*: 2-Way ANOVA, stress $F_{(1,73)} = 9.6$, $p < 0.005$; genotype $F_{(1,73)} = 8.9$, $p < 0.005$, Bonferroni post-test, $p < 0.05$)(Figure 17B). Next we assessed the effect of CSDS on anxiety-related behavior in control and *Crh*$^{CNS\text{-}COE}$ mice. As expected, *Crh*$^{CNS\text{-}COE}$ mice displayed decreased anxiety and/or increased risk-assessment behavior under basal conditions in the EPM (2-Way ANOVA, genotype x stress $F_{(1,74)} = 14.5$, $p < 0.0005$; genotype $F_{(1,74)} = 17.9$, $p < 0.0001$; stress $F_{(1,74)} = 37.0$, $p < 0.0001$; Bonferroni post-test, $p < 0.05$) (Figure 17C). However, CSDS induced a strikingly severe increase in anxiety-related behavior in *Crh*$^{CNS\text{-}COE}$ compared to control littermates. Whereas open arm time was reduced by approximately 4% in controls, a decrease of nearly 17% was observed in *Crh*$^{CNS\text{-}COE}$ mice (Delta, 24.7, $p < 0.0001$). A similar effect was observed for the number of open arm entries (2-Way ANOVA, genotype x stress $F_{(1,74)} = 2.4$, $p = 0.1$; genotype $F_{(1,74)} = 6.1$, $p < 0.05$; stress $F_{(1,74)} = 17.1$, $p < 0.0001$; Bonferroni post-test, $p < 0.05$), latency to enter the open arms (2-Way ANOVA, genotype $F_{(1,74)} = 4.8$, $p < 0.05$; stress $F_{(1,74)} = 15.1$, $p < 0.0005$; Bonferroni post-test, $p < 0.05$), distance travelled (2-Way ANOVA, genotype x stress $F_{(1,74)} = 22.8$, $p < 0.0001$; genotype $F_{(1,74)} = 15.4$, $p < 0.0005$; stress $F_{(1,74)} = 48.9$, $p < 0.0001$, Bonferroni post-test, $p < 0.05$) and immobility (2-Way ANOVA, genotype x stress $F_{(1,74)} = 24.8$, $p < 0.0001$; genotype $F_{(1,74)} = 16.0$, $p < 0.0005$; stress $F_{(1,74)} = 45.3$, $p < 0.0001$; Bonferroni post-test, $p < 0.05$) (Figure 17C). Enhanced chronic-stress induced anxiety could additionally be confirmed for *Crh*$^{CNS\text{-}COE}$ mice in the DaLi (Figure 17D).

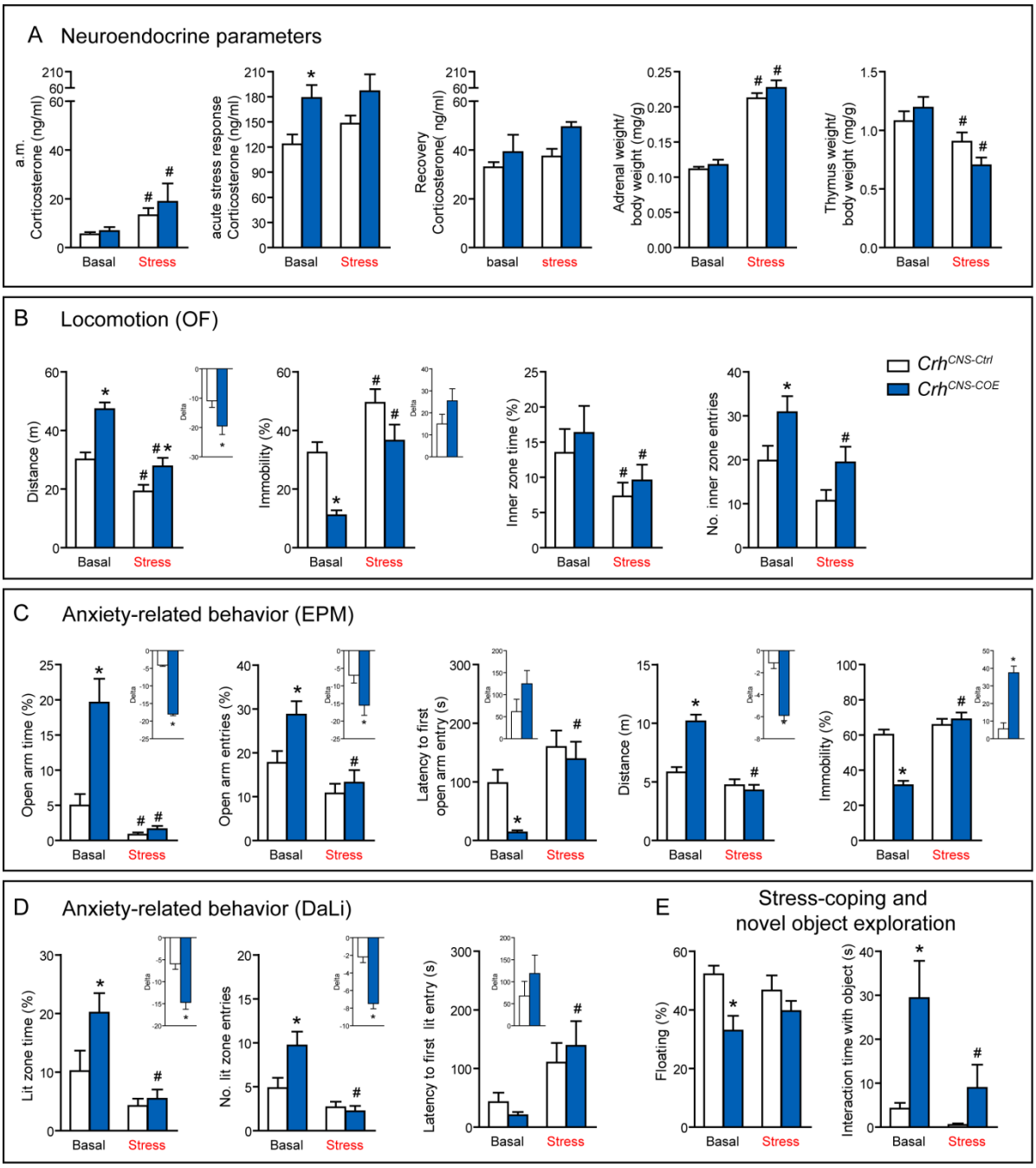

Figure 17: CSDS induces a switch from mania- to depression-like behavior in *Crh*$^{CNS\text{-}COE}$ mice.
(A) CSDS led to an increase in basal corticosterone levels and adrenal gland weights, and induced a decrease in thymus size independent of genotype. CSDS had no significant effect on acute stress-response and recovery levels. **(B)** CSDS induced a greater locomotion-decrease in *Crh*$^{CNS\text{-}COE}$ than control mice; however *Crh*$^{CNS\text{-}COE}$ mice still retained their hyperactivity. *Crh*$^{CNS\text{-}COE}$ mice also showed a slightly larger increase in CSDS-induced immobility compared to controls. Inner zone time and entries were not differentially affected by CSDS. **(C)** Open arm time and open arm entries in the EPM were reduced by CSDS to a greater extent in *Crh*$^{CNS\text{-}COE}$ than in control mice. A similar effect is depicted for the latency to open arm entry, distance travelled and immobility. **(D)** Enhanced CSDS-induced anxiety in *Crh*$^{CNS\text{-}COE}$ mice was also observed in the DaLi. CSDS reduced the amount of lit zone time and number of lit entries, which was more strongly pronounced in *Crh*$^{CNS\text{-}COE}$ than control mice. The latency to enter the lit zone was enhanced by CSDS to a similar degree in *Crh*$^{CNS\text{-}COE}$ and control mice. **(E)** Decreased floating time in the FST and increased novel object exploration were observed in *Crh*$^{CNS\text{-}COE}$ mice, but these were not differentially affected by CSDS. *Significant from control of the same condition, # significant from the chronically stressed group of the same genotype; RM-ANOVA

for time, analysis $p < 0.05$; 2-Way ANOVA for group analysis, $p < 0.05$; Bonferroni post-test, $p < 0.05$; Delta = each CSDS-group normalized to the corresponding basal group, Student's t-test, $p < 0.05$, *t* trend, $p \leq 0.1$; n = 10-12.

Aversive lit zone time was decreased to a greater extent in $Crh^{CNS\text{-}COE}$ than control mice (2-Way ANOVA, genotype x stress $F_{(1,40)} = 2.5$, $p = 0.12$; genotype $F_{(1,40)} = 4.1$, $p < 0.05$; stress $F_{(1,40)} = 13.9$, $p < 0.0005$; Bonferroni post-test, $p < 0.05$). The same was observed for the number of lit zone entries (2-Way ANOVA, genotype x stress $F_{(1,40)} = 5.8$, $p < 0.05$; genotype $F_{(1,40)} = 4.0$, $p = 0.051$; stress $F_{(1,40)} = 19.4$, $p < 0.0001$; Bonferroni post-test, $p < 0.05$) but not for the latency to enter the lit compartment (2-Way ANOVA, stress $F_{(1,40)} = 11.8$, $p < 0.005$; Bonferroni post-test, $p < 0.05$). Importantly, anxiety-levels in the EPM and DaLi were slightly lower in chronically stressed $Crh^{CNS\text{-}COE}$ compared to basal $Crh^{CNS\text{-}Ctrl}$ mice. (Figure 17C-D) Thus, CSDS did no simply repress the manic state (or normalize it like lithium), but actually induced endophenotypes of depression in $Crh^{CNS\text{-}COE}$ mice. As previously shown (Figure 16), novel object exploration was significantly enhanced in $Crh^{CNS\text{-}COE}$ mice compared to controls, which still remained the case following CSDS (2-Way ANOVA, genotype $F_{(1,28)} = 8.6$, $p < 0.05$; stress $F_{(1,28)} = 4.4$, $p < 0.05$; Bonferroni post-test, $p < 0.05$)(Figure 17E). Floating time in the FST was only affected by genotype (2-Way ANOVA, genotype $F_{(1,40)} = 9.7$, $p < 0.005$)(Figure 17E). Overall our results suggest that CSDS can induce a switch from a manic- to a depressive-like state in $Crh^{CNS\text{-}COE}$ mice especially with regards to anxiety-related behavior.

4.1.3. Region- and neurotransmitter-specific CRH overexpressing mice reveal dual properties of the CRH system

So far our results have demonstrated that HPA axis hyperdrive on its own, independent of alterations in the central CRH system is not sufficient to alter emotional behavior. Importantly the behavioral changes observed in *Crh*$^{CNS\text{-}COE}$ mice further confirm that central CRH can exert its effects independent of basal HPA axis activation. However, even in *Crh*$^{CNS\text{-}COE}$ mice the HPA axis does not remain unaffected by central CRH overexpression, resulting in heightened stress sensitivity. Once more, this emphasizes the difficulty to completely uncouple central from peripheral CRH actions. In order to further uncover the underlying neuronal circuits and brain regions mediating emotional behavior via CRH, we set out to generate additional, site- and neurotransmitter-specific conditional CRH-overxpressing mouse mutants (Figure 18). We took advantage of the increasing number of available brain site- and neurotransmitter-specific Cre recombinase expressing mouse lines, to address CRH function in a spatially and temporally restricted manner. For example, mouse lines expressing Cre recombinases selectively in neurons of a specific neurotransmitter type allow for gene targeting of specific populations of neurons. Moreover, increasing availability of mouse lines expressing the tamoxifen-inducible Cre recombinase variant *CreERT2* offers additional temporal control and avoids obscurities due to developmental functions of targeted genes.

First, we used conditional mutagenesis to genetically dissect the main brain regions involved in mediating the behavioral effects of CRH. As described in the previous sections we initially crossed *R26*$^{flopCrh/flopCrh}$ mice with *Delter-Cre*, *Pomc-Cre* and *Nestin-Cre* to generate ubiquitous (*Crh*$^{Del\text{-}COE}$), anterior pituitary- (*Crh*$^{APit\text{-}COE}$) and CNS-specific (*Crh*$^{CNS\text{-}COE}$) CRH overexpressing mice (Section 4.1.1 and 4.1.2). In order assess the effects of CRH overexpression in the forebrain (*Crh*$^{FB\text{-}COE}$) and mid-hindbrain (*Crh*$^{MHB\text{-}COE}$), *R26*$^{flopCrh/flopCrh}$ mice were additionally bred to the *Camk2α-Cre* (calcium/calmodulin dependent protein kinase II apha) transgenic mice and *En1-Cre* (engrailed-1) knockin mice respectively (Minichiello et al., 1999; Kimmel et al., 2000) (Figure 18). *Camk2α-Cre* activation occurs around postnatal day 18, thereby circumventing major developmental compensatory adaptations. However, crossing *R26*$^{flopCrh/flopCrh}$ with inducible *Camk2α-CreERT2* mice (*Crh*$^{iFB\text{-}COE}$) allowed us to further discriminate between early and late adult effects of forebrain-restricted CRH overexpression, which also includes limbic structures known to regulate emotional behavior (Erdmann et al., 2007). In addition, gradual deletion processes are avoided with inducible Cre-lines.

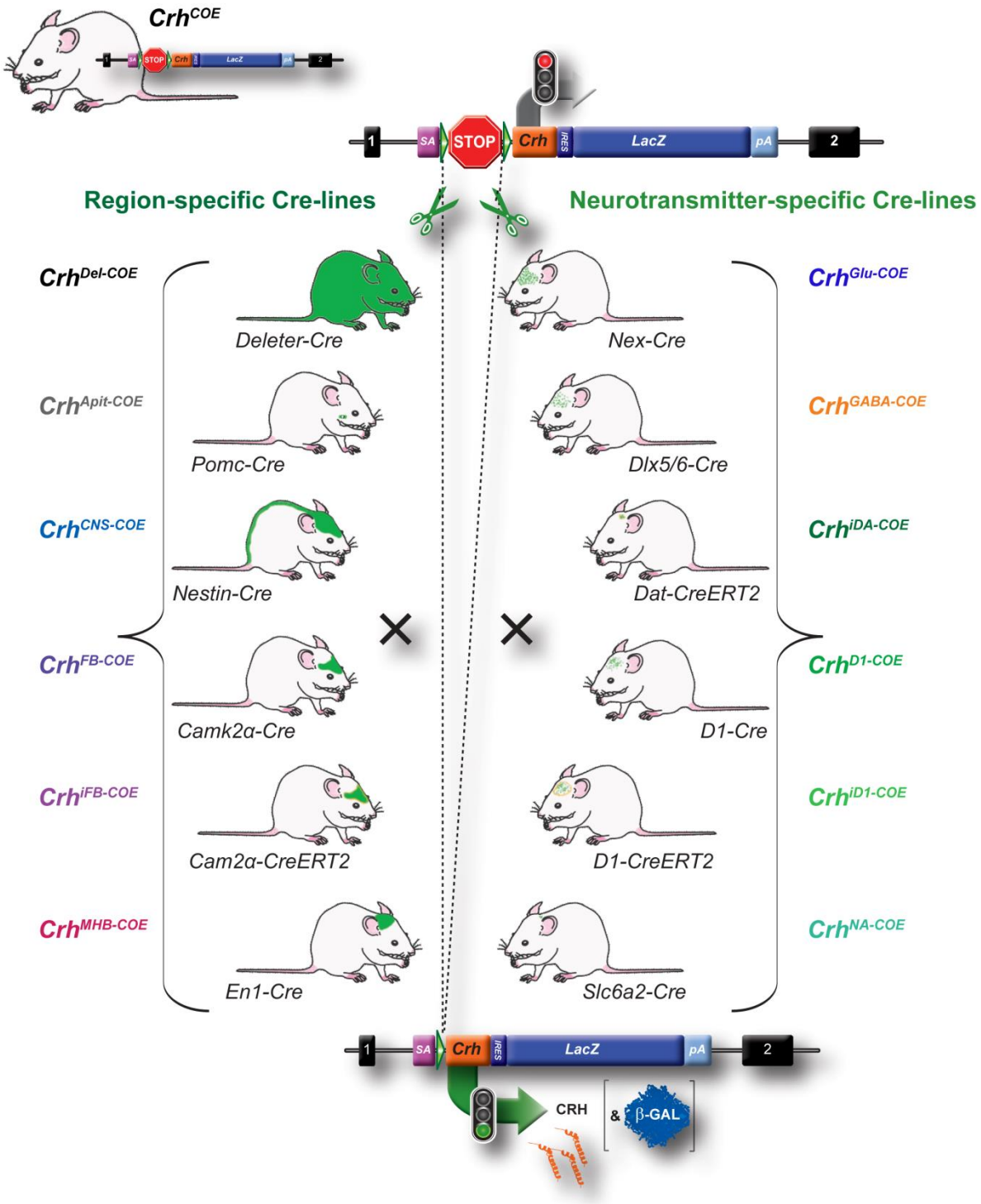

Figure 18: Strategy for conditional, region- and neurotransmitter-specific CRH overexpression.
Schematic representation of the *ROSA26* locus, which was engineered to harbour a Cre-inducible *Crh-LacZ* expression unit. Breeding to different region- and neurotransmitter-specifc Cre-mice leads to removal of the transcriptional terminator sequence (STOP), resulting in specific CRH overexpression patterns (Cre-recombinase expression pattern depicted in green). Generated mouse lines: $Crh^{Del\text{-}COE}$ (ubiqitious), $Crh^{CNS\text{-}COE}$ (CNS/ *Nestin-Cre*), $Crh^{APit\text{-}COE}$ (anterior pituitary / *Pomc-Cre*), $Crh^{FB\text{-}COE}$ (forebrain / *Camk2α-Cre*), $Crh^{iFB\text{-}COE}$ (inducible forebrain / *Camk2α-CreERT2*), $Crh^{MHB\text{-}COE}$ (mid-hindbrain / *En1-Cre*), $Crh^{Glu\text{-}COE}$ (glutamatergic / *Nex-Cre*), $Crh^{GABA\text{-}COE}$ (GABAergic / *Dlx5/6-Cre*), $Crh^{iDA\text{-}COE}$ (inducible dopamingeric / *Dat-CreERT2*), $Crh^{D1\text{-}COE}$ (D1-dopaminoceptive / *D1-Cre*), $Crh^{iD1\text{-}COE}$ (inducible D1-dopaminoceptive / *D1-CreERT2*), $Crh^{NA\text{-}COE}$ (noradrenergic / *Slc6a2-Cre*). *R26* exons are indicated as black boxes, the transcriptional terminator as a STOP sign and *loxP*

sites as green arrowheads. Splice acceptor (SA), internal ribosomal entry side (IRES), poly A signal (pA), conditional CRH overexpression (COE).

Camk2α-CreERT2 expression was initiated between postnatal weeks 8-10 via two weeks of oral tamoxifen application. The pattern of brain-region specific CRH overexpression is perfectly mirrored by *LacZ* reporter gene expression, which is co-activated upon Cre-mediated excision of the transcriptional terminator sequence (Figure 1 and Figure 18). In both $Crh^{Del\text{-}COE}$ and $Crh^{CNS\text{-}COE}$ mice *LacZ* mRNA expression was detected throughout the brain (Figure 19, Figure 7 and Figure 11). In contrast, CRH overexpression in $Crh^{FB\text{-}COE}$ mice was restricted to forebrain projection neurons, which predominantly include excitatory pyramidal neurons of the cortex and hippocampus (Murray et al., 2008), but also principal neurons of the amygdala, olfactory bulb, bed nucleus of the stria terminalis, septum, geniculate nucleus and medium spiny neurons of the caudate putamen and nucleus accumbens (Figure 19). Notably, the *LacZ* mRNA expression pattern observed in inducible $Crh^{iFB\text{-}COE}$ mice did not fully recapitulate that of $Crh^{FB\text{-}COE}$ mice. The slight alterations in recombination-patterns between the *Camk2α-Cre* and the inducible *Camk2α-CreERT2,* might be attributed to differences in the utilized promoter elements, or the presence of endogenous enhancers in the vicinity of the transgenic integration site, which is most likely different for the two Cre lines. Consequently, *Camk2α-CreERT2* does not recombine in the caudate putamen, nucleus accumbens, BNST and amygdala to the same extent as the non-inducible *Camk2α-Cre,* which is supported by the diminished number of *LacZ*-positive neurons in those regions in $Crh^{iFB\text{-}COE}$ mice. On the other hand, additional recombination in the raphe nucleus and an increased number of *LacZ* expressing neurons in the hippocampus was observed in $Crh^{iFB\text{-}COE}$ compared to in $Crh^{FB\text{-}COE}$ mice (Figure 19). CRH overexpression in $Crh^{MHB\text{-}COE}$ mice is initiated at prenatal day 8 (Davis and Joyner, 1988) and was restricted to the caudal midbrain and anterior hindbrain domain of *En1* including the substantia nigra, ventral tegmental area, periaqueductal central gray, superior olive, superior and inferior colliculus, and the cerebellum (Figure 19).

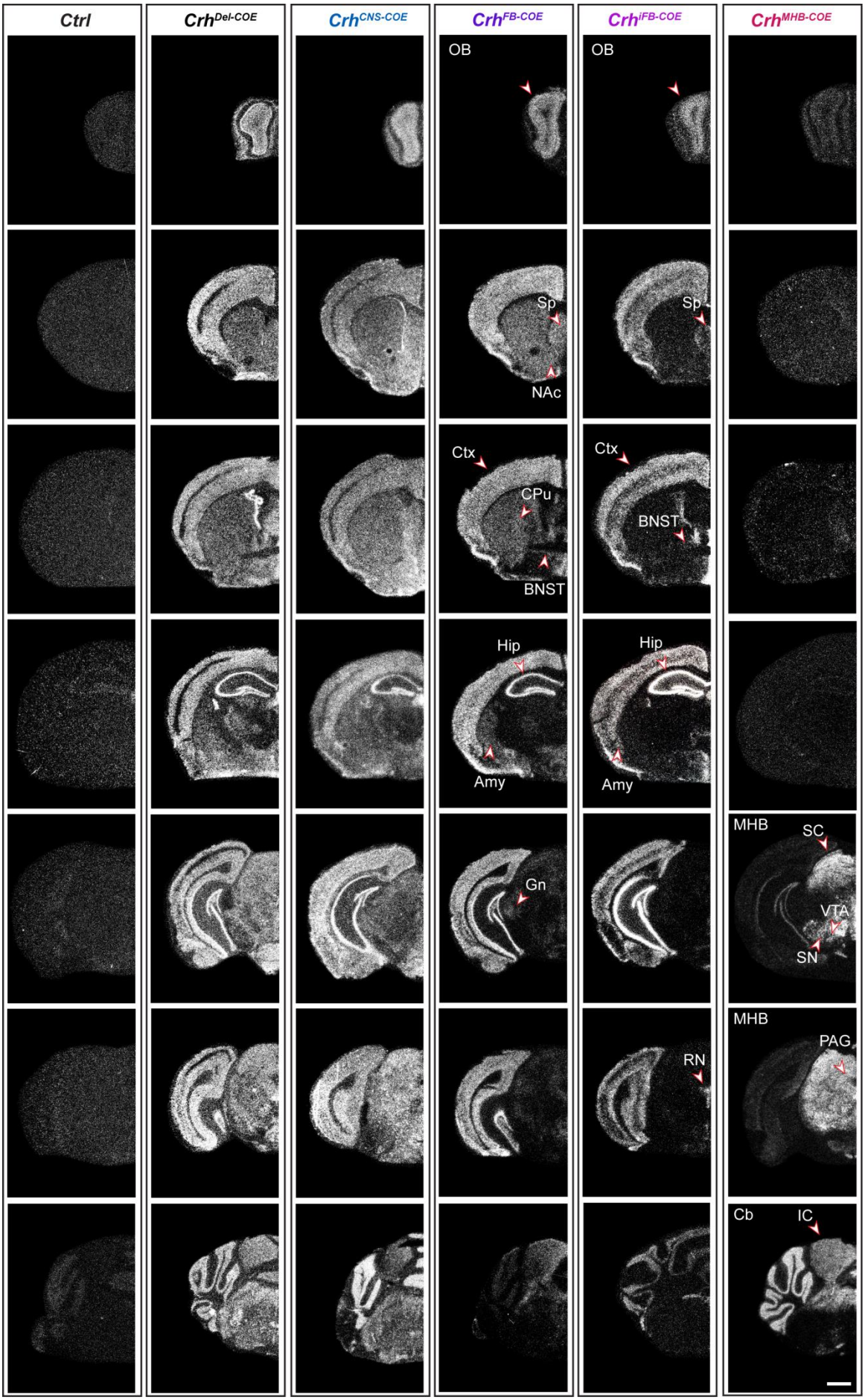
Ctrl
Crh Del-COE
Crh CNS-COE
Crh FB-COE
Crh iFB-COE
Crh MHB-COE
OB
Sp
NAc
Ctx
CPu
BNST
Hip
Amy
Gn
MHB
SC
VTA
SN
RN
PAG
Cb
IC

Figure 19: Brain-region specific CRH overexpressing mouse lines.
ISH using a *LacZ*-specific riboprobe, which detects the *Crh-LacZ* fusion transcript, confirmed the specific patterns of exogenous CRH expression in $Crh^{Del\text{-}COE}$ (ubiqitious), $Crh^{CNS\text{-}COE}$ (CNS/ *Nestin-Cre*), $Crh^{APit\text{-}COE}$ (anterior pituitary / *Pomc-Cre*), $Crh^{FB\text{-}COE}$ (forebrain / *Camk2α-Cre*), $Crh^{iFB\text{-}COE}$ (inducible forebrain / *Camk2α-CreERT2*), and $Crh^{MHB\text{-}COE}$ (mid-hindbrain / *En1-Cre*) mice. Abbreviations: amygdala (Amy), bed nucleus of the stria terminalis (BNST), cerebellum (Cb), caudate putamen (CPu), cortex (Ctx), geniculate nucleus (Gn), hippocampus (Hip), inferior colliculus (IC), mid-hindbrain (MHB), nucleus accumbens (NAc), olfactory bulb (OB), raphe nucleus (RN), superior colliculus (SC), substantia nigra (SN), septum (Sp), periaqueductal grey (PAG), ventral tegmental area (VTA). Scale bar represents 1 mm.

Although brain-region specificity in the context of CRH overexpression is crucial to further uncover CRH effects that modulate emotional behavior, it tells us little about possible CRH-neurotransmitter interactions. The neurochemical identity of CRH neurons remains largely unknown, and has so far only been mapped to GABAergic neurons of the hippocampus, cortex and the central amygdala (Day et al., 1999; Kubota et al., 2011; Chen et al., 2012b). The ability of CRH to potentiate noradrenergic neurotransmission is widely accepted, but the interaction with other neurotransmitter-circuits is less well described. In order to address a wider range of potential CRH-neurotransmitter interactions in the modulation of emotional behavior, we overexpressed CRH in a cell-type specific manner (Figure 18 and Figure 20). Overexpression of CRH in glutamatergic neurons was achieved by mating $R26^{flopCrh/flopCrh}$ mice with the *Nex-Cre* knockin line (Goebbels et al., 2006) generating $Crh^{Glu\text{-}COE}$ mice. In this line Cre expression starts during development (E11.5), and is under the control of the regulatory sequences of *NeuroD6* (*Nex*), which encodes a neuronal basic helix-loop-helix (bHLH) protein. CRH overexpression was primarily detected in glutamatergic neurons of the neocortex and hippocampus, but also in the basolateral amygdala, the mitral layer of the OB and the parabrachial nucleus (Figure 20). CRH overexpression in GABAergic neurons was obtained by breeding $R26^{flopCrh/flopCrh}$ mice to the *Dlx5/6-Cre* transgenic line (Zerucha et al., 2000; Stuhmer et al., 2002; Monory et al., 2006), where Cre is driven by the regulatory sequences of the Dlx5/Dlx6 homeobox genes expressed in migrating forebrain GABAergic neurons during development (E10). CRH overexpression in $Crh^{GABA\text{-}COE}$ mice was detected most strongly in GABAergic neurons of the olfactory bulb, and caudate putamen and bed nucleus of the stria terminalis, but also in the cortex, hippocampus, reticular thalmic nucleus, amygdala and unexpectedly in the locus coeruleus (Figure 20). To assess the involvement of CRH in dopaminergic neurons, $R26^{flopCrh/flopCrh}$ were mated with inducible *Dat-CreERT2* mice (Engblom et al., 2008) to obtain the $Crh^{iDA\text{-}COE}$ transgenic line.

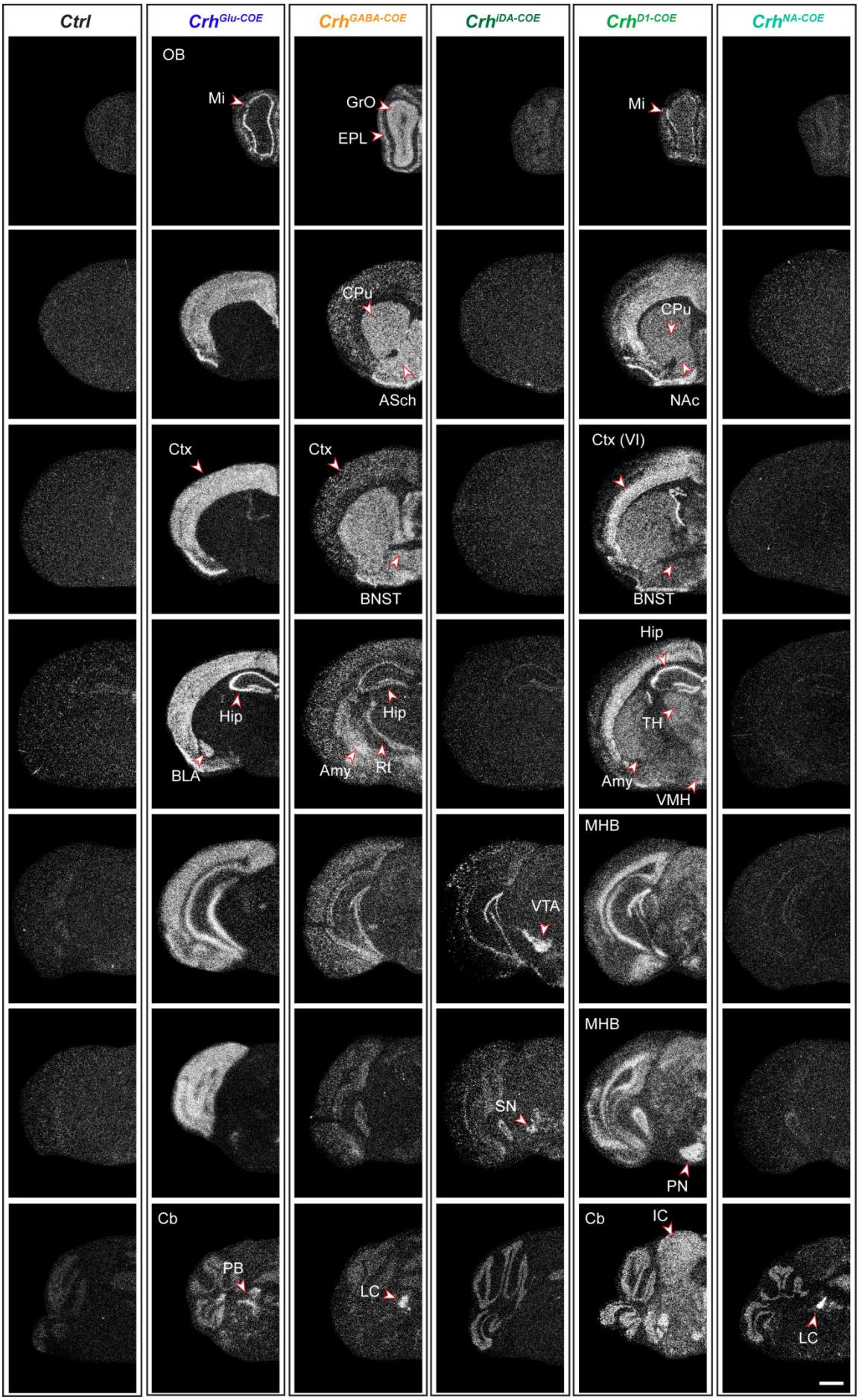
Ctrl
CrhGlu-COE
CrhGABA-COE
CrhiDA-COE
CrhD1-COE
CrhNA-COE
OB
Mi
GrO
EPL
Mi
CPu
ASch
CPu
NAc
Ctx
Ctx
Ctx (VI)
BNST
BNST
Hip
Hip
Hip
TH
BLA
Amy
Rt
Amy
VMH
MHB
VTA
MHB
SN
PN
Cb
PB
LC
Cb
IC
LC

Figure 20: Neurotransmitter-specific CRH overexpressing mouse lines.
ISH using a *LacZ*-specific riboprobe, which detects the *Crh-LacZ* fusion transcript, confirmed the distinctive patterns of exogenous CRH expression in $Crh^{Glu\text{-}COE}$ (glutamatergic / *Nex-Cre*), $Crh^{GABA\text{-}COE}$ (GABAergic/ *Dlx5/6-Cre*), $Crh^{iDA\text{-}COE}$ (inducible dopamingeric / *Dat-CreERT2*), $Crh^{D1\text{-}COE}$ (D1-dopaminoceptive / *D1-Cre*), and $Crh^{NA\text{-}COE}$ (noradrenergic / *Slc6a2-Cre*) mice. Abbreviations: amygdala (Amy), basolateral amygdala (BLA), bed nucleus of the stria terminalis (BNST), cerebellum (Cb), caudate putamen (CPu), cortex (Ctx), hippocampus (Hip), inferior colliculus (IC), locus coeruleus (LC), mid/hind brain (MHB), nucleus accumbens (NAc), olfactory bulb (OB), olfactory bulb external plexiform layer (EPL), olfactory bulb granule cell layer (GrO), olfactory bulb mitral layer (Mi) parabrachial nucleus (PB), reticular thalmic nucleus (Rt), substantia nigra (SN), ventral tegmental area (VTA). Scale bar represents 1 mm.

In this line the inducible Cre-recombinase is controlled by regulatory elements of the dopamine transporter (DAT) and is mainly expressed in midbrain dopaminergic neurons, which is also depicted by *LacZ* mRNA expression in the substantia nigra and ventral tegmental area of $Crh^{iDA\text{-}COE}$ mice (Figure 20). *Dat-CreERT2* expression was initiated between postnatal weeks 8-10 via two weeks of tamoxifen food application. To further investigate the interaction between CRH and the dopaminergic system we sought to overexpress CRH not only in dopamine-producing neurons, but also in dopaminergic projection sites. For this, we bred $R26^{flopCrh/flopCrh}$ to *D1-Cre* and inducible *D1-CreERT2* mice (Mantamadiotis et al., 2002; Lemberger et al., 2007), generating $Crh^{D1\text{-}COE}$ and $Crh^{iD1\text{-}COE}$ mice respectively. This allowed us to address possible differences between pre- and postnatal CRH overexpression in D1-positive neurons. *D1-Cre* expression is directed by the promoter of the dopamine receptor D1A gene (*Drd1a*), starting at E16 in few striosomal neurons of the striatum and progresses until adulthood (Mantamadiotis et al., 2002; Lemberger et al., 2007). High levels of *LacZ* expression were detected in the caudate putamen, nucleus accumbens, hippocampus and layer VI of the cortex. In addition *D1-Cre* recombination was observed in limbic regions including the CeA and BNST, the ventral-medial hypothalamus, pontine nucleus, inferior colliculus, the olfactory bulb and cerebellum (Figure 20), which is largely in line with the endogenous D1 expression pattern (Weiner et al., 1991; Fremeau, Jr. et al., 1991). *D1-CreERT2* expression (and hence CRH overexpression) was initiated in $Crh^{iD1\text{-}COE}$ mice between postnatal weeks 8-10 via two weeks of tamoxifen food application, and mirrored the expression map of $Crh^{D1\text{-}COE}$ mice (data not shown). Last, the noradrenergic system was targeted by breeding $R26^{flopCrh/flopCrh}$ to *Scl6a2-Cre* transgenic mice (Gong et al., 2007). Cre expression is controlled by promoter elements of the *Slc6a2* gene, encoding the noradrenaline transporter, which is detectable as early as E9.5 (Ren et al., 2003). CRH overexpression was only detected in the locus coeruleus of $Crh^{NA\text{-}COE}$ mice (Figure 20).

4.1.3.1. Overexpression of CRH in forebrain Camk2α-positive and GABAergic neurons induces opposing anxiogenic and anxiolytic effects

Having established a complementary set of region- and neurotransmitter restricted CRH overexpressing mouse lines, we set out to specify the brain regions and neurochemical substrates underlying the manic- and depression-like properties observed in *Crh*$^{Del\text{-}COE}$ and *Crh*$^{CNS\text{-}COE}$ mice (Section 4.1.1 and 4.1.2). Strongly pronounced alterations in body weight were only observed in the previously mentioned *Crh*$^{Del\text{-}COE}$ and *Crh*$^{CNS\text{-}COE}$ lines, the former resulting from Chushing-like symptoms due to constantly elevated glucocorticoid secretion (Figure 8 and Figure 21). Diminished body weight in *Crh*$^{CNS\text{-}COE}$ mice is likely a consequence of hyperactivity, decreased liquid intake (Section 4.1.2) and/or alterations in metabolic rate due to overexpression of CRH in hypothalamic nuclei. Importantly, the absence of visible physiological alterations in the other mouse lines argues against developmental defects possible caused by pre- and/or postnatal CRH overexpression.

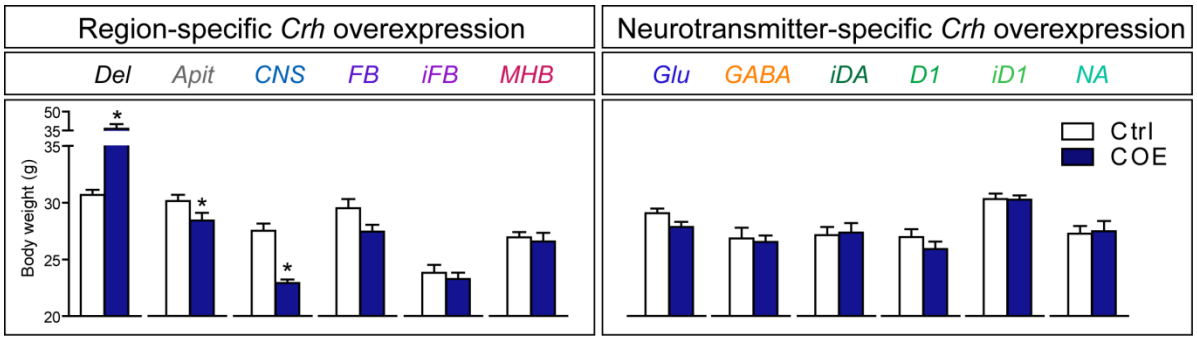

Figure 21: Assessment of body weight in region- and neurotransmitter-specific CRH overexpressing mice. Ubiquitous CRH overexpression resulted in increased body weight, while CNS-restricted overexpression produced the opposite effect. Overexpression of CRH from other brain regions and circuits had no effect on body weight. Abbreviations: control (Ctrl), conditional CRH overexpression (COE), ubiquitous *Crh-OE* (Del), CNS-specific *Crh-OE* (CNS), forebrain-specific *Crh-OE* (FB), inducible forebrain-specific *Crh-OE* (iFB), mid/hindbrain-specific *Crh-OE* (MHB), *Crh-OE* in glutamatergic neurons (Glu), *Crh-OE* in GABAergic neurons (GABA), inducible *Crh-OE* in dopaminergic neurons (iDA), *Crh-OE* in D1-dopaminoceptive neurons (D1), inducible *Crh-OE* in D1-dopaminoceptive neurons (iD1), *Crh-OE* in noradrenergic neurons (NA). Refer to the main text for a detailed description of the conditional mouse lines. Student's t-test, $p < 0.05$, n = 10-12.

In order to analyze possible alterations in HPA axis function, we measured morning, evening, stress-response (following 10 min of restraint stress) and recovery corticosterone levels in all region- and neurotransmitter-specific mouse lines (Figure 22). As shown in the previous section (Section 4.1.1), the most drastic effects on HPA axis function were observed upon ubiquitous and anterior pituitary-restricted CRH overexpression. In both mouse lines, CRH hyperdrive resulted in enhanced basal corticosterone secretion due to activation of CRHR1 in

the pituitary. In contrast, CNS-restricted overexpression resulted in stress-induced hypersecretion of corticosterone, without affecting basal and recovery levels (Figure 22). Interestingly, forebrain-specific CRH overexpression in principal *Camk2α*-positive neurons (*Crh*$^{FB\text{-}COE}$) led to a slight, but not significant increase in HPA axis activity (Figure 22). This would suggest that peripheral CRH actions are not primarily mediated via CRH in principal neurons. However, compensatory downregulation of endogenous CRH or alterations in CRHR1/CRHR2 expression might have restored initial HPA axis changes, which could also hold true for the other overexpressing lines and was already reported for *Crh*$^{CNS\text{-}COE}$ mice (Lu et al., 2008). Contrastingly, CRH overexpression induced in late adulthood (postnatal week 10) in forebrain principal *Camk2α*-positive neurons (*Crh*$^{iFB\text{-}COE}$) lead to a slight decrease in morning ($t = 2.3$, $p < 0.05$) and evening ($t = 2.3$, $p = 0.07$) corticosterone levels (Figure 22). This is rather surprising and might be attributed to an initial, strongly pronounced compensatory downregulation of endogenous CRH, which probably also occurred in non-inducible *Crh*$^{FB\text{-}COE}$. However, the degree to which *Crh*$^{iFB\text{-}COE}$ mice can compensate for the induced changes is debatable given the limited occurrence of structural plasticity in the adult brain. On the other hand, differences in recombination patterns between the *Camk2α-Cre* and *Camk2α-CreERT2* might also account for differences in HPA axis activity between *Crh*$^{FB\text{-}COE}$ and *Crh*$^{iFB\text{-}COE}$ mice (Figure 20). Mice overexpressing CRH in the mid-hindbrain displayed an enhanced stress-response ($t = 2.5$, $p < 0.05$) and elevated morning and evening plasma corticosterone levels (*a.m.*: $t = 2.7$, $p < 0.05$ / *p.m.*: $t = 2.1$, $p < 0.05$), which might result from enhanced noradrenergic activation (Figure 22). Apart from indirect regulation of adrenal gland function via the HPA axis, CRH can also modulate glucocorticoid secretion via the autonomic nervous system by activating noradrenergic neurons within the LC, which in turn innervate all components of the HPA axis (Herman and Cullinan, 1997; Hwang et al., 1998). However, most evidence points towards CRH-innervation of the LC, rather than local expression (Pammer et al., 1990; Keegan et al., 1994; Tjoumakaris et al., 2003; Jedema and Grace, 2004; Alon et al., 2009). The fact that specific overexpression in the LC (*Crh*$^{NA\text{-}COE}$ mice) failed to alter corticosterone secretion further supports that CRH-containing cell bodies within the LC are not responsible for noradrenergic regulation of the HPA axis (Figure 22). Nevertheless, our results suggest that CRH-expressing neurons in the mid-hindbrain are modulating HPA axis function, possibly via direct or indirect innervation of the LC. Neurotransmitter-specific overexpression of CRH revealed no significant alterations in morning, evening and recovery corticosterone levels in any of the assessed mouse lines (Figure 22).

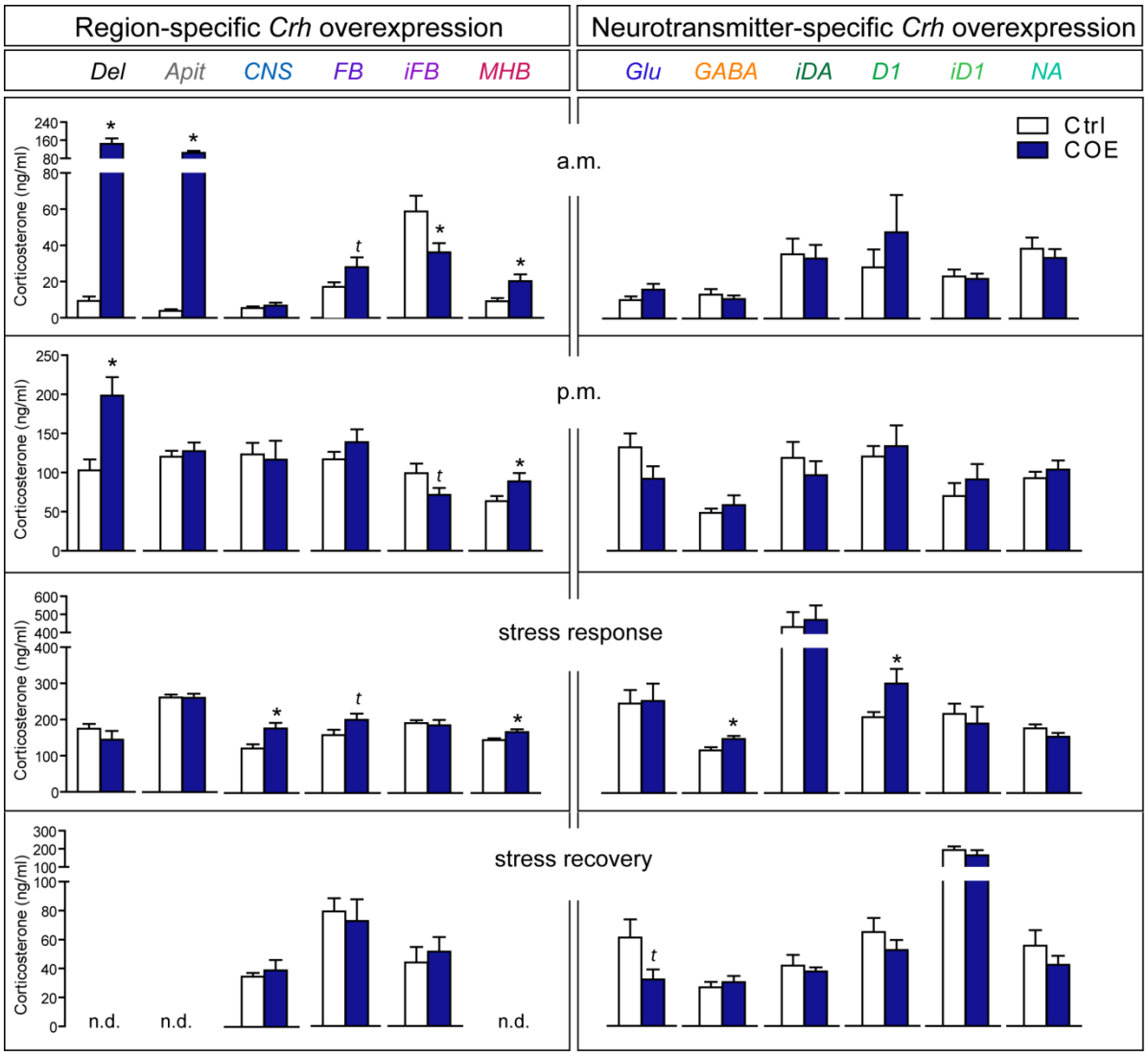

Figure 22: HPA axis regulation in region- and neurotransmitter-specific CRH overexpressing mice.
HPA axis activity is most profoundly affected by ubiquitous and anterior-pituitary specific CRH overexpression, depicted by strongly elevated morning plasma corticosterone levels. Stress response and recovery levels were measured 10 and 90 min after restraint stress respectively. Abbreviations: control (Ctrl), conditional CRH overexpression (COE), not determined (n.d.), ubiquitous *Crh-OE* (*Del*), CNS-specific *Crh-OE* (*CNS*), forebrain-specific *Crh-OE* (*FB*), inducible forebrain-specific *Crh-OE* (*iFB*), mid/hindbrain-specific *Crh-OE* (*MHB*), *Crh-OE* in glutamatergic neurons (*Glu*), *Crh-OE* in GABAergic neurons (*GABA*), inducible *Crh-OE* in dopaminergic neurons (*iDA*), *Crh-OE* in D1-dopaminoceptive neurons (*D1*), inducible *Crh-OE* in D1-dopaminoceptive neurons (*iD1*), *Crh-OE* in noradrenergic neurons (*NA*). Refer to main text for detailed description of conditional mouse lines. *Significant from control, Student's t-test, $p < 0.05$, *t* trend $p \leq 0.1$; n = 10-12.

However, overexpression in GABAergic and D1-dopaminoceptive neurons lead to an enhanced stress response ($Crh^{GABA\text{-}COE}$: $t = 2.6$, $p < 0.05$ / $Crh^{D1\text{-}COE}$: $t = 2.4$, $p < 0.05$). Interestingly, $Crh^{GABA\text{-}COE}$ and $Crh^{D1\text{-}COE}$ mice displayed a similar HPA axis profile as $Crh^{CNS\text{-}COE}$ mice. Considering that the D1 receptors are expressed in many GABAergic neurons, including medium spiny neurons of the striatum and nucleus accumbens (Valjent et al., 2009; Matamales et al., 2009; Gangarossa et al., 2012), infers that HPA axis hyperactivity in $Crh^{CNS\text{-}COE}$ mice might be caused

by CRH overexpression in GABAergic D1-positive neurons. However, D1-restricted overexpression in adulthood did not result in an enhanced stress response (Figure 22).This may again be caused by differences in compensatory mechanisms, given that *D1-CreERT2* expression was induced between postnatal weeks 8-10, whereas *D1-Cre* expression is initiated at E16.

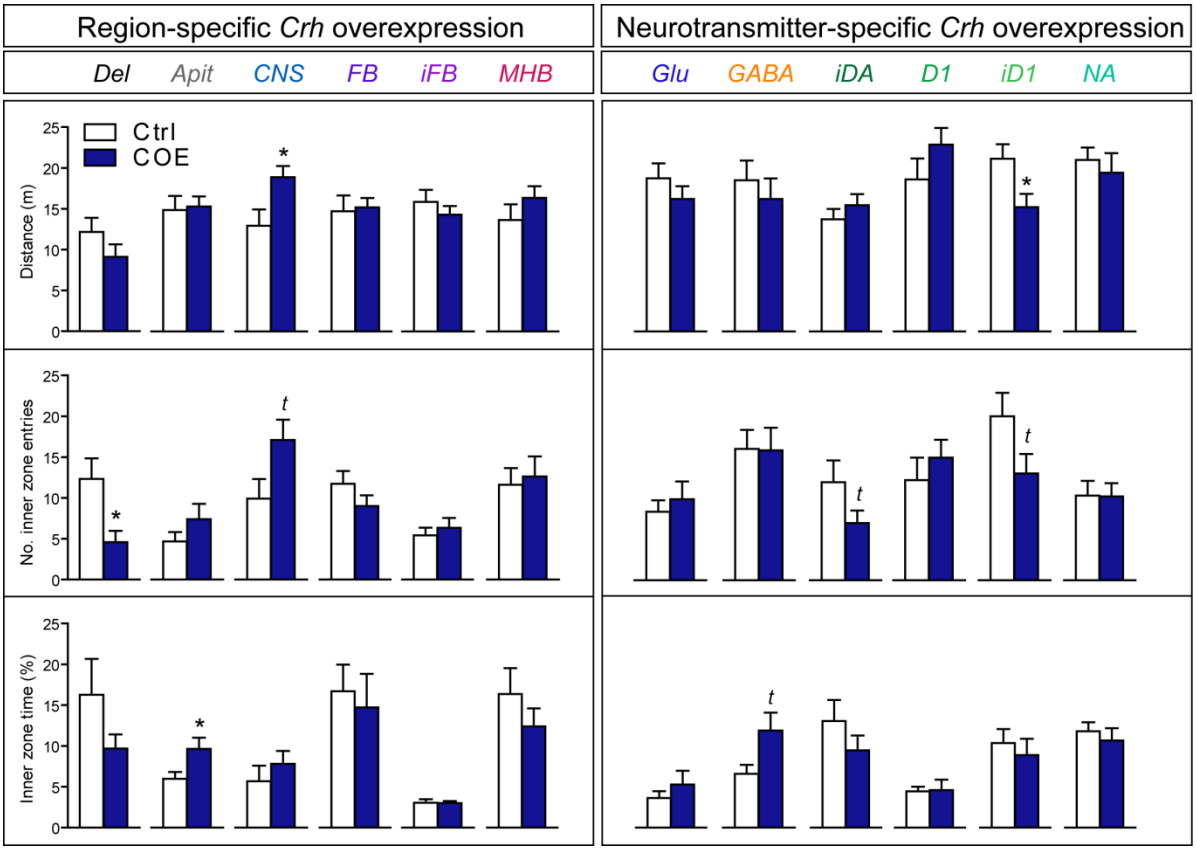

Figure 23: Effects of region- and neurotransmitter-specific CRH overexpression on locomotion in the OF. *CNS*-specific CRH overexpression induces hyperactivity. The opposite effect was observed in mice overexpressing CRH in *D1*-dopaminoceptive neurons during adulthood. $Crh^{Del\text{-}COE}$ mice displayed enhanced anxiety-related behavior by entering the inner zone less frequently; while the opposite was observed in $Crh^{APit\text{-}COE}$ mice which spent more time in the inner zone (also see section 3.1.1.). OF duration-5min. Abbreviations: control (Ctrl), conditional CRH overexpression (COE), ubiquitous *Crh-OE* (*Del*), *CNS*-specific *Crh-OE* (*CNS*), forebrain-specific *Crh-OE* (*FB*), inducible forebrain-specific *Crh-OE* (*iFB*), mid/hindbrain-specific *Crh-OE* (*MHB*), *Crh-OE* in glutamatergic neurons (*Glu*), *Crh-OE* in GABAergic neurons (*GABA*), inducible *Crh-OE* in dopaminergic neurons (*iDA*), *Crh-OE* in D1-dopaminoceptive neurons (*D1*), inducible *Crh-OE* in D1-dopaminoceptive neurons (*iD1*), *Crh-OE* in noradrenergic neurons (*NA*). Refer to the main text for detailed description of the conditional mouse lines. *Significant from control; Student's t-test, $p < 0.05$, *t* trend, $p \leq 0.1$; n = 10-12.

Importantly, considerable differences in morning, evening, response and recovery levels were observed between the control groups ($Crh^{flopCrh/flopCrh}$-white bars). This can be attributed to the fact that the experiments were performed over the time course of three years, using different radioimmunoassay kits. Moreover, not all of the mouse lines were bred and assessed in the

same animal facility, which might have differentially impacted corticosterone levels. This emphasizes the importance of utilizing littermate controls for all mouse lines.

In order to specify the brain regions and neurotransmitter circuits responsible for regulating emotional behavior via CRH, a general behavioral screen was performed for all of the above mentioned mouse mutants, including the OF, FST, EPM and DaLi test. Hyperlocomotion observed in $Crh^{CNS\text{-}COE}$ mice (Section 4.1.2.1) was not observed in any of the other mouse lines (Figure 23). However, a significant decrease in distance travelled was shown in $Crh^{iD1\text{-}COE}$ mice ($t = 2.5$, $p < 0.05$). Anxiety-related parameters of the OF, including the time and number of inner zone entries were only significantly altered in $Crh^{Del\text{-}COE}$ and $Crh^{APit\text{-}COE}$ mice, as previously discussed (Section 4.1.1).

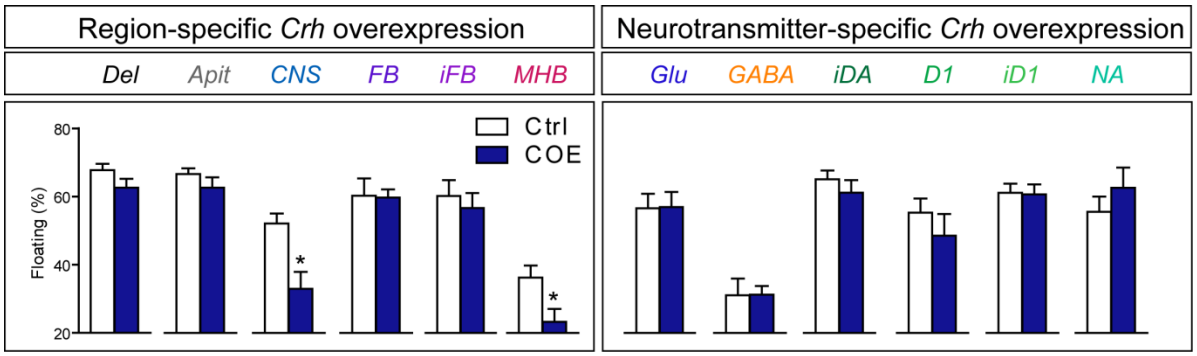

Figure 24: Enhanced active stress-coping behavior is mediated by CRH overexpression in the mid-hindbrain, but not the locus coeruleus.

Floating time in the FST was significantly decreased in $Crh^{CNS\text{-}COE}$ and $Crh^{MHB\text{-}COE}$ mice. Abbreviations: control (Ctrl), conditional CRH overexpression (COE), ubiquitous *Crh-OE* (*Del*), *CNS*-specific *Crh-OE* (*CNS*), forebrain-specific *Crh-OE* (*FB*), inducible forebrain-specific *Crh-OE* (*iFB*), mid/hindbrain-specific *Crh-OE* (*MHB*), *Crh-OE* in glutamatergic neurons (*Glu*), *Crh-OE* in GABAergic neurons (*GABA*), inducible *Crh-OE* in dopaminergic neurons (*iDA*), *Crh-OE* in D1-dopaminoceptive neurons (*D1*), inducible *Crh-OE* in D1-dopaminoceptive neurons (*iD1*), *Crh-OE* in noradrenergic neurons (*NA*). Refer to the main text for detailed description of the conditional mouse lines. *Significant from control; Student's t-test, $p < 0.05$; $n = 10\text{-}12$.

Active stress-coping behavior, assessed with the FST was only significantly altered in $Crh^{CNS\text{-}COE}$ ($t = 3.5$, $p < 0.005$) and $Crh^{MHB\text{-}COE}$ mice ($t = 2.4$, $p < 0.05$) (Figure 24). Importantly, this further supports that CRH overexpression in caudal brain nuclei within the MHB promotes reduced immobility in the FST. Enhanced noradrenergic activation of the LC in $Crh^{CNS\text{-}COE}$ mice (Lu et al., 2008) probably also underlies the immobility phenotype in $Crh^{MHB\text{-}COE}$ mice. However, CRH overexpression within the LC is not responsible for alterations in FST-behavior, given that $Crh^{NA\text{-}COE}$ mice displayed no significant changes in floating time (Figure 24). Our result further support that noradrenergic activation is probably not caused by CRH expressing neurons within the LC, but rather by direct or indirect CRH innervations originating in other nuclei of the MHB.

However, this has to be confirmed, preferentially via *in vivo* microdialysis and/or analysis of immediate early gene (IEG) activation following acute stress in $Crh^{MHB\text{-}COE}$ and $Crh^{NA\text{-}COE}$ mice. Alterations in the CRH-system are commonly associated with changes in anxiety-related behavior. As shown in Section 4.1.1.1, ubiquitous CRH overexpression enhances anxiety, which has also been reported by others (Stenzel-Poore et al., 1994). To further specify the brain regions and neurotransmitter circuits responsible for regulating anxiety via central CRH, the EPM and DaLi test were conducted for the above described mouse lines.

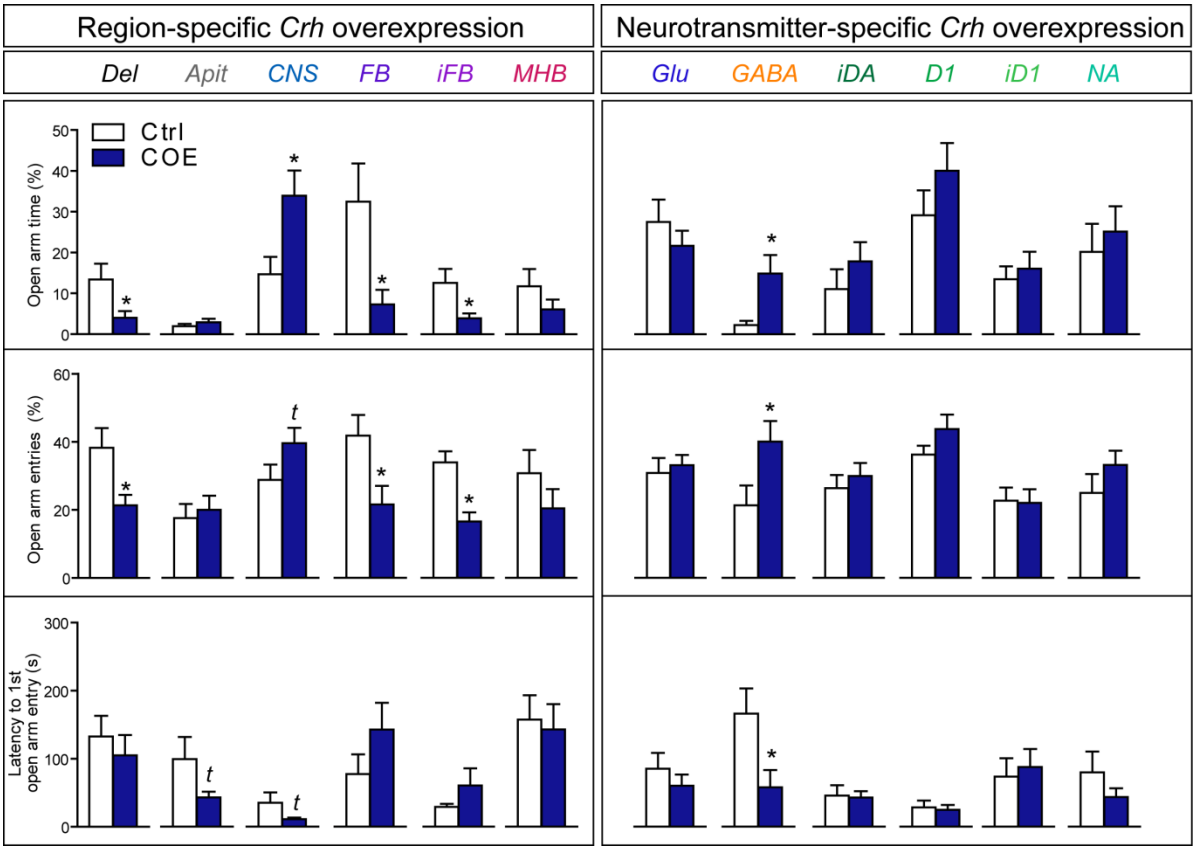

Figure 25: Overexpression of CRH in forebrain CAMK2α-positive and GABAergic neurons induces opposing anxiogenic and anxiolytic effects in the EPM.
$Crh^{FB\text{-}COE}$ and $Crh^{iFB\text{-}COE}$ mice spent less time on the aversive open arms of the EPM and entered these less frequently. The opposite was observed in $Crh^{GABA\text{-}COE}$ mice. Abbreviations: control (Ctrl), conditional CRH overexpression (COE), ubiquitous *Crh-OE* (*Del*), *CNS*-specific *Crh-OE* (*CNS*), forebrain-specific *Crh-OE* (*FB*), inducible forebrain-specific *Crh-OE* (*iFB*), mid/hindbrain-specific *Crh-OE* (*MHB*), *Crh-OE* in glutamatergic neurons (*Glu*), *Crh-OE* in GABAergic neurons (*GABA*), inducible *Crh-OE* in dopaminergic neurons (*iDA*), *Crh-OE* in D1-dopaminoceptive neurons (*D1*), inducible *Crh-OE* in D1-dopaminoceptive neurons (*iD1*), *Crh-OE* in noradrenergic neurons (*NA*). Refer to the main text for detailed description of the conditional mouse lines. *Significant from control; Student's t-test, $p < 0.05$, *t* trend, $p \leq 0.1$; n = 10-12.

Apart from ubiquitous CRH overexpressing mice, only $Crh^{FB\text{-}COE}$ and $Crh^{iFB\text{-}COE}$ mice displayed enhanced anxiety-related behavior depicted by decreased open arm time and entries in the EPM ($Crh^{FB\text{-}COE}$ *open arm time*: $t = 2.5$, $p < 0.05$; *open entries*: $t = 2.5$, $p < 0.05$ / $Crh^{iFB\text{-}COE}$ *open*

arm time: t = 2.4, p < 0.05; *open entries*: t = 4.1, p < 0.001) (Figure 25) and reduced lit zone time and number of entries in the DaLi (*Crh*$^{FB\text{-}COE}$ *lit zone time*: t = 2.8, p < 0.01; *lit entries*: t = 2.0, p = 0.06 / *Crh*$^{iFB\text{-}COE}$ *lit zone time*: t = 3.0, p < 0.01; *lit entries*: t = 2.3, p < 0.05) (Figure 26). This suggests an anxiogenic effect of CRH hyperdrive in forebrain limbic structures. In addition, these results mirror the low anxiety levels previously reported for forebrain-specific *Crhr1* knockout (*Crhr1*$^{FB\text{-}CKO}$) mice (Muller et al., 2003).

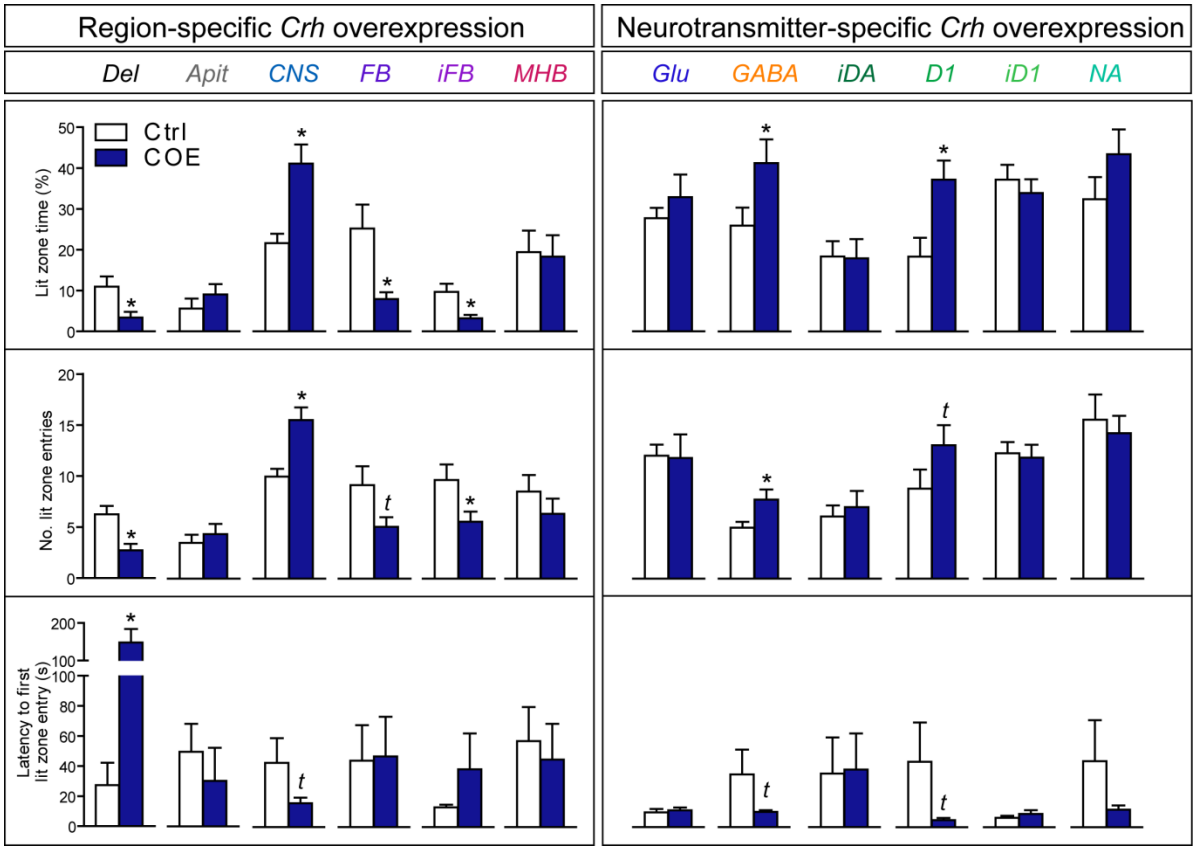

Figure 26: Overexpression of CRH in forebrain CAMK2α-positive and GABAergic neurons induces opposing anxiogenic and anxiolytic effects in the DaLi.
Crh$^{FB\text{-}COE}$ and *Crh*$^{iFB\text{-}COE}$ mice spent less time in, and made fewer entries to the aversive lit zone of the DaLi. The opposite was observed in *Crh*$^{GABA\text{-}COE}$ and *Crh*$^{D1\text{-}COE}$ mice. Abbreviations: control (Ctrl), conditional CRH overexpression (COE), ubiquitous *Crh-OE* (*Del*), *CNS*-specific *Crh-OE* (*CNS*), forebrain-specific *Crh-OE* (*FB*), inducible forebrain-specific *Crh-OE* (*iFB*), mid/hind brain-specific *CRH*-OE (*MHB*), *Crh-OE* in glutamatergic neurons (*Glu*), *Crh-OE* in GABAergic neurons (*GABA*), inducible *Crh-OE* in dopaminergic neurons (*iDA*), *Crh-OE* in D1-dopaminoceptive neurons (*D1*), inducible *Crh-OE* in D1-dopaminoceptive neurons (*iD1*), *Crh-OE* in noradrenergic neurons (*NA*). Refer to the main text for detailed description of the conditional mouse lines. *Significant from control; Student's t-test, p < 0.05, *t* trend, p ≤ 0.1; n = 10-12.

Importantly, *Camk2α*-mediated overexpression/deletion of *Crh/Crhr1* occurs during the second week of postnatal life (Minichiello et al., 1999; Refojo et al., 2011), or even later in case of *Camk2α-CreERT2*-mediated recombination. Thus, manipulations of the CRH/CRHR1 system during adulthood are responsible for the observed behavioral changes. In addition, similar

anxiety, but contrasting HPA-axis profiles of *Crhr1*$^{FB\text{-}CKO}$ and *Crhr1*$^{iFB\text{-}CKO}$ mice further support that behavioral alterations mediated by CRH occur independent of peripheral glucocorticoid action. Considering that CAMK2α is largely expressed in glutamatergic principal neurons of the cortex and hippocampus, it is surprising that anxiety remained unaffected in *Crh*$^{Glu\text{-}COE}$ mice which share a similar overexpression pattern with *Crh*$^{FB\text{-}COE}$ and *Crh*$^{iFB\text{-}COE}$ mice (Figure 19, 20 and 26). However, CAMK2α expression is also reported in GABAergic medium-spiny neurons of the striatum (Erondu and Kennedy, 1985; Mayford et al., 1996; Picconi et al., 2004; Klug et al., 2012), which is in line with the *LacZ*-expression maps (Figure 20). In addition, *Camk2α*-driven (in contrast to *Nex*-driven) CRH overexpression is present throughout the amygdala, BNST and septum (Figure 20). But whether these represent excitatory glutamatergic neurons is largely unknown. Thus, CRH overexpression from a distinct *Camk2α*-positive subpopulation of neurons seems to be inducing anxiety-enhancing effects. Further assessment of neurotransmitter-specific CRH-COE mouse lines revealed previously unidentified anxiolytic properties of CRH when overexpressed in GABAergic and/or D1-dopaminoceptive neurons. Both, *Crh*$^{GABA\text{-}COE}$ and *Crh*$^{D1\text{-}COE}$ mice made more entries and spent more time in the lit zone of the DaLi (*Crh*$^{GABA\text{-}COE}$ *lit zone time*: $t = 2.1$, $p < 0.05$; *lit entries*: $t = 2.4$, $p < 0.05$ / *Crh*$^{D1\text{-}COE}$ *lit zone time*: $t = 2.9$, $p < 0.05$; *lit entries*: $t = 1.6$, $p = 0.1$) (Figure 26). However, this decrease in anxiety-related behavior could only be confirmed for *Crh*$^{GABA\text{-}COE}$ mice in the EPM (*Crh*$^{GABA\text{-}COE}$ *open arm time*: $t = 2.7$, $p < 0.05$; *open arm entries*: $t = 2.2$, $p < 0.05$) (Figure 25). In addition, anxiety was not affected in inducible *Crh*$^{iD1\text{-}COE}$ mice, suggesting that CRH overexpression during development in *D1*-positive neurons is mediating the anxiolytic effect observed in the DaLi. Importantly, *Crh*$^{GABA\text{-}COE}$ mice show a strikingly similar anxiety and HPA-axis profile to that of *Crh*$^{CNS\text{-}COE}$ mice, which is further illustrated in Figure 28. However, the fact that locomotion was not changed in *Crh*$^{GABA\text{-}COE}$ mice argues against locomotor-induced alterations in anxiety. In addition, stress-coping behavior in the FST was also not affected in *Crh*$^{GABA\text{-}COE}$ mice, supporting that the decreased anxiety phenotype is not caused by a manic-like state previously observed in *Crh*$^{CNS\text{-}COE}$ mice (Figure 24 and Figure 28C). The pattern of CRH overexpression was verified in *Crh*$^{iFB\text{-}COE}$ and *Crh*$^{GABA\text{-}COE}$ mice by *ISH* using a riboprobe that detects endogenous as well as exogenous *Crh*, and is in line with Lu et al., 2008 (Figure 27). Importantly, differences in locomotion, stress-coping and anxiety-related behavior between the respective control groups (*Crh*$^{flopCrh/flopCrh}$ - white bars) are probably caused by the fact that not all behavioral experiments were performed in the same laboratory.

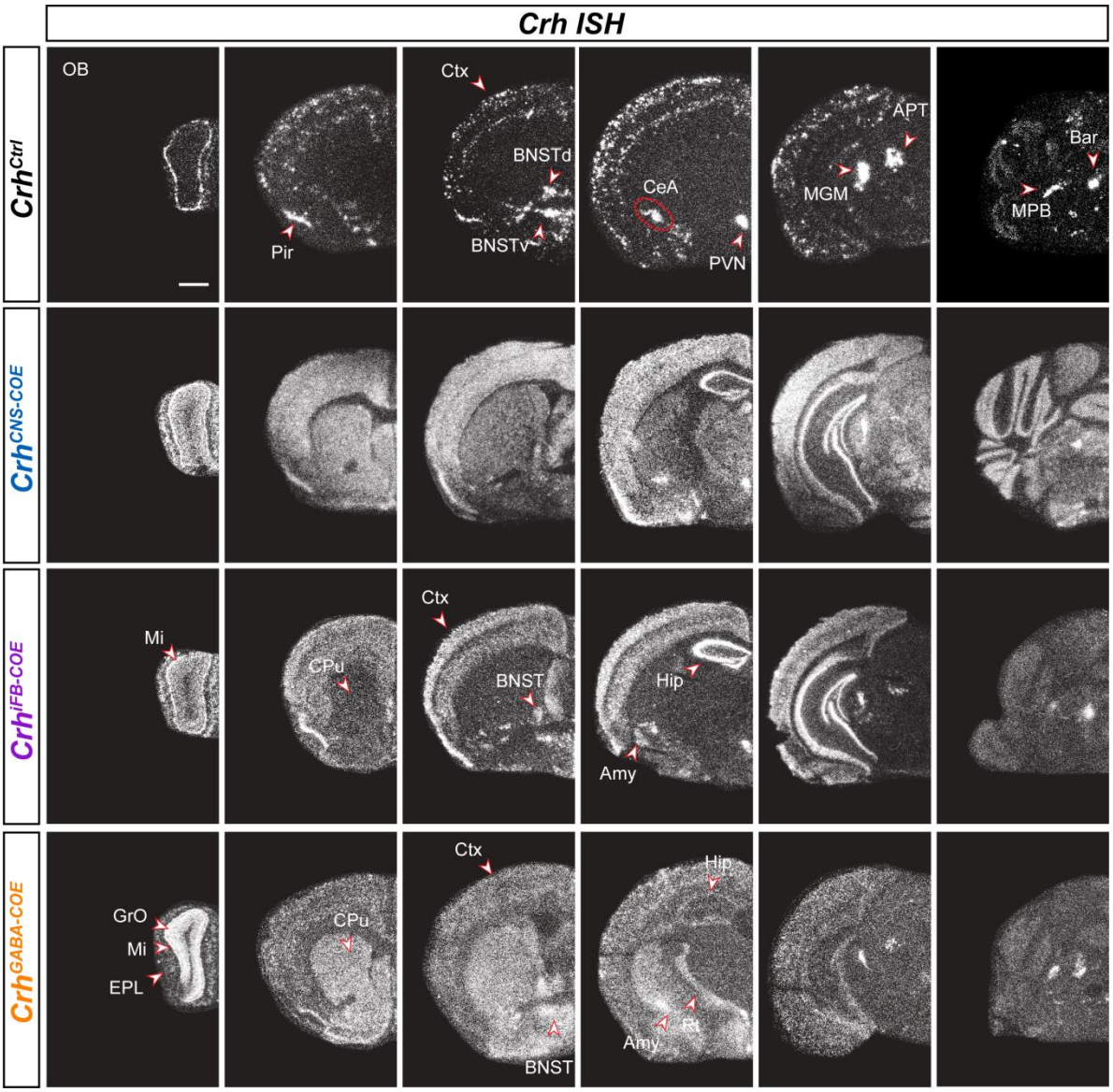

Figure 27: Confirmation of CRH overexpression in *Crh*$^{CNS\text{-}COE}$, *Crh*$^{iFB\text{-}COE}$, and *Crh*$^{GABA\text{-}COE}$ mice.
ISH using a *Crh*-specific riboprobe, which detects endogenous and exogenous *Crh*, confirmed distinctive overexpression patterns previously observed for *LacZ ISH* (Section 4.1.3). *Crh*$^{CNS\text{-}COE}$ (*CNS / Nestin-Cre*), *Crh*$^{iFB\text{-}COE}$ (inducible forebrain / *Camk2α-CreERT2*), *Crh*$^{GABA\text{-}COE}$ (GABAergic / *Dlx5/6-Cre*). Abbreviations: amygdala (Amy), anterior pretectal nucleus (APT), Barrington's nucleus (Bar), bed nucleus of the stria terminalis dorsal/ventral (BNSTd/v), cerebellum (Cb), central amygdala (CeA) caudate putamen (CPu), cortex (Ctx), hippocampus (Hip), medium geniculate nucleus (MGM), medial parabrachial nucleus (MPB), olfactory bulb (OB), olfactory bulb external plexiform layer (EPL), olfactory bulb granule cell layer (GrO), olfactory bulb mitral layer (Mi), piriform cortex (Pir), paraventricular nucleus of the hypothalamus (PVN), reticular thalmic nucleus (Rt). Scale bar represents 1 mm.

Moreover, due to space limitations many of the mouse lines were not bred and housed in the same animal facility, which might also have impacted baseline behavior. However, by utilizing littermate controls for all mouse lines in all experiments, we were able to control for these limitations. In conclusion, CRH overexpression in forebrain principal neurons enhances anxiety-related behavior whereas overexpression in GABAergic neurons produces the opposite effect

(Figure 28). These results highlight the ability of CRH to modulate anxiety-related behavior in opposite directions via different neurotransmitter circuits.

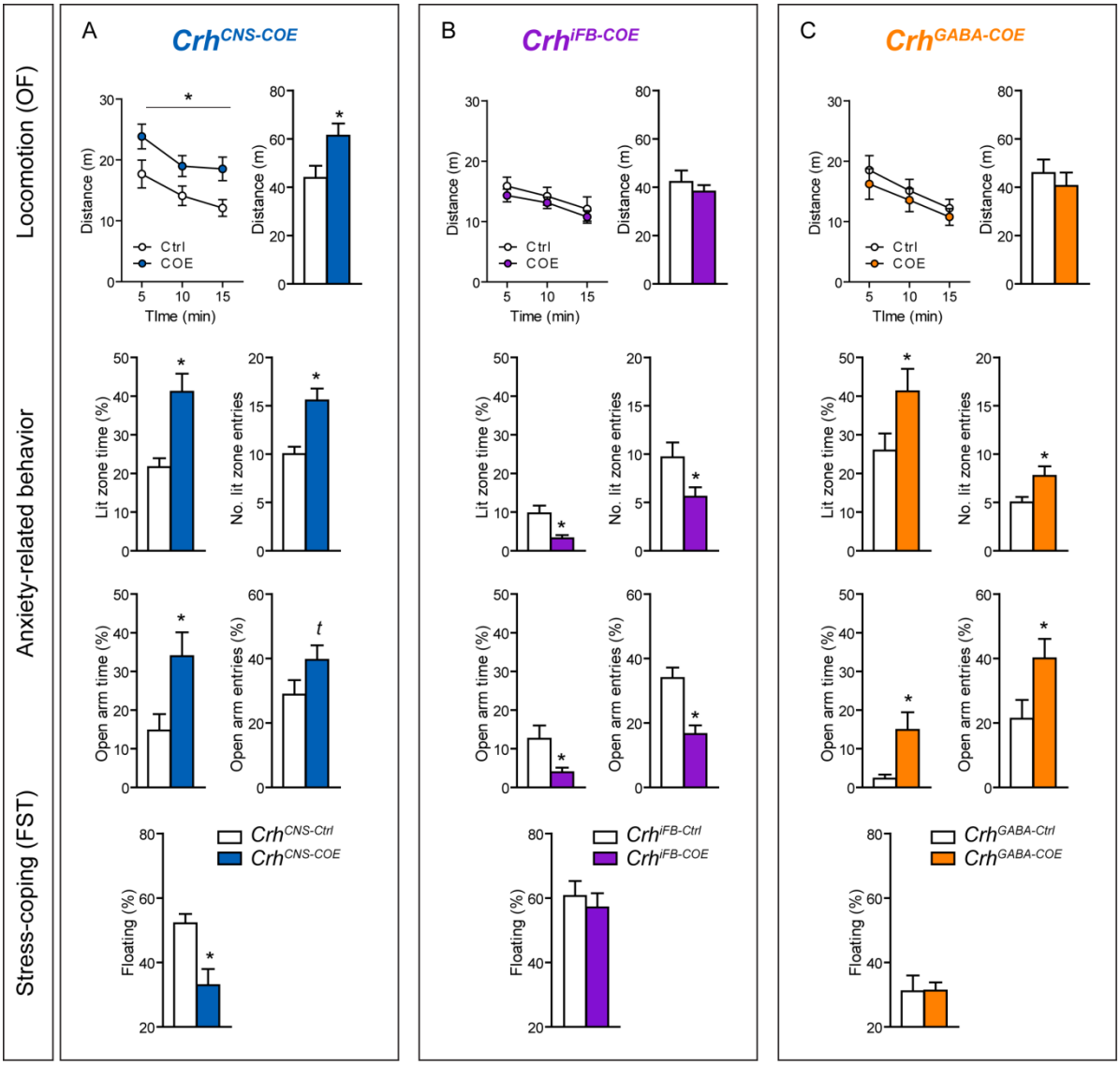

Figure 28: Overexpression of CRH in forebrain CAMK2α-positive and GABAergic neurons induces opposing anxiogenic and anxiolytic effects.

(A) Recapitulation of the manic-like phenotype in *Crh*$^{CNS\text{-}COE}$ mice, which display hyperactivity, decreased anxiety-related behavior and/or enhanced risk-assessment and increased active stress-coping behavior in the FST (decreased floating). **(B)** CRH overexpression in forebrain *Camk2α*-positive neurons enhances anxiety in the DaLi (*lit zone time*: t = 3.0, p < 0.01; *lit entries*: t = 2.3, p < 0.05) and EPM (*open arm time*: t = 2.4, p < 0.05; *open entries*: t = 4.1, p < 0.001) without altering locomotion and stress-coping behavior. **(C)** Contrastingly, overexpression in forebrain GABAergic neurons reduces anxiety in the DaLi (*lit zone time*: t = 2.1, p < 0.05; *lit entries*: t= 2.4, p < 0.05) and EPM (*open arm time*: t = 2.7, p < 0.05; *open entries*: t = 2.2, p < 0.05) without altering locomotion and active stress-coping behavior. *Significant from control; RM-ANOVA for time-dependent analysis, p < 0.05; Student's t-test, p < 0.05, *t* trend, p ≤ 0.1; n = 10-12.

4.1.3.2. Overexpression of CRH in GABAergic neurons enhances dopamine release in the PFC

The behavioral characterization of *Crh*$^{GABA\text{-}COE}$ mice revealed an unexpected anxiolytic phenotype, which has thus far not been described in other models of CRH excess or for exogenous CRH application. In most cases (and as shown in this study), CRH hyperdrive enhances arousal and induces anxiogenic-like behavior (Stenzel-Poore et al., 1994; Heinrichs and Joppa, 2001; Heinrichs and Koob, 2004). To assess whether CRH overexpression in GABAergic neurons would also alter stress-induced anxiety behavior, we subjected control and *Crh*$^{GABA\text{-}COE}$ mice to 15 min acute restrain stress. Anxiety-related behavior was analyzed in the 0-Maze one hour after restraint onset. Although the observed basal effects were milder than in the first batch (Figure 28), ANOVA revealed a significant genotype effect for all parameters, indicating decreased anxiety in *Crh*$^{GABA\text{-}COE}$ mice under basal and acute-stress conditions (Figure 30A). The fact that CNS-specific CRH overexpression decreases basal, but augments chronic stress-induced anxiety (Section 4.1.2.4) further suggest that modulation of different neurocircuits underlies the phenotype of *Crh*$^{GABA\text{-}COE}$ and *Crh*$^{CNS\text{-}COE}$ mice. In order to assess whether CRH overexpression in GABergic neurons acts via CRHR1 or CRHR2 to decrease anxiety, we applied a conditional strategy to overexpress UCN2 in GABAergic neurons (*Ucn2*$^{GABA\text{-}COE}$). UCN2 is a specific CRHR2-ligand and endogenously expressed in the PVN, supraoptice nucleus, LC and the brainstem of mice (Ryabinin et al., 2012). Although *Ucn2*$^{GABA\text{-}COE}$ displayed a trend towards decreased anxiety in the EPM, the effects did not reach statistical significance (Figure 29). Thus, the diminished anxiety-phenotype observed in *Crh*$^{GABA\text{-}COE}$ mice is primarily mediated via CRHR1.

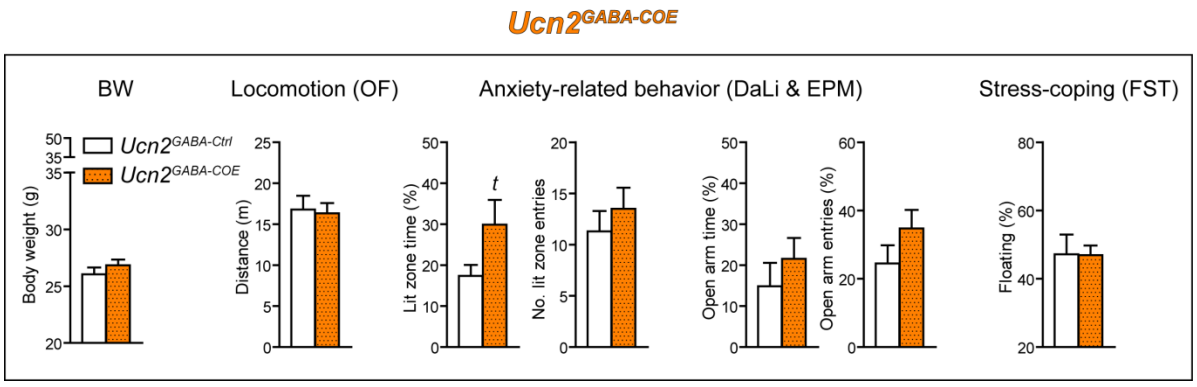

Figure 29: UCN2 overexpression in GABAergic neurons does not alter emotional behavior.
Body weight, locomotion, anxiety-related and stress-coping behavior were not altered *Ucn2*$^{GABA\text{-}COE}$ mice compared to control littermates. *t* trend, $p \leq 0.1$, Student's t-test; n = 12.

To further substantiate this, and considering that *Crh*$^{CNS\text{-}COE}$ mice display enhanced stress-induced noradrenaline release (unpublished data), we performed *in vivo* microdialysis to assess possible alterations in neurotransmitter release in *Crh*$^{CNS\text{-}COE}$ mice.The great advantage of microdialysis, compared to electrophysiological approaches or whole tissue-analysis, is that it enables the measurement of neurotransmitter concentrations in the extracellular space within the desired brain region of a living, freely moving animal (Anderzhanova and Wotjak, 2013). In this case, dopamine, serotonin, noradrenaline as well as their metabolites were measured in the prefrontal cortex (including the cingulate, prelimbic and infralimbic cortex) (Figure 30B). After probe implantation, mice were allowed to recover for one day in order to get accustomed to the wiring. To induce and mimic the emotional response displayed during behavioral testing in the EPM and/or DaLi, mice were placed onto a small circular but highly elevated platform (EP) for 20 min. In addition, this should raise the basal neurotransmitter content, which can drop below the analytical detection limit in resting, non-engaging animals (Anderzhanova and Wotjak, 2013). Dialysates samples were collected every 20 min. Basal neurotransmitter release is represented by the first six samples, collected prior to acute EP-stress. Additional seven samples were collected following acute-stress application. Neurotransmitter concentrations were subsequently determined using high performance liquid chromatography (HPLC) with an electrochemical detection system.

Dopamine release in the PFC was significantly elevated in *Crh*$^{GABA\text{-}COE}$ compared to control mice following EP-stress, illustrated by time-dependent dopamine (DA) measures (RM-ANOVA, time $F_{(12,288)} = 2.0$, $p < 0.05$; genotype $F_{(1,288)} = 7.4$, $p < 0.05$; Bonferroni post-test $p < 0.05$) as well as area under the curve (AUC) values ($t = 3.0$, $p < 0.01$)(Figure 30B). Similarly, dopamine metabolites, 3,4-dihydroxyphenylacetic acid (DOPAC) and homovanillic acid (HVA) were also elevated in acutely stressed *Crh*$^{GABA\text{-}COE}$ mice (*DOPAC:* RM-ANOVA, time $F_{(12,72)} = 2.4$, $p < 0.05$; genotype $F_{(1,72)} = 5.4$, $p = 0.058$ / *HVA:* RM-ANOVA, genotype $F_{(1,72)} = 4.9$, $p = 0.068$; time x genotype $F_{(12,72)} = 1.6$, $p = 0.09$ (Figure 30D). Importantly, noradrenaline and serotonin release were not affected by CRH overexpression in GABAergic neurons, which proves that different neurotransmitter circuits are affected by CNS-specific and GABAergic CRH overexpression (Figure 30C). Consequently, CRH appears to modulate anxiety-related behavior via the dopaminergic system whereas arousal/hyperactivity, as observed in manic-like *Crh*$^{CNS\text{-}COE}$ mice results from CRH-mediated activation of the noradrenergic system.

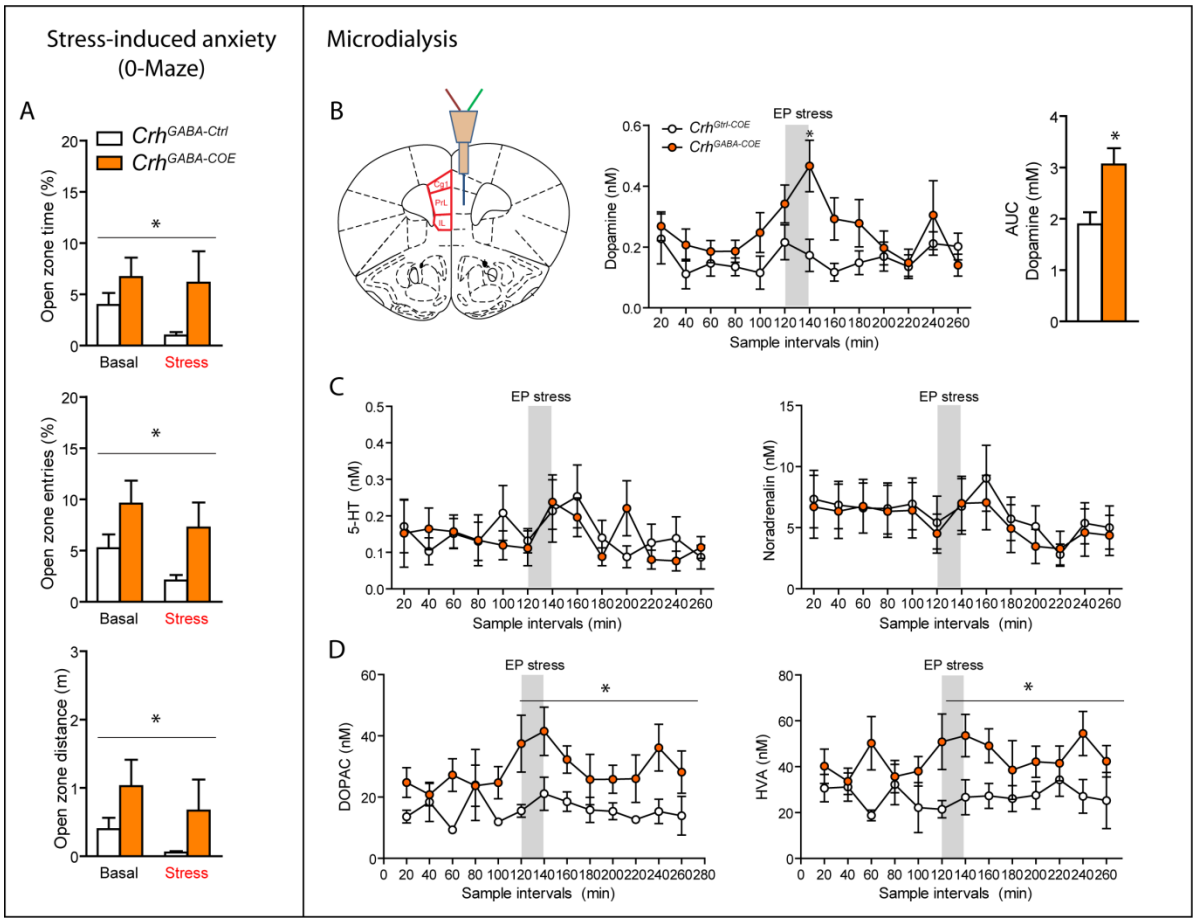

Figure 30: *Crh*$^{GABA\text{-}COE}$ mice display reduced susceptibility to acute restraint stress and enhanced stress-induced dopamine release in the prefrontal cortex.

(A) Open arm time (2-Way ANOVA, genotype $F_{(1,44)} = 4.2$, $p < 0.05$), open arm entries (2-Way ANOVA, genotype $F_{(1,44)} = 6.7$, $p < 0.05$), and open arm distance (2-Way ANOVA, genotype $F_{(1,44)} = 3.9$, $p = 0.05$) were increased in *Crh*$^{GABA\text{-}COE}$ mice under basal and acute-stress conditions. **(B)** Microdialysis probes were implanted in the PFC. Dopamine release was significantly enhanced in *Crh*$^{GABA\text{-}COE}$ mice following EP-stress. **(C)** Serotonin (5-HT) and noradrenalin concentration were not differentially affected in *Crh*$^{GABA\text{-}COE}$ mice. **(D)** Dopamine metabolites were increased in *Crh*$^{GABA\text{-}COE}$ mice following EP-stress. Abbreviations: area under the curve (AUC), conditional overexpression (COE), elevated platform (EP), 3,4-dihydroxyphenylacetic acid (DOPAC), homovanillic acid (HVA). *Significant from control; RM-ANOVA or 2-Way ANOVA, $p < 0.05$; Bonferroni post-test, $p < 0.05$; Student's t-test for AUC, $p < 0.05$; n = 10-13.

4.2. Glutamatergic and dopaminergic neurons mediate anxiogenic and anxiolytic effects of CRHR1

The results depicted in the previous sections demonstrate the versatility of conditional CRH overexpressing mice. For one, we could show that CNS-specific CRH overexpressing mice represent a disease models with strong face and predictive validity, which is highly relevant considering that depression and anxiety-related disorders, are often accompanied by excessive glucocorticoids and elevated CRH levels in the cerebrospinal fluid (Nemeroff et al., 1984; Lowy et al., 1984; Peeters et al., 2004). Second, the generated region- and neurotransmitter-specific CRH overexpressing lines represent highly valuable genetic tools, aiding in the dissection of the organism's major stress-integrating system. In this regard, we could show that CRH has the ability to induce negative and positive emotional responses depending on the site of overexpression. However, the lack of construct validity and uncertainties that arise with ectopic CRH expression cannot be neglected and represent a major disadvantage of the above described overexpression mouse models. This makes it extremely difficult to accurately address endogenous CRH circuits, considering that we are ectopically expressing CRH in neurons which normally do not synthesize it, possibly resulting in non-physiological activation of both CRHR1 and CRHR2. Importantly, one fundamental question cannot be completely resolved with the overexpression-approach, that is: Which receptors are mediating the observed effects and where are they located? Mutant CRHR1 mice have provided crucial information in this regard. Total and forebrain-specific CRHR1 knockout mice exhibit reduced anxiety-related behavior, which is not influenced by CNS-effects of circulating stress hormones (Timpl et al., 1998; Muller et al., 2003). In addition, forebrain CRHR1 deficiency has been shown to attenuate chronic stress-induced cognitive deficits and dendritic remodeling (Wang et al., 2011a). Importantly, while the effects of CRHR1 on anxiety are well established, the role of CRHR2 in mood-related behavior is debated. However, the exact brain structures and circuits mediating anxiety-like behavior via CRHR1 remain largely unknown. To tackle this, it was of utter importance to first identify the neurochemical identity of CRHR1-expressing neurons, which is not easy given the low endogenous expression levels of CRHR1 and the lack of reliable antibodies (Refojo et al., 2011). Thus, two strategies were applied in our lab to solve these questions. First, a sensitive double *ISH* method was established and used to assess the co-localization between *Crhr1* and different neurotransmitter markers at the mRNA level. Second, a new CRHR1 knockin mouse line, which reports *Crhr1* expression via GFP ($Crhr1^{\Delta Egfp}$) was generated (Refojo et al., 2011). To unravel the neurochemical identity of CRHR1 neurons,

double IHC was applied using antibodies against neuronal identity markers and against GFP in *Crhr1*$^{\Delta Egfp}$ mice. CRHR1 was shown to be primarily expressed in glutamatergic (Glu) neurons of the cortex, hippocampus and basolateral amygdala; in GABAergic neurons of the olfactory bulb, reticular thalamic nucleus, globus pallidus, and septum; and in dopaminergic neurons of the substantia nigra pars compacta (SNpc) and ventral tegmental area.

	Relative expression strength		Colocalization Score	NT specific *Crhr1-KO* line showing Crhr1 deletion
Brain Region	Crhr1	NT		
Olfactory bulb (OB)	++++	Glu ++ GABA ++++	+ +++	*Crhr1*$^{GABA\text{-}CKO}$
Cortical layer (II/III, IV)	+++	Glu +++ GABA ++	+++ +	*Crhr1*$^{Glu\text{-}CKO}$
Hippoocampus (Hip)	+++	Glu +++ GABA +	+++ -/+	*Crhr1*$^{Glu\text{-}CKO}$
Reticular thalamic nucleus (RTN)	+++	GABA ++++	++++	*Crhr1*$^{GABA\text{-}CKO}$
Zona incerta (Zi)	++	GABA ++	++	*Crhr1*$^{GABA\text{-}CKO}$
Medial septum (MS)	+++	GABA ++++	+++	*Crhr1*$^{GABA\text{-}CKO}$
Lateral septum (LS)	++	GABA ++	++	*Crhr1*$^{GABA\text{-}CKO}$
Bed nucleus of the stria terminalis (BNST)	+++	GABA ++	++	*Crhr1*$^{GABA\text{-}CKO}$
Basolateral amygdal (BLA)	+++	Glu ++	++	*Crhr1*$^{Glu\text{-}CKO}$
Medial amygdala (MeA)	++	GABA ++	++	*Crhr1*$^{GABA\text{-}CKO}$
Globus pallidus (GP)	++++	GABA ++++	++++	*Crhr1*$^{GABA\text{-}CKO}$
Substantia nigra (SN) pars compacta	+++	DA ++++	++++	*Crhr1*$^{DA\text{-}CKO}$
Substantia nigra (SN) pars reticularis	++	GABA +++	+	-
Ventral tegmental area (VTA)	+++	DA +++	+++	*Crhr1*$^{DA\text{-}CKO}$
Raphe nuclei (RN)	+	5HT +++	+	-

Table 18: Expression map and neurochemical identity of CRHR1-positive neurons in the mouse brain.
Summary of double ISH and double IHC expression studies illustrating the strength, distribution and NT-colocalization of *Crhr1* mRNA as well as the deletion pattern found in the NT-specific *Crhr1*^{CKO} lines. *Crhr1* expression levels are indicated with crosses in the second column and the signal intensity observed for the NT-specific markers is indicated with crosses in the third column. Ratings reflect primarily the density of positive neurons with (-) representing a lack of staining, (+) isolated positively labelled cells and (++++) labelling in a substantial majority of cells in a given cell group or fields. From Refojo et al., 2011.

Just a very few serotonergic neurons of the dorsal and medial raphe nuclei expressed CRHR1 (Refojo et al., 2011). A systematic neurochemical map of CRHR1 expression in different

neurotransmitter populations is shown in Table 18. Bearing in mind that limbic *Crhr1* knockout mice display reduced anxiety-related behavior, and the fact that we observed bidirectional modulated of anxiety in different CRH overexpressing mice, we wanted to specifically address the underlying neurotransmitter circuits that modulate this specific emotional response via CRHR1. In order to genetically dissect the specific involvement of CRHR1 in distinct neuronal populations conditional mutagenesis was applied (Figure 31). Previously generated *Crhr1*$^{flox/flox}$ mice (Muller et al., 2003) were mated with different neurotransmitter-specific Cre lines to obtain *Crhr1*$^{Glu\text{-}CKO}$ (*Crhr1* deletion in forebrain glutamatergic neurons using *Nex-Cre* mice), *Crhr1*$^{GABA\text{-}CKO}$ (*Crhr1* deletion in forebrain GABAergic neurons using *Dlx5/6-Cre* mice), *Crhr1*$^{iDA\text{-}CKO}$ (inducible *Crhr1* deletion in midbrain dopaminergic neurons using *Dat-CreERT2* mice), and *Crhr1*$^{5\text{-}HT\text{-}CKO}$ (*Crhr1* deletion in brainstem serotonergic neurons using *ePet-Cre* mice) (Figure 31). The pattern of *Crhr1* deletion in all conditional knockout lines perfectly mirrored the expression maps traced with the histochemical mapping (Table 18) and emphasizes the selectivity of the neurotransmitter-specific deletion properties of the Cre-recombinase lines (Refojo et al., 2011).

To functionally dissect the neuronal subpopulations mediating the effects of CRHR1 on anxiety-related behavior, neurotransmitter-specific CKO mice were subjected to the OF, EPM, DaLi, modified hole board (MHB) and novel object exploration test (NOET). *Crhr1*$^{Glu\text{-}CKO}$ mice showed reduced anxiety-like behavior compared to control littermates, which is depicted by increased lit compartment time and number of entries in the DaLi (Figure 32B), and enhanced open arm time and number of entries in the EPM (*DaLi*: lit time, $U = 25.0$, $p < 0.01$; lit entries, $U = 33.5$, $p < 0.05$ / *EPM*: open arm time, $U = 35$, $p < 0.05$; open arm entries, $U = 32.0$, $p < 0.01$)(Figure 32C). *Crhr1*$^{Glu\text{-}CKO}$ mice also spent more time exploring the novel object, further confirming the diminished anxiety phenotype ($U = 2.1$, $p < 0.05$)(Figure 32E). In addition, *Crhr1*$^{Glu\text{-}CKO}$ mice spent more time on the board ($t = 1.63$, $p = 0.11$) and also showed more entries ($t = 1.44$, $p = 0.16$) during the MHB test. Consequently, previously reported anxiogenic effects of limbic CRHR1 are mediated by CRHR1 on forebrain glutamatergic neurons. In addition, limbic forebrain-specific deletion of *Crhr1* was initiated during postnatal week 2, suggesting that manipulation of the CRH/CRHR1-system during adulthood is responsible for the behavioral changes observed in *Crhr1*$^{Glu\text{-}CKO}$ mice. No changes in anxiety-related behavior were observed in *Crhr1*$^{GABA\text{-}CKO}$ and *Crhr1*$^{5\text{-}HT\text{-}CKO}$ mice (Refojo et al., 2011).

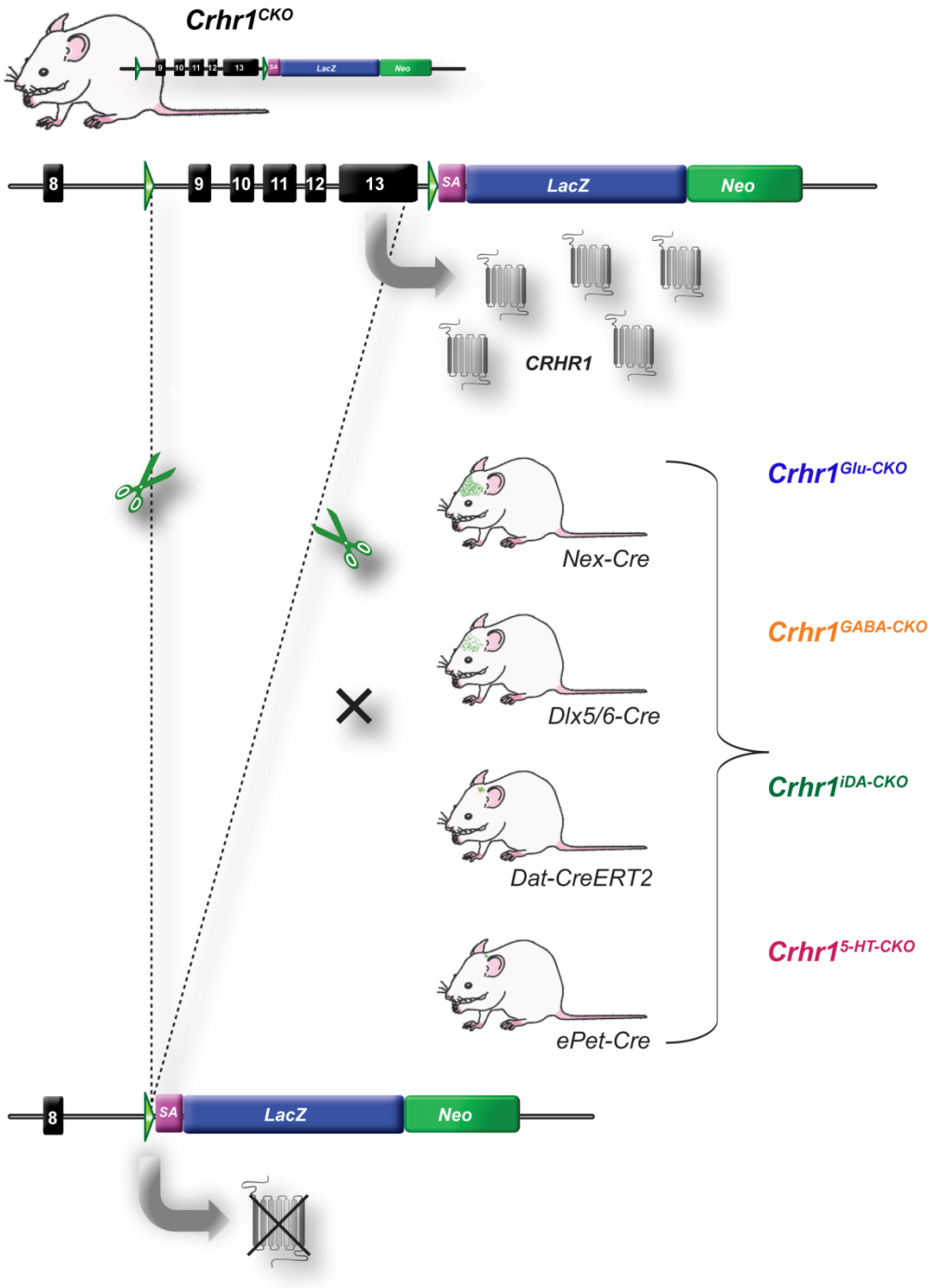

Figure 31: Strategy for conditional, neurotransmitter-specific deletion of *Crhr1*.
Schematic representation of previously established conditional inactivation of the *Crhr1* gene (Muller et al., 2003). Exons 9-13 are flanked by *loxP* sites. An engrailed 2 splice-acceptor (*SA*) fused to a β-galactosidase and a PGK-neomycin cassette is located 3' of exon 13. Breeding to different Cre-lines (Cre-recombinase expression pattern depicted in green) cleaves exons 9-13, resulting in *Crhr1* inactivation. Generated mouse lines: $Crhr1^{Glu\text{-}CKO}$ (deletion in glutamatergic neurons / *Nex-Cre*), $Crhr1^{GABA\text{-}CKO}$ (deletion in GABAergic neurons / *Dlx5/6-Cre*), $Crhr1^{iDA\text{-}CKO}$ (inducible *Crhr1* deletion in dopaminergic neurons / *Dat-CreERT2*), and $Crhr1^{5\text{-}HT\text{-}CKO}$ (deletion in serotonergic neurons / *ePet-Cre*). *Crhr1* exons are indicated as black boxes, the *loxP* sites as green arrowheads.

Interestingly, deletion of *Crhr1* from midbrain dopaminergic neurons increased anxiety-related behavior in the DaLi, EPM, NOET and MHB (*DaLi*: lit time, U = 48.5, p < 0.05; lit entries, U = 37.0, p < 0.01 / *EPM*: open arm time, U = 80, p < 0.05; open arm entries, U = 74.5, p < 0.05 / *MHB*: board time, t = 2.1, p < 0.05; board entries, t = 1.9, p < 0.05 / *NOET*: time, t = 2.5, p < 0.05) (Figure 32G).

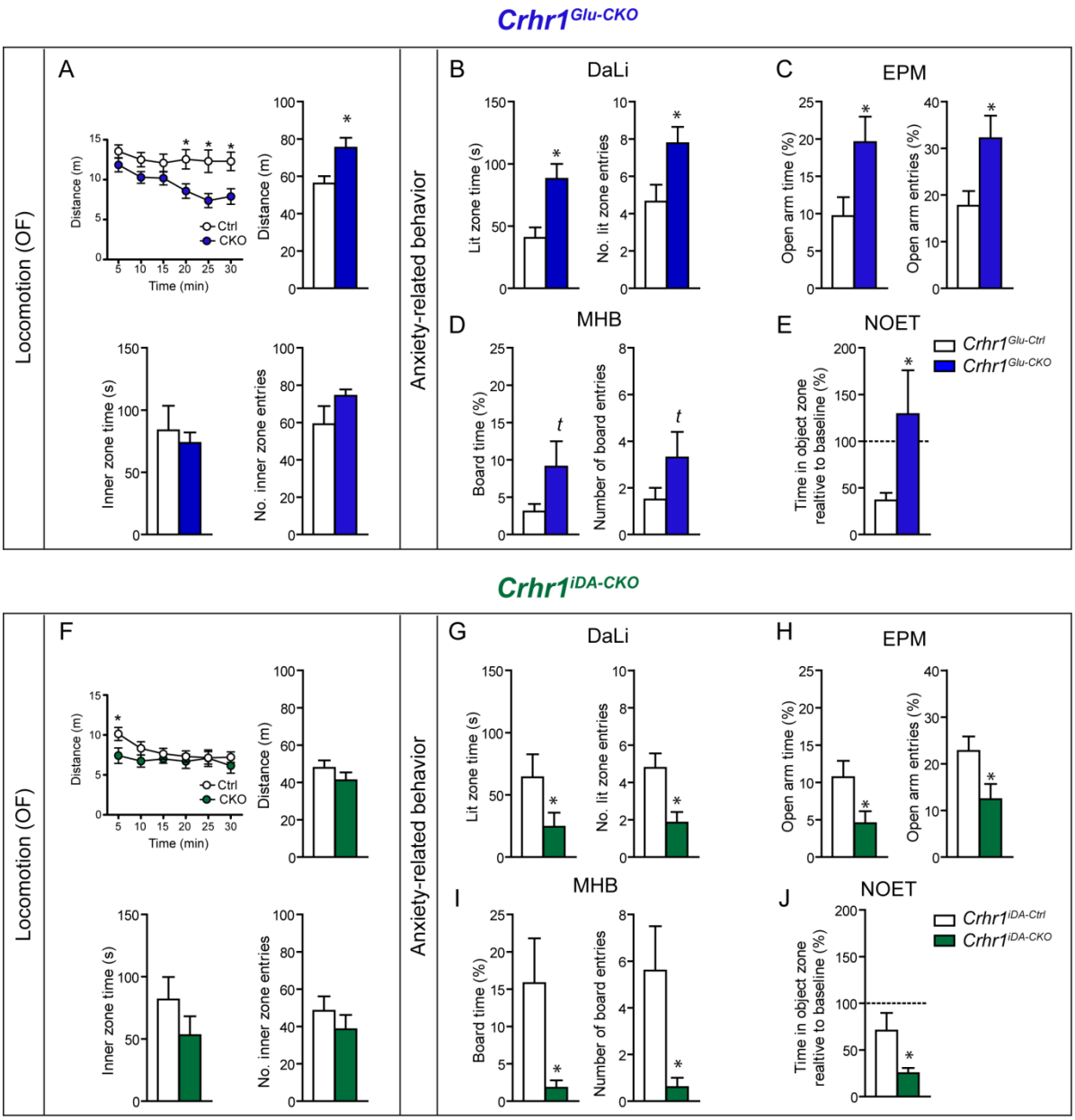

Figure 32: *Crhr1* exerts anxiogenic and anxiolytic effects via glutamatergic and dopaminergic neurons.
(A) Deletion of *Crhr1* from forebrain glutamatergic neurons decreased locomotion during the last segments of the OF, but had no effect on inner zone time or number of entries. **(B-E)** $Crhr1^{Glu\text{-}CKO}$ mice exhibited reduced anxiety-related behavior in several paradigms including the DaLi, EPM, MHB and NOET. **(F)** Deletion of *Crhr1* from dopaminergic neurons reduced locomotion during the 1st 5min, but had not effect on inner zone time or number of entries. **(G-J)** $Crhr1^{iDA\text{-}CKO}$ mice showed increased anxiety-related behavior in the DaLi, EPM, MHB and NOET. *Significant from control; RM-ANOVA for time-dependent analysis, p < 0.05; Student's t-test for parametric data, p < 0.05; Mann-Whitney test for non-parametric data; p < 0.05; *t* trend, p ≤ 0.1; n = 10-16. Published in Refojo et al., 2011.

Crhr1$^{iDA\text{-}CKO}$ additionally displayed decreased locomotion during the first 5 min of the open field test, suggesting increased novelty-induced anxiety (Figure 32F), which was not observed in *Crhr1*$^{Glu\text{-}CKO}$ mice (Figure 32A). However, *Crhr1*$^{Glu\text{-}CKO}$ mice exhibited reduced locomotion during the last segment of the OF (Figure 32A). However, this does not confine the interpretation of the previous tests, because the effect was established 20 min after test onset, whereas anxiety is assessed during the initial 5-10 min of apparatus exposure. Importantly, the observed behavioral differences were independent of alterations in HPA axis, which was indistinguishable between knockout and control mice (Refojo et al., 2011). Further behavioral analysis of tone-dependent fear conditioning did not demonstrate significant differences between any of the NT-knockout lines and their respective controls (Refojo et al., 2011). Along these lines, active stress-coping behavior was also not affected by neurotransmitter-specific deletion of the receptor, suggesting a specific role of glutamatergic and dopaminergic *Crhr1* in anxiety. To unravel possible molecular correlates of behavior and to further assess the interaction between *Crhr1* and glutamatergic/dopaminergic neurotransmission, electrophysiological recordings and microdialysis were applied. These experiments additionally revealed that CRH enhances excitatory neurotransmission in the BLA via *Crhr1* on glutamatergic neurons (Refojo et al., 2011). Furthermore, activation of *Crhr1* (which would occur during responses to stress) specifically modulates glutamatergic neurotransmission, producing an amplification of neuronal excitation in the hippocampal DG-CA3-CA1 network (Refojo et al., 2011). *In vivo* microdialysis revealed a decreased response to stress-induced dopamine-release in the PFC of *Crhr1*$^{iDA\text{-}CKO}$ mice compared to controls (RM-ANOVA, time $F_{(5,70)}$ = 11.2, $p < 0.0001$; genotype time $F_{(1, 70)}$ = 6.5, $p < 0.05$) as shown in Figure 33 (Refojo et al., 2011).

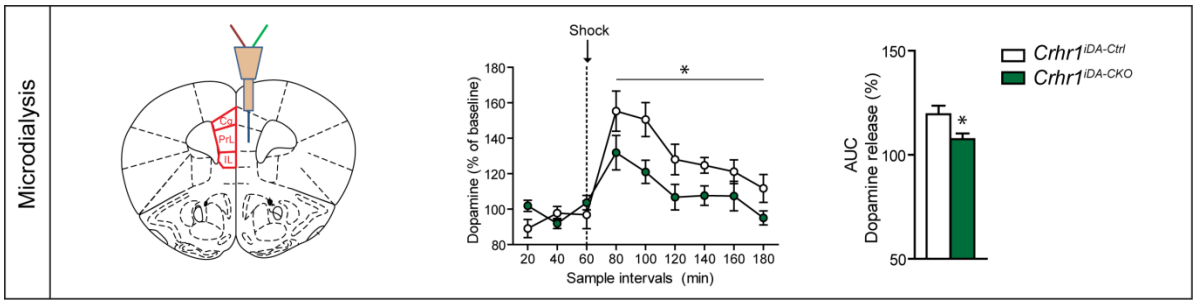

Figure 33: *Crhr1*$^{iDA\text{-}CKO}$ mice exhibit diminished stress-induced dopamine release in the PFC.
Microdialysis probes were implanted in the PFC - including the cingulate cortex (Cg), prilimbic cortex (PrL) and infralimbic cortex (IL). Dopamine release was significantly reduced in *Crhr1*$^{iDA\text{-}COE}$ mice following single footshock-stress, which is depicted by the dopamine-release curve and area under the curve (AUC) statistics ($t = 2.6$, $p < 0.05$). Experiments performed by Stefani Ehrenberg. Published in Refojo et al., 2011.

Our results highlight once more the dual role of the CRH/CRHR1 system in anxiety-modulation. Whereas deletion of CRHR1 from glutamatergic neurons reduced anxiety, the opposite was observed upon ablation of the receptor from dopaminergic neurons. This suggests that under physiological conditions, CRH/CRHR1-controlled glutamatergic and dopaminergic systems might function in a concerted but antagonistic manner to keep adaptive anxiety responses to stressful situations in balance (Refojo et al., 2011). Thus, CRH hyperactivity, which is observed in many patients suffering from emotional disorders, might not be general but restricted to particular neuronal circuits, triggering symptoms by generating an imbalance between CRHR1-controlled glutamatergic and dopaminergic systems involved in emotional behavior (Refojo et al., 2011). Notably, the ability of CRH to produce positive emotional responses was also observed in neurotransmitter-specific CRH overexpressing mice (Section 4.1.3). The involvement of the dopaminergic system in CRH-mediated positive emotional responses appears especially interesting, considering that CRH x dopamine interactions were thus far mainly implicated in the context of addiction (George et al., 2012; Haass-Koffler and Bartlett, 2012). The fact that *Crh*$^{GABA\text{-}COE}$ mice display reduced anxiety and increased dopamine release promotes the hypothesis that CRH, released from GABAergic projection neurons, activates dopaminergic CRHR1 receptors in the VTA/SNc, which in turn modulate dopamine release. The ability of CRH to potentiate dopaminergic neurotransmission has been shown by previous studies; but whether this occurs via direct or indirect activation of the VTA is still a matter of debate (Rodaros et al., 2007; Wise and Morales, 2010; George et al., 2012; Lemos et al., 2012; Silberman et al., 2013). Thus, two important questions arise at this point. First: Are the observed effects really mediated by GABAergic neurons which endogenously express CRH (which might not be the case in *Crh*$^{GABA\text{-}COE}$ mice)? Second: To which structures can we trace these CRH neurons? Consequently, a precise neurochemical characterization of CRH neurons, as well as a systematic analysis of their projection sites is mandatory in order to identify the “anxiogenic” and “anxiolytic” CRH neurons.

4.3. Spiny CAMK2α-expressing CRH neurons are required for positive emotional responses

4.3.1. CRH is expressed in GABAergic interneurons and long-range projection neurons

As demonstrated in the previous section, our group was able to identify anxiety-regulating CRHR1-sites, illustrating opposing effects of the receptor in glutamatergic and dopaminergic neurons. In order to locate the responsible CRH-producing neurons, we first set out to determine their neurochemical identity. To date the cellular and subcellular localization of CRH has mainly been investigated in the hippocampus, where its expression has been assigned to GAD65/67-positive GABAergic interneurons including parvalbumin co-expressing basket cells (Yan et al., 1998; Chen et al., 2004c). However, only a few studies have investigated the cellular subpopulation of other CRH-expressing brain regions. In the cortex, CRH expression was localized predominately to vasoactive intestinal polypeptide (VIP) and/or cholecystokinin (CCK)-positive GABAergic neurons (Gallopin et al., 2006; Kubota et al., 2011). Similarly, CRH-expressing cells in the central amygdala (CeA) and oval bed nucleus of the stria terminalis (BNST) are predominately GABAergic (Day et al., 1999). Using a sensitive double *ISH* method, we set out to analyze the neurochemical-identity of CRH expressing neurons more thoroughly. This method was preferred to a double IHC-approach considering that neuropeptides are located predominately in fibers, making it difficult to identify the CRH-producing soma. Another disadvantage is given by the lack of reliable CRH-antibodies. Simultaneous detection of ^{35}S-labeled CRH and DIG-labeled, glutamic acid decarboxylase 65 and 67 (*Gad65/67*) riboprobes revealed predominant expression of *Crh* in GABAergic neurons of the cortex and most limbic structures. Approximately 80-90% of *Crh*-expressing neurons in the olfactory bulb (OB), dorsal/ventral BNST, nucleus accumbens shell (AscSh), CeA, lateral hypothalamic area (LHA), hippocampus (Hip), and about 60-70% in the cortex/prefrontal cortex (PFC) co-localized with the GABAergic markers *Gad65/67* (Figure 34). Minimal to no co-expression was observed in the piriform cortex (Pir), PVN, medial geniculate nucleus (MGM), anterior pretectal area (APT) and Barrington's nucleus (Bar) (Figure 34). Co-localization scores for each structure are additionally summarized in Table 19, Section 4.3.5. Importantly, these numbers are based on rough estimations and need to be verified by exact cell counts in the future.

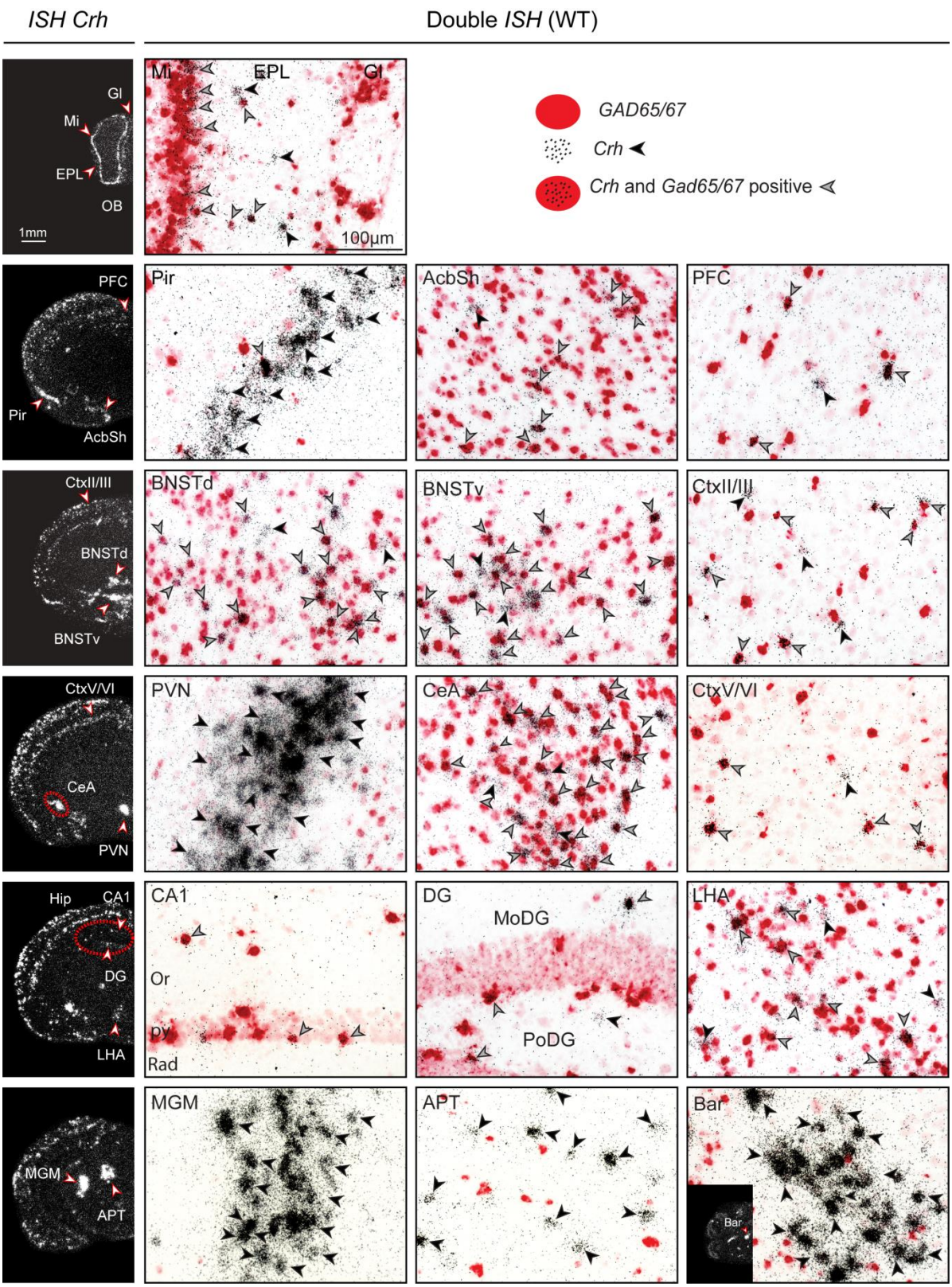

Figure 34: Limbic *Crh* is expressed in *Gad65/67*-positive GABAergic neurons.
The first left column depicts dark-field photomicrographs of the *Crh* mRNA expression pattern in brain sections of wild-type mice. Regions of interest are highlighted with red arrowheads and dashed lines. The additional columns represent bright field photomicrographs of coronal wild-type brain sections showing double *ISH* of *Crh* mRNA (silver grains) together with the glutamic acid decarboxylase 65 and 67 (*Gad65/67,* red staining). Black arrowheads indicate cells only expressing *Crh* (silver grains). Grey arrowheads indicate cells co-expressing *Crh* and *Gad65/67*. Abbreviations: nucleus accumbens shell (AcbSh), anterior pretectal

nucleus (APT), Barrington's nucleus (Bar), bed nucleus of the stria terminalis dorsal/ventral (BNSTd/v), central nucleus of the amygdala (CeA), cortical layers (CtxII/III, CtxV/VI), dentate gyrus (DG), molecular layer of DG (MoDG), polymorph DG (PoDG), hippocampus (Hip), hippocampal CA1 (CA1), pyramidal layer Hip (py), radiatum layer Hip (Rad), oriens layer Hip (Or), lateral hypothalamic area (LHA), medial geniculate nucleus (MGM), olfactory bulb (OB), olfactory bulb external plexiform layer (EPL), olfactory bulb granule cell layer (Gl), olfactory bulb mitral layer (Mi), piriform cortex (Pir), prefrontal cortex (PFC), paraventricular nucleus of the hypothalamus (PVN).

In order to determine whether some of the non-GABAergic CRH neurons express glutamatergic markers, additional double *ISHs* were performed against *Crh* and the vesicular glutamate transporter 1 (*VGlut1*) encoded by the *Slc17a*7 gene. The majority of *Crh*-expressing cells in the Pir co-localized with *VGlut1* (Figure 35). However, only a few single *Crh* neurons in the OB, Ctx, PFC, LHA, MGM, and hippocampus were glutamatergic. Minimal to no co-localization was observed in the CeA, BNST, PVN, APT, and Bar (Figure 35). Our results demonstrate that CRH expression in the cortex, PFC, BNST, CeA, Hip and LHA is predominately restricted to *Gad65/67*-positve, GABAergic neurons, which is in line with previous studies (Day et al., 1999; Kubota et al., 2011; Chen et al., 2012b). Notably, roughly 30-40% of cortical *Crh* neurons did not co-express *Gad65/67*. The fact that only few cortical *Crh* cells expressed *VGlut1* might indicate the presence of an additional subpopulation of yet uncharacterized CRH neurons. Importantly, *VGlut1* is predominately expressed in the cortex, hippocampus, and cerebellum which emphasizes the necessity of co-localization studies with additional glutamatergic markers such *VGlut2*, which is mainly synthesized in the thalamus and hypothalamus (Fremeau, Jr. et al., 2001; Fremeau, Jr. et al., 2004).

The majority of published data support the notion that cortical, hippocampal and amygdalar CRH is contained within GABAergic interneurons (Kubota et al., 2011; Chen et al., 2012b), whereas its post-synaptic element, CRHR1, resides in excitatory glutamatergic neurons (Refojo et al., 2011). However, CRH release sites and modes of travel to target receptors remain largely unknown. In addition, consensus is missing as to whether CRHR1 is located perisomatically, in axon-initial segments, dendritic spine heads, dendritic shafts, or all of the mentioned. Tallie Z. Baram and colleagues proposed the so called "mis-matched" hippocampal CRH synapse. Their data supports the notion that CRH is released from interneurons in the hippocampal pyramidal cell layer where it diffuses locally, via volume transmission to act on CRHR1 at relatively distant post-synaptic sites (Chen et al., 2012b). However, the specific and differential effects observed in our CRH overexpressing mouse lines argue against the idea that CRH effects are mediated via volume transmission over larger distances, but rather favor a mechanism involving specific synaptic release.

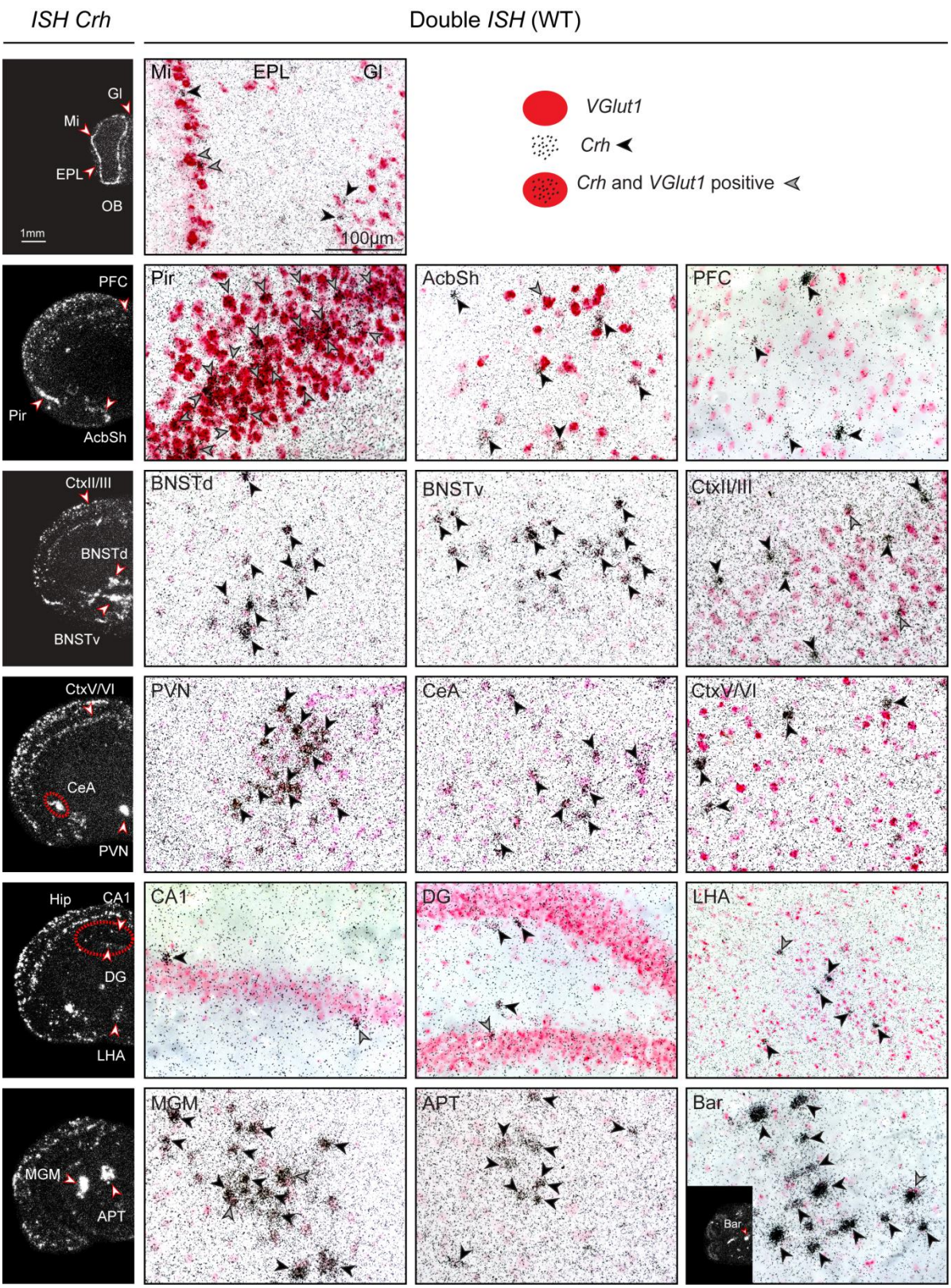

Figure 35: *Crh* is expressed in *VGlut1*-positive, glutamatergic neurons of the piriform cortex.
The first left column depicts dark-field photomicrographs of the *Crh* mRNA expression pattern in brain sections of wild-type mice. Regions of interest are highlighted with red arrowheads and dashed lines. The additional columns represent bright field photomicrographs of coronal wild-type brain sections showing double *ISH* of *Crh* mRNA (silver grains) together with the vesicular glutamate transporter 1 (*VGlut1,* red staining). Black arrowheads indicate cells only expressing *Crh* (silver grains). Grey arrowheads indicate cells coexpressing *Crh* and *VGlut1*. Abbreviations: nucleus accumbens shell (AcbSh), anterior pretectal nucleus

(APT), Barrington's nucleus (Bar), bed nucleus of the stria terminalis dorsal/ventral (BNSTd/v), central nucleus of the amygdala (CeA), cortical layers (CtxII/III, CtxV/VI), dentate gyrus (DG), molecular layer of DG (MoDG), polymorph DG (PoDG), hippocampus (Hip), hippocampal CA1 (CA1), pyramidal layer Hip (py), radiatum layer Hip (Rad), oriens layer Hip (Or), lateral hypothalamic area (LHA), medial geniculate nucleus (MGM), olfactory bulb (OB), olfactory bulb external plexiform layer (EPL), olfactory bulb granule cell layer (Gl), olfactory bulb mitral layer (Mi), piriform cortex (Pir), prefrontal cortex (PFC), paraventricular nucleus of the hypothalamus (PVN).

Furthermore, our results undermine the notion that CRH-regulated emotional responses are solely attributable to its locale release from interneurons. Overexpression of CRH in forebrain GABAergic, and deletion of CRHR1 from midbrain dopaminergic neurons altered stress-induced dopamine release and anxiety behavior, proposing the idea that CRH-positive GABAergic-VTA projection neurons are regulating emotional responses. The assumption that limbic, and not local, CRH neurons act on dopaminergic CRH receptors is further supported by the fact that overexpression of CRH in the mid-hindbrain, and more specifically in dopaminergic neurons themselves, failed to alter anxiety (Section 4.1.3.1). To further substantiate this hypothesis, we set out to investigate the morphology and release sites of cortical and limbic CRH neurons. We made use of the recently generated *Crh-IRES-Cre* knockin driver line, in which a Cre coding cassette was inserted immediately after the translational STOP codon of the endogenous *Crh* gene (Taniguchi et al., 2011). Thus, Cre expression is regulated by the endogenous *Crh* promoter, without compromising its expression. To assess the recombination pattern, *Crh-IRES-Cre* mice were bred to the *Ai9* mice harboring a CAG promoter driven *loxP-STOP-loxP-tdTomato* reporter allele, located in the *Rosa26* locus (Madisen et al., 2010). Tomato fluorescence strongly resembled the endogenous *Crh* mRNA expression pattern (Figure 36). As previously reported (Taniguchi et al., 2011), the *Crh-IRES-Cre* driver targeted the major CRH-expression sites in the brain, including the OB, Pir, Ctx, BNST, PVN, CeA, MGM and inferior olive (IO) (Figure 36). More detailed assessment of the *Crh-IRES-Cre:Ai9* mice revealed forebrain-VTA projecting CRH axons, as well as projection fibers in and around the CeA (Figure 37). IHC against tyrosine hydroxylase (TH) in *Crh-IRES-Cre:Ai9* mice confirmed that the dense immunofluorescence in and around the VTA is in fact a result of innervating projections and not local CRH expressing neurons (Figure 37 and 38). CRHR1 is densely expressed in dopaminergic neurons of the VTA and SNc (Kuhne et al., 2012). However, only a few CRH-expressing cell bodies were detected in the VTA of *Crh-IRES-Cre:Ai9* mice, and a negligible portion of those co-localized with TH (Figure 38). This additionally suggests that the effects on anxiety and dopamine release in $Crhr1^{iDA\text{-}CKO}$ and $Crh^{GABA\text{-}COE}$ mice are most likely not caused by few CRH-synthesizing cells of the VTA, but rather by CRH neurons with distal projection origins.

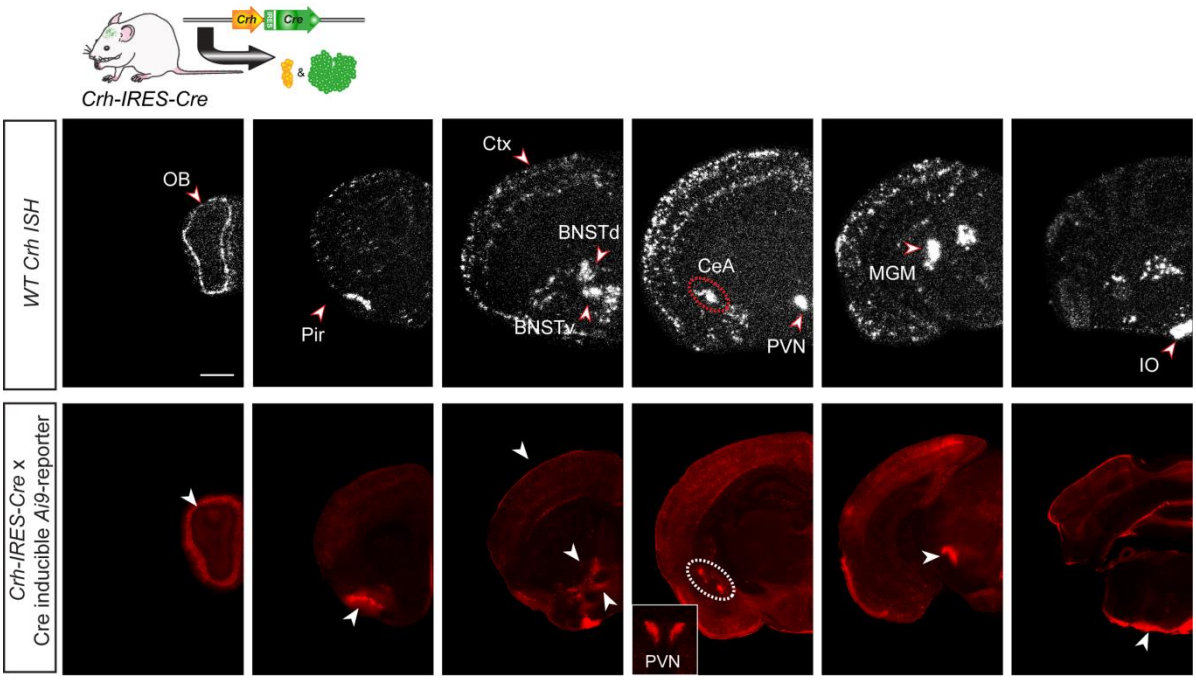

Figure 36: Validation of recombination-specificity in *Crh-IRES-Cre* driver mice.
Top row depicts dark-field photomicrographs of the *Crh* mRNA expression pattern in brain sections of wild-type adult mice. *Crh-IRES-Cre* driver (Taniguchi et al., 2011) bred to the *Ai9* (*loxP-STOP-loxP-tdTomato*) reporter (Madisen et al., 2010) are shown at the bottom. Endogenous tomato expression mirrors the endogenous *Crh* mRNA pattern. Regions of interest are highlighted with arrowheads and dashed lines. Abbreviations: bed nucleus of the stria terminalis dorsal/ventral (BNSTd/v), central nucleus of the amygdala (CeA), cortex (Ctx), inferior olive (IO), medium geniculate nucleus (MGM), olfactory bulb (OB), piriform cortex (Pir), paraventricular nucleus of the hypothalamus (PVN). Scale bar represents 1 mm.

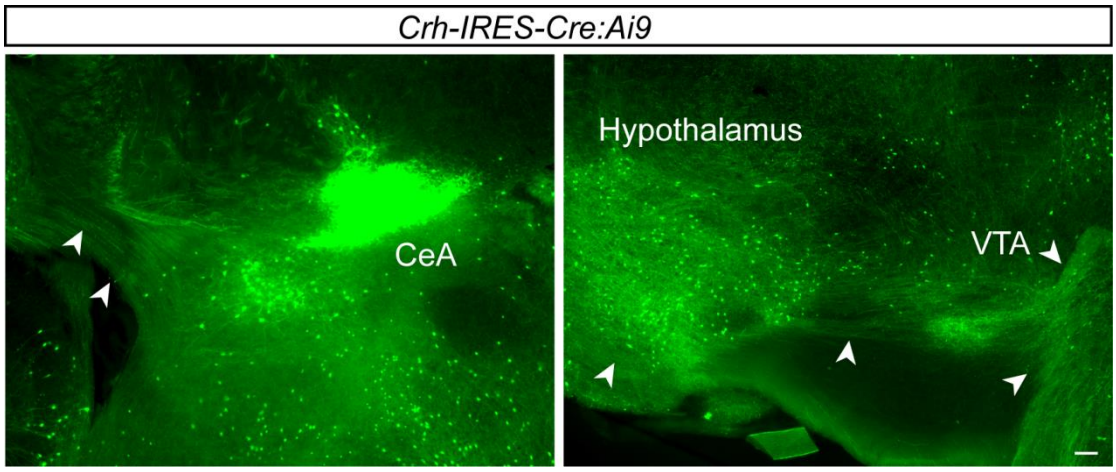

Figure 37: CRH neurons have long-projection axons.
(A) Sagittal vibratom sections from a *Crh-IRES-Cre*:*Ai9* mouse brain depicts long-range projection axons in and around the central amygdala (CeA). **(B)** Similarly, long-range CRH projections innervate the ventral tegmental area (VTA). Endogenous tomato expression is shown in green. Projections are highlighted with white arrowheads. Scale bar represents 100 µm.

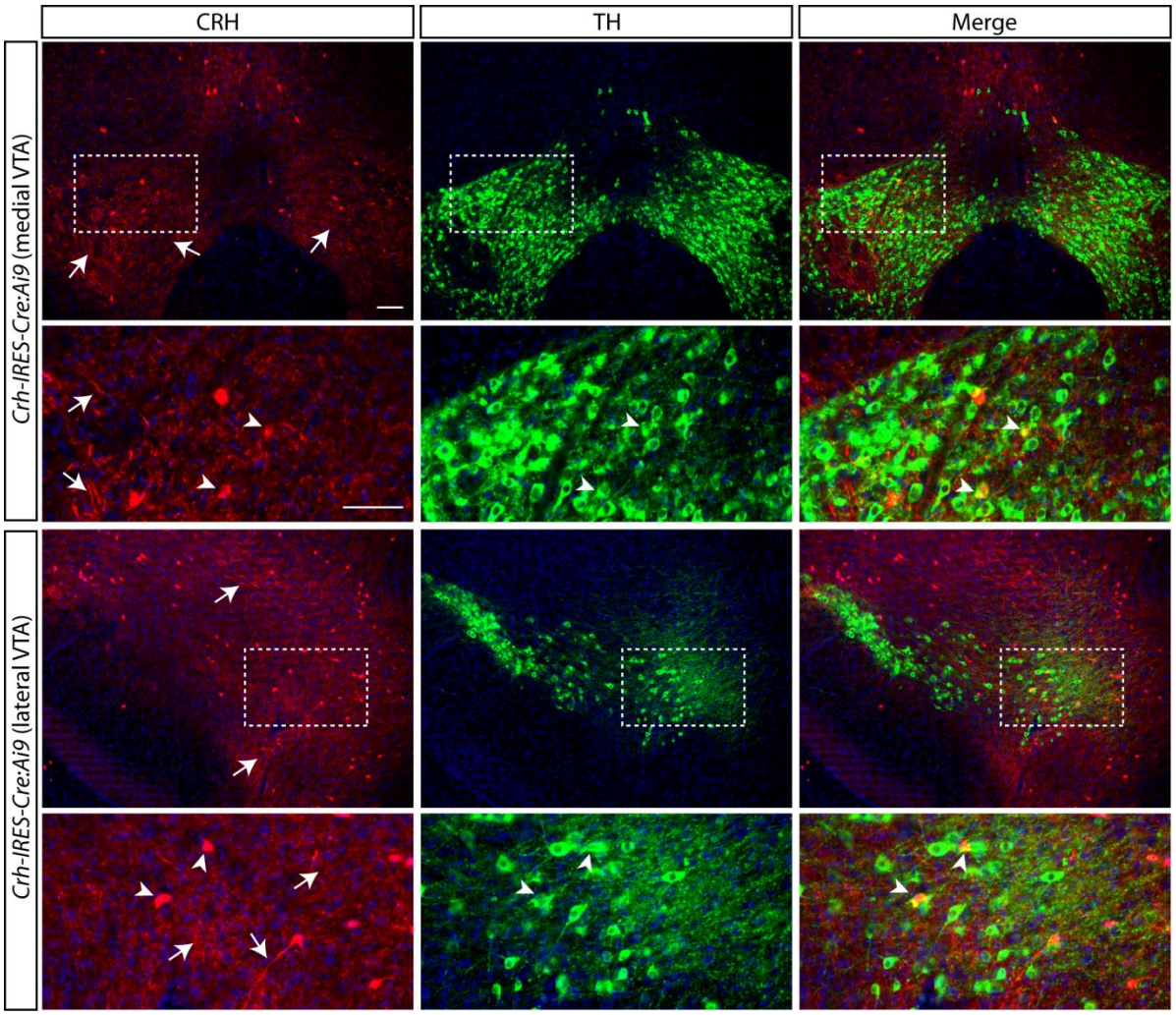

Figure 38: CRH is expressed in few dopaminergic VTA neurons.
Sagittal vibratom sections from *Crh-IRES-Cre*:*Ai9* mice were stained against the dopaminergic marker tyrosine hydroxylase (TH-green). A small number of CRH expressing neurons (red) were identified in the medial and lateral parts of the VTA (white arrowheads). Only a few of those were dopaminergic. In contrast, significant levels of CRH-immunoreactive fibers were observed in the VTA (white arrows). Cell bodies, marked by white arrowheads are shown in the magnification of the boxed region. Scale bar represents 100 µm.

In order to corroborate this, we examined whether limbic CRH sites, which we and others have shown to be involved in anxiety, project monosynaptically onto VTA neurons. We choose to specifically investigate VTA-projecting BNST neurons (Georges and Aston-Jones, 2002; Jalabert et al., 2009; Kudo et al., 2012), given the recently emphasized bidirectional involvement of the BNST in anxiety (Kim et al., 2013; Jennings et al., 2013; Deisseroth, 2014), and the strong CRH expression within this region (see previous results). In addition, BNST-CRH signaling was shown to regulate excitatory neurotransmission of VTA-projecting BNST neurons (Silberman et al., 2013). Single injection of adeno-associated viruses (AAV) to the dorsal and ventral BNST of *Crh-IRES-Cre* mice were used to anterogradely label presynaptic terminals via expression of a Cre-dependent synaptophysin-eGFP fusion protein (AAV-Syn-floxed-eGFP) (Figure 39A).

Synaptophysin, also known as the major synaptic vesicle protein, is expressed in virtually all neurons of the brain and spinal cord, and is commonly used to label synapses. In this case, anterograde labeling of synapses, and hence projection sites, is enabled by fusion of synaptophysin to eGFP. The fusion-protein is expressed from a flip-excision (*FLEX*) vector, under the control of the ubiquitous human *EF1a* promoter. The *FLEX*-switch system makes use of two pairs of heterotypic, antiparallel *loxP*-type recombination sites, which first undergo Cre-dependent inversion of the coding sequence, followed by excision of two of the *loxP* sites (Atasoy et al., 2008). Thus, each of the orthogonal recombination sites ends up oppositely oriented and incapable of further recombination. The type of labeled neurons/synapses is therefore defined by the Cre-expression pattern, and is in this case restricted to CRH neurons. Four weeks after unilateral stereotactic injection of *AAV-Syn-floxed-eGFP* to the dorsal and ventral BNST of *Crh-IRES-Cre* mice, labeled CRH projections were detected in the VTA and surrounding midbrain regions including the periaqueductal gray (PAG), parabrachial pigmented nucleus (PBP) and the medial mammillary nucleus (MM) (Figure 39B). In addition, labeled presynaptic terminals were observed in the lateral septum, lateral hypothalamus, median eminence, stria terminalis and posterior PVN (data not shown). Local projections within the BNST were also extensively labeled (Figure 39A). In addition, somatic and dendritic localization of synaptophysin-eGFP around the injection site was observed, possibly due to large amounts of synthesized proteins, which has also been reported by others (Li et al., 2010). Nonetheless, our results clearly indicate that a subpopulation of CRH neurons within the BNST monosynoptically innervate the VTA. These possibly represent long-range GABAergic projection neurons, since the majority of CRH-expressing cells in the BNST co-express *Gad65/67* (see above). Importantly, BNST projection neurons in the rat can be distinguished from local interneurons based on differences in electrophysiological membrane currents (Egli and Winder, 2003; Hammack et al., 2007; Silberman et al., 2013). In addition, CRH BNST neurons were previously classified into at least three different categories based on their voltage responses to transient current steps (Silberman et al., 2013). Taking this into account, our results suggest that CRH is expressed in at least two distinct subpopulations of BNST neurons, including GABAergic interneurons and GABAergic long-range projection neurons.

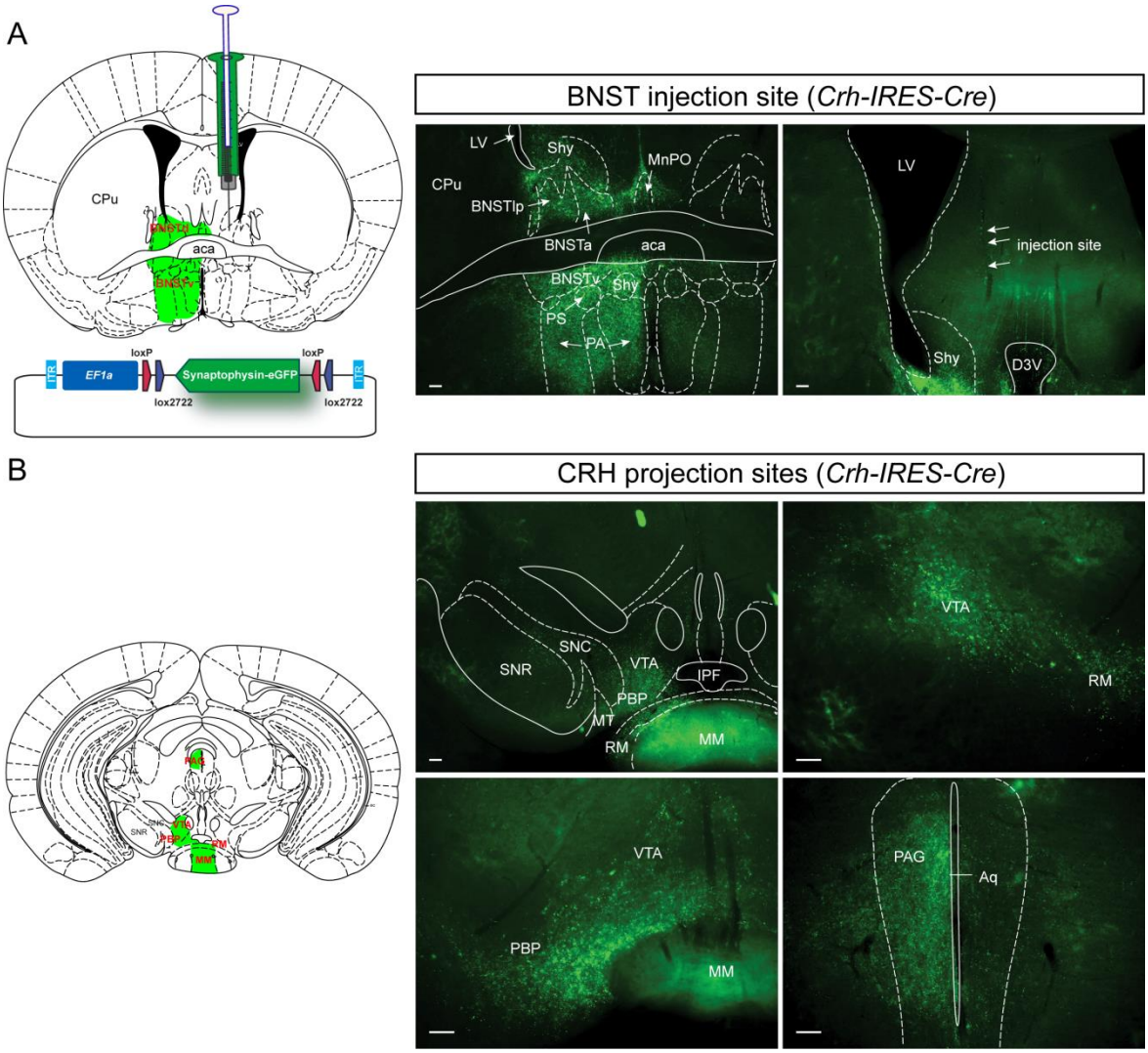

Figure 39: Evidence for direct projections of CRH neurons from the BNST to the VTA.
(A) An AAV-delivered *FLEX*-switch vector for synaptophysin-eGFP was injected into the BNST of *Crh-IRES-Cre* mice (schematic drawing). Coronal vibratome sections of Cre-dependent synaptophysin-eGFP expression in *Crh-IRES-Cre* mice depict local CRH projections within the BNST. Bed nucleus of stria terminalis (BNST), ventral (BNSTv), anterior (BNSTa), lateral posterior division (BNSTlp), caudate putamen (CPu), lateral ventricle (LV), dorsal 3rd ventricle (D3V), anterior commissure (aca), aqueduct (Aq), median preoptic nucleus (MnPO), preoptic area (PA), parastrial nucleus (PS), septohypothalmic nucleus (Shy). **(B)** Strong axonal labelling was also observed in distant midbrain nuclei, including the ventral tegmental area (VTA), parabrachial pigmented nucleus (PBP), medial mammillary nucleus (MM), retromammillary nucleus (RM), and periaqueductal gray (PAG). Scale bars represent 100 µm.

4.3.2. A subpopulation of CAMK2α-positive CRH neurons exhibit dendritic spines

In the previous section we established that the majority of limbic and cortical CRH neurons are GABAergic, and that some of these project over long distances. Next, we decided to have a closer look at the morphology of cortical and limbic CRH neurons. Mammalian neocortical neurons are usually classified as pyramidal or nonpyramidal based on their morphology. Pyramidal neurons are excitatory projection neurons, which usually exhibit a high density of dendritic spines, form asymmetrical synapses, and express the vesicular transporter VGLUT1 (Andjelic et al., 2009). Non-pyramidal cell subtypes usually express GABAergic markers and project locally (Kubota, 2013). They are morphologically classified according to their distinct axonal and dendritic aborization patterns into basket cells, chandelier cells, Martinotti cells, double bouquet cells, neuroglia-form cells, and others (Kubota, 2013; DeFelipe et al., 2013). In addition, expression of distinct markers including parvalbumin (PV), calretinin (CR), somatostatin (SOM), vasoactive intestinal polypeptide (VIP), as well as different firing properties are also observed in cortical non-pyramidal cell subtypes (Kubota, 2013; Taniguchi, 2014). Previous studies reported cortical CRH expression in GABAergic double bouquet cells, and descending basket cells with narrow columnar axonal arbors (Kubota et al., 2011; Kubota, 2013). CRH-expressing interneurons of the hippocampus are commonly classified as parvalbumin-expressing basket cells (Chen et al., 2012b). Using high-magnification light and confocal microscopy we assessed neuronal morphology of CRH neurons in the cortex, CeA and BNST of *Crh-IRES-Cre* mice bred to *Ai32* mice harboring a CAG promoter driven l*oxP-STOP-loxP-channelrhodopsin2-eYFP* allele *(ChR2-eYFP* or *Ai32)*, located in the *Rosa26* locus. *Ai32* mice were used to improve the visualization of dendritic arbors and axonal projections, since channelrhodopsins are trafficked to the membrane where they functions as light-gated channels. *ChR2-eYFP* expressing CRH neurons were observed throughout the cortex, most densely in upper layers II/III and the lower layers V/VI (Figure 40). Most CRH neurons displayed a bitufted/bipolar morphology (Figure 40A, E), characteristic of double bouquet cells and vasoactive intestinal peptide (VIP)-expressing interneurons. In addition, a few neurons were shaped like small basket cells and/or Martinotti-like cells (Figure 40B, D). Notably, Martinotti-like GABAergic neurons are known to exhibit dendritic spines, and project to other cortical areas (Kubota, 2013; Caputi et al., 2013).

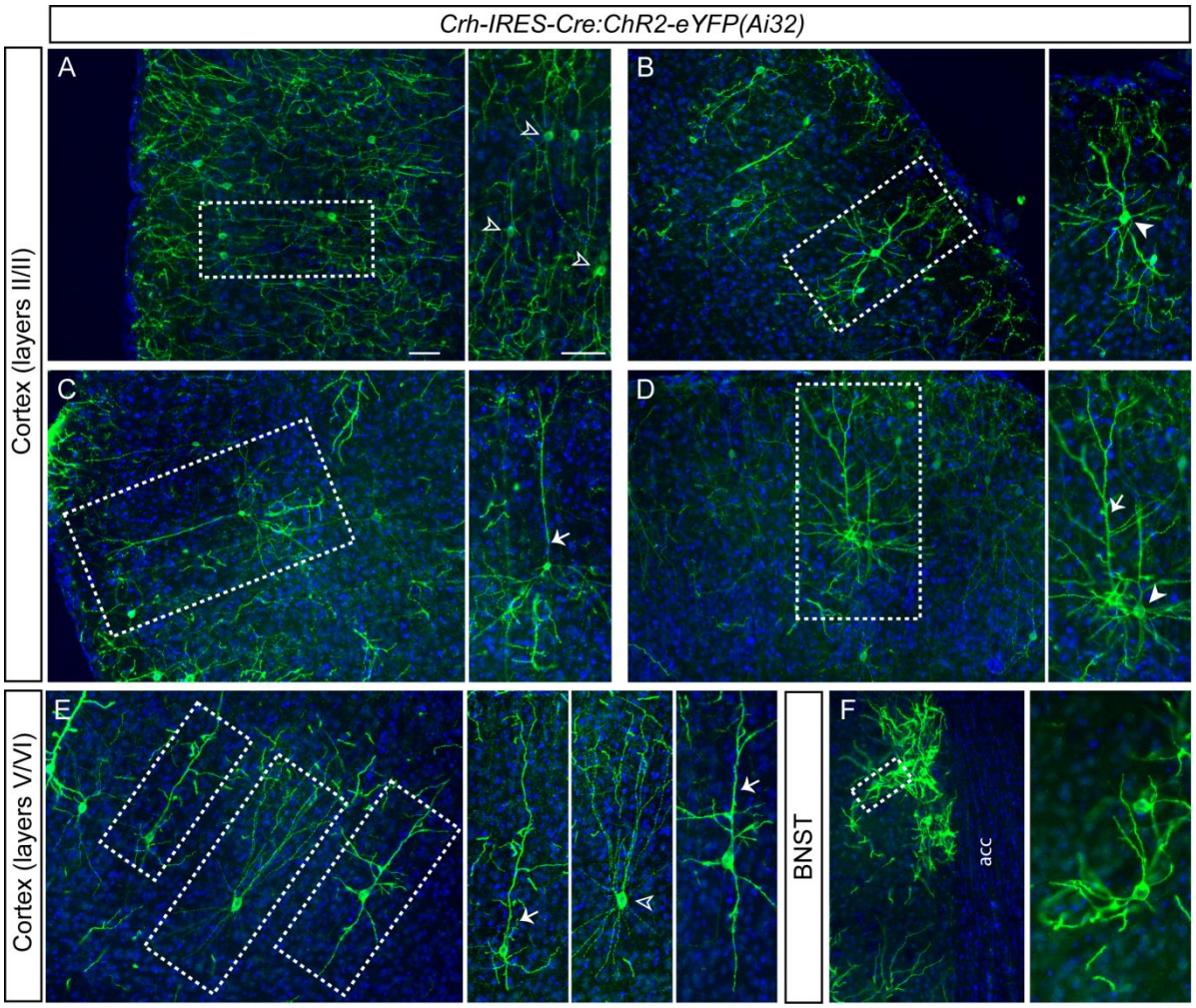

Figure 40: CRH is expressed in non-pyramidal and pyramidal neurons of the cortex.
Adult brains of *Crh-IRES-Cre:ChR2-eYFP(Ai32)* mice were fixed and immunofluorescence staining against GFP was performed on vibratome sections. *CRH/ChR2-eYFP* expression was mainly detected in bipolar double-bouqet (**A**, **E**, arrow heads) and small basket cells and/or Martinotti-like cells (**B**, **D**, filled arrow heads) in cortical layers II/III and V/VI. A few CRH-cells exhibited pyramidal-like morphologies, marked by the presence of a prominent apical dendrite (**C**, **D**, **E**, arrows). **(F)** Typical multipolar morphology of *CRH/ChR2-eYFP* neurons in the BNST. Magnifications of neurons in the boxed regions are shown on the right of each image. Anterior commissure (aca). Scale bar represents 50 µm.

However, additional co-localization studies with other GABAergic markers, as well as the assessment of axonal projections are necessary to further specify the morphological characteristics of CRH neurons. More surprisingly, eYFP expression was additionally observed in few pyramidal-like cells, showing a prominent apical dendrite extending vertically from a conical soma toward the pial surface (Jones, 1975), which has thus far not been reported for CRH neurons (Figure 40C-E). These possibly represent the small number of VGLUT1-positive, glutamatergic cortical CRH neurons previously detected by double *ISH* (Figure 35). To corroborate our findings we subsequently examined the presence of dendritic spines in pyramidal-like CRH neurons.

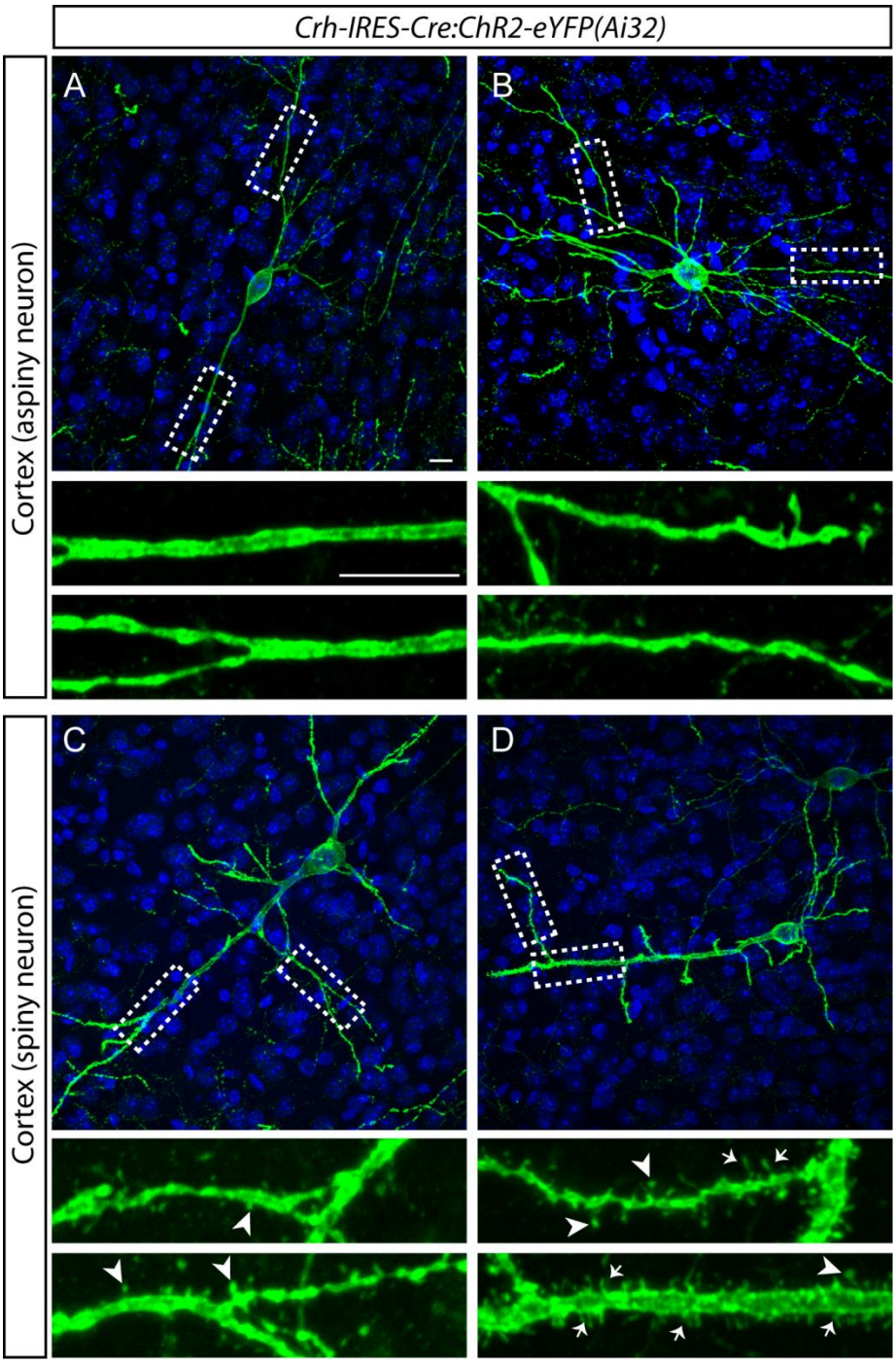

Figure 41: Pyramidal-like CRH neurons contain dendritic spines.
Adult brains of *Crh-IRES-Cre:ChR2-eYFP(Ai32)* mice were fixed and immunofluorescence staining against GFP was performed on vibratome sections. Bipolar double-bouqet **(A)** and small basket cells and/or Martinotti-like CRH cells **(B)** exhibited no dendritic spines. **(C-D)** In contrast, pyramidal-like CRH neurons are decorated with thin (arrows) and mushroom-like (arrowheads) spines. Magnifications of selected dendrites in the boxed regions are shown below each image. Scale bar represents 10 µm.

Bipolar double bouquet, and small basket cells and/or Martinotti-like CRH cells displayed no dendritic spines (Figure 41A-B). On the other hand, thin and mushroom-like spines were observed in pyramidal-like CRH neurons (Figure 41C-D). However, only a subset of cortical cells

was assessed until now. Thus, we cannot entirely exclude the presence of spines in all nonpyramidal CRH neurons. This is important, considering that not all glutamatergic spiny neurons are pyramidal-shaped, and that some even express both excitatory and inhibitory markers (Jones, 1975; Andjelic et al., 2009). Overall, our results suggest the presence of a diverse set of cortical CRH-expressing neurons which might exhibit specific and distinct behavioral functions. Keeping in mind that limbic, rather than cortical CRH sites are believed to control emotional responses in mice, we assessed the presence of dendritic spines in CRH-expressing neurons of the CeA and BNST.

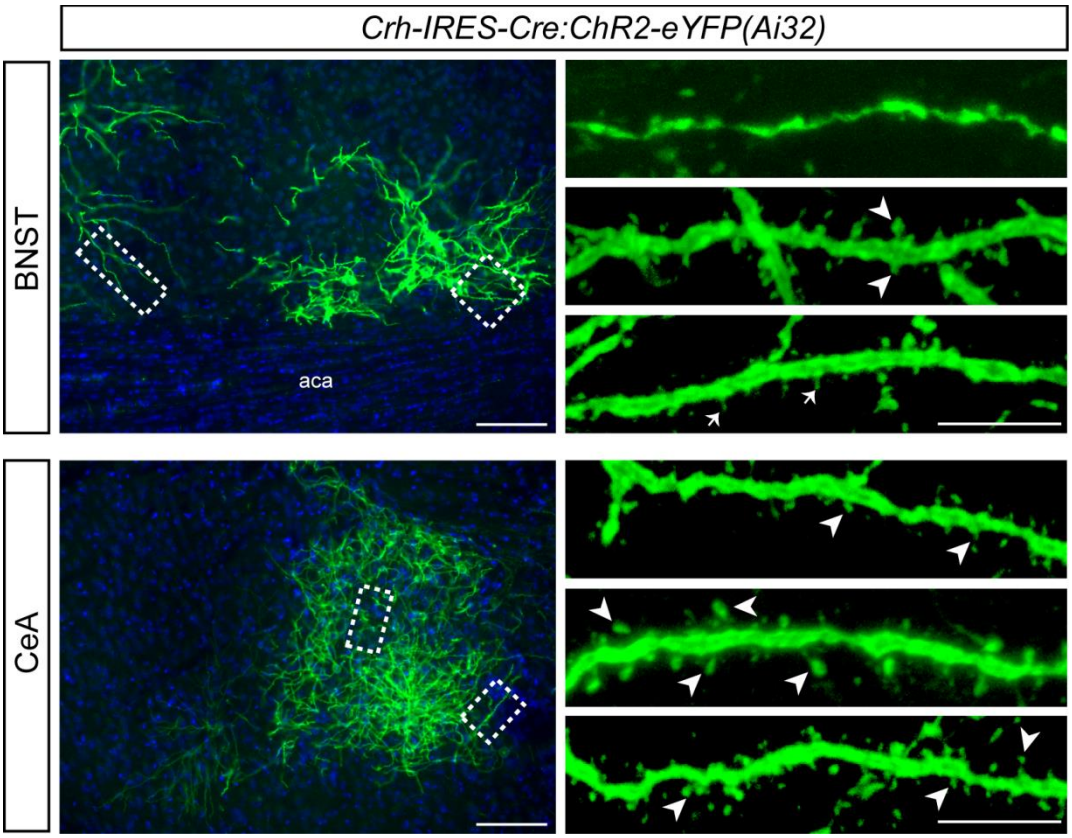

Figure 42: CRH is expressed in spiny neurons of the BNST and CeA.
Adult brains of *Crh-IRES-Cre:ChR2-eYFP(Ai32)* mice were fixed and immunoflurosence staining against GFP was performed on vibratome sections. Thin (arrows) and mushroom-like spines (arrowheads) were present on dendrites of *ChR-eYFP*-expressing CRH neurons in the BNST and CeA. Magnifications of selected dendrites in the boxed regions are shown on the right side of each image. Anterior commissure (aca). Scale bars; overview - 100 µm, spines - 10 µm.

Morphological studies in these brain regions have been challenging due to the complex interconnected network of cells and lack of specific markers. Accordingly, the dense population of CRH-expressing neurons in the BNST and CeA made it extremely difficult to assess their neuronal morphology. In the BNST, many CRH neurons were multipolar with 3-4 primary dendrites (Figure 40F), which was also observed for the CeA (data not shown). Compared to

the cortex, a far greater population of CRH neurons in the BNST and CeA exhibited dendritic spines (Figure 42). The spine density ranged from spares to moderate including thin and mushroom-like spines. Previous studies have reported the presence of spiny multipolar and bipolar spindle-shaped neurons in the amygdala and BNST (Larriva-Sahd, 2004; Chieng et al., 2006), but their neuronal identity remains largely unknown. CRH neurons in the BNST and CeA are predominately *Gad65/67*-positive (Section 4.3.1), which suggests the presence of a subpopulation of spiny GABAergic-CRH neurons in these limbic structures. In order to further classify this neuronal subpopulation, we searched for additional neurochemical markers. A well described population of spiny GABAergic neurons are medium-spiny projection neurons of the striatum, which integrate cortical input with dopaminergic signaling to regulate the selection of motor and cognitive action patterns (Gerfen and Surmeier, 2011). Interestingly, striatal-like spiny neurons have also been reported for the amygdala and BNST (Larriva-Sahd, 2004; Chieng et al., 2006). CAMK2α is expressed in forebrain excitatory projection neurons as well as in GABAergic medium spiny projection neurons of the striatum/caudate putamen (Erondu and Kennedy, 1985; Liu and Murray, 2012; Klug et al., 2012). In addition, recent optogentic studies revealed that photostimulation of CAMK2α-positive BNST-VTA projections produced both glutamatergic and GABAergic currents in VTA neurons (Jennings et al., 2013). In Section 4.1.3.1 we showed that overexpression of CRH in Camk2α-positive neurons enhanced anxiety, whereas overexpression in glutamatergic neurons produced no effect. This lead us to speculate, that hyperdrive of CRH in CAMK2α-positive, non-glutamatergic cells might mediate the observed effects. Double *ISH* showed strong co-localization of *Camk2α* and *Crh* in the piriform cortex (Figure 43), which was expected considering that CRH-expression within this structure was found in glutamatergic, *VGlut1*-positive neurons. Interestingly, a substantial amount of *Crh* neurons in the BNST (~40%) and CeA (~40%) also expressed *Camk2α* (Figure 43). In addition, co-localization was observed in most CRH expressing structures including the OB, AcbSh, PFC, Ctx, LHA, Hip, MGM and APT. Accordingly, *Camk2α*-positive CRH neurons might represent the subpopulation of spiny neurons observed in the BNST, CeA and cortex. To asses this, we again made use of the *FLEX*-switch system. Single injections of Cre-dependent *AAV-Camk2α-floxed-eYFP* into the BNST, CeA and PFC of *Crh-IRES-Cre* mice were used to label *Camk2α*-positive CRH neurons. More specifically, eYFP expression, which is driven by the *Camk2α* promoter, is induced only upon Cre-mediated inversion of the *FLEX*-construct.

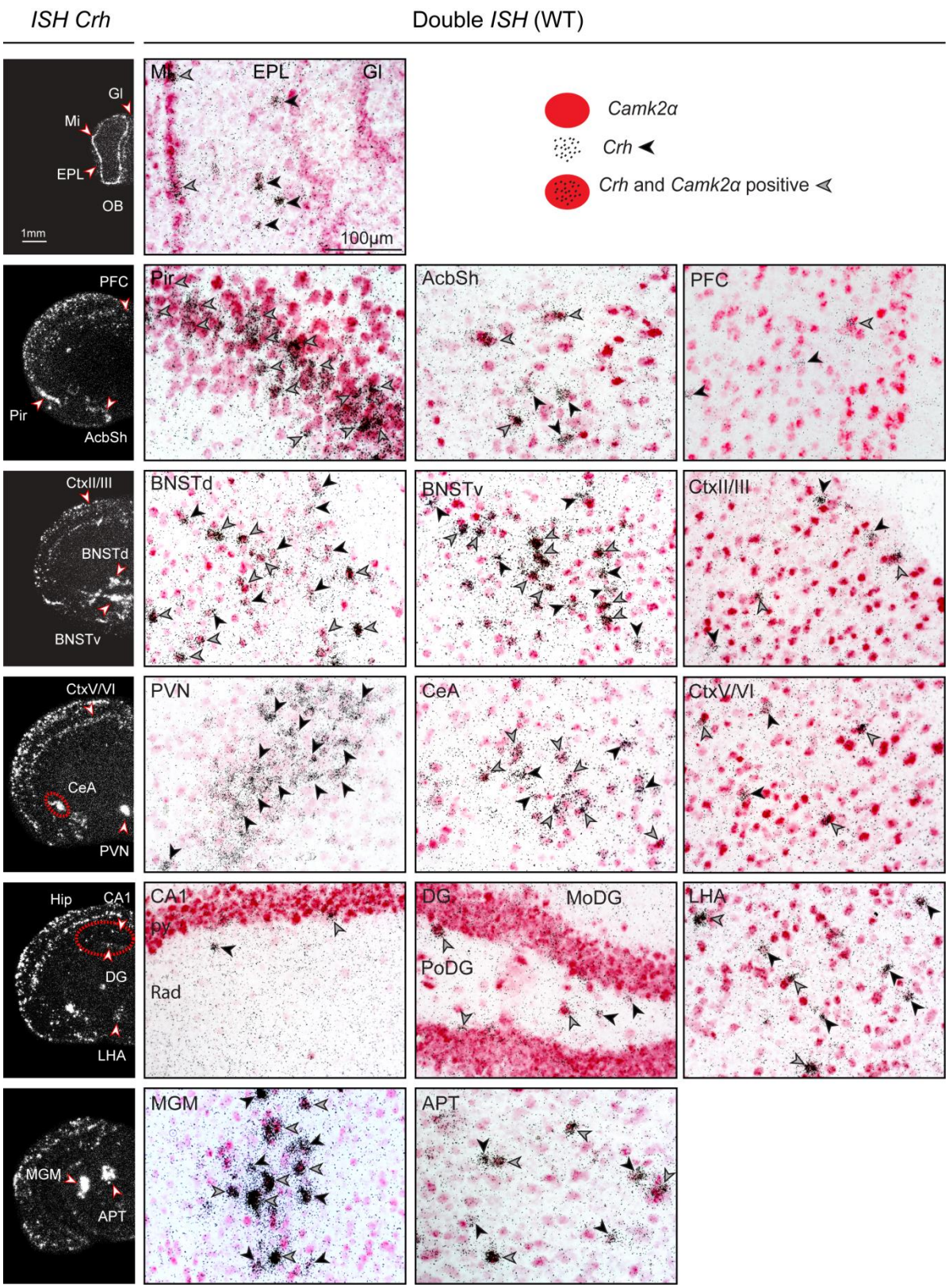

Figure 43: A subpopulation of *Crh* neurons co-expresses *Camk2α*.

The first left column depicts dark-field photomicrographs of the *Crh* mRNA expression pattern in brain sections of wild-type mice. Regions of interest are highlighted with red arrowheads and dashed lines. The additional columns represent bright field photomicrographs of coronal wild-type brain sections showing double *ISH* of *Crh* mRNA (silver grains) together with the calmodulin calcium-dependent kinase 2α (*Camk2α,* red staining). Black arrowheads indicate cells only expressing *Crh* (silver grains). Grey arrowheads indicate cells coexpressing *Crh* and *Camk2α*. Abbreviations: nucleus accumbens shell (AcbSh), anterior pretectal

nucleus (APT), bed nucleus of the stria terminalis dorsal/ventral (BNSTd/v), central nucleus nucleus of the amygdala (CeA), cortical layers (CtxII/III, CtxV/VI), dentate gyrus (DG), molecular layer of DG (MoDG), polymorph DG (PoDG), hippocampus (Hip), hippocampal CA1 (CA1), pyramidal layer Hip (py), radiatum layer Hip (Rad), oriens layer Hip (Or), lateral hypothalamic area (LHA), medial geniculate nucleus (MGM), olfactory bulb (OB), olfactory bulb external plexiform layer (EPL), olfactory bulb granule cell layer (Gl), olfactory bulb mitral layer (Mi), piriform cortex (Pir), prefrontal cortex (PFC), paraventricular nucleus of the hypothalamus (PVN).

Bearing in mind that Cre-expression is controlled by the endogenous CRH promoter, eYFP fluorescence will only be observed in CAMK2α-positive CRH neurons. In the BNST and CeA, dendrites of the majority of eYFP-fluorescent, CAMK2α-positive CRH neurons were decorated with spines (Figure 44). Again, the density and shape of spines varied from spares to moderate and thin to mushroom-like respectively. Furthermore, a substantial amount of long-range axons was observed in the BNST of *AAV-Camk2α-floxed-eYFP* injected *Crh-IRES-Cre* mice, suggesting that CAMK2α-positive CRH neurons are able to project over long distances (Figure 45). Dendritic spines were also observed in CAMK2α-positive CRH neurons of the PFC (Figure 46). However, this time it proved difficult to categorize them into pyramidal or nonpyramidal cells, due to incomplete labeling of most neurons. eYFP is most likely not as effectively transported to fibers and axons as the previously employed membrane-recruited channelrhodopsin2-eYFP fusion protein. Based on these results and earlier morphological assessment, cortical, spiny CAMK2α-expressing CRH neurons most likely represent excitatory pyramidal neurons. Interestingly, *Camk2α-eYFP* expression was also detected in aspiny CRH neurons of the PFC (Figure 46), suggesting that CAMK2α is expressed in GABAergic cells apart from striatal medium spiny neurons. To assess this in more detail, double *ISH* was performed against *Gad65/67* and *tomato* in *Camk2αCreERT2:Ai9* mice. In this case, tomato expression is driven by the *Camk2α* promoter upon tamoxifen application. Interestingly, about 5-10% of cortical and hippocampal *Gad65/67*-positive neurons co-expressed *tomato/Camk2α* (Figure 47). Even more GABAergic neurons co-localized with *Camk2α* in the BNST and CeA (~50%). The presence of *Camk2α* in *Gad65/67*-positive neurons of the caudate putamen was confirmed and is in line with previous reports (Erondu and Kennedy, 1985). Only a few double-positive cells were detected in the PVN, Hip and Pir (Figure 47). Co-localization was absent in the MGM and cerebellum. These results further support the presence of triple positive, GABAergic, CAMK2α-expressing CRH neurons. Taking all results into account concludes that CRH expression in the cortex, CeA and BNST is largely restricted to GABAergic neurons. With the exception of the piriform cortex, only a few glutamatergic CRH neurons were observed in other cortical structures. These were usually pyramidal-shaped and exhibited dendritic spines.

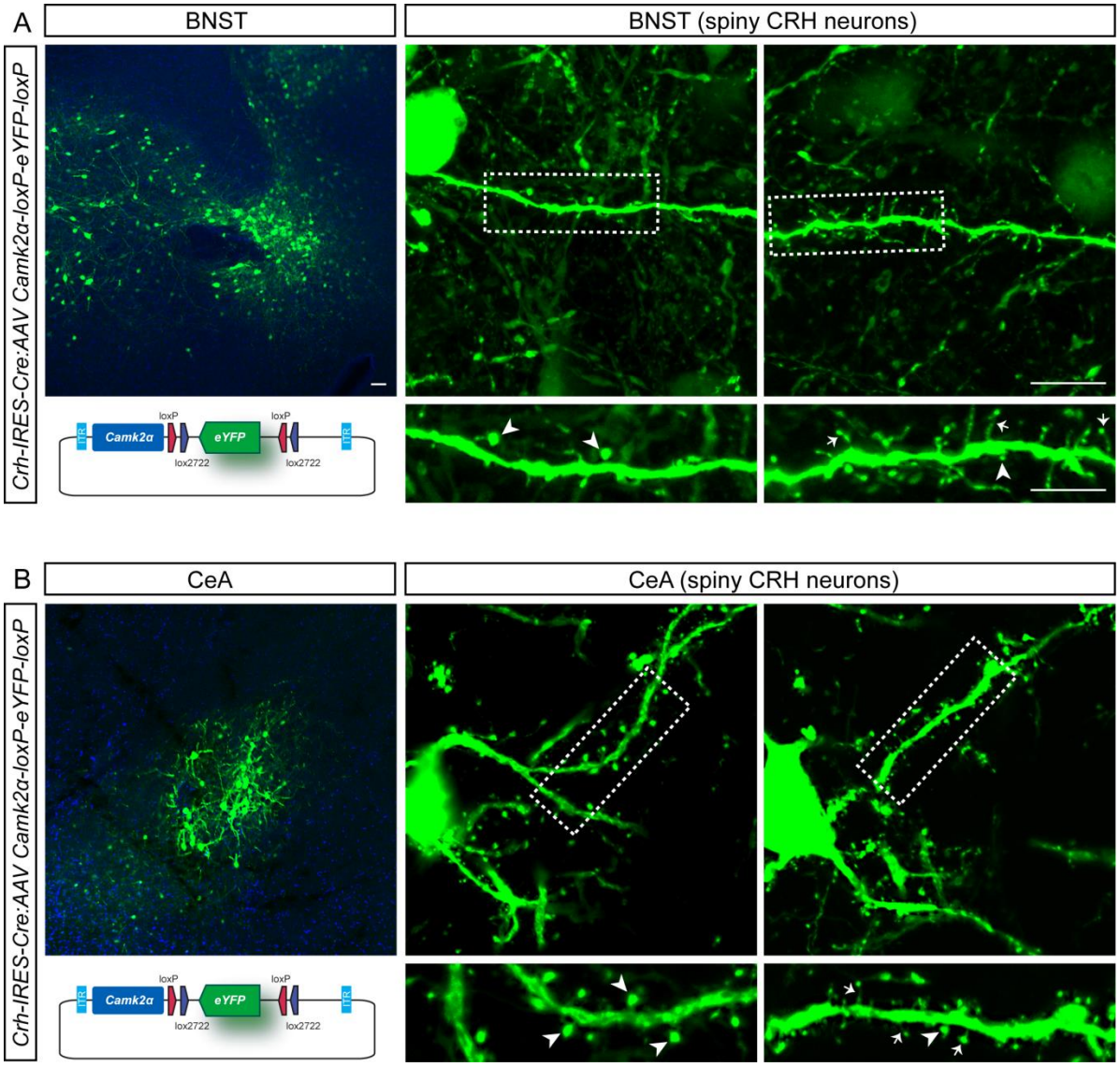

Figure 44: Spiny CRH neurons in the BNST and CeA express CAMK2α
AAVs delivering a *Camk2α-eYFP* FLEX vector (schematic drawing) were unilaterally injected into the dorsal and ventral BNST **(A)**, and CeA **(B)** of *Crh-IRES-Cre* mice. Coronal vibratome sections of Cre-dependent *Camk2α-eYFP* expression in *Crh-IRES-Cre* mice depict dendritic thin (arrows) and mushroom-like spines (arrowheads) in CRH neurons of the BNST and CeA. Magnifications of selected dendrites in the boxed regions are shown at the bottom of each image. Scale bars: overview BNST/CeA - 50 µm, overview spines - 25 µm, magnification spines - 10 µm.

Nevertheless, the presence of spiny, cortical GABAergic CRH neurons can thus far not be excluded. Previous experiments showed that CRH neurons in the BNST (and possibly also in other regions) have long-range axons which allow them to monsynaptically project to midbrain regions such as the VTA (Section 4.3.1). Furthermore, a subpopulation of CRH neurons in the BNST and CeA, characterized by the expression of *Camk2α*, exhibits dendritic spines. Importantly, long-distance axons were also observed in *Camk2α*-positive CRH neurons of the BNST.

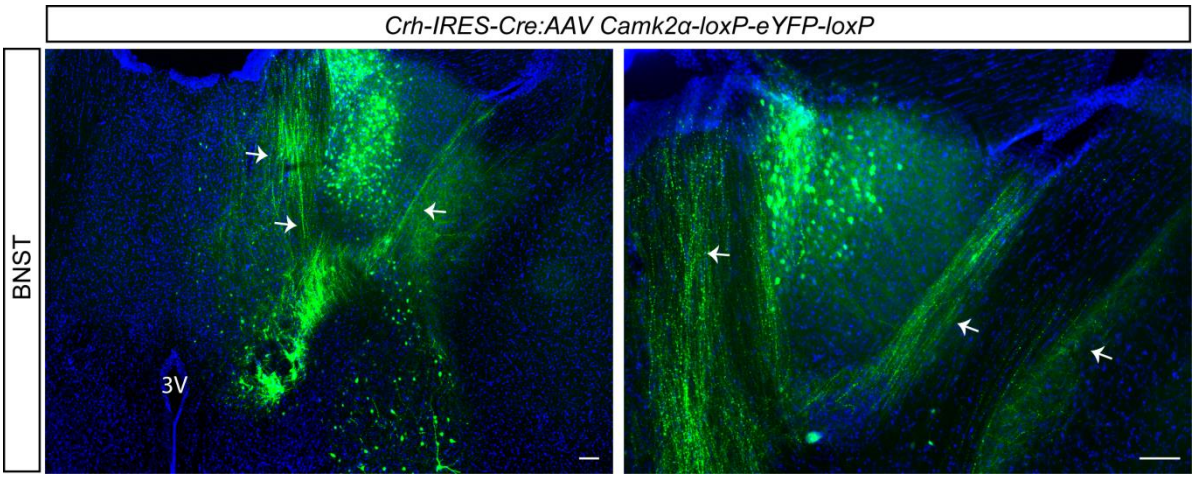

Figure 45: CRH is expressed in CAMK2α-positive long-range projection neurons of the BNST.
AAVs delivering a *Camk2α-eYFP* FLEX vector were unilaterally injected into the dorsal and ventral BNST of *Crh-IRES-Cre* mice. Coronal vibratome sections of Cre-dependent *Camk2α-eYFP* expression in *Crh-IRES-Cre* mice depict strong labelling of long-range projecting CRH axons. Scale bars represents 100 µm.

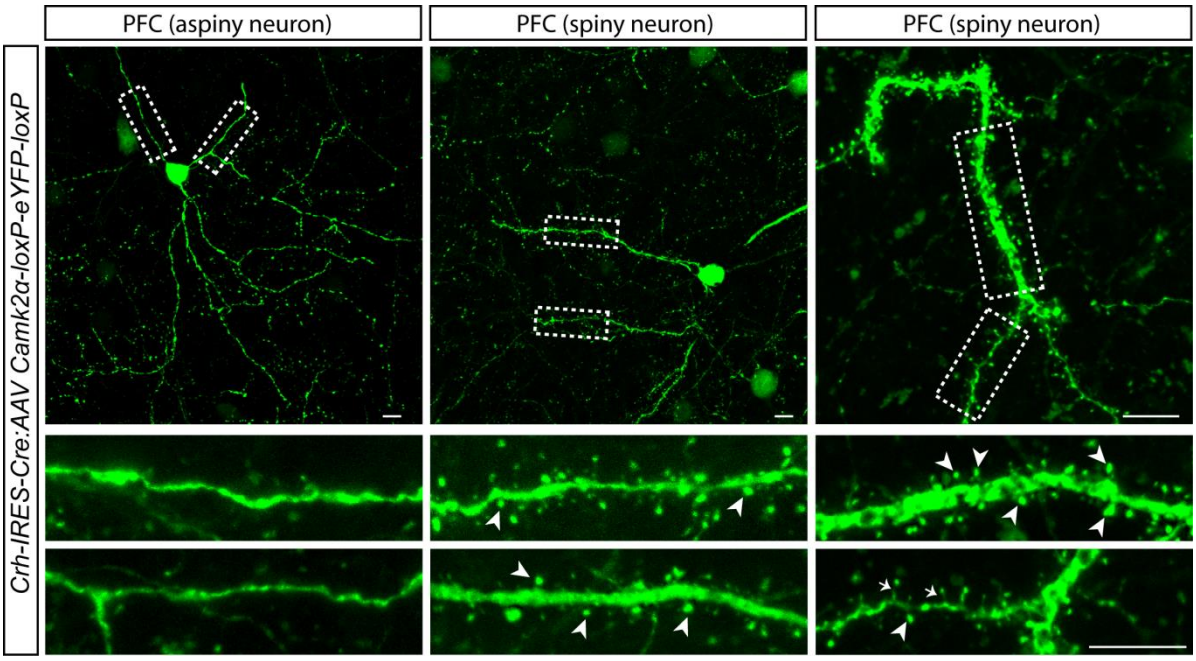

Figure 46: Localization of spiny and aspiny CAMK2α-positive CRH neurons in the PFC.
AAVs delivering a *Camk2α-eYFP* FLEX vector were unilaterally injected into the PFC of *Crh-IRES-Cre* mice. Coronal vibratome sections of Cre-dependent *Camk2α-eYFP* expression in *Crh-IRES-Cre* mice highlight the presence of spiny and aspiny cortical *Camk2α*-positive *Crh* neurons. Thin (arrows) and mushroom-like spines (arrowheads) were located on the dendrites. Magnifications of selected dendrites in the boxed regions are shown at the bottom of each image. Scale bars represent 10 µm.

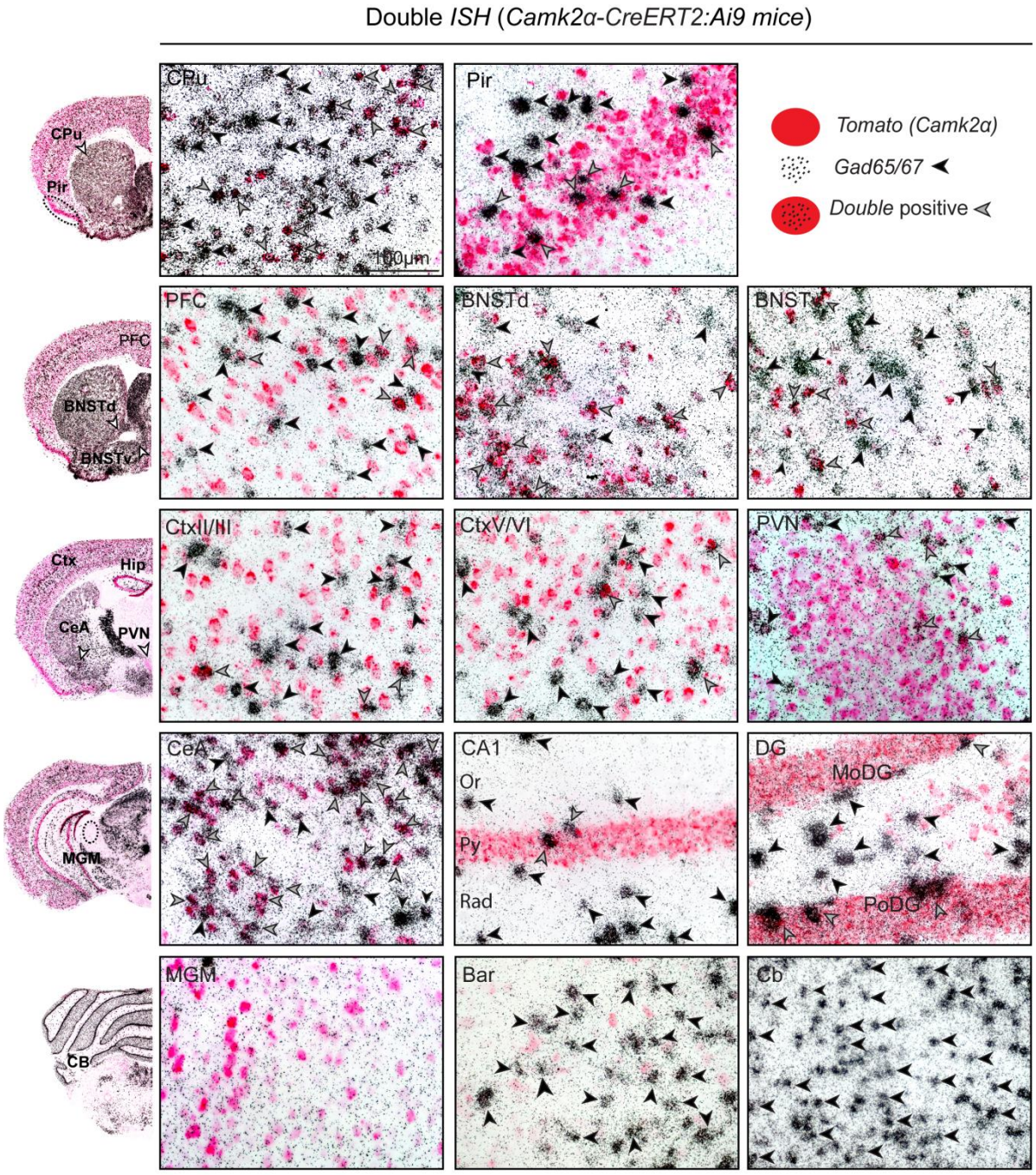

Figure 47: *Camk2α* is expressed in cortical and limbic GABAergic neurons.
The first left column depicts overview bright-field photomicrographs of coronal brain sections of *Camk2αCreERT2:floxedAi9* mice, showing double *ISH* of *Gad75/76* mRNA (silver grains) together with tomato (red staining). Tomato expression was initiated upon oral tamoxifen administration starting at postnatal week 8, and is restricted to *Camk2α-CreERT2* expressing cells. Areas of interest are highlighted with arrowheads and dashed lines. The additional columns represent higher magnifications of selected regions of the bright field photomicrographs. Black arrowheads indicate cells only expressing *Gad65/67* (silver grains). Grey arrowheads indicate cells co-expressing *Gad65/67* and *tomato*. Abbreviations: Barrington's nucleus (Bar), bed nucleus of the stria terminalis dorsal/ventral (BNSTd/v), cerebellum (Cb), central nucleus of the amygdala (CeA), cortical layers (CtxII/III, CtxV/VI), dentate gyrus (DG), molecular layer of DG (MoDG), polymorph DG (PoDG), hippocampus (Hip), hippocampal CA1 (CA1), pyramidal layer Hip (py), radiatum layer Hip (Rad), oriens layer Hip (Or), medium geniculate nucleus (MGM), prefrontal cortex (PFC), paraventricular nucleus of the hypothalamus (PVN).

In view of the fact that CAMK2α is generally expressed in projection neurons (cortical/hippocampal excitatory projection neurons and striatal GABAergic medium spiny projection neurons), gives rise to the hypothesis that GABAegic, CAMK2α-positive CRH cells represent a subpopulation of long-range projection neurons. However, triple labeling approaches are necessary to confirm that CAMK2α-expressing CRH neurons are in fact GABAergic. Additional labeling experiments are also required to assess whether CAMK2α-positive CRH neurons monosynaptically innervate more distant brain regions, such as the VTA. This will be realized in the future via AAV-delivered, Cre-dependent *Camk2α*-driven synaptophysin-eGFP protein expression in *Crh-IRES-Cre* mice.

4.3.3. Generation of conditional *Crh* knockout mice

Conditional CRH overexpressing mouse lines as well as neurotransmitter-specific CRHR1 knockout mice revealed the bidirectional nature of the CRH/CRHR1 system in anxiety-related behavior. More precisely, CRHR1 in forebrain glutamatergic and midbrain dopaminergic neurons is mediating anxiogenic and anxiolytic effects, respectively (Section 4.2). However, the source of CRH appears to be restricted to forebrain spiny and/or aspiny GABAergic and/or CAMK2α-positive neurons, of which some project over long distances. To circumvent the problems of ectopic expression associated with CRH overexpressing mice, and to specifically address the role of CRH in emotional behavior, we set out to target CRH itself. Initial attempts were already made in 1995 in Joseph Majzoub's lab, by generating the first, and so far only, constitutive CRH knockout mice (Muglia et al., 1995). The study revealed fetal glucocorticoid requirement for lung maturation, which was severely impaired in CRH deficient mice obtained from homozygous breedings, resulting in death within the first 12 hours of life (Muglia et al., 1995). In addition, *Crh* knockout mice exhibited diminished HPA axis activity, evident by severely reduced basal and stress-induced corticosterone levels. More surprisingly, CRH deficient mice displayed no major alterations in depression- and anxiety-like behavior (Weninger et al., 1999; Muglia et al., 2001). However, compensatory mechanism and basal HPA axis alterations might obscure the interpretation of the role of central CRH in emotional behavior. Consequently, we set out to generate conditional CRH knockout mice (produced by Claudia Kühne), which will additionally enable a more precise assessment of CRH x neurotransmitter interactions. The applied targeting strategy is based on a previously described method used to generate *Crhr1*-reporter and conditional knockout mice (Kuhne et al., 2012).

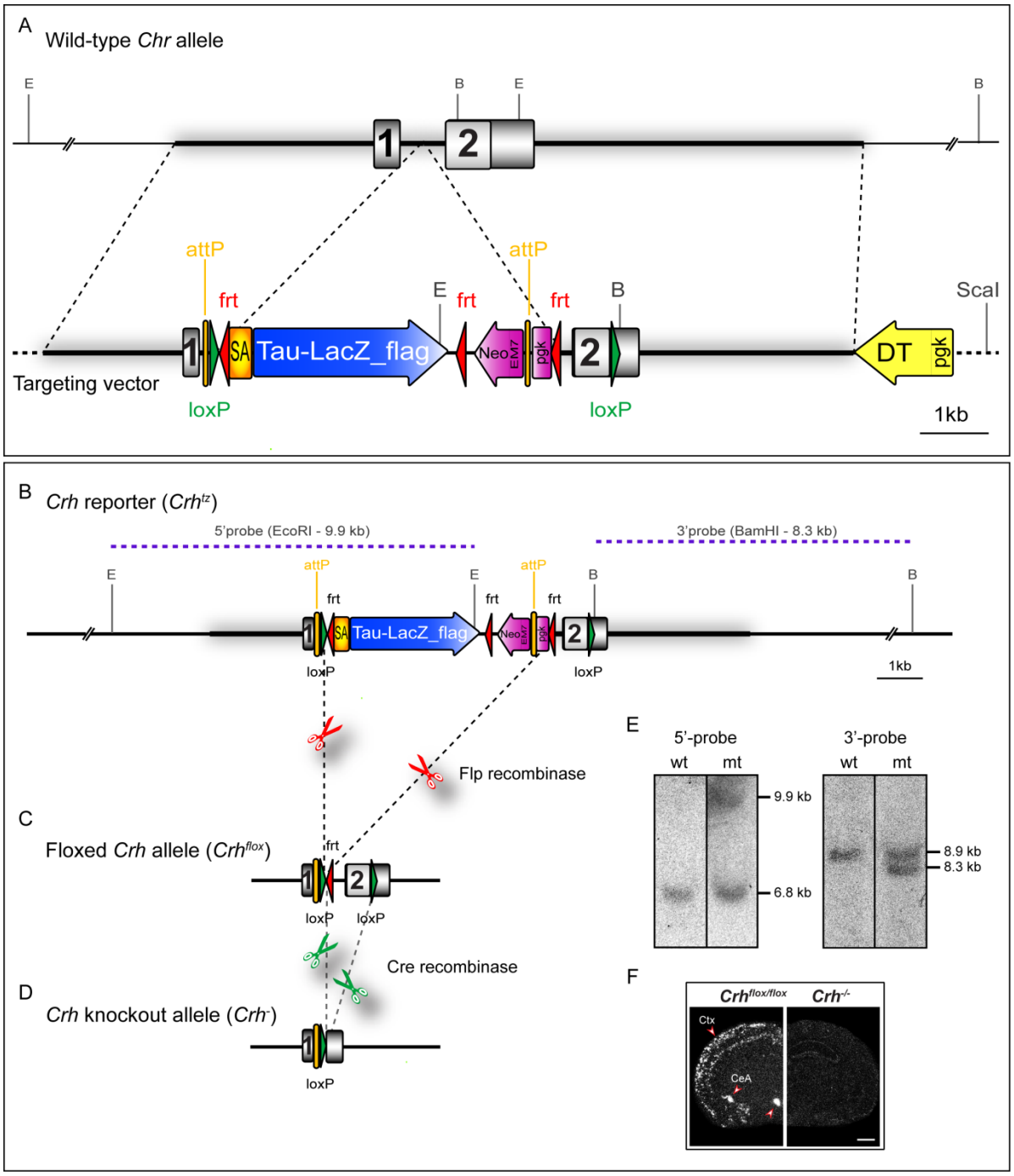

Figure 48: Generation of conditional *Crh* knockout mice.
Strategy for targeted manipulation of the *Crh* locus, based on Kühne et al., 2012. **(A)** Partial restriction maps of the wild-type locus and targeting vector. **(B)** Recombined reporter allele (Crh^{tz}) following homologous recombination in ES cells. **(C)** Recombined floxed allele (Crh^{CKO}) following removal of the *frt*-flanked reporter-selection cassette and conditional knockout allele (Crh^{-}) following Cre-meadited excision of the *loxP*-flanked exon 2 **(D)**. **(E)** Southern blot analysis of WT and targeted ES cell clones. The external *Crh* 5'-probe was hybridized to *EcoRI*-digested genomic ES cell DNA. The targeted allele is indicated by the presence of an additional mutant 9.9 kb fragment. The *Crh* 3'-probe was hybridized to *BamHI*-digested DNA from the same ES cell clone confirming homologous recombination by detection of an additional mutant fragment at 8.3 kb. **(F)** *ISH*, performed with a 3'UTR-specific *Crh* riboprobe, illustrates the absence of *Crh* mRNA throughout the brain of $Crh^{-/-}$ mice. Scale bar represents 1 mm. Mice were generated by Claudia Kühne.

A reporter-selection cassette was introduced into intron 1 of the murine *Crh* gene via homologous recombination in embryonic stem cells (ES) (Figure 48). This cassette, excluding the *Pgk* promoter, is flanked by *attP* sites, which allow for subsequent C31 integrase-mediated cassette exchange (Kuhne et al., 2012). In this configuration *Crh* exon 1 should be spliced to the strong adenoviral splice acceptor of the reporter, which utilizes its own initiation codon given that that the translational start of *Crh* is located in exon 2. This should enable stable *tau-LacZ* (*tZ*) expression under the control of the endogenous *Crh* promoter. At the same time, exon 2 was flanked by loxP sites (Figure 48A). TBV2 ES cells (129S2) were electroporated with the linearized (*ScaI*) targeting vector and mutant ES cell clones were identified by Southern blot analysis of genomic ES cell DNA digested with *EcoRI* (5'-probe) and *BamHI* (3'-probe), respectively (Figure 48). Mutant ES cells were used to generate chimeric mice by blastocyst injection. Male chimeras were bred to wildtype C57BL/6J mice to obtain germline transmission of the modified *Crh* allele (*tZ* reporter allele (Crh^{tZ}), which is a null allele) in F_1 offspring. For unknown reasons the insertion of the reporter-selection cassette into intron 1 of the murine *Crh* gene did not yield proper expression of the reporter. Reverse transcription PCR (forward primer located in *Crh* exon 1 and the reverse at the start of the *tau-LacZ* sequence) and subsequent sequencing analysis revealed the presence of a transcript which included *Crh* exon 1, the first *loxP* and *frt* site as well as the sequence of the *SA* and the start of *tau-LacZ* (data not shown). This indicated the absence of functional splicing of *Crh* exon 1 to the inserted adenoviral *SA*. However, the *tau-Lacz* cassette was designed to harbour its own ATG start codon, which should have enabled β-galactosidase expression even in the absence of functional splicing. Subsequent Lacz-stainings and *ISH* analyses revealed neither *LacZ* mRNA nor β-galactosidase protein expression in Crh^{tz} mice (data not shown). This suggests the presence of an unstable mRNA product, possibly due to ineffective splicing, ultimately resulting in degradation shortly after transcription. Importantly, *Crh* function can be restored by breeding Crh^{tz} mice to *Flpe-deleter* mice (Rodriguez et al., 2000), implying functionality of the inserted targeting vector. This leads to the removal of the reporter-selection cassette flanked by the outermost *frt* sites, which in turn restores *Crh* function and leaves exon 2 flanked by *loxP* sites (Crh^{flox}) (Figure 48B-C). Spatial and/or temporal inactivation of *Crh* expression is enabled by Cre-mediated deletion of the floxed exon 2 (Figure 48D). The novel conditional Crh^{flox} allele was evaluated by breeding $Crh^{flox/flox}$ mice to *Cre-deleter* mice, expressing Cre recombinase from the ROSA26 locus, to obtain $Crh^{flox/-}$ mice. The latter were intercrossed to obtain homozygous *Crh* knockout mice. *ISH*, using a riboprobe complementary

to the 3'UTR of *Crh*, showed identical expression of *Crh* mRNA in $Crh^{flox/flox}$ mice compared to wild type animals (data not shown). Expectedly, no *Crh* transcript was detected throughout the brain of $Crh^{-/-}$ compared to $Crh^{flox/flox}$ mice (Figure 48E). In addition, basal and stress-induced plasma corticosterone levels were analyzed. $Crh^{flox/flox}$ mice displayed normal circadian fluctuations of corticosterone levels, evident by enhanced afternoon (p.m.) compared to morning (a.m.) values. They also displayed a normal stress-response and recovery. Contrastingly, corticosterone levels in *Crh* knockout mice were barely detectable, further indicating the absence of a functional CRH allele (Figure 49).

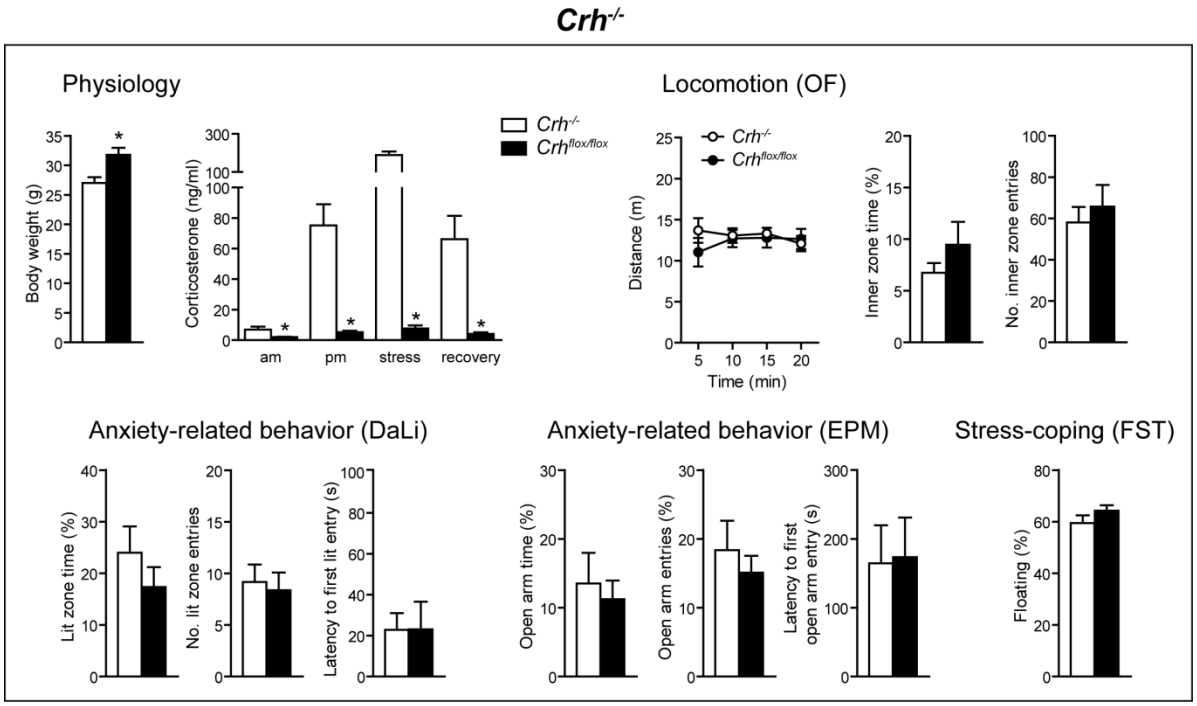

Figure 49: Constitutive *Crh* deficiency does not alter basal emotionality.
$Crh^{-/-}$ mice displayed increased body weight and strongly diminished HPA axis activity. Locomotion, anxiety and stress-coping behavior were not altered upon complete *Crh* depletion. *Significant from control, Student's t-test, $p < 0.05$; n = 10-12.

Finally, we assessed possible behavioral alterations in *Crh* deficient mice. Due to the fact that heterozygous mattings ($Crh^{flox/-}$ x $Crh^{flox/-}$) did not yield enough homozygous knockouts, additional $Crh^{-/-}$ mice were obtained from homozygous breeding pairs ($Crh^{-/-}$ x $Crh^{-/-}$). Given the fetal glucocorticoid need for lung maturation, corticosterone was supplied to the drinking water of $Crh^{-/-}$ mothers until weaning. Exogenous glucocorticoid supply during development likely explains the enhanced body weight in $Crh^{-/-}$ mice (Figure 49), which also showed a mild Cushing-like phenotype at 3 months of age (data not shown). Locomotion, stress-coping and anxiety-related behavior were not significantly altered in $Crh^{-/-}$ compared to $Crh^{flox/flox}$ mice

(*Crh*$^{Ctrl\text{-}CKO}$)(Figure 49), which is in agreement with the results obtained by Muglia and colleagues (Weninger et al., 1999).

4.3.4. Deletion of *Crh* from GABAegic neurons diminishes stress susceptibility

Having established that CRH is primarily expressed in GABAergic neurons of forebrain limbic structures and the cortex, as well as glutamatergic neurons of the piriform cortex, we made use of conditional mutagenesis to specifically dissect the involvement of CRH in these distinct neuronal populations. *Crh*$^{flox/flox}$ mice were crossed with *Dlx5/6-Cre* and *Nex-Cre* mice leading to *Crh* deletion in forebrain GABAergic neurons (*Crh*$^{GABA\text{-}CKO}$) and glutamatergic neurons (*Crh*$^{Glu\text{-}CKO}$), respectively. The pattern of *Crh* deletion in *Crh*$^{GABA\text{-}CKO}$ and *Crh*$^{Glu\text{-}CKO}$ mice was largely in line with the expression maps obtained with double *ISH* (Figure 50). Thus, lack of *Crh* expression was observed in the OB, BNST, CeA, hippocampus and throughout the cortex of *Crh*$^{GABA\text{-}CKO}$ mice. In contrast, *Crh*$^{Glu\text{-}CKO}$ mice displayed absence of *Crh* mRNA in the OB, piriform cortex and medial vestibular nucleus (MVe) (Figure 50). Co-localization scores and deletion patterns are additionally summarized in Table 19 (Section 4.3.5). Importantly, neither the *Dlx5/6-Cre* nor the *Nex-Cre* recombined in CRH-expressing neurons of the PVN, resulting in unaltered HPA axis activity in both mouse lines (Figure 50 and Figure 51). Thus, preserved CRH expression in the PVN is sufficient for normal HPA axis regulation. To functionally dissect whether GABAergic and/or glutamatergic neurons are mediating the effects of CRH on emotional behavior, *Crh*$^{GABA\text{-}CKO}$ and *Crh*$^{Glu\text{-}CKO}$ mice were subjected to a series of behavioral tests. The fact that deletion of *Crhr1* alters emotional behavior, suggests that ablation of the main ligand/CRH would produce similar effects. Expectedly *Crh*$^{Glu\text{-}CKO}$ mice displayed no alterations in locomotion, anxiety and stress-coping behavior (Figure 51), since *Crh*-deletion was mainly restricted to the piriform cortex and MVe; brain structures which are rarely implicated in emotional behavior. More surprisingly, *Crh* deletion from GABAergic neurons, which results in *Crh* absence from all limbic structures, also failed to alter behavioral responses (Figure 51). To exclude the possibility that *Crh* in more caudal brain regions is regulating anxiety, locomotion and stress-coping behavior, we crossed *Crh*$^{flox/flox}$ with *En1-Cre* mice to generate mid/hindbrain-specific *Crh* knockout mice (*Crh*$^{MHB\text{-}CKO}$). Lack of *Crh* expression was detected in most MHB regions including the anterior pretectal nucleus, parabrachial nucleus and Barrington's nucleus (Figure 50). However, body weight, HPA axis activity and emotional behavior were not altered in *Crh*$^{MHB\text{-}CKO}$ mice (Figure 52).

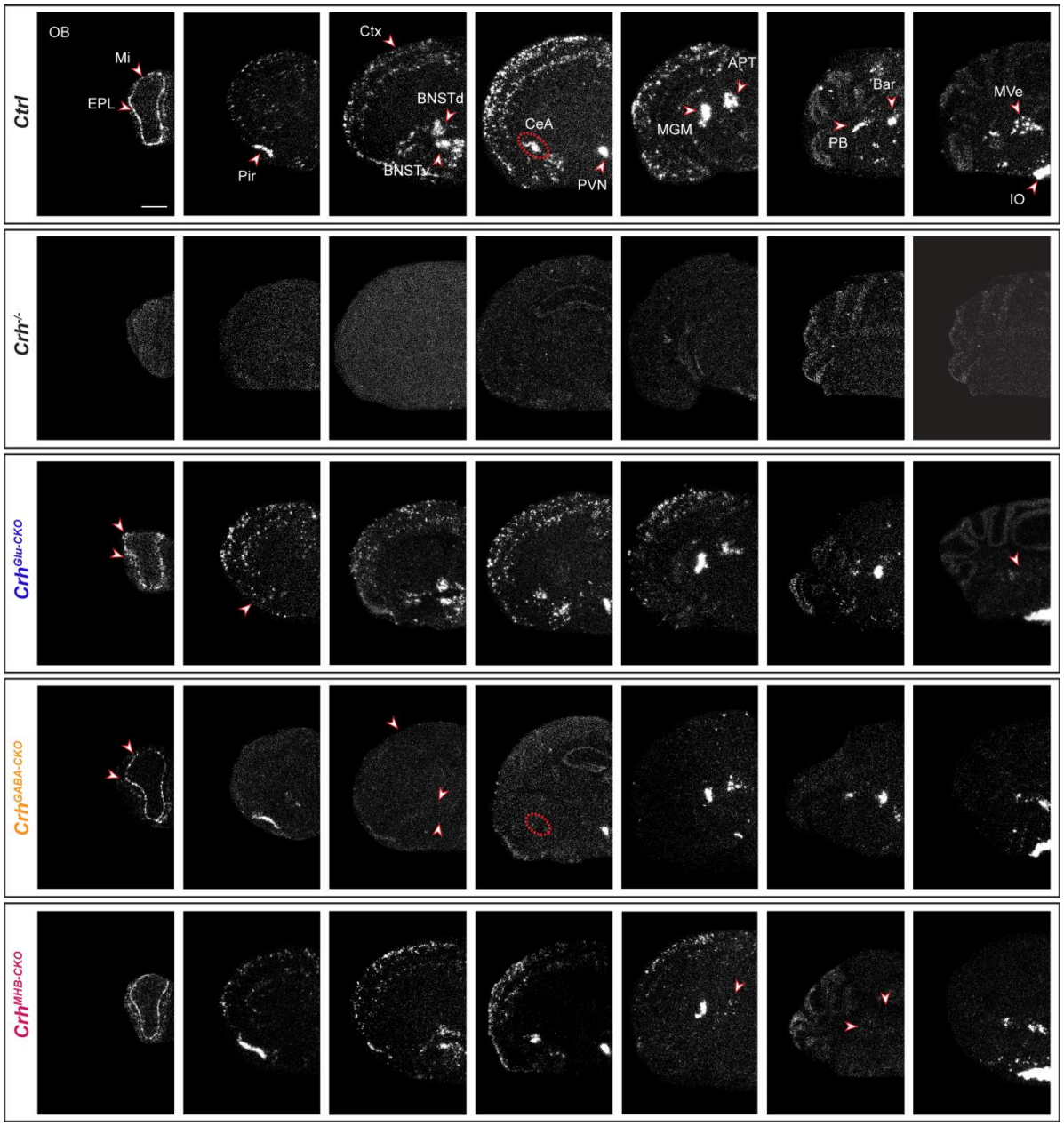

Figure 50: Conditional *Crh*^{CKO} lines lack *Crh* in a region and cell-type specific manner.
Expression of *Crh* mRNA was assessed by *ISH* in control and conditional knockout lines, using a riboprobe, which detects the *3'UTR* of *Crh*. Dark-field photomicrographs depict the specific patterns of *Crh* deletion in *Crh*$^{-/-}$ (ubiqitious), *Crh*$^{Glu\text{-}CKO}$ (glutamatergic / *Nex-Cre*), *Crh*$^{GABA\text{-}CKO}$ (GABAergic / *Dlx5/6-Cre*), and *Crh*$^{MHB\text{-}CKO}$ (mid-hind brain / *En1-Cre*) mice. Areas of interest are highlighted with arrowheads and dashed lines. Abbreviations: anterior pretectal nucleus (APT), Barrington's nucleus (Bar), central amygdala (CeA), bed nucleus of the stria terminalis dorsal/ventral (BNST), cortical layers (CtxII/III, CtxV/VI), inferior olive (IO), medium geniculate nucleus (MGM), medial vestibular nucleus (MVe), olfactory bulb external plexiform layer (EPL), olfactory bulb mitral layer (Mi), parabrachial nucleus (PB), piriform cortex (Pir), paraventricular nucleus of the hypothalamus (PVN). Scale bar represents 1 mm.

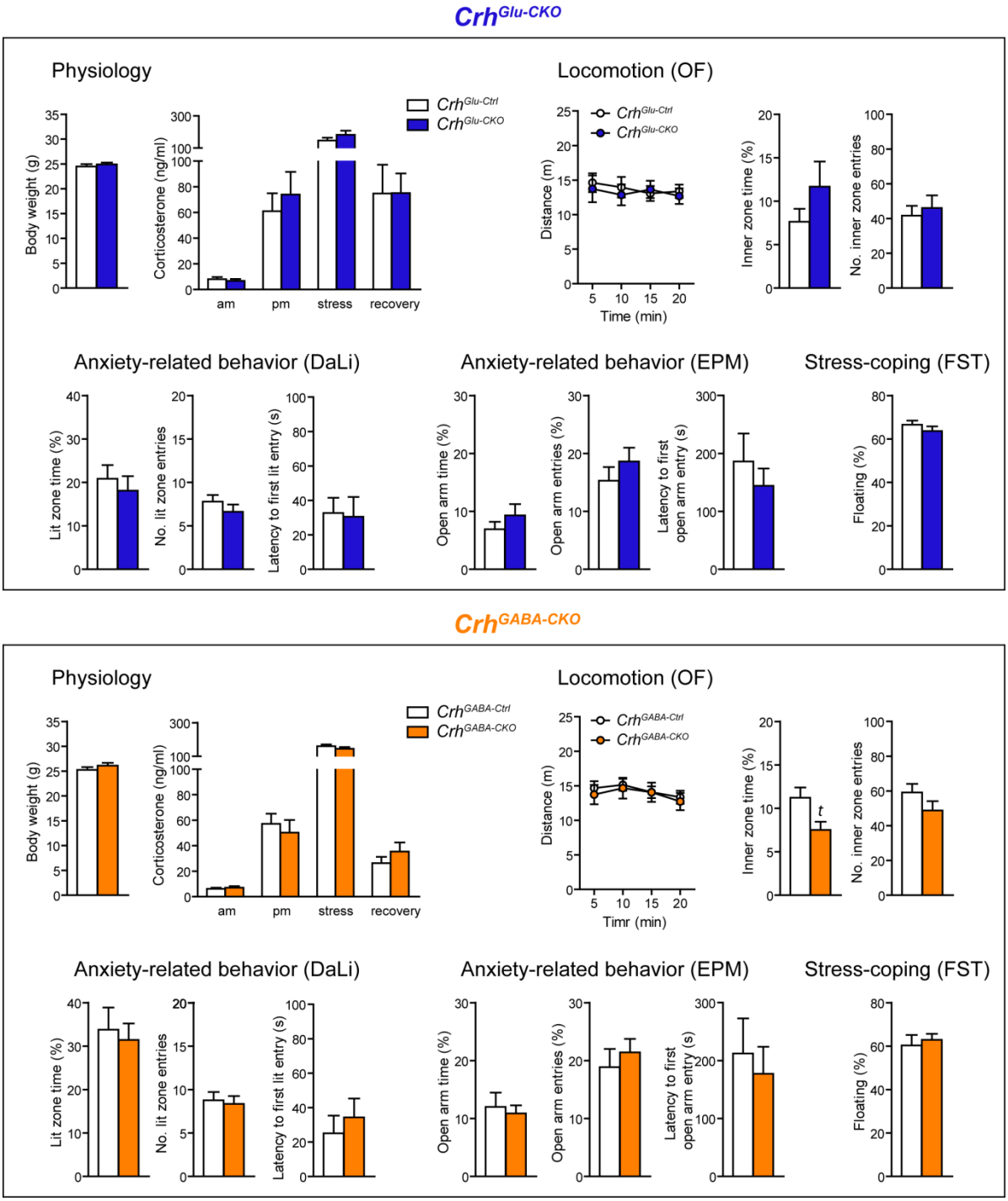

Figure 51: HPA axis activity and emotional behavior are not altered in *Crh*$^{Glu\text{-}CKO}$ and *Crh*$^{GABA\text{-}CKO}$ mice.
Body weight, HPA axis activity, general locomotion, anxiety-related behavior and active stress-coping behavior were not significantly altered upon *Crh* deletion of from glutamatergic (*Nex-Cre*) or GABAergic (*Dlx5/6-Cre*) neurons. Students t-test, *t* trend, $p \leq 0.01$.

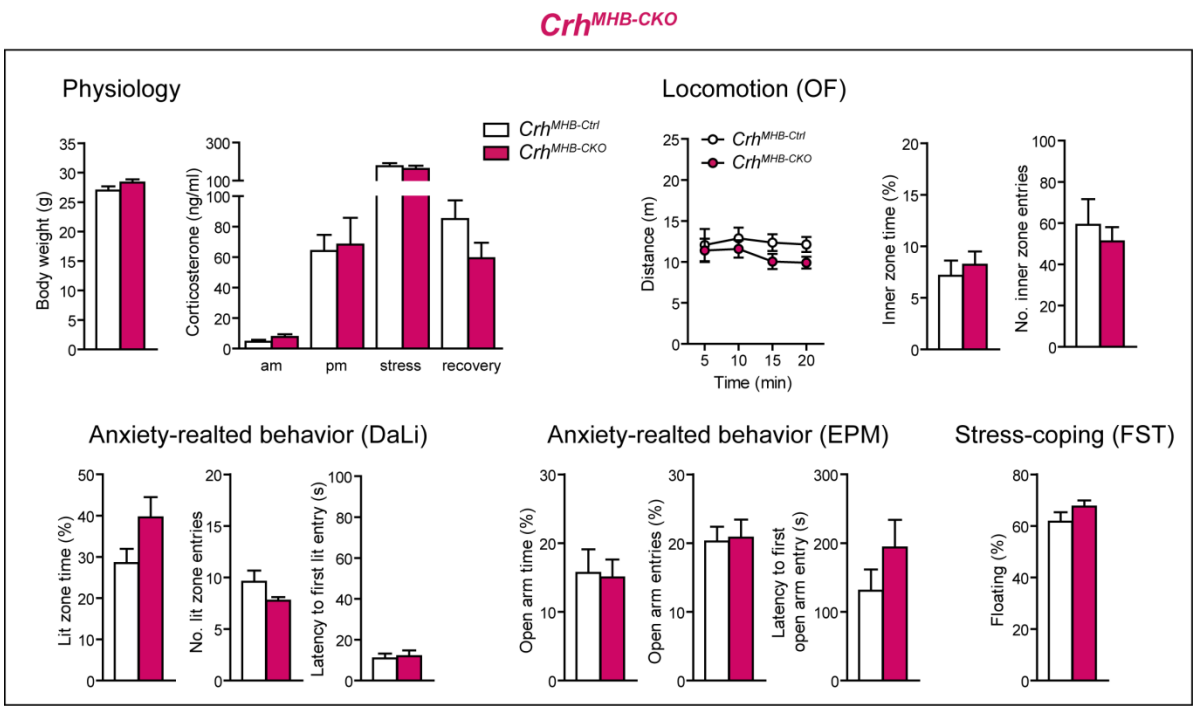

Figure 52: Deletion of *Crh* from mid/hindbrain regions does not alter emotional behavior.
Body weight, HPA axis activity, general locomotion, anxiety-related behavior and active stress-coping behavior were not significantly altered upon *Crh* deletion from the mid/hindbrain regions (*En1-Cre*).

The lack of behavioral effects in $Crh^{GABA\text{-}CKO}$ mice might be explained by one, or a combination of the following. 1st) Recombination of the *Dlx5/6-Cre* during development (E10) might have initiated early compensatory mechanisms. To date, UCN1, which is primarily expressed in the Edinger Westphal nucleus, represents the only additional CRHR1 ligand (Vaughan et al., 1995; Fekete and Zorrilla, 2007). Although this structure was shown to innervate numerous brain regions (Klooster et al., 1993), it is questionable whether UCN1 alone can compensate for limbic and cortical CRH deletion. 2nd) However, the presence of an additional, so far unknown CRHR1 ligand might explain the lack of behavioral effects in total and conditional *Crh* deficient mice. Considering that the mouse genome has been sequenced, and the efficacy of current bioinformatic tools to detect alternative agonists, would point towards a novel ligand which is structurally different from *Crh* and the UCNs. 3rd) Constitutive activity of CRHR1 and CRHR2, which are G-protein coupled receptors (GPCRs), is probably the more likely explanation. Constitutive activity describes the intracellular metabolic tone, associated with many GPCRs that does not require the presence of an agonist (Seifert and Wenzel-Seifert, 2002). Thus, CRHR1 might exhibit constant tonic activity, even in the absence of a ligand, resulting in the initiation of downstream signaling events. This could explain the consistent behavioral effects in conditional and total *Crhr1* knockout mice, as well as the absence of behavioral effects in *Crh*

deficient mice. Importantly, constitutive activity of CRHR1 would imply that CRH exerts its effects mainly during stress, when it is most strongly released. Along these lines, CRHR1 antagonist application was shown to block stress-induced anxiety behavior and cognitive deficits in mice (Liebsch et al., 1995; Ivy et al., 2010; Wang et al., 2011a; Wang et al., 2013). To assess whether deletion of *Crh* from cortical and limbic structures would alter stress susceptibility, $Crh^{GABA\text{-}CKO}$ mice were subjected to three weeks of chronic social defeat stress. As previously mentioned, CSDS is able to induce and exacerbate mood-related psychopathologies. Basal and acute-stress induced corticosterone levels were significantly elevated in chronically stressed mice independent of genotype (*Basal*: 2-Way ANOVA, stress $F_{(1,46)} = 10.4$, $p < 0.005$; Bonferroni post-test, $p < 0.05$ / *Response*: 2-Way ANOVA, stress $F_{(1,44)} = 20.4$, $p < 0.0001$; Bonferroni post-test, $p < 0.05$) (Figure 53A). In addition, CSDS resulted in enhanced adrenal gland weight and decreased thymus weight in stressed $Crh^{GABA\text{-}Ctrl}$ and $Crh^{GABA\text{-}CKO}$ mice (*AG*: 2-Way ANOVA, stress $F_{(1,48)} = 42.5$, $p < 0.0001$; Bonferroni post-test, $p < 0.05$ / *Thymus*: 2-Way ANOVA, stress $F_{(1,48)} = 58.9$, $p < 0.0001$; Bonferroni post-test, $p < 0.05$)(Figure 53A). These robust stress markers demonstrate the effectiveness of the paradigm as observed in section 4.1.2.4 and reported by others (Wagner et al., 2011; Hartmann et al., 2012a; Hartmann et al., 2012b; Wang et al., 2013). A mild genotype effect was detected for recovery corticosterone levels, implying alterations in HPA axis feedback in $Crh^{GABA\text{-}CKO}$ mice (2-Way ANOVA, genotype $F_{(1,44)} = 6.2$, $p < 0.05$) (Figure 53A). General locomotion and exploration in the OF was significantly reduced in $Crh^{GABA\text{-}Ctrl}$ and $Crh^{GABA\text{-}CKO}$ mice following CSDS (Figure 53B), whereas inner zone time and number of entries were not affected (RM-ANOVA, time x stress $F_{(1,47)} = 4.8$, $p < 0.05$; stress $F_{(1,48)} = 16.9$, $p < 0.0001$; Bonferroni post-test, $p < 0.05$). Interestingly, $Crh^{GABA\text{-}CKO}$ mice were less vulnerable to the anxiety-inducing effects of CSDS. The latencies to enter the aversive lit zone of the DaLi and open arms of the EPM were significantly increased in chronically stressed $Crh^{GABA\text{-}Ctrl}$ but not $Crh^{GABA\text{-}CKO}$ mice (*DaLi*: 2-Way ANOVA, genotype x stress $F_{(1,43)} = 4.3$, $p < 0.05$; stress $F_{(1,43)} = 4.2$, $p < 0.05$; Bonferroni post-test, $p < 0.05$ / *EPM*: 2-Way ANOVA, genotype $F_{(1,44)} = 4.6$, $p < 0.05$; stress $F_{(1,44)} = 4.0$, $p = 0.051$; Bonferroni post-test, $p < 0.05$)(Figure 53D-E). In accordance, lit zone time and number of entries were significantly reduced in $Crh^{GABA\text{-}Ctrl}$ following CSDS; this stress effect was absent in $Crh^{GABA\text{-}CKO}$ mice (*time*: 2-Way ANOVA, stress $F_{(1,44)} = 4.9$, $p < 0.05$; Bonferroni post-test, $p < 0.05$ / *entries*: 2-Way ANOVA, stress $F_{(1,44)} = 12.2$, $p < 0.005$; Bonferroni post-test, $p < 0.05$).

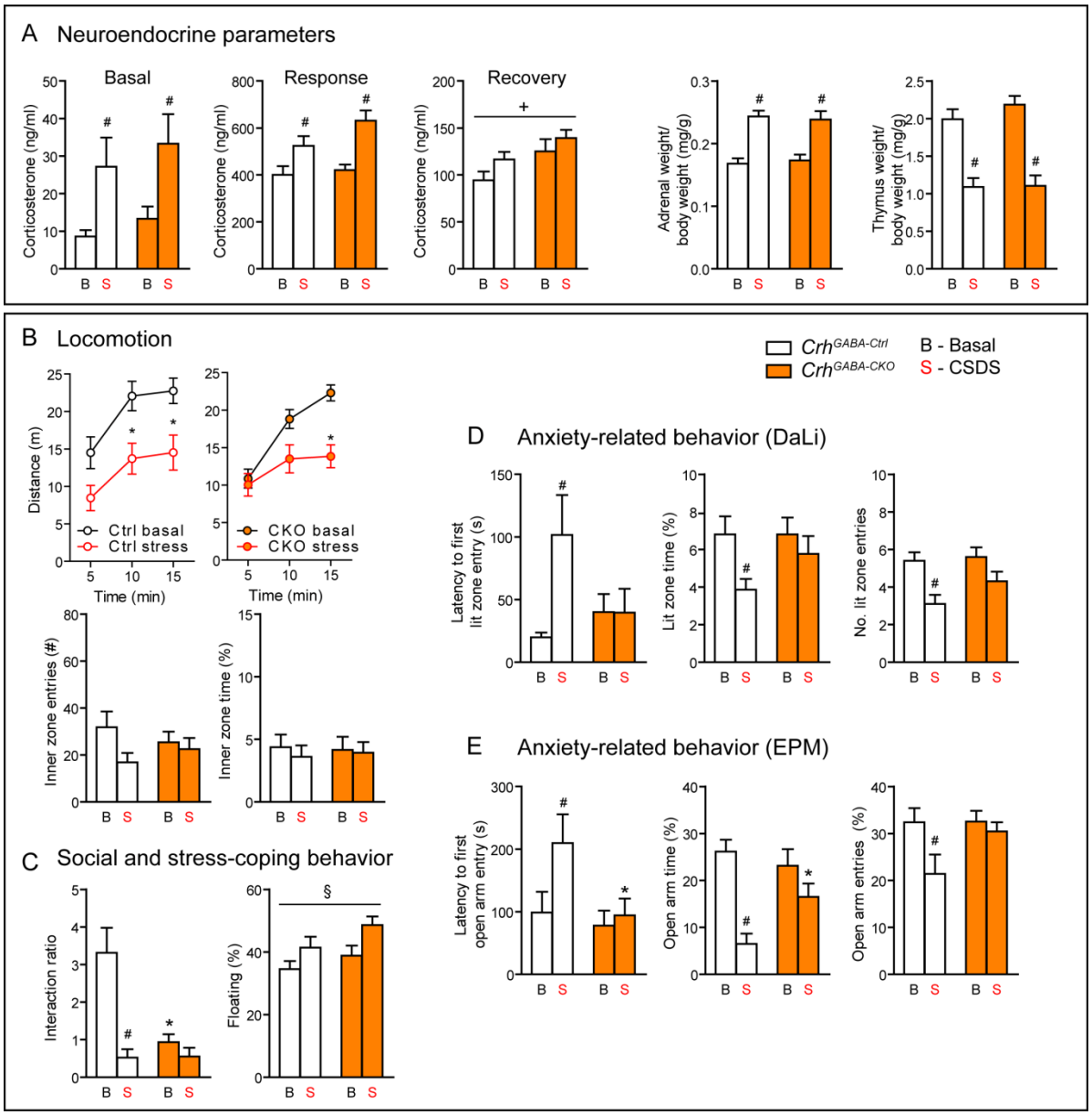

Figure 53: *Crh* deletion in GABAergic neurons reduces susceptibility to chronic social defeat stress.
(A) Control and *Crh*$^{GABA\text{-}CKO}$ mice showed enhanced basal and stress-induced response (30 min post FST stress) corticosterone levels, increased adrenal gland weight and decreased thymus weight following CSDS. Recovery from FST-stress was slightly enhanced in *Crh*$^{GABA\text{-}CKO}$ mice independent of condition. **(B)** CSDS reduced locomotion independent of genotype. **(C)** CSDS reduced interaction ratios in control mice during the social avoidance test. This effect was absent in *Crh*$^{GABA\text{-}CKO}$ mice, which displayed reduced baseline interaction. Active stress-coping behavior in the FST was not affected by genotype and/or condition. **(D-E)** Anxiety-related behavior in the DaLi and EPM was significantly enhanced in control, but not *Crh*$^{GABA\text{-}CKO}$ mice. This is depicted by increased latencies to enter the aversive lit zone of the DaLi and open arms of the EPM, as well as reduced lit/open arm time and entries in control but not *Crh*$^{GABA\text{-}CKO}$ mice. *Significant from control of the same condition, # significant from the chronically stressed group of the same genotype, + significant genotype effect; § significant condition effect; RM-ANOVA or 2-Way ANOVA, $p < 0.05$; Bonferroni post-test, $p < 0.05$; n = 11-13.

Similarly, chronically stressed *Crh*$^{GABA\text{-}Ctrl}$ mice spent less time on the open arms of the EPM and entered these less frequently, which was not observed upon deletion of *Crh* from GABAergic neurons (*time*: 2-Way ANOVA, genotype x stress $F_{(1,44)} = 4.4$, $p < 0.05$; stress $F_{(1,44)} = 18.2$, $p < 0.0001$; Bonferroni post-test, $p < 0.05$ / *entries*: 2-Way ANOVA, genotype x stress $F_{(1,44)} = 2.5$, $p = 0.12$; stress $F_{(1,44)} = 5.4$, $p < 0.05$; Bonferroni post-test, $p < 0.05$)(Figure 53E). As initially reported, genotype alterations were not observed under basal conditions (Figure 51 and Figure 53). Thus, CSDS enhanced anxiety-related behavior in control but not *Crh*$^{GABA\text{-}CKO}$ mice. Alterations in social behavior are observed in many psychiatric disorders including, major depressive disorder, bipolar disorder, schizophrenia and autism (Nestler and Hyman, 2010). In addition, CSDS is able to reduce social interaction and enhance avoidance behavior (Berton et al., 2006). To test whether *Crh*-deletion from GABAergic neurons would affect social behavior under basal and chronic stress conditions, we performed the social avoidance test. Chronically stressed control mice spent significantly less time in close proximity to a social counterpart, indicated by a decreased interaction ratio (Figure 53C). Interestingly, reduced social interaction was observed in *Crh*$^{GABA\text{-}CKO}$ mice compared to controls already under basal conditions, and was not further aggravated following CSDS (2-Way ANOVA, genotype x stress $F_{(1,41)} = 9.8$, $p < 0.005$; stress $F_{(1,41)} = 17.0$, $p < 0.0005$; genotype $F_{(1,41)} = 9.3$, $p < 0.005$; Bonferroni post-test, $p < 0.05$). This implies that CRH in GABAergic neurons is required for the expression of “normal” social behavior. Active stress-coping behavior in the FST was decreased following CSDS independent of genotype (Figure 53C). Overall, our results indicate that CRH in GABAergic neurons is mediating the effects of CSDS on anxiety-related behavior.

To date, no specific downstream targets of CRH/CRHR1-signalling have been discovered, which makes it extremely difficult to assess the underlying molecular alterations of “chronic stress-resistant” *Crh*$^{GABA\text{-}CKO}$ mice. Many studies have utilized the expression of immediate early genes, especially *c-fos*, to evaluate stress-induced patterns of neuronal activation (Kollack-Walker et al., 1997; Martinez et al., 2002). We applied a similar approach, by analyzing *c-fos* and *zif268* expression in *Crh*$^{GABA\text{-}Ctrl}$ and *Crh*$^{GABA\text{-}CKO}$ mice following 30 min of acute FST-stress. Basal *c-fos* and *zif268* expression is consistently low in brains of resting rodents, and was not significantly different between *Crh*$^{GABA\text{-}Ctrl}$ and *Crh*$^{GABA\text{-}CKO}$ mice (data not shown). Following acute FST-stress, a marked increase of *c-fos* and *zif268* expression was detected throughout the brain of *Crh*$^{GABA\text{-}Ctrl}$ and *Crh*$^{GABA\text{-}CKO}$ mice (Figure 54). However, diminished *c-fos* expression was observed in the hippocampus, and most cortical sites of *Crh*$^{GABA\text{-}CKO}$ compared to control mice (Figure 54).

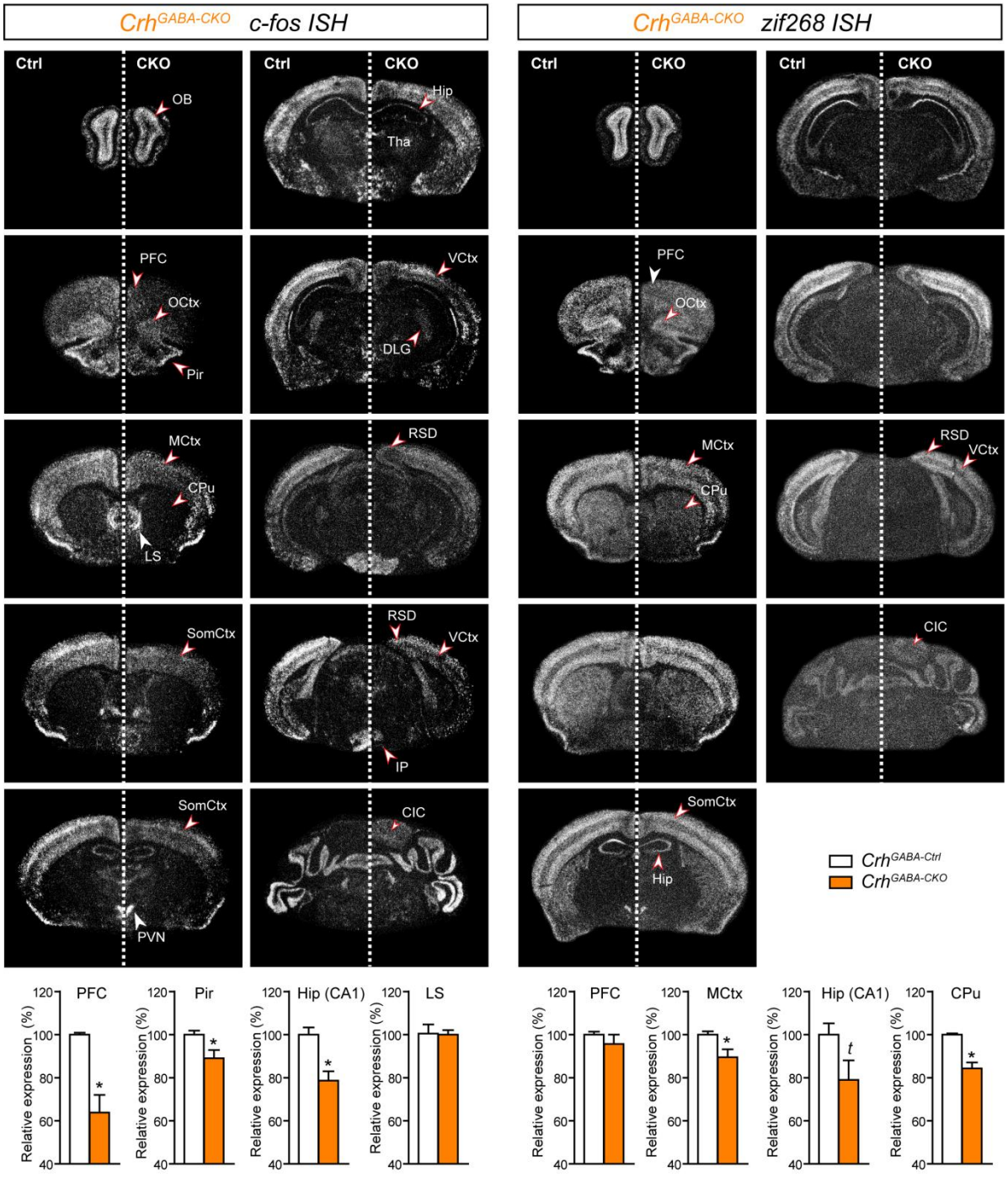

Figure 54: Stress-induced neuronal activation is diminished in *Crh*$^{GABA\text{-}CKO}$ mice.
Forced swim stress induced a significantly stronger expression of *c-fos* and *zif268* mRNA in the hippocampus ($t_{(21)}$ = 3.9, p < 0.005), caudate putamen ($t_{(18)}$ = 5.6, p < 0.0001) and throughout the cortex ($t_{(22)}$ = 4.4, p < 0.0005) of *Crh*$^{GABA\text{-}CKO}$ than of *Crh*$^{GABA\text{-}Ctrl}$ mice, determined by *ISH*. Quantification of the respective *c-fos* and *zif268* mRNA expression in distinct brain regions is shown below the representative dark-field photomicrographs. *Significantly different from control; Student's t-test, p < 0.05; *t* trend, p ≤ 0.01; Scale bar represents 1mm.

Similar effects were observed for *zif268* expression, where decreased activation was additionally detected in the caudate putamen of *Crh*$^{GABA\text{-}CKO}$ mice (Figure 54). These results suggest that CRH depletion in GABAergic neurons reduces stress-dependent neuronal

activation in CRHR1-expressing brain regions such as the cortex and hippocampus. This is further supported by the fact that *c-fos* expression was not differentially altered in the PVN of $Crh^{GABA\text{-}CKO}$ mice, a structure which barely contains *Crhr1* and where *Crh*-expression remained intact. Given its ability to facilitate excitatory neurotransmission in regions such as the amygdala and hippocampus, CRH can be denoted as an activating neuropeptide (Aldenhoff et al., 1983; Hollrigel et al., 1998; Giesbrecht et al., 2010; Refojo et al., 2011). CRH administration into different brain regions is able to induce *c-fos* expression and mimic acute-stress effects (Dunn and Berridge, 1990; Liebsch et al., 1995; Rostkowski et al., 2013). In addition, CNS-specific CRH overexpressing mice demonstrate enhanced activation of the locus coeruleus following forced-swim stress (Lu et al., 2008). Thus, it seems plausible that deletion of *Crh* from most cortical and all limbic regions should produce a net inhibitory effect, exhibited by decreased stress-induced *c-fos* activation. The necessity to uncover the precise mechanisms by which CRH acts in an excitatory fashion becomes evident in view of the fact that CRH is primarily released from inhibitory GABAergic neurons. Overall our data suggests that deletion of *Crh* in GABAergic neurons protects from the adverse effects of CSDS, possibly by reducing stress-induced neuronal activation. The absence of basal behavioral alterations in conditional *Crh* knockout mice further supports the idea that *Crh*-induced changes in mood-related behavior are primarily initiated during stress.

4.3.5. CAMK2α-expressing CRH neurons are required for positive emotional responses

Although we could show that GABAergic-CRH neurons control stress-induced emotional behavior, it should be kept in mind that *Crh* is entirely deleted from the cortex and all limbic structures of $Crh^{GABA\text{-}CKO}$ mice. These neurons most probably represent the *Crh*-source for both anxiogenic and anxiolytic *Crhr1* in glutamatergic and dopaminergic neurons respectively. We have already postulated that under physiological conditions, CRHR1-controlled glutamatergic and dopaminergic systems might function in a concerted but antagonistic manner to keep adaptive anxiety responses to stressful situations in balance (Refojo et al., 2011). This is additionally supported by the fact that deletion of *Crhr1* in both neurotransmitter systems ($Crhr1^{CNS\text{-}CKO}$) fails to alter mood-related behavior (Refojo et al., 2011). Correspondingly, depletion of *Crh* required for glutamatergic and dopaminergic CRHR1 activation, might lead to the same outcome, and thereby additionally explain the absence of basal behavioral effects in $Crh^{GABA\text{-}CKO}$ mice. Thus, different subpopulations of CRH neurons within the same brain

structure probably activate different classes of receptors. We could already show that *Crh* is expressed in at least two distinct neuronal subgroups consisting of spiny and aspiny neurons, some of which are able to project over long distances (Section 4.3.2). Considering the vast co-localization of *Crh* with *Gad65/67*, as well as its absence in limbic and cortical structures of $Crh^{GABA\text{-}CKO}$ mice, suggests that spiny and aspiny CRH neurons are predominantly GABAergic. Importantly, we identified CAMK2α as a potential marker of spiny, long-projecting CRH-neurons. Therefore, we decided to specifically address the involvement of CAMK2α-positive CRH neurons in emotional behavior. $Crh^{flox/flox}$ mice were crossed with inducible (largerly forebrain-restricted) *Camk2α-CreERT2* mice to generate the $Crh^{iFB\text{-}CKO}$ line. Deletion was induced during postnatal week 10 via 2 weeks of oral tamoxifen application. Importantly, this allowed us to address the role of *Crh* during adulthood, circumventing possible compensatory mechanisms associated with developmental deletion. An additional advantage is achived by the absence of gradual deletion processes, which frequently occur in non-inducible Cre lines, and have been demonstrated for *Camk2α-Cre* mice (Refojo et al., 2011). In order to verify that *Camk2α-CreERT2* recombines solely in endogenously *Camk2α*-expressing neurons, we performed double *ISH*. Co-expression patterns of *Crh* and tomato in *Camk2α-CreERT* mice bred to *Ai9*-reporter mice were compared to double *ISHs* performed against *Crh* and endogenous *Camk2α* in wild-type mice. A similar degree of co-localization was observed in representative structures including the Pir, Ctx, CeA and PVN, arguing against ectopic *Camk2α-CreERT2* expression in *Camk2α-CreERT2:Ai9* mice (Figure 55). However, an additional control would include double *ISH* against endogenous *Camk2α* and tomato in *Camk2α-CreERT2:Ai9* mice. Next, we assessed the *Crh* deletion pattern in $Crh^{iFB\text{-}CKO}$ mice. Lack, but not complete absence of *Crh* expression in the OB, Pir, Ctx, BNST, CeA, PVN, APT, MGM and PB was observed in $Crh^{iFB\text{-}CKO}$ mice compared to controls (Figure 56A). The pattern of *Crh* deletion perfectly mirrors the expression map obtained with double *ISH*, which further emphasizes the substantial population of *Camk2α*-positive CRH neurons (Figure 43 and Table 19). $Crh^{iFB\text{-}CKO}$ mice exhibited no alterations in body weight compared to littermate controls (Figure 56B). Although *Crh* expression was absent in few *Camk2α*-positive neurons of the PVN, basal and stress-induced HPA axis activity remained unchanged in $Crh^{iFB\text{-}CKO}$ mice (Figure 56B). Subsequently, we aimed to dissect the involvement of *Camk2α*-positive CRH neurons in mood-related behavior. $Crh^{iFB\text{-}CKO}$ mice showed slightly reduced locomotion in the OF test, but this did not reach statistical significance (Figure 56C). Active stress-coping behavior in the FST was also not significantly affected in $Crh^{iFB\text{-}CKO}$ mice.

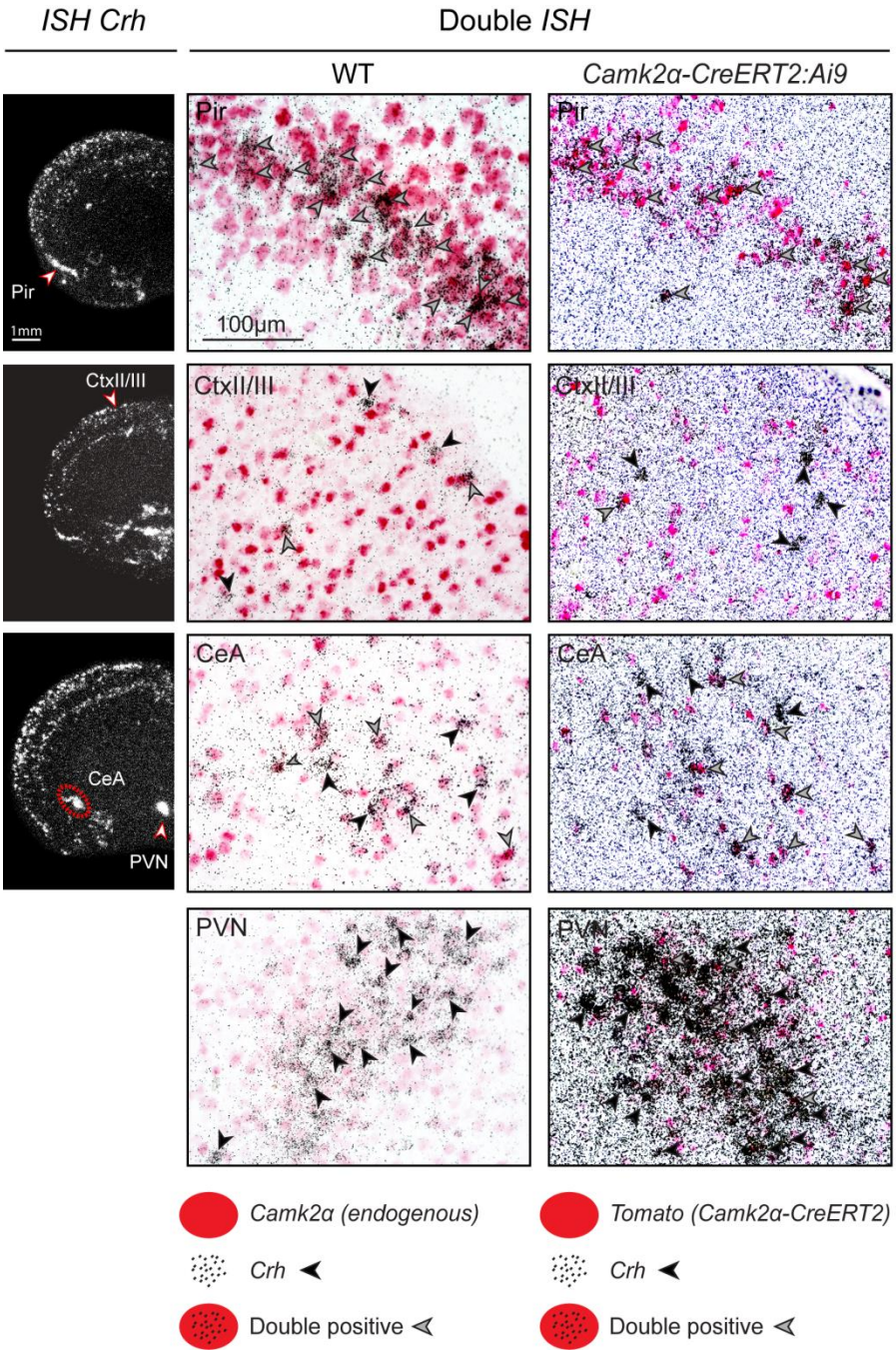

Figure 55: Validation of cell-type specific recombination in *Camk2α-CreERT2* mice.
The first left column depicts dark-field photomicrographs of the *Crh* mRNA expression pattern in brain sections of wild-type mice. Regions of interest are highlighted with red arrowheads and dashed lines. The second column represent bright field photomicrographs of coronal wild-type brain sections showing double *ISH* of *Crh* mRNA (silver grains) together with the calmodulin calcium-dependent kinase 2α (*Camk2α,* red staining). Black arrowheads indicate cells only expressing *Crh* (silver grains). Grey arrowheads indicate cells co-expressing *Crh* and *Camk2α*. The third column shows bright field photomicrographs of coronal brain sections obtained from *Camk2α-CreERT2* mice bred to *Ai9* reporter mice (*Camk2αCreERT2:Ai9*). Double *ISH* of *Crh* mRNA (silver grains) together with the tomato (red staining) is shown. Black arrowheads indicate cells only expressing *Crh* (silver grains). Grey arrowheads indicate cells expressing *Crh* and *tomato*. The co-localization pattern is simillar in both lines. Abbreviations: central nucleus of the amygdala (CeA), cortical layers (CtxII/III, CtxV/VI), paraventricular nucleus of the hypothalamus (PVN), piriform cortex (Pir).

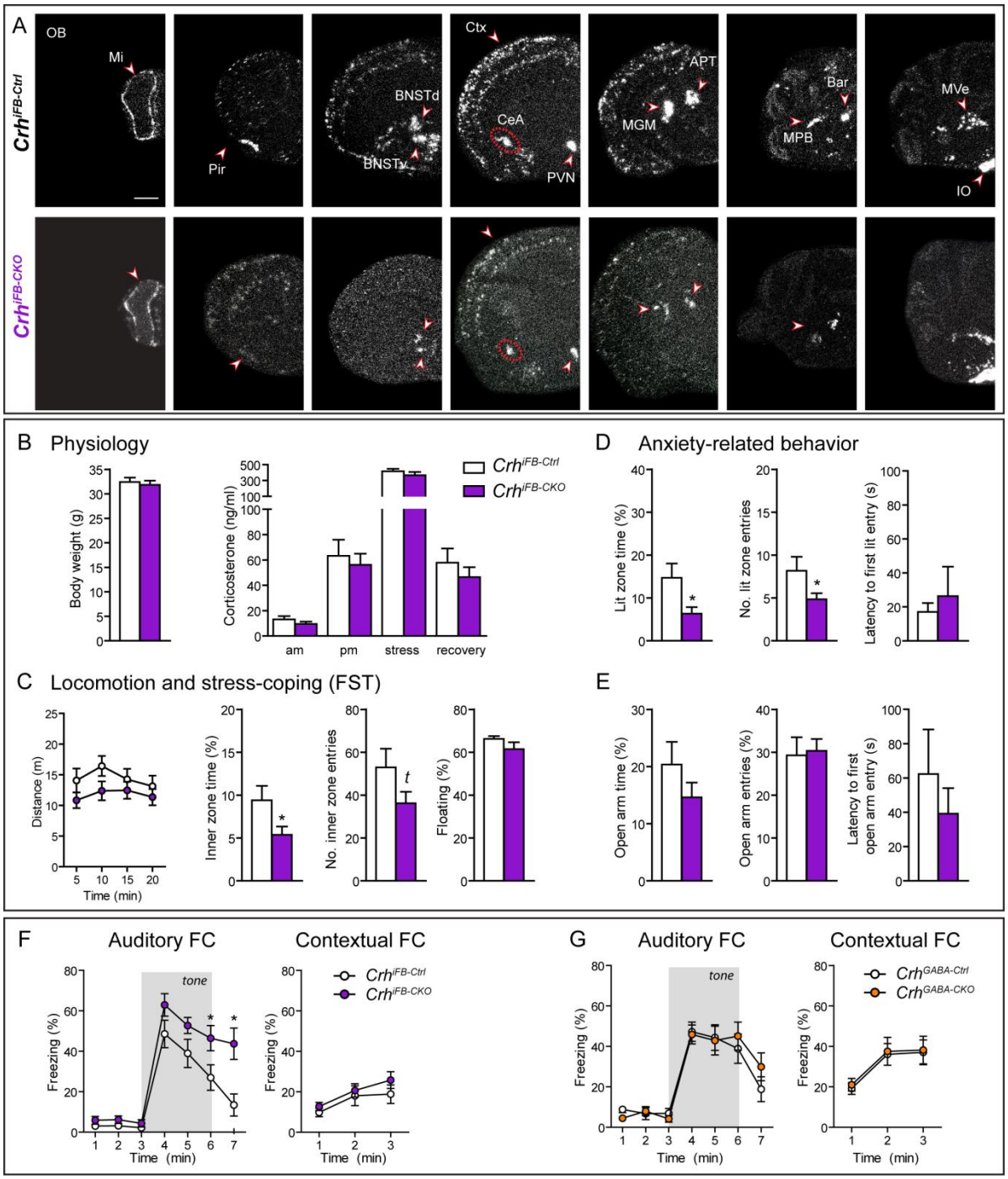

Figure 56: Deletion of *Crh* in *Camk2α*-positive neurons enhances anxiety-related behavior.
(A) Dark-field photomicrographs of *ISH* depict the specific pattern of *Crh* deletion in control and conditional knockout mice lacking *Crh* in *Camk2α*-positive neurons ($Crh^{iFB\text{-}CKO}$ / *Camk2α-CreERT2*). Areas of interest are highlighted with arrowheads and dashed lines. **(B)** Body weight and HPA axis remained unchanged in $Crh^{iFB\text{-}CKO}$ mice. **(C)** Inner zone time in the OF was significantly reduced in $Crh^{iFB\text{-}CKO}$ mice. Time floating in the FST was simillar between genotypes. **(D-E)** $Crh^{iFB\text{-}CKO}$ mice displayed enhanced anxiety-related behavior in the DaLi, but not in the EPM. **(F-G)** Expression of auditory fear memory was significantly increased in $Crh^{iFB\text{-}CKO}$ but not $Crh^{GABA\text{-}CKO}$ mice. Abbreviations: anterior pretectal nucleus (APT), Barrington's nucleus (Bar), central nucleus of the amygdala (CeA), bed nucleus of the stria terminalis dorsal/ventral (BNST), cortical layers (CtxII/III, CtxV/VI), inferior olive (IO), medium geniculate nucleus (MGM), medial vestibular nucleus (MVe), olfactory bulb mitral layer (Mi), piriform cortex (Pir), paraventricular nucleus of the hypothalamus (PVN). *Significant from control; RM-ANOVA + Bonferroni post-test for time-dependent analysis, $p < 0.05$; Student's t-test, $p < 0.05$; *t* trend, $p \leq 0.1$; Scale bar represents 1 mm.

Brain Region	Relative expression strength: Crh	Relative expression strength: Marker	Colocalization Score	Conditional *Crh-KO* lines showing *Crh* deletion
Olfactory bulb (OB)	+	Glu ++ Camk2α++ GABA ++++	+ + ++	$Crh^{Glu\text{-}CKO}$ ↓ $Crh^{iFB\text{-}CKO}$ ↓ $Crh^{GABA\text{-}CKO}$ ↓
Cortical layers (II/III, IV) including the PFC	++	Glu +++ Camk2α +++ GABA ++	+ ++ +++	$Crh^{iFB\text{-}CKO}$ ↓↓ $Crhr1^{GABA\text{-}CKO}$ —
Piriform cortex (Pir)	++++	Glu +++ Camk2α +++ GABA +	++++ ++++ -/+	$Crh^{Glu\text{-}CKO}$ ↓↓↓ $Crh^{iFB\text{-}CKO}$ —
Nucleus accumbens shell (AcbSh)	+	Glu + Camk2α ++ GABA +++	- ++ ++++	$Crh^{iFB\text{-}CKO}$ — $Crhr1^{GABA\text{-}CKO}$ —
Bed nucleus of the stria terminalis (BNST)	+++	Camk2α + GABA +++	++ ++++	$Crh^{iFB\text{-}CKO}$ — $Crhr1^{GABA\text{-}CKO}$ —
Central amygdala (CeA)	+++	Camk2α + GABA +++	++ ++++	$Crh^{iFB\text{-}CKO}$ ↓↓ $Crhr1^{GABA\text{-}CKO}$ —
Hippocampus (CA 1/3, DG)	S.C.	Glu +++ Camk2α +++ GABA +	- + ++	$Crh^{iFB\text{-}CKO}$ ↓↓↓ $Crhr1^{GABA\text{-}CKO}$ —
Paraventricular hypothalamic n. (PVN)	++++	Glu + Camk2α + GABA +	- -/? -	$Crh^{iFB\text{-}CKO}$ ↓
Lateral hypothalamic area (LHA)	+++	Camk2α ++ GABA ++	+ ++	$Crh^{iFB\text{-}CKO}$ ↓
Medial part of med. geniculate (MGM)	+++	Glu + Camk2α +	- +	$Crh^{iFB\text{-}CKO}$ ↓
Anterior pretectal nucleus (APT)	+	Camk2α + GABA +	+ -	$Crh^{Glu\text{-}CKO}$ ↓↓ $Crh^{iFB\text{-}CKO}$ ↓↓↓ $Crh^{MHB\text{-}CKO}$ —
Barrington's nucleus (Bar)	++++	Glu + GABA +	- -	$Crh^{MHB\text{-}CKO}$ —

Table 19: Expression map and neurochemical identity of CRH-positive neurons in the mouse brain.
Summary of double *ISH* studies illustrating the strength, distribution and cell-type localization of *Crh* mRNA as well as the deletion pattern found in the region and cell-type specific Crh^{CKO} lines. *Crh* expression levels are indicated with crosses in the second column and the signal intensity observed for the cell-type specific markers is indicated with crosses in the third column. Ratings reflect primarily the density of positive neurons with (-) representing a lack of staining/lack of co-cozalization, (+) isolated positively labelled cells and (+++) labelling in a substantial majority of cells in a given cell group or field. Arrows in the last column indicate the relative decrease of *Crh* mRNA signal intensity in the specifc Crh^{CKO} line for a given region; (-) complete loss of *Crh* signal intensity, (↓) isolated single cells, (↓↓↓) substantial majority of *Crh* cells.

Interestingly, $Crh^{iFB\text{-}CKO}$ mice spent significantly less time in the aversive inner zone of the OF, and entered it less frequently (Figure 56C), which implies enhanced anxiety (*time*: $t = 2.2$, $p < 0.05$; *entries*: $t = 1.7$, $p = 0.1$). To further confirm this, the DaLi and EPM tests were performed. $Crh^{iFB\text{-}CKO}$ mice spent less time, and made fewer entries into the lit zone, suggesting increased anxiety-related behavior (*time*: $t = 2.4$, $p < 0.05$ / *entries*: $t = 2.2$, $p < 0.05$)(Figure 56D).

However, no significant differences were observed in the EPM (Figure 56E). Enhanced responses of pre-established fear memories are additional indicators for pathological anxiety. Moreover, the CRH/CRHR1-system has been widely implicated in memory-consolidation processes (Radulovic et al., 1999b; Roozendaal et al., 2008; Thoeringer et al., 2012; Isogawa et al., 2013). Thus, we decided to assess auditory and contextual fear conditioning in $Crh^{iFB\text{-}CKO}$ mice. On day 0, mice were placed in a cubic-shaped chamber with metal grid floors for 3 min. After 180s, a sine wave tone (80 dB, 9 kHz) was presented for 20s, which co-terminated with a 2s scrambled electric footshock of 1.5 mA. A neutral context consisting of a Plexiglas cylinder with bedding was used to investigate auditory (tone-dependent) fear memory on the following day. Contextual (associative) fear-memory was tested by re-exposing the animals to the conditioning grid chamber for 3 min on day 2. $Crh^{iFB\text{-}CKO}$ mice displayed enhanced tone-dependent freezing behavior, which even persisted after withdrawal of the stimulus (RM-ANOVA, genotype x time $F_{(6,156)} = 3.9$, $p < 0.005$; genotype $F_{(1,156)} = 6.8$, $p < 0.05$; time $F_{(6,156)} = 5.5$, $p < 0.0001$; Bonferroni post-test, $p < 0.05$) (Figure 56F). The fact that context-dependent freezing behavior was not altered argues against generalized fear responses in $Crh^{iFB\text{-}CKO}$ mice. In addition, freezing behavior in a neutral context before tone-application was also not significantly changed in $Crh^{iFB\text{-}CKO}$ compared to control mice. Importantly, $Crh^{GABA\text{-}CKO}$ mice showed no alterations in auditory and contextual fear-memory, suggesting that *Crh* depletion in general is not responsible for the observed effects (Figure 56G). Thus, our results support the notion that CRH, specifically in CAMK2α-positive neurons, is required for positive emotional responses and stable fear memory expression. Keeping in mind that $Crhr1^{iDA\text{-}CKO}$ exhibited similar behavioral alterations, might imply that CAMK2α-positive CRH neurons target dopaminergic CRHR1 receptors. However, auditory fear conditioning was not altered in $Crhr1^{iDA\text{-}CKO}$ mice (Refojo et al., 2011), suggesting the involvement of additional neurotransmitter circuits in CRH-controlled fear memory expression.

The ability of CRH to induce positive emotional responses was also demonstrated by Lemos et al. Their data indicate that CRH acts in the nucleus accumbens to produce a positive affective state, by increasing dopamine release (Lemos et al., 2012). However, severe stress was able to initiate a persistent dysregulation of positive CRH-dopamine interactions, resulting in aversive behavior (Lemos et al., 2012). Thus we investigated whether chronic social defeat stress would switch CRH action in CAMK2α-positive neurons from anxiolytic to anxiogenic. As demonstrated for $Crh^{GABA\text{-}CKO}$ mice, CSDS induced robust stress-markers including elevated basal corticosterone levels, increased adrenal gland weight and decreased thymus weight

independent of genotype (*Corticosterone*: 2-Way ANOVA, stress $F_{(1,45)} = 6.1$, $p < 0.05$ / *AG*: 2-Way ANOVA, stress $F_{(1,46)} = 28.9$, $p < 0.0001$ / *Thymus*: stress $F_{(1,45)} = 17.0$, $p < 0.0005$; Bonferroni post-test, $p < 0.05$) (Figure 57A). Social interaction, locomotion, inner zone time and number of entries in the OF were decreased to a similar degree in control and $Crh^{iFB\text{-}CKO}$ mice following CSDS (*SA*: 2-Way ANOVA, stress $F_{(1,46)} = 12.8$, $p < 0.005$; genotype $F_{(1,46)} = 4.8$, $p < 0.05$/ *AG*: 2-Way ANOVA, stress $F_{(1,46)} = 28.9$, $p < 0.0001$ / *Distance*: RM-ANOVA, time x stress $F_{(1,46)} = 4.4$, $p < 0.05$; stress $F_{(1,46)} = 10.5$, $p < 0.001$, Bonferroni post-test, $p < 0.05$ / *Inner zone time*: 2-Way ANOVA, stress $F_{(1,44)} = 5.9$, $p < 0.05$ / *entries*: 2-Way ANOVA, stress $F_{(1,44)} = 6.5$, $p < 0.05$) (Figure 57B-C). Stress coping behavior in the FST was not significantly affected by genotype or condition (Figure 57B). Expectedly, anxiety-related behavior in the DaLi was increased in naïve $Crh^{iFB\text{-}CKO}$ mice compared to their respective controls (Figure 57D). An overall genotype effect was also observed for open zone time in the 0-Maze, additionally supporting increased anxiety in $Crh^{iFB\text{-}CKO}$ mice (2-Way ANOVA, genotype $F_{(1,45)} = 5.2$, $p < 0.05$; stress $F_{(1,45)} = 3.4$, $p = 0.07$) (Figure 57E). Control mice made fewer entries and spent less time in the lit zone of the DaLi following CSDS (2-Way ANOVA: *time*, genotype x stress $F_{(1,42)} = 5.3$, $p < 0.05$; stress $F_{(1,42)} = 3.7$, $p = 0.06$; genotype $F_{(1,42)} = 10.3$, $p < 0.005$ / *entries*, genotype x stress $F_{(1,42)} = 4.2$, $p < 0.05$; stress $F_{(1,42)} = 6.1$, $p < 0.05$; genotype $F_{(1,42)} = 10.0$, $p < 0.005$) (Figure 57D). This effect was absent in $Crh^{iFB\text{-}CKO}$ mice, suggesting reduced susceptibility to CSDS. However, the fact that $Crh^{iFB\text{-}CKO}$ mice display increased anxiety already under basal conditions rather points towards a floor effect, which cannot be further intensified by CSDS. In addition, significant overall stress effects were observed for the latency to enter the lit zone and open arms of the 0-Maze as well as the number of open zone entries (2-Way ANOVA: *DaLi latency*, stress $F_{(1,44)} = 5.1$, $p < 0.05$ / *0-Maze latency*, stress $F_{(1,42)} = 6.2$, $p < 0.05$ / *0-Maze entries*, stress $F_{(1,45)} = 7.7$, $p < 0.01$) (Figure 57D-E). Overall we could replicate our previous results, showing that $Crh^{iFB\text{-}CKO}$ mice exhibit enhanced anxiety under physiological conditions. However, CSDS induced similar changes in control and $Crh^{iFB\text{-}CKO}$ mice, failing to switch CRH action in CAMK2α-positive neurons from anxiolytic to anxiogenic. Nevertheless, the fact that deletion of *Crh* from GABAergic neurons is able to decrease susceptibility to CSDS further demonstrates the ability of CRH to induce opposing behavioral effects under basal and severe stress conditions. Importantly, the results support the existence of anxiolytic and anxiogenic CRH-releasing neurons.

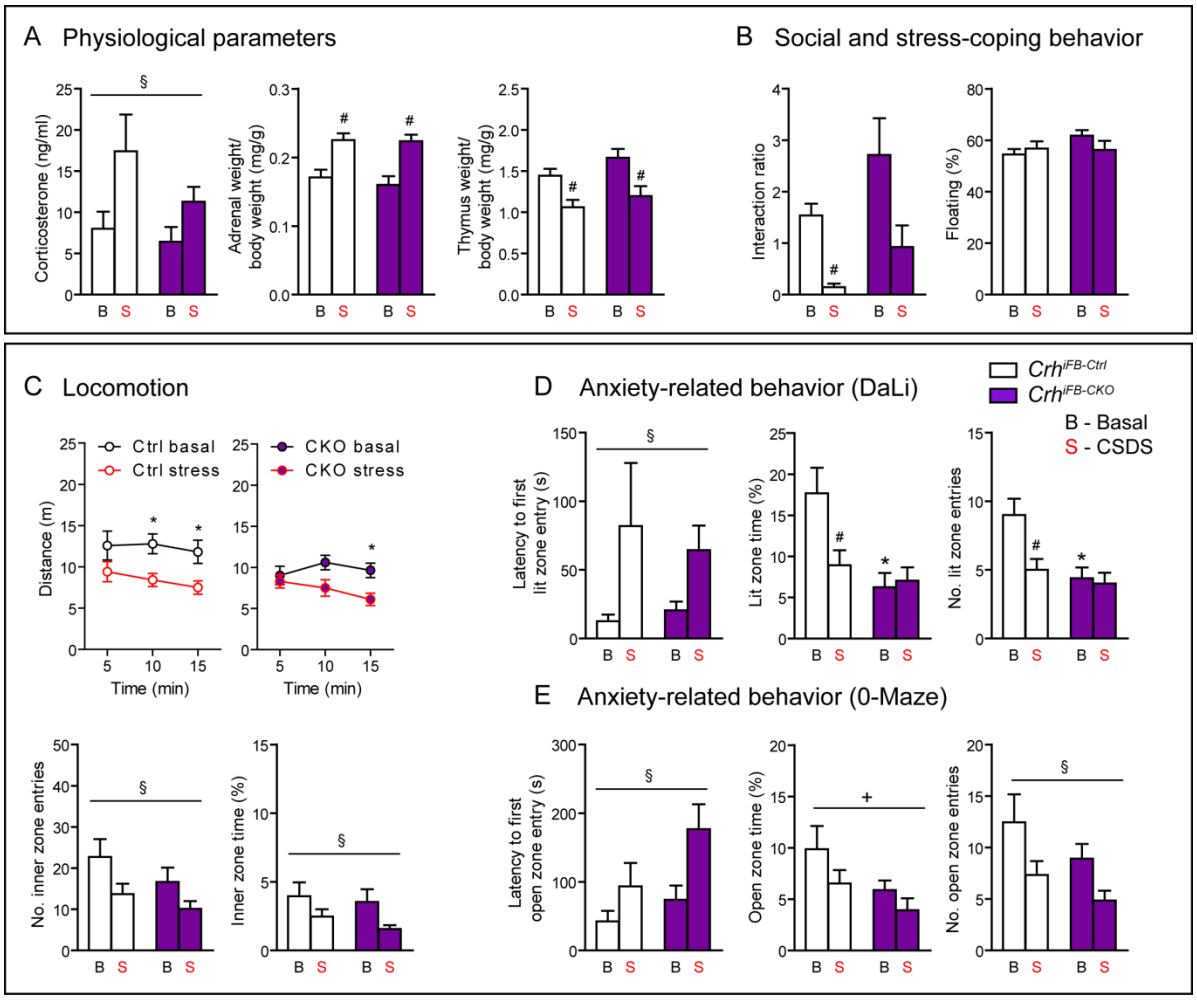

Figure 57: *Crh*$^{iFB\text{-}CKO}$ mice are not differentially affected by chronic social defeat stress.
(A) Control and *Crh*$^{iFB\text{-}CKO}$ mice (CKO induced with *Camk2α-CreERT2*) showed enhanced basal corticosterone levels, increased adrenal gland weight and decreased thymus weight following CSDS. **(B)** CSDS reduced interaction ratios during the social avoidance test independent of genotype. Active stress-coping behavior in the FST was not affected by genotype and/or condition. **(C)** CSDS reduced locomotion, inner zone time and entries independent of genotype. **(D)** Anxiety-related behavior in the DaLi was significantly enhanced in *Crh*$^{iFB\text{-}CKO}$ mice under basal conditions, depicted by reduced lit time and entries. CSDS-induced anxiety was more prominent in control than *Crh*$^{iFB\text{-}CKO}$ mice. **(E)** CSDS enhanced anxiety-related behavior in the 0-Maze indepenet of genotype. However, in general *Crh*$^{iFB\text{-}CKO}$ mice spent less time in the aversive open zone. *Significant from control of the same condition, # significant from the chronically stressed group of the same genotype, + significant genotype effect, § significant stress effect; RM-ANOVA or 2-Way ANOVA, $p < 0.05$, Bonfferoni post-test, $p < 0.05$; n = 11-13.

4.4. Working model of CRH/CRHR1-dopamine interactions in anxiety

The CRH/CRHR-system plays a key role in the regulation of neuroendocrine and behavioral responses to stress. Accordingly, CRH is commonly perceived as an anxiolytic and/or stress-inducing neuropeptide. However, our data supports a bidirectional mode of action for the CRH/CRHR1 system in emotional behavior. Using genetic gain- and loss-of-function approaches, we could show that CRH, most likely released from GABAergic inter-, and/or projection neurons, modulates anxiogenic and anxiolytic responses via CRHR1 on glutamatergic, and dopaminergic neurons respectively. The involvement of limbic forebrain CRH/CRHR1 in emotional behavior has been extensively studied; however the crosstalk between CRH/CRHR1 and the dopaminergic system has scarcely been investigated in the context of mood-related behavior. Collectively our date leads to the following hypothesis: A subpopulation of limbic BNST and/or CeA CRH-expressing GABAergic neurons project to CRHR1-expressing dopaminergic neurons of the VTA to modulate dopamine release and regulate emotional behavior (Figure 58A). This is implicated by the fact that deletion of CRHR1 from dopaminergic neurons (*Crhr1*$^{iDα\text{-}CKO}$ mice) reduces stress-induced dopamine release and enhances anxiety-related behavior (Figure 58B). The same effect on anxiety is observed upon deletion of CRH from *Camk2α*-positive neurons (*Crh*$^{iFB\text{-}CKO}$ mice) (Figure 58C). Considering the morphological analyses and tracing studies (Section 4.3.1 and 4.3.2), VTA-projecting CRH neurons most likely represent spiny GABAergic, CAMK2α-expressing neurons of the BNST and/or CeA, which maintain a positive emotional state under physiological conditions. However, additional microdialysis experiments will need to unravel whether dopaminergic neurotransmission is altered in *Crh*$^{iFB\text{-}CKO}$ mice. Astoundingly, deletion and overexpression of CRH in *Camk2α*-positive neurons both result in increased anxiety. One explanation could be that enhanced receptor stimulation in CRH overexpressing mice overshadows normal patterns of endogenous CRH release that are triggered naturally by environmental stimuli. Additionally, co-activation of CRHR2 cannot be excluded in *Crh*$^{iFB\text{-}COE}$ mice, which might contribute to the anxiogenic phenotype. Anxiety-regulated modulation of the dopaminergic system via CRH is further depicted in *Crh*$^{GABA\text{-}CKO}$ mice. In this case, CRH hyperdrive in GABAergic neurons enhances stress-induced dopamine release and reduces anxiety-related behavior (Figure 59A). This might be due to enhanced CRH function in CAMK2α-positive neurons. Although the results obtained from CRH overexpressing mice have to be interpreted with caution, they still demonstrate the bidirectional properties of the CRH/CRHR1 system.

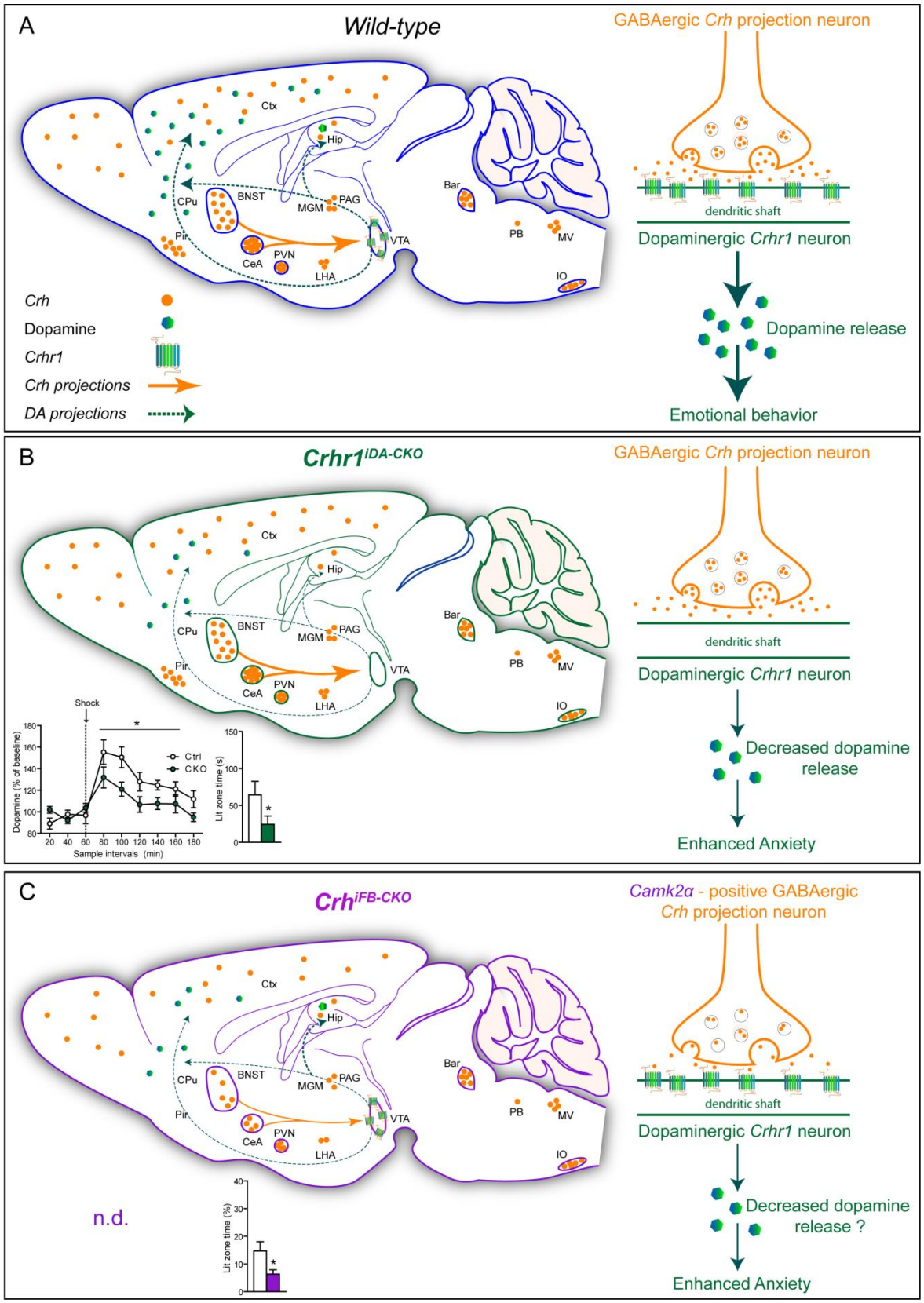

Figure 58: Proposed model of CRH/CRHR1-dopamine interactions under basal conditions.
(A) Limbic long-range GABAergic CRH projections synapse on dopaminergic CRHR1-positive neurons. These regulate emotional behavior by modulating dopamine release. **(B)** Deletion of dopaminergic *Crhr1* receptors diminishes dopamine release and enhances anxiety behavior. **(C)** The same effect on anxiety is observed when *Crh* is deleted from VTA-projecting, CAMK2α-positive neurons. Not determined (n.d.).

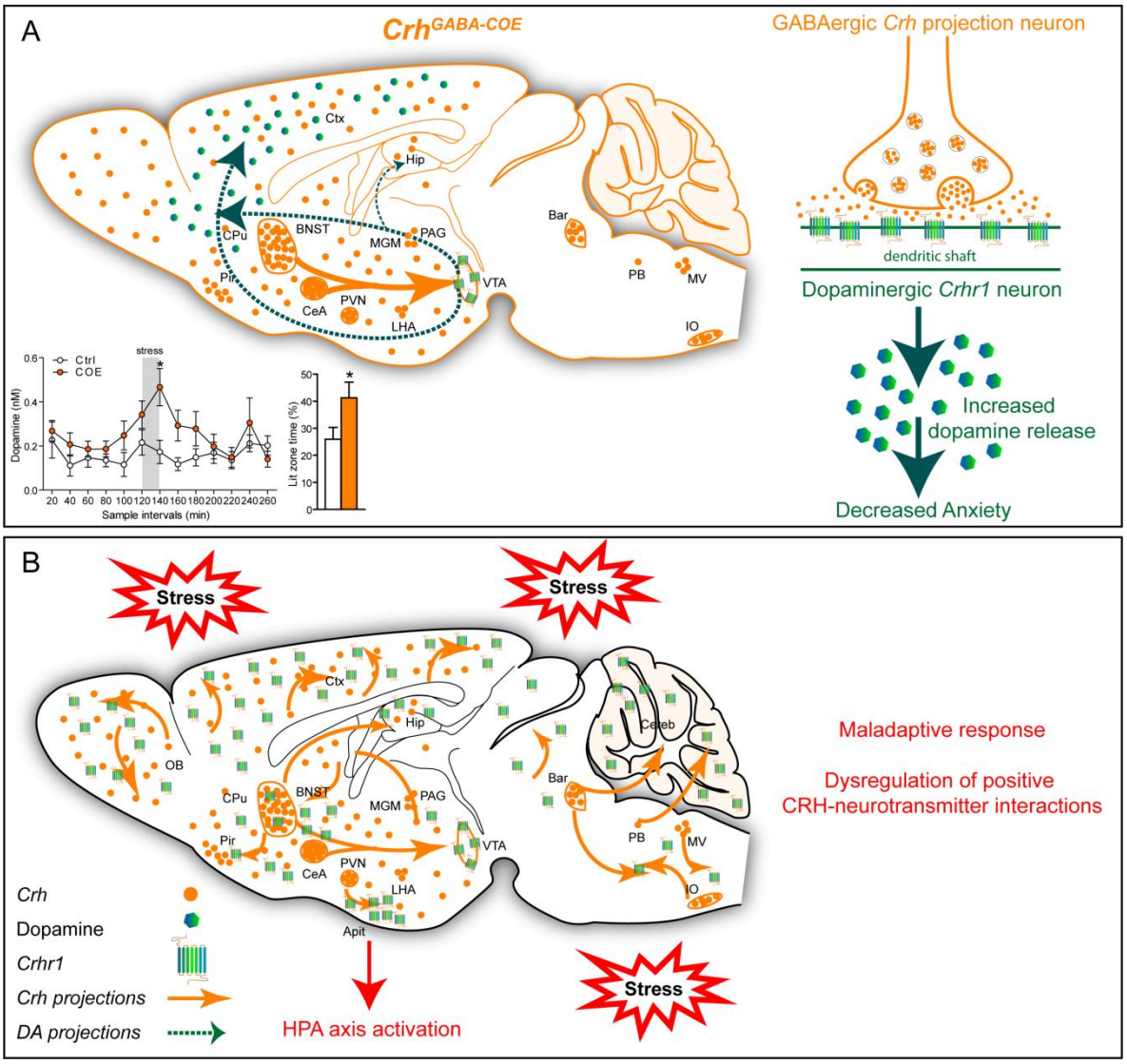

Figure 59: Proposed model of CRH/CRHR1-dopamine interactions following CRH hyperdrive and/or stress. **(A)** CRH overexpression in limbic long-range projecting GABAergic neurons enhances dopamine-release and diminishes anxiety-related behavior via prolonged activation of CRHR1 on dopaminergic neurons. **(B)** CRH loses the ability to induce positive emotional responses under severe stress conditions, due to HPA axis hyperdrive and persistent activation of anxiolytic and anxiogenic CRH receptors.

Importantly, the subcellular localization of CRHR1 in dopaminergic VTA neurons remains far from clear. Thus, CRH release could occur at axosomatic, axoaxonic and/or axodendritic shaft and/or spine synapses. Considering that GABAergic axons rarely target spine heads favors the idea that CRH neurons synapse onto dendritic shafts (illustrated in the working-model), axons and/or soma of CRHR1-expressing dopaminergic neurons. However, inhibitory spine synapses have also been reported (Knott et al., 2002; van Versendaal et al., 2012; Chen et al., 2012a) and cannot be excluded for CRH neurons.

So far our result revealed anxiety-inducing and anxiety-repressing CRH/CRHR1 circuits under physiological conditions. Another level of complexity is added when the system if faced with severe stress. Persistent CRH hyperdrive caused by chronic stress exposure can result in maladaptive responses in the long run. This might be caused by overactivation of both anxiogenic, and anxiolytic CRH receptors, resulting in persistent dysregulation of positive CRH-neurotransmitter interactions (Figure 59B). In addition, enhanced secretion of glucocorticoids due to HPA axis hyperdrive may further exacerbate the aversive outcomes. The fact that deletion of CRH from limbic and most cortical structures blunts the adverse effects of CSDS suggests differential behavioral modulation via the CRH/CRHR1 system under physiological and chronic stress conditions. Simply put, CRH loses the ability to induce positive emotional responses under severe stress conditions. Importantly, the bidirectional nature of the CRH system may account for the low efficacy of CRHR1-antagonist to ameliorate symptoms of anxiety and depression in most clinical trials (Paez-Pereda et al., 2011). Overall, our results contributed to further unravel CRH-controlled neurocircuitries of stress, which is of crucial relevance for the improvement of future treatment strategies for stress-related psychiatric disorders.

5. DISCUSSION

In the past years, chronic stress has been repeatedly implicated in altered brain function, which can eventually result in mental illnesses such as anxiety, depression, mania and/or schizophrenia. Consequently, the assessment of stress-related neurocircuitries has been a primary focus of many studies. CRH, UCN1-3, and their cognate receptors represent the brain's major stress-integrating system, and are widely distributed throughout the CNS (Swanson et al., 1983; Van Pett et al., 2000; Ryabinin et al., 2012; Kuhne et al., 2012). Particularly alterations in the expression of CRH and its high-affinity receptor (CRHR1) have been linked to the development of mood and anxiety disorders (Arborelius et al., 1999; Holsboer, 1999; Deussing and Wurst, 2005; de Kloet et al., 2005a). In this regard, CRH functions as both, a neuroendocrine hormone within the line of the HPA axis (Vale et al., 1981) and a neuromodulator via hypothalamic and extrahypothalamic neuronal pathways (Gallagher et al., 2008). Elevated levels of CRH in the cerebrospinal fluid, hypersecretion of CRH from the paraventricular nucleus of the hypothalamus, elevated circulating cortisol as well as an impaired glucocorticoid receptor (GR)-mediated negative feedback are consistently replicated findings in patients with major depression (Nemeroff et al., 1984; Lowy et al., 1984; Nemeroff et al., 1988; Fossey et al., 1996; Holsboer, 2000; Binder and Nemeroff, 2010; Ozbolt and Nemeroff, 2013). In rats and mice, intracerebroventricular administration of CRH produces behavioral effects comparable to those induced by stress, including hyperlocomotion, anxiety-related behavior, anorexia, changes in sexual behavior and altered cognitive performance (Sirinathsinghji et al., 1983; Dunn and Berridge, 1990; Baldwin et al., 1991; Koob et al., 1993; Menzaghi et al., 1993b; Zorrilla et al., 2002). Along these lines, CRH overexpressing mice display elevated plasma corticosterone levels, enhanced anxiety and stress-induced cognitive impairments possibly due to CRH hyperdrive in limbic structures (Stenzel-Poore et al., 1992; Stenzel-Poore et al., 1994; Kolber et al., 2010; Wang et al., 2011b). This is further supported by constitutive and forebrain-specific *Crhr1*-knockout mice, which show reduced anxiety-behavior and attenuated chronic-stress induced cognitive deficits (Timpl et al., 1998; Muller et al., 2003; Wang et al., 2011a; Wang et al., 2011b; Wang et al., 2013).

This study aimed to further unravel stress-related CRH neurocircuitries using genetic loss- and gain-of-function approaches. The first aim was to discriminate between direct effects of centrally hypersecreted CRH from those resulting from HPA axis activation on mood-related behavior. Second, the potential to model certain aspects of mood-disorders was assessed in CNS-specific CRH overexpressing mice ($Crh^{CNS\text{-}COE}$), which do not display basal HPA axis

alterations. Thus, effects on basal and stress-induced emotional behavior and cognitive performance were analyzed in *Crh*$^{CNS\text{-}COE}$ mice. In addition, predictive validity was evaluated by assessing physiological and behavioral response to the mood-stabilizer lithium. Third, the underlying brain regions and neuronal circuits mediating emotional behavior via CRH were analyzed using conditional mutagenesis by overexpressing CRH in a region and neurotransmitter-specific manner. Possible physiological, neuroendocrine and behavioral alterations were investigated in all conditional mouse lines. Fourth, conditional *Crhr1*-knockout mice were used to locate the receptors controlling CRH-mediated behavioral alterations. More specifically, *Crhr1* was deleted in different neurochemical subpopulations, enabling the analyses of CRH-neurotransmitter interactions. Finally, the study aimed to assess the identity, morphology and projection sites of CRH neurons. To circumvent the problems of ectopic expression associated with CRH overexpressing mice, and to specifically address the role of CRH in emotional behavior, conditional *Crh* mice were generated. These were subsequently bred to different site- and neurotransmitter-specific Cre-mouse lines, and investigated for basal and stress-induced neuroendocrine and behavioral alterations.

5.1. Conditional CRH overexpressing mice model endophenotypes of stress-related neuropsychopathologies

Chronic-stress-associated hyperactivity of the CRH/CRHR1 system has been implicated in mood and anxiety disorders (Arborelius et al., 1999; Koob and Heinrichs, 1999; Holsboer, 2000; Holsboer, 2001; Heinrichs and Koob, 2004; Deussing and Wurst, 2005; de Kloet et al., 2005a; Deussing, 2006; Holsboer and Ising, 2008; Binder and Nemeroff, 2010; Ozbolt and Nemeroff, 2013). To specifically dissect CRH-controlled brain regions and neurotransmitter circuits on physiology, anxiety-related and stress-coping behavior, we made use of a previously generated mouse model that allows CRH overexpression at different levels in a spatially restricted manner. This conditional approach provides the opportunity to create different CRH-overexpressing mouse lines, avoiding well-known variables inherent to classical transgenesis such as copy number or site of transgene insertion (Lu et al., 2008). In all generated mouse lines, the pattern of CRH overexpression depends solely on the spatial and/or temporal properties of the introduced Cre recombinase whereas the transcriptional control via the endogenous Rosa26 *(R26)* promoter guarantees stable and fully reproducible expression levels. Moreover, it allows the overexpression of CRH at two different dosages - from a single or both R26 alleles, respectively. It is of note that the homozygous disruption of the *R26* locus has no

phenotypic consequences. Hence, the *R26* locus is the most widely used genomic location for reliable gene expression.

5.1.1. Hypercorticosteroidism unaccompanied by CNS-specific CRH hyperdrive is not sufficient to alter mood-related behavior

Multiple lines of evidence suggest that a dysregulation of the HPA axis plays an important role in the pathogenesis of mood and anxiety disorders (Holsboer, 1999; Heinrichs and Koob, 2004; Holsboer and Ising, 2008; Bonfiglio et al., 2011). However, it has been challenging to discriminate between effects of centrally hypersecreted CRH from those resulting from downstream peripheral effects due to HPA axis activation. To unequivocally dissect central from peripheral effects of CRH on physiology, anxiety-related and stress-coping behavior, we generated two mouse lines of HPA axis hyperdrive with and without direct alteration of central CRH expression. This enabled a more precise discrimination between the effects of CRH and corticosterone on the physiology and mood-related behavior. As expected, chronic and ubiquitous overexpression of exogenous CRH led to prominent endocrine and physiological changes in $Crh^{Del\text{-}COE}$ mice reminiscent of those observed in patients with Cushing's syndrome and largely identical to those observed in mice overexpressing CRH from the broadly active metallothionine 1 promoter (CRF-OE^{Mt1}) (Stenzel-Poore et al., 1992). These included excess fat accumulation, thin skin, hair loss and severely elevated plasma corticosterone levels. Chronic stress-like alterations, such as enlarged adrenal glands and decreased thymus weight caused by excessive production and circulating levels of glucocorticoids (van den Brandt J. et al., 2007; Wagner et al., 2011; Hartmann et al., 2012b), were also observed in $Crh^{Del\text{-}COE}$ mice. Circadian rhythmicity of corticosterone secretion was virtually absent in male but not female $Crh^{Del\text{-}COE}$ mice. Circadian variation in HPA axis activity is known to differ between genders, and could also explain the variations observed between male and female $Crh^{Del\text{-}COE}$ animals (Seale et al., 2004; Atkinson et al., 2010). Generally, corticosterone levels were higher in females compared to males, which is most likely attributed to differences in gonadal steroid levels (Rhees et al., 1999; Drossopoulou et al., 2004; Andreano and Cahill, 2009; Garcia-Caceres et al., 2010). As displayed by control mice of both lines, gender-specific HPA axis differences are not only found at baseline but also in response to acute stress. In contrast, restraint stress was not able to elicit a corticosterone response in neither male nor female $Crh^{Del\text{-}COE}$ mice. It has been suggested that chronic HPA axis activation desensitizes the HPA system to further stress-dependent stimulation (Coste et al., 2001). However, the fact that homozygous $Crh^{APit\text{-}COE}$ mice,

which also show elevated glucocorticoid levels, are still able to respond to a stressor, favors the conclusion that the absence of a stress response in *Crh*$^{Del\text{-}COE}$ mice might rather reflect a ceiling effect caused by sustained HPA axis hyperactivity. Besides the mentioned endocrine abnormalities, *Crh*$^{Del\text{-}COE}$ mice exhibited increased anxiety-related behavior in the EPM and DaLi test, which was also observed in CRF-OE^{Mt1} mice (Stenzel-Poore et al., 1994). We did not see differences in general locomotor activity in the OF and EPM, which might otherwise obscure the interpretation of anxiety-related behavior. The observation that *Crh*$^{Del\text{-}COE}$ mice made less entries into the inner zone of the OF additionally supports the phenotype of increased anxiety-related behavior. In the FST, *Crh*$^{Del\text{-}COE}$ showed increased active stress-coping behavior compared to *Crh*$^{Del\text{-}Ctrl}$ mice. However, these effects were not as strong as previously observed in CRF-OE^{Mt1} mice, which showed a much more pronounced decrease in immobility (van Gaalen et al., 2002). Similarly, intracerebroventricular application of CRH or cortagine, a potent CRHR1 agonist, decreases immobility in the FST (Garcia-Lecumberri and Ambrosio, 2000; Tezval et al., 2004). Along these lines, CNS-restricted CRH overexpression (*Crh*$^{CNS\text{-}COE}$) also induces a dosage-dependent reduction in immobility, which is not an effect of excessive basal corticosterone secretion since circulating corticosteroids are normal in *Crh*$^{CNS\text{-}COE}$ mice (Lu et al., 2008). In contrast, CRH overexpression from the *Thy1.2* promoter (CRH-OE$^{Thy1.2}$) did not induce alterations in FST behavior (Dirks et al., 2001). These discrepancies might in the first instance be related to the applied promoters, which differ with respect to their spatial and temporal properties driving CRH expression but also with respect to their strength and subsequently triggered compensatory mechanisms. In addition, the behavioral test conditions and genetic background might explain some of the observed behavioral differences. In contrast to *Crh*$^{Del\text{-}COE}$ mice, chronic exposure to exogenous corticosterone has been shown to reduce active stress-coping behavior and to increase immobility (Murray et al., 2008), suggesting once more that enhanced active stress-coping behavior in *Crh*$^{Del\text{-}COE}$ and CRF-OE^{Mt1} mice is a consequence of central CRH hyperdrive. However, a mouse line-specific synergistic effect of hypercorticosteroidism and CRH overproduction on FST behavior cannot be ruled out. Along these lines, it is also not entirely clear whether the observed anxiogenic phenotype in *Crh*$^{Del\text{-}COE}$ and *CRF-OE*^{Mt1}mice is caused by a dysregulation and overproduction of central CRH, secondary effects of glucocorticoids, or a combination of both. Numerous lines of evidence suggest that CRH and CRHR1 regulate behavior in response to stressors and under basal conditions independent of downstream glucocorticoid action (Muller et al., 2003; Lu et al., 2008; Kolber et al., 2010; Flandreau et al., 2011). In addition, application of a CRHR1 antagonist

reverted the anxiogenic state observed in CRF-OE^{Mt1}mice (Stenzel-Poore et al., 1994) as well as the active stress-coping phenotype in *Crh*$^{CNS\text{-}COE}$ mice (Lu et al., 2008). Furthermore, Heinrichs and colleagues showed that adrenalectomy, leading to normalisation of plasma corticosterone levels, did not attenuate the anxiogenic effect of CRH overproduction (Heinrichs et al., 1997). At the same time, long-term exposure to exogenous corticosterone in rodents has been shown to induce anxiety/depression-like changes in behavior, neurochemistry, and brain morphology (Ardayfio and Kim, 2006; Gourley et al., 2008; Murray et al., 2008; David et al., 2009). However, chronic application of corticosterone analogues hardly fulfills the criteria of construct validity and is often applied at high and non-physiological concentrations.

In order to address the impact of excess glucocorticoids on physiology and behavior without directly altering central CRH expression, we bred CRH-overexpressing mice to *Pomc-Cre* mice (Akagi et al., 1997). In this mouse line, CRH overexpression is mainly restricted to the anterior and intermediate lobe of the pituitary as well as to a subset of neurons of the arcuate nucleus. Similarly to *Crh*$^{Del\text{-}COE}$ mice, heterozygous and homozygous *Crh*$^{APit\text{-}COE}$ mice displayed enlarged adrenal glands and an atrophy of the thymus as a result of enhanced corticosterone secretion, which is most likely a consequence of CRH acting in a paracrine fashion directly within the pituitary. Despite elevated plasma corticosterone levels, homozygous *Crh*$^{APit\text{-}COE}$ mice showed only a mild Cushing-like phenotype, which became apparent only after 5-6 months of age. This was associated with hair loss and thinning of skin, but not with excessive fat accumulation. On the contrary, homozygous *Crh*$^{APit\text{-}COE}$ mice were significantly lighter than control littermates. This is probably the result of *Pomc*-directed CRH overexpression in the arcuate nucleus, which is involved in the regulation of appetite (Schwartz et al., 2000) and where CRH might have elicited its well-known anorectic effects (Heinrichs and Richard, 1999). The fact that high glucocorticoid levels have not been associated with a reduction of food intake in experimental animals (Warwick and Romsos, 1988; Nieuwenhuizen and Rutters, 2008) favors the assumption that CRH overexpression in the arcuate nucleus is responsible for the observed body weight alteration. It has been described that hypothalamic CRH inhibits food intake, and the orexigenic effects of NPY in the PVN independently of the HPA axis (Heinrichs et al., 1993; Menzaghi et al., 1993a; Zorrilla et al., 2003). In addition, CRF-OE^{Mt1} mice exhibit reduced food intake in response to fasting due to neuronal activation in the arcuate nucleus (Stengel et al., 2009). A possible explanation why *Crh*$^{Del\text{-}COE}$ mice display substantial weight gain may be linked to the heightened constitutive overexpression of brain CRH-signaling pathways that override the NPY signals in the arcuate nucleus, and the general anorexigenic effects of CRH. In

addition, *Crh*$^{Del\text{-}COE}$ mice showed constantly elevated corticosterone levels. These are probably high enough to induce hyperphagia, which is also observed after central glucocorticoid administration. However, the exact mechanism by which CRH overexpression in neurons of the arcuate nucleus regulates weight loss/gain is subject of further investigations. As already mentioned, dosage-dependent differences in corticosterone levels between heterozygous and homozygous *Crh*$^{APit\text{-}COE}$ mice and respective *Crh*$^{APit\text{-}Ctrl}$ mice were only detectable at the circadian trough. Although this led to disrupted circadian corticosterone rhythmicity in male and female homozygous *Crh*$^{APit\text{-}COE}$ mice, these animals still displayed a comparatively normal neuroendocrine stress response.

Similarly to *Crh*$^{Del\text{-}COE}$ mice, gender-specific differences in HPA axis activity were also observed in this mouse line. Interestingly, we observed no alterations in locomotor activity and anxiety-related behavior in male *Crh*$^{APit\text{-}COE}$ mice, suggesting that chronic hypercorticosteroidism on its own is not sufficient to alter anxiety-related behavior. In support of this, conditional GR knockout mice, which also display increased basal plasma corticosterone levels and signs of a Cushing-like phenotype, show reduced anxiety (Tronche et al., 1999). Along these lines, *Fkbp51* knockout mice, which show decreased basal corticosterone levels as well as an enhanced recovery following acute and chronic stress exposure, do not display alterations in anxiety-related behavior (Touma et al., 2011; Hartmann et al., 2012b). This supports the notion that the anxiogenic effects observed in *Crh*$^{Del\text{-}COE}$ and CRF-OE^{Mt1} mice are not solely caused by elevated glucocorticoids, but rather by central CRH hyperdrive or a synergistic effect of both. However, the process by which central CRH and glucocorticoids may synergistically modulate anxiety-related behavior is largely unknown. Notably, these observations are not in line with studies of chronic corticosterone application, where anxiety-related behavior is induced upon exogenous glucocorticoid application (Ardayfio and Kim, 2006; Murray et al., 2008; David et al., 2009). However, the assessment of hypercorticosteroidism-induced behavioral effects via exogenous glucocorticoid administration faces major drawbacks: differential effects strongly depend on the duration and dose of treatment (Brotto et al., 2001; Gregus et al., 2005); HPA axis activity is downregulated which bears little resemblance to disease etiology; observed outcomes have not been replicated by many studies and are often contradictory especially concerning effects of corticosterone application on the stress-coping behavior in the FST (Brotto et al., 2001; Murray et al., 2008; Stone and Lin, 2008; David et al., 2009). Moreover, exogenous corticosteroids can have acute antidepressant and anti-stress effects (Reuter, 2002; Het and Wolf, 2007; Stone and Lin, 2008), but have also been shown to induce depression-like

behavior in humans and animals (Brown and Suppes, 1998; Celano et al., 2011). These controversies render the interpretation of the mild FST phenotype in homozygous *Crh*$^{APit\text{-}COE}$ mice difficult. Additionally, it should be noted that CRH overexpression in the anterior and intermediate lobes of the pituitary is driven by the *Pomc* promoter, which is active from early development onwards. Moreover, expression of *Pomc* in a subset of trophoblast giant cells has been reported (Zhu and Pintar, 1998), which could result in a transient overexpression of CRH during gestation. Therefore, expression of *Pomc-Cre* in the placenta needs to be analysed in the future. In this regard, adaptive processes and compensatory mechanisms in circuitries involved in anxiety-related behavior and feeding cannot be ruled out. Furthermore, expression levels and sensitivity of glucocorticoid and mineralocorticoid receptors might be altered in homozygous *Crh*$^{APit\text{-}COE}$ mice, partially blunting the effect of elevated corticosterone levels, and thereby sustaining HPA axis reactivity. Hence, the generation of inducible pituitary-specific CRH-overexpressing mice would more precisely assess the role of elevated glucocorticoids during adulthood.

To our knowledge, *Crh*$^{APit\text{-}COE}$ mice represent the first animal model of hypercorticosteroidism independent of direct genetic alterations in the brain. In this regard, *Crh*$^{APit\text{-}COE}$ mice offer valuable additional insights regarding the physiological and behavioral effects of excessive corticosterone production. Further studies will be necessary to investigate, whether endogenous ACTH levels are increased in response to chronic CRH overproduction in *Crh*$^{Del\text{-}COE}$ and *Crh*$^{APit\text{-}COE}$ mice, or whether the effects are attributed to a hyper-responsiveness of the adrenal cortex to ACTH. We only investigated CRH overexpression and HPA axis hyperdrive in the context of anxiety-related and stress-coping behavior. However, alterations in cognitive, social and reward-seeking behavior also represent core endophenotypes of mental disorders, and remain to be assessed in *Crh*$^{Del\text{-}COE}$ and *Crh*$^{APit\text{-}COE}$ mice. Moreover, stress in combination with genetic predisposition can increase the risk to develop psychiatric disorders (de Kloet et al., 2005a) and should be examined in both mouse models. In conclusion, the above described mouse lines represent useful tools to address behavioural and neuroendocrine effects of chronic CRH overproduction and HPA axis activation. However, the generation of additional, site- and neurotransmitter-specific conditional CRH-overexpressing mouse mutants allowed us to more clearly define the underlying neuronal circuits and brain regions involved in mediating anxiety-related behavior via CRH, and will be discussed next.

5.1.2. CNS-specific CRH overexpressing mice model mania-like behavior

Ubiquitous overexpression of CRH enhanced anxiety-related behavior and corticosterone secretion, whereas HPA-axis activation on its own failed to produce similar effects. However, we cannot fully exclude a synergistic effect of central CRH hyperdrive and elevated glucocorticoid levels on behavioral outcomes. In order to specifically address the role of central CRH in the pathophysiology of psychiatric disorders, we assessed conditional CNS-specific CRH overexpressing mice. *Crh*$^{CNS\text{-}COE}$ mice were previously reported to elicit hypersensitive HPA-axis activity and increased active stress-coping behavior in the FST and TST, mediated by enhanced noradrenergic activation (Lu et al., 2008). This was further confirmed by microdialysis experiments, revealing enhanced stress-induced noradrenaline release in the hippocampus of *Crh*$^{CNS\text{-}COE}$ mice compared to controls (unpublished data). In addition, *Crh*$^{CNS\text{-}COE}$ mice displayed alterations in sleep architecture evident by constantly enhanced REM sleep (Kimura et al., 2010). Changes in stress-reactivity, sleep, and monoaminergic function are commonly observed in anxiety and mood disorders (Dedic et al., 2011; Bonfiglio et al., 2011; Arnett et al., 2011). This study extended the physiological, molecular and behavioral characterization of *Crh*$^{CNS\text{-}COE}$ mice, revealing marked hyperactivity in most of the performed tests including the OF. In addition, CNS-specific CRH overexpression resulted in decreased anxiety-related behavior and enhanced novel object exploration. Initially, this was rather surprising considering that *Crh*$^{Del\text{-}COE}$ mice showed enhanced anxiety without changes in locomotion. Hence, synergistic effects of central CRH hyperdrive and elevated glucocorticoids seem to be responsible for the observed effects in *Crh*$^{Del\text{-}COE}$ mice. Moreover, *Crh*$^{CNS\text{-}COE}$ mice displayed deficits in object recognition memory and were unable to perform an operant learning task. However, hippocampus-dependent spatial memory, glutamatergic neurotransmission and synaptic plasticity at CA3-CA1 synapses remained unaffected. In addition, a slight decrease in prepulse inhibition was observed in *Crh*$^{CNS\text{-}COE}$ mice, which also failed to show a characteristic habituation of the acoustic startle response during the PPI-sessions. Overall, the behavioral profile of *Crh*$^{CNS\text{-}COE}$ mice resembles several behavioral dimensions of bipolar patients in the manic state, which include hyperactivity, increased impulsivity, psychomotor agitation, decreased sleep, and decreased PPI (Chen et al., 2010a; Young et al., 2011)(Table 16). Furthermore, prominent genetic models of mania phenocopy many of the changes observed in *Crh*$^{CNS\text{-}COE}$ mice (Prickaerts et al., 2006; Roybal et al., 2007; Shaltiel et al., 2008; Maeng et al., 2008; Kirshenbaum et al., 2011; Han et al., 2013).

Increased locomotor activity represents the main characteristic of animal models of mania (Young et al., 2007). This is owed to the fact that psychostimulants such as amphetamine (which induce hyperactivity in rodents) produce mania-like symptoms in normal healthy subjects and aggravate symptoms in patients (Meyendorff et al., 1985; Peet and Peters, 1995; Hasler et al., 2006). A recent study demonstrated greater motor activity, extensive and unpredictable patters of exploration, and more object exploration in manic BP patients compared to healthy volunteers in a human behavioral pattern monitor (Minassian et al., 2011). Importantly, *Crh*$^{CNS\text{-}COE}$ mice also displayed enhanced novel object exploration, stressing the involvement of altered CRH-function in mania-like behavior. However, hyperactivity measures have also been used as an indicator for other neuropsychiatric disorders including schizophrenia and attention-deficit hyperactivity disorder (ADHS)(Young et al., 2007). CRH-induced enhancement in locomotion is well documented (Diamant and De, 1991; Koob et al., 1993), but the underlying neuronal mechanisms remain largely unknown. Intracerebroventricular administration of CRH leads to a dose-dependent increase in locomotion, which can be reversed by central CRHR1-antagonist treatment (Zorrilla et al., 2002). Importantly, these effects are independent of changes in downstream HPA axis function, given that hypophysectomy or systemic dexamethasone injections fail to alter locomotor-enhancing properties of CRH (Eaves et al., 1985; Britton et al., 1986). Enhanced noradrenergic activation in *Crh*$^{CNS\text{-}COE}$ mice might represent one of the mechanisms by which central CRH hyperdrive induces endophenotypes of mania including hyperactivity. This is further supported by the fact that *Crh*$^{CNS\text{-}COE}$ mice display increased active stress-coping behavior in the FST and TST, which is commonly observed upon acute and/or chronic monoaminergic antidepressant treatment. Importantly, pharmacological blockade of catecholamine synthesis by AMPT could partially reverse the phenotype (Lu et al., 2008). Moreover, infusion of CRH into the locus coeruleus was shown to increase nonambulatory locomotion and active stress-coping behavior in the FST (Butler et al., 1990). However, hyperactivity could also arise due to activation of CRHR1-expressing neurons in brainstem structures responsible for motor-coordination. Additional experiments will clarify whether amphetamine can further intensify locomotion in *Crh*$^{CNS\text{-}COE}$ mice. In general, amphetamine-induced hyperactivity is considered the 'gold-standard' rodent model of mania. However, genetic mania-models including *Crh*$^{CNS\text{-}COE}$ mice, have the advantage of exhibiting long term alterations of a broad range of behaviors, which are more likely to mimic disease progression. Importantly, the fact that *Crh*$^{CNS\text{-}COE}$ mice exhibited slightly reduced home-cage activity points

towards novelty-induced exacerbation of locomotion. Environmental novelty is an important aspect in BPD and critical in the assessment of rodent mania models. Complex and/or novel environments were shown to disrupt a subject's circadian rhythm, resulting in manic episodes in predisposed subjects (Ehlers et al., 1988; Malkoff-Schwartz et al., 1998; Young et al., 2011). Similarly, novelty seems to induce a manic-like state in *Crh*$^{CNS\text{-}COE}$ mice, leading to hyperactivity. Thus, prolonged durations spent in the aversive compartments of the EPM and DaLi are more likely implying increased risk-taking and behavioral impulsivity in novel environments, rather than decreased anxiety.

Deficits in sensorimotor gating, revealed by impaired prepulse inhibition of the acoustic startle reflex are observed in many psychotic-like disorders (Braff et al., 2001; Geyer et al., 2001; Young et al., 2011). PPI represent a cross-species measure where a response to a startling stimulus (such as a loud noise) is inhibited by a previous presentation of a low intensity prepulse (Braff et al., 1978; Swerdlow et al., 2002). Earlier studies demonstrated that gating deficits are highly correlated with measures of thought disturbance (Braff et al., 1999). Moreover, mood stabilizers were shown to increase PPI in naïve mice (Ong et al., 2005; Flood et al., 2009), and ameliorate PPI deficits in mania models (Powell et al., 2008). *Crh*$^{CNS\text{-}COE}$ mice displayed a slight overall reduction in PPI, which was most strongly pronounced at lower prepulse intensities. Although no differences were observed in the acoustic startle reflex at different decibel intensities, *Crh*$^{CNS\text{-}COE}$ mice failed to display startle-habituation during the PPI trials. The inability to habituate to a repeatedly presented startling stimulus has been observed in individuals with schizophrenia, which share similar clinical symptoms with bipolar patients experiencing an acute manic phase (Braff et al., 1999; Perry et al., 2001). Moreover, CRH overexpression (CRF-OE^{Thy1} mice) and acute CRH infusion into the CNS are able to induce deficits in PPI and acoustic startle response, which are caused by central CRHR1, and not glucocorticoid receptor activation (Dirks et al., 2002b; Vinkers et al., 2007; Groenink et al., 2008). Importantly, Toth and colleagues could show that forebrain-specific CRH overexpression during development mediates impairments in PPI in these mice (Toth et al., 2014).

Cognitive dysfunction is observed in a wide set of psychiatric disorders including, depression, BPD, schizophrenia, autism etc. CRF-OE^{Mt1} mice exhibit learning deficits in spatial memory tasks such as the T-Maze and Morris water maze, which can be reversed upon benzodiazepine treatment (Heinrichs et al., 1996). In contrast, central CRH hyperdrive in this study impaired object recognition memory and operant reward learning, but had no effect on spatial navigation in the Y-Maze. Although cognitive performance was impaired in both mouse

models, concurrent baseline HPA axis hyperactivity in CRF-OE^{Mt1} mice may account for the discrepancies in spatial learning abilities. Enhanced arousal observed in *Crh*$^{CNS\text{-}COE}$ mice, could have additionally confounded learning processes, as observed in other studies (Greene et al., 2014; Riediger et al., 2014). Most individuals suffering from mood-disorders exhibit specific rather than general cognitive impairments. Bipolar patients often display executive dysfunction, but can also show deficits in vigilance, working memory, verbal fluency and verbal recall and recognition (Sax et al., 1999; Borkowska and Rybakowski, 2001; Fleck et al., 2003; Martinez-Aran et al., 2004; Savitz et al., 2005). Interestingly, reports of memory impairments in genetic models of mania have been limited.

The mechanisms by which CRH modulates synaptic transmission and cognitive performance have been extensively studied in the past. CRH actions in the hippocampus and BLA are generally excitatory and mediated via CRHR1 on glutamategic neurons (Refojo et al., 2011; Chen et al., 2012b). Furthermore, activation of CRHR1 specifically modulates glutamatergic neurotransmission, producing an amplification of neuronal excitation in the hippocampal DG-CA3-CA1 network (Refojo et al., 2011). Importantly, opposing effects on cognitive performance are proposed depending on the length and exposure of CRH-release. Thus, acute CRH release is able to excite synapses and augment synaptic plasticity, which promotes learning and memory during aversive situations and is in line with activating memory-promoting effects of acute stress (Chen et al., 2012b). However, chronic CRH hyperdrive, which occurs as a consequence of persistent stress exposure, results in cognitive impairments. This is further highlighted by the fact that conditional forebrain CRHR1 deficiency attenuates chronic-stress induced cognitive deficits (Wang et al., 2011a). Along these lines, CRH infusions into the lateral amygdala impair consolidation of memory for fear conditioning but enhance the expression of pre-established fear memories. Although *Crh*$^{CNS\text{-}COE}$ mice displayed cognitive deficits, these were not caused by changes in glutamatergic neruotransmisson, which remained unaltered as assessed with input-output measurements and paired-pulse facilitation in the hippocampus. In addition, LTP recordings at CA3-CA1 synapses showed no effects of central CRH overexpression on synaptic plasticity. These results likely explain intact hippocampal-dependent spatial memory performance in *Crh*$^{CNS\text{-}COE}$ mice. However, deficits in object recognition memory and operant reward learning might reflect functional changes in the perirhinal cortex, prefrontal cortex and/or amygdala rather than the hippocampus. Moreover, enhanced hippocampal stress-induced noradrenaline release, detected in *Crh*$^{CNS\text{-}COE}$ mice, could account for alterations in cognitive functioning independent of changes in glutamatergic neurotransmission. The

assessment of potential alterations in glutamatergic and noradrenergic neurotransmission in regions other than the hippocampus will be mandatory in the future. This is due to the fact that a vast amount of studies are starting to implicate altered synaptic function with neuropsychiatric disorders such as BPD, schizophrenia, autism, intellectual disability and obsessive compulsive disorder. Alterations in excitatory/inhibitory balance, due to increased SHANK3 expression, are proposed to cause hyperkinetic neuropathologies such as BPD (Han et al., 2013). Interestingly, mania-like behavior in SHANK3 overexpressing mice was rescued by valproate, but not lithium treatment, implying a unique pharmacokinetic profile for this specific model. Other studies have specifically linked altered glutamatergic function with BPD. Human imaging and postmortem studies point to altered glutamin/glutamate rations, and glutamate receptor levels in individuals with BPD (Hashimoto et al., 2007; Lan et al., 2009; Eastwood and Harrison, 2010). In addition, human post-mortem studies showed reduced glutamate receptor 6 (*GLUR6*) expression in several brain regions of BPD patients (Beneyto et al., 2007). Accordingly, *Glur6* knockout mice display behavioral alterations related to symptoms of mania including hyperactivity, aggressiveness, risk-taking and sensitivity to psychostimulants (Shaltiel et al., 2008).

Central noradrenaline, primarily synthesized in cell bodies of the locus coeruleus (LC), can modulate various behaviors including arousal, attention, motivation, reward as well as learning and memory (Chamberlain and Robbins, 2013). This is owed to the broad innervation by LC-projections, including the cortex, amygdala, thalamus, hypothalamus, hippocampus and cerebellum (Swanson and Hartman, 1975). Stimulation of the noradrenergic system is generally associated with positive effects on cognition and emotion. Although findings in humans are less consistent, animal studies strongly suggest that noradrenergic activation improves working memory and cognitive flexibility (Chamberlain and Robbins, 2013). However, excessive noradrenaline-release has also been associated with spatial memory deficits (Arnsten et al., 1999; McAllister, 2001; Zhang and Cai, 2005). Importantly, the LC is strongly implicated in prompting and maintaining arousal, and acts on various aspects of attention (Valentino and Van Bockstaele, 2008). Heightened arousal during stressful situations is primarily linked to elevations in noradrenaline release, which ultimately leads to a narrowing of intentional focuses (Chamberlain and Robbins, 2013). On account of that, an inverted U-shaped relationship has been proposed for arousal (or noradrenaline status) and cognition. Thus, for a given “cognitive function, there exists an optimal level of activity to facilitate maximal behavioral performance” (Robbins, 2000; Chamberlain and Robbins, 2013).

Accordingly, many of the behavioral abnormalities in *Crh*$^{CNS\text{-}COE}$ mice are likely a result of enhanced arousal due to increased stress-induced LC-activation and consequently elevated noradrenaline-release. For example, object recognition memory and operant learning require sustained attention, which is decreased upon enhance noradrenaline-release. Thus, the observed impairments in *Crh*$^{CNS\text{-}COE}$ mice in these cognitive tasks may be a result of noradrenaline-induced attention deficits. Noradrenaline-mediated alterations in attention and cognition seem to depend on the firing properties of LC neurons; tonic or phasic. Whereas the phasic mode enables focused attention, tonic firing can facilitate task disengagement. Thus, impaired object recognition memory and operant learning may be a result of generally enhanced tonic LC-firing in *Crh*$^{CNS\text{-}COE}$ mice, due to persistently activated LC-neurons. Additionally, previous studies have shown that LC tonic discharge positively correlates with the state of arousal (Foote et al., 1980; Aston-Jones and Bloom, 1981), and that CRH can bias LC activity towards a tonic mode (Valentino and Van Bockstaele, 2008).

Enhanced noradrenergic action in *Crh*$^{CNS\text{-}COE}$ mice is likely a consequence of CRH-mediated activation of LC-neurons, and is discussed in Lu et al. (2008). Although CRH receptor localization in the LC is debated, the ability of CRH to activate the noradrenergic system is well documented. Importantly, enhanced arousal due to CRH activation of the LC is proposed to alter attention in response to stress (Valentino and Wehby, 1988; Valentino and Van Bockstaele, 2008). However, the potential effects off HPA-axis hyperactivity on behavioral outcomes should not be neglected, considering numerous reports on the involvement of glucocorticoids in anxiety and mood disorders. Apart from indirect regulation of adrenal gland function via the HPA axis, CRH can also modulate glucocorticoid secretion via the autonomic nervous system by activating noradrenergic neurons within the LC, which in turn innervate all components of the HPA axis (Herman and Cullinan, 1997; Hwang et al., 1998). Retrograd tracing studies have revealed PVN-LC projecting CRH neurons, which are distinct from those that innervate the median eminence. This suggests one of two possibilities: 1) Central CRH overexpression triggers HPA axis hypersensitivity via direct and/or indirect activation of PVN neurons, which project to the LC to stimulate noradrenaline release. 2) Central CRH hyperdrive triggers enhanced activation of the noradrenergic system, which in turn drives HPA axis hyperactivity. Considering that stress-induced corticosterone levels were elevated upon CRH overexpression in the mid/hindbrain, but not the forebrain (discussed in detail below) would favor the latter. However, CRH overexpression in GABAergic and D1-positive neurons, which are vastly expressed in the forebrain, also increased stress-reactivity (discussed in detail in

section 5.1.3). Thus, a synergistic effect of both modes of actions is likely. The ability of the HPA axis and the noradrenergic system to synergistically modulate emotional behavior and memory performance has also been proposed by others (Roozendaal and McGaugh, 2011).
Alterations in circadian rhythms and molecular clock genes are also frequently associated with BPD, given that the majority of patients display changes in circadian function including sleep, activity, hormonal secretion and appetite (Belmaker, 2004). In support, CLOCK mutant mice show mania-like behavior, including hyperactivity, decreased sleep, decreased immobility in the FST, risk-taking, and an increase in reward value for cocaine, sucrose and medial forebrain bundle stimulation (Roybal et al., 2007). Notably, circadian rhythmicity of corticosterone secretion was not affected by central CRH overexpression; however $Crh^{CNS\text{-}COE}$ mice displayed a hypersensitive HPA axis in response to stress. Importantly, $Crh^{CNS\text{-}COE}$ mice exhibited alterations in sleep, characterized by enhanced REM sleep independent of HPA axis hyperactivity. These findings further establish $Crh^{CNS\text{-}COE}$ mice as a potential model of human mania.

Although associations of the CRH-system with bipolar disorder are limited compared with anxiety or depression (Binder and Nemeroff, 2010), several studies have linked CRH hypersecretion to psychotic symptoms. Decreased CRH-binding protein expression was seen in the amygdala of schizophrenia patients. In addition, CRH receptors are implicated in stress-induced relapse to drug-seeking, and modulation of mesolimbic dopaminergic projections; pathways relevant during the onset of psychosis (Izzo et al., 2005; Moffett and Goeders, 2007; Groenink et al., 2008). On the other hand, lack of linkage between CRH and bipolar affective disorder has also been reported (Stratakis et al., 1997). Overall our results support the involvement of CRH in the manifestation of mania-like behavior. This is further emphasized by the ability of lithium to revert many of the observed alterations in $Crh^{CNS\text{-}COE}$ mice. Hyperactivity, enhanced risk taking, novel object exploration, and diminished PPI and startle habituation were reversed to control levels following 10 days of chronic lithium treatment. However, the mechanisms by which lithium improves CRH-induced behavioral alterations are not clear at this point. Chronic valporic acid and lithium administration were previously reported to alter CRH and CRHR expression in the amygdala, cortex and PVN, suggesting that therapeutic actions of these mood-stabilizers may in part result from their actions on central CRH neurons (Gilmor et al., 2003). Whether CRH and CRH receptor expression is altered in $Crh^{CNS\text{-}COE}$ mice following lithium treatment remains to be investigated. More importantly, the effects of chronic lithium treatment on CRH-mediated noradrenergic activation in $Crh^{CNS\text{-}COE}$ mice need to be determined. LiCl did not alter spatial memory performance in the Y-maze, but

whether it can ameliorate deficits in object recognition memory and operant learning in *Crh*$^{CNS\text{-}COE}$ mice, will be addressed in the future. In addition, effects of lithium on HPA-axis function in control and *Crh*$^{CNS\text{-}COE}$ mice are still missing. So far, only a few studies have investigated the effects of lithium on glucocorticoid secretion, demonstrating enhanced activation of the HPA axis, possibly due to stimulation of arginine vasopressine (Sugawara et al., 1988; Adli et al., 2009).

Lithium is a commonly used mood-stabilizer that is particularly effective in treating mania, and is often prescribed to depressed patients that do not respond to first-line antidepressant medication (Bauer et al., 2002). Lithium is believed to exert its therapeutic effects via inhibition of glycogen synthase kinase 3 β (GSK-3β) and other related phosphomonoesterases of the Wnt- and AKT-pathway, although the exact mechanisms are still far from clear (Berridge et al., 1989; Klein and Melton, 1996). This is further supported by GSK-3β overexpressing mice, which display features of mania including hyperactivity and reduced habituation (Prickaerts et al., 2006). So far CRH/CRHR1-dependent signal transduction mechanisms are only partially understood. CRH actions are largely mediated through Gs-coupling and activation of the cAMP/adenylyl cyclase-protein kinase A (PKA) pathway, and/or stimulation of ERK-mitogen-activated Protein (MAP) kinase signaling events (Hauger et al., 2006; Grammatopoulos, 2012). However, the effects of CRH/CRHR1 can diverge through activation of other downstream molecules such as GSK-3β. CRHR1 was shown to mediate phosphorylation of GSK-3β at Ser^{9}, possibly via activation of PKA (Brar et al., 2002; Facci et al., 2003; Khattak et al., 2010). However, phosphorylation of Ser^{9} and Ser^{21} results in GSK-3β inhibition (which is constitutively active in cells), and subsequent propagation of intracellular signals (Cohen and Frame, 2001). This would imply similar actions of lithium and CRH on GSK-3β activity. However, these experiments are based on acute CRH application in cells and may differ from chronic CRH hyperdrive *in vivo*. Whether CRH can also enhance GSK-3β activity, and thereby induce mania-like features, remains to be elucidated. Consequently, behavioral alteration in *Crh*$^{CNS\text{-}COE}$ mice are possibly the result of interactions with GSK-3β regulated pathways, which can be modulated by lithium treatment.

Although only a few susceptibility genes were discussed here, many other targets have been associated with BPD in recent years, including *ERK1*, *SLC6A4*, *BDNF*, *DAOA*, *DTNBP1*, *NRG1*, *DISC1*, *ANK3* and *CACNA1C*, which strongly suggests that this illness arises from the complex inheritance of multiple susceptibility genes. In order to assess whether any of the mentioned

genes and/or pathways are altered in *Crh*$^{CNS\text{-}COE}$ mice, and to identify possible new target genes regulated by CRH/CRHR1 signaling, a non-hypothesis driven approach using microarray technology was applied. Microarrays provide a powerful tool for studying the genetic contribution to complex disorders (Bunney et al., 2003). This method enables the analyses of gene expression levels across the genome in specific tissues. Our results revealed increased expression of *Aqp4* across the brain of *Crh*$^{CNS\text{-}COE}$ mice. AQP4 represents the main water channel in the CNS and is primarily localized in glia cells including astrocyte processes and ependymocytes (Nagelhus and Ottersen, 2013). Aquaporins facilitate the bidirectional transfer of water, and small molecules such as glycerol, across biological membranes. To date, 13 AQP members have been identified, but only AQP1 and AQP9 are additionally found in the brain (Papadopoulos and Verkman, 2013). In contrast to the broad expression of *Aqp4* (Figure 14), *Aqp1* is mainly localized in the choroid plexus, and *Aqp9* in circumventricular regions and catecholaminergic neurons of the hindbrain (Badaut and Regli, 2004; Oshio et al., 2006). AQP4 has recently been implicated in diverse neuropathologies, which is not surprising considering the growing evidence on astrocyte dysfunction in CNS disorders (Seifert et al., 2006). Antidepressant effects and fluoxetine-induced hippocampal neurogenesis are abolished in *Aqp4* knockout mice (Kong et al., 2009). In addition, *Aqp4* deficient mice displayed alterations in hippocampal and amygdalar synaptic plasticity, and deficits in object recognition and associative fear memory (Skucas et al., 2011; Li et al., 2012). Changes in *AQP4* expression were also observed in brain tissue of Alzheimer patients, and decreased *AQP4* mRNA levels were detected in the plasma of individuals with Parkinson's disease (Wilcock et al., 2009; Thenral and Vanisree, 2012). The versatility of AQP4 actions is owed to its ability to modulate astrocyte function. Thus, AQP4 is involved in the maintenance of CNS water homeostasis, potassium spatial buffering, calcium signal transduction and regulation of neurotransmission (Xiao and Hu, 2014). The last point is of particular interest, considering that glutamate clearance is primarily controlled by astrocytes, following its uptake via excitatory amino-acid transporters. Studies in *Aqp4* knockout mice demonstrated impairments in glutamate uptake ability and decreased expression of glutamate transporter I in astrocytes (Zeng et al., 2007; Li et al., 2012). As described above, BPD is often associated with altered glutamatergic function. Thus, up-regulation of *Aqp4* in *Crh*$^{CNS\text{-}COE}$ mice might represent a compensatory mechanism, aimed to restore initially altered glutamatergic neurotransmission caused by CRH overexpression. Importantly, differential and region-specific alterations in dopamine, serotonin and noradrenaline levels were reported for *Aqp4* knockout mice (Fan et al., 2005; Ding et al., 2007).

This further demonstrates the ability of AQP4 to modulate neurotransmission, which may be of relevance, considering that hippocampal noradrenaline levels were increased in $Crh^{CNS\text{-}COE}$ mice.

Küppers and co-workers demonstrated a clear involvement of AQP4 in the regulation of striatal astrocyte proliferation *in vitro* (Kuppers et al., 2008). Interestingly, there is also evidence that changes in glial cell numbers are involved in the neuropathology of major depression and bipolar disorders (Rajkowska and Miguel-Hidalgo, 2007). The ability of AQP4 to modulate proliferation and structural changes in astrocytes is of particular interest, considering reports of hippocampal volume changes in depression (Czeh and Lucassen, 2007). Accordingly, increased *Aqp4 ISH* signal intensity observed in $Crh^{CNS\text{-}COE}$ mice might be a consequence of astrocytic proliferation rather than enhanced mRNA expression. This will be investigated in the future via expression analysis of the glial fibrillary acidic protein (GFAP), a marker for differentiated astrocytes. Additional evidence also suggests a critical role for AQP4 in astrocyte migration and activation (Papadopoulos et al., 2008). Thus, enhanced AQP4 expression may reflect overall increased astrocyte reactivity, which is observed in many CNS disorders. However, the precise mechanism by which CRH hyperdrive regulates AQP4 expression and/or astrocyte proliferation remains to be investigated. In addition, future experiments will have to assess the effects of lithium on AQP4 expression and/or astrocyte proliferation in $Crh^{CNS\text{-}COE}$ mice. This will help to reveal whether upregulation of this water channel (and/or astrocyte proliferation) is causing mania-like behavior in $Crh^{CNS\text{-}COE}$ mice or occurs in response to it.

Our result indicated that $Crh^{CNS\text{-}COE}$ mice model many aspects of human mania. However, BPD represents a complex disease in which patients alternate between episodes of mania and depression. Thus far, researchers did not succeed to successfully model these alternations in animals. As previously described, manic episodes are characterized by euphoric or irritable mood, thought disturbances, and behavioral symptoms, including hyperactivity, risk-taking, aggressive behavior, increased goal-directed behavior, excessive involvement in pleasurable activities as well as the propensity toward drug abuse. On the other hand, episodes of depression are characterized by depressed or irritable mood, diminished interest or pleasure in everyday activities, psychomotor agitation or retardation, alternations in body weight or appetite, cognitive dysfunction, and recurrent thoughts of death or suicide (Goodwin FK and Jamison KR, 2007). Euthymic/remitted phases occur between the manic and depressive state in which patients remain vulnerable to the reappearance of one of the mood episodes.

Importantly, relapses from one state to another can be triggered by physical and socio-psychological stressors, although spontaneous alternations were also reported (Goodwin FK and Jamison KR, 2007). In addition to genetic predisposition, chronic stress represents a major risk factor for the majority of psychiatric diseases including depression and BPD. Interestingly, clinical studies have demonstrated the ability of glucocorticoids to trigger both depressive and manic episodes in BP individuals (Goodwin FK and Jamison KR, 2007). To determine whether depression-like symptoms can be induced by an environmental trigger, $Crh^{CNS\text{-}COE}$ mice were exposed to three weeks of chronic socials defeat stress (CSDS). A more profound increase in chronic stress-induced anxiety was observed in $Crh^{CNS\text{-}COE}$ mice compared to controls. Under basal condition, $Crh^{CNS\text{-}COE}$ mice spent significantly more time in the lit zone of the DaLi, and one the open arms of the EPM, indicating enhanced impulsivity and risk-taking. Following CSDS, anxiety levels were increased in both groups, but were now indistinguishable between genotypes, indicating enhanced stress susceptibility in $Crh^{CNS\text{-}COE}$ mice. This might indicate the ability of $Crh^{CNS\text{-}COE}$ mice to cycle between manic and depressive episodes. However, differential effects of CSDS were not observed for all investigated parameters. Thus, HPA axis hyperactivity and increased novel object exploration were retained in $Crh^{CNS\text{-}COE}$ mice following CSDS. Moreover, possible CSDS-induced alterations in *Aqp4* expression need to be investigated in $Crh^{CNS\text{-}COE}$ mice. Along these lines, cognitive parameters, startle reactivity and PPI were thus far not assessed following CSDS. These additional tests will help to unravel whether CSDS-induced behavioral alterations in $Crh^{CNS\text{-}COE}$ mice are specific to anxiety.

Taken together, our results clearly implicate the involvement of the CRH-system in bipolar disorder. The behavioral profile of $Crh^{CNS\text{-}COE}$ mice was strikingly similar to other mania models and recapitulates several aspects of human BP patients in the manic state. Accordingly, many of the behavioral changes could be reversed with chronic lithium treatment. Although the exact underlying mechanisms remain to be elucidated, they are likely linked to enhanced noradrenergic function. Moreover, microarray analysis revealed increased *Aqp4* expression in $Crh^{CNS\text{-}COE}$ mice which might point to alterations in astrocyte function. However, the most striking feature of $Crh^{CNS\text{-}COE}$ mice is the ability to switch from manic to depressive-like behavior following chronic stress exposure. Although the alternation was specific to anxiety-related behavior, $Crh^{CNS\text{-}COE}$ mice potentially represent one of the first genetic models of BPD to cycle between manic and depressive endophenotypes.

5.1.3. Region and neurotransmitter-specific CRH overexpressing mice reveal bidirectional properties of the CRH system

Thus far we could establish a role of central CRH in the modulation of diverse behavioral domains, which are often altered in stress-related psychiatric disorders. Subsequently we aimed to uncover the underlying brain regions and neuronal circuits involved in mediating behavioral alterations via CRH. Importantly, this would enable us to specify and distinguish the brain regions and neuronal circuits responsible for the modulation of mania- and depression-like behavior in $Crh^{CNS\text{-}COE}$ and $Crh^{Del\text{-}COE}$ mice. Conditional mutagenesis, and the vast availability of region- and cell type-specific Cre recombinases, allowed us to address CRH function in a spatially and temporally restricted manner. Conditional, floxed $R26^{flopCrh/flopCrh}$ mice were bred to various region and neurotransmitter-specific Cre lines in order to generate mice overexpressing CRH selectively in the forebrain (using the *Camk2α-Cre* / $Crh^{FB\text{-}COE}$ and the inducible *Camk2α-CreERT2* / $Crh^{iFB\text{-}COE}$), mid/hindbrain (using the *En1-Cre* / $Crh^{MHB\text{-}COE}$), (using the *En1-Cre* / $Crh^{MHB\text{-}COE}$), in glutamatergic neurons (using the *Nex-Cre* / $Crh^{Glu\text{-}COE}$), GABAergic neurons (using the Dlx5/6-*Cre* / $Crh^{GABA\text{-}COE}$), dopaminergic neurons (using the inducible *Dat-CreERT2* / $Crh^{iDA\text{-}COE}$), dopaminoceptive neurons (using the *D1-Cre* / $Crh^{D1\text{-}COE}$ and the inducible *D1-CreERT2* / $Crh^{iD1\text{-}COE}$), and noradrenergic neurons (using the *Slc6a2-Cre* / $Crh^{NA\text{-}COE}$). The specific and distinct CRH overexpression patterns (reflecting the specificity of the applied Cre promoters) were confirmed for each mouse line via *ISH*. HPA axis function, locomotion, anxiety and stress-coping behavior were additionally assessed for all mouse lines.

Alterations in HPA axis activity were analyzed by measuring corticosterone levels at circadian nadir (a.m.), peak (p.m.), and after 10 min of restraint stress (stress response). HPA axis feedback was assessed by measuring plasma corticosterone levels 90 min following 10 min of restraint stress. Changes in circulating corticosterone were detected in some of the mouse lines; however the strongest effects were observed upon ubiquitous and anterior pituitary-restricted CRH overexpression (as previously discussed). In both $Crh^{Del\text{-}COE}$ and $Crh^{APit\text{-}COE}$ mice, enhanced basal corticosterone levels were caused by CRH overexpression in the pituitary, leading to persistent activation of CRHR1 in corticotroph cells. CRH is normally not synthesized in corticotroph cells of the anterior pituitary, making it difficult for the system to adjust to the employed changes. Corticosterone levels in forebrain-specific CRH overexpressing mice ($Crh^{FB\text{-}COE}$) were slightly increased under basal and stress conditions, but this did not reach statistical significance. These results are in line with recently generated inducible forebrain-

specific CRH overexpressing mice, which also displayed a mild increase in basal corticosterone levels. However, this transgenic line was engineered using the inducible rtTA/tetO system controlled by doxycycline. Although overexpression was restricted to CAMKα-positive neurons, the employed promoter driving CRH expression was not the same, likely resulting in different CRH brain levels compared to our mouse lines. Nevertheless, these results suggest that CRH in CAMKα-neurons is not majorly involved in the regulation of peripheral HPA axis effects. As already mentioned, compensatory downregulation of endogenous CRH might have restored initial changes, which has previously been reported for $Crh^{CNS\text{-}COE}$ mice (Lu et al., 2008). Such adaptive changes were also observed in other forebrain-specific CRH overexpressing mice, which showed decreased CRH levels in the PVN (Kolber et al., 2010). In addition, alterations in CRHR1/CRHR2 and glucocorticoid receptor expression might be counterbalancing initial changes induced by CRH hyperdrive. Interestingly, slightly decreased basal corticosterone levels were detected when CRH was overexpressed CAMKα-positive neurons later on in adulthood ($Crh^{iFB\text{-}COE}$), starting at postnatal week 8-10. These results are partially in line with the study of Kolber et al., demonstrating that early exposure to CRH in forebrain structures elevates HPA axis activity. Again, this might be attributed to an initially pronounced downregulation of endogenous CRH and/or alterations in CRH and glucocorticoid receptor expression. However, HPA axis parameters were assessed five weeks after tamoxifen-initiated overexpression, and it is questionable whether this relatively short time period is sufficient for adaptive changes to take place, especially during adulthood when brain-plasticity is limited. In addition, differences in recombination patterns (although mild) between the *Camk2α-Cre* and *Camk2α-CreERT2* might also account for dissimilarities in HPA axis profiles between $Crh^{FB\text{-}COE}$ and $Crh^{iFB\text{-}COE}$ mice.

Enhanced basal and afternoon corticosterone levels were also detected upon overexpression in the mid/hindbrain. Furthermore, $Crh^{MHB\text{-}COE}$ mice showed an increased stress response but no changes in stress recovery. In addition to the effects on HPA axis function, stress can also activate the noradrenergic system; and restraint, footstock and auditory stress have all been shown to increase extracellular noradrenaline levels in LC terminal regions (Valentino and Van Bockstaele, 2008). CRH is considered a potential mediator of stress-elicited LC activation. CRH-immunoreactive fibers densely innervate the nuclear core of the LC (Valentino et al., 1992). However the inability of many *ISH* studies to detect CRHR mRNA in the LC argues against a direct action of CRH on these neurons (Van Pett et al., 2000). In contrast, electrophysiological analyses imply a direct action of CRH on LC neurons (Jedema and Grace, 2004), and more

recent work using electron microscopy has identified CRHR1-immunoreactivty in LC dendrites (Reyes et al., 2006; Reyes et al., 2007).

As previously mentioned, LC innervations also include many components of the HPA axis, and can thus indirectly affect stress hormone secretion. Consequently, enhanced basal and stress-induced corticosterone levels in $Crh^{MHB\text{-}COE}$ mice are most likely the result of augmented CRH-mediated activation of the LC, which in turn stimulates HPA axis hyperfunction. It is generally accepted that CRH afferents, from forebrain and hindbrain structures to the LC, are eliciting stress-induced effects on the noradrenergic-system, although a few studies have also localized CRH-expressing cell bodies in the LC itself (Bittencourt and Sawchenko, 2000). Our results support the former, since overexpression of CRH specifically in noradrenergic neurons of the LC ($Crh^{NA\text{-}COE}$) failed to elicit any changes in HPA axis function or behavior. Until now, CRH projections to the LC were traced to the CeA, BNST, PVN, Barrington's nucleus (Bar) and the nucleus paragigantocellularis (Gi) (Valentino and Van Bockstaele, 2008). Interestingly, this might imply that CRH hyperdrive in Bar and Gi nuclei drives LC-mediated HPA activity. However, activation of LC neurons via projections from ectopically expressing CRH neurons cannot be excluded in $Crh^{MHB\text{-}COE}$ mice. More importantly, the involvement of the noradrenergic system in $Crh^{MHB\text{-}COE}$ mice is only speculative and needs to be verified in the future.

Overexpression of CRH in GABAergic and D1-positve neurons resulted in stress-induced HPA axis hyperactivity, without altering basal or recovery corticosterone levels. This profile is strikingly similar to $Crh^{CNS\text{-}COE}$ mice, suggesting that CRH overexpression in a subpopulation of GABAergic D1-positive neurons might be driving HPA axis hyperactivity in centrally CRH overexpressing mice. Earlier we proposed enhanced noradrenergic activation as the cause for elevated stress-induced corticosterone levels in $Crh^{CNS\text{-}COE}$ mice. CRH neurons of the CeA and BNST were shown to project to the LC (Tjoumakaris et al., 2003), which in turn innervates the PVN to modulate HPA axis function (and both $Crh^{GABA\text{-}COE}$ and $Crh^{D1\text{-}COE}$ mice overexpress CRH in the CeA and BNST). However, $Crh^{GABA\text{-}COE}$ mice showed no significant changes in stress-induced noradrenaline release (discussed below). However, the latter was measured in the prefrontal cortex, in contrast to hippocampal levels assessed in $Crh^{CNS\text{-}COE}$ mice. Thus we cannot exclude alterations of the noradrenergic system in other brain regions. Importantly, possible changes in neurotransmitter-release in $Crh^{D1\text{-}COE}$ mice need to be investigated. A likely alternative is that HPA axis hyperdrive in $Crh^{GABA\text{-}COE}$ and $Crh^{D1\text{-}COE}$ mice is independent of alterations in the noradrenergic system. GABAergic and D1-positve neurons are both expressed in the central

nucleus of the amygdala and the BNST (Weiner et al., 1991; Fremeau, Jr. et al., 1991; Day et al., 1999), which endogenously harbor a dense population of CRH neurons. Previous work has postulated that CRH in the amygdala and BNST is able to prompt HPA axis drive (Redgate and Fahringer, 1973; Choi et al., 2007). Along these lines, chronic stress-induced elevations in circulating glucocorticoids are often accompanied by increased CRH expression in the CeA. The CeA projects to the fusiform nucleus of the BNST, which is involved in the activation of the HPA axis (Choi et al., 2007). Thus, CRH hyperdrive in CeA and/or BNST-neurons may augment HPA axis activity during stress. It is of note that CRH overexpression initiated during adulthood (postnatal weeks 8-10) in D1-positive neurons failed to alter stress reactivity. Keeping in mind that *D1-Cre* expression is initiated at E16 further emphasizes that early exposure to elevated CRH levels is responsible for increased HPA axis activity during adulthood. Along these lines, early-life stress often results in elevated glucocorticoid levels during adulthood.

Overall, our results demonstrate that CRH overexpression differentially modulates HPA axis function depending on the brain region and cell-type. Although CRH in extrahypothalmic sites is able to modulate HPA axis activity, the strongest regulation occurs via CRH in the PVN and CRHR1 in the anterior pituitary. This is also supported by studies with conventional and conditional CRHR1 mutants. Whereas deletion of CRHR1 in forebrain, glutamatergic, GABAergic, dopaminergic and serotonergic neurons resulted in mild or no changes in HPA axis function, inactivation of the receptor in peripheral sites including the pituitary strongly diminished corticosterone secretion. Future studies will investigate whether endogenous ACTH levers are increased in response to chronic CRH overprouction in region and neurotransmitter-specific mice, or whether some of the effects are attributed to a hyper-responsiveness of the adrenal cortex to ACTH.

Lcomotor activity, assessed with the open field (OF) test, was only significantly altered in $Crh^{CNS\text{-}COE}$ mice, as discussed above. The absence of effects in the other lines suggests that changes in locomotion are primarily observed upon a vast activation of the system, integrating the majority of CRH circuits. The fact that ubiquitously CRH overexpressing mice showed no alterations in the travelled distance suggests a synergistic effect of central CRH and elevated glucocorticoids on behavior, which was also observed in CRF-OE^{Thy1} and CRF-OE^{Mt1} mice. Locomotion effects were also absent in other forebrain-specific CRH overexpressing mice which is in line with our results (Vicentini et al., 2009; Kolber et al., 2010). In addition, total and forebrain-specific *Crhr1* knockout mice also exhibited no alterations in locomotion. Initial studies by Sutton and colleagues found that i.c.v. application of CRH is able to elicit dose-

dependent increases in locomotor activity in familiar environments, which was independent of peripheral HPA axis activity (Sutton et al., 1982), and was later on confirmed by a number of studies. However, these activating effects of CRH on behavior were absent in animals which were exposed to a novel, stressful environment. In this case, CRH administration produced behavioral inhibition, resulting in reduced locomotion. Opposing effects on locomotion caused by environmental familiarity/novelty were also observed upon site-specific CRH administration into the CeA (Tazi et al., 1987; Liang and Lee, 1988; Wiersma et al., 1995). These results are not in line with our observations, where central CRH hyperdrive resulted in novelty-induced hyperlocomotion. However, such comparisons have to be made with caution given that behavioral effects in transgenic mice result from lifelong CRH overexpression. In contrast, locomotor effects measured after i.c.v. application or site-specific CRH injections reflect acute responses, which are likely to differ from adaptive processes initiated by chronic activation of the system. In addition, studies assessing the behavioral effects of exogenous CRH administration need to be interpreted with caution, since the obtained CRH levels often reflect non-physiological concentrations. The molecular mechanisms underlying CRH-mediated locomotor alterations are still not clear, however interactions with the dopaminergic and noradrenergic systems have been proposed. Importantly, the OF tests were conducted for only 5 min for many of the overexpressing mouse models, thus primarily assessing novelty-induced changes in locomotion. Consequently, possible alterations in habituation cannot be excluded for the tested mouse lines. Moreover, general alterations in locomotion, which are not confounded by novelty or anxiety, are commonly measured in the home cage and will be assessed in the future.

In earlier days, the Porsolt forced swim test (FST) was regarded as a typical depression-like paradigm, considering that it was developed to screen monoamine-based antidepressant drugs (Porsolt et al., 1977; Porsolt et al., 1978). This is currently a matter of debate, since the test assesses the response to an acute inescapable stressor, provoking despair-based behavior/immobility or active vs. passive stress-coping behavior rather than depression-like behavior (Nestler and Hyman, 2010). The FST makes use of the fact that rodents eventually develop immobility when being placed in a cylinder of water after they have stopped active escape behaviors, such as climbing or swimming. The question whether immobility should be interpreted as passive stress-coping, behavioral despair or even depression-like behavior remains controversial, although it is very unlikely that such a short period of inescapable stress is able to induce a depression-like state in rodents. One aspect favoring the stress-coping

rather than depression-like aspect of the FST is the fact that CRH overexpressing animals as well as central application of CRH result in decreased immobility (Butler et al., 1990; van Gaalen et al., 2002). Similarly, *Crh*$^{CNS\text{-}COE}$ mice also display enhanced active stress-coping behavior, which was linked to increased LC-noradrenergic activation (Lu et al., 2008), and was also confirmed in this study (previously discussed). The fact that this phenotype was only additionally observed in *Crh*$^{MHB\text{-}COE}$ mice supports that CRH hyperdrive in mid-hindbrain regions modulates stress-coping behavior. Importantly, the endogenous CRH system does not seem to influence FST behavior under basal non-stressed conditions, as neither deletion of *Crhr1* (Refojo et al., 2011) or *Crh* (see later) affects immobility in the FST. This implies that ectopic overexpression of CRH in *Crh*$^{CNS\text{-}COE}$ and *Crh*$^{MHB\text{-}COE}$ mice mimics the behavioral consequences of stress-mediated activation of the endogenous CRH system on FST behavior. This is additionally supported by experiments showing that activation of the endogenous CRH system before the FST decreases immobility in control, but not in *Crhr1* knockout mice (Lu et al., 2008). This might also hold true for *Crh* knockout mice and will be the subject of future studies.

A principal role of CRH is the regulation of anxiety. Chronic and acute activation of the CRH system generally results in anxiogenic effects in mice and rats. Original studies reported enhanced anxiety-related behavior in a variety of approach-avoidance conflict tests, including the EPM, following i.c.v. administration of CRH (Dunn and Berridge, 1990). Accordingly, constitutive CRH overexpressing mice spent less time in the aversive open arms of the EPM, which could be reversed with central CRHR-antagonist treatment (Stenzel-Poore et al., 1994). We confirmed the anxiogenic phenotype in our ubiquitously CRH overexpressing mice, and further showed that these effects are not caused by augmented HPA axis function (previously discussed). In an attempt to further specify the responsible brain regions and neurotransmitter circuits, we revealed that overexpression of CRH in forebrain principal CAMK2α-positive neurons (*Crh*$^{FB\text{-}COE}$) is driving anxiogenic responses. Similar observations were reported in two recently generated forebrain-specific CRH overexpressing mouse lines (Vicentini et al., 2009; Kolber et al., 2010). Expectedly, opposite anxiolytic effects are observed upon disruption of *Crhr1* in CAMK2α-positive neurons (Muller et al., 2003). All these results point towards the involvement of CRH/CRHR1-dependent pathways in forebrain structures, including the limbic system, in the control of emotional behavior. Importantly, CAMK2α-dependent deletion/overexpression occurs during the second week of postnatal life, underlining that manipulations of the CRH/CRHR1-system during adulthood are mediating the observed behavioral changes. This is additionally supported by the observation that CRH overexpression

in forebrain *Camk2α*-positive neurons, induced in late adulthood between postnatal weeks 10-12, results in the same phenotype. Importantly, overexpression in the MHB did not induce differential effects in the EPM or DaLi, highlighting a role for caudal CRH in arousal and stress-coping, but not anxiety. The fact that $Crh^{FB\text{-}COE}$ and $Crh^{iFB\text{-}COE}$ mice displayed similar behavioral, but not HPA axis profiles further supports that CRH-mediated effects on emotionality are largely independent of glucocorticoid action. According to the literature, CAMK2α is mainly expressed in forebrain projection neurons, which predominately include excitatory pyramidal neurons of the cortex and hippocampus (Liu and Murray, 2012). This is further supported by similar *LacZ* mRNA expression patterns in $Crh^{iFB\text{-}COE}$/$Crh^{FB\text{-}COE}$ and $Crh^{Glu\text{-}COE}$ mice, which are driven by the glutamatergic *Camk2α-Cre* and *Nex-Cre* respectively. However, double *ISHs* revealed that a substantial amount of *Camk2α*-positive neurons co-localize with the GABAergic markers *Gad65/67*, implying a similar, but not identical recombination pattern of the *Nex*-Cre and *Camk2α*-Cre. Consequently, we observed *Camk2α*-driven (in contrast to *Nex*-driven) CRH overexpression throughout the central amygdala, BNST and septum. In addition, *Camk2α* expression is also reported in GABAergic medium-spiny neurons of the striatum (Kennedy et al., 1983; Erondu and Kennedy, 1985; Klug et al., 2012), which is in line with the *LacZ* mRNA expression maps. Considering that $Crh^{Glu\text{-}COE}$ mice displayed no behavioral abnormalities suggests that CRH overexpression from a distinct CAMK2α-positive neuronal subpopulation produces anxiogenic responses. Two CRH-expressing brain regions most likely responsible for the detected effects are the CeA and BNST. The amygdala is an important mediator of fear and anxiety and has been extensively investigated for its role in the effects of CRH on mood related behavior. Injection of CRH into the basolateral amygdala (which harbors CRHR1) leads to reduced social interaction and increased anxiety-related behavior (Rainnie et al., 2004). The BNST is heavily innervated by the amygdala, and recent optogenetic studies have revealed a crucial role of this structure in the modulation of anxiety (Kim et al., 2013). Microinfusions of CRH into the BNST enhance anxiety in the EPM (Sahuque et al., 2006), retention in an inhibitory avoidance task (Liang et al., 2001), and startle amplitude (Lee and Davis, 1997). However, other structures, including the hippocampus, have also been implicated in the modulation of anxiety-behavior via CRH. Pentkowski and colleagues reported decreased open arm time in the EPM following CRH application to the ventral hippocampus (Pentkowski et al., 2009). Thus, it seems even more astounding that we observed anxiolytic effects in mice overexpressing CRH in GABAergic neurons. Similarly to manic-like $Crh^{CNS\text{-}COE}$ mice, the HPA axis in $Crh^{GABA\text{-}COE}$ mice was hyper-reactive to stress. However, the fact that $Crh^{GABA\text{-}COE}$ mice

displayed no alterations in locomotion or stress-coping behavior argues against a manic-like phenotype. Moreover, anxiety-responses induced by 15 min of acute restraint stress were more strongly pronounced in controls than *Crh*$^{GABA\text{-}COE}$ mice. Although some overlap exists between *Camk2α* and GABAergic markers, the two essentially characterize mutually exclusive neuronal subpopulations. However, CRH is expressed in both, *Camk2α* and GABAergic neurons of the cortex and limbic structures. This suggests that different CRH-subpopulations within the same brain region modulate opposing behavioral effects (discussed in section 5.3).

Microdialyis experiments were performed to assess whether changes in neurotransmitter release underlie CRH-induced behavioral alterations in *Crh*$^{GABA\text{-}COE}$ mice. Dopamine and its metabolites DOPAC (3,4-dihydroxyphenylacetic acid) and HVA (homovanilic acid) were significantly increased in *Crh*$^{GABA\text{-}COE}$ mice following elevated platform stress. The fact that noradrenaline levels were not changed further suggests that different neurocircuits are activated by CRH in *Crh*$^{GABA\text{-}COE}$ and *Crh*$^{CNS\text{-}COE}$ mice to modulate anxiolytic and manic-like behavior respectively. CRH-dopamine interactions have been extensively studied in the context of addiction, but so far little evidence exists for the involvement in anxiety. The ability of CRH to potentiate dopaminergic firing and release has been linked to stress-induced relapse in drug-seeking (George et al., 2012). The extended amygdala, consisting of the BNST, central and medial amygdala, and medial portions of the nucleus accumbens, is hypothesized to play a role in the reinforcing actions of drugs. Importantly, CRH is expressed in GABAergic neurons of the extended amygdala (discussed later), but whether these are responsible for alterations in anxiety remains to be investigated. The possible mechanism by which GABAergic CRH neurons regulate dopamine release and emotional behavior will be extensively discussed later on. However, *Crh*$^{GABA\text{-}COE}$ mice ectopically express CRH in the striatum and nucleus accumbens, which regulates dopaminergic input via direct projections to the VTA and substantia nigra (Gerfen and Surmeier, 2011). This could also explain the mild anxiolytic phenotype of *Crh*$^{D1\text{-}COE}$ mice, although the effects were only observed in the DaLi. Although dopamine receptor 1 (Drd1)-expressing spiny projection neurons innervate the substantia nigra (Gerfen and Surmeier, 2011), it is not clear whether the dopamine-system is altered in *Crh*$^{D1\text{-}COE}$ mice. Importantly, CRH can also act via CRHR2 to affect anxiety, although inconsistent findings have been reported in the past. Overexpression of UCN2, a selective CRHR2 ligand, in GABAergic neurons allowed us to dissect the involvement of the two receptors in CRH-mediated anxiolytic behavior. Although the effects were not significant, *Ucn2*$^{GABA\text{-}COE}$ displayed a mild trend towards decreased anxiety in the EPM. These results imply a major (but not sole) involvement

of CRHR1 in the anxiolytic-phenotype observed in *Crh*$^{GABA\text{-}COE}$ mice. Importantly, the effects of CRH overexpression in *Crh*$^{GABA\text{-}COE}$ mice on GABA transmission itself need to be evaluated. Along these lines, CRH application in brain slices was shown to increase pre- and postsynaptic GABAergic transmission onto serotonergic neurons, which was differentially mediated by CRHR1 and CRHR2 (Kirby et al., 2008). Overall our results highlight the ability of CRH to modulate anxiety-related behavior in opposite directions via different neurotransmitter circuits. CRH overexpression in forebrain *Camk2α*-positive neurons enhances anxiety-related behavior whereas overexpression in GABAergic neurons produces the opposite effect. Interestingly, hyper-activation of the entire CRH circuitry (as it occurs in CNS-specific overexpressing mice) results in manic/depressive-like behavior which incorporates many of the phenotypes observed in region and neurotransmitter-specific CRH overexpressing mice.

5.2. Glutamatergic and dopaminergic neurons mediate anxiogenic and anxiolytic effects of CRHR1

The conditional CRH overexpressing mouse lines characterized in this study, highlight the importance of the CRH-system in the regulation of stress-related neuroendocrine and behavioral responses. The applied gain-of-function approach, revealed the ability of CRH to generate negative and positive emotional responses when overexpressed in CAMK2α-positive and GABAergic neurons respectively. However, the results have to be interpreted with caution considering the uncertainties that go along with ectopic gene expression. Importantly, the outcomes tell us little about the involved receptors and their location. Although experiments with *Ucn2*$^{GABA\text{-}COE}$ mice revealed a primary role for CRHR1 in the anxiolytic effects of CRH in GABAergic neurons, does not necessarily mean that it is true for the other conditional mutants. In order to determine whether the *endogenous* CRH system interacts with different neurotransmitter circuits to modulate emotional behavior in a bidirectional manner, we applied conditional mutagenesis to knockout *Crhr1* in distinct neurochemical subpopulations. Previous studies have established a crucial role for limbic CRHR1 in mood-related behaviors. Forebrain-specific *Crhr1* knockout mice display reduced anxiety-related behavior (Muller et al., 2003; Wang et al., 2012), and decreased susceptibility to stress-induced cognitive deficits (Wang et al., 2011a; Wang et al., 2011b; Wang et al., 2013). Furthermore, suppression of amygdalar *Crhr1* via antisense oligonucleotides (Liebsch et al., 1995) or viral-mediated RNA interference (Sztainberg et al., 2010) also reduces anxiety. These results revealed the ability of limbic CRHR1 to induce negative emotional responses, which explains past efforts to develop

selective CRHR1 antagonists as potential therapeutics for anxiety and depression. However, the identity of CRHR1 neurons, and the exact neurotransmitter circuits that are modulated by the receptor to alter emotional behavior were so far unknown. Our group was able to neurochemically characterize CRHR1 neurons using double labeling methods against different neurotransmitter markers and *Crhr1*, or *Egfp* in *Crhr1*$^{\Delta Egfp}$ mice (Refojo et al., 2011). Principally, *Crhr1* expression was found in glutamatergic neurons of the cortex, hippocampus and basolateral amygdala; in GABAergic neurons of the olfactory bulb, reticular thalmic nucleus, globus pallidus, and septum; in dopaminergic neurons of the ventral tegmental area (VTA) and substantia nigra pars compacta; and in a few serotonergic neurons of the raphe nucleus (Refojo et al., 2011). Subsequently, conditional mutagenesis was applied to specifically delete *Crhr1* in glutamatergic (*Crhr1*$^{Glu\text{-}CKO}$), GABAergic (*Crhr1*$^{GABA\text{-}CKO}$), serotonergic (*Crhr1*$^{5\text{-}HT\text{-}CKO}$), and dopaminergic neurons (*Crhr1*$^{iDA\text{-}CKO}$). In accordance with the CRH-overexpression data, CRHR1 was able to modulate emotionality in a bidirectional manner. Whereas inactivation of *Crhr1* from glutamatergic neurons decreased anxiety-related behavior, deletion from dopaminergic neurons produced the opposite outcome. The effects were consistent across a variety of tests, and were independent of HPA axis function, which was indistinguishable between control and CKO mice (Refojo et al., 2011). Thus, previously reported anxiogenic properties of limbic CRHR1 are primarily mediated by forebrain glutamatergic neurons. Importantly, deletion of limbic *Crhr1* in forebrain principal neurons is driven by the *Camk2α-Cre*, and thus initiated during the second week of postnatal life. Along these lines, forebrain-specific CRH overexpression during adulthood produced increased anxiety-like behavior. These results suggest that manipulation of the CRH/CRHR1-system during adulthood is responsible for the observed effects, even though *Nex-Cre* mediated deletion of *Crhr1* in *Crhr1*$^{Glu\text{-}CKO}$ mice is initiated during early development, starting at E11.5. Additional experiments in our group revealed that CRH enhances excitatory neurotransmission in the basolateral amygdala via *Crhr1* on glutamatergic neurons (Refojo et al., 2011). Moreover, activation of *Crhr1* was able to amplify neuronal excitation in the hippocampal DG-CA3-CA1 network of control but not *Crhr1*$^{Glu\text{-}CKO}$ mice (Refojo et al., 2011). These results imply that glutamatergic CRH type 1 receptors regulate behavioral stress-responses by augmenting excitatory neurotransmission in the amygdala and hippocampus, two critical limbic regions in the neurobiology of mood-disorders. This is in agreement with previous data, showing that application of CRH to hippocampal slices increases the firing rates of pyramidal neurons by suppressing the after-hyperpolarization (Aldenhoff et al., 1983), and enhances the activity propagation through the

hippocampal formation (von Wolff et al., 2011). But whether CRHR1-mediated changes in excitatory activity translate into structural alterations is still a matter of debate. In fact, CRHR1-antagonist treatment results in exuberant dendritic branching and increased dendritic length (Chen et al., 2004b; Chen et al., 2008). Contrastingly, these effects were not observed in forebrain-specific *Crhr1* knockout mice; however the susceptibility to chronic stress-induced dendritic atrophy was reduced in these animals (Wang et al., 2011a). Although the CRH/CRHR1-system was shown to play an important role in cognitive performance, there is still missing consensus as to whether it affects long-term potentiation, the major *in vitro* correlate for processes related to memory. A more recent study found CRH to increase population spikes in somatic and dendritic regions of CA1 by stimulating Schaffer-collaterals, while neither affecting field excitatory postsynaptic potentials (fEPSP) nor LTP (Kratzer et al., 2013). Importantly, fEPSPs evoked by electrical stimulation of Schaffer-collaterals reflect processes of synaptic transmission that are below the threshold of action-potential (AP) generation in most of the target cells. However, when Schaffer-collaterals were excited via APs generated by stimulation of CA3 pyramidal neurons, CRH increased fEPSP amplitudes and the magnitude of LTP in the CA1 region (Kratzer et al., 2013). Kratzer et al., further demonstrated that these effects were mediated exclusively by CRHR1 on glutamatergic neurons. The evaluation of further experiments lead to the hypothesis that CRH does not increase neuronal excitability by affecting synaptic transmission per se, but via the modulation of somatic voltage-gated ionic currents important for the generation of APs (Kratzer et al., 2013).

5.2.1. The CRH/CRHR1-system interacts with dopaminergic circuits to modulate mood-related behavior

In addition to the anxiogenic effect of CRHR1 in forebrain glutamatergic neurons, our experiments revealed novel anxiolytic properties for CRHR1 on dopaminergic neurons. Keeping in mind that dopaminergic *Crhr1*-deletion was induced in adulthood, additionally argues against developmental effects of receptor inactivation on the observed effects. We propose that under physiological conditions CRH/CRHR1-controlled glutamatergic and dopaminergic systems function in a concerted but antagonistic manner to keep adaptive anxiety processes to stressful situations in balance. Thus, CRH hyperactivity, which is observed in many patients suffering from emotional disorders, might not be general but restricted to particular neuronal circuits, triggering symptoms by generating an imbalance between CRHR1-controlled glutamatergic and dopaminergic systems involved in emotional behavior (Refojo et al., 2011).

This is further supported by the observation that neurotransmitter-specific CRH overexpressing mice were also able to induced anxiogenic and anxiolytic effects. Our data strongly implicates alterations of the dopaminergic system in CRH-mediated negative and positive emotional responses. Whereas deletion of *Crhr1* specifically in dopaminergic neurons decreased dopamine-release in the PFC and enhanced anxiety, overexpression of CRH in GABAergic neurons enhanced PFC dopamine-release and diminished anxiety. This lead to the hypothesis that CRH released from GABAergic projection neurons, targets dopaminergic CRHR1 receptors in the VTA/SNc, to modulate dopamine release and consequently affect emotional behavior (see Working-model section 4.4). Using double *ISH*, we found *Crh* to be predominantly expressed in cortical and limbic GABAergic neurons, including the CeA, BNST, hippocampus and nucleus accumbens shell. Only cells of the piriform cortex and a few single neurons of the cerebral cortex expressed the glutamatergic marker *VGlut1*. Thus, it is very likely that CRH hyperdrive in endogenously CRH-expressing GABAergic neurons is responsible for the anxiolytic phenotype and enhanced dopamine release in $Crh^{GABA\text{-}COE}$ mice.

The dopaminergic projection system is commonly subdivided into the nigrostriatal, mesocortical, and mesolimbic pathway (Moore and Bloom, 1978; Wise and Rompre, 1989; Dunlop and Nemeroff, 2007; Russo and Nestler, 2013). The nigrostriatal pathway is characterized by substantia nigra-striatum projections, which are primarily associated with motor control. The mesolimbc pathway, which comprises dopaminergic VTA neurons that project to the nucleus accumbens, PFC, amygdala and hippocampus, represents the best described reward circuit in the brain (Russo and Nestler, 2013). The mesocortical pathway also arises from the VTA and projects to the frontal and temporal cortices, to regulate specific cognitive functions. The last two are often referred to as the mesocorticolimbic dopaminergic system. In addition, dopamine can regulate the secretion of certain hormones such as prolactin via local hypothalamic projections of the tuberoinfundibular pathway. Importantly, increased anxiety-related behavior was recently reported in mice lacking CRHR1 in the globus pallidus (GP) (Sztainberg et al., 2011), a major output source of the nigrostriatal circuit. Therefore we cannot entirely exclude that activation of these receptors via CRH in GABAergic neurons is responsible for the behavioral alterations observed in $Crh^{GABA\text{-}COE}$ mice. Moreover, $Crh^{GABA\text{-}COE}$ mice ectopically express CRH in striatal medium spiny neurons, which directly innervate the GP (Gerfen and Surmeier, 2011). This direct pathway originates from *Drd1*-expressing spiny neurons that project to the GP and substantia nigra output nuclei (Gerfen and Surmeier, 2011). Overexpression of CRH in D1-positive neurons might partially underlie the mild anxiolytic

phenotype of *Crh*$^{D1\text{-}COE}$ mice, assuming that enhanced dopaminergic activation in these animals represents the responsible mechanism for alterations in anxiety. On the other hand, *Crh*$^{D1\text{-}COE}$ and *Crh*$^{GABA\text{-}COE}$ mice also overexpress CRH in endogenously CRH-expressing GABAergic neurons of the nucleus accumbens shell, BNST and CeA. Interestingly, VTA projections have been reported for all these regions (Geisler and Zahm, 2005; Jalabert et al., 2009; Kaufling et al., 2009; Zahm et al., 2011; Xia et al., 2011), which strengthens the idea that CRH-positive GABAergic-VTA projecting neurons regulate emotional behavior via modulation of dopamine release in limbic structures. However, this is based on the assumption that CRH is expressed in long-range GABAergic projection neurons, which have thus far not been described. Most cortical and hippocampal CRH neurons are classified as local projecting interneurons (Kubota et al., 2011; Chen et al., 2012b), but whether this is also the case in other limbic regions, including the BNST and CeA, is not entirely clear. In order to visualize the presence of potential CRH long-range axons, we made use of recently generated *Crh-IRES-Cre* mice in which Cre recombination is driven by the endogenous *Crh* promoter (Taniguchi et al., 2011). *Crh-IRES-Cre* mice were bred to *Ai9* mice harboring a *loxP-STOP-loxP-tdTomato* reported allele (Madisen et al., 2010), which exhibits strong endogenous fluorescence, enabling the visualization of soma, dendrites and axonal projections. Detailed assessment of *Crh-IRES-Cre:Ai9* mice revealed forebrain-VTA projecting axons, and significant levels of CRH-immunoreactive fibers in and around the CeA. Using anterograde tracing methods, we then examined more specifically whether limbic CRH neurons project monosynaptically to the VTA. Single injection of adeno-associated viruses (AAV) to the dorsal and ventral BNST of *Crh-IRES-Cre* mice were used to anterogradely label presynaptic CRH terminals via expression of a Cre-dependent synaptophysin-eGFP fusion protein (*AAV-Syn-floxed-eGFP*). Labeled CRH projections were detected in the VTA and surrounding midbrain regions including the periaqueductal gray, parabrachial pigmented nucleus, medial mammillary nucleus, lateral septum, lateral hypothalamus, median eminence and the PVN. These results clearly indicate that a subpopulation of CRH neurons within the BNST monosynaptically innervates the VTA, but also other distant brain regions. Considering that most *Crh* neurons in the BNST co-localized with *Gad65/67*, favors the assumption that these represent GABAergic long-range projection neurons. Future tracing experiments will elucidate the presence of CRH projection neurons in other regions, including the cortex, CeA and hippocampus.

BNST outputs to the VTA have been extensively characterized in the past (Dong et al., 2001; Georges and Aston-Jones, 2002; Dong and Swanson, 2004; Geisler and Zahm, 2005; Dong and

Swanson, 2006; Jalabert et al., 2009; Zahm et al., 2011; Sartor and Aston-Jones, 2012; Kudo et al., 2012), and CRH application to the BNST was shown to alter mood-related behavior, including anxiety (Sahuque et al., 2006; Lee et al., 2008). Nevertheless, we do not know whether VTA-projecting CRH neurons of the BNST are mediating the effect observed in $Crh^{GABA\text{-}COE}$ mice. Recent optogenetic analysis demonstrated that distinct BNST subregions exert opposite features of anxiety (Kim et al., 2013). Whereas oval BNST activity promotes an anxiogenic state, anterodorsal BNST-associated activity exerts anxiolytic influences (Kim et al., 2013). Notably, anterodorsal BNST-neurons were shown to project to the lateral hypothalamus, parabrachial nucleus and VTA to implement anxiolysis (Kim et al., 2013). Interestingly, we detected similar projection sites for BNST CRH neurons. CRH expressing neurons are located throughout the BNST, including the oval and dorsolateral regions (Olschowka et al., 1982b; Cummings et al., 1983; Sakanaka et al., 1987; Morin et al., 1999). This might imply that CRH-expressing GABAergic neurons of the anterodorsal BNST project to the VTA to modulate dopamine-release and promote anxiolytic responses. On the other hand, CRH neurons of the oval BNST might drive anxiogenic properties via activation of glutamatergic CRHR1 receptors in limbic structures. Due to high infection rates of the *AAV-Syn-floxed-eGFP* virus it was not possible to specify the BNST nuclei that harbor CRH-VTA projecting neurons in our study. Importantly, the idea that CRH is not only released locally from interneurons, but also from long-projecting axons, is not new and has been shown by other groups. As previously mentioned, the LC receives CRH afferents from the CeA, PVN, BNST and Barrington's nucleus (Valentino et al., 1992; Valentino et al., 1996; Van Bockstaele et al., 1998; Reyes et al., 2005). Rodaros and colleagues reported CRH-positive VTA projections in the PVN, CeA, and BNST using fluorescent retrograde tracers and CRH immunohistochemistry (Rodaros et al., 2007). This shows that the source of CRF input to the VTA is not entirely restricted to the BNST. Additional inputs onto CRHR1-positive dopaminergic neurons could be ideally investigated via injections of retrograde rabies viruses, harboring Cre-dependent tracers, into the VTA of *Crhr1-Cre* mice. However, the current unavailability of *Crhr1-Cre* mice has made this approach challenging. Importantly, CRH neurons in the BNST can also modulate dopaminergic activity via indirect mechanisms. Silberman and colleagues propose a feedback loop in which dopamine enhances CRH release from BNST interneurons, which in turn enhance excitatory neurotransmission on VTA-projecting neurons (Silberman et al., 2013). This pathway is suggested to regulate stress-induced drug-seeking behavior. A closer look at the literature revealed no indication that CRH exerts its effects via release from local VTA neurons. In fact,

most mapping studies have not localized CRH in dopaminergic neurons of the VTA. Interestingly, we detected a few disperse CRH-expressing cell bodies in the VTA of *Crh-IRES-Cre:Ai9* mice, which might not have been detected with conventional *in situ* and immunohistochemistry methods. A small number of these cells co-expressed the dopaminergic marker tyrosin hydroxylase. However, it is rather unlikely that these few CRH-expressing neurons are solely mediating the observed behavioral effects, considering the vast amount of CRH innervating fibers in this region. In addition, alterations in dopaminergic neurotransmission were observed in $Crh^{GABA\text{-}COE}$ mice, which do not overexpressed CRH in the VTA or in other midbrain dopaminergic nuclei. Nevertheless, CRH released from few VTA neurons could activate a large number of receptors via volume transmission. A similar mode of action is proposed for the hippocampus, where few GABAergic neurons release CRH, which diffuses locally to target CRHR1 at distant excitatory post-synaptic sites (Chen et al., 2012b). Importantly, upon Cre/loxP recombination-mediated removal of the transcriptional STOP cassette, tomato-reporter expression is continuously driven by the strong CAG promoter, and detected in all neurons that have expressed CRH at any given time point. Thus, we cannot exclude the possibility that some of tomato-fluorescent VTA neurons initially expressed CRH during development, but seized to do so during adulthood. Of course the opposite scenario is also likely.

Multiple lines of evidence have implicated altered dopaminergic neurotransmission in mood-related disorders. However studies on the role of dopamine in depression have largely been overshadowed by research on noradrenergic- and serotonergic-circuits (Dunlop and Nemeroff, 2007). This is largely owed to the fact that most antidepressant treatments do not directly target dopaminergic neurotransmission. However, depression is often characterized by impairments in motivation, psychomotor speed, concentrations and the ability to experience pleasure (anhedonia), which are all partially regulated by dopaminergic circuits (Dunlop and Nemeroff, 2007). In contrast to schizophrenia, which is associated with enhanced dopaminergic functioning, the dopamine-system is believed to be hypoactive in depression. Several studies reported reduced concentrations of dopamine metabolites in the cerebrospinal fluid of depressed patients (Korf and Van Praag, 1971; Mendels et al., 1972; Goodwin et al., 1973; Banki, 1977; Dunlop and Nemeroff, 2007). However, contradicting results have also been reported (Vestergaard et al., 1978; Gjerris et al., 1987). The conflicting results may arise from the fact that depressed subjects often exhibit certain psychotic or manic features, which are frequently associated with excessive dopaminergic activity (Swerdlow and Koob, 1987; Reith et

al., 1994; Pearlson et al., 1995; Cubells et al., 2002). A few postmortem studies have demonstrated altered dopaminergic functioning in depressed subjects. Reduced dopamine transporter (DAT) density and elevated D_2/D_3 receptor binding in the amygdala was reported for depressed patients that have died of suicide (Klimek et al., 2002). Another indicator for the involvement of the dopaminergic system in mood disorders is the markedly high frequency of depression among patients with Parkinson disease (Tandberg et al., 1996; Aarsland et al., 2012). Animal studies have clearly linked altered dopaminergic signaling with depression-like endophenotypes, however the mode of action remains controversial. Optogenetic stimulation of VTA dopaminergic neurons was shown to reverse stress-induced behavioral deficits in sucrose preference and stress-coping behavior, which could be blocked by treatment with dopamine receptor antagonists (Tye et al., 2013). Thus, the authors implicate decreased dopaminergic activation with depression-like behavior, which is in line with our results. On the other hand, studies distinguishing CSDS-susceptible from resilient animals, have reported increased firing rates of dopaminergic neurons in susceptible, but not resilient mice (Berton et al., 2006; Krishnan et al., 2007; Cao et al., 2010). Importantly, the alterations in dopaminergic firing rates were pathway specific. VTA-nucleus accumbens (NAc) projecting neurons exhibited increased firing rates in susceptible mice, whereas VTA-medial PFC (mPFC) projecting neurons exhibited decreased firing rates (Chaudhury et al., 2013). Consequently, Chaudhury and colleagues proposed opposite roles for VTA-PFC and VTA-NAc pathways in the modulation of depression-like endophentoypes. They suggest a functional role for the VTA-NAc circuitry, but not VTA-mPFC pathway in encoding reward-related information in the context of depression (Chaudhury et al., 2013). Thus, the VTA-mPFC circuit is possibly regulating other behavioral domains, such as anxiety, and activation of this pathway might be beneficial in the context of stress. In fact, the PFC represents a critical structure in the regulation of anxiety (Shin and Liberzon, 2010; Adhikari et al., 2010; Etkin et al., 2011; Myers-Schulz and Koenigs, 2012). Considering that we observed decreased dopamine-release in the PFC of “anxiogenic” *Crhr1*$^{iDA\text{-}CKO}$ mice, and enhanced dopamine-release in the PFC of “anxiolytic” *Crh*$^{GABA\text{-}CKO}$ mice, further supports the involvement of VTA-mPFC pathways in anxiety. Moreover, our data implies that CRH-dopamine interactions are required for a positive emotional state in naïve animals. Nevertheless, analysis of VTA-NAc circuits and anhedonic-like behavior in *Crh*$^{GABA\text{-}CKO}$ and *Crhr1*$^{iDA\text{-}CKO}$ mice will be mandatory in the future. As a matter of fact, Lemos and co-workers recently demonstrated that CRH application into the NAc enhances dopamine release in this region through coactivation of CRHR1 and CRHR2 on dopaminergic terminals and NAc

cell bodies (Lemos et al., 2012). Interestingly, this resulted in a positive affective state, characterized by conditioned place preference for the CRH-paired context (Lemos et al., 2012). However, under severe stress-conditions CRH lost the ability to promote appetitive behavior, resulting in an aversive emotional state, revealed by conditioned-place aversion and decreased novel object interaction (Lemos et al., 2012). Importantly, chronic stress disabled CRH-mediated positive regulation of dopamine release. Consequently, the authors propose that chronic stress initiates a persistent dysregulation of CRH-dopamine interactions that normally produce a positive affective state (Lemos et al., 2012). A more recent study suggested that CRH exerts its detrimental effects by increasing BDNF signaling in the NAc during stress (Walsh et al., 2014). Our results additionally highlight that disruption of CRH-dopamine circuits (via *Crhr1* deletion on dopaminergic neurons) under baseline conditions is sufficient to produce a negative emotional state similar to that following severe stress. It will be of interest to see whether persistent stress can obscure the ability of CRH to positively regulate dopamine release in $Crh^{GABA\text{-}CKO}$ mice.

A substantial number of patients suffering from mood-disorders exhibit deficits in several aspects of reward (Nestler and Carlezon, Jr., 2006; Russo and Nestler, 2013). The most prominent is anhedonia, which is observed in the majority of depressed patients. It has been estimated that over 20% of individuals with mood or anxiety disorder also fulfill criteria for drug addiction (Conway et al., 2006). As previously mentioned, the best characterized reward circuits in the brain is the mesocorticolimbic dopaminergic pathway, with special emphasis on VTA-NAc projections. With the exception of opioids, most drugs of abuse acutely stimulate the dopaminergic system and increase dopamine release in the NAc (Wise, 1980; Volkow et al., 1997; George et al., 2012). However, decreased activity of the mesolimbic dopamine system is observed during drug withdrawal, which is associated with fatigue, diminished mood, and psychomotor retardation in humans, and with decreased motivation to work for natural rewards, elevations in reward thresholds and decreased locomotor activity in rodents (Pulvirenti and Koob, 1993; Koob and Le, 1997; Barr and Phillips, 1999; Koob and Le, 2005; Le and Koob, 2007; George et al., 2012). Importantly, human and animal studies have consistently implicated stress as a critical factor in the drug addiction processes, including that it triggers relapse. Consequently, the CRH/CRHR1-system has been repeatedly associated with stress-induced drug reinforcement, where it acts to facilitate relapse and increase anxiety during acute and chronic withdrawal (George et al., 2012). CRH-expressing neurons of the extended amygdala, including BNST, NAc and CeA, were shown to mediate many of the effects, possibly

through modulation of dopaminergic neurotransmission via direct VTA-projections. Accordingly, CRH was shown to increase dopamine neuron firing and dopamine release (Kalivas et al., 1987; Bagosi et al., 2006; Muramatsu et al., 2006; Wanat et al., 2008; Lemos et al., 2012), which is in line with our data. George and colleagues suggest that exposure to drugs of abuse may sensitize the dopaminergic system to the effects of CRH to facilitate relapse in drug-dependent subjects (George et al., 2012). However, the exact mechanism by which CRH regulates dopaminergic neurotransmission remains unknown. This can be largely attributed to the fact that the subcellular localization of dopaminergic CRH receptors has not been determined, given the lack of specific antibodies and appropriate genetic tools. We assume that CRH long-range projection neurons synapse on dendritic spines, shafts and/or soma of CRHR1-expressing dopaminergic neurons. CRH application to VTA slices was shown to facilitate NMDA-dependent synaptic responses, suggesting a postsynaptic mechanism of action, although this was attributed to CRHR2 (Ungless et al., 2003). But presynaptic localization of the receptor cannot be excluded. VTA neurons project to CRH-containing brain regions including the CeA, BNST, NAc and cortex (Kudo et al., 2012; Russo and Nestler, 2013), which might enable CRH-expressing interneurons to regulate dopaminergic transmission locally in case of presynaptic receptor expression. In fact, this mode of action is supported by Lemos and colleagues, demonstrating colocalization of CRHR1 and CRHR2 with TH-positive fibers in the NAc (Lemos et al., 2012). However, the expression of CRHR2 in the VTA, and CRHR1 and CRHR2 in the NAc is controversial, considering that this was determined with antibodies, which are largely believed to exert low specificity (Refojo et al., 2011; Kuhne et al., 2012). Accordingly, most *ISH* studies do not support these results.

The other unanswered question is how CRH modulates excitatory neurotransmission and dopamine-release in the limbic forebrain considering that it is predominantly expressed in inhibitory GABAergic neurons? Notably, release of neuropeptides neurokinin B (NKB) and cholecystokinin (CCK) from GABAergic interneurons was also reported to increase excitability of the neocortical network (Gallopin et al., 2006). One possibility is that stress-activated GABAergic CRH neurons inhibit other inhibitory neurons that are keeping stress circuits basally inactive, leading to a net disinhibition of specific pathways in order to adapt to environmental challenges. However, this would imply that CRH axons primarily synapse onto other GABAergic neurons, which is supported by the expression of CRHR1 on GABAergic neurons, but not on glutamatergic and dopaminergic neurons, which constitute the majority of CRHR1-expressing cells. Along these lines, CRH might be exerting excitatory effects by dampening GABA

transmission via autoregulatory mechanisms, but this would most likely involve presynaptic CRHR1 on GABAergic neurons. However, the complementary expression patterns of CRH and CRHR1 argue against this mode of action. CRHR1 has been found on cell bodies and dendritic shafts of hippocampal neurons (Chen et al., 2004c; Chen et al., 2010b). However, Tallie Baram's group has also repeatedly localized CRHR1 in dendritic spines of hippocampal pyramidal neurons (Chen et al., 2004c; Chen et al., 2010b). Notably, GABAergic synapses are usually not located on dendritic spines but are predominately found on dendritic shafts (Somogyi et al., 1998; Megias et al., 2001; Dumitriu et al., 2007). Thus, it was proposed that CRH is released from inhibitory pre-synaptic terminals and diffuses locally via volume transmission to target receptors on dendritic spines of excitatory pyramidal neurons (Chen et al., 2012b). Volume transmission represents a common mode of travel, observed in many neuropeptides (van den Pol, 2012; Fuxe et al., 2013). However, consensus hasn't been reached as to whether neuropeptides diffuse over long-distances, or act via local diffusion on cells near the release sites, with a distance of action of a few microns (van den Pol, 2012). Arguing against long-distance release is the fact that CRH is synthesized and released by a number of distinct neurons (discussed later) in different regions of the brain. Thus, any specific role of CRH in a given neuronal subgroup would be compromised if it was diffusing over long distances from other brain regions. Furthermore, the complex system of astrocytic processes that surrounds many axodendritic synaptic complexes tends to attenuate long-distance transmitter diffusion (van den Pol, 2012). In addition, the distinct behavioral effects observed in our CRH overexpressing mouse lines support the idea that CRH action involves specific synaptic release, which might be restricted to the soma, axonal initial segment, dendrites or even spines. Although GABAergic synapses are primarily located on dendritic shafts, a subset was also shown to target spine heads (Kubota et al., 2007; van Versendaal et al., 2012; Chen et al., 2012a; Chiu et al., 2013). Interestingly, some of these targeted spines on pyramidal neurons and expressed the marker vasoactive intestinal peptide (VIP), which co-localizes with the majority of cortical CRH neurons (Kawaguchi and Kubota, 1996; Kawaguchi and Kubota, 1997; Gallopin et al., 2006; Kubota et al., 2011). As a result we cannot exclude the possibility that GABAergic CRH axons directly target CRHR1 on dendritic spines. Importantly, recent studies have demonstrated that inhibitory spine synapses, including the recipient spine, are highly plastic in repose to certain environmental stimuli, including visual experience and whisker stimulation (Knott et al., 2002; van Versendaal et al., 2012; Chen et al., 2012a). Direct release onto inhibitory spine-synapses might constitute a mechanism by which CRH provokes

dendritic spine retraction/loss during stress (Chen et al., 2008; Wang et al., 2013; Chen et al., 2013a). Several lines of evidence have additionally suggested local somatic and dendritic release for certain neuropeptides, including oxytocin and vasopressin (Morris and Pow, 1991; van den Pol, 2012). This can have autoregulatory functions or serve to increase/decrease activity of nearby neurons. A key feature of endocannabinoid modulation is release from postsynaptic neurons and retrograde diffusion to modulate neurotransmitter release from presynaptic terminals (Lovinger, 2008). Whether CRH is released from somatodendritc compartments is not known at this point. We postulate that CRH release and mode of travel may vary depending on the neuronal subtype. For example; CRH released from hippocampal interneurons might be acting via local volume transmission, which has been postulated by others (Chen et al., 2012b). On the other hand, release from long-range GABAergic projection neurons or glutamatergic neurons is probably restricted to the synaptic compartment.

In summary, analyses of neurotransmitter-specific CRHR1 knockout mice additionally highlight the bidirectional role of the CRH/CRHR1-system in emotional behavior. Thus, anxiogenic and anxiolytic effects of CRHR1 are mediated by forebrain glutamatergic and midbrain dopaminergic neurons respectively. We propose that CRH, released from limbic GABAergic projection neurons, activates CRHR1 on VTA dopaminergic neurons to regulate anxiety-related behavior through modulation of dopamine-release in the prefrontal cortex.

5.3. Neurochemical identity and morphology of CRH neurons

In Section 4.3.1 we established that the majority of limbic and cortical CRH neurons are GABAergic. As a reminder, approximately 80-90% of *Crh*-expressing neurons in the olfactory bulb (OB), dorsal/ventral bed nucleus of the stria terminalis (BNST), accumbens shell (AscSh), central amygdala (CeA), lateral hypothalamic area (LHA), hippocampus (Hip), and about 60-70% in the cortex/prefrontal cortex (PFC) co-localized with the GABAergic markers *Gad65/67*. Strong co-expression of *Crh* and the glutamatergic marker *VGlut1* was observed in the piriform cortex (Pir). Only a few disperse glutamatergic *Crh* neurons were detected in the OB, Ctx, PFC, LHA, medium geniculate nucleus (MGM), and hippocampus. Minimal to no co-localization was observed in the CeA, BNST, PVN, anterior pretectal nucleus (APT), and Barrigton's nucleus. Our results are largely in line with previous studies, reporting CRH in GABAergic neurons of the cortex, hippocampus, central amygdala and BNST (Day et al., 1999; Kubota et al., 2011; Chen et al., 2012b). The identity of the remaining non-GABAergic CRH neurons in the cortex and limbic regions is currently unclear. 30-40% of cortical *Crh* neurons did not co-localize with *Gad65/67*

and only a few expressed *Vglut1*, indicating the presence of additional subpopulations of yet uncharacterized CRH neurons. These might represent *VGlut2*- or *VGlut3*-positive neurons, considering that these markers are usually not co-expressed with *Vglut1* (Fremeau, Jr. et al., 2001; Fremeau, Jr. et al., 2004; Kudo et al., 2012). In fact, the patterns of *Vglut1* and *Vglut2* are complementary; the former is predominately expressed in the cortex, hippocampus and basolateral amygdala, whereas the latter is mainly found in the thalamus and hypothalamus (Fremeau, Jr. et al., 2001; Fremeau, Jr. et al., 2004; Kudo et al., 2012). The absence of *Vglut2* in the cortex and the fact that *Vglut3* mRNA is only scarcely expressed in the cortex and hippocampus, argues against a remaining glutamatergic CRH population. In addition, *Crh* was not detected in *Vglut2*-expressing neurons of the BNST (Dabrowska et al., 2013). The fact that cortical and limbic *Crh* mRNA expression is completely abolished in $Crh^{GABA\text{-}CKO}$ mice (driven by the *Dlx5/6-Cre*) strongly supports that the remaining limbic and cortical *Gad65/67*-negative *Crh* neurons are GABAergic. One explanation could be low expression levels of *Gad65/67* mRNA in a subset of GABAergic neurons, which are not detectable with current double *ISH* protocols. These neurons are likely expressing additional GABAergic markers including, parvalbumin (PV), calretinin (CR), cholecystokinin (CCK), somatostatin (SOM), alpha-actinin-2 (AAc), calbindin (CB), or vasoactive intestinal polypeptide (VIP). Recent work by Kubota and colleagues has shown that CRH neurons represent roughly 20% of cortical GABAergic cells (Kubota et al., 2011). Most CRH cells were co-localized with VIP, some of which also co-expressed CR or CCK (Demeulemeester et al., 1988; Taki et al., 2000; Karube et al., 2004; Gallopin et al., 2006; Kubota et al., 2011). In addition, a substantial number of layer V/VI CRH-expressing cells co-express SOM (Kubota et al., 2011). Interestingly, SOM-positive CRH neurons rarely co-expressed any of the other markers. Many CRH neurons in the hippocampus were shown to co-express PV (Yan et al., 1998; Chen et al., 2004c). However, a systematic co-expression analysis for CRH and different GABAergic markers is still missing for limbic regions such as the BNST and CeA. In addition, the identity of mid/hindbrain-expressing CRH neurons is also far from clear.

In contrast to excitatory pyramidal cells, the diversity of non-pyramidal GABAergic neurons has made it difficult to reach conclusive agreements about the classification criteria. Currently, GABAergic neurons are characterized based on morphology, neurochemical marker expression, electrophysiological properties and/or connectivity (Kawaguchi and Kubota, 1997; Karube et al., 2004; Markram et al., 2004; Klausberger and Somogyi, 2008; Kubota et al., 2011; Kubota, 2013; DeFelipe et al., 2013; Taniguchi, 2014). Cortical GABAergic sub-types are

morphologically classified into basket cells, double bouquet cells, Martinotti cells and neuroglia-form cells, which innervate different domains of target neurons (Karube et al., 2004; DeFelipe et al., 2013; Kubota, 2013). As mentioned above, most cortical GABAergic neurons express at least one of the following markers: PV, VIP, CCK, CR, CB, AAc and/or SOM (Kubota, 2013; Taniguchi, 2014). Electrophysiological classification differentiates between fast spiking (FS), late spiking (LS), and regular spiking (RS) firing patters following step-current injections (Kawaguchi and Kubota, 1996; Kubota et al., 2011; Kubota, 2013). However, none of the proposed classification criteria are entirely satisfactory given the partial overlap of some features. For example, double bouquet cells can express VIP, CR and/or CCK and display similar or distinct firing properties (Kubota, 2013). Thus, GABAergic neurons often possess specific combinations of markers and firing patterns, which can differ depending on the brain region (Kubota et al., 2011). In addition, most characterization studies on GABAergic structure and function have been performed in the cortex and may not necessarily apply to other brain regions. We set out to morphologically characterize cortical and limbic CRH neurons in *Crh-IRES-Cre* mice bred to Cre-dependent channelrhodopsin2-eYFP reporter mice (*floxed ChR2-eYFP* (*Ai32*)). We took advantage of the fact that the channelrhodopsin2-eYFP fusion protein is trafficked to membranes, enabling the visualization of dendritic arbors and axonal projections. eYFP fluorescence is directly visible and restricted to CRH expressing cells. Additional immunoflorescent staining was performed against GFP in order to improve the visualization of cell bodies. *ChR2-eYFP* expressing CRH neurons were observed throughout the cortex, most densely in upper layers II/III and the lower layers V/VI. In accordance with previous studies (Kubota et al., 2011), most CRH neurons displayed a bitufted/bipolar morphology, characteristic of double bouquet cells and vasoactive intestinal peptide (VIP)-expressing interneurons. In addition, a few neurons were shaped like small basket cells and/or Martinotti-like cells. More surprisingly, eYFP expression was additionally observed in few pyramidal-like cells, showing a prominent apical dendrite extending vertically from a conical soma toward the pial surface (Jones, 1975), which has thus far not been reported for cortical CRH neurons. Accordingly, these neurons exhibited thin and mushroom-like spines characteristic for excitatory pyramidal cells. These possibly represent the small number of *Vglut1*-positive, glutamatergic cortical CRH neurons previously detected with double *ISH*. Past morphological analyses relied on immunohistochemistry, which can be ambiguous owing to the lack of antibody specificity or weak somatic staining due to synaptic transport of neuropeptides/neurotransmitters. Using transgenic mice, we and others were able to

genetically target CRH neurons, thereby substantially improving the visualization of morphological features. Importantly, eYFP is consistently produced in cells that have expressed CRH at any given time point. Thus, we cannot exclude the possibility that pyramidal-like CRH cells only expressed CRH during development. Up to now, we observed no dendritic spines on bipolar double bouquet and basket/Martinotti-like CRH neurons. However, only subsets of cortical CRH neurons were assessed thus far. Dendritic spines are conventionally believed to be largely absent from inhibitory neurons; however an increasing number of studies are staring to report the presence of spines on cortical and limbic GABAergic neurons (Peters and Regidor, 1981; Freund and Buzsaki, 1996; Azouz et al., 1997; Martinez et al., 1999; Larriva-Sahd, 2004; Kawaguchi et al., 2006; Chieng et al., 2006; Kuhlman and Huang, 2008; Keck et al., 2011; Kubota et al., 2011). Importantly, SOM-positive Martinotti cells were shown to exhibit dendritic spines (Kawaguchi et al., 2006; Kubota et al., 2011). Thus, we cannot exclude the presence of spiny GABAergic CRH neurons, considering that CRH is co-expressed with SOM in cortical layers V/VI (Gallopin et al., 2006; Kubota et al., 2011; DeFelipe et al., 2013). Notably, spiny SOM-expressing neurons frequently express neuropeptide Y (NPY). Contrastingly, CRH and NPY are not co-expressed in the cortex (Kubota et al., 2011). Overall, the morphological assessment performed in this study supports the presence at least three different types of cortical CRH-expressing neurons, including aspiny double bouquet and small basket and/or Martinotti-like cells (which represent GABAergic interneurons) as well as spiny pyramidal-like neurons. Additional co-localization studies are being performed for CRH and different GABAergic markers in order to further specify our findings. Future studies will have to determine the precise target domains of different cortical CRH neurons.

Considering that limbic, rather than cortical CRH is believed to shape emotional responses in mice, we assessed the morphology of CRH-expressing neurons in the CeA and BNST. These two brain regions are densely populated with GABAergic neurons (Cullinan et al., 1993; Sun and Cassell, 1993; Poulin et al., 2009). This is further reflected by the vast co-localization between *Crh* and *Gad65/67* in the CeA and BNST, which was also reported by others (Day et al., 1999). As mentioned above, *Vglut2* is expressed in the BNST and amygdala (Poulin et al., 2008; Poulin et al., 2009; Kudo et al., 2012) and could constitute the identity of the remaining CRH neurons. However, Dabrowska and colleagues reported no co-localization between CRH and VGLUT2 in the BNST (Dabrowska et al., 2013). In contrast, CRH-neurons of the PVN largely co-localize with VGLUT2, but not VGLUT1, which is in line with our results (Dabrowska et al., 2013) and demonstrates the specificity of the double *ISH*. Morphological studies of CRH-expressing BNST

and CeA neurons have been challenging due to the complex interconnected network of cells and lack of specific markers. Accordingly, the dense population of CRH-expressing neurons in the BNST and CeA made it extremely difficult to assess their neuronal morphology. In the BNST, many CRH neurons were multipolar with 3-4 primary dendrites, which was also observed for the CeA. Compared to the cortex, a far greater population of spiny CRH neurons was detected in the BNST and CeA. The spine density was generally lower than in cortical and/or hippocampal pyramidal neurons, ranging from spares to moderate including thin and mushroom-like spines. Whether these spines form synapses with functional glutamatergic and/or GABAergic terminals remains to be investigated. Previous studies have reported the presence of spiny multipolar and bipolar spindle-shaped neurons in the amygdala and BNST (Larriva-Sahd, 2004; Chieng et al., 2006), but their identity remains largely unknown. Most of these represent local-projecting interneurons. However, we also observed long-range projecting CRH neurons in the BNST, some of which targeted the VTA. The vast co-expression of CRH and GAD65/67 in these regions implies that these are GABAergic projection neurons, although we cannot be certain at this point. In support of this, Kudo and colleagues identified three neurochemical types of BNST-VTA projections using anterograde labeling techniques, and the majority originated from GABAergic neurons expressing GAD67 (Kudo et al., 2012). More specifically, ~90% of BNST-VTA projecting neurons were GAD67-positive, while only ~4.3% expressed the glutamatergic marker VGLUT2 (Kudo et al., 2012). The remaining 3.7% co-expressed GAD67 and VGLUT3 (Kudo et al., 2012). Then again, neuroanatomical studies have co-localized CRH in GABAergic but also in glutamatergic (VGLUT2-positive) afferents and synapses with dopaminergic as well as non-dopaminergic neurons in the VTA (Tagliaferro and Morales, 2008). The origins of glutamatergic CRH afferents were not investigated by Tagliaferro and Morales, and might constitute VGLUT2-positve cells in limbic regions, even though Dabrowska *et al.,* did not detect VGLUT2-CRH co-expressing neurons in the BNST (Dabrowska et al., 2013). On the other hand, GABAergic neurons were also shown to co-innervate excitatory spine synapses, which might explain the presence of CRH at glutamatergic terminals. Importantly, CRH-release at glutamatergic and GABAergic synapses implies that CRHR1 is localized at dendritic shafts as well as spines. Notably, GABAergic BNST neurons preferentially innervate VTA GABAergic neurons, and only ~15% target VTA dopaminergic neurons (Kudo et al., 2012). These might represent the CRH-positive subpopulation, considering that CRHR1 is primarily expressed on dopaminergic VTA neurons. Overall, we suggest the presence of at least two distinct subpopulations of CRH neurons in the BNST;

Inhibitory interneurons, and GABAergic long-range projection neurons, which might be exerting opposing effects on emotionality (as previously discussed). Whether both types carry dendritic spines remains to be investigated. Previous studies have distinguished local interneurons from projection neurons in the BNST based on electrophysiological membrane currents, but the precise physiological properties of CRH neurons are still far from clear (Egli and Winder, 2003; Hammack et al., 2007; Hazra et al., 2011; Silberman et al., 2013). At this point it is unclear whether different populations of CRH BNST neurons project to specific targets or whether a single population of CRH neurons within the BNST can simultaneously project to multiple brain regions. Although we observed similar morphological properties between CRH neurons of the BNST and CeA, their projections targets are likely to be different and thereby initiate specific functions. The presence of physiologicaly distinct CRH neurons in the brain was recently demonstrated by Dabrowska and colleagues. They propose distinct functions for CRH neurons in the PVN and BNST, which can be distinguished based on unique neurochemical expression patterns, and electrophysiological properties (Dabrowska et al., 2013). They revealed that PVN CRH neurons are predominantly glutamatergic (VGLUT2-positve) whereas BNST CRH neurons are primarily GABAergic. In line with our results, VGLUT1-expression was not detected in PVN neurons (Herzog et al., 2001; Ziegler et al., 2002; Singru et al., 2012). Interestingly, we did not observed diminished CRH expression in the PVN of conditional *Crh* knockout mice bred to the glutamatergic *Nex-Cre* mice ($Crh^{Glu\text{-}CKO}$). This is probably due to the fact the *Nex-Cre* recombination is largely restricted to *VGLUT1*-positve neurons of the cortex, hippocampus and basolateral amygdala. The absence of *LacZ* mRNA expression in the BNST, CeA, PVN and thalamic regions of $Crh^{Glu\text{-}COE}$ mice additionally supports this (Figure 20).

To the best of our knowledge, this is the first study to describe the presence of spiny CRH neurons in the cortex, CeA and BNST. At this point we hypothesized that spiny CRH neurons in the CeA and BNST represent long-range GABAergic projection neurons, which exert distinct functions compared to CRH-expressing interneurons. This assumption was based on the fact that GABAergic medium-spiny neurons (MSN) of the striatum innervate distant brain regions via long-range axons. As a matter of fact, MSN represent the best characterized spiny GABAergic population in the brain and comprise approximately 90% of striatal neurons (Gerfen and Surmeier, 2011). They serve to integrate excitatory cortical input with dopaminergic signaling to regulate a selection of motor and cognitive action patterns (Matamales et al., 2009; Gerfen and Surmeier, 2011). Loss of dendritic spines in striatal MSN is linked to

neurodegenerative disorders including Parkinson disease (McNeill et al., 1988; Zaja-Milatovic et al., 2005; Stephens et al., 2005; Deutch, 2006). At most excitatory synapses, LTP is triggered by Ca^{2+} entry into the postsynaptic compartment. Several lines of evidence indicate that the Ca^{2+}/calmodulin-dependent kinase II (CAMK2) detects this Ca^{2+} elevation and initiates biochemical cascades that potentiate synaptic transmission and influence synaptic plasticity (Lisman et al., 2002; Elgersma et al., 2002; Elgersma et al., 2004; Irvine et al., 2006; Lucchesi et al., 2011; Coultrap and Bayer, 2012). Accordingly, this specific kinase is enriched at spine synapses and represents one of the main proteins of the postsynaptic density (Kennedy et al., 1983; Lisman et al., 2002). Thus, it is not surprising that CAMK2 is predominantly expressed in glutamatergic neurons of the cortex and hippocampus. Multiple studies are proposing lack of CAMK2-expression in GABAergic neurons (mainly in the cortex and hippocampus), which are largely deprived of dendritic spines (Jones et al., 1994; Sik et al., 1998; Liu and Murray, 2012). One exception are CAMK2-expressing striatal GABAergic MSN neurons, where Ca^{2+}/calmodulin-dependent signaling cascades are required at excitatory spine synapses to modulate synaptic plasticity in response to glutamatergic and dopaminergic input (Erondu and Kennedy, 1985; Mayford et al., 1996; Picconi et al., 2004; Klug et al., 2012). In mammals, CAMK2 comprises homooligomeric and heterooligomeric complexes that are the product of four closely related genes: α, β, δ and γ. CAMK2α and CAMK2β represent the predominant isoforms in the brain, but only the former has been extensively studied in relation to memory function (Lisman et al., 2002; Elgersma et al., 2002; Elgersma et al., 2004). Although CAMK2/CAMK2α is expressed in striatal GABAergic MSNs (Erondu and Kennedy, 1985; Picconi et al., 2004), little is known about how it modulates neuronal function in the striatum. Recent studies illustrated that abnormal CAMK2α autophosphorylation plays a causal role in the alterations of striatal plasticity and motor behavior that follow dopamine-denervation (Picconi et al., 2004). Considering the lack of CAMK2α-expression in cortical and hippocampal GABAergic neurons, we hypothesized that this kinase may serve as a marker for excitatory pyramidal projection neurons, but also spiny GABAergic projection neurons such as striatal MSNs. Notably, striatal-like spiny neurons have also been reported for the amygdala and BNST (Larriva-Sahd, 2004; Chieng et al., 2006). Using double *ISH*, we observed considerable co-expression of *Crh* and *Camk2α* in the BNST (~40%) and CeA (~40%). In addition, double-labeled cells were observed in other *Crh* expressing regions including the OB, AchSh, PFC, Ctx, LHA, Hip, MGM and APT, although these were fewer than in the BNST and CeA. Accordingly, CAMK2α-positive CRH neurons might represent the subpopulation of spiny neurons observed

in the BNST and CeA, which are most likely GABAergic. This would suggest that CAMK2α is expressed in GABAergic neurons apart from striatal medium spiny neurons. To assess this, double *ISH* was performed against *Gad65/67* and *tomato* in *Camk2αCreERT2:Ai9* mice, where tomato expression is driven by the inducible *Camk2α* promoter. Interestingly, about 5-10% of cortical and hippocampal *Gad65/67*-positive neurons co-expressed *tomato/Camk2α.* Even more GABAergic neurons co-localized with *Camk2α* in the BNST and CeA (~50%). The presence of *Camk2α* in *Gad65/67*-positive MSNs of the caudate putamen was confirmed and is in line with previous reports (Erondu and Kennedy, 1985; Picconi et al., 2004). Importantly, the specificity of the double *ISH* is further confirmed by the fact nearly all *Crh* neurons in the piriform cortex (which are mainly glutamatergic) co-expressed *Camk2α*. Only few *Camk2α*-positive *Crh* neurons were detected in the cerebral cortex, but at this point it is not clear whether these are GABAergic or glutamatergic. As previously mentioned, Jennings and colleagues reported that optogenetic-mediated activation of CAMK2α-expressing BNST-VTA projection neurons produced both glutamatergic and GABAergic currents in VTA neurons (Jennings et al., 2013). This additionally supports the presence of long-range CAMK2α-positive GABAergic projection neurons. Additional triple labeling approaches are necessary to determine the exact number of GABAergic CAMK2α-expressing CRH neurons in limbic and cortical structures.

In order to specifically assess, whether CAMK2α-positive CRH neurons carry dendritic spines; we made use of the FLEX-switch system (described in 4.3.1). Single injections of Cre-dependent *AAV-Camk2α-floxed-eYFP* vectors to the BNST, CeA and PFC of *Crh-IRES-Cre* mice were used to label CAMK2α-positive CRH neurons. In this case, eYFP expression is driven by the CAMK2α promoter, and induced only upon Cre-mediated inversion of the FLEX-construct. Bearing in mind that Cre-expression is controlled by the endogenous CRH promoter, eYFP fluorescence is only observed in CAMK2α-positive CRH neurons. In the BNST and CeA, dendrites of the majority of eYFP-fluorescent, CAMK2α-positive CRH neurons were decorated with spines. Again, the density and shape of spines varied from spares to moderate and thin to mushroom-like respectively. Furthermore, a substantial amount of long-range axons were observed in the BNST of *AAV-Camk2α-floxed-eYFP* injected *Crh-IRES-Cre* mice, suggesting that CAMK2α-positive CRH neurons are able to project over long distances. Whether this neuronal subgroup also projects to more distant brain regions, including the VTA, will be investigated with anterograde viral tracers, expressing CAMK2α-driven synaptophysin-eYFP fusion proteins. Dendritic spines were also observed in CAMK2α-positive CRH neurons of the PFC. As

mentioned earlier, in most cases it was not possible to classify them into pyramidal or nonpyramidal cells, due to incomplete labeling of the majority of neurons. Importantly, Camk2α-eYFP expression was also detected in aspiny cortical CRH neurons, which were basket-cell shaped. In contrast to our earlier assumption, this implies that CAMK2α is not only expressed in spiny glutamatergic and GABAergic neurons, but presumably also in few aspiny interneurons. The fact that a small number of cortical neurons co-expressed *Gad65/67* and *Camk2α* further supports this.

Overall, our results give rise to the hypothesis that CAMK2α-expressing GABAergic CRH neurons represent a subpopulation of spiny long-range projection neurons. Studies on GABAergic cells have mainly focused on local interneurons neglecting those inhibitory neurons projecting to distant brain areas. However, clear-cut criteria for "long-range" versus "short-range" GABAergic neurons are still missing. Caputi and colleagues considered GABAergic cells as being "long-range" when they interconnect brain areas associated with distinct functions (Caputi et al., 2013). As previously stated, the best characterized are MSNs in the striatum but also Purkinje cells in the cerebellum. In addition, long-range bidirectional GABAergic connectivity was observed between the hippocampus and medial septum, as well as the hippocampus and entorhinal cortex (Toth and Freund, 1992; Toth et al., 1993; Takacs et al., 2008; Melzer et al., 2012). Interestingly, a recent study reported VTA-NAc long-range GABAergic projections, which enhance stimulus-outcome learning following optogentic-mediated activation (Brown et al., 2012). Neocortical long-range GABAergic connections have also been identified (McDonald and Burkhalter, 1993; Tomioka et al., 2005; Tomioka and Rockland, 2007), many of which express SOM, NPY and/or nitric oxide synthase (Caputi et al., 2013). Notably, dendritic spines are found on a number of cortical SOM and NPY expressing neurons (Kawaguchi et al., 2006; Kubota, 2013). However, it is unclear whether cortical and/or limbic GABAergic projection neurons generally exhibit dendritic spines, as is the case in striatal MSNs. An intriguing class of hippocampal long-range GABAergic neurons are the so-called "hub-cells". A subset of these neurons exhibited both, long-range and short-range axons, which enable them to control nearby and distant neuronal networks (Picardo et al., 2011). Whether this dual mode of innervation exists for other GABAergic projection neurons is currently not clear. From diverse immunohistochemical and genetic analyses it can be inferred that long-range GABAergic cells do not constitute a homogenous class in most brain regions (Caputi et al., 2013). Fate-mapping studies demonstrated that the diversity of GABAergic interneurons is strongly determined by the site and time of birth (Marin and Rubenstein, 2003;

Caputi et al., 2013). The three major sites that give rise to GABAergic cells are the medial ganglionic eminence (MGE), lateral ganglionic eminence (LGE) and caudal ganglionic eminence (CGE). The peak time of generation of GABAergic neurons in rodents is between E11 and 14 (Marin and Rubenstein, 2003). So far it is not clear when and where GABAergic CRH neurons are generated, and whether this is different for CRH-expressing interneurons and long-range projection neurons. Future studies will have to validate the morphological characteristics and identify the target areas of CRH projection neurons. Assessment of electrophysiological properties and/or optogenetic stimulation/inhibition of projecting CRH neurons will help to uncover the functional relevance of this neuronal subpopulation.

Our results support the presence of distinct CRH-expressing neuronal subpopulations in the mouse brain. We believe that each of these carry out specific functions under basal conditions and in response to stress. We revealed that CRH-expression in the cortex and limbic regions is primarily restricted to GABAergic neurons. These can be further subdividing into local CRH-expressing interneurons, and GABAergic long-range projection neurons. In addition, a large number of limbic CRH neurons, characterized by the expression of CAMK2α, exhibited dendritic spines. We propose that GABAergic/CAMK2α CRH neurons represent a subset of spiny long-range projection neurons similar to GABAergic medium spiny neurons of the striatum. The functional role of this subpopulation will be discussed in the following section.

5.4. Conditional *Crh* knockout mice highlight the bidirectional modulation of anxiety via the CRH/CRHR1-system

Conditional CRH overexpressing mice played a substantial role in unraveling the bidirectional nature of the CRH/CRHR1 system in anxiety, which was further confirmed in neurotransmitter-specific *Crhr1* knockout mice. However, overexpression studies are limited in their ability to accurately reflect the endogenous function of specific CRH subpopulations, which is primarily due to ectopic and non-physiological expression of the peptide in the brain. Thus, a loss of function approach, targeting *Crhr1* and/or *Crh*, is more likely to reveal physiologically relevant effects of the CRH/CRHR1-system on behavior. As a reminder, we observed that CRHR1 in forebrain glutamatergic and midbrain dopaminergic neurons is mediating anxiogenic and anxiolytic effects respectively. Importantly, genetic labeling and tracing studies suggest that the source of CRH is restricted to forebrain spiny and/or aspiny GABAergic and/or CAMK2α-positive neurons, some of which project over long distances. To circumvent the problems of

ectopic expression associated with CRH overexpressing mice, and to more accurately address the role of CRH in emotional behavior, we generated conditional *Crh* knockout mice (produced by Claudia Kühne).

A reporter-selection cassette flanked by *frt* sites, followed by a floxed *Crh* exon 2, was introduced into intron 1 of the murine *Crh* gene via homologous recombination in embryonic stem cells (for details see Section 4.3.3). In this constellation, *Crh* expression is prevented (null alle), but can be restored upon removal of the *frt*-flanked reporter-selection cassette, resulting in a functional floxed *Crh* allele (Crh^{flox}). Spatial and/or temporal inactivation of *Crh* expression is enabled by Cre-mediated inactivation of the floxed exon 2. The novel conditional Crh^{flox} allele was evaluated by breeding $Crh^{flox/flox}$ mice to ubiquitous *Cre-deleter* mice to obtain heterozygous *Crh* knockout animals ($Crh^{flox/-}$). The latter were intercrossed to yield viable homozygous *Crh* knockout mice ($Crh^{-/-}$) at an expected mendelian frequency. $Crh^{-/-}$ mice obtained from heterozygous breedings were fertile and displayed no obvious physiological alterations compared to control littermates. However, mating between homozygous *Crh* knockout mice yielded progeny which died within the first day of life. This was also observed in conventional *Crh* knockout mice (*Crh-KO*) generated by Muglia and colleagues, and resulted from fetal glucocorticoid need for lung maturation (Muglia et al., 1995). Exogenous supply of corticosterone to the drinking water of homozygous mothers prevented the effects, underscoring the ability of glucocorticoids to cross the placenta. More importantly, this suggested that glucocorticoids are primarily required during fetal and not postnatal life (Muglia et al., 1995). Expectedly, no *Crh* transcript was detected throughout the brain of $Crh^{-/-}$ compared to $Crh^{flox/flox}$ mice. In addition, basal and stress-induced plasma corticosterone levels were scarcely detectable in $Crh^{-/-}$ mice, further indicating the absence of a functional *Crh* allele. This nicely mirrors the reduced HPA axis function in total *Crhr1* knockout mice (Timpl et al., 1998). In contrast to the anxiolytic response observed in constitutive *Crhr1* knockout mice (Timpl et al., 1998), CRH deficiency produced no alterations in locomotion, anxiety or stress-coping behavior. This contradictive finding is in line with earlier studies reporting normal baseline locomotor activity, exploration, anxiety, startle response and learning in *Crh-KO* mice (Weninger et al., 1999). However, compensatory mechanisms and basal HPA axis alterations might obscure the interpretation of the role of central CRH in emotional behavior. Thus, we decided to specifically dissect the involvement of CRH in distinct neuronal subpopulations. Having established that CRH is primarily expressed in GABAergic neurons of forebrain limbic structures and the cortex, as well as glutamatergic neurons of the piriform cortex, we initially

bred *Crh*$^{flox/flox}$ mice to *Dlx5/6-Cre* and *Nex-Cre* mice to induce *Crh* deficiency in GABAergic (*Crh*$^{GABA\text{-}CKO}$) and glutamatergic neurons (*Crh*$^{Glu\text{-}CKO}$) respectively. The pattern of *Crh* deletion in *Crh*$^{GABA\text{-}CKO}$ and *Crh*$^{Glu\text{-}CKO}$ mice was largely in line with the expression maps obtained with double *ISH,* which emphasizes the specificity of the Cre lines. Importantly, neither the *Dlx5/6-Cre* nor the *Nex-Cre* recombined in CRH-expressing neurons of the PVN, resulting in unaltered HPA axis activity in both mouse lines. This emphasizes that CRH in the PVN, but not extrahypothalamic sites, is required for normal HPA axis function. However, CRH hyperdrive in extrahypothalamic regions has the ability to potentiate HPA axis activity, as previously demonstrated in a subset of region and neurotransmitter-specific CRH overexpressing mouse lines. Similar to constitutive *Crh* knockout mice, *Crh*$^{Glu\text{-}CKO}$ mice displayed no behavioral alterations, which is not unexpected considering that glutamatergic CRH neurons are primarily localized in the piriform cortex, a brain structure which is rarely implicated in emotional behavior. More surprising was the fact that *Crh* deletion in GABAergic neurons (resulting in *Crh* absence from the cortex and all limbic structures) also failed to alter locomotion, anxiety and stress-coping behavior. To exclude the possibility that CRH in more caudal brain regions is regulating emotional behavior, we bred *Crh*$^{flox/flox}$ mice to *En1-Cre* mice to obtain conditional knockout mice lacking *Crh* in the mid/hindbrain (*Crh*$^{MHB\text{-}CKO}$). Similarly, these mice displayed no physiological or behavioral alterations compared to controls. Thus, we could not recapitulate the effects observed in conditional *Crhr1* knockout mice by genetically depleting *Crh* levels in a region- and neurotransmitter-specific manner. Consequently this supports that CRHR1, but not CRH, is modulating the expression of emotional behavior under baseline conditions. Importantly, *Crh-KO* mice exhibit normal acute stress-induced behavior, which can be specifically blocked by CRHR1-antagonist treatment (Weninger et al., 1999). This initially suggested compensations by other related neuropeptides. Considering that recombination of the *Dlx5/6-Cre*, *Nex-Cre* and *En1-Cre* occurs prenatally, favors the idea of early compensatory mechanism. However, the only other known mammalian CRHR1 ligand is urocortin 1 (UCN1), which is primarily confined to the Edinger-Westphal nucleus (EW), lateral superior olive and supraoptic nucleus (Vaughan et al., 1995; Fekete and Zorrilla, 2007). UCN1-immunoreactive fibers are found throughout the brain including the lateral septum, several motor nuclei in the brainstem, the olivocochlear fiber pathway, and the spinal cord (Bittencourt et al., 1999). However, UCN1-expressing fibers were not detected in limbic regions known to modulate mood-related behavior, which makes it rather unlikely that this neuropeptide could compensate for limbic and cortical CRH deficiency. Along these lines, UCN1 mRNA expression

was not significantly altered in constitutive *Crh-KO* mice compared to controls (Weninger et al., 1999). On the other hand, central administration of UCN1 results in similar behavioral effects to those observed following CRH application. These include increased arousal and anxiety-related behavior, altered locomotor activity and food intake, diminished sexual behavior and sleep disturbances (Moreau et al., 1997; Koob and Heinrichs, 1999; Benoit et al., 2000; Spiga et al., 2006; Sztainberg and Chen, 2012). Thus, we cannot exclude the possibility that UCN1 reaches CRHR1 receptors via volume transmission to induce CRH-like responses. In addition, both UCN1 and CRH were shown to mediate dopamine release through activation of CRHR1 in striatal slices (Bagosi et al., 2006). However, UCN1 can activate both CRH receptor subtypes. Consequently, central UCN1 administration might activate receptors non-selectively in areas where endogenous UCN1 may not exist. In order to investigate the specific role of UCN1, three conventional *Ucn1* knockout mice have been independently generated in the past (Vetter et al., 2002; Wang et al., 2002; Zalutskaya et al., 2007). All displayed no gross alterations in glucocorticoid secretion, supporting the view that CRH/CRHR1 is primarily involved in HPA axis regulation. However, the behavioral phenotype of *Ucn1-KO* mice remains controversial. Whereas Wang *et al.,* observed no changes in anxiety (Wang et al., 2002), Vetter and colleagues detected increased anxiety-related behavior in *Ucn1-KO* mice (Vetter et al., 2002). Based on the receptor's affinity and behavioral effects, UCN1 seems to have the ability to compensate for CRH deficiency, but its non-limbic distribution makes this rather unlikely to occur endogenously. Additional studies with double knockout mice, lacking CRH and UCN1 will help to shed light on this.

If UCN1 is not compensating for CRH deficiency, then this might suggest that an unidentified CRHR1 ligand is participating in basal and stress-induced mood-related behavior. Considering that the mouse genome has been sequenced, and the efficacy of current bioinformatics tools to detect alternative agonists, suggests a novel ligand which is structurally different from CRH and the UCNs. The teneurin C-terminal-associated peptide 1 (TCAP-1) was initially believed to represent a potential candidate. TCAPs were originally identified in a rainbow trout cDNA library screen for potential CRH homologs, and although they share a number of structural similarities with the CRH family of peptides, they have less than 20% sequence similarity (Wang et al., 2005; Lovejoy et al., 2006; Chen et al., 2013b). TCAPs are highly expressed in hypothalamic nuclei, and limbic regions, including the hippocampus, central and basolateral amygdala (Wang et al., 2005). TCAP-1 is able to block CRH-induced c-*fos* activation and behavioral alterations, but has little effect on behavior on its own (Tan et al., 2009). However,

the neuromodulatory role of TCAP-1 on elements of CRH signaling is not caused by TCAP-1-CRHR1 binding. Previous studies showed that CRHR1 receptor antagonist treatment does not block TCAP-1-induced downstream effects (in this case cAMP elevation) suggesting the presence of independent signaling pathways (Wang et al., 2005; Chen et al., 2013b). Similarly to the CRH binding protein (CRH-BP), TCAP-1 might be exerting its neuromodulatory functions by directly inhibiting CRH expression, but this has not been proven so far. Whether TCAP-1 and CRH-BP are capable of activating CRHR1/CRHR2 in case of CRH deficiency is currently unknown.

Another explanation for the lack of effects in total and conditional *Crh* knockout mice might be the presence of constitutively active CRH receptors. Constitutive activity defines the intracellular metabolic tone, associated with many GPCRs, that does not require the presence of an agonist (Seifert and Wenzel-Seifert, 2002). In other words, it describes the ability of GPCRs to undergo agonist-independent isomerization from an inactive (R) to an active (R*) state. In the R state, GPCRs are uncoupled from G proteins, whereas in the R* state, GPCRs can couple to, and activate, G-proteins (Seifert and Wenzel-Seifert, 2002). Full agonists maximally stabilize the R* state. However, in constitutively active GPCRs, the R- to R* isomerization can also occur spontaneously, or be triggered by homo- and/or heterodimerization with other receptors, i.e., independently of an agonist (Seifert and Wenzel-Seifert, 2002). Notably, many of the constitutively active wild-type GPCRs are receptors for neurotransmitters and neuromodulators including noradrenaline, 5-hydoxytryptamin, melatonin, dopamine, acetylcholine, histamine, adenosine, opioid peptides, neurokinins, neuropeptide Y and glutamate (Seifert and Wenzel-Seifert, 2002). As a matter of fact, non-peptidergic CRHR1 antagonist application to the amygdala facilitates evoked excitatory post-synaptic responses, suggesting tonic activation of CRH receptors by endogenous ligands and/or the presence of constitutively active receptors who's basal activity can be affected by antagonists (Orozco-Cabal et al., 2006). Similar effects were also observed in the lateral septum (Orozco-Cabal et al., 2006), but a systematic analysis is still lacking for most brain regions. Thus, CRHR1 might be constitutively active, resulting in the initiation of downstream signaling events even in the absence of a ligand. This could explain the consistent behavioral effects in conditional and total *Crhr1* knockout mice, as well as the absence of behavioral effects in *Crh* deficient mice. Constitutive activity of CRHR1 might arise spontaneously or from ligand-independent interactions with other synaptic proteins/receptors. Another possibility is that tonic release of CRH itself might keep CRHR1 basally active (similar to dopamine-D1/2 receptor system), which

would also be blocked by the application of an antagonist. The fact that *Crh* knockout mice display no substantial behavioral alterations would imply that such effects are not of high relevance for emotional behavior. However, enhanced CRH-release, as it occurs during stress, might alter the tonic mode to initiate changes in receptor confirmation and downstream signaling, which might eventually result in altered behavioral outcomes. Importantly, constitutive and/or tonic activation of CRHR1 would imply that CRH exerts its effects mainly during stress, when it is most strongly released. A large body of work has demonstrated the ability of CRHR1 antagonists to block stress-induced behavioral alterations (Cole et al., 1990; Heinrichs et al., 1992; Swiergiel et al., 1993; Liebsch et al., 1995; Koob and Le, 1997; Shaham et al., 1998; Weninger et al., 1999; Habib et al., 2000; Griebel et al., 2002; Zorrilla et al., 2002; Ducottet et al., 2003; Robison et al., 2004; Le and Koob, 2007; Roozendaal et al., 2008; Bruijnzeel et al., 2009; Ivy et al., 2010; Koob and Zorrilla, 2010; Zorrilla and Koob, 2010). Thus we assessed whether deletion of *Crh* from GABAergic neurons, and hence all limbic regions, would alter the behavioral susceptibility to chronic social defeat stress (CSDS). CSDS has been extensively used to model mood-related psychopathologies in mice (Berton et al., 2006; Nestler and Hyman, 2010). In accordance with the protective effects of CRHR1-antagonists on stress-induced behavior, CSDS enhanced anxiety-related behavior in control but not $Crh^{GABA\text{-}CKO}$ mice. The effects were independent of altered locomotion or HPA axis function, which were equally affected by CSDS in control and $Crh^{GABA\text{-}CKO}$ mice. Moreover, acute-stress induced expression of immediate early genes *c-fos* and *zif268* was significantly reduced in CRHR1-expressing brain regions including the hippocampus, caudate putamen and cortex of $Crh^{GABA\text{-}CKO}$ mice compared to controls. Decreased stress-induced neuronal activation in $Crh^{GABA\text{-}CKO}$ mice nicely mirrors the activating effects of central CRH application on *c-fos* expression (Dunn and Berridge, 1990; Liebsch et al., 1995; Benoit et al., 2000; Bittencourt and Sawchenko, 2000; Rostkowski et al., 2013). Accordingly, CRHR1-antagonist treatment was shown to block CRH- and stress-induced increase in *c-fos* expression (Doyon et al., 2007; Skorzewska et al., 2008). Decreased neuronal activation in stressed $Crh^{GABA\text{-}CKO}$ mice further reinforces the activating properties of CRH. Along these lines, forebrain-specific deletion of *Crhr1* decreases the susceptibility to chronic stress-induced cognitive deficits (Wang et al., 2011a; Wang et al., 2011b; Wang et al., 2012; Wang et al., 2013). To date, no specific downstream targets of CRH/CRHR1 signaling are known, which makes it extremely difficult to specifically assess the molecular mechanism underlying “chronic stress-resistance” in $Crh^{GABA\text{-}CKO}$ mice. Microarray and proteomic analysis in conditional *Crh* knockout mice could aid

in this undertaking. The possible mechanisms by which CRH-release from GABAergic neurons acts in an excitatory fashion were previously discussed (Section 5.2.1). Importantly, our data suggests that deletion of *Crh* in GABAergic neurons protects from the adverse effects of CSDS, possibly by reducing stress-induced neuronal activation. However, the protective effects were only observed in relation to anxiety-related behavior. Neither locomotion nor immobility in the FST were differentially affected by CSDS in control and $Crh^{GABA\text{-}CKO}$ mice. Contrastingly, anxiety-related behavior was similarly enhanced in control and constitutive *Crh* knockout mice following acute restraint stress (Weninger et al., 1999). This might suggest that chronic, but not acute, activation of the CRH-system shapes behavioral stress-responses. Thus, other systems might be able to compensate for CRH deficiency during acute but not chronic stress exposure. On the other hand, we have to keep in mind that constitutive *Crh* knockout mice display reduced HPA axis activity, which might mask potential phenotypes. At this point we cannot exclude that constitutive *Crh* knockout mice might also display enhanced resilience to CSDS. Moreover, the effects of acute stress in $Crh^{GABA\text{-}CKO}$ mice will elucidate whether CRH is primarily involved in modulating behavioral responses to chronic stress.

Considering that social behavior is altered in many psychiatric disorders including, MDD, BPD, schizophrenia and autism (Nestler and Hyman, 2010), we additionally assessed social interaction in $Crh^{GABA\text{-}CKO}$ mice. CSDS is able to reduce social interaction and enhance avoidance behavior in mice (Berton et al., 2006). Interestingly, $Crh^{GABA\text{-}CKO}$ mice exhibited significantly reduced social interaction compared to controls already under basal conditions. This was not further aggravated by CSDS most likely due to the established floor effect under basal conditions. The results suggest that CRH in GABAergic neurons is required for the expression of "normal" social behavior. This is partially in line with the work of Kasahara and colleagues, which demonstrated enhanced social investigation in CRH overexpressing mice (Kasahara et al., 2011). On the other hand, central, BNST and amygdala-specific CRH administration were shown to decrease social interaction (Dunn and File, 1987; Sajdyk et al., 1999; Lee et al., 2008). Along these lines, CRH infusion into the NAc propagates stress-induced social avoidance (mimicked by optogenetic activation of VTA-NAc projections). However, in the absence of stress or optical stimulation, CRH application to the NAc produced no alterations in social behavior (Walsh et al., 2014). Similarly, knockdown of *Crh* in the PVN attenuated social avoidance in chronic social defeated mice, without altering social interaction under basal conditions (Elliott et al., 2010). However, the authors did not assess possible alterations in HPA axis function, which could have been caused by *Crh* knockdown in the PVN. Thus, it cannot be

exclude that the observed phenotype is partially caused by reduced glucocorticoid levels. Importantly, the results obtained after exogenous CRH application have to be interpreted with caution considering that these experiments are only mimicking acute effects of CRH hyperdrive. In addition, enhanced receptor activation following exogenous CRH application or overexpression might overshadow normal patterns of endogenous CRH release. Furthermore, co-activation of CRHR2 might obscure the relevance of CRH-CRHR1 signaling in social behavior. This is supported by the fact that mice deficient for *Ucn3*, *Ucn2* (specific CRHR2 ligands) and *Crhr2* display alterations in social behavior (Deussing et al., 2010; Breu et al., 2012). Importantly, social avoidance/approach paradigms are often confounded by anxiety, such that anxious animals are more likely to display reduced social engagement. As observed for anxiety-related behavior, distinct CRH circuits might also differently regulate social behavior, which can be further altered by stress. Additional tests assessing sociability and social group interaction will further specify the role of GABAergic CRH circuits in social behavior. Consequently, we have to contradict our earlier statement that mood-related behavior is not altered in $Crh^{GABA\text{-}CKO}$ mice. Deficits in social behavior support the notion that *Crh* depletion in GABAergic neurons is able to alter specific mood-related behaviors already under basal conditions. Whether this also applies to other non-investigated paradigms (for example those assessing cognition, attention, etc.) will be assessed in the future. Of note, fear memory acquisition, consolidation and expression were not affected in $Crh^{GABA\text{-}CKO}$ mice (discussed later). It is still not understood how the brain incorporates the CRH/CRHR1-system to translate stressful stimuli into a final autonomic and behavioral response. A recent study reported demethylation of the CRH-promoter region, which resulted in enhanced *Crh* gene expression in the PVN of mice that were susceptible to CSDS (Elliott et al., 2010). Knockdown of *Crh* in the PVN attenuated CSDS-induced behavioral alterations. The fact that CRH expression is preserved in the PVN of $Crh^{GABA\text{-}CKO}$ mice might partially explain the absence of CSDS-induced effects on other behaviors such as locomotion and immobility in the FST. Whether CSDS also alters *Crh* methylation in other brain regions is currently unknown. Thus, epigenetic regulation of CRH may constitute a mechanism by which the brain regulates long-term behavioral responses to stress.

Overall, *Crh* deletion in GABAergic neurons decreased CSDS-induced anxiety without altering baseline behaviors in most of the performed tests. This further supports the idea that CRH in GABAergic neurons modulates chronic stress-induced changes in anxiety as well as basal social behavior. Importantly, possible changes in CRH-neurotransmitter interactions (especially with

regards to the dopaminergic system; Section 5.2.1) have to be investigate in *Crh*$^{GABA\text{-}CKO}$ mice under basal and chronic stress conditions.

5.4.1. CAMK2α-expressing CRH neurons are required for positive emotional responses

Earlier we established that a subpopulation of GABAergic *Crh* neurons expresses *Camk2α*. These triple-positive neurons likely represent a subset of spiny long-range projection neurons similar to GABAergic medium spiny neurons of the striatum. Hence, we aimed to investigate the specific role of CAMK2α-positive CRH neurons on emotional behavior. Although we could show that GABAergic-CRH neurons control stress-induced emotional behavior, it should be kept in mind that *Crh* is entirely deleted from the cortex and all limbic structures of *Crh*$^{GABA\text{-}CKO}$ mice. Thus, it is probable that the source of CRH is depleted for both, anxiogenic and anxiolytic CRH type 1 receptors in glutamatergic and dopaminergic neurons respectively. We have already postulated that under physiological conditions, CRHR1-controlled glutamatergic and dopaminergic systems might function in a concerted but antagonistic manner to keep adaptive anxiety responses to stressful situations in balance. This is additionally supported by the fact that deletion of *Crhr1* in both neurotransmitter systems (*Crhr1*$^{CNS\text{-}CKO}$) fails to alter mood-related behavior. Correspondingly, depletion of *Crh* required for glutamatergic and dopaminergic-CRHR1 activation, might lead to the same outcome, and thereby additionally explain the absence of strong basal behavioral effects in *Crh*$^{GABA\text{-}CKO}$ mice. We postulate that different subpopulations of CRH neurons, within the same brain structures, are able to activate different classes of receptors. Spiny CAMK2α-positive GABAergic cells probably represent one specific subgroup of CRH neurons. In order to investigate the involvement of CAMK2α-positive CRH neurons in emotional behavior, *Crh*$^{flox/flox}$ mice were crossed with inducible *Camk2α-CreERT2* mice to generate the *Crh*$^{iFB\text{-}CKO}$ line. Deletion was induced during postnatal week 10 via 2 weeks of oral tamoxifen application. Importantly, this allowed us to address the role of CRH during adulthood, circumventing possible compensatory mechanisms associated with developmental deletion which might have occurred in all of the above described *Crh* knockout lines. An additional advantage is obtained by the absence of gradual deletion processes, which frequently occur in non-inducible Cre lines, and have been demonstrated for *Camk2α-Cre* mice (Refojo et al., 2011). The *Crh*-deletion pattern in *Crh*$^{iFB\text{-}CKO}$ mice nicely mirrored the expression maps obtained with double *ISH*. Consequently, a reduction, but not complete absence of *Crh* mRNA was observed in the OB, Pir, Ctx, BNST, CeA, PVN, APT, MGM and PB of *Crh*$^{iFB\text{-}CKO}$ mice.

Interestingly, deletion of *Crh* from *Camk2α*-positive neurons resulted in increased anxiety-related behavior in the EPM and OF, stressing the necessity of specific CRH circuits for positive emotional behavior. Consequently, CRH signaling during adulthood is not only conveying the negative effects of stress, but might also be required to transmit and integrate the positive aspects of acutely stressful life-events. These observations are in line with the anxiogenic phenotype of $Crhr1^{iDA\text{-}CKO}$ mice, and suggest that GABAergic, CAMK2α-positive CRH neurons (possibly located in the BNST) innervate CRHR1-expressing dopaminergic neurons in the VTA to modulate dopamine release and thus induce anxiolytic responses. In support, channelrhodopsin-2-assisted circuit mapping revealed that stimulation of glutamatergic BNST-VTA projections resulted in aversive and anxiogenic behavioral phenotypes. Conversly, activation of GABAergic BNST-VTA projections produced rewarding and anxiolytic phenotypes (Jennings et al., 2013). Optogenetic-mediated activation/inhibition of BNST CAMK2α-positive CRH projections will clarify whether this presumably GABAergic subpopulation is responsible for the anxiolytic and rewarding effects. One important question arises at this point: Which CRH neurons activate glutamatergic CRH type 1 receptors to enhance anxiety under basal conditions? These could represent CRH-positive GABAergic interneurons that do no express CAMK2α. Whether deletion of *Crh* specifically from limbic non-*Camk2α*-expressing neurons would result in decreased anxiety (which is observed upon deletion of *Crhr1* from glutamatergic neurons) remains unknown and is hampered by the unavailability of appropriate markers and hence Cre-lines that target this specific cell population. Thus, the absence of basal behavioral effects in $Crh^{GABA\text{-}CKO}$ mice could result from deletion of CRH from both, anxiety-causing GABAergic interneurons and anxiety-inhibiting GABAergic/CAMK2α CRH neurons. The fact that $Crh^{GABA\text{-}CKO}$ mice display decreased stress-susceptibility clearly supports the presence of “anxiogenic” CRH circuits. However, these might be specifically activated by stress, as proposed above. Importantly, our results support the existence of anxiolytic and anxiogenic CRH-releasing neurons.

In support of anxiolytic CRH-releasing neurons, the expression of auditory fear memory was significantly enhanced in $Crh^{iFB\text{-}CKO}$ mice compared to controls. The phenotype was not reflective of generalized fear responses since freezing behavior in a neutral context, and context-dependent freezing were not altered $Crh^{iFB\text{-}CKO}$ mice compared to controls. Notably, enhanced responses of pre-established fear memories can serve as additional indicators for pathological anxiety. Accordingly, the CRH/CRHR1 system has been widely implicated in hippocampal-dependent contextual fear-memory as well as in amygdala-dependent auditory

fear memory, although many of the results are contradictory. Most studies, using CRHR1 antagonists or *Crhr1*-knockout mice have demonstrated impairments in fear memory consolidation and/or expression, which might be beneficial in case of pathologically sustained fear responses (Butler et al., 1990; Radulovic et al., 1999b; Hikichi et al., 2000; Hubbard et al., 2007; Kolber et al., 2008; Roozendaal et al., 2008; Pitts et al., 2009; Thoeringer et al., 2012). This body of work supports the idea that CRH is necessary for the formation of fear memories, which is not in line with our data. On the contrary, deletion of *Crh* from *Camk2α*-positive neurons even enhanced tone-dependent freezing behavior. Importantly, $Crh^{GABA\text{-}CKO}$ mice showed no alterations in auditory and contextual fear-memory, suggesting that *Crh* depletion specifically from *Camk2α*-positive neurons is responsible for the observed effects. However, we cannot exclude the possibility that compensatory mechanisms, due to developmental CRH deletion in $Crh^{GABA\text{-}CKO}$ mice, are masking potential effects. In contrast to the reported fear-enhancing properties of CRH, Isogawa and colleagues have recently observed that pre-training and post-training infusions of CRH into the basolateral amygdala impair the formation of fear memories, which is partially supported by our data (Isogawa et al., 2013). In line with these observations, Tovote et al., reported lower acquisition of auditory fear memory in CRH overexpressing mice (Tovote et al., 2005). Overall it becomes evident that interference as well as enhancement of CRH function can result in impairments in memory consolidation. Isogawa and colleagues suggest that receptor stimulation by exogenous CRH application might overshadow normal patterns of endogenous CRH release that are triggered naturally by the fear conditioning experience. In other words, exogenous CRH might be overshadowing the endogenous signal that would normally support fear memory formation. Our data does not support this notion, since both $Crh^{GABA\text{-}CKO}$ mice and $Crh^{iFB\text{-}CKO}$ mice displayed no deficits in auditory and contextual fear memory formation. In support, deletion of *Crhr1* from glutamatergic, GABAergic, dopaminergic and serotonergic neruons failed to alter tone-dependent freezing behavior (Refojo et al., 2011). Similarly, forebrain-specific *Crhr1* knockout mice ($Crhr1^{FB\text{-}CKO}$) displayed no alterations in contextual or auditory fear memory consolidation. However, forebrain-specific deletion of *Crhr1* did attenuate remote fear memory consolidation processes investigated four weeks after training (Thoeringer et al., 2012). Fear and anxiety are tightly interconnected and often difficult to dissociate. Thus $Crh^{iFB\text{-}CKO}$ mice might be exhibiting enhanced anxiety in response to an aversive event-coupled stimulus (tone). This is supported by studies in mice bred for high anxiety, which displayed enhanced contextual and auditory fear memory compared to controls (Sartori et al., 2011). Importantly, enhanced fear

expression in *Crh*$^{iFB\text{-}CKO}$ mice was not generalized, implying that CAMK2α-positive neurons modulate very specific, amygdala-dependent fear circuits. In fact, optogenetic dissection of different nuclei within the central amygdala revealed heterogeneous GABAergic neuronal subpopulations that gate specific conditioned fear responses (Haubensak et al., 2010). Considering that fear and anxiety are closely related, might suggest that fear memory formation is also regulated in a bidirectional manner by the CRH/CRHR1-system. Thus, specific CRH/CRHR1-circuits might be required for consolidation processes of aversive experiences, while others might specifically block it. This could serve to specifically "gate" the strength of memories, deciding which experience should be thoroughly remembered and which should not. The duration of CRH/CRHR1 activation is also likely to influence fear memory processes. This is supported by the fact that acute stress and short treatment with CRH enhances memory, which might constitute an adaptive mechanism that promotes learning and remembering during threatening situations (Wang et al., 1998; Blank et al., 2002; Joels and Baram, 2009; Chen et al., 2012b). On the other hand prolonged stress and CRH treatment lead to cognitive impairments, often accompanied by diminished synaptic integrity (Heinrichs et al., 1996; Radulovic et al., 1999b; Chen et al., 2012b). Importantly, the majority of published studies have assessed acute effects of CRH/CRHR1 activation and/or blockade which might not accurately reflect the endogenous CRH/CRHR1 circuitry in the context of stress-induced fear-memory formation. This emphasizes the necessity for more elaborate analyses of fear-memory pathways in conditional *Crh* and *Crhr1* mouse mutants.

Astoundingly, deletion (*Crh*$^{iFB\text{-}CKO}$) and overexpression (*Crh*$^{iFB\text{-}COE}$) of *Crh* in *Camk2α*-positive neurons both result in increased anxiety. As already postulated, this could be cause by enhanced receptor stimulation in CRH overexpressing mice, which overshadows normal patterns of endogenous CRH release that are triggered naturally by environmental stimuli. Additionally, co-activation of CRHR2 might contribute to the anxiogenic phenotype and cannot be excluded in *Crh*$^{iFB\text{-}COE}$ mice. In fact, optogenetic activation of CRHR2-expressing GABAergic neurons of the septum promotes persistent anxious behaviors (Anthony et al., 2014). The expression pattern of the *Crh-LacZ* fusion transcript indicates that *Crh* is ectopically expressed in the septum of *Crh*$^{iFB\text{-}COE}$ mice (Figure 19). Overexpression of UCN2 (a selective CRHR2 ligand) in CAMK2α-positive neurons will clarify to which extend CRHR2 is involved in the observed phenotype. Another explanation for the similar phenotypes could be that the effect of CRH on anxiety follows an inverted U-shaped relationship under basal conditions. Thus, "normal

anxiety responses" might require an optimal level of CRH release, and anything below or above could result in an altered emotional state.

Overall our results propose that CRH, specifically in CAMK2α-positive neurons, is required for positive emotional responses and stable fear memory expression. Keeping in mind that *Crhr1*$^{iDA\text{-}CKO}$ exhibited similar behavioral alterations, might imply that CAMK2α-expressing CRH neurons in limbic nuclei target dopaminergic CRHR1 receptors (refer to working model in section 4.4). In fact, our results suggest that CAMK2α-positive CRH neurons comprise a subpopulation of GABAergic long-range projection neurons. In consequence it seems plausible that deletion of anxiolytic CRH type 1 receptors from dopaminergic neurons or *Crh* from VTA-input neurons yield a similar behavioral profile. However, additional microdialysis experiments will need to unravel whether dopaminergic neurotransmission is altered in *Crh*$^{iFB\text{-}CKO}$ mice. Importantly, auditory fear conditioning was not affected in *Crhr1*$^{iDA\text{-}CKO}$ mice suggesting the involvement of additional (not dopamine-related) neurotransmitter circuits in CRH-controlled fear memory expression.

We have already extensively discussed the possibility by which CRH interacts with the dopaminergic system to regulate emotional behavior. In this context, Lemos and colleagues suggest that severe stress is able to initiate a persistent dysregulation of CRH-dopamine interactions that normally modulate positive emotional responses (Lemos et al., 2012). However, CSDS induced similar changes in control and *Crh*$^{iFB\text{-}CKO}$ mice, failing to switch CRH action in CAMK2α-positive neurons from anxiolytic to anxiogenic. On the other hand, deletion of *Crh* from GABAergic neurons (which also encompasses most limbic CAMK2α-positive CRH neurons) diminished chronic stress-susceptibility. Consequently, we propose that the CRH/CRHR1-system has the ability to modulate emotional responses in a bidirectional manner under physiological conditions. The ability is lost under severe stress condition, where activation of the CRH-system is generally aversive, resulting in the suppression of positive behavioral responses. However, we are just staring to comprehend the complexity of CRH-neurotransmitter interactions, which appear to be differentially regulated under basal and severe-stress conditions. Further assessment of the described mouse models (e.g. exposure of neurotransmitter-specific *Crhr1* knockout mice to CSDS) will strengthen our understating of CRH/CRHR1-neurocircuitries in the context of mood-related psychopathologies.

6. CONCLUSION AND OUTLOOK

CRH and CRHR1 are widely distributed throughout the brain where they orchestrate the neuroendocrine, autonomic and behavioral responses to stress. However, little is known about CRH/CRHR1-regulated neurotransmitter-circuits in the context of adaptive and maladaptive stress-related behavior. We addressed this issue using a variety of neurochemical, molecular and genetic tools.

Using gain-of-function models, we initially established that central CRH hyperdrive on its own, or in combination with elevated glucocorticoids, is able to regulate aspects of stress-related behavior including anxiety. In addition, many of the generated CRH overexpressing mice displayed endophenotypes of stress-related disorders. For instance, the behavioral profile of CNS-specific CRH overexpressing mice is strikingly similar to other mania models and recapitulates several aspects of human BP patients in the manic state. Accordingly, many of the behavioral changes could be reversed with chronic lithium treatment. Although the exact underlying mechanisms remain to be elucidated, they are likely linked to enhanced noradrenergic function. However, the most striking feature of $Crh^{CNS\text{-}COE}$ mice is the ability to switch from manic to depressive-like behavior following chronic stress exposure. Although the alternation was specific to anxiety behavior, $Crh^{CNS\text{-}COE}$ mice potentially represent one of the first genetic models of BPD to cycle between manic and depressive endophenotypes.

The additional generation of region- and neurotransmitter-specific CRH overexpressing mice demonstrated the ability of CRH to induce positive and negative emotional responses depending on the site of overexpression. However, the lack of construct validity and uncertainties that arise with ectopic CRH expression cannot be neglected and represent a major disadvantage of the described overexpression models. With respect to clinical findings and in order to fully understand the effects of CRH hyperdrive in the context of stress-related neuropathologies, the generation of mice overexpressing CRH under its endogenous promoter represents a matter of particular importance. We are currently establishing this by breeding recently generated *CRH-IRES-Cre* mice to our conditional CRH overexpressing mouse mutants. A more selective approach will constitute an AAV-mediated overexpression system in combination with the *Crh-IRES-Cre* mouse line. We recently developed an AAV containing a floxed *Crh-IRES-eGFP* expression cassette under the control of the *EF1a* promoter, which will be selectively expressed in CRH positive neurons upon stereotaxical injection of the virus within discrete limbic brain regions of *Crh-IRES-Cre* mice. This will enable us to dissect the underlying brain regions involved in mediating CRH hyperdrive-induced behavioral alterations.

Nevertheless, we believe that the already established overexpressing lines will represent valid disease models, which can be used to predict the efficacy of newly developed drugs that target depression-, mania- or anxiety-like symptoms.

Loss-of-function approaches were subsequently applied to unravel the underlying neurotransmitter circuits controlled by CRH/CRHR1 that modulate stress-related behavior. We revealed that deletion of *Crhr1* from glutamatergic (*Crhr1*$^{Glu\text{-}CKO}$) neurons reduced anxiety-related behavior, which is in agreement with the previously established phenotype of forebrain-specific *Crhr1* knockout mice, and the anxiolytic properties of CRHR1-antagonists. Moreover, studies in our group revealed that this phenotype is associated with impaired glutamatergic neurotransmission in the amygdala and hippocampus. Unexpectedly, deletion of the receptor from dopaminergic neurons (*Crhr1*$^{DA\text{-}CKO}$) increased anxiety-related behavior, which was linked to diminished dopamine release in the PFC. The ability of CRH to positively regulate dopamine release and decrease anxiety was demonstrated upon CRH-overexpression in GABAergic neurons. But whether this occurs in endogenously activated GABAergic CRH circuits remains to be investigated. Consequently our results suggest that under physiological conditions, CRH/CRHR1-controlled glutamatergic and dopaminergic systems might function in a concerted but antagonistic manner to keep adaptive anxiety responses to stressful situations in balance. Thus, CRH hyperactivity, which is observed in many patients suffering from emotional disorders, might not be general but restricted to particular neuronal circuits, triggering symptoms by generating an imbalance between CRHR1-controlled glutamatergic and dopaminergic systems involved in emotional behavior.

In order to locate the CRH-producing neurons responsible for modulating behavioral responses in a bidirectional manner, we set out to determine their neurochemical identity and morphology. The majority of *Crh*-expressing cells in the cortex and limbic structures co-expressed the GABAergic markers *Gad65/67*. In contrast, glutamatergic *Crh* neurons were primarily located in the piriform cortex. GABAergic CRH neurons exhibited distinct morphologies depending on the brain region (e.g. cortical CRH neurons were primarily aspiny double-bouquet or small-basket shaped, in contrast to limbic CRH neurons which displayed spiny multipolar morphologies). Next we performed AAV-mediated anterograde tracing studies in *Crh-IRES-Cre* mice to determine the origins of CRH neurons that target dopaminergic CRH type 1 receptors in the VTA. We found that a subgroup of CRH neurons within the BNST project monosynaptically to the VTA. Additional neurochemical studies revealed that a substantial number of limbic CRH neurons express CAMK2α and contain dendritic spines. Interestingly,

these neurons were also shown to exhibit long-range axons. Considering that the majority of limbic *Crh* cells co-express *Gad65/67*, we believe that that CAMK2α-positive CRH neurons might represent a subpopulation of spiny GABAergic long-range projection neurons. Triple labeling approaches will clarify the degree of overlap. For example, viral-delivery of Cre-dependent *Camk2α-eYFP* constructs into *Crh-IRES-Cre* mice will label CAMK2α-positve CRH neurons. Subsequent immunohistochemistry against GAD65/67 or GABA will enable the visualization of triple-positive cells. Co-localization studies with additional GABAergic makers such as VIP, SOM, CCK or PV will help to further characterize different CRH subpopulations. The identification of distinct electrophysiological properties will also be mandatory in the future. Moreover, anterograde viral tracers expressing *Camk2α*-driven synaptophysin-eGFP fusion proteins will be injected into limbic regions of *Crh-IRES-Cre* mice in order to determine whether CAMK2α-positive CRH projections target the VTA.

Having described different subpopulations of CRH neurons we aimed to assess their role in emotional behavior by generating conditional *Crh* knockout mice. Deletion of *Crh* from *Camk2α*-positive neurons enhanced anxiety and fear memory expression, implicating that this specific CRH pathway is required under physiological conditions to maintain a positive emotional state. Considering that deletion of *Crhr1* from dopaminergic neurons produces similar effects, suggests that limbic, triple-positive CAMK2α-CRH-expressing GABAergic projection neurons target dopaminergic CRH type 1 receptors to modulate emotional behavior by altering dopamine release. Consequently, the deletion of either the receptor from dopaminergic VTA neurons or the ligand from VTA-projecting limbic neurons results in the same anxiogenic response, which is likely a result of diminished dopamine release. To address this more accurately, we will implement optogenetic tools to activate or inhibit CRH projections that innervate the VTA. For this, *Crh-IRES-Cre* mice will be crossed with floxed channelrhodopsin or halorhodopsin/archaerhodopsin mice in order to induce expression of the light-sensitive channels specifically in CRH neurons. Concurrent implantation of microdialysis probes will enable us to monitor dopamine release *in vivo* upon stimulation/inhibition of VTA-projecting CRH terminals. Specific targeting of CAMK2α-positive CRH projections can be achieved by injecting a Cre-inducible AAV vector, which expresses *Camk2α*-driven opsins, into *Crh-IRES-Cre* mice. In addition, we aim to selectively delete *Crh* from *Camk2α*-positive neurons that project to the VTA. For this, we will inject AAV vectors that express the *Camk2*-driven Cre recombinase and undergo retrograde transport, into the VTA of floxed *Crh* mice. Consequently, Cre-mediated deletion of *Crh* will only take place in *Camk2α*-

positive neurons that project to the VTA. In order to precisely map all VTA projecting CRH neurons, Cre-dependent retrograde tracing systems using rabies viruses will be applied. However, this requires the availability of a *Crhr1-Cre* mouse line, which is currently being generated in our group.

So far our results have revealed the presence of anxiety-inducing and anxiety-repressing CRH/CRHR1 circuits under physiological conditions, which are required for adaptive emotional responses to stress. Remarkably the ability of CRH to positively regulate behavior is lost upon prolonged exposure to severe stress. This was demonstrated by the fact that deletion of *Crh* from most cortical and limbic structures diminished the susceptibility to chronic social defeat stress most probably by blunting stress-induced neuronal activation, which was mirrored by reduced c-*fos* expression. The switch to an "all-aversive" effect of CRH during chronic stress is likely caused by over-activation of both anxiogenic and anxiolytic CRH receptors, resulting in a persistent dysregulation of positive CRH-neurotransmitter interactions as well as the initiation of HPA axis hyperfunction. Optogentic-mediated activation/inhibition of specific CRH-circuits during chronic stress exposure will provide more insight into the underlying molecular mechanisms. Moreover, precise mapping of ligand-activated CRHR1-neurons *in vivo* is essential to further comprehend complex CRH/CRHR1 circuits. To achieve this we aim to combine the recently developed TANGO GPCR assay with the targeted recombination in active populations (TRAP) method. This combination will facilitate temporally controlled labeling of ligand-activated CRHR1-expressing cells, and can be applied to assess specific activation patterns upon exposure to different stressors. Another matter of importance will be the close assessment of CRHR2 and urocortin expression in all our *Crh* knockout lines in order to assess possible compensatory or adaptive mechanisms. Although most of the behavioral alterations in conditional *Crh* knockout mice were HPA axis independent, we can not rule out possible changes in central glucocorticoid and mineralocorticoid receptor expression, which might have taken place to compensate for initial changes in HPA axis function. Moreover, we are planning to investigate spatial and object recognition memory in CRH deficient mice, considering the differential impact of acute and chronic stress on cognitive performance.

Our results provided novel and comprehensive insights into the CRH/CRHR1-system, but they also opened up a number of questions: What is the precise subcellular localization of CRHR1 in different neuronal subpopulations? How does CRH, which is primarily expressed from inhibitory GABAergic neurons, potentiate excitatory neurotransmission? And to what extend does it influence GABA release? What are the specific-downstream targets of CRHR1, and do

they differ under basal and chronic stress conditions? Does CRHR1 display constitutive activity which would allow it to signal independent of ligand-binding, and does this occur via heteromerization with other GPCRs? What is the functional role of CRHR2 and the urocortins in emotional stress-responses? We hope to address many of these questions in the near future using the large battery of transgenic lines generated in this study. We believe that these models represent highly valuable tools for studying stress- and CRH-modulated neuronal function.

Overall this study provided a comprehensive assessment of the major mammalian stress-integrating system. It defined the ability of the CRH/CRHR1-circuitry to modulate emotional behavior in a bidirectional fashion, renouncing the common belief that CRH action is generally aversive. As pointed out by Wylie Vale: *"The idea is not to abolish the CRFR1 receptor's response to the brains's stress hormone but to bring it into the normal range so that it would have appropriate levels of anxiety and stress as conditions dictate."*

Wylie W. Vale (1941-2012)

7. ADDENDUM

7.1. CACNA1C differentially regulates cognition, emotional behavior and stress susceptibility during development and adulthood

Nina Dedic[1,2], Divya Mehta[1], Benedikt Bedenk[1], Michael Metzger[1], Jakob Hartmann[1], Angela Jurik[1], Klaus Wagner[1], Marcel Schieven[1], Sven Moosmang[4], Franz Hofmann[4], Carsten T. Wotjak[1], Gerhard Rammes[1], Kerry J. Ressler[3], Mathias V. Schmidt[1], Wolfgang Wurst[2], Elisabeth B. Binder[1], Jan M. Deussing[1]

[1] *Max Planck Institute of Psychiatry, Kraepelinstr. 2-10, 80804 Munich, Germany*

[2] *Institute of Developmental Genetics, Helmholtz Zentrum München, German Research Center for Enviormental Health, Ingolstädter Landstr. 1, 85764 Neuherberg, Germany*

[3] *Department of Psychiatry and Behavioral Sciences, Emory University School of Medicine, Atlanta, USA*

[4] *Technische Universität München, IPT – Institute für Pharmakologie und Toxikologie, Biedersteiner Str. 29, 80802 Munich, Germany Germany*

Manuscript in preparation

Abstract

Voltage-gated L-type Ca^{2+} channels (LTCCs) play a pivotal role in modulating neuronal excitability, synaptic plasticity, and gene expression. Until now many rodent studies have focused on the involvement of LTCCs in learning and memory, but emerging evidence from genome-wide association studies (GWAS) and meta-analyses of GWAS support the association of single nucleotide polymorphisms (SNPs) in the pore-forming subunit α1C (*CACNA1C*) of $Ca_v1.2$ with major depressive disorder, bipolar disorder and schizophrenia. However, the causality and mechanisms of how genetic alterations in *CACNA1C* affect the risk for an entire spectrum of psychiatric disorders remain largely unknown. Here we show that *Cacna1c* depletion during embryonic and early postnatal development, specifically in forebrain glutamatergic neurons promotes the manifestation of endophenotypes related to psychiatric disorders, while deletion during adulthood ceases to do so, and even improves cognitive parameters. In addition we could show that *Cacna1c* strongly interacts with chronic stress to shape behavioral outcomes. In a gene x environment design, *Cacna1c* haploinsuficiency enhanced the susceptibility to chronic social defeat stress, while adult deletion in forebrain excitatory projection neurons produced resilience. Importantly, we report that *CACNA1C* also significantly interacts with adult trauma to predict depressive symptoms in humans.

Introduction

Family, twin and epidemiological studies provide clear evidence for a major genetic contribution in the risk to develop psychiatric disorders such as major depressive disorder (MDD), bipolar disorder (BPD) or schizophrenia (SCZ). However, the identification of susceptibility genes has been challenging given that many initial discoveries failed replication, which is largely owed to the inherent phenotypic and genetic heterogeneity of psychiatric disorders as well as to the difficulty to control for environmental factors, which interfere with disease etiology.

One of the most consistent and robust genetic findings from GWAS are the associations of single nucleotide polymorphisms (SNPs) in the α1 subunit of the L-type Ca^{2+} channel $Ca_v1.2$ (*CACNA1C*) with BPD, SCZ and MDD (Sklar et al., 2008; Ferreira et al., 2008; Green et al., 2010; Liu et al., 2011; Schaaf et al., 2011). In support of this, a number of follow up clinical studies have associated the primary disease-associated *CACNA1C* risk allele, rs1006737, with variations in human brain function and structure in patients, but also in healthy subjects (Erk et al., 2010; Bhat et al., 2012). Hence, the available GWAS and clinical data suggest that *CACNA1C* might represent a shared susceptibility factor which influences disease susceptibility for MDD, BPD and SCZ across DSM diagnostic boundaries (Bhat et al., 2012).

Voltage-gated L-type Ca^{2+} channels (LTCCs) are Ca^{2+} selective pores linked to voltage-sensing domains that couple membrane depolarization to intracellular signaling events and thereby influence various processes in the central nervous system. Functional LTCCs are heterooligomeric complexes consisting of multiple subunits: α1, β, α2δ, and/or γ. The voltage-sensor, selectivity filter, ion-conduction pore and binding site for all available calcium channel blockers is encoded by the α1 subunit. Until now mainly $Ca_v1.2$ and $Ca_v1.3$, have been shown to play a prominent role in the brain (Calin-Jageman and Lee, 2008), with $Ca_v1.2$ representing the most abundant LTCC (Sinnegger-Brauns et al., 2004). In light of this it is not surprising that an increasing effort is being made to uncover how $Ca_v1.2$ exerts its effects on behavior in order to gain a better understanding of its role in the development of psychiatric disorders. The constitutive inactivation of *Cacna1c* in the mouse results in early embryonic lethality (Seisenberger et al., 2000). Whereas previous animal studies have implicated inactivation of $Ca_v1.2$ in forebrain structures with impairments in cognitive function (Moosmang et al., 2005; White et al., 2008; Jeon et al., 2010; Langwieser et al., 2010) the role of $Ca_v1.2$ in the development of core endophenotypes of MDD, BPD and SCZ has scarcely been investigated. Recently it was shown that haploinsufficiency as well as forebrain-specific deletion of *Cacna1c*

was associated with anxiety-like behavior in mice (Dao et al., 2010; Lee et al., 2012). Yet, the neurochemical identity of $Ca_v1.2$-positive neurons that exert these effects and whether this occurs during development or adulthood remains largely unknown. Applying a main-effect approach, the present study aimed to first assess the direct outcome of a temporal, region and neurotransmitter-specific deletion of *Cacna1c* on the development of MDD-, BPD- and SCZ-related endophenotypes, which show a considerable amount of overlap (Chadman et al., 2009; Nestler and Hyman, 2010; Adam, 2013). Keeping in mind that psychiatric disorders are not solely genetically influenced, and that chronic stress and/or trauma were shown to represent additional risk factors (Caspi et al., 2003; de Kloet et al., 2005a; Klengel et al., 2013; Mehta et al., 2013), we also aimed to examine the involvement of *CACNA1C* in the development of MDD, BPD and SCZ-related endophenotypes in the context of gene x environment interactions, both in mice and humans.

Materials and Methods

Animals

Adult male CNS-specific *Cancna1c* knockout mice and control littermates were obtained by breeding *Cacna1c*$^{lox/lox}$ mice with *Cacna1c*$^{-/+}$ *Nestin-Cre* mice; *Cav1.2*$^{CNS\text{-}Ctrl}$ (*Cacna1c*$^{+/lox}$ *Nestin-Cre)* and *Cav1.2*$^{CNS\text{-}CKO}$ (*Cacna1c*$^{-/lox}$ *Nestin-Cre*) (Seisenberger et al., 2000; Langwieser et al., 2010). Heterozygous *Cav1*.2 mice and their control littermates were obtained from the same breedings; *Cav1.2*^{Ctrl} (*Cacna1c*$^{+/lox}$) and *Cav1.2*^{Het} (*Cacna1c*$^{-/lox}$). Inactivation of *Cacna1c* from forebrain glutamatergic neurons was achived by breeding *Cacna1c*$^{lox/lox}$ mice to transgenic *Nex-Cre* mice (Goebbels et al., 2006) to obtain *Cav1.2*$^{Glu\text{-}Ctl}$ (*Cacna1c*$^{lox/lox}$) and *Cav1.2*$^{Glu\text{-}CKO}$ (*Cacna1c*$^{lox/lox}$ *Nex-Cre*). Mice were 14-16 weeks old at the start of the behavioral experiments. Deletion of *Cacna1c* from forebrain excitatory projection neurons was achived by breeding *Cacna1c*$^{lox/lox}$ mice to transgenic *Camk2α-CreERT2 (Erdmann et al., 2007)* mice to obtain *Cav1.2*$^{FB\text{-}Crtl}$ (*Cacna1c*$^{lox/lox}$) and *Cav1.2*$^{FB\text{-}CKO}$ (*Cacna1*$^{lox/lox}$ *Camk2α-CreERT2*). *Cacna1c* inactivation was induced via two weeks of oral tamoxifen administration initiated between postnatal weeks 12 and 13. Behavioural tests were conducted 4 weeks post induction. All animals were kept under standard laboratory conditions and were maintained on a 12 h light-dark cycle (lights on from 7:00 am to 7:00 pm), with food and water provided ad libitum. All experiments were conducted in accordance with the Guide for the Care and Use of Laboratory Animals of the Government of Upper Bavaria, Germany.

Open field test

The OF was used to characterize locomotor activity in a novel environment. Testing was performed in an open field arena (50 x 50 x 50 cm) dimly illuminated with 10 lux in order to minimize anxiety effects on locomotion. All mice were placed into a corner of the apparatus at the beginning of the trial. The distance traveled and time spent in the outer and inner zones was assessed with the ANY-maze software.

Dark-light box test

The DaLi test was performed in a rectangular apparatus (15 x 20 x 25 cm) consisting of an aversive brightly lit compartment (700 lux) and a more protective dark compartment (5 lux). At the start of the test, all mice were placed in the dark compartment and were allowed to freely explore the apparatus for 5 min.

Forced swim test (FST) and acute stress response

The FST was used to assess stress-coping behaviour and corticosterone levels in response to an acute stressor in animals subjected to the chronic social defeat stress paradigm. Each mouse was placed into a 2 l glass beaker filled with tap water (21 ± 1 °C) for a test period of 5 min. After the FST, all mice were placed into a novel cage and blood samples were collected by tail cut 30 min after the onset of the FST. Stress response and basal blood plasma concentrations obtained from trunk blood were measured using a commercially available radioimmunoassay according to the manufactures manual (MP Biomedicals Inc; sensitivity 6.25 ng/ml).

Sociability test

The sociability test was performed using a three chamber apparatus, as previously described (Moy et al., 2004; Hartmann et al., 2012a). Briefly, during the sociability trial an unfamiliar male C57BL/6J mouse was introduced into one of the chambers, enclosed in a wire cage, while a toy mouse was placed in the opposite chamber (alteration occurred after 3 consecutive trials). The time spent interacting with mouse and object was scored for 10-minute by a trained observer.

Water cross maze (WCM)

The WCM was implemented to assess spatial memory performance, and was performed as previously described (Kleinknecht et al., 2012). Similarly to the classical Morris water maze, the WCM makes use of water-based motivation, but additionally allows for the simple assessment of learning strategies by means of the standard parameters accuracy and start bias scores. The maze consists of two intersecting arms, forming a cross, made from clear acrylic glass to enable visual orientation within the room. A submerged platform was located in one on of the arms, 1 cm under the water surface, invisible to the mice. Every animal performed six trials a day for five consecutive days. During this time the platform was always located in the same arm (for example east), whereas the starting position of the mice alternated between South and North in a pseudorandom manner. The latency to reach the platform was set to 1 min. Learning performance was assessed by accuracy, number of wrong platform visits, latency to reach the platform and start bias.

Accuracy: A trial was considered accurate (i.e., value 1), if the animal directly entered the arm containing the platform and climbed onto it. Aberrant behavior was considred as non-accurate (i.e., value 0). Thus, accuracy reflects the percentage of accurate trials on each day per animal.

An animal reached the criterion of an accurate learner, if it accomplished more than 83% accurate trials per day (i.e., ≥5 out of 6 trials).

Start bias: The start bias was described as the absolute value of the sum of accurate trials from the South arm minus the sum of accurate trials from the North arm $|\sum(\text{accurate North trials}) - \sum(\text{accurate South trials})|$. An animal with a daily score ≥2 was considered to be biased, suggesting a response-, rather than spatial-based learning strategy.

Spatial object recognition memory task

Spatial object memory was assessed in the OF arena under low illumination (10 lux). During the acquisition trial, mice were presented with two identical objects (salt shakers) and allowed to freely explore the object for 10 min. Following a 30 min intertrial interval, mice were presented with a nondisplaced object and a relocated one. Spatial cues were provided during both trials. The percentage of time exploring the displaced objects was calculated. A higher preference for the displaced object reflects intact spatial recognition memory.

Chronic social defeat stress (CSDS) paradigm

The CSDS paradigm is commonly applied to induce anxiety- and depression-related endophenotypes in mice, and was performed as previously described (Wagner et al., 2011; Hartmann et al., 2012b; Wang et al., 2013). Experimental mice (9-13 male mice per group between 11-13 weeks of age) were submitted to chronic social defeat stress for 21 consecutive days. They were introduced into the home cage (45 cm x 25 cm) of a dominant CD1 resident for no longer than 5 min, and were subsequently defeated. Following defeat, animals spent 24 hours in the same cage, which was separated via a holed steel partition, enabling sensory but not physical contact. Every day experimental mice were exposed to a new unfamiliar resident. Defeat encounters were randomized, with variations in starting time in order to decrease the predictability to the stressor and minimize habituation effects. Control animals were housed in their home cages throughout the course of the experiment. All animals were handled daily; weight and fur status were assessed every 3-4 days. Behavioral testing was conducted during the last week of the CSDS paradigm.

In situ hybridization (ISH)

Brains were sectioned coronally at 20 µm at -20 °C in a cryotome. The sections were thaw-mounted on superfrost slides, dried, and kept at -80 °C. *ISH* hybridization was performed as previously described (Lu et al., 2008; Refojo et al., 2011).

Western blot analysis

For western blot analysis tissue was lysed in RIPA buffer containing protease inhibitors (Roche), 20 µM NEM 1,10-OPT (Sigma Aldrich). Protein samples were separated by 8% SDS-PAGE and transferred to 0.45-µm PVDF membranes (Millipore). The membranes were then incubated with the $Ca_v1.2$ primary antibody (Moosmang et al., 2005) and a secondary HRP-conjugated antibody. Chemiluminescence signals were visualized in a ChemiDoc station (BioRad) and analysed using Image Lab (Bio-Rad).

Electrophysiology

The influence of *Cacna1c* deficiency on hippocampal long-term potentiation (LTP) was conducted as previously described (Kratzer et al., 2013). Control (n = 6) and and *Cav1.2*$^{FB\text{-}CKO}$ (n = 7) mice were anesthetized with isoflurane and decapitated shortly after. The brains were removed and quickly transferred into ice-cold carbogenated (95% O_2/5% CO_2) artificial cerebrospinal fluid (aCSF). Sagittal hippocampal slices (350µm) were obtained using a vibratome (HM 650V, Microm International, Walldorf, Germany). The slices were allowed to recover for at least 1h at 34°C before being transferred to the recording chamber where they were continuously superfused with aCSF at a rate of 5ml/min. The aCSF contained: NaCl, 124 mM; KCl, 3 mM; $NaHCO_3$, 26 mM; $CaCl_2$,2 mM; $MgSO_4$, 1 mM; D-glucose, 25 mM; NaH_2PO_4, 1.25 mM, and was saturated with a mixture of (95% O2/5% CO2, final pH7.3). Field excitatory postsynaptic potentials (fEPSPs) at synapses between Schaffer collateral-commissural pathway (SCCP) and CA1 pyramidal cells were recorded extracellularly in the stratum radiatum of CA1. High-frequency stimulation (HFS) of 1 x 100 Hz/100 pulses to the SCCP were delivered to induce LTP. The recordings were amplified, filtered (3 kHz) and digitized (9 kHz) using a laboratory interface board (ITC-16, Instrutech), and stored with the acquisition program Pulse, version 8.5 (Heka Electronik). Data were analyzed offline with the analysis program IgorPro v.6 (WaveMetrics) software. Measurements of the amplitude of the fEPSP were taken and normalized with respect to the 30 min control period before tetanic stimulation.

Statistical analysis

All results are presented as mean ± standard error of the mean (SEM). Behavioral phenotypic differences were evaluated with Students T-test. Time-dependent measures such as locomotion and fur state progressions were assessed with multi-factorial analysis of variance (ANOVA) with repeated measures (RM-ANOVA). The effects of genotype and condition on all other behavioral and neuroendocrine parameters were assessed by two factorial analysis of

variance (two-way ANOVA). Whenever significant main or interaction effects were found by the ANOVAs, Bonferroni post-hoc tests were carried out to locate simple effects. Statistical significance was defined as $p < 0.05$.

Human samples

Participants in this study belonged to a larger cohort (Grady Trauma Project) investigating the role of genetic and environmental factors in predicting outcomes to stressful life events (Binder et al., 2008; Klengel et al., 2013; Mehta et al., 2013). Phenotypes and genotypes were available for a total of 3075 individuals, predominantly African-Americans belonging to a highly traumatized, urban population of low socioeconomic status. All procedures were approved by the institutional review boards of Emory University School of Medicine and Grady Memorial Hospital.

Trauma events inventory (TEI)

The TEI in this study assesses lifetime history of trauma exposure to a range of traumatic events excluding childhood abuse (Mehta et al., 2013). Individuals were divided into three groups for each of the three genotypes according to the absence and severity of trauma exposure: 0 = no adult trauma, 1 = 1 or 2 types of adult trauma, 2 = 3 or more types of adult trauma. Although the TEI also includes exposure to non-child abuse traumatic events in childhood, the mean age of exposure was 20, thus referred to as adult trauma.

Beck depression inventory (BDI)

The 21-item BDI is a psychometrically validated, commonly used measure of depressive symptoms (BECK et al., 1961), and was also applied in this study.

Expression analysis

The gene expression experiments were performed on Illumina Human HT-12 v3 arrays and the genotypes were obtained from the Omni express v2 and Omni 1M arrays. All experimental procedures were performed according to the manufacturer's protocol. The minor allele frequencies of the 2 tested SNPs in the GWAS/mQTL were as follows: rs7297582 - 0.1204/0.139 and rs1024582 - 0.1169/0.1082. Effects of *CACNA1C* SNPs and adult trauma (ie. SNP x trauma interaction) on BDI were assessed using generalized regression models (additive genotype effect) in PLINK. The results were corrected for multiple testing using the Bonferroni threshold ($p = 0.05/2 = 0.0250$) of significance. Phenotypes were regressed against genotypes, after adjusting for PCA (population principal components for ancestry), gender and age.

Methylation analysis

The effect of trauma-genotype interaction on DNA methylation of the *CACNA1C* locus in peripheral blood cells was assessed in 344 individuals belonging to the Grady trauma project using the Illumina 450 k Human Methylation array. The methylation results represents a subset of a previously analysed dataset, with similar distributions of phenotypes (Mehta et al., 2013). Data was analysed using generalized regression models (additive genotype effect) in PLINK. Methylation beta values were regressed against genotypes, after adjusting for PCA, gender and age.

Results

Previously two independent studies have shown that deletion of *Cacna1c* in mice enhances anxiety-related behavior (Dao et al., 2010; Lee et al., 2012), a core endophenotype of MDD and BPD (Nestler and Hyman, 2010). In light of this, we first crossed floxed *Cacna1c* mice to the *Nestin-Cre* mice (Tronche et al., 1999), in order to assess the effects of a central nervous system (CNS)-specific elimination of $Ca_v1.2$ (*Cav1.2*$^{CNS\text{-}CKO}$) on a range of behavioral outcomes known to be altered in MDD, BPD and SCZ, including locomotion/exploration, anxiety, cognition, social and stress-coping behavior. Using *in situ* hybridisation (*ISH*) and western blot analysis we verified the complete absence of *Cacna1c* expression in the brain of *Cav1.2*$^{CNS\text{-}CKO}$ compared to *Cav1.2*$^{CNS\text{-}Ctrl}$ mice (Figure 1A and S1). First we conducted an open field test (OF) under low illumination conditions (15 lux) in order to assess locomotion/exploration more accurately, which is often obscured by heightened anxiety in brighter illuminated arenas. Deletion of *Cacna1c* in the CNS increased locomotion during the last segments of the open field (OF) (RM-ANOVA, time: $F_{5,90} = 11.01$, $p < 0.0001$; interaction: $F_{5,90} = 4.10$, $p = 0.002$; Bonferroni $p < 0.05$) and decreased overall immobility ($t_{18} = 2.4$, $p < 0.05$) (Figure 1B and S2B), whereas total inner zone time was not affected (Figure S2B). Anxiety-related behavior was specifically addressed with the dark-light box test (DaLi), showing that *Cav1.2*$^{CNS\text{-}CKO}$ mice spent significantly less time ($t_{20} = 2.2$, $p < 0.04$) and made fewer entries into the lit zone compared to controls ($t_{20} = 3.7$, $p < 0.005$) (Figure 1C), which is in agreement with the above mentioned studies. Deletion of *Cacna1c* from the CNS also resulted in significantly enhanced active stress-coping behavior during the forced swim test (FST), depicted by a decrease in floating time ($t_{20} = 2.7$, $p < 0.05$) (Figure 1D), which was also reported for heterozygous mice by Dao et al. (2010) and is in line with studies demonstrating antidepressant-like effects for LTCC blockers (Mogilnicka et al., 1987; Sinnegger-Brauns et al., 2009; Dao et al., 2010). Both, enhanced locomotor activity and decreased floating behavior in the FST have often been described in mouse models of mania (Prickaerts et al., 2006; Roybal et al., 2007; Shaltiel et al., 2008; Kirshenbaum et al., 2011; Han et al., 2013). Given the fact that alterations in social behavior are also often observed in patients with BPD, SCZ, and MDD, we additionally performed the sociability test. *Cav1.2*$^{CNS\text{-}CKO}$ mice displayed reduced sociability, depicted by a decreased preference for a novel mouse compared to a toy object ($t_{26} = 4.0$, $p < 0.0005$) (Figure 1D). Finally, spatial learning and memory was analysed in *Cav1.2*$^{CNS\text{-}CKO}$ using the water-cross maze task (WCM) (Kleinknecht et al., 2012).

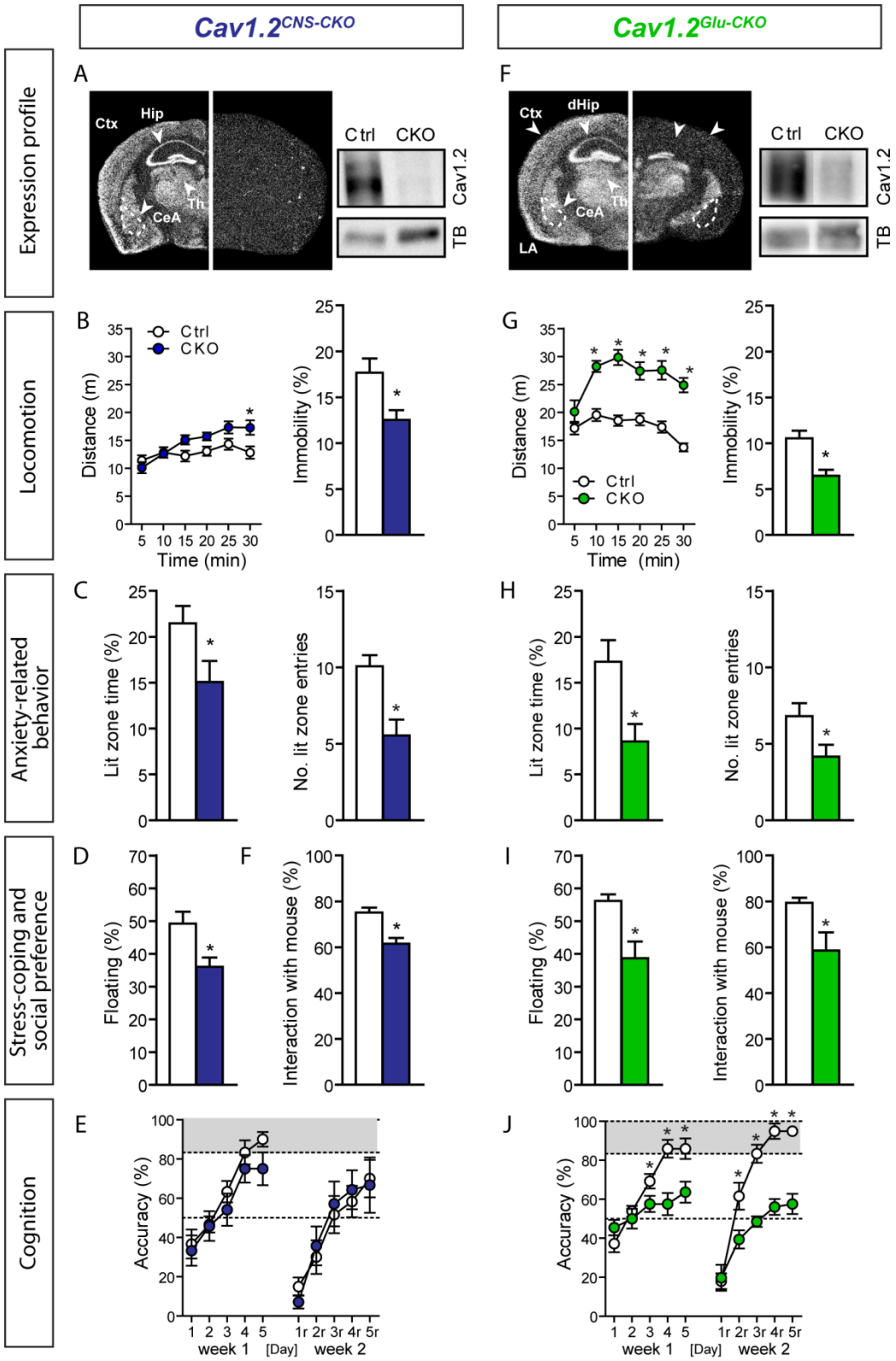

Figure 1: Deletion of *Cacna1c* from the CNS and forebrain glutamatergic neurons induces behavioral alterations reminiscent of BPD, MDD and SCZ. (A and **F)** Expression of *Cacna1c* mRNA and hippocampal protein levels were assessed by *ISH* and WB in *Cav1.2*$^{CNS\text{-}CKO}$ and *Cav1.2*$^{Glu\text{-}CKO}$ mice respectively. Areas of interest are highlighted with arrowheads and dashed lines. *Cav1.2*$^{CNS\text{-}CKO}$ displayed enhanced locomotion (RM-ANOVA + Bonferroni post-test, $p < 0.05$) and decreased immobility in the OF **(B)**, which was even more strongly pronounced in *Cav1.2*$^{Glu\text{-}CKO}$ mice **(G)**. Both *Cav1.2*$^{CNS\text{-}CKO}$ and *Cav1.2*$^{Glu\text{-}CKO}$ mice displayed enhanced anxiety-related behavior in the DaLi **(C** and **H)**, decreased floating in the FST and reduced social interaction in

the sociability test **(D** and **I)**. Spatial learning and memory, assessed with the WCM was slightly impaired in *Cav1.2*$^{CNS\text{-}CKO}$ **(E)** in contrast to *Cav1.2*$^{Glu\text{-}CKO}$ mice, which showed more severe deficits **(J)**. Student's t-test,*p < 0.05; n = 10-13. Amygdala (Amy), cortex (Ctx), dorsal hippocampus (dHip), tubulin (TB), thalamus (Th).

Given that many studies have shown that deletion of *Cacna1c* from forebrain structures leads to memory impairment, *Cav1.2*$^{CNS\text{-}CKO}$ displayed only mildly impaired learning during the 1st week. This became evident by decreased accuracy (RM-ANOVA, time: $F_{4,64}$ = 22.3, p < 0.0001; genotype: $F_{1,64}$ = 2.1, p = 0.16) and wrong platform visits (RM-ANOVA, time: $F_{4,64}$ = 28.3, p < 0.0001; genotype: $F_{1,64}$ = 2.8, p = 0.11) on d5 (Figure S2B) as well as by an overall increase in the latency to reach the platform during learning (RM-ANOVA, time: $F_{4,64}$ = 21.2, p < 0.0001; genotype: $F_{1,64}$ = 7.6, p < 0.05) and relearning (RM-ANOVA, time: $F_{4,60}$ = 32.3, p < 0.0001; genotype: $F_{1,60}$ = 3.3, p = 0.08) (Fig. 1E and S2A).

To genetically define the Ca_v1.2-expressing brain regions and neuronal populations responsible for the observed behavioral alterations, floxed *Cacna1c* mice were bred to *Nex-Cre* mice (Goebbels et al., 2006) to generate conditional knockout animals with a specific deletion of *Cacna1c* in forebrain excitatory (glutamatergic) neurons (*Cav1.2*$^{Glu\text{-}CKO}$). *Cav1.2*$^{Glu\text{-}CKO}$ mice display a complete loss of *Cacna1c* mRNA signal from the piriform cortex, parts of the lateral amygdala, the CA1, CA2 and CA3 of the hippocampus, and the cerebral cortex (Figure 1F and S1). This was confirmed at the protein level, showing only a faint Ca_v1.2 band in hippocampal extracts, which can be ascribed to the Ca_v1.2-positive GABAergic neurons and cells of the DG (Figure 1F). The behavioral phenotype of *Cav1.2*$^{Glu\text{-}CKO}$ mice strongly resembled that of CNS-specific *Cacna1c* knockout animals, suggesting that Ca_v1.2 in glutamatergic forebrain neurons is likely mediating the observed effects in *Cav1.2*$^{CNS\text{-}CKO}$ mice. *Cav1.2*$^{Glu\text{-}CKO}$ exhibited enhanced anxiety-related (lit time: t_{26} = 2.7, p < 0.05; lit entries: t_{26} = 2.2, p < 0.05), and active stress-coping behavior (t_{26} = 3.6, p < 0.005), as well as decreased sociability (t_{26} = 2.9, p < 0.05) compared to *Cav1.2*$^{Glu\text{-}Ctrl}$ mice (Figure 1H-I). However, deletion of *Cacna1c* from glutamatergic neurons lead to an extremely pronounced hyperlocomotion in the OF (RM-ANOVA, time: $F_{5,130}$ = 13.4, p < 0.0001; genotype: $F_{1,130}$ = 45.9, p < 0.001; interaction: $F_{5,130}$ = 5.7, p < 0.0001; Bonferroni, p < 0.05), which was however, not observed during the initial 5 min were novelty-induced anxiety is most prominent (Figure 1G). Cognitive performance in the WCM task was also drastically impaired in *Cav1.2*$^{Glu\text{-}CKO}$ mice, showing accuracy levels that barely surpassed the chance level of 50%, both during learning and relearning, suggesting random performance of these animals (RM-ANOVA, time: $F_{4,88}$ = 26.9, p < 0.0001; genotype: $F_{1,88}$ = 7.5, p < 0.05; interaction: $F_{4,88}$ = 7.3, p < 0.0001; Bonferroni, p < 0.05) (Figure 1J and S2C). Merely 3 out of 11 *Cav1.2*$^{Glu\text{-}CKO}$ mice in the 1st and 2nd week achieved the accurate learner criterion as compared

to 10/13 and 13/13 controls (learning: $\chi 2 = \geq 5.9$, $p < 0.05$; relearning: $\chi 2 = \geq 14.2$, $p < 0.0005$). Although *Cav1.2*$^{Glu\text{-}CKO}$ mice displayed an overall increased number of wrong platform visits, both groups displayed a comparable decrease in wrong platform visits and escape latencies over the course of learning and relearning (Figure S2C). It seemed that the majority of *Cav1.2*$^{Glu\text{-}CKO}$ mice developed a clear turn-bias: Animals performed the same turn, left or right, irrespective of the starting position, which is depicted by an increased start bias (Figure S2C). At the beginning of training, both *Cav1.2*$^{Glu\text{-}Ctrl}$ and *Cav1.2*$^{Glu\text{-}CKO}$ mice seemed to acquire a response strategy, which was characterized by an increased start bias. Upon the course of training, control mice switched to place learning (spatial learning), as indicated by a decrease in start bias, whereas *Cav1.2*$^{Glu\text{-}CKO}$ displayed persistant high levels during learning and relearning. The development of such a response-based strategy compared to place learning explains the decrease in wrong platform visits and escape latencies in *Cav1.2*$^{Glu\text{-}CKO}$ mice over the course of training. Overall *Cav1.2*$^{Glu\text{-}CKO}$ displayed enhanced anxiety-related behavior, reduced social and cognitive performance which are considered core endophenotypes of MDD and/or the depressive phase of BPD, whereas increased locomotion and FST activity are often associated with the manic phase of BPD. Importantly, hyperlocomotion, altered social behavior, and learning and memory impairments, are also analogous to negative and cognitive symptoms of SCZ respectively (Jones et al., 2011).

Our results clearly implicate a depletion of *Cacna1c* in the brains main excitatory system with behavioral alterations reminiscent of MDD, BPD and SCZ endophenotypes. Bearing in mind that both, *Nestin*- and *Nex-Cre* recombinase activity is initiate around embryonic day 8 and 11.5 respectively (Goebbels et al., 2006; Dubois et al., 2006), the question arises, whether developmental or adult *Cacna1c* depletion leads to the observed neurobiological changes. Thus, we bred floxed *Cacna1c* mice to inducible *Camkα-CreERT2* mice (Erdmann et al., 2007) with the aim of deleting *Cacna1c* in forebrain principal neurons during adulthood (*Cav1.2*$^{FB\text{-}CKO}$). We deliberately chose the *Camkα-CreERT2* line because of the strongly overlapping expression pattern with the *Nex-Cre*. $Ca_v1.2$ was inactivated upon tamoxifen administration only in forebrain projection neurons, which predominantly include excitatory pyramidal neurons of the cortex and hippocampus, but also principal neurons of the amygdala and thalamus. As expected, the deletion pattern strongly resembled that of *Cav1.2*$^{Glu\text{-}CKO}$ mice, with absence of *Cacna1c* mRNA signal from the cerebral cortex, the lateral amygdala, as well as the entire hippocampus and cortex (Figure 2A and S1), which was also confirmed at the protein level (Figure 2A). In addition, deletion of *Cacna1c* mRNA expression was observed in

the central amygdala (CaA), geniculate nucleus (Gn) and parts of the thalamus and putamen (Figure 2A and S1). *Cav1.2*$^{FB\text{-}CKO}$ mice also displayed enhanced locomotion in the OF, although this was not as strongly pronounced as in *Cav1.2*$^{Glu\text{-}CKO}$ mice (RM-ANOVA, time: $F_{5,130} = 9.94$, $p < 0.0001$; genotype: $F_{1,130} = 9.06$, $p < 0.05$; Bonferroni, $p < 0.05$) (Figure 2B and S2F).

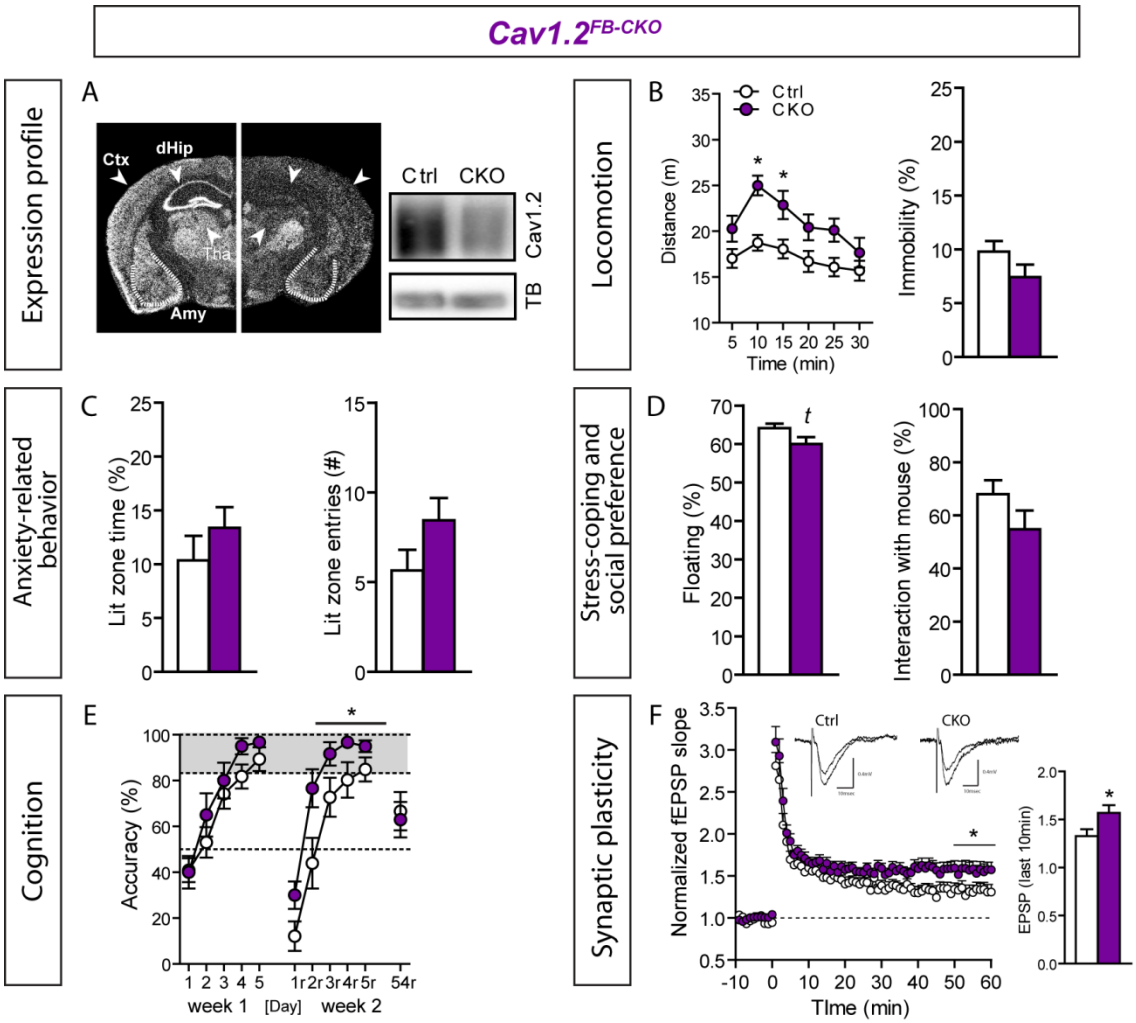

Figure 2: Inactivation of *Cacna1c* from forebrain principal neurons during adulthood improves spatial relearning and enhances hippocampal LTP. (A) Expression of *Cacna1c* mRNA and hippocampal protein levels assessed by *ISH* and WB in *Cav1.2*$^{FB\text{-}CKO}$ mice. Areas of interest are highlighted with arrowheads and dashed lines. *Cav1.2*$^{FB\text{-}CKO}$ mice displayed enhanced locomotion in the OF (RM-ANOVA + Bonferroni post-test, $p < 0.05$) **(B)**, no alterations in anxiety-related behavior in the DaLi **(C)**, a trend towards decreased floating and reduced social interaction in the FST and sociability test respectively **(D)**. *Cav1.2*$^{FB\text{-}CKO}$ mice exhibited intact spatial memory performance during the first week of learning and performed even slightly better during relearning **(E)**. **(F)** *Cav1.2*$^{FB\text{-}CKO}$ mice showed enhanced Schaffer collateral/CA1-LTP (n = 13-15 slices from 6-7 animals per group; RM-ANOVA + Bonferroni post-test, $p < 0.05$). Student's t-test, *$p < 0.05$, *t* (trend) $p \leq 0.1$; n = 10-13. Amygdala (Amy), cortex (Ctx), dorsal hippocampus (dHip), tubulin (TB), thalamus (Th).

Along these lines, floating time in the FST and sociability were decreased, but this did not reach statistical significance, as was the case for *Cav1.2*$^{CNS\text{-}CKO}$ and *Cav1.2*$^{Glu\text{-}CKO}$ mice (Figure 2D). Surprisingly, deletion of *Cacna1c* during adulthood did not affect anxiety-related behavior and

spatial memory (Figure 2C, E and S2F). On the contrary, *Cav1.2*$^{FB\text{-}CKO}$ mice even displayed a marginal increase in lit zone time and entries, and performed slightly better during relearning of the WCM compared to controls (RM-ANOVA, time: $F_{4,80} = 63.4$ $p < 0.0001$; genotype: $F_{1,80} = 4.36$, $p < 0.05$; Bonferroni, $p < 0.05$) (Figure 2C, 2E and S2F). Since deletion of forebrain *Cacna1c* was suggested to impair long-term memory (White et al., 2008), we re-exposed the animals to the WCM 30 days after relearning, but did not observed any differences between *Cav1.2*$^{FB\text{-}CKO}$ and *Cav1.2*$^{FB\text{-}Ctrl}$ mice (Figure S3E). In view of the fact that early inactivation of *Cacna1c* from glutamatergic neurons decreases NMDA receptor-independent synaptic plasticity and impairs spatial memory, we additionally assessed long-term potentiation (LTP) in *Cav1.2*$^{FB\text{-}CKO}$ mice. One hour after a 100 Hz tetanus stimulation, *Cav1.2*$^{FB\text{-}CKO}$ showed increased LTP compared to *Cav1.2*$^{FB\text{-}Ctrl}$ mice (RM-ANOVA, time: $F_{69,1863} = 70.0$ $p < 0.0001$; genotype: $F_{1,1863} = 5.5$, $p < 0.05$; interaction: $F_{69,1863} = 1.38$, $p < 0.05$) (Figure 2F). Our results demonstrate that deletion of *Cacna1c* during development and adulthood, presumably in glutamatergic principal neurons differentially affects spatial memory and anxiety-related behavior. Whereas early deletion of *Cacna1c* from the CNS and glutamatergic neurons increased anxiety and impaired cognition, inactivation of the LTCC during adulthood ceased to alter anxiety and even enhanced spatial memory and synaptic plasticity. Importantly, these changes were not caused by alterations in hypothalamic-pituitary-adrenocortical (HPA) axis function, since corticosterone levels were indistinguishable between all mouse lines (Figure S2B, D and F).

To date genetic predisposition alone has failed to account for the manifestation of many psychiatry disorders. Chronic stress and/or traumatic life events have been shown to represent additional risk factors. Thus we investigated if *Cacna1c* interacts with chronic stress to affect behavioral outcomes; more specifically we assessed whether developmental and adult-specific depletion of *Cacna1c* would differentially affect stress susceptibility. Since *Cav1.2*$^{CNS\text{-}CKO}$ and *Cav1.2*$^{Glu\text{-}CKO}$ *mice* displayed a wide range of behavioral alterations already under basal conditions, we assessed heterozygous knockout mice *Cav1.2*^{HET} which were only reported to show mild changes (Dao et al., 2010; Lee et al., 2012), and are also more prone to mimic a possible clinical situation, where complete absence of $Ca_v1.2$ would rather be unlikely. An overall reduction of *Cacna1c* mRNA expression was confirmed by in situ hybridisation and WB (Figure S1 and S3A). *Cav1.2*^{Ctrl} and *Cav1.2*^{Het} mice were subjected to three weeks of chronic social defeat stress (CSDS). In accordance with other studies, we were able to detect robust physiological and neuroendocrine changes evoked by CSDS independent of genotype, demonstrating the efficacy of the paradigm (Wagner et al., 2011; Wang et al., 2011a;

Hartmann et al., 2012a; Hartmann et al., 2012b; Wang et al., 2013). These included a progressive fur quality decrease, thymus atrophy, adrenal gland enlargement as well as an enhanced corticosterone response (Figure S3B-E). Consequently, we analysed the effect of CSDS on *Cav1.2*^{Het} mice in a number of behavioural tasks. Chronically stressed *Cav1.2*^{Ctrl} animals showed an expected decrease in locomotion compared to non-stressed *Cav1.2*^{Ctrl} mice during the last segments of the OF. However, this effect was more strongly pronounced in stressed *Cav1.2*^{Het} mice, which displayed drastically reduced locomotion throughout the entire test duration compared to both, non-stressed *Cav1.2*^{Het} and stressed *Cav1.2*^{Ctrl} mice (RM-ANOVA, time: $F_{2,46} = 13.3$, $p < 0.0001$; time x condition: $F_{2,46} = 7.1$, $p < 0.005$; time x genotype x condition: $F_{2,46} = 4.8$, $p < 0.05$; Genotype: $F_{1,47} = 23.1$, $p < 0.0001$; Condition: $F_{1,47} = 24.6$, $p < 0.0001$, genotype x condition: $F_{2,46} = 2.8$, $p = 0.099$ Bonferroni: $p < 0.05$) (Figure 3A and S3F). This is further depicted in total immobility time, which was also strongly increased in stressed *Cav1.2*^{Het} mice (2-way ANOVA, stress x genotype: $F_{1,46} = 27.76$, $p < 0.0001$; stress: $F_{1,46} = 70.4$, $p < 0.0001$; genotype: $F_{1,46} = 66.3.54$, $p < 0.0001$; Bonferroni: $p < 0.05$) (Figure 3B). In addition, only chronically stressed *Cav1.2*^{Het} mice showed a significant reduction in the number of inner zone entries (2-way ANOVA, stress x genotype: $F_{1,42} = 5.2$, $p < 0.05$; stress: $F_{1,42} = 18.1$, $p < 0.0005$ genotype: $F_{1,42} = 16.9$, $p < 0.0005$; Bonferroni: $p < 0.05$) and inner zone time (2-way ANOVA, stress x genotype: $F_{1,42} = 5.4$, $p < 0.05$; stress: $F_{1,42} = 11.8$, $p < 0.005$ genotype: $F_{1,42} = 5.4$, $p < 0.05$; Bonferroni: $p < 0.05$) of the OF, which indicates increased anxiety-related behavior (Figure 3B and S3G). Importantly, a decrease in locomotion was also observed under basal conditions between *Cav1.2*^{Het} and Cav1.2^{Ctrl} mice during the last segment of the OF (Figure 3A). Similarly to *Cav1.2*$^{CNS\text{-}CKO}$ and *Cav1.2*$^{Glu\text{-}CKO}$ mice, *Cav1.2*^{Het} animals were less immobile in the FST under basal conditions, while no difference was observed following CSDS, which argues against possible motor deficits due to peripheral *Cacna1c* deletion in heterozygous *Cav1.2* mice (2-way ANOVA, genotype: $F_{1,32} = 5.62$, $p < 0.05$, Bonferroni: $p < 0.05$) (Figure 3D). An enhanced anxiety-response to CSDS in *Cav1.2*^{Het} mice was also observed in the DaLi (Figure 3C and S3H).

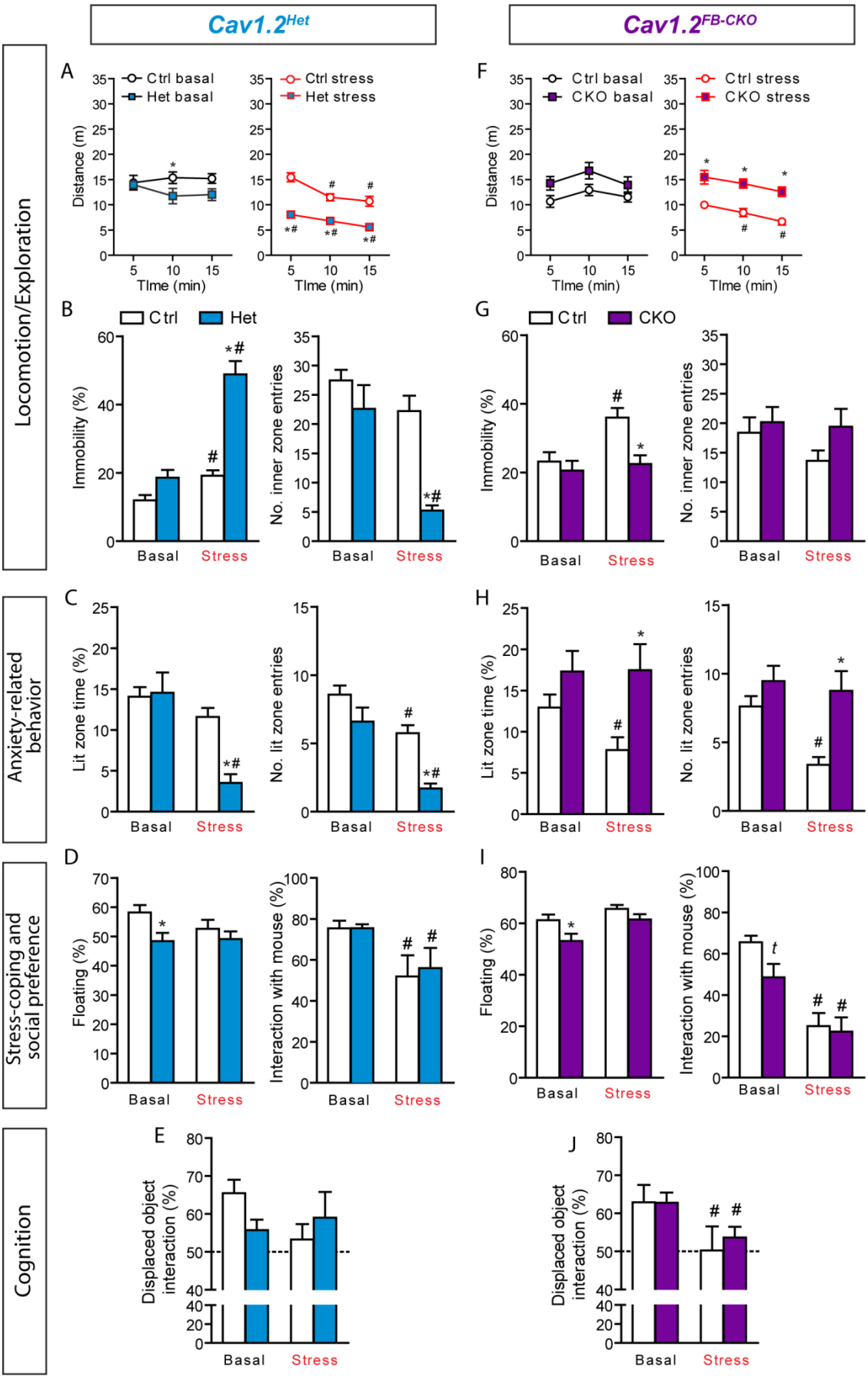

Figure 3: *Cacna1c* critically impacts stress susceptibility. *Cacna1c* heterozygosity enhances CSDS-induced anxiety, which was not observed upon forebrain specific deletion of *Cacna1c* in adulthood. **(A-B** and **F-G)** The

CSDS-induced decrease in locomotion was more prominent in *Cav1.2*^{Het} than *Cav1.2*^{Ctrl} mice. CSDS reduced locomotion in *Cav1.2*$^{FB\text{-}Ctrl}$ but not *Cav1.2*$^{FB\text{-}CKO}$ mice. Following CSDS, immobility time in the OF was significantly enhanced in *Cav1.2*^{Het} compared to *Cav1.2*^{Ctrl} mice while the number of inner zone entries was significantly reduced in *Cav1.2*^{Het} but not *Cav1.2*^{Ctrl} animals. In contrast, CSDS enhanced immobility only in *Cav1.2*$^{FB\text{-}Ctrl}$ but not in *Cav1.2*$^{FB\text{-}CKO}$ mice. **(C** and **H)** Compared to littermate controls, *Cav1.2*^{Het} mice displayed severely enhanced anxiety-related behavior in the DaLi following CSDS. This effect was not observed in *Cav1.2*$^{FB\text{-}CKO}$, which displayed no alterations in anxiety following CSDS compared to *Cav1.2*$^{FB\text{-}Ctrl}$ animals. **(D** and **I)** Both, *Cav1.2*^{Het} and *Cav1.2*$^{FB\text{-}Ctrl}$ mice exhibited reduced floating in the FST under basal but not stress conditions compared to their respective controls. Sociability in *Cav1.2*^{Het} and *Cav1.2*$^{FB\text{-}CKO}$ mice was similarly affected by CSDS. **(E** and **J)** Spatial object recognition memory was not significantly altered in *Cav1.2*^{Het} and *Cav1.2*$^{FB\text{-}CKO}$ mice under basal and stress conditions compared to their respective controls. 2-way ANOVA + Bonferoni post-test; *significantly different from the control group of the same condition, $p < 0.05$; # significantly different from the basal condition of the same genotype, $p < 0.05$; n = 10-13.

CSDS increased the latency to enter the lit zone, and decreased the lit zone time and number of entries to a much greater extend in *Cav1.2*^{Het} than *Cav1.2*^{Ctrl} mice (Lit zone time: 2-way ANOVA, stress x genotype: $F_{1,45} = 9.7$, $p < 0.005$; stress: $F_{1,45} = 20.5$, $p < 0.0001$; Bonferroni: $p < 0.05$; Lit zone entries: 2-way ANOVA, stress x genotype: $F_{1,45} = 2.2$, $p = 0.15$; stress: $F_{1,45} = 28.9$, $p < 0.0001$; genotype: $F_{1,45} = 17.7$, $p < 0.0005$; Bonferroni: $p < 0.05$). This is in line with the results of the OF and points towards enhanced stress-vulnerability of *Cav1.2*^{Het} mice, especially with regards to anxiety measures, which is further strengthened by the observation that sociability was solely affected by chronic stress, but not genotype (2-way ANOVA, condition: $F_{1,34} = 8.02$, $p < 0.01$; Bonferroni: $p < 0.05$) (Figure 3D). The ability to identify the displaced object during the spatial object recognition task was reduced to chance level in chronically stressed *Cav1.2*^{Ctrl} mice, but was already decreased in *Cav1.2*^{Het} animals under basal conditions, without reaching statistical significance (2-way ANOVA, stress x genotype: $F_{1,31} = 2.9$, $p = 0.1$). In contrast to the results obtained following *Cacna1c* depletion in the CNS and glutamatergic neurons, the findings indicate, and further confirm, that *Cacna1c* haploinsufficiency only results in mild behavioral alterations under basal conditions. However, the interaction between *Cacna1c* heterozygosity and chronic defeat stress resulted in a severe anxiety phenotype. Thus, we asked whether deletion of *Cacna1c* in excitatory forebrain projection neurons during adulthood would also induce stress vulnerability.

Cav1.2$^{FB\text{-}CKO}$ and *Cav1.2*$^{FB\text{-}Ctrl}$ mice were subjected to the same CSDS procedure and analysed in an identical test battery. As opposed to *Cav1.2*^{Het} mice, adult-induced *Cacna1c* inactivation in excitatory forebrain projection neurons resulted in stress resilience with regards to anxiety measures. This is depicted in the DaLi, where only *Cav1.2*$^{FB\text{-}Ctrl}$ mice responded to CSDS with a decreased amount of lit zone time and number of entries (Lit zone time: 2-way ANOVA; genotype: $F_{1,45} = 9.3$, $p < 0.005$; Bonferroni: $p < 0.05$; Lit zone entries: 2-way ANOVA, stress x

genotype: $F_{1,45}$ = 2.9, p = 0.0.9; stress: F1,45 = 5.8, p < 0.05; genotype: $F_{1,45}$ = 12.3, p < 0.005; Bonferroni: p < 0.05) (Figure 3H). Similarly, locomotion, immobility and inner zone entries were only altered in stressed *Cav1.2*$^{FB\text{-}Ctrl}$ but not stressed *Cav1.2*$^{FB\text{-}CKO}$ mice (Figure 3F-G). However, fur state quality, neuroendocrine parameters, FST behavior, sociability and spatial memory were similarly affected by CSDS in *Cav1.2*$^{FB\text{-}Ctrl}$ and *Cav1.2*$^{FB\text{-}CKO}$ mice (Figure 3I-J and S3I-L). This goes to show, that *Cacna1c* is able to interact with chronic stress to differentially alter anxiety-related behavior depending on the inactivation time point.

These results raised the question, whether *CACNA1C* also interacts with the environment to alter depressive symptomatology in humans. So far four SNPs (rs7297582, rs1006737, rs4765913 and rs4765905) in the *CACNA1C* gene have been associated with psychiatric disorders, reaching genome-wide significance (Ferreira et al., 2008; Sklar et al., 2008; Liu et al., 2011; Ripke et al., 2011; Sklar et al., 2011; Hamshere et al., 2013). However, a study examining stress-or trauma-specific genetic associations for these polymorphisms is still missing. The four mentioned SNPs are located in two separate linkage disequilibrium blocks (1st block= rs7297582, rs1006737 and rs4765905 and 2nd block = rs4765913) (Figure 4A). In our analysis rs7297582 was used for the 1st, and rs1024583, which is in linkage disequilibrium with rs4765913 in Yorubans, for the 2nd block (Figure 4A). We choose to specifically investigate the interplay between *CACNA1C* SNPs and adult trauma considering that *Cav1.2*^{Het} and *Cav1.2*$^{FB\text{-}CKO}$ mice were subjected to CSDS during adulthood. We first assessed the effect of the two *CACNA1C* SNPs and adult trauma on depressive symptoms, determined by the Beck Depression Inventory (BDI) in an African-American cohort of non-psychiatric clinical patients (N = 3075) from the Grady trauma project (Binder et al., 2008; Klengel et al., 2013; Mehta et al., 2013). Clinical and epidemiological demographics of participants across the three genotypes for each SNP are depicted in Table S1. The trauma events inventory (TEI) represents a measure of non-child abuse trauma, summing up the total number of different types of trauma among the participants into a continuous variable (0 = no adult trauma, 1 = 1 or 2 types of adult trauma, 2 = 3 or more types of adult trauma). Our analysis shows that both SNPs, rs7297582 and rs1024582 significantly interacted with adult trauma to predict depressive symptoms (p = 0.009159, p = 0.01424 respectively) without a main effect on BDI scores (Table S1). Notably, a BDI score of ≥ 16 significantly correlated with depression diagnosis in our and several other studies.

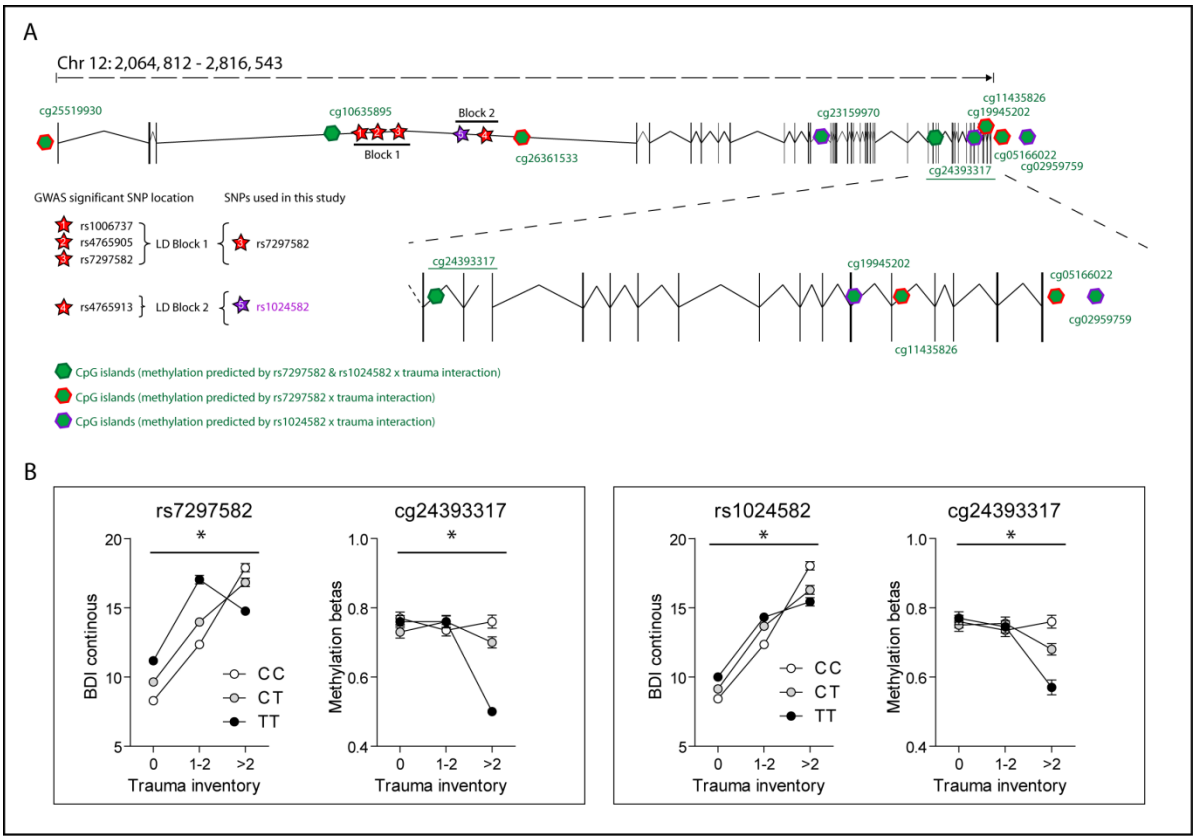

Figure 4: *CACNA1C* interacts with adult trauma to predict depressive symptoms in humans. (A) SNP and CpG site location in the human *CACNA1C* locus. Exons are indicated with vertical bars. **(B)** rs7297582 ($p < 0.01$) and rs1024582 ($p < 0.05$) significantly interacted with adult trauma to predict BDI scores and methylation of different CpGs including cg24393317 ($p < 0.005$) which is located distal to the transcription start site.

Interestingly, whereas homozygous SNP carriers (TT) with no trauma history and/or 1 or 2 trauma exposures displayed the highest BDI scores compared to the other two groups, the opposite was observed for homozygous SNP carriers having experienced 3 or more traumatic events (Figure 4B). To investigate the possibility that *CACNA1C* x adult trauma interactions are mediated by epigenetic modifications, we performed DNA methylation analysis using the Illumina 450 k HumanMethylation array. Bisulfite-treated genomic DNA extracts from peripheral blood cells were pyrosequenced from 344 individuals selected from the Grady trauma project, as previously described (Mehta et al., 2013). DNA from individuals having experienced no trauma was compared with DNA from individuals with 1-2, or 3 or more types of adult trauma for each SNP. The SNP rs7297582 significantly interacted with adult trauma to predict methylation levels of 6 CpGs (cg05166022, $p = 0.04626$; cg11435826, $p = 0.01508$; cg25519930, $p = 0.0191$; cg26361533, $p = 0.02246$; cg24393317, $p = 0.003517$ and cg10635895, $p = 0.04562$), while rs1024582 significantly interacted with adult trauma to predict methylation levels of 5 CpGs (cg02959759, $p = 0.04788$; cg19945202, $p = 0.04115$;

cg23159970, p = 0.04675; cg24393317, p = 0.003524 and cg10635895 p = 0.03421 (Figure 4A-B). In case of both SNPs, a significant decrease in DNA methylation was detected for cg24393317 in SNP carriers exposed to 3 or more types of adult trauma compared to the other two groups (Figure 4B). These changes in DNA methylation might be of functional relevance and mediate possible changes in *CACNA1C* gene expression. Thus, with an increasing number of trauma exposures, rs7297582 and rs1024582 switch from a risk allele status to a protective genotype, which also goes along with the strongest changes in methylation. The human data additionally supports an interaction between *CACNA1C* and adult trauma in the development of depressive symptoms, and further points towards an involvement of *CACNA1C* in the development of psychiatry disorders.

Discussion

The current study supports a role for $Ca_v1.2$ in the development of endophenotypes related to MDD, BPD and SCZ. Depletion of *Cacna1c* during development in the entire CNS and/or specifically in forebrain glutamatergic neurons results in hyperlocomotion, enhanced anxiety and active stress-coping behavior, reduced sociability and impaired spatial working memory, all representing key endophenotypes of MDD, BPD and SCZ. Enhanced locomotion in the OF, and active stress-coping behavior in the FST are frequently observed in mouse models of mania whereas increased anxiety, cognitive and social disturbances are more often associated with the depressive phase of BPD and with MDD itself (Nestler and Hyman, 2010). Notably, hyperactivity, altered social behavior, and cognitive impairments are also characteristic endophenotypes of SCZ (Jones et al., 2011), supporting the notion that *CACNA1C* represents a shared susceptibility factor for MDD, BPD and SCZ. However, a broader range of behavioral tests are necessary to more specifically address the manic-depressive aspects of BPD, and the positive, negative and cognitive symptoms of SCZ in our mouse models. Interestingly, the extent to which locomotion and memory performance were affected differed considerably between *Cav1.2*$^{CNS\text{-}CKO}$ and *Cav1.2*$^{Glu\text{-}CKO}$ mice. As opposed to a CNS-specific deletion, removal of *Cacna1c* from glutamatergic neurons impaired spatial memory to a far greater extend, and resulted in sever hyperlocomotion. This might be caused by different compensatory mechanisms, given that *Cacna1c* is specifically deleted from excitatory circuits in *Cav1.2*$^{Glu\text{-}CKO}$ mice, and not the whole brain (Figure S1). It should also be kept in mind, that even though inactivation of *Cacna1c* takes place during embryonic development in both mouse lines, deletion still occurs at a later time point in *Cav1.2*$^{Glu\text{-}CKO}$ than in *Cav1.2*$^{CNS\text{-}CKO}$ mice (E11.5 vs. E8), when neurons are further specified/committed (Goebbels et al., 2006; Dubois et al., 2006). Another possibility is that *Cacna1c* exerts different, and perhaps even opposing roles in particular brain regions and/or specific neuronal circuits, which might function in a concerted but antagonistic manner to keep neurobiological processes related to locomotion and cognition in balance.

In order to determine whether deletion of *Cacna1c* during adulthood would result in similar behavioral changes, we applied an inducible strategy to inactivate *Cacna1c* upon tamoxifen administration during adulthood only in forebrain principal neurons. Similarly as in *Cav1.2*$^{Glu\text{-}CKO}$ mice, locomotion was also enhanced in *Cav1.2*$^{FB\text{-}CKO}$ animals, and social and active stress-coping behavior mildly affected, suggesting that these endophenotypes are partly regulated by

forebrain-$Ca_v1.2$ during development and adulthood. However, anxiety-related behavior was not altered upon deletion of *Cacna1c* from forebrain principal neurons, while hippocampus-dependent spatial learning during the WCM was even slightly improved, without affecting long-term memory. In accordance, LTP, which is considered the cellular equivalent of learning and memory (Kandel, 2001) was enhanced in $Cav1.2^{FB\text{-}CKO}$ mice compared to controls. This is especially interesting, considering that deletion of *Cacna1c* from glutamatergic neurons impaired synaptic plasticity (Moosmang et al., 2005). However, while we observed changes in NMDA receptor (NMDAR)-dependent LTP, by stimulating with 100 Hz, Moosmang and colleagues showed that in the presence of NMDAR antagonists, only NMDAR-independent LTP was affected upon inactivation of *Cacna1c* from glutamatergic neurons (Moosmang et al., 2005). There are three main Ca^{2+} sources for induction of synaptic plasticity, NMDARs, VDCCs, and intracellular stores (ICS), the latter being mainly controlled by ryanodine receptors (RyRs) (Foster, 2012). Electrophysiological and pharmacological data have indicated that LTP induction is mainly initiated through NMDAR-activity but can also include NMDAR-independent and VGCC-dependent mechanisms. While high frequency stimulations between 25-100 Hz induce a rise in intracellular Ca^{2+} mainly through activation of NMDARs, higher frequency stimulation (200 Hz) was shown to induce LTP independent of NMDARs, due to increases in Ca^{2+} from VGCCs, particularly L-type channels (Grover and Teyler, 1990; Cavus and Teyler, 1996). However our study shows that NMDAR-dependent LTP can be potentiated upon deletion of *Cacna1c* in adult mice. Although we can only speculate about the underlying molecular mechanism at this point, it should be kept in mind that alterations in Ca^{2+} homeostasis are proposed to underlie age-dependent cognitive decline, which has been widely accepted as the “calcium hypothesis of aging” (Khachaturian, 1989a; Khachaturian, 1989b; Foster and Norris, 1997; Thibault et al., 2007; Foster, 2012). Such age-related changes in Ca^{2+} regulation include diminished NMDAR function and increased Ca^{2+} availability from VGCC and ICS. Thus, the decline of some memory processes is attributed to the shift from NMDAR-dependent to VGCC-ICS-dependent regulation of synaptic plasticity (Foster and Norris, 1997; Norris et al., 1998; Kumar and Foster, 2007). Although we did not assess aged animals, it can be speculated that ablation of $Ca_v1.2$ mice in adulthood partially blocks an evolving shift towards VGCC-ICS-dependent regulation of synaptic plasticity, hence facilitating NMDAR-LTP. Although NMDAR-LTP was not altered when *Cacna1c* was deleted during development from glutamatergic neurons, spatial memory was still impaired due to depletion of VGCC-dependent LTP mechanisms (Moosmang et al., 2005). This might suggest that $Ca_v1.2$ is required during

development, but not in adulthood for hippocampal-dependent spatial memory formation. This is further supported by White et al., where *Cacna1c* was conditionally deleted from forebrain principal neurons using a non-inducible *Camk2α-Cre*, which was shown to impair long-term spatial memory (White et al., 2008). In addition calcium channel antagonists were shown to ameliorate age-related deficits in hippocampal-dependent memory, possibly mediated through facilitation of NMDAR-LTP or inhibition of long-term depression (LTD) (Ban et al., 1990; Sandin et al., 1990; Riekkinen et al., 1997; Norris et al., 1998; Kumar and Foster, 2004; Trompet et al., 2008). We cannot entirely rule out that behavioral differences between *Cav1.2*$^{FB\text{-}CKO}$ and *Cav1.2*$^{Glu\text{-}CKO}$ are not partially caused by minor discrepancies in deletion patterns, such as in the DG, CeA, CPu and thalamus. However, the fact that forebrain elimination of *Cacna1c*, using a non-inducible *Camk2α-CreERT2* also results in enhanced anxiety-like behavior (Lee et al., 2012) favours opposing roles for $Ca_v1.2$ in anxiety during adulthood and embryonic/postnatal development. However Le et al., used a CaMKII-Cre T50 line from Jackson Laboratories, where Cre expression is activated at p18, thereby circumventing major developmental compensatory adaptations (Lee et al., 2012). Considering that deletion in this study was initiated between p84-91 would suggest that the beneficial effects of *Cacna1c* deletion on spatial memory occur at a much later time point in adulthood. However, it has also been shown that inactivation of *Cacna1c* in the anterior cingulate cortex via knockdown in adulthood, impaired observational fear learning, without altering anxiety-related behavior, novel object recognition memory and classical fear conditioning (Jeon et al., 2010). This additionally supports that developmental and early postnatal inactivation of *Cacna1c* regulate anxiety, but not all aspects of learning and memory.

So far our results favour the assumption that a strong genetic component, involving *Cacna1c*, underlies the development of key endophenotypes of MDD, BPD and SCZ. However SNPs in *CACNA1C* were also shown to affect measures of anxiety, depression, psychosocial functioning and cognitive aspects in healthy controls, which might represent increased susceptibility factors for psychiatric disorders upon exposure to adverse environments (Erk et al., 2010). Thus, we asked whether *Cacna1c* depletion can predispose towards disease development when the genetic component on its own does not strongly impact behavior. In other words, do stressful life events interact with *Cacna1c* to cause disease? To investigate this, we subjected *Cav1.2*^{Het} and *Cav1.2*$^{FB\text{-}CKO}$ mice to three weeks of CSDS. We choose heterozygous knockout mice to investigate the impact of early *Cacna1c* depletion on stress susceptibility, since both *Cav1.2*$^{CNS\text{-}CKO}$ and *Cav1.2*$^{Glu\text{-}CKO}$ mice already displayed strong behavioral alterations under basal

conditions, which may not be further aggravated by stress. *Cav1.2*^{Het} mice displayed reduced floating in the FST, but only showed a mild decrease in locomotion and cognitive performance under basal conditions, without displaying alterations in anxiety-related and social behavior. Peripheral deletion of *Cacna1c* in *Cav1.2*^{Het} mice might account for the decrease in locomotion under basal conditions, considering that the opposite effect was observed in the other mouse lines (*Cav1.2*$^{CNS\text{-}CKO}$, *Cav1.2*$^{Glu\text{-}CKO}$ and *Cav1.2*$^{FB\text{-}CKO}$). Overall our results are largely in line with the characterization of heterozygous *Cacna1c* mice performed by Dao and colleagues (Dao et al., 2010). However, the latter observe more pronounced changes in female Het mice. Along these lines, more recent work by Lee et al. (2012) demonstrated enhanced anxiety-related behavior in heterozygous *Cacna1c* male mice in the EPM, but not the DaLi, without observing changes in locomotion. Despite these conflicting observations, all studies implicate CACNA1C as a susceptibility gene for psychiatric disorders. In fact, the mild behavioral phenotype in *Cav1.2*^{Het} mice might represent a presymptomatic disease stage, rendering them more vulnerable to CSDS. More specifically, our findings demonstrate that heterozygosity of *Cacna1c* induces a severe increase in anxiety-related behavior in the OF, EPM and DaLi following chronic stress exposure, which is considered a major risk factor for the development of many psychiatric diseases. We observed no significant genotype-mediated differences in sociability, stress-coping behavior and spatial memory following CSDS, which highlights a specific role for $Ca_v1.2$ in stress-induced anxiety. However, different behavioral readouts might reveal additional effects of *Cacna1c* depletion CSDS-induced behavioral changes. This would not be surprising considering the fact that $Ca_v1.2$ is broadly expressed throughout the brain and accounts for approximately 85% of the LTCCs (Sinnegger-Brauns et al., 2009). However, the underlying molecular mechanisms which constitute the enhanced stress-vulnerability in *Cav1.2*^{Het} mice remain to be elucidated. It has previously been reported that decreased levels of $Ca_v1.2$ are not compensated by upregulation of $Ca_v1.3$, the other major LTCC in the brain (Dao et al., 2010; Enes et al., 2010; Langwieser et al., 2010). But whether this is also the case under chronic stress conditions has to be investigated. A previous study reported an upregulation of *Cacna1c* expression in the basolateral amygdala and hippocampus of adult male rats following chronic restraint stress, which was partially normalized by electroconvulsive stimulations (Maigaard et al., 2012). In addition $Ca_v1.2$ protein levels were increased in the amygdala of fear-conditioned rats (Shinnick-Gallagher et al., 2003). This might rather suggest a protective role for decreased $Ca_v1.2$ expression, which is also proposed by Dao et al. (2010). In order to assess, whether deletion of *Cacna1c* can also protect from the adverse effects of chronic

stress, we subjected *Cav1.2*$^{FB\text{-}CKO}$ to CSDS, given that this mouse line displayed slightly improved cognitive performance and enhanced synaptic plasticity under basal conditions. Notably, deletion of *Cacna1c* in adulthood from forebrain principal neurons resulted in a protective effect on CSDS-induced anxiety. While locomotion and anxiety were not affected in chronically stressed *Cav1.2*$^{FB\text{-}CKO}$ mice, sociability, stress-coping behavior and spatial memory were altered to a similar degree, in both *Cav1.2*$^{FB\text{-}Ctrl}$ and *Cav1.2*$^{FB\text{-}CKO}$. Given the enhanced LTP in *Cav1.2*$^{FB\text{-}CKO}$ mice, we initially expected a protective role on spatial memory following CSDS. However, a more elaborate memory analysis, including a wide spectrum of cognitive tests is required to further substantiate the results. This data further supports opposing roles for developmental and adult *Cacna1c* in the development of psychiatric endophenotypes, more specifically anxiety-related behavior. Nevertheless, we cannot entirely exclude that the observed phenotype in chronically stressed *Cav1.2*^{Het} mice is not partially caused by peripheral deletion of *Cacna1c*. However, the fact that an even greater reduction of central *Cacna1c*, as is the case in *Cav1.2*$^{CNS\text{-}CKO}$ and *Cav1.2*$^{Glu\text{-}CKO}$ mice, already induces behavioral impairments reminiscent of those observed in chronically stressed *Cav1.2*^{Het} mice, argues against that. Along these lines, the protective effect observed in *Cav1.2*$^{FB\text{-}CKO}$ mice is most likely not caused by differences in spatial deletion patterns, since embryonic inactivation of *Cacna1c* from forebrain glutamatergic neurons (*Cav1.2*$^{Glu\text{-}CKO}$), which results in a similar deletion pattern, failed to produce analogous effects.

To the best of our knowledge, this is the first study to systematically assess the interaction between *Canca1c* and chronic stress exposure on the development of MDD, BPD and SCZ-related endophenotypes. Since *Canca1c* interacted with CSDS to specifically affect anxiety in mice, a key endophenotype of MDD and BPD, but not necessarily SCZ, we chose to investigate the effect of *CACNA1C* SNPs and adult trauma on depressive symptomatology in humans. We found that two SNPs, rs7297582 and rs1024582, which are located in separate linkage disequilibrium blocks, significantly interact with adult trauma to predict depressive symptoms and methylation status of 9 different CpGs, which were located throughout the gene (Figure 4). In general, the risk to develop depressive symptoms was increased with exposure to adult trauma. BDI scores were higher in risk allele carriers (rs7297582 (TT) and rs1024582 (TT)) with no trauma, and following one or two trauma exposures. This goes in the direction of the GWAS data, which has associated rs1006737 (and genetic variants in LD with it) with MDD and BPD, and with enhanced depression and anxiety score in the absence of disease (Erk et al., 2010). However, in the presence of severe (3 or more) trauma exposures, the risk-alleles rs7297582

(TT) and rs1024582 (TT) switched into to a protective genotype. This potentially explains the missing main genetic effect of *CACNA1C* rs7297582 and rs1024582 on total BDI. This is rather unusual, and might imply different neurobiological changes in depressed SNP carriers depending on the presence and severity of previous trauma exposure. This idea was previously proposed by Metha and colleagues showing distinct biological modifications in post-traumatic stress disorder (PTSD) in the presence or absence of exposure to childhood abuse (Mehta et al., 2013). In support of this, significant changes in methylation were only observed in rs7297582 and rs1024582 SNP carriers with 3 or more trauma exposures, implying possible functional differences at the expression level. Epigenetic mechanisms, such as DNA methylation have been implicated with long-lasting consequences of early trauma (Gunnar and Quevedo, 2007; McGowan et al., 2009; Murgatroyd et al., 2009; Davies et al., 2012; Mehta et al., 2013). However, the relation between DNA methylation and gene expression is not straight-forward, as both negative and positive correlations were observed depending on the location of the CpGs (Chuang et al., 2012; Mehta et al., 2013). Due to low *CACNA1C* expression levels in peripheral blood, we were not able to assess possible changes in *CACNA1C* mRNA expression amongst the different groups. So far, the risk-associated SNP rs1006737 was shown to predict increased and decreased *CACNA1C* expression in human post mortem prefrontal cortex and cerebellar tissue respectively (Bigos et al., 2010; Gershon et al., 2013), which might imply changes in regulatory function between different brain regions and/or cell types. Although DNA methylation profiles are often tissue-specific, previous studies have shown that changes in the blood can mirror some of the DNA methylation changes in the brain (Sommershof et al., 2009; Provencal et al., 2012; Mehta et al., 2013). Overall we could show that two widely associated *CACNA1C* SNPs can differently impact depressive outcome depending on the presence and degree of previous trauma history. This is especially interesting considering that many GWAS studies do not control for previous trauma history. Nevertheless, future analysis in a larger cohort is necessary to validate the findings.

We propose that the association of *CACNA1C* with multiple psychiatric disorders is related to its broad expression within key neuronal circuits relevant to emotion, motivation and cognition, and that alteration in $Ca_v1.2$ gene expression during development and adulthood can result in diverging behavioral outcomes. Moreover, inactivation of *Cacna1c* is able to induce stress vulnerability and resilience depending on the temporal and spatial deletion pattern. Importantly, our mouse data is further supported by human genetic analyses, which clearly support an interaction between *CACNA1C* and adult stress exposure such as trauma.

Supplementary Information

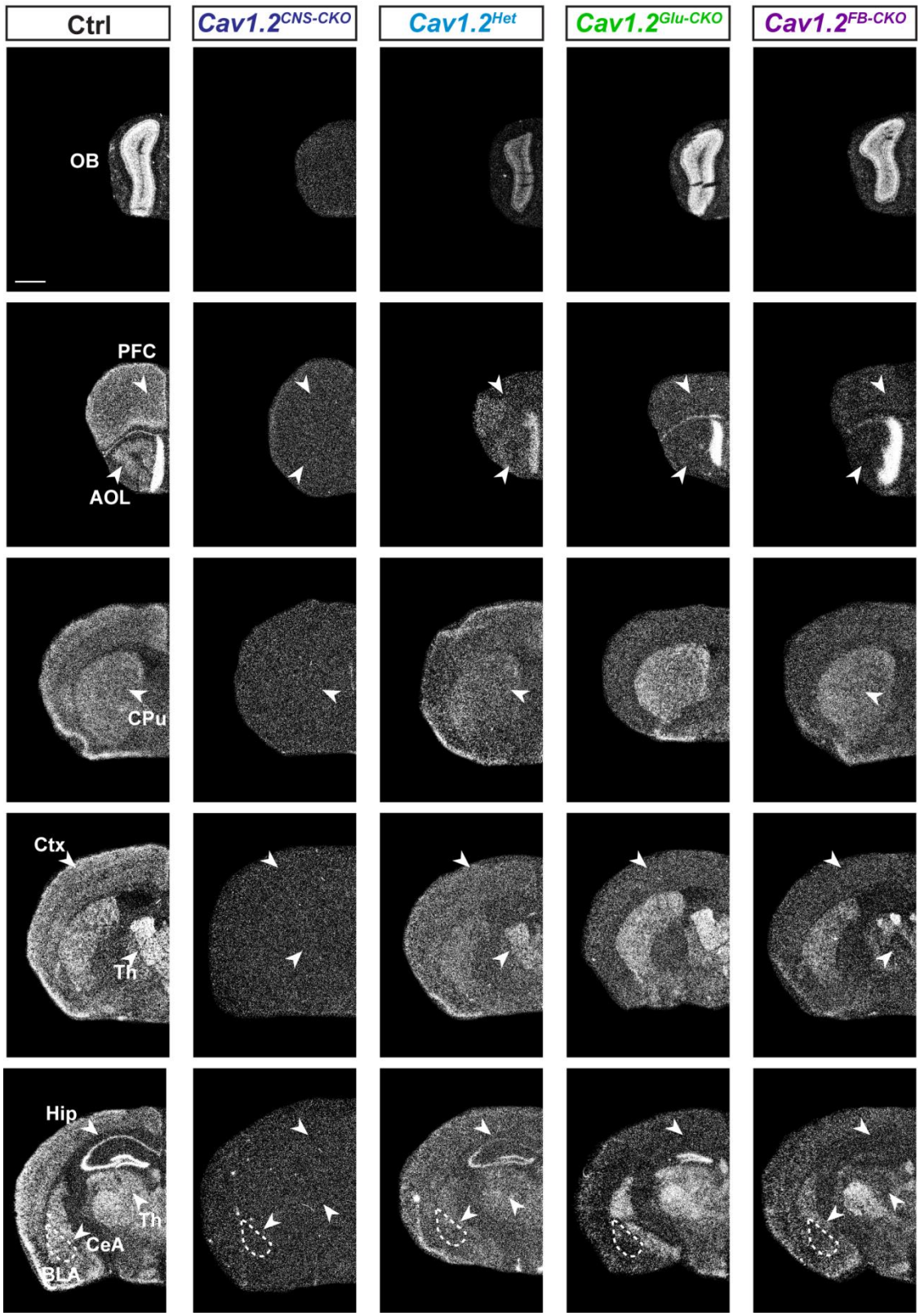

Supplementary Figure 1: Specific deletion pattern of *Cacna1c* mRNA throughout the brain of different conditional *Cav1.2*^{CKO} lines.

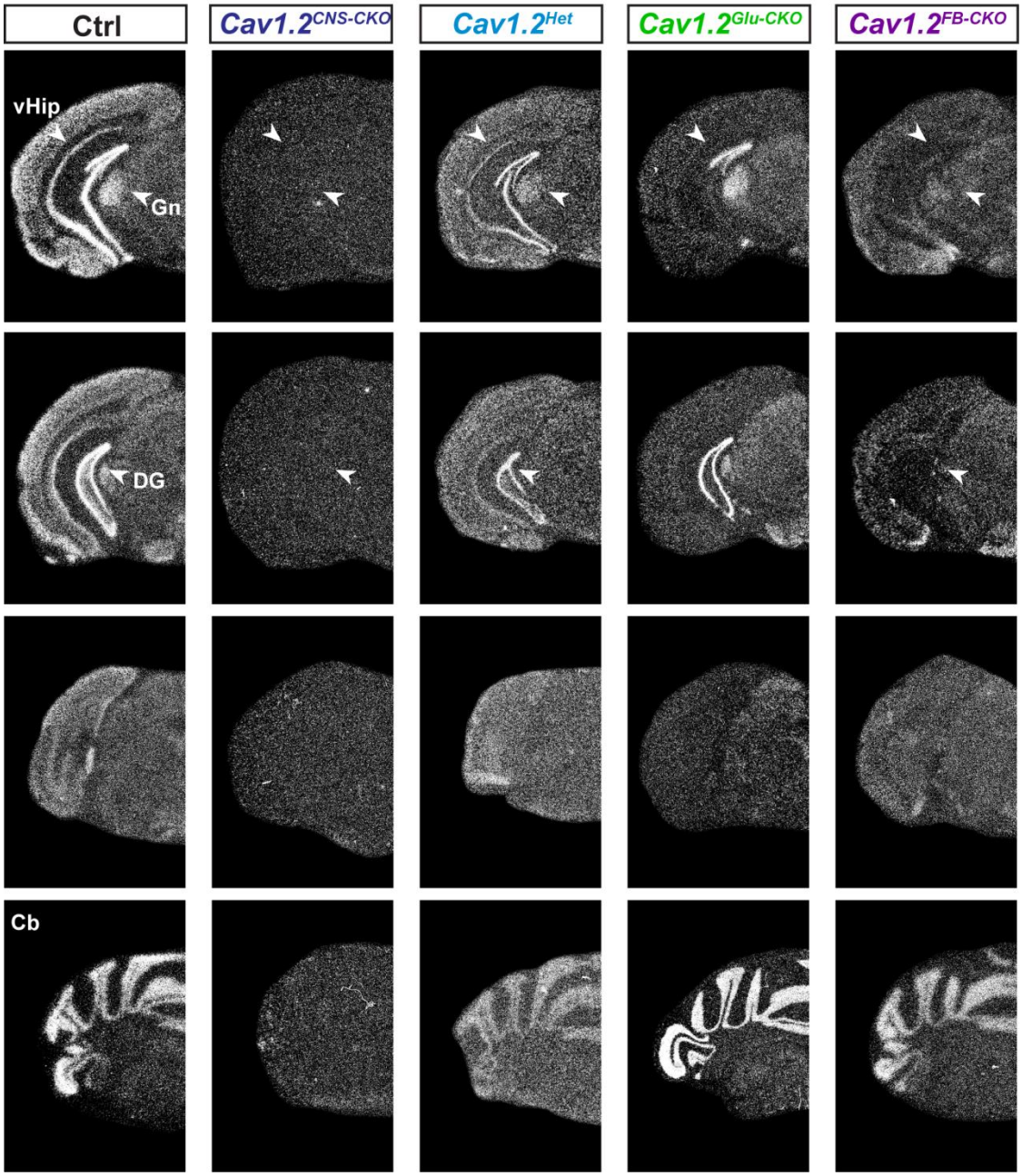

Supplementary Figure 1 continued: Specific deletion pattern of *Cacna1c* mRNA throughout the brain of different conditional *Cav1.2*^{CKO} lines. Representative radioactive *in situ* hybridization dark-field photomicrographs show *Cacna1c* mRNA expression in coronal brain sections of control *Cav1.2*$^{CNS\text{-}CKO}$, *Cav1.2*^{Het}, *Cav1.2*$^{Glu\text{-}CKO}$ and *Cav1.2*$^{FB\text{-}CKO}$ mouse lines. Noticeable areas are highlighted with arrowheads. Specific deletion of the *Cacna1c* gene in forebrain glutamatergic neurons (*Cav1.2*$^{Glu\text{-}CKO}$) renders complete loss of *Cacna1c* mRNA expression in the cerebral cortex (Ctx), hippocampal formation (Hip), and lateral divisions of the amygdala including the basolateral nucleus of the amygdala (BLA). A similar deletion pattern was observed in *Cav1.2*$^{FB\text{-}CKO}$ mice, lacking *Cacna1c* in forebrain *Camk2α*-positive principal neurons; however additional signal loss was observed throughout the caudate putamen (CPu), thalamus (Th), dentate gyrus (DG), central nucleus of the amygdala (CeA) and geniculate nucleus of the midbrain (Gn). Anterior olfactory area (AOL), caudate putamen / striatum (CPu), cerebellum (Cb), prefrontal cortex (PFC), olfactory bulb (OPB), ventral hippocampus (vHip). Scale bar represents 1 mm.

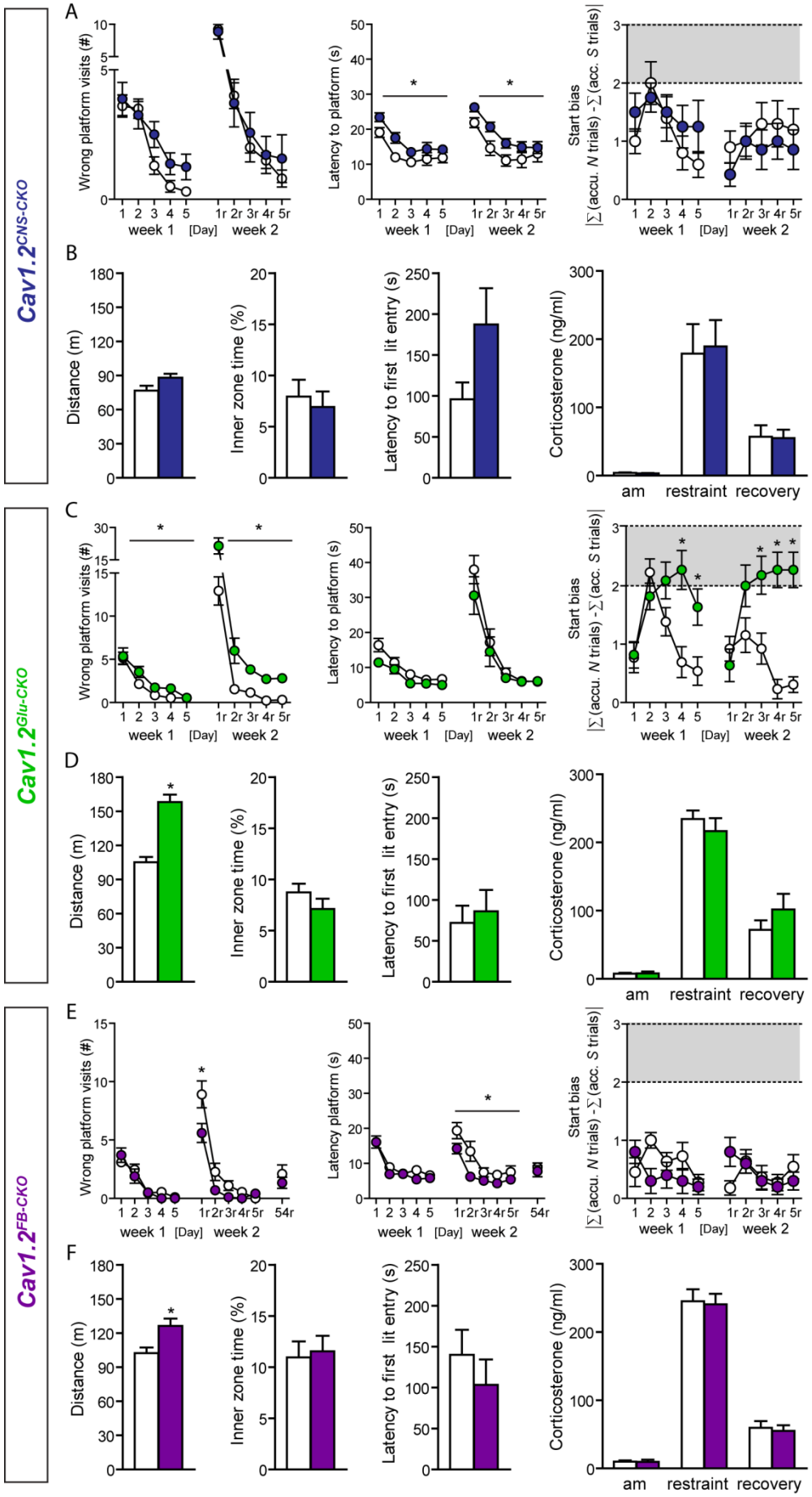
Cav1.2CNS-CKO
Cav1.2Glu-CKO
Cav1.2FB-CKO
A
B
C
D
E
F
Wrong platform visits (#)
Latency to platform (s)
Start bias
|∑(accu. N trials) - ∑(acc. S trials)|
week 1
[Day]
week 2
Distance (m)
Inner zone time (%)
Latency to first lit entry (s)
Corticosterone (ng/ml)
am
restraint
recovery

Supplementary Figure 2: Additional behavioral and neuroendocrine parameters in *Cav1.2*$^{CNS\text{-}CKO}$, *Cav1.2*$^{Glu\text{-}CKO}$ and *Cav1.2*$^{FB\text{-}CKO}$ mice. (A) *Cav1.2*$^{CNS\text{-}CKO}$ showed increased latencies to reach the platform during learning (RM-ANOVA, genotype: $F_{1,64}$ = 7.6, p < 0.05) and relearning (RM-ANOVA; genotype, $F_{1,60}$ = 7.6, p = 0.08) of the WCM task, while the start bias and number of wrong platform visits did not differ between genotypes. Total distance travelled and inner zone time in the OF did not significantly different between genotypes, while the latency to enter the lit zone of the DaLi was slightly increased. HPA axis function was not altered in *Cav1.2*$^{CNS\text{-}CKO}$ mice. **(B)** *Cav1.2*$^{Glu\text{-}CKO}$ exhibited an increased number of wrong platform visits during learning (RM-ANOVA, genotype: $F_{1,88}$ = 4.5, p < 0.05) and relearning (RM-ANOVA; genotype, $F_{1,88}$ = 27.7, p < 0.0001), without showing alterations in latencies. In addition, *Cav1.2*$^{Glu\text{-}CKO}$ mice displayed a strong start bias, which suggest the utilization of a response rather than spatially-based learning strategy in these animals (learning: RM-ANOVA; interaction, $F_{4,88}$ = 5.5, p < 0.005; genotype, $F_{1,88}$ = 7.6, p < 0.05; time, $F_{4,88}$ = 8.4, p < 0.0001 / relearning: RM-ANOVA; interaction, $F_{4,88}$ = 9.3, p <0.0001; genotype, $F_{1,88}$ = 21.2, p <0.0005, time: $F_{4,88}$ = 4.2, p <0.005; Bonferroni post-test, p < 0.05). Total distance travelled was strongly increased in *Cav1.2*$^{Glu\text{-}CKO}$ compared to *Cav1.2*$^{Glu\text{-}Ctrl}$ mice (t_{26} = 6.8, p < 0.05), while no differences were observed in inner zone time of the OF, the latency to enter the lit compartment of the DaLi or HPA axis parameters. **(C)** *Cav1.2*$^{FB\text{-}CKO}$ made fewer wrong platform visits (RM-ANOVA; interaction, $F_{4,80}$ = 4.3, p < 0.005; genotype, $F_{1,80}$ = 4.6, p < 0.05; time, $F_{4,80}$ = 76.6, p < 0.0001, Bonferroni post-test, p < 0.05) during relearning and displayed shorter latencies to reach the platform (RM-ANOVA; genotype, $F_{1,80}$ = 4.4, p < 0.05) while the start bias did not differ between the groups. No differences were observed between genotypes in the remote memory trial performed 30 days after the last relearning episode (d54). Total distance travelled was increased in *Cav1.2*$^{FB\text{-}CKO}$ compared to *Cav1.2*$^{FB\text{-}Ctrl}$ mice (t_{26} = 3.0, p < 0.01), while no differences were observed in inner zone time of the OF, the latency to enter the lit compartment of the DaLi or HPA axis parameters.

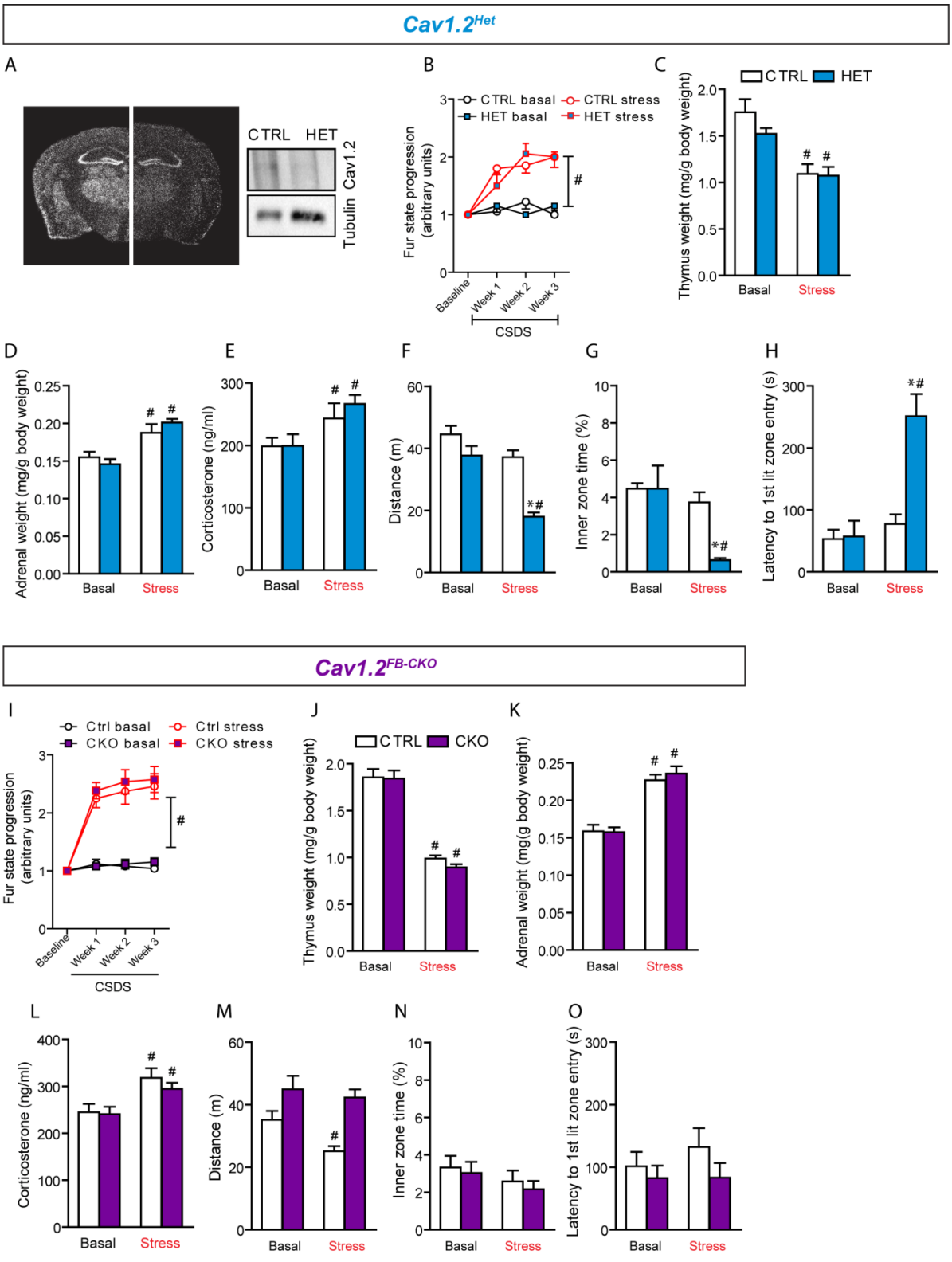

Supplementary Figure 3: CSDS induced similar physiological and neuroendocrine alterations in *Cav1.2*^{Het} and *Cav1.2*$^{FB\text{-}CKO}$ compared to control littermates. (A) *Cav1.2*^{Het} mice displayed ~ 50% reduction in *Cacna1c* mRNA and hippocampal protein levels assessed by *ISH* and WB respectively. **(B)** CSDS led to a robust decrease in fur state quality depicted by a progressive increase in fur coat status (RM-ANOVA; time x condition, $F_{3,32} = 28.0$, $p < 0.0001$; condition, $F_{1,34} = 75.3$, $p < 0.0001$). **(C-E)** Similarly, CSDS induced thymus atrophy (2-way ANOVA; condition, $F_{1,34} = 28.0$, $p < 0.0001$), adrenal gland enlargement (2-way ANOVA; condition, $F_{1,34} = 28.2$, $p < 0.0001$), and an increased corticosterone response (2-way ANOVA; condition, $F_{1,33} = 8.5$, $p < 0.01$) independent of genotype. **(I-L)** The same was observed in *Cav1.2*$^{FB\text{-}CKO}$ mice (fur state

progression: RM-ANOVA, time x condition: $F_{3,46}$ = 29.0, $p < 0.0001$; condition: $F_{1,46}$ = 80.2, $p < 0.0001$ / thymus: 2-way ANOVA; condition, $F_{1,46}$ = 187.0, $p < 0.0001$ / adrenal glands: 2-way ANOVA, condition, $F_{1,46}$ = 79.7, $p < 0.0001$ / corticosterone response: 2-way ANOVA; condition, $F_{1,45}$ = 14.9, $p < 0.0005$). **(F-G)** Compared to *Cav1.2*^{Ctrl}, *Cav1.2*^{Het} mice showed decreased locomotion and inner zone time in the OF following CSDS (2-way ANOVA; interaction, $F_{1,46}$ = 2.9, $p = 0.09$; condition, $F_{1,46}$ = 23.6, $p < 0.0001$, genotype, $F_{1,46}$ = 22.7, $p < 0.0001$; Bonferroni post-test, $p < 0.05$). **(H)** The latency to enter the lit compartment of the DaLi was drastically enhanced in chronically stressed *Cav1.2*^{Het} but not *Cav1.2*^{Ctrl} mice (2-way ANOVA; interaction, $F_{1,43}$ = 15.0, $p < 0.0005$; condition, $F_{1,44}$ = 24.9, $p < 0.0005$; genotype, $F_{1,44}$ = 16.5, $p < 0.0005$, Bonferroni post-test, $p < 0.05$). **(M)** On the other hand, *Cav1.2*$^{FB\text{-}CKO}$ displayed no reduction in locomotion following CSDS (2-way ANOVA; condition, $F_{1,43}$ = 4.4, $p < 0.05$; genotype, $F_{1,43}$ = 19.6, $p < 0.0001$, Bonferroni post-test, $p < 0.05$). **(N-O)** No genotype- or condition-mediated differences were observed for the inner zone time, and latency to enter the lit compartment.

	All	rs72975821			rs1024582			P-value rs72975821	P-value rs1024582
		CC	CT	TT	CC	CT	TT		
	N = 3075	N = 2409	N = 625	N = 41	N =2460	N = 530	N = 80		
	Mean (SD/%)	Mean (SD/%)	Mean (SD/%)	Mean (SD/%)	Mean (SD/%)	Mean (SD/%)	Mean (SD/%)		
Gender - Males Females	987 (32.1%) 2088 (67.9%)	752 (31.2%) 1655 (68.8%)	222 (35.6%) 402 (64.4%)	12 (29.3%) 29 (70.7%)	768 (31.3%) 1683 (68.7%)	190 (35.8%) 340 (64.2%)	23 (28.7%) 57 (71.3%)	0.219	0.156
Age	39.50 (0.26)	39.36 (0.29)	40.06 (0.50)	39.0 (2.3)	39.35 (0.28)	40.17 (0.63)	40.05 (1.6)	0.5	0.654
Race - African Americans	2882 (93.7%)	2305 (95.8%)	548 (87.8%)	26 (63.4%)	2337 (95.3%)	468 (88.3%)	64 (80%)	0.19	0.34
Substance abuse current	110 (3.6%)	88 (3.7%)	18 (2.9%)	3 (7.3%)	88 (3.7%)	18 (3.4%)	4 (5%)	0.194	0.74
Total types of adult trauma exposure	2.52 (0.04)	2.51 (0.04)	2.55 (0.08)	2.70 (0.32)	2.51 (0.04)	2.59 (0.09)	2.4 (0.22)	0.491	0.518
0 types 1 to 2 types 3 or more types	478 (15.5%) 1250 (40.7%) 1347 (43.8%)	373 (16%) 998 (41%) 1038 (43%)	99 (16%) 235 (38%) 291 (46%)	6 (15%) 17 (41%) 18 (44%)	373 (15%) 1022 (42%) 1065 (43%)	90 (17%) 190 (36%) 250 (47%)	14 (17.5%) 34 (42.5%) 32 (40%)	0.766	0.4
BDI total score	14.24 (0.22)	14.13 (0.25)	14.63 (0.48)	15.17 (1.6)	14.29 (0.25)	14.15 (0.50)	14.01 (1.2)	0.393	0.597
N (%) with BDI total score	868 (28.2%)	679 (28.2%)	176 (28.2%)	13 (31.7%)	700 (28.5%)	146 (27.5%)	22 (27.5%)	0.701	0.167
Total PTSD symptom score	12.91 (0.23)	13.02 (0.26)	12.49 (0.49)	13.12 (1.7)	13.00 (0.26)	12.57 (0.54)	12.63 (1.35)	0.678	0.492

Supplementary Table 1: Sample description of the Grady trauma project cohort. P-values are calculated across the 3 genotypes for each SNP. Beck Depression Inventory (BDI), Traumatic Events Inventory (TEI). A BDI score of ≥ 16 significantly correlated with Depression diagnosis in this and several other studies. The methylation dataset was a subset of a previous dataset with similar distributions of phenotypes (Mehta et al., 2013).

LIST OF ABBREVIATIONS

^{35}S	Isotope 35 of sulfur
5-HT	5-hydroxytryptamine (serotonin)
AAc	Alpha-actinin-2
AAV	Adeno-associated virus
AcbSh	Nucleus accumbens shell
ACTH	Adrenocorticotropin
ADHS	Attention-deficit/hyperactivity disorder
AMP	Adenosine monophosphate
Amy	Amygdala
ANK3	Ankyrin-3
ANOVA	Analysis of variance
AOL	Anterior olfactory area
Apit	Anterior pituitary
APT	Anterior pretectal area
AQP4	Aquaporine 4
aRNA	Amplified ribonucleic acid
ASD	Autism spectrum disorder
ASR	Acoustic startle response
ATP	Adenosine triphosphate
AVP	Arginine vasopressin
BAG1	BAG family molecular chaperone regulator 1
Bar	Barrington's nucleus
BDI	Beck depression inventory
BDNF	Brain-derived neurotrophic factor
BLA	Basolateral nucleus of the amygdala
BNST	Bed nucleus of the stria terminalis
bp	Basepairs
BPD	Bipolar disorder
CA 1/2/3	Cornu ammonis area
Ca^{2+}	Calcium
CACNA1C	Gene encoding the $Ca_v1.2$ calcium channel
CAMK2α	Calcium/calmodulin-dependent protein kinase type II alpha
Cas	CRISP-associated protein
$Ca_v1.2$	L-type, voltage-dependent calcium channel, alpha 1C subunit
$Ca_v1.3$	L-type, voltage-dependent calcium channel, alpha 1D subunit
CB	Calbindin
CCK	Cholecystokinin
cDNA	Copy DNA
CeA	Central nucleus of the amygdala
CGE	Caudal ganglionic eminence
ChETA	Channelrhodopsin 2-E123T accelerated

ChIEF	Chimeric hybrids of ChR1 and ChR2
ChR	Channelrhodopsin
CK	Calretinin
CKO	Conditional knockout
CLOCK (gene)	Circadian Locomotor Output Cycles Kaput (transcription factor)
CMV	Cytomegalovirus
CNS	Central nervous system
COE	Conditional overexpression
Cp	Crossing point
Cpm	Counts per minute
CPu	Caudate putamen
Cre	Cyclization recombina-tion
CREB	cAMP response element-binding protein
CRH	Corticotropin-releasing hormone
CRHBP	Corticotropin-releasing hormone binding protein
CRHR	Corticotropin-releasing hormone receptor
CRISP	Clustered regulatory interspaced short palindromic repeats
CSDS	Chronic social defeat stress
CSF	Cerebrospinal fluid
CSF	Cerebrospinal fluid
Ctrl	Control
CTSQ	Cathepsin
Ctx	cortex
D1 / DRD1	Dopamine receptor 1
DA	Dopamine
DAG	Diacylglycerol
DaLi	Dark-light box
DAOA	D-Amino acid oxidase activator
DAPI	4’,6-diamidino-2-phenylindole
DAT/SLC6A3	Dopamine transporter
dB	Decibel
Del	Deleter
DEPC	Diethylpyrocarbonate
DG	Dentate gyrus
dHip	Dorsal hippocampus
DIO	Double-floxed inverted open reading frame
DISC1	Disrupted in schizophrenia 1
DLX5*/6*	Homeodomain transcription factor (s) related to the Drosophila distal-les (Dll) gene
DMSO	Dimethyl sulfoxide
DNA	Deoxyribonucleic acid
dNTP	Desoxyribonucleotide triphosphate
Dock 10	Dedicator of cytokinesis protein 10
DOPAC	3,4-dihydroxyphenylacetic acid

Dox	Doxycycline
DSB	Double strand break
DSM 4/5	Diagnostic and Statistical Manual of Mental Disorders 4/5
DST	Dexamethasone suppression test
DTNBP1	Dysbindin 1
DTT	1,4-dithiothreitol
E	Embryonic
E. coli	*Escherichia coli*
EDTA	Ethylenediaminetetraacetic acid
EF1α	Expression of elongation factor 1α
EN1	Engrailed 1
ePet	Enhancer of the ETS-domain transcription factor Pet-1
EPL	External plexiform layer of the olfactory bulb
EPM	Elevated plus-maze
ER	Estrogen receptor
ERK	Extracellular-signal-regulated kinase
ES cells	Embryonic stem cells
EtOH	Ethanol
eYFP	enhanced Yellow fluorescent protein
FB	Forebrain
fEPSP	Field excitatory post-synaptic potential
FGF	Fibroblast growth factor
FKBP5	FK506 binding protein 5
FLEX	Flip-excision
flop	Floxed stop
Flp	Flipase
FR	Fixed ratio
frt	Flp recognition target
FST	Forced swim test
g	Gram
GABA	γ-Aminobutyric acid
Gad65	Glutamic acid decarboxylase (molecular weight 65 kDa)
Gad67	Glutamic acid decarboxylase (molecular weight 67 kDa)
GCs	Glucocorticoids
GFAP	Glial fibrillary acidic protein
GFP	Green fluorescent protein
GI	Glomerular layer of the olfactory bulb
Gi	Nucleus paragigantocellularis
Glu	Glutamate
Glur6	Glutamate receptor, ionotropic, kainite 2
Gn	Geniculate nucleus
GPCR	G-protein coupled receptor
GR	Glucocorticoid receptor
GSK-3β	Glycogen synthase kinase 3β

GWAS	Genom-wide association study
h	Hour
HB	Habenula nucleus
HDR	Homology directed repair
Het	Heterozygous
HFS	High frequency stimulation
Hip	Hippocampus
Hom	Homozygous
HPA	Hypothalamic-pituitary-adrenocortical
HVA	Homovanilic acid
HY	Hypothalamus
Hz	Hertz
IC	Inferior colliculus
ICS	Intracellular calcium stores
ICV / i.c.v.	Intracerebroventricular
iDA	Inducible dopaminergic (Cre)
IEG	Immediate early gene
iFB	Inducible forebrain-specific (Cre)
Ifitm1	Interferon-induced transmembrane protein
IHC	Immunohistochemistry
IO	Inferior olive
IP_3	Inositol 1,4,5-trisphosphate
IRES	Internal ribosome entry site
ISH	*In situ* hybridization
kb	Kilobasepairs
kDa	Kilodalton
KO	Knockout
KW	Kruskal Wallis test
LacZ	Gene encoding β-galactosidase
LB	Lysogeny broth
LBD	Ligand binding domain
LC	Locus coeruleus
LGE	Lateral ganglionic eminence
LHA	Lateral hypothalamic area
LiCl	Lithium chloride
Lmol	Stratum lacunosum
loxP	Locus of crossover [x] of P1
LTCC	L-type calcium channel
LTD	Long-term depression
LTP	Long-term potentiation
L-type	Long-lasting type
LV	Lentivirus
M	Molar
MDD	Major depressive disorder

MeA	Medial nucleus of the amygdala
mEPSP	Miniature excitatory post-synaptic potential
$MgCl_2$	Magnesium chloride
MGM	Medial ganglionic eminence
MHB	Mid/hindbrain
Mi	Mitral layer of the olfactory bulb
min	Minute
MM	Mammillary nucleus
MoDG	moleculare layer of the dentate gyrus
MR	Mineralocorticoid receptor
mRNA	Messenger ribonucleic acid
MSN	Medium spiny neurons
Mt1	Metallothionine 1
MWM	Morris water-maze
Myk	Myshkin
NA	Noradrenaline
NAc	Nucleus accumbens
Neo	Neomycin
NET/SLC6A2	Norepinephrine transporter
Nex	Helix-loop-helix transcription factor
Nfib	Nuclear factor I/B
NHEJ	Non-homologous end joining
NHS	N-hydroxysuccinimid
NMDA	*N*-Methyl-D-aspartic acid
NMDAR	*N*-Methyl-D-aspartic acid receptor
NPY	Neuropeptide Y
NRG1	Neuregulin 1
NT	Neurotransmitter
o.n.	Over night
OB	Olfactory bulb
OD	Optical density
OE	Overexpression
OF	Open field
ONPG	Ortho-nitrophenyl-β-galactoside
Or	Oriens layer of the hippocampus
ORF	Open reading frame
P	Postnatal
P/S	Penicillin/streptomycin
pA	Polyadenylation
PAG	Periaqueductal grey
PB	Parabrachial nucleus
PBS	Phosphate buffered saline
PCP	Phencyclidine
PCR	Polymerase chain reaction

PFA	Paraformaldehyde
PFC	Prefrontal cortex
Pir	Piriform cortex
PN	Pontine nucleus
PoDG	Polymorph DG
POMC	Proopiomelanocortin
PPI	Prepulse inhibition
PR	Progressive ratio
PSD-95	Pos-tsynaptic density protein 95
PTSD	Post-traumatic stress disorder
PV	parvalbumin
PVC	Polyvinyl chloride
PVN	Paraventricular nucleus of the hypothalamus
qRT-PCR	Quantitative real-time polymerase chain reaction
r	relearning
REM	Rapid eye movement
RGN	RNA-guided endonucleases
RM-ANOVA	Repeated measures analysis of variance
RN	Raphe nucleus
RNA	Ribonucleic acid
Rpm	Rounds per minute
Rt	Room temperature
RyR	Ryanodine receptor
s	Second
SA	Social avoidance
SA	Splice acceptor
SC	Superior colliculus
SCP	Stresscopin
SCZ	Schizophrenia
SEM	Standard error of mean
SFO	step-function opsins
SHANK3	SH3 and multiple ankyrin repeat domains 3
shRNA	short hairpin RNA
SN	Substantia nigra
SNP	Single nucleotide polymorphism
SOC	Super optimal broth
SOM	Somatostatin
Sp	Septum
SSC	Standard saline citrate
Syn	Synaptophysin
TAE	Tris acetate EDTA
TALEN	transcription activator-like effector nucleases
TB	Tubulin
TCAP-1	Teneurin C-terminal-associated peptide 1

TEA	Triethanolamine
TEI	Traumatic events inventory
tetO	Tetracycline operator
tg	Transgenic
TH	Thalamus
TH	Tyrosine hydroxylase
Thy1	Also known as CD90 (cluster of differentiation 90)
TRAP	Targeted recombination in active populations
Tris	Trisaminomethane
TRKB	Tyrosine kinase B receptor
TSE	Tail suspension test
tTA	Tetracycline transactivator
U	Unit(s)
UCN (1-3)	Urocortin (1-3)
UTP	Uridine triphosphate
UV	Ultra violet
VDCC	Voltage-dependent calcium channel
VGlut (1-3)	Vesicular glutamate transporter (1-3)
vHip	Ventral hippocampus
VIP	Vasoactive intestinal peptide
VTA	Ventral tegmental area
WB	Western blot
WCM	Water-cross maze
wt	Wild-type
X-Gal	5-bromo-4-chloro-3-indolyl-beta-D-galactopyranoside

REFERENCES

Aarsland D, Pahlhagen S, Ballard CG, Ehrt U, Svenningsson P (2012) Depression in Parkinson disease--epidemiology, mechanisms and management. Nat Rev Neurol 8:35-47.

Adam D (2013) Mental health: On the spectrum. Nature 496:416-418.

Adhikari A, Topiwala MA, Gordon JA (2010) Synchronized activity between the ventral hippocampus and the medial prefrontal cortex during anxiety. Neuron 65:257-269.

Adler NE, Ostrove JM (1999) Socioeconomic status and health: what we know and what we don't. Ann N Y Acad Sci 896:3-15.

Adli M, Bschor T, Bauer M, Lucka C, Lewitzka U, Ising M, Uhr M, Mueller-Oerlinghausen B, Baethge C (2009) Long-term outcome after lithium augmentation in unipolar depression: focus on HPA system activity. Neuropsychobiology 60:23-30.

Akagi K, Sandig V, Vooijs M, Van d, V, Giovannini M, Strauss M, Berns A (1997) Cre-mediated somatic site-specific recombination in mice. Nucleic Acids Res 25:1766-1773.

Aldenhoff JB, Gruol DL, Rivier J, Vale W, Siggins GR (1983) Corticotropin releasing factor decreases postburst hyperpolarizations and excites hippocampal neurons. Science 221:875-877.

Alon T, Zhou L, Perez CA, Garfield AS, Friedman JM, Heisler LK (2009) Transgenic mice expressing green fluorescent protein under the control of the corticotropin-releasing hormone promoter. Endocrinology 150:5626-5632.

Anderzhanova E, Wotjak CT (2013) Brain microdialysis and its applications in experimental neurochemistry. Cell Tissue Res.

Anderzhanova EA, Bachli H, Buneeva OA, Narkevich VB, Medvedev AE, Thoeringer CK, Wotjak CT, Kudrin VS (2013) Strain differences in profiles of dopaminergic neurotransmission in the prefrontal cortex of the BALB/C vs. C57Bl/6 mice: consequences of stress and afobazole. Eur J Pharmacol 708:95-104.

Andjelic S, Gallopin T, Cauli B, Hill EL, Roux L, Badr S, Hu E, Tamas G, Lambolez B (2009) Glutamatergic nonpyramidal neurons from neocortical layer VI and their comparison with pyramidal and spiny stellate neurons. J Neurophysiol 101:641-654.

Andreano JM, Cahill L (2009) Sex influences on the neurobiology of learning and memory. Learn Mem 16:248-266.

Andreasen NC (1995) Symptoms, signs, and diagnosis of schizophrenia. Lancet 346:477-481.

Andreasen NC, Olsen S (1982) Negative v positive schizophrenia. Definition and validation. Arch Gen Psychiatry 39:789-794.

Anthony TE, Dee N, Bernard A, Lerchner W, Heintz N, Anderson DJ (2014) Control of stress-induced persistent anxiety by an extra-amygdala septohypothalamic circuit. Cell 156:522-536.

APA (2013) Diagnostic and Statistical Manual of Mental Disorders. Arlington, VA: American Psychiatric Publishing.

Arborelius L, Owens MJ, Plotsky PM, Nemeroff CB (1999) The role of corticotropin-releasing factor in depression and anxiety disorders. J Endocrinol 160:1-12.

Ardayfio P, Kim KS (2006) Anxiogenic-like effect of chronic corticosterone in the light-dark emergence task in mice. Behav Neurosci 120:249-256.

Arenkiel BR, Peca J, Davison IG, Feliciano C, Deisseroth K, Augustine GJ, Ehlers MD, Feng G (2007) In vivo light-induced activation of neural circuitry in transgenic mice expressing channelrhodopsin-2. Neuron 54:205-218.

Argos P, Landy A, Abremski K, Egan JB, Haggard-Ljungquist E, Hoess RH, Kahn ML, Kalionis B, Narayana SV, Pierson LS, III, . (1986) The integrase family of site-specific recombinases: regional similarities and global diversity. EMBO J 5:433-440.

Arguello PA, Markx S, Gogos JA, Karayiorgou M (2010) Development of animal models for schizophrenia. Dis Model Mech 3:22-26.

Arnett MG, Kolber BJ, Boyle MP, Muglia LJ (2011) Behavioral insights from mouse models of forebrain--and amygdala-specific glucocorticoid receptor genetic disruption. Mol Cell Endocrinol 336:2-5.

Arnsten AF, Mathew R, Ubriani R, Taylor JR, Li BM (1999) Alpha-1 noradrenergic receptor stimulation impairs prefrontal cortical cognitive function. Biol Psychiatry 45:26-31.

Aston-Jones G, Bloom FE (1981) Activity of norepinephrine-containing locus coeruleus neurons in behaving rats anticipates fluctuations in the sleep-waking cycle. J Neurosci 1:876-886.

Atasoy D, Aponte Y, Su HH, Sternson SM (2008) A FLEX switch targets Channelrhodopsin-2 to multiple cell types for imaging and long-range circuit mapping. J Neurosci 28:7025-7030.

Atkinson HC, Leggett JD, Wood SA, Castrique ES, Kershaw YM, Lightman SL (2010) Regulation of the hypothalamic-pituitary-adrenal axis circadian rhythm by endocannabinoids is sexually diergic. Endocrinology 151:3720-3727.

Azouz R, Gray CM, Nowak LG, McCormick DA (1997) Physiological properties of inhibitory interneurons in cat striate cortex. Cereb Cortex 7:534-545.

Badaut J, Regli L (2004) Distribution and possible roles of aquaporin 9 in the brain. Neuroscience 129:971-981.

Baekelandt V, Claeys A, Eggermont K, Lauwers E, De SB, Nuttin B, Debyser Z (2002) Characterization of lentiviral vector-mediated gene transfer in adult mouse brain. Hum Gene Ther 13:841-853.

Baekelandt V, Eggermont K, Michiels M, Nuttin B, Debyser Z (2003) Optimized lentiviral vector production and purification procedure prevents immune response after transduction of mouse brain. Gene Ther 10:1933-1940.

Bagosi Z, Jaszberenyi M, Bujdoso E, Telegdy G (2006) The effects of corticoptropin-releasing factor and the urocortins on striatal dopamine release induced by electrical stimulation-an in vitro superfusion study. Neurochem Res 31:209-213.

Baldwin HA, Rassnick S, Rivier J, Koob GF, Britton KT (1991) CRF antagonist reverses the "anxiogenic" response to ethanol withdrawal in the rat. Psychopharmacology (Berl) 103:227-232.

Bale TL, Contarino A, Smith GW, Chan R, Gold LH, Sawchenko PE, Koob GF, Vale WW, Lee KF (2000) Mice deficient for corticotropin-releasing hormone receptor-2 display anxiety-like behaviour and are hypersensitive to stress. Nat Genet 24:410-414.

Bale TL, Picetti R, Contarino A, Koob GF, Vale WW, Lee KF (2002) Mice deficient for both corticotropin-releasing factor receptor 1 (CRFR1) and CRFR2 have an impaired stress response and display sexually dichotomous anxiety-like behavior. J Neurosci 22:193-199.

Ban TA, Morey L, Aguglia E, Azzarelli O, Balsano F, Marigliano V, Caglieris N, Sterlicchio M, Capurso A, Tomasi NA, . (1990) Nimodipine in the treatment of old age dementias. Prog Neuropsychopharmacol Biol Psychiatry 14:525-551.

Banki CM (1977) Correlation between cerebrospinal fluid amine metabolites and psychomotor activity in affective disorders. J Neurochem 28:255-257.

Bardo MT, Bevins RA (2000) Conditioned place preference: what does it add to our preclinical understanding of drug reward? Psychopharmacology (Berl) 153:31-43.

Barnes CA (1979) Memory deficits associated with senescence: a neurophysiological and behavioral study in the rat. J Comp Physiol Psychol 93:74-104.

Barr AM, Phillips AG (1999) Withdrawal following repeated exposure to d-amphetamine decreases responding for a sucrose solution as measured by a progressive ratio schedule of reinforcement. Psychopharmacology (Berl) 141:99-106.

Bartel MA, Weinstein JR, Schaffer DV (2012) Directed evolution of novel adeno-associated viruses for therapeutic gene delivery. Gene Ther 19:694-700.

Bauer M, Whybrow PC, Angst J, Versiani M, Moller HJ (2002) World Federation of Societies of Biological Psychiatry (WFSBP) Guidelines for Biological Treatment of Unipolar Depressive Disorders, Part 1: Acute and continuation treatment of major depressive disorder. World J Biol Psychiatry 3:5-43.

BECK AT, WARD CH, MENDELSON M, MOCK J, ERBAUGH J (1961) An inventory for measuring depression. Arch Gen Psychiatry 4:561-571.

Behan DP, De Souza EB, Lowry PJ, Potter E, Sawchenko P, Vale WW (1995) Corticotropin releasing factor (CRF) binding protein: a novel regulator of CRF and related peptides. Front Neuroendocrinol 16:362-382.

Belmaker RH (2004) Bipolar disorder. N Engl J Med 351:476-486.

Belmaker RH, Bersudsky Y (2004) Bipolar disorder: Mania and depression. Discov Med 4:239-245.

Belzung C, Pineau N, Beuzen A, Misslin R (1994) PD135158, a CCK-B antagonist, reduces "state," but not "trait" anxiety in mice. Pharmacol Biochem Behav 49:433-436.

Benabarre A, Vieta E, Colom F, Martinez-Aran A, Reinares M, Gasto C (2001) Bipolar disorder, schizoaffective disorder and schizophrenia: epidemiologic, clinical and prognostic differences. Eur Psychiatry 16:167-172.

Beneyto M, Kristiansen LV, Oni-Orisan A, McCullumsmith RE, Meador-Woodruff JH (2007) Abnormal glutamate receptor expression in the medial temporal lobe in schizophrenia and mood disorders. Neuropsychopharmacology 32:1888-1902.

Benoit SC, Thiele TE, Heinrichs SC, Rushing PA, Blake KA, Steeley RJ (2000) Comparison of central administration of corticotropin-releasing hormone and urocortin on food intake, conditioned taste aversion, and c-Fos expression. Peptides 21:345-351.

Berrettini WH (2000) Are schizophrenic and bipolar disorders related? A review of family and molecular studies. Biol Psychiatry 48:531-538.

Berridge MJ, Downes CP, Hanley MR (1989) Neural and developmental actions of lithium: a unifying hypothesis. Cell 59:411-419.

Berton O, Hahn CG, Thase ME (2012) Are we getting closer to valid translational models for major depression? Science 338:75-79.

Berton O, McClung CA, Dileone RJ, Krishnan V, Renthal W, Russo SJ, Graham D, Tsankova NM, Bolanos CA, Rios M, Monteggia LM, Self DW, Nestler EJ (2006) Essential role of BDNF in the mesolimbic dopamine pathway in social defeat stress. Science 311:864-868.

Berton O, Nestler EJ (2006) New approaches to antidepressant drug discovery: beyond monoamines. Nat Rev Neurosci 7:137-151.

Bessis N, GarciaCozar FJ, Boissier MC (2004) Immune responses to gene therapy vectors: influence on vector function and effector mechanisms. Gene Ther 11 Suppl 1:S10-S17.

Betley JN, Sternson SM (2011) Adeno-associated viral vectors for mapping, monitoring, and manipulating neural circuits. Hum Gene Ther 22:669-677.

Bhat S, Dao DT, Terrillion CE, Arad M, Smith RJ, Soldatov NM, Gould TD (2012) CACNA1C (Ca(v)1.2) in the pathophysiology of psychiatric disease. Prog Neurobiol.

Bi A, Cui J, Ma YP, Olshevskaya E, Pu M, Dizhoor AM, Pan ZH (2006) Ectopic expression of a microbial-type rhodopsin restores visual responses in mice with photoreceptor degeneration. Neuron 50:23-33.

Bienvenu OJ, Stein MB, Samuels JF, Onyike CU, Eaton WW, Nestadt G (2009) Personality disorder traits as predictors of subsequent first-onset panic disorder or agoraphobia. Compr Psychiatry 50:209-214.

Bigos KL, Mattay VS, Callicott JH, Straub RE, Vakkalanka R, Kolachana B, Hyde TM, Lipska BK, Kleinman JE, Weinberger DR (2010) Genetic variation in CACNA1C affects brain circuitries related to mental illness. Arch Gen Psychiatry 67:939-945.

Binder EB, Bradley RG, Liu W, Epstein MP, Deveau TC, Mercer KB, Tang Y, Gillespie CF, Heim CM, Nemeroff CB, Schwartz AC, Cubells JF, Ressler KJ (2008) Association of FKBP5 polymorphisms and childhood abuse with risk of posttraumatic stress disorder symptoms in adults. JAMA 299:1291-1305.

Binder EB, Nemeroff CB (2010) The CRF system, stress, depression and anxiety-insights from human genetic studies. Mol Psychiatry 15:574-588.

Bissette G, Klimek V, Pan J, Stockmeier C, Ordway G (2003) Elevated concentrations of CRF in the locus coeruleus of depressed subjects. Neuropsychopharmacology 28:1328-1335.

Bittencourt JC, Sawchenko PE (2000) Do centrally administered neuropeptides access cognate receptors?: an analysis in the central corticotropin-releasing factor system. J Neurosci 20:1142-1156.

Bittencourt JC, Vaughan J, Arias C, Rissman RA, Vale WW, Sawchenko PE (1999) Urocortin expression in rat brain: evidence against a pervasive relationship of urocortin-containing projections with targets bearing type 2 CRF receptors. J Comp Neurol 415:285-312.

Blank T, Nijholt I, Eckart K, Spiess J (2002) Priming of long-term potentiation in mouse hippocampus by corticotropin-releasing factor and acute stress: implications for hippocampus-dependent learning. J Neurosci 22:3788-3794.

Bonfiglio JJ, Inda C, Refojo D, Holsboer F, Arzt E, Silberstein S (2011) The corticotropin-releasing hormone network and the hypothalamic-pituitary-adrenal axis: molecular and cellular mechanisms involved. Neuroendocrinology 94:12-20.

Borkowska A, Rybakowski JK (2001) Neuropsychological frontal lobe tests indicate that bipolar depressed patients are more impaired than unipolar. Bipolar Disord 3:88-94.

Bourin M, Lambert O, Guitton B (2005) Treatment of acute mania--from clinical trials to recommendations for clinical practice. Hum Psychopharmacol 20:15-26.

Boyden ES, Zhang F, Bamberg E, Nagel G, Deisseroth K (2005) Millisecond-timescale, genetically targeted optical control of neural activity. Nat Neurosci 8:1263-1268.

Braff D, Stone C, Callaway E, Geyer M, Glick I, Bali L (1978) Prestimulus effects on human startle reflex in normals and schizophrenics. Psychophysiology 15:339-343.

Braff DL, Geyer MA, Swerdlow NR (2001) Human studies of prepulse inhibition of startle: normal subjects, patient groups, and pharmacological studies. Psychopharmacology (Berl) 156:234-258.

Braff DL, Swerdlow NR, Geyer MA (1999) Symptom correlates of prepulse inhibition deficits in male schizophrenic patients. Am J Psychiatry 156:596-602.

Branda CS, Dymecki SM (2004) Talking about a revolution: The impact of site-specific recombinases on genetic analyses in mice. Dev Cell 6:7-28.

Brar BK, Stephanou A, Knight R, Latchman DS (2002) Activation of protein kinase B/Akt by urocortin is essential for its ability to protect cardiac cells against hypoxia/reoxygenation-induced cell death. J Mol Cell Cardiol 34:483-492.

Breu J, Touma C, Holter SM, Knapman A, Wurst W, Deussing JM (2012) Urocortin 2 modulates aspects of social behaviour in mice. Behav Brain Res 233:331-336.

Britton DR, Varela M, Garcia A, Rosenthal M (1986) Dexamethasone suppresses pituitary-adrenal but not behavioral effects of centrally administered CRF. Life Sci 38:211-216.

Brotto LA, Gorzalka BB, Barr AM (2001) Paradoxical effects of chronic corticosterone on forced swim behaviours in aged male and female rats. Eur J Pharmacol 424:203-209.

Brown ES, Suppes T (1998) Mood symptoms during corticosteroid therapy: a review. Harv Rev Psychiatry 5:239-246.

Brown GW, Bifulco A, Harris TO (1987) Life events, vulnerability and onset of depression: some refinements. Br J Psychiatry 150:30-42.

Brown MT, Tan KR, O'Connor EC, Nikonenko I, Muller D, Luscher C (2012) Ventral tegmental area GABA projections pause accumbal cholinergic interneurons to enhance associative learning. Nature 492:452-456.

Bruijnzeel AW, Prado M, Isaac S (2009) Corticotropin-releasing factor-1 receptor activation mediates nicotine withdrawal-induced deficit in brain reward function and stress-induced relapse. Biol Psychiatry 66:110-117.

Buckley PF, Miller BJ, Lehrer DS, Castle DJ (2009) Psychiatric comorbidities and schizophrenia. Schizophr Bull 35:383-402.

Bunney WE, Bunney BG, Vawter MP, Tomita H, Li J, Evans SJ, Choudary PV, Myers RM, Jones EG, Watson SJ, Akil H (2003) Microarray technology: a review of new strategies to discover candidate vulnerability genes in psychiatric disorders. Am J Psychiatry 160:657-666.

Burcusa SL, Iacono WG (2007) Risk for recurrence in depression. Clin Psychol Rev 27:959-985.

Burger C, Gorbatyuk OS, Velardo MJ, Peden CS, Williams P, Zolotukhin S, Reier PJ, Mandel RJ, Muzyczka N (2004) Recombinant AAV viral vectors pseudotyped with viral capsids from serotypes 1, 2, and 5 display differential efficiency and cell tropism after delivery to different regions of the central nervous system. Mol Ther 10:302-317.

Buss C, Entringer S, Wadhwa PD (2012) Fetal programming of brain development: intrauterine stress and susceptibility to psychopathology. Sci Signal 5:t7.

Butler PD, Weiss JM, Stout JC, Nemeroff CB (1990) Corticotropin-releasing factor produces fear-enhancing and behavioral activating effects following infusion into the locus coeruleus. J Neurosci 10:176-183.

Buttgereit F, Burmester GR, Lipworth BJ (2009) Inflammation, glucocorticoids and risk of cardiovascular disease. Nat Clin Pract Rheumatol 5:18-19.

Calin-Jageman I, Lee A (2008) Ca(v)1 L-type Ca2+ channel signaling complexes in neurons. J Neurochem 105:573-583.

Cannon TD, Thompson PM, Van Erp TG, Toga AW, Poutanen VP, Huttunen M, Lonnqvist J, Standerskjold-Nordenstam CG, Narr KL, Khaledy M, Zoumalan CI, Dail R, Kaprio J (2002) Cortex mapping reveals regionally specific patterns of genetic and disease-specific gray-matter deficits in twins discordant for schizophrenia. Proc Natl Acad Sci U S A 99:3228-3233.

Cannon WB (1932) The Wisdom of the Body. New York: W.W. Norton & Company, Inc.

Cao JL, Covington HE, III, Friedman AK, Wilkinson MB, Walsh JJ, Cooper DC, Nestler EJ, Han MH (2010) Mesolimbic dopamine neurons in the brain reward circuit mediate susceptibility to social defeat and antidepressant action. J Neurosci 30:16453-16458.

Caputi A, Melzer S, Michael M, Monyer H (2013) The long and short of GABAergic neurons. Curr Opin Neurobiol 23:179-186.

Carpenter LL, Tyrka AR, McDougle CJ, Malison RT, Owens MJ, Nemeroff CB, Price LH (2004) Cerebrospinal fluid corticotropin-releasing factor and perceived early-life stress in depressed patients and healthy control subjects. Neuropsychopharmacology 29:777-784.

Carter ME, de LL (2011) Optogenetic investigation of neural circuits in vivo. Trends Mol Med 17:197-206.

Caspi A, Sugden K, Moffitt TE, Taylor A, Craig IW, Harrington H, McClay J, Mill J, Martin J, Braithwaite A, Poulton R (2003) Influence of life stress on depression: moderation by a polymorphism in the 5-HTT gene. Science 301:386-389.

Cavus I, Teyler T (1996) Two forms of long-term potentiation in area CA1 activate different signal transduction cascades. J Neurophysiol 76:3038-3047.

Cearley CN, Vandenberghe LH, Parente MK, Carnish ER, Wilson JM, Wolfe JH (2008) Expanded repertoire of AAV vector serotypes mediate unique patterns of transduction in mouse brain. Mol Ther 16:1710-1718.

Celano CM, Freudenreich O, Fernandez-Robles C, Stern TA, Caro MA, Huffman JC (2011) Depressogenic effects of medications: a review. Dialogues Clin Neurosci 13:109-125.

Chadman KK, Yang M, Crawley JN (2009) Criteria for validating mouse models of psychiatric diseases. Am J Med Genet B Neuropsychiatr Genet 150B:1-11.

Chamberlain SR, Robbins TW (2013) Noradrenergic modulation of cognition: therapeutic implications. J Psychopharmacol 27:694-718.

Chang CP, Pearse RV, O'Connell S, Rosenfeld MG (1993) Identification of a seven transmembrane helix receptor for corticotropin-releasing factor and sauvagine in mammalian brain. Neuron 11:1187-1195.

Chaudhury D, et al. (2013) Rapid regulation of depression-related behaviours by control of midbrain dopamine neurons. Nature 493:532-536.

Chen A, Blount A, Vaughan J, Brar B, Vale W (2004a) Urocortin II gene is highly expressed in mouse skin and skeletal muscle tissues: localization, basal expression in corticotropin-releasing factor receptor (CRFR) 1- and CRFR2-null mice, and regulation by glucocorticoids. Endocrinology 145:2445-2457.

Chen A, Zorrilla E, Smith S, Rousso D, Levy C, Vaughan J, Donaldson C, Roberts A, Lee KF, Vale W (2006) Urocortin 2-deficient mice exhibit gender-specific alterations in circadian hypothalamus-pituitary-adrenal axis and depressive-like behavior. J Neurosci 26:5500-5510.

Chen AM, Perrin MH, Digruccio MR, Vaughan JM, Brar BK, Arias CM, Lewis KA, Rivier JE, Sawchenko PE, Vale WW (2005) A soluble mouse brain splice variant of type 2alpha corticotropin-releasing factor (CRF) receptor binds ligands and modulates their activity. Proc Natl Acad Sci U S A 102:2620-2625.

Chen G, Henter ID, Manji HK (2010a) Translational research in bipolar disorder: emerging insights from genetically based models. Mol Psychiatry 15:883-895.

Chen JL, Villa KL, Cha JW, So PT, Kubota Y, Nedivi E (2012a) Clustered dynamics of inhibitory synapses and dendritic spines in the adult neocortex. Neuron 74:361-373.

Chen R, Lewis KA, Perrin MH, Vale WW (1993) Expression cloning of a human corticotropin-releasing-factor receptor. Proc Natl Acad Sci U S A 90:8967-8971.

Chen Y, Andres AL, Frotscher M, Baram TZ (2012b) Tuning synaptic transmission in the hippocampus by stress: the CRH system. Front Cell Neurosci 6:13.

Chen Y, Bender RA, Brunson KL, Pomper JK, Grigoriadis DE, Wurst W, Baram TZ (2004b) Modulation of dendritic differentiation by corticotropin-releasing factor in the developing hippocampus. Proc Natl Acad Sci U S A 101:15782-15787.

Chen Y, Brunson KL, Adelmann G, Bender RA, Frotscher M, Baram TZ (2004c) Hippocampal corticotropin releasing hormone: pre- and postsynaptic location and release by stress. Neuroscience 126:533-540.

Chen Y, Dube CM, Rice CJ, Baram TZ (2008) Rapid loss of dendritic spines after stress involves derangement of spine dynamics by corticotropin-releasing hormone. J Neurosci 28:2903-2911.

Chen Y, Kramar EA, Chen LY, Babayan AH, Andres AL, Gall CM, Lynch G, Baram TZ (2013a) Impairment of synaptic plasticity by the stress mediator CRH involves selective destruction of thin dendritic spines via RhoA signaling. Mol Psychiatry 18:485-496.

Chen Y, Rex CS, Rice CJ, Dube CM, Gall CM, Lynch G, Baram TZ (2010b) Correlated memory defects and hippocampal dendritic spine loss after acute stress involve corticotropin-releasing hormone signaling. Proc Natl Acad Sci U S A 107:13123-13128.

Chen Y, Xu M, De AR, Lovejoy DA (2013b) Teneurin C-terminal associated peptides (TCAP): modulators of corticotropin-releasing factor (CRF) physiology and behavior. Front Neurosci 7:166.

Chieng BC, Christie MJ, Osborne PB (2006) Characterization of neurons in the rat central nucleus of the amygdala: cellular physiology, morphology, and opioid sensitivity. J Comp Neurol 497:910-927.

Chiu CQ, Lur G, Morse TM, Carnevale NT, Ellis-Davies GC, Higley MJ (2013) Compartmentalization of GABAergic inhibition by dendritic spines. Science 340:759-762.

Choi DC, Furay AR, Evanson NK, Ostrander MM, Ulrich-Lai YM, Herman JP (2007) Bed nucleus of the stria terminalis subregions differentially regulate hypothalamic-pituitary-adrenal axis activity: implications for the integration of limbic inputs. J Neurosci 27:2025-2034.

Chrousos GP (2009) Stress and disorders of the stress system. Nat Rev Endocrinol 5:374-381.

Chuang TJ, Chen FC, Chen YZ (2012) Position-dependent correlations between DNA methylation and the evolutionary rates of mammalian coding exons. Proc Natl Acad Sci U S A 109:15841-15846.

Cohen JD, Servan-Schreiber D (1992) Context, cortex, and dopamine: a connectionist approach to behavior and biology in schizophrenia. Psychol Rev 99:45-77.

Cohen P, Frame S (2001) The renaissance of GSK3. Nat Rev Mol Cell Biol 2:769-776.

Cohen S, Janicki-Deverts D, Miller GE (2007) Psychological stress and disease. JAMA 298:1685-1687.

Cole BJ, Cador M, Stinus L, Rivier J, Vale W, Koob GF, Le MM (1990) Central administration of a CRF antagonist blocks the development of stress-induced behavioral sensitization. Brain Res 512:343-346.

Collins PY, et al. (2011) Grand challenges in global mental health. Nature 475:27-30.

Conrad CD, Galea LA, Kuroda Y, McEwen BS (1996) Chronic stress impairs rat spatial memory on the Y maze, and this effect is blocked by tianeptine pretreatment. Behav Neurosci 110:1321-1334.

Contarino A, Dellu F, Koob GF, Smith GW, Lee KF, Vale W, Gold LH (1999) Reduced anxiety-like and cognitive performance in mice lacking the corticotropin-releasing factor receptor 1. Brain Res 835:1-9.

Conway KP, Compton W, Stinson FS, Grant BF (2006) Lifetime comorbidity of DSM-IV mood and anxiety disorders and specific drug use disorders: results from the National Epidemiologic Survey on Alcohol and Related Conditions. J Clin Psychiatry 67:247-257.

Corcoran C, Walker E, Huot R, Mittal V, Tessner K, Kestler L, Malaspina D (2003) The stress cascade and schizophrenia: etiology and onset. Schizophr Bull 29:671-692.

Coste SC, Kesterson RA, Heldwein KA, Stevens SL, Heard AD, Hollis JH, Murray SE, Hill JK, Pantely GA, Hohimer AR, Hatton DC, Phillips TJ, Finn DA, Low MJ, Rittenberg MB, Stenzel P, Stenzel-Poore MP (2000) Abnormal adaptations to stress and impaired cardiovascular function in mice lacking corticotropin-releasing hormone receptor-2. Nat Genet 24:403-409.

Coste SC, Murray SE, Stenzel-Poore MP (2001) Animal models of CRH excess and CRH receptor deficiency display altered adaptations to stress. Peptides 22:733-741.

Coultrap SJ, Bayer KU (2012) CaMKII regulation in information processing and storage. Trends Neurosci 35:607-618.

Craddock N, O'Donovan MC, Owen MJ (2006) Genes for schizophrenia and bipolar disorder? Implications for psychiatric nosology. Schizophr Bull 32:9-16.

Craddock N, Owen MJ (2010a) Data and clinical utility should be the drivers of changes to psychiatric classification. Br J Psychiatry 197:158-159.

Craddock N, Owen MJ (2010b) The Kraepelinian dichotomy - going, going... but still not gone. Br J Psychiatry 196:92-95.

Cryan JF, Holmes A (2005) The ascent of mouse: advances in modelling human depression and anxiety. Nat Rev Drug Discov 4:775-790.

Cryan JF, Mombereau C (2004) In search of a depressed mouse: utility of models for studying depression-related behavior in genetically modified mice. Mol Psychiatry 9:326-357.

Cryan JF, Mombereau C, Vassout A (2005) The tail suspension test as a model for assessing antidepressant activity: review of pharmacological and genetic studies in mice. Neurosci Biobehav Rev 29:571-625.

Cubells JF, Price LH, Meyers BS, Anderson GM, Zabetian CP, Alexopoulos GS, Nelson JC, Sanacora G, Kirwin P, Carpenter L, Malison RT, Gelernter J (2002) Genotype-controlled analysis of plasma dopamine beta-hydroxylase activity in psychotic unipolar major depression. Biol Psychiatry 51:358-364.

Cullinan WE, Herman JP, Watson SJ (1993) Ventral subicular interaction with the hypothalamic paraventricular nucleus: evidence for a relay in the bed nucleus of the stria terminalis. J Comp Neurol 332:1-20.

Cummings S, Elde R, Ells J, Lindall A (1983) Corticotropin-releasing factor immunoreactivity is widely distributed within the central nervous system of the rat: an immunohistochemical study. J Neurosci 3:1355-1368.

Czeh B, Lucassen PJ (2007) What causes the hippocampal volume decrease in depression? Are neurogenesis, glial changes and apoptosis implicated? Eur Arch Psychiatry Clin Neurosci 257:250-260.

D'Hooge R, De Deyn PP (2001) Applications of the Morris water maze in the study of learning and memory. Brain Res Brain Res Rev 36:60-90.

Dabrowska J, Hazra R, Guo JD, Dewitt S, Rainnie DG (2013) Central CRF neurons are not created equal: phenotypic differences in CRF-containing neurons of the rat paraventricular hypothalamus and the bed nucleus of the stria terminalis. Front Neurosci 7:156.

Danielian PS, Muccino D, Rowitch DH, Michael SK, McMahon AP (1998) Modification of gene activity in mouse embryos in utero by a tamoxifen-inducible form of Cre recombinase. Curr Biol 8:1323-1326.

Dao DT, Mahon PB, Cai X, Kovacsics CE, Blackwell RA, Arad M, Shi J, Zandi PP, O'Donnell P, Knowles JA, Weissman MM, Coryell W, Scheftner WA, Lawson WB, Levinson DF, Thompson SM, Potash JB, Gould TD (2010) Mood disorder susceptibility gene CACNA1C modifies mood-related behaviors in mice and interacts with sex to influence behavior in mice and diagnosis in humans. Biol Psychiatry 68:801-810.

Dautzenberg FM, Hauger RL (2002) The CRF peptide family and their receptors: yet more partners discovered. Trends Pharmacol Sci 23:71-77.

David DJ, Samuels BA, Rainer Q, Wang JW, Marsteller D, Mendez I, Drew M, Craig DA, Guiard BP, Guilloux JP, Artymyshyn RP, Gardier AM, Gerald C, Antonijevic IA, Leonardo ED, Hen R (2009) Neurogenesis-dependent and -independent effects of fluoxetine in an animal model of anxiety/depression. Neuron 62:479-493.

Davidson BL, Breakefield XO (2003) Viral vectors for gene delivery to the nervous system. Nat Rev Neurosci 4:353-364.

Davies MN, Volta M, Pidsley R, Lunnon K, Dixit A, Lovestone S, Coarfa C, Harris RA, Milosavljevic A, Troakes C, Al-Sarraj S, Dobson R, Schalkwyk LC, Mill J (2012) Functional annotation of the human brain methylome identifies tissue-specific epigenetic variation across brain and blood. Genome Biol 13:R43.

Davis CA, Joyner AL (1988) Expression patterns of the homeo box-containing genes En-1 and En-2 and the proto-oncogene int-1 diverge during mouse development. Genes Dev 2:1736-1744.

Davis M (1990) Animal models of anxiety based on classical conditioning: the conditioned emotional response (CER) and the fear-potentiated startle effect. Pharmacol Ther 47:147-165.

Day HE, Curran EJ, Watson SJ, Jr., Akil H (1999) Distinct neurochemical populations in the rat central nucleus of the amygdala and bed nucleus of the stria terminalis: evidence for their selective activation by interleukin-1beta. J Comp Neurol 413:113-128.

de Kloet ER (2004) Hormones and the stressed brain. Ann N Y Acad Sci 1018:1-15.

de Kloet ER, Joels M, Holsboer F (2005a) Stress and the brain: from adaptation to disease. Nat Rev Neurosci 6:463-475.

de Kloet ER, Sibug RM, Helmerhorst FM, Schmidt MV (2005b) Stress, genes and the mechanism of programming the brain for later life. Neurosci Biobehav Rev 29:271-281.

DeBold CR, Sheldon WR, DeCherney GS, Jackson RV, Alexander AN, Vale W, Rivier J, Orth DN (1984) Arginine vasopressin potentiates adrenocorticotropin release induced by ovine corticotropin-releasing factor. J Clin Invest 73:533-538.

Dedic N, Walser S, Deussing J (2011) Mouse Models of Depression, Psychiatric Disorders - Trends and Developments, Toru Uehara (Ed.). ISBN: 978-953-307-745-1.

DeFelipe J, et al. (2013) New insights into the classification and nomenclature of cortical GABAergic interneurons. Nat Rev Neurosci 14:202-216.

Dehpour AR, Sadr SS, Azizi MR, Namiranian K, Farahani M, Javidan AN (2002) Lithium inhibits the development of physical dependence to clonidine in mice. Pharmacol Toxicol 90:89-93.

Deisseroth K (2010) Controlling the brain with light. Sci Am 303:48-55.

Deisseroth K (2011) Optogenetics. Nat Methods 8:26-29.

Deisseroth K (2014) Circuit dynamics of adaptive and maladaptive behaviour. Nature 505:309-317.

Deisseroth K, Feng G, Majewska AK, Miesenbock G, Ting A, Schnitzer MJ (2006) Next-generation optical technologies for illuminating genetically targeted brain circuits. J Neurosci 26:10380-10386.

Dellu F, Contarino A, Simon H, Koob GF, Gold LH (2000) Genetic differences in response to novelty and spatial memory using a two-trial recognition task in mice. Neurobiol Learn Mem 73:31-48.

Demeulemeester H, Vandesande F, Orban GA, Brandon C, Vanderhaeghen JJ (1988) Heterogeneity of GABAergic cells in cat visual cortex. J Neurosci 8:988-1000.

Deussing JM (2006) Animal models of depression. Drug discovery today 3:375-383.

Deussing JM (2013) Targeted mutagenesis tools for modelling psychiatric disorders. Cell Tissue Res 354:9-25.

Deussing JM, Breu J, Kuhne C, Kallnik M, Bunck M, Glasl L, Yen YC, Schmidt MV, Zurmuhlen R, Vogl AM, Gailus-Durner V, Fuchs H, Holter SM, Wotjak CT, Landgraf R, de Angelis MH, Holsboer F, Wurst W (2010) Urocortin 3 modulates social discrimination abilities via corticotropin-releasing hormone receptor type 2. J Neurosci 30:9103-9116.

Deussing JM, Wurst W (2005) Dissecting the genetic effect of the CRH system on anxiety and stress-related behaviour. Comptes Rendus Biologies 328:199-212.

Deutch AY (2006) Striatal plasticity in parkinsonism: dystrophic changes in medium spiny neurons and progression in Parkinson's disease. J Neural Transm Suppl67-70.

Diamant M, De WD (1991) Autonomic and behavioral effects of centrally administered corticotropin-releasing factor in rats. Endocrinology 129:446-454.

Dias BG, Ressler KJ (2014) Parental olfactory experience influences behavior and neural structure in subsequent generations. Nat Neurosci 17:89-96.

Dine J, Ionescu IA, Stepan J, Yen YC, Holsboer F, Landgraf R, Eder M, Schmidt U (2013) Identification of a role for the ventral hippocampus in neuropeptide S-elicited anxiolysis. PLoS One 8:e60219.

Ding JH, Sha LL, Chang J, Zhou XQ, Fan Y, Hu G (2007) Alterations of striatal neurotransmitter release in aquaporin-4 deficient mice: An in vivo microdialysis study. Neurosci Lett 422:175-180.

Dirks A, Groenink L, Bouwknecht JA, Hijzen TH, Van Der GJ, Ronken E, Verbeek JS, Veening JG, Dederen PJ, Korosi A, Schoolderman LF, Roubos EW, Olivier B (2002a) Overexpression of corticotropin-releasing hormone in transgenic mice and chronic stress-like autonomic and physiological alterations. Eur J Neurosci 16:1751-1760.

Dirks A, Groenink L, Schipholt MI, Van Der GJ, Hijzen TH, Geyer MA, Olivier B (2002b) Reduced startle reactivity and plasticity in transgenic mice overexpressing corticotropin-releasing hormone. Biol Psychiatry 51:583-590.

Dirks A, Groenink L, Verdouw MP., Schipholt M., Gugten Jvd, Hijzen T, Olivier B (2001) Behavioural analysis of transgenic mice overexpressing corticotropin-releasing hormone in paradigms emulating aspects of stress, anxiety, and depression. International Journal of Comparative Psychology123-135.

Dong HW, Petrovich GD, Watts AG, Swanson LW (2001) Basic organization of projections from the oval and fusiform nuclei of the bed nuclei of the stria terminalis in adult rat brain. J Comp Neurol 436:430-455.

Dong HW, Swanson LW (2004) Organization of axonal projections from the anterolateral area of the bed nuclei of the stria terminalis. J Comp Neurol 468:277-298.

Dong HW, Swanson LW (2006) Projections from bed nuclei of the stria terminalis, anteromedial area: cerebral hemisphere integration of neuroendocrine, autonomic, and behavioral aspects of energy balance. J Comp Neurol 494:142-178.

Doyon C, Samson P, Lalonde J, Richard D (2007) Effects of the CRF1 receptor antagonist SSR125543 on energy balance and food deprivation-induced neuronal activation in obese Zucker rats. J Endocrinol 193:11-19.

Drossopoulou G, Antoniou K, Kitraki E, Papathanasiou G, Papalexi E, Dalla C, Papadopoulou-Daifoti Z (2004) Sex differences in behavioral, neurochemical and neuroendocrine effects induced by the forced swim test in rats. Neuroscience 126:849-857.

Dubois NC, Hofmann D, Kaloulis K, Bishop JM, Trumpp A (2006) Nestin-Cre transgenic mouse line Nes-Cre1 mediates highly efficient Cre/loxP mediated recombination in the nervous system, kidney, and somite-derived tissues. Genesis 44:355-360.

Ducottet C, Griebel G, Belzung C (2003) Effects of the selective nonpeptide corticotropin-releasing factor receptor 1 antagonist antalarmin in the chronic mild stress model of depression in mice. Prog Neuropsychopharmacol Biol Psychiatry 27:625-631.

Duman RS (2005) Neurotrophic factors and regulation of mood: role of exercise, diet and metabolism. Neurobiol Aging 26 Suppl 1:88-93.

Dumitriu D, Cossart R, Huang J, Yuste R (2007) Correlation between axonal morphologies and synaptic input kinetics of interneurons from mouse visual cortex. Cereb Cortex 17:81-91.

Dunlop BW, Nemeroff CB (2007) The role of dopamine in the pathophysiology of depression. Arch Gen Psychiatry 64:327-337.

Dunn AJ, Berridge CW (1990) Physiological and behavioral responses to corticotropin-releasing factor administration: is CRF a mediator of anxiety or stress responses? Brain Res Brain Res Rev 15:71-100.

Dunn AJ, File SE (1987) Corticotropin-releasing factor has an anxiogenic action in the social interaction test. Horm Behav 21:193-202.

Dunner DL, Patrick V, Fieve RR (1979) Life events at the onset of bipolar affective illness. Am J Psychiatry 136:508-511.

Eastwood SL, Harrison PJ (2010) Markers of glutamate synaptic transmission and plasticity are increased in the anterior cingulate cortex in bipolar disorder. Biol Psychiatry 67:1010-1016.

Eaves M, Thatcher-Britton K, Rivier J, Vale W, Koob GF (1985) Effects of corticotropin releasing factor on locomotor activity in hypophysectomized rats. Peptides 6:923-926.

Egli RE, Winder DG (2003) Dorsal and ventral distribution of excitable and synaptic properties of neurons of the bed nucleus of the stria terminalis. J Neurophysiol 90:405-414.

Ehlers CL, Frank E, Kupfer DJ (1988) Social zeitgebers and biological rhythms. A unified approach to understanding the etiology of depression. Arch Gen Psychiatry 45:948-952.

Einat H, Manji HK (2006) Cellular plasticity cascades: genes-to-behavior pathways in animal models of bipolar disorder. Biol Psychiatry 59:1160-1171.

Elgersma Y, Fedorov NB, Ikonen S, Choi ES, Elgersma M, Carvalho OM, Giese KP, Silva AJ (2002) Inhibitory autophosphorylation of CaMKII controls PSD association, plasticity, and learning. Neuron 36:493-505.

Elgersma Y, Sweatt JD, Giese KP (2004) Mouse genetic approaches to investigating calcium/calmodulin-dependent protein kinase II function in plasticity and cognition. J Neurosci 24:8410-8415.

Elliott E, Ezra-Nevo G, Regev L, Neufeld-Cohen A, Chen A (2010) Resilience to social stress coincides with functional DNA methylation of the Crf gene in adult mice. Nat Neurosci 13:1351-1353.

Enes J, Langwieser N, Ruschel J, Carballosa-Gonzalez MM, Klug A, Traut MH, Ylera B, Tahirovic S, Hofmann F, Stein V, Moosmang S, Hentall ID, Bradke F (2010) Electrical activity suppresses axon growth through Ca(v)1.2 channels in adult primary sensory neurons. Curr Biol 20:1154-1164.

Engblom D, Bilbao A, Sanchis-Segura C, Dahan L, Perreau-Lenz S, Balland B, Parkitna JR, Lujan R, Halbout B, Mameli M, Parlato R, Sprengel R, Luscher C, Schutz G, Spanagel R (2008) Glutamate receptors on dopamine neurons control the persistence of cocaine seeking. Neuron 59:497-508.

Erb S, Stewart J (1999) A role for the bed nucleus of the stria terminalis, but not the amygdala, in the effects of corticotropin-releasing factor on stress-induced reinstatement of cocaine seeking. J Neurosci 19:RC35.

Erdmann G, Schutz G, Berger S (2007) Inducible gene inactivation in neurons of the adult mouse forebrain. BMC Neurosci 8:63.

Erk S, Meyer-Lindenberg A, Schnell K, Opitz von BC, Esslinger C, Kirsch P, Grimm O, Arnold C, Haddad L, Witt SH, Cichon S, Nothen MM, Rietschel M, Walter H (2010) Brain function in carriers of a genome-wide supported bipolar disorder variant. Arch Gen Psychiatry 67:803-811.

Erondu NE, Kennedy MB (1985) Regional distribution of type II Ca2+/calmodulin-dependent protein kinase in rat brain. J Neurosci 5:3270-3277.

Etkin A, Egner T, Kalisch R (2011) Emotional processing in anterior cingulate and medial prefrontal cortex. Trends Cogn Sci 15:85-93.

Evans RT, Seasholtz AF (2009) Soluble corticotropin-releasing hormone receptor 2alpha splice variant is efficiently translated but not trafficked for secretion. Endocrinology 150:4191-4202.

Facci L, Stevens DA, Pangallo M, Franceschini D, Skaper SD, Strijbos PJ (2003) Corticotropin-releasing factor (CRF) and related peptides confer neuroprotection via type 1 CRF receptors. Neuropharmacology 45:623-636.

Fan Y, Zhang J, Sun XL, Gao L, Zeng XN, Ding JH, Cao C, Niu L, Hu G (2005) Sex- and region-specific alterations of basal amino acid and monoamine metabolism in the brain of aquaporin-4 knockout mice. J Neurosci Res 82:458-464.

Fanselow MS (1980) Conditioned and unconditional components of post-shock freezing. Pavlov J Biol Sci 15:177-182.

Feil R, Brocard J, Mascrez B, LeMeur M, Metzger D, Chambon P (1996) Ligand-activated site-specific recombination in mice. Proc Natl Acad Sci U S A 93:10887-10890.

Fekete EM, Zorrilla EP (2007) Physiology, pharmacology, and therapeutic relevance of urocortins in mammals: ancient CRF paralogs. Front Neuroendocrinol 28:1-27.

Fendt M, Fanselow MS (1999) The neuroanatomical and neurochemical basis of conditioned fear. Neurosci Biobehav Rev 23:743-760.

Fenoglio KA, Brunson KL, Baram TZ (2006) Hippocampal neuroplasticity induced by early-life stress: functional and molecular aspects. Front Neuroendocrinol 27:180-192.

Fernando AB, Robbins TW (2011) Animal models of neuropsychiatric disorders. Annu Rev Clin Psychol 7:39-61.

Ferreira MA, et al. (2008) Collaborative genome-wide association analysis supports a role for ANK3 and CACNA1C in bipolar disorder. Nat Genet 40:1056-1058.

Flandreau EI, Ressler KJ, Owens MJ, Nemeroff CB (2011) Chronic overexpression of corticotropin-releasing factor from the central amygdala produces HPA axis hyperactivity and behavioral anxiety associated with gene-expression changes in the hippocampus and paraventricular nucleus of the hypothalamus. Psychoneuroendocrinology.

Fleck DE, Shear PK, Zimmerman ME, Getz GE, Corey KB, Jak A, Lebowitz BK, Strakowski SM (2003) Verbal memory in mania: effects of clinical state and task requirements. Bipolar Disord 5:375-380.

Flood DG, Choinski M, Marino MJ, Gasior M (2009) Mood stabilizers increase prepulse inhibition in DBA/2NCrl mice. Psychopharmacology (Berl) 205:369-377.

Fone KC, Porkess MV (2008) Behavioural and neurochemical effects of post-weaning social isolation in rodents-relevance to developmental neuropsychiatric disorders. Neurosci Biobehav Rev 32:1087-1102.

Foote SL, Aston-Jones G, Bloom FE (1980) Impulse activity of locus coeruleus neurons in awake rats and monkeys is a function of sensory stimulation and arousal. Proc Natl Acad Sci U S A 77:3033-3037.

Fossey MD, Lydiard RB, Ballenger JC, Laraia MT, Bissette G, Nemeroff CB (1996) Cerebrospinal fluid corticotropin-releasing factor concentrations in patients with anxiety disorders and normal comparison subjects. Biol Psychiatry 39:703-707.

Foster TC (2012) Dissecting the age-related decline on spatial learning and memory tasks in rodent models: N-methyl-D-aspartate receptors and voltage-dependent Ca2+ channels in senescent synaptic plasticity. Prog Neurobiol 96:283-303.

Foster TC, Norris CM (1997) Age-associated changes in Ca(2+)-dependent processes: relation to hippocampal synaptic plasticity. Hippocampus 7:602-612.

Fremeau RT, Jr., Duncan GE, Fornaretto MG, Dearry A, Gingrich JA, Breese GR, Caron MG (1991) Localization of D1 dopamine receptor mRNA in brain supports a role in cognitive, affective, and neuroendocrine aspects of dopaminergic neurotransmission. Proc Natl Acad Sci U S A 88:3772-3776.

Fremeau RT, Jr., Kam K, Qureshi T, Johnson J, Copenhagen DR, Storm-Mathisen J, Chaudhry FA, Nicoll RA, Edwards RH (2004) Vesicular glutamate transporters 1 and 2 target to functionally distinct synaptic release sites. Science 304:1815-1819.

Fremeau RT, Jr., Troyer MD, Pahner I, Nygaard GO, Tran CH, Reimer RJ, Bellocchio EE, Fortin D, Storm-Mathisen J, Edwards RH (2001) The expression of vesicular glutamate transporters defines two classes of excitatory synapse. Neuron 31:247-260.

Freund TF, Buzsaki G (1996) Interneurons of the hippocampus. Hippocampus 6:347-470.

Furay AR, Bruestle AE, Herman JP (2008) The role of the forebrain glucocorticoid receptor in acute and chronic stress. Endocrinology 149:5482-5490.

Fuxe K, Borroto-Escuela DO, Romero-Fernandez W, Zhang WB, Agnati LF (2013) Volume transmission and its different forms in the central nervous system. Chin J Integr Med 19:323-329.

Gaj T, Gersbach CA, Barbas CF, III (2013) ZFN, TALEN, and CRISPR/Cas-based methods for genome engineering. Trends Biotechnol 31:397-405.

Gallagher JP, Orozco-Cabal LF, Liu J, Shinnick-Gallagher P (2008) Synaptic physiology of central CRH system. Eur J Pharmacol 583:215-225.

Gallopin T, Geoffroy H, Rossier J, Lambolez B (2006) Cortical sources of CRF, NKB, and CCK and their effects on pyramidal cells in the neocortex. Cereb Cortex 16:1440-1452.

Gangarossa G, Longueville S, De BD, Perroy J, Herve D, Girault JA, Valjent E (2012) Characterization of dopamine D1 and D2 receptor-expressing neurons in the mouse hippocampus. Hippocampus 22:2199-2207.

Garcia-Caceres C, Lagunas N, Calmarza-Font I, Azcoitia I, Diz-Chaves Y, Garcia-Segura LM, Baquedano E, Frago LM, Argente J, Chowen JA (2010) Gender differences in the long-term effects of chronic prenatal stress on the HPA axis and hypothalamic structure in rats. Psychoneuroendocrinology 35:1525-1535.

Garcia-Lecumberri C, Ambrosio E (2000) Differential effect of low doses of intracerebroventricular corticotropin-releasing factor in forced swimming test. Pharmacol Biochem Behav 67:519-525.

Gaveriaux-Ruff C, Kieffer BL (2007) Conditional gene targeting in the mouse nervous system: Insights into brain function and diseases. Pharmacol Ther 113:619-634.

Geisler S, Zahm DS (2005) Afferents of the ventral tegmental area in the rat-anatomical substratum for integrative functions. J Comp Neurol 490:270-294.

George O, Le MM, Koob GF (2012) Allostasis and addiction: role of the dopamine and corticotropin-releasing factor systems. Physiol Behav 106:58-64.

Georges F, Aston-Jones G (2002) Activation of ventral tegmental area cells by the bed nucleus of the stria terminalis: a novel excitatory amino acid input to midbrain dopamine neurons. J Neurosci 22:5173-5187.

Gerfen CR, Surmeier DJ (2011) Modulation of striatal projection systems by dopamine. Annu Rev Neurosci 34:441-466.

Gershon ES, Grennan K, Busnello J, Badner JA, Ovsiew F, Memon S, liey-Rodriguez N, Cooper J, Romanos B, Liu C (2013) A rare mutation of CACNA1C in a patient with bipolar disorder, and decreased gene expression associated with a bipolar-associated common SNP of CACNA1C in brain. Mol Psychiatry.

Geyer MA, Krebs-Thomson K, Braff DL, Swerdlow NR (2001) Pharmacological studies of prepulse inhibition models of sensorimotor gating deficits in schizophrenia: a decade in review. Psychopharmacology (Berl) 156:117-154.

Giesbrecht CJ, Mackay JP, Silveira HB, Urban JH, Colmers WF (2010) Countervailing modulation of Ih by neuropeptide Y and corticotrophin-releasing factor in basolateral amygdala as a possible mechanism for their effects on stress-related behaviors. J Neurosci 30:16970-16982.

Gillespie CF, Nemeroff CB (2005) Hypercortisolemia and depression. Psychosom Med 67 Suppl 1:S26-S28.

Gilmor ML, Skelton KH, Nemeroff CB, Owens MJ (2003) The effects of chronic treatment with the mood stabilizers valproic acid and lithium on corticotropin-releasing factor neuronal systems. J Pharmacol Exp Ther 305:434-439.

Giros B, Jaber M, Jones SR, Wightman RM, Caron MG (1996) Hyperlocomotion and indifference to cocaine and amphetamine in mice lacking the dopamine transporter. Nature 379:606-612.

Gjerris A, Werdelin L, Rafaelsen OJ, Alling C, Christensen NJ (1987) CSF dopamine increased in depression: CSF dopamine, noradrenaline and their metabolites in depressed patients and in controls. J Affect Disord 13:279-286.

Goebbels S, Bormuth I, Bode U, Hermanson O, Schwab MH, Nave KA (2006) Genetic targeting of principal neurons in neocortex and hippocampus of NEX-Cre mice. Genesis 44:611-621.

Gold PW, Chrousos GP (2002) Organization of the stress system and its dysregulation in melancholic and atypical depression: high vs low CRH/NE states. Mol Psychiatry 7:254-275.

Golden SA, Covington HE, III, Berton O, Russo SJ (2011) A standardized protocol for repeated social defeat stress in mice. Nat Protoc 6:1183-1191.

Golub Y, Mauch CP, Dahlhoff M, Wotjak CT (2009) Consequences of extinction training on associative and non-associative fear in a mouse model of Posttraumatic Stress Disorder (PTSD). Behav Brain Res 205:544-549.

Gong S, Doughty M, Harbaugh CR, Cummins A, Hatten ME, Heintz N, Gerfen CR (2007) Targeting Cre recombinase to specific neuron populations with bacterial artificial chromosome constructs. J Neurosci 27:9817-9823.

Goodwin FK, Jamison KR (2007) Manic-Depressive Illness: Bipolar and Recurrent Unipolar Disorders. New York: Oxford University Press.

Goodwin FK, Post RM, Dunner DL, Gordon EK (1973) Cerebrospinal fluid amine metabolites in affective illness: the probenecid technique. Am J Psychiatry 130:73-79.

Goshen I, Brodsky M, Prakash R, Wallace J, Gradinaru V, Ramakrishnan C, Deisseroth K (2011) Dynamics of retrieval strategies for remote memories. Cell 147:678-689.

Gossen M, Bujard H (1992) Tight control of gene expression in mammalian cells by tetracycline-responsive promoters. Proc Natl Acad Sci U S A 89:5547-5551.

Goto Y, Grace AA (2007) The dopamine system and the pathophysiology of schizophrenia: a basic science perspective. Int Rev Neurobiol 78:41-68.

Goto Y, Otani S, Grace AA (2007) The Yin and Yang of dopamine release: a new perspective. Neuropharmacology 53:583-587.

Gould TD, Gottesman II (2006) Psychiatric endophenotypes and the development of valid animal models. Genes Brain Behav 5:113-119.

Gourley SL, Wu FJ, Kiraly DD, Ploski JE, Kedves AT, Duman RS, Taylor JR (2008) Regionally specific regulation of ERK MAP kinase in a model of antidepressant-sensitive chronic depression. Biol Psychiatry 63:353-359.

Grammatopoulos DK (2012) Insights into mechanisms of corticotropin-releasing hormone receptor signal transduction. Br J Pharmacol 166:85-97.

Grandjean EM, Aubry JM (2009) Lithium: updated human knowledge using an evidence-based approach: Part I: Clinical efficacy in bipolar disorder. CNS Drugs 23:225-240.

Green EK, Grozeva D, Jones I, Jones L, Kirov G, Caesar S, Gordon-Smith K, Fraser C, Forty L, Russell E, Hamshere ML, Moskvina V, Nikolov I, Farmer A, McGuffin P, Holmans PA, Owen MJ, O'Donovan MC, Craddock N (2010) The bipolar disorder risk allele at CACNA1C also confers risk of recurrent major depression and of schizophrenia. Mol Psychiatry 15:1016-1022.

Greene CM, Flannery O, Soto D (2014) Distinct parietal sites mediate the influences of mood, arousal, and their interaction on human recognition memory. Cogn Affect Behav Neurosci.

Gregus A, Wintink AJ, Davis AC, Kalynchuk LE (2005) Effect of repeated corticosterone injections and restraint stress on anxiety and depression-like behavior in male rats. Behav Brain Res 156:105-114.

Griebel G, Belzung C, Misslin R, Vogel E (1993) The free-exploratory paradigm: an effective method for measuring neophobic behaviour in mice and testing potential neophobia-reducing drugs. Behav Pharmacol 4:637-644.

Griebel G, Simiand J, Steinberg R, Jung M, Gully D, Roger P, Geslin M, Scatton B, Maffrand JP, Soubrie P (2002) 4-(2-Chloro-4-methoxy-5-methylphenyl)-N-[(1S)-2-cyclopropyl-1-(3-fluoro-4-methylp henyl)ethyl]5-methyl-N-(2-propynyl)-1, 3-thiazol-2-amine hydrochloride (SSR125543A), a potent and selective corticotrophin-releasing factor(1) receptor antagonist. II. Characterization in rodent models of stress-related disorders. J Pharmacol Exp Ther 301:333-345.

Grinevich V, Brecht M, Osten P (2005) Monosynaptic pathway from rat vibrissa motor cortex to facial motor neurons revealed by lentivirus-based axonal tracing. J Neurosci 25:8250-8258.

Groeneweg FL, Karst H, de Kloet ER, Joels M (2012) Mineralocorticoid and glucocorticoid receptors at the neuronal membrane, regulators of nongenomic corticosteroid signalling. Mol Cell Endocrinol 350:299-309.

Groenink L, Dirks A, Verdouw PM, de GM, Peeters BW, Millan MJ, Olivier B (2008) CRF1 not glucocorticoid receptors mediate prepulse inhibition deficits in mice overexpressing CRF. Biol Psychiatry 63:360-368.

Groenink L, Dirks A, Verdouw PM, Schipholt M, Veening JG, Van Der GJ, Olivier B (2002) HPA axis dysregulation in mice overexpressing corticotropin releasing hormone. Biol Psychiatry 51:875-881.

Grover LM, Teyler TJ (1990) Differential effects of NMDA receptor antagonist APV on tetanic stimulation induced and calcium induced potentiation. Neurosci Lett 113:309-314.

Groves JO (2007) Is it time to reassess the BDNF hypothesis of depression? Mol Psychiatry 12:1079-1088.

Guidotti A, Auta J, Davis JM, Di-Giorgi-Gerevini V, Dwivedi Y, Grayson DR, Impagnatiello F, Pandey G, Pesold C, Sharma R, Uzunov D, Costa E (2000) Decrease in reelin and glutamic acid decarboxylase67 (GAD67) expression in schizophrenia and bipolar disorder: a postmortem brain study. Arch Gen Psychiatry 57:1061-1069.

Gunaydin LA, Yizhar O, Berndt A, Sohal VS, Deisseroth K, Hegemann P (2010) Ultrafast optogenetic control. Nat Neurosci 13:387-392.

Gunnar M, Quevedo K (2007) The neurobiology of stress and development. Annu Rev Psychol 58:145-173.

Haass-Koffler CL, Bartlett SE (2012) Stress and addiction: contribution of the corticotropin releasing factor (CRF) system in neuroplasticity. Front Mol Neurosci 5:91.

Habib KE, Weld KP, Rice KC, Pushkas J, Champoux M, Listwak S, Webster EL, Atkinson AJ, Schulkin J, Contoreggi C, Chrousos GP, McCann SM, Suomi SJ, Higley JD, Gold PW (2000) Oral administration of a corticotropin-releasing hormone receptor antagonist significantly attenuates behavioral, neuroendocrine, and autonomic responses to stress in primates. Proc Natl Acad Sci U S A 97:6079-6084.

Haenisch B, Bilkei-Gorzo A, Caron MG, Bonisch H (2009) Knockout of the norepinephrine transporter and pharmacologically diverse antidepressants prevent behavioral and brain neurotrophin alterations in two chronic stress models of depression. J Neurochem 111:403-416.

Haenisch B, Bonisch H (2011) Depression and antidepressants: insights from knockout of dopamine, serotonin or noradrenaline re-uptake transporters. Pharmacol Ther 129:352-368.

Hammack SE, Mania I, Rainnie DG (2007) Differential expression of intrinsic membrane currents in defined cell types of the anterolateral bed nucleus of the stria terminalis. J Neurophysiol 98:638-656.

Hammen C (2006) Stress generation in depression: reflections on origins, research, and future directions. J Clin Psychol 62:1065-1082.

Hamshere ML, et al. (2013) Genome-wide significant associations in schizophrenia to ITIH3/4, CACNA1C and SDCCAG8, and extensive replication of associations reported by the Schizophrenia PGC. Mol Psychiatry 18:708-712.

Han K, Holder JL, Jr., Schaaf CP, Lu H, Chen H, Kang H, Tang J, Wu Z, Hao S, Cheung SW, Yu P, Sun H, Breman AM, Patel A, Lu HC, Zoghbi HY (2013) SHANK3 overexpression causes manic-like behaviour with unique pharmacogenetic properties. Nature 503:72-77.

Handley SL, Mithani S (1984) Effects of alpha-adrenoceptor agonists and antagonists in a maze-exploration model of 'fear'-motivated behaviour. Naunyn Schmiedebergs Arch Pharmacol 327:1-5.

Harris JA, Oh SW, Zeng H (2012) Adeno-associated viral vectors for anterograde axonal tracing with fluorescent proteins in nontransgenic and cre driver mice. Curr Protoc Neurosci Chapter 1:Unit-18.

Hartmann J, Wagner KV, Dedic N, Marinescu D, Scharf SH, Wang XD, Deussing JM, Hausch F, Rein T, Schmidt U, Holsboer F, Muller MB, Schmidt MV (2012a) Fkbp52 heterozygosity alters behavioral, endocrine and neurogenetic parameters under basal and chronic stress conditions in mice. Psychoneuroendocrinology.

Hartmann J, Wagner KV, Liebl C, Scharf SH, Wang XD, Wolf M, Hausch F, Rein T, Schmidt U, Touma C, Cheung-Flynn J, Cox MB, Smith DF, Holsboer F, Muller MB, Schmidt MV (2012b) The involvement of FK506-binding protein 51 (FKBP5) in the behavioral and neuroendocrine effects of chronic social defeat stress. Neuropharmacology 62:332-339.

Hasan MT, Schonig K, Berger S, Graewe W, Bujard H (2001) Long-term, noninvasive imaging of regulated gene expression in living mice. Genesis 29:116-122.

Hascoet M, Bourin M, Nic Dhonnchadha BA (2001) The mouse light-dark paradigm: a review. Prog Neuropsychopharmacol Biol Psychiatry 25:141-166.

Hashimoto K, Sawa A, Iyo M (2007) Increased levels of glutamate in brains from patients with mood disorders. Biol Psychiatry 62:1310-1316.

Hasler G, Drevets WC, Gould TD, Gottesman II, Manji HK (2006) Toward constructing an endophenotype strategy for bipolar disorders. Biol Psychiatry 60:93-105.

Hasler G, Drevets WC, Manji HK, Charney DS (2004) Discovering endophenotypes for major depression. Neuropsychopharmacology 29:1765-1781.

Haubensak W, Kunwar PS, Cai H, Ciocchi S, Wall NR, Ponnusamy R, Biag J, Dong HW, Deisseroth K, Callaway EM, Fanselow MS, Luthi A, Anderson DJ (2010) Genetic dissection of an amygdala microcircuit that gates conditioned fear. Nature 468:270-276.

Hauger RL, Risbrough V, Brauns O, Dautzenberg FM (2006) Corticotropin releasing factor (CRF) receptor signaling in the central nervous system: new molecular targets. CNS Neurol Disord Drug Targets 5:453-479.

Hazra R, Guo JD, Ryan SJ, Jasnow AM, Dabrowska J, Rainnie DG (2011) A transcriptomic analysis of type I-III neurons in the bed nucleus of the stria terminalis. Mol Cell Neurosci 46:699-709.

Heard E, Martienssen RA (2014) Transgenerational epigenetic inheritance: myths and mechanisms. Cell 157:95-109.

Heinrichs SC, Joppa M (2001) Dissociation of arousal-like from anxiogenic-like actions of brain corticotropin-releasing factor receptor ligands in rats. Behav Brain Res 122:43-50.

Heinrichs SC, Koob GF (2004) Corticotropin-releasing factor in brain: a role in activation, arousal, and affect regulation. J Pharmacol Exp Ther 311:427-440.

Heinrichs SC, Menzaghi F, Pich EM, Hauger RL, Koob GF (1993) Corticotropin-releasing factor in the paraventricular nucleus modulates feeding induced by neuropeptide Y. Brain Res 611:18-24.

Heinrichs SC, Min H, Tamraz S, Carmouche M, Boehme SA, Vale WW (1997) Anti-sexual and anxiogenic behavioral consequences of corticotropin-releasing factor overexpression are centrally mediated. Psychoneuroendocrinology 22:215-224.

Heinrichs SC, Pich EM, Miczek KA, Britton KT, Koob GF (1992) Corticotropin-releasing factor antagonist reduces emotionality in socially defeated rats via direct neurotropic action. Brain Res 581:190-197.

Heinrichs SC, Richard D (1999) The role of corticotropin-releasing factor and urocortin in the modulation of ingestive behavior. Neuropeptides 33:350-359.

Heinrichs SC, Stenzel-Poore MP, Gold LH, Battenberg E, Bloom FE, Koob GF, Vale WW, Pich EM (1996) Learning impairment in transgenic mice with central overexpression of corticotropin-releasing factor. Neuroscience 74:303-311.

Herman JP, Cullinan WE (1997) Neurocircuitry of stress: central control of the hypothalamo-pituitary-adrenocortical axis. Trends Neurosci 20:78-84.

Herzog E, Bellenchi GC, Gras C, Bernard V, Ravassard P, Bedet C, Gasnier B, Giros B, El MS (2001) The existence of a second vesicular glutamate transporter specifies subpopulations of glutamatergic neurons. J Neurosci 21:RC181.

Het S, Wolf OT (2007) Mood changes in response to psychosocial stress in healthy young women: effects of pretreatment with cortisol. Behav Neurosci 121:11-20.

Hikichi T, Akiyoshi J, Yamamoto Y, Tsutsumi T, Isogawa K, Nagayama H (2000) Suppression of conditioned fear by administration of CRF receptor antagonist CP-154,526. Pharmacopsychiatry 33:189-193.

Hodgkinson CA, Goldman D, Jaeger J, Persaud S, Kane JM, Lipsky RH, Malhotra AK (2004) Disrupted in schizophrenia 1 (DISC1): association with schizophrenia, schizoaffective disorder, and bipolar disorder. Am J Hum Genet 75:862-872.

Hoess RH, Ziese M, Sternberg N (1982) P1 site-specific recombination: nucleotide sequence of the recombining sites. Proc Natl Acad Sci U S A 79:3398-3402.

Hollrigel GS, Chen K, Baram TZ, Soltesz I (1998) The pro-convulsant actions of corticotropin-releasing hormone in the hippocampus of infant rats. Neuroscience 84:71-79.

Holsboer F (1999) The rationale for corticotropin-releasing hormone receptor (CRH-R) antagonists to treat depression and anxiety. J Psychiatr Res 33:181-214.

Holsboer F (2000) The corticosteroid receptor hypothesis of depression. Neuropsychopharmacology 23:477-501.

Holsboer F (2001) Stress, hypercortisolism and corticosteroid receptors in depression: implications for therapy. J Affect Disord 62:77-91.

Holsboer F, Ising M (2008) Central CRH system in depression and anxiety--evidence from clinical studies with CRH1 receptor antagonists. Eur J Pharmacol 583:350-357.

Hommel JD, Sears RM, Georgescu D, Simmons DL, Dileone RJ (2003) Local gene knockdown in the brain using viral-mediated RNA interference. Nat Med 9:1539-1544.

Hsu SY, Hsueh AJ (2001) Human stresscopin and stresscopin-related peptide are selective ligands for the type 2 corticotropin-releasing hormone receptor. Nat Med 7:605-611.

Hubbard DT, Nakashima BR, Lee I, Takahashi LK (2007) Activation of basolateral amygdala corticotropin-releasing factor 1 receptors modulates the consolidation of contextual fear. Neuroscience 150:818-828.

Hwang KR, Chan SH, Chan JY (1998) Noradrenergic neurotransmission at PVN in locus ceruleus-induced baroreflex suppression in rats. Am J Physiol 274:H1284-H1292.

Irvine EE, von Hertzen LS, Plattner F, Giese KP (2006) alphaCaMKII autophosphorylation: a fast track to memory. Trends Neurosci 29:459-465.

Ishizuka T, Kakuda M, Araki R, Yawo H (2006) Kinetic evaluation of photosensitivity in genetically engineered neurons expressing green algae light-gated channels. Neurosci Res 54:85-94.

Ising M, Holsboer F (2006) Genetics of stress response and stress-related disorders. Dialogues Clin Neurosci 8:433-444.

Isogawa K, Bush DE, LeDoux JE (2013) Contrasting effects of pretraining, posttraining, and pretesting infusions of corticotropin-releasing factor into the lateral amygdala: attenuation of fear memory formation but facilitation of its expression. Biol Psychiatry 73:353-359.

Ivy AS, Rex CS, Chen Y, Dube C, Maras PM, Grigoriadis DE, Gall CM, Lynch G, Baram TZ (2010) Hippocampal dysfunction and cognitive impairments provoked by chronic early-life stress involve excessive activation of CRH receptors. J Neurosci 30:13005-13015.

Izzo E, Sanna PP, Koob GF (2005) Impairment of dopaminergic system function after chronic treatment with corticotropin-releasing factor. Pharmacol Biochem Behav 81:701-708.

Jaaro-Peled H (2009) Gene models of schizophrenia: DISC1 mouse models. Prog Brain Res 179:75-86.

Jaaro-Peled H, Hayashi-Takagi A, Seshadri S, Kamiya A, Brandon NJ, Sawa A (2009) Neurodevelopmental mechanisms of schizophrenia: understanding disturbed postnatal brain maturation through neuregulin-1-ErbB4 and DISC1. Trends Neurosci 32:485-495.

Jalabert M, Aston-Jones G, Herzog E, Manzoni O, Georges F (2009) Role of the bed nucleus of the stria terminalis in the control of ventral tegmental area dopamine neurons. Prog Neuropsychopharmacol Biol Psychiatry 33:1336-1346.

Jedema HP, Grace AA (2004) Corticotropin-releasing hormone directly activates noradrenergic neurons of the locus ceruleus recorded in vitro. J Neurosci 24:9703-9713.

Jennings JH, Sparta DR, Stamatakis AM, Ung RL, Pleil KE, Kash TL, Stuber GD (2013) Distinct extended amygdala circuits for divergent motivational states. Nature 496:224-228.

Jeon D, Kim S, Chetana M, Jo D, Ruley HE, Lin SY, Rabah D, Kinet JP, Shin HS (2010) Observational fear learning involves affective pain system and Cav1.2 Ca2+ channels in ACC. Nat Neurosci 13:482-488.

Joels M, Baram TZ (2009) The neuro-symphony of stress. Nat Rev Neurosci 10:459-466.

Joels M, Pu Z, Wiegert O, Oitzl MS, Krugers HJ (2006) Learning under stress: how does it work? Trends Cogn Sci 10:152-158.

Jones CA, Watson DJ, Fone KC (2011) Animal models of schizophrenia. Br J Pharmacol 164:1162-1194.

Jones EG (1975) Varieties and distribution of non-pyramidal cells in the somatic sensory cortex of the squirrel monkey. J Comp Neurol 160:205-267.

Jones EG, Huntley GW, Benson DL (1994) Alpha calcium/calmodulin-dependent protein kinase II selectively expressed in a subpopulation of excitatory neurons in monkey sensory-motor cortex: comparison with GAD-67 expression. J Neurosci 14:611-629.

Justice NJ, Yuan ZF, Sawchenko PE, Vale W (2008) Type 1 corticotropin-releasing factor receptor expression reported in BAC transgenic mice: implications for reconciling ligand-receptor mismatch in the central corticotropin-releasing factor system. J Comp Neurol 511:479-496.

Kalivas PW, Duffy P, Latimer LG (1987) Neurochemical and behavioral effects of corticotropin-releasing factor in the ventral tegmental area of the rat. J Pharmacol Exp Ther 242:757-763.

Kalueff AV, Murphy DL (2007) The importance of cognitive phenotypes in experimental modeling of animal anxiety and depression. Neural Plast 2007:52087.

Kamprath K, Wotjak CT (2004) Nonassociative learning processes determine expression and extinction of conditioned fear in mice. Learn Mem 11:770-786.

Kandel ER (2001) The molecular biology of memory storage: a dialog between genes and synapses. Biosci Rep 21:565-611.

Karube F, Kubota Y, Kawaguchi Y (2004) Axon branching and synaptic bouton phenotypes in GABAergic nonpyramidal cell subtypes. J Neurosci 24:2853-2865.

Kasahara M, Groenink L, Kas MJ, Bijlsma EY, Olivier B, Sarnyai Z (2011) Influence of transgenic corticotropin-releasing factor (CRF) over-expression on social recognition memory in mice. Behav Brain Res 218:357-362.

Kaufling J, Veinante P, Pawlowski SA, Freund-Mercier MJ, Barrot M (2009) Afferents to the GABAergic tail of the ventral tegmental area in the rat. J Comp Neurol 513:597-621.

Kawaguchi Y, Karube F, Kubota Y (2006) Dendritic branch typing and spine expression patterns in cortical nonpyramidal cells. Cereb Cortex 16:696-711.

Kawaguchi Y, Kubota Y (1996) Physiological and morphological identification of somatostatin- or vasoactive intestinal polypeptide-containing cells among GABAergic cell subtypes in rat frontal cortex. J Neurosci 16:2701-2715.

Kawaguchi Y, Kubota Y (1997) GABAergic cell subtypes and their synaptic connections in rat frontal cortex. Cereb Cortex 7:476-486.

Keck T, Scheuss V, Jacobsen RI, Wierenga CJ, Eysel UT, Bonhoeffer T, Hubener M (2011) Loss of sensory input causes rapid structural changes of inhibitory neurons in adult mouse visual cortex. Neuron 71:869-882.

Keefe RS, Bilder RM, Davis SM, Harvey PD, Palmer BW, Gold JM, Meltzer HY, Green MF, Capuano G, Stroup TS, McEvoy JP, Swartz MS, Rosenheck RA, Perkins DO, Davis CE, Hsiao JK, Lieberman JA (2007) Neurocognitive effects of antipsychotic medications in patients with chronic schizophrenia in the CATIE Trial. Arch Gen Psychiatry 64:633-647.

Keegan CE, Karolyi IJ, Knapp LT, Bourbonais FJ, Camper SA, Seasholtz AF (1994) Expression of corticotropin-releasing hormone transgenes in neurons of adult and developing mice. Mol Cell Neurosci 5:505-514.

Kegeles LS, Abi-Dargham A, Frankle WG, Gil R, Cooper TB, Slifstein M, Hwang DR, Huang Y, Haber SN, Laruelle M (2010) Increased synaptic dopamine function in associative regions of the striatum in schizophrenia. Arch Gen Psychiatry 67:231-239.

Kendler KS (1995) Adversity, Stress and Psychopathology - A Psychiatric Genetic Perspective. International Journal of Methods in Psychiatric Research 5:163-170.

Kendler KS, Karkowski LM, Prescott CA (1999) Causal relationship between stressful life events and the onset of major depression. American Journal of Psychiatry 156:837-841.

Kennedy MB, Bennett MK, Erondu NE (1983) Biochemical and immunochemical evidence that the "major postsynaptic density protein" is a subunit of a calmodulin-dependent protein kinase. Proc Natl Acad Sci U S A 80:7357-7361.

Kessler RC, Avenevoli S, Costello EJ, Georgiades K, Green JG, Gruber MJ, He JP, Koretz D, McLaughlin KA, Petukhova M, Sampson NA, Zaslavsky AM, Merikangas KR (2012) Prevalence, persistence, and sociodemographic correlates of DSM-IV disorders in the National Comorbidity Survey Replication Adolescent Supplement. Arch Gen Psychiatry 69:372-380.

Kessler RC, Chiu WT, Demler O, Merikangas KR, Walters EE (2005) Prevalence, severity, and comorbidity of 12-month DSM-IV disorders in the National Comorbidity Survey Replication. Arch Gen Psychiatry 62:617-627.

Khachaturian ZS (1989a) Calcium, membranes, aging, and Alzheimer's disease. Introduction and overview. Ann N Y Acad Sci 568:1-4.

Khachaturian ZS (1989b) The role of calcium regulation in brain aging: reexamination of a hypothesis. Aging (Milano) 1:17-34.

Khattak MN, Buchfelder M, Kleindienst A, Schofl C, Kremenevskaja N (2010) CRH and SRIF have opposite effects on the Wnt/beta-catenin signalling pathway through PKA/GSK-3beta in corticotroph pituitary cells. Cancer Invest 28:797-805.

Kilby NJ, Snaith MR, Murray JA (1993) Site-specific recombinases: tools for genome engineering. Trends Genet 9:413-421.

Kim SY, Adhikari A, Lee SY, Marshel JH, Kim CK, Mallory CS, Lo M, Pak S, Mattis J, Lim BK, Malenka RC, Warden MR, Neve R, Tye KM, Deisseroth K (2013) Diverging neural pathways assemble a behavioural state from separable features in anxiety. Nature 496:219-223.

Kimmel RA, Turnbull DH, Blanquet V, Wurst W, Loomis CA, Joyner AL (2000) Two lineage boundaries coordinate vertebrate apical ectodermal ridge formation. Genes Dev 14:1377-1389.

Kimura M, Muller-Preuss P, Lu A, Wiesner E, Flachskamm C, Wurst W, Holsboer F, Deussing JM (2010) Conditional corticotropin-releasing hormone overexpression in the mouse forebrain enhances rapid eye movement sleep. Mol Psychiatry 15:154-165.

King LS, Kozono D, Agre P (2004) From structure to disease: the evolving tale of aquaporin biology. Nat Rev Mol Cell Biol 5:687-698.

Kirby ED, Muroy SE, Sun WG, Covarrubias D, Leong MJ, Barchas LA, Kaufer D (2013) Acute stress enhances adult rat hippocampal neurogenesis and activation of newborn neurons via secreted astrocytic FGF2. Elife 2:e00362.

Kirby LG, Freeman-Daniels E, Lemos JC, Nunan JD, Lamy C, Akanwa A, Beck SG (2008) Corticotropin-releasing factor increases GABA synaptic activity and induces inward current in 5-hydroxytryptamine dorsal raphe neurons. J Neurosci 28:12927-12937.

Kirshenbaum GS, Clapcote SJ, Duffy S, Burgess CR, Petersen J, Jarowek KJ, Yucel YH, Cortez MA, Snead OC, III, Vilsen B, Peever JH, Ralph MR, Roder JC (2011) Mania-like behavior induced by genetic dysfunction of the neuron-specific Na+,K+-ATPase alpha3 sodium pump. Proc Natl Acad Sci U S A 108:18144-18149.

Kishimoto T, Radulovic J, Radulovic M, Lin CR, Schrick C, Hooshmand F, Hermanson O, Rosenfeld MG, Spiess J (2000) Deletion of crhr2 reveals an anxiolytic role for corticotropin-releasing hormone receptor-2. Nat Genet 24:415-419.

Kistner A, Gossen M, Zimmermann F, Jerecic J, Ullmer C, Lubbert H, Bujard H (1996) Doxycycline-mediated quantitative and tissue-specific control of gene expression in transgenic mice. Proc Natl Acad Sci U S A 93:10933-10938.

Klausberger T, Somogyi P (2008) Neuronal diversity and temporal dynamics: the unity of hippocampal circuit operations. Science 321:53-57.

Klein PS, Melton DA (1996) A molecular mechanism for the effect of lithium on development. Proc Natl Acad Sci U S A 93:8455-8459.

Kleinhammer A, Wurst W, Kuhn R (2010) Gene knockdown in the mouse through RNAi. Methods Enzymol 477:387-414.

Kleinknecht KR, Bedenk BT, Kaltwasser SF, Grunecker B, Yen YC, Czisch M, Wotjak CT (2012) Hippocampus-dependent place learning enables spatial flexibility in C57BL6/N mice. Front Behav Neurosci 6:87.

Klengel T, Mehta D, Anacker C, Rex-Haffner M, Pruessner JC, Pariante CM, Pace TW, Mercer KB, Mayberg HS, Bradley B, Nemeroff CB, Holsboer F, Heim CM, Ressler KJ, Rein T, Binder EB (2013) Allele-specific FKBP5 DNA demethylation mediates gene-childhood trauma interactions. Nat Neurosci 16:33-41.

Klimek V, Schenck JE, Han H, Stockmeier CA, Ordway GA (2002) Dopaminergic abnormalities in amygdaloid nuclei in major depression: a postmortem study. Biol Psychiatry 52:740-748.

Klooster J, Beckers HJ, Vrensen GF, van der Want JJ (1993) The peripheral and central projections of the Edinger-Westphal nucleus in the rat. A light and electron microscopic tracing study. Brain Res 632:260-273.

Klug JR, Mathur BN, Kash TL, Wang HD, Matthews RT, Robison AJ, Anderson ME, Deutch AY, Lovinger DM, Colbran RJ, Winder DG (2012) Genetic inhibition of CaMKII in dorsal striatal medium spiny neurons reduces functional excitatory synapses and enhances intrinsic excitability. PLoS One 7:e45323.

Knobloch HS, Charlet A, Hoffmann LC, Eliava M, Khrulev S, Cetin AH, Osten P, Schwarz MK, Seeburg PH, Stoop R, Grinevich V (2012) Evoked axonal oxytocin release in the central amygdala attenuates fear response. Neuron 73:553-566.

Knott GW, Quairiaux C, Genoud C, Welker E (2002) Formation of dendritic spines with GABAergic synapses induced by whisker stimulation in adult mice. Neuron 34:265-273.

Kolber BJ, Boyle MP, Wieczorek L, Kelley CL, Onwuzurike CC, Nettles SA, Vogt SK, Muglia LJ (2010) Transient early-life forebrain corticotropin-releasing hormone elevation causes long-lasting anxiogenic and despair-like changes in mice. J Neurosci 30:2571-2581.

Kolber BJ, Wieczorek L, Muglia LJ (2008) Hypothalamic-pituitary-adrenal axis dysregulation and behavioral analysis of mouse mutants with altered glucocorticoid or mineralocorticoid receptor function. Stress 11:321-338.

Kollack-Walker S, Watson SJ, Akil H (1997) Social stress in hamsters: defeat activates specific neurocircuits within the brain. J Neurosci 17:8842-8855.

Kong H, Sha LL, Fan Y, Xiao M, Ding JH, Wu J, Hu G (2009) Requirement of AQP4 for antidepressive efficiency of fluoxetine: implication in adult hippocampal neurogenesis. Neuropsychopharmacology 34:1263-1276.

Koob GF (2008) A role for brain stress systems in addiction. Neuron 59:11-34.

Koob GF (2012) Animal models of psychiatric disorders. Handb Clin Neurol 106:137-166.

Koob GF, Heinrichs SC (1999) A role for corticotropin releasing factor and urocortin in behavioral responses to stressors. Brain Res 848:141-152.

Koob GF, Heinrichs SC, Pich EM, Menzaghi F, Baldwin H, Miczek K, Britton KT (1993) The role of corticotropin-releasing factor in behavioural responses to stress. Ciba Found Symp 172:277-289.

Koob GF, Le MM (1997) Drug abuse: hedonic homeostatic dysregulation. Science 278:52-58.

Koob GF, Le MM (2005) Plasticity of reward neurocircuitry and the 'dark side' of drug addiction. Nat Neurosci 8:1442-1444.

Koob GF, Swerdlow N, Seeligson M, Eaves M, Sutton R, Rivier J, Vale W (1984) Effects of alpha-flupenthixol and naloxone on CRF-induced locomotor activation. Neuroendocrinology 39:459-464.

Koob GF, Zorrilla EP (2010) Neurobiological mechanisms of addiction: focus on corticotropin-releasing factor. Curr Opin Investig Drugs 11:63-71.

Koolhaas JM, Bartolomucci A, Buwalda B, de Boer SF, Flugge G, Korte SM, Meerlo P, Murison R, Olivier B, Palanza P, Richter-Levin G, Sgoifo A, Steimer T, Stiedl O, van DG, Wohr M, Fuchs E (2011) Stress revisited: a critical evaluation of the stress concept. Neurosci Biobehav Rev 35:1291-1301.

Koolhaas JM, de Boer SF, De Rutter AJ, Meerlo P, Sgoifo A (1997) Social stress in rats and mice. Acta Physiol Scand Suppl 640:69-72.

Korf J, Van Praag HM (1971) Retarded depression and the dopamine metabolism. Psychopharmacologia 19:199-203.

Krahn DD, Gosnell BA, Grace M, Levine AS (1986) CRF antagonist partially reverses CRF- and stress-induced effects on feeding. Brain Res Bull 17:285-289.

Kratzer S, Mattusch C, Metzger MW, Dedic N, Noll-Hussong M, Kafitz KW, Eder M, Deussing JM, Holsboer F, Kochs E, Rammes G (2013) Activation of CRH receptor type 1 expressed on glutamatergic neurons increases excitability of CA1 pyramidal neurons by the modulation of voltage-gated ion channels. Front Cell Neurosci 7:91.

Kravitz AV, Freeze BS, Parker PR, Kay K, Thwin MT, Deisseroth K, Kreitzer AC (2010) Regulation of parkinsonian motor behaviours by optogenetic control of basal ganglia circuitry. Nature 466:622-626.

Krishnan V, et al. (2007) Molecular adaptations underlying susceptibility and resistance to social defeat in brain reward regions. Cell 131:391-404.

Krishnan V, Nestler EJ (2008) The molecular neurobiology of depression. Nature 455:894-902.

Krishnan V, Nestler EJ (2011) Animal models of depression: molecular perspectives. Curr Top Behav Neurosci 7:121-147.

Kubota Y (2013) Untangling GABAergic wiring in the cortical microcircuit. Curr Opin Neurobiol 26C:7-14.

Kubota Y, Hatada S, Kondo S, Karube F, Kawaguchi Y (2007) Neocortical inhibitory terminals innervate dendritic spines targeted by thalamocortical afferents. J Neurosci 27:1139-1150.

Kubota Y, Shigematsu N, Karube F, Sekigawa A, Kato S, Yamaguchi N, Hirai Y, Morishima M, Kawaguchi Y (2011) Selective coexpression of multiple chemical markers defines discrete populations of neocortical GABAergic neurons. Cereb Cortex 21:1803-1817.

Kudo T, Uchigashima M, Miyazaki T, Konno K, Yamasaki M, Yanagawa Y, Minami M, Watanabe M (2012) Three types of neurochemical projection from the bed nucleus of the stria terminalis to the ventral tegmental area in adult mice. J Neurosci 32:18035-18046.

Kudryavtseva NN, Bakshtanovskaya IV, Koryakina LA (1991) Social model of depression in mice of C57BL/6J strain. Pharmacol Biochem Behav 38:315-320.

Kuhlman SJ, Huang ZJ (2008) High-resolution labeling and functional manipulation of specific neuron types in mouse brain by Cre-activated viral gene expression. PLoS One 3:e2005.

Kühn R, Wurst W (2008) Overview on Mouse Mutagenesis. In: Gene Knockout Protocols: (Kühn R, Wurst W, eds), Springer Protocols.

Kuhne C, Puk O, Graw J, de Angelis MH, Schutz G, Wurst W, Deussing JM (2012) Visualizing Corticotropin-Releasing Hormone Receptor Type 1 Expression and Neuronal Connectivities in the Mouse Using a Novel Multifunctional Allele. Journal of Comparative Neurology 520:3150-3180.

Kumar A, Foster TC (2004) Enhanced long-term potentiation during aging is masked by processes involving intracellular calcium stores. J Neurophysiol 91:2437-2444.

Kumar A, Foster TC (2007) Shift in induction mechanisms underlies an age-dependent increase in DHPG-induced synaptic depression at CA3 CA1 synapses. J Neurophysiol 98:2729-2736.

Kuperman Y, Chen A (2008) Urocortins: emerging metabolic and energy homeostasis perspectives. Trends Endocrinol Metab 19:122-129.

Kuppers E, Gleiser C, Brito V, Wachter B, Pauly T, Hirt B, Grissmer S (2008) AQP4 expression in striatal primary cultures is regulated by dopamine--implications for proliferation of astrocytes. Eur J Neurosci 28:2173-2182.

Lan MJ, McLoughlin GA, Griffin JL, Tsang TM, Huang JT, Yuan P, Manji H, Holmes E, Bahn S (2009) Metabonomic analysis identifies molecular changes associated with the pathophysiology and drug treatment of bipolar disorder. Mol Psychiatry 14:269-279.

Langwieser N, Christel CJ, Kleppisch T, Hofmann F, Wotjak CT, Moosmang S (2010) Homeostatic switch in hebbian plasticity and fear learning after sustained loss of Cav1.2 calcium channels. J Neurosci 30:8367-8375.

Lapiz MD, Fulford A, Muchimapura S, Mason R, Parker T, Marsden CA (2003) Influence of postweaning social isolation in the rat on brain development, conditioned behavior, and neurotransmission. Neurosci Behav Physiol 33:13-29.

Larriva-Sahd J (2004) Juxtacapsular nucleus of the stria terminalis of the adult rat: extrinsic inputs, cell types, and neuronal modules: a combined Golgi and electron microscopic study. J Comp Neurol 475:220-237.

Le MM, Koob GF (2007) Drug addiction: pathways to the disease and pathophysiological perspectives. Eur Neuropsychopharmacol 17:377-393.

Lee AS, Ra S, Rajadhyaksha AM, Britt JK, De Jesus-Cortes H, Gonzales KL, Lee A, Moosmang S, Hofmann F, Pieper AA, Rajadhyaksha AM (2012) Forebrain elimination of cacna1c mediates anxiety-like behavior in mice. Mol Psychiatry.

Lee SH, et al. (2013) Genetic relationship between five psychiatric disorders estimated from genome-wide SNPs. Nat Genet 45:984-994.

Lee Y, Davis M (1997) Role of the hippocampus, the bed nucleus of the stria terminalis, and the amygdala in the excitatory effect of corticotropin-releasing hormone on the acoustic startle reflex. J Neurosci 17:6434-6446.

Lee Y, Fitz S, Johnson PL, Shekhar A (2008) Repeated stimulation of CRF receptors in the BNST of rats selectively induces social but not panic-like anxiety. Neuropsychopharmacology 33:2586-2594.

Lemberger T, Parlato R, Dassesse D, Westphal M, Casanova E, Turiault M, Tronche F, Schiffmann SN, Schutz G (2007) Expression of Cre recombinase in dopaminoceptive neurons. BMC Neurosci 8:4.

Lemos JC, Wanat MJ, Smith JS, Reyes BA, Hollon NG, Van Bockstaele EJ, Chavkin C, Phillips PE (2012) Severe stress switches CRF action in the nucleus accumbens from appetitive to aversive. Nature 490:402-406.

Lentz TB, Gray SJ, Samulski RJ (2012) Viral vectors for gene delivery to the central nervous system. Neurobiol Dis 48:179-188.

Leonardo ED, Hen R (2008) Anxiety as a developmental disorder. Neuropsychopharmacology 33:134-140.

Lepine JP, Briley M (2011) The increasing burden of depression. Neuropsychiatr Dis Treat 7:3-7.

Lewis DA, Levitt P (2002) Schizophrenia as a disorder of neurodevelopment. Annu Rev Neurosci 25:409-432.

Lewis DA, Sweet RA (2009) Schizophrenia from a neural circuitry perspective: advancing toward rational pharmacological therapies. J Clin Invest 119:706-716.

Lewis K, Li C, Perrin MH, Blount A, Kunitake K, Donaldson C, Vaughan J, Reyes TM, Gulyas J, Fischer W, Bilezikjian L, Rivier J, Sawchenko PE, Vale WW (2001) Identification of urocortin III, an additional member of the corticotropin-releasing factor (CRF) family with high affinity for the CRF2 receptor. Proc Natl Acad Sci U S A 98:7570-7575.

Li C, Chen P, Vaughan J, Blount A, Chen A, Jamieson PM, Rivier J, Smith MS, Vale W (2003) Urocortin III is expressed in pancreatic beta-cells and stimulates insulin and glucagon secretion. Endocrinology 144:3216-3224.

Li L, Tasic B, Micheva KD, Ivanov VM, Spletter ML, Smith SJ, Luo L (2010) Visualizing the distribution of synapses from individual neurons in the mouse brain. PLoS One 5:e11503.

Li X, Gutierrez DV, Hanson MG, Han J, Mark MD, Chiel H, Hegemann P, Landmesser LT, Herlitze S (2005) Fast noninvasive activation and inhibition of neural and network activity by vertebrate rhodopsin and green algae channelrhodopsin. Proc Natl Acad Sci U S A 102:17816-17821.

Li YK, Wang F, Wang W, Luo Y, Wu PF, Xiao JL, Hu ZL, Jin Y, Hu G, Chen JG (2012) Aquaporin-4 deficiency impairs synaptic plasticity and associative fear memory in the lateral amygdala: involvement of downregulation of glutamate transporter-1 expression. Neuropsychopharmacology 37:1867-1878.

Liang KC, Chen HC, Chen DY (2001) Posttraining infusion of norepinephrine and corticotropin releasing factor into the bed nucleus of the stria terminalis enhanced retention in an inhibitory avoidance task. Chin J Physiol 44:33-43.

Liang KC, Lee EH (1988) Intra-amygdala injections of corticotropin releasing factor facilitate inhibitory avoidance learning and reduce exploratory behavior in rats. Psychopharmacology (Berl) 96:232-236.

Liebsch G, Landgraf R, Gerstberger R, Probst JC, Wotjak CT, Engelmann M, Holsboer F, Montkowski A (1995) Chronic infusion of a CRH1 receptor antisense oligodeoxynucleotide into the central nucleus of the amygdala reduced anxiety-related behavior in socially defeated rats. Regul Pept 59:229-239.

Lin JY, Lin MZ, Steinbach P, Tsien RY (2009) Characterization of engineered channelrhodopsin variants with improved properties and kinetics. Biophys J 96:1803-1814.

Lisman J, Schulman H, Cline H (2002) The molecular basis of CaMKII function in synaptic and behavioural memory. Nat Rev Neurosci 3:175-190.

Lister RG (1987) The use of a plus-maze to measure anxiety in the mouse. Psychopharmacology (Berl) 92:180-185.

Liu XB, Murray KD (2012) Neuronal excitability and calcium/calmodulin-dependent protein kinase type II: location, location, location. Epilepsia 53 Suppl 1:45-52.

Liu Y, et al. (2011) Meta-analysis of genome-wide association data of bipolar disorder and major depressive disorder. Mol Psychiatry 16:2-4.

Livak KJ, Schmittgen TD (2001) Analysis of relative gene expression data using real-time quantitative PCR and the 2(-Delta Delta C(T)) Method. Methods 25:402-408.

Lo L, Anderson DJ (2011) A Cre-dependent, anterograde transsynaptic viral tracer for mapping output pathways of genetically marked neurons. Neuron 72:938-950.

Lovejoy DA, Al CA, Cadinouche MZ (2006) Teneurin C-terminal associated peptides: an enigmatic family of neuropeptides with structural similarity to the corticotropin-releasing factor and calcitonin families of peptides. Gen Comp Endocrinol 148:299-305.

Lovenberg TW, Chalmers DT, Liu C, De Souza EB (1995) CRF2 alpha and CRF2 beta receptor mRNAs are differentially distributed between the rat central nervous system and peripheral tissues. Endocrinology 136:4139-4142.

Lovinger DM (2008) Presynaptic modulation by endocannabinoids. Handb Exp Pharmacol435-477.

Lowy MT, Reder AT, Antel JP, Meltzer HY (1984) Glucocorticoid resistance in depression: the dexamethasone suppression test and lymphocyte sensitivity to dexamethasone. Am J Psychiatry 141:1365-1370.

Lu A, Steiner MA, Whittle N, Vogl AM, Walser SM, Ableitner M, Refojo D, Ekker M, Rubenstein JL, Stalla GK, Singewald N, Holsboer F, Wotjak CT, Wurst W, Deussing JM (2008) Conditional mouse mutants highlight mechanisms of corticotropin-releasing hormone effects on stress-coping behavior. Mol Psychiatry 13:1028-1042.

Lucchesi W, Mizuno K, Giese KP (2011) Novel insights into CaMKII function and regulation during memory formation. Brain Res Bull 85:2-8.

Lupien SJ, McEwen BS, Gunnar MR, Heim C (2009) Effects of stress throughout the lifespan on the brain, behaviour and cognition. Nat Rev Neurosci 10:434-445.

Madisen L, et al. (2012) A toolbox of Cre-dependent optogenetic transgenic mice for light-induced activation and silencing. Nat Neurosci 15:793-802.

Madisen L, Zwingman TA, Sunkin SM, Oh SW, Zariwala HA, Gu H, Ng LL, Palmiter RD, Hawrylycz MJ, Jones AR, Lein ES, Zeng H (2010) A robust and high-throughput Cre reporting and characterization system for the whole mouse brain. Nat Neurosci 13:133-140.

Maeng S, Hunsberger JG, Pearson B, Yuan P, Wang Y, Wei Y, McCammon J, Schloesser RJ, Zhou R, Du J, Chen G, McEwen B, Reed JC, Manji HK (2008) BAG1 plays a critical role in regulating recovery from both manic-like and depression-like behavioral impairments. Proc Natl Acad Sci U S A 105:8766-8771.

Maher B (2008) Personal genomes: The case of the missing heritability. Nature 456:18-21.

Maigaard K, Hageman I, Jorgensen A, Jorgensen MB, Wortwein G (2012) Electroconvulsive stimulations prevent chronic stress-induced increases in L-type calcium channel mRNAs in the hippocampus and basolateral amygdala. Neurosci Lett 516:24-28.

Maj M (2005) "Psychiatric comorbidity": an artefact of current diagnostic systems? Br J Psychiatry 186:182-184.

Malkesman O, Austin DR, Chen G, Manji HK (2009) Reverse translational strategies for developing animal models of bipolar disorder. Dis Model Mech 2:238-245.

Malkoff-Schwartz S, Frank E, Anderson B, Sherrill JT, Siegel L, Patterson D, Kupfer DJ (1998) Stressful life events and social rhythm disruption in the onset of manic and depressive bipolar episodes: a preliminary investigation. Arch Gen Psychiatry 55:702-707.

Mantamadiotis T, Lemberger T, Bleckmann SC, Kern H, Kretz O, Martin VA, Tronche F, Kellendonk C, Gau D, Kapfhammer J, Otto C, Schmid W, Schutz G (2002) Disruption of CREB function in brain leads to neurodegeneration. Nat Genet 31:47-54.

Marcaida MJ, Munoz IG, Blanco FJ, Prieto J, Montoya G (2010) Homing endonucleases: from basics to therapeutic applications. Cell Mol Life Sci 67:727-748.

Maren S (2001) Neurobiology of Pavlovian fear conditioning. Annu Rev Neurosci 24:897-931.

Marin O, Rubenstein JL (2003) Cell migration in the forebrain. Annu Rev Neurosci 26:441-483.

Markram H, Toledo-Rodriguez M, Wang Y, Gupta A, Silberberg G, Wu C (2004) Interneurons of the neocortical inhibitory system. Nat Rev Neurosci 5:793-807.

Martinez A, Ruiz M, Soriano E (1999) Spiny calretinin-immunoreactive neurons in the hilus and CA3 region of the rat hippocampus: local axon circuits, synaptic connections, and glutamic acid decarboxylase 65/67 mRNA expression. J Comp Neurol 404:438-448.

Martinez M, Calvo-Torrent A, Herbert J (2002) Mapping brain response to social stress in rodents with c-fos expression: a review. Stress 5:3-13.

Martinez-Aran A, Vieta E, Reinares M, Colom F, Torrent C, Sanchez-Moreno J, Benabarre A, Goikolea JM, Comes M, Salamero M (2004) Cognitive function across manic or hypomanic, depressed, and euthymic states in bipolar disorder. Am J Psychiatry 161:262-270.

Matamales M, Bertran-Gonzalez J, Salomon L, Degos B, Deniau JM, Valjent E, Herve D, Girault JA (2009) Striatal medium-sized spiny neurons: identification by nuclear staining and study of neuronal subpopulations in BAC transgenic mice. PLoS One 4:e4770.

Mattis J, Tye KM, Ferenczi EA, Ramakrishnan C, O'Shea DJ, Prakash R, Gunaydin LA, Hyun M, Fenno LE, Gradinaru V, Yizhar O, Deisseroth K (2012) Principles for applying optogenetic tools derived from direct comparative analysis of microbial opsins. Nat Methods 9:159-172.

Mayford M, Bach ME, Huang YY, Wang L, Hawkins RD, Kandel ER (1996) Control of memory formation through regulated expression of a CaMKII transgene. Science 274:1678-1683.

McAllister KH (2001) The alpha 2 adrenoceptor antagonists RX 821002 and yohimbine delay-dependently impair choice accuracy in a delayed non-matching-to-position task in rats. Psychopharmacology (Berl) 155:379-388.

McClure DJ (1966) The diurnal variation of plasma cortisol levels in depression. J Psychosom Res 10:189-195.

McDonald CT, Burkhalter A (1993) Organization of long-range inhibitory connections with rat visual cortex. J Neurosci 13:768-781.

McEwen BS (1998) Stress, adaptation, and disease. Allostasis and allostatic load. Ann N Y Acad Sci 840:33-44.

McEwen BS (2004) Protection and damage from acute and chronic stress: allostasis and allostatic overload and relevance to the pathophysiology of psychiatric disorders. Ann N Y Acad Sci 1032:1-7.

McEwen BS (2007) Physiology and neurobiology of stress and adaptation: central role of the brain. Physiol Rev 87:873-904.

McEwen BS, Gianaros PJ (2010) Central role of the brain in stress and adaptation: links to socioeconomic status, health, and disease. Ann N Y Acad Sci 1186:190-222.

McGowan PO, Sasaki A, D'Alessio AC, Dymov S, Labonte B, Szyf M, Turecki G, Meaney MJ (2009) Epigenetic regulation of the glucocorticoid receptor in human brain associates with childhood abuse. Nat Neurosci 12:342-348.

McIlwain KL, Merriweather MY, Yuva-Paylor LA, Paylor R (2001) The use of behavioral test batteries: effects of training history. Physiol Behav 73:705-717.

McKinney WT, Jr., Bunney WE, Jr. (1969) Animal model of depression. I. Review of evidence: implications for research. Arch Gen Psychiatry 21:240-248.

McNeill TH, Brown SA, Rafols JA, Shoulson I (1988) Atrophy of medium spiny I striatal dendrites in advanced Parkinson's disease. Brain Res 455:148-152.

Meaney MJ (2001) Maternal care, gene expression, and the transmission of individual differences in stress reactivity across generations. Annu Rev Neurosci 24:1161-1192.

Megias M, Emri Z, Freund TF, Gulyas AI (2001) Total number and distribution of inhibitory and excitatory synapses on hippocampal CA1 pyramidal cells. Neuroscience 102:527-540.

Mehta D, Klengel T, Conneely KN, Smith AK, Altmann A, Pace TW, Rex-Haffner M, Loeschner A, Gonik M, Mercer KB, Bradley B, Muller-Myhsok B, Ressler KJ, Binder EB (2013) Childhood maltreatment is associated with distinct genomic and epigenetic profiles in posttraumatic stress disorder. Proc Natl Acad Sci U S A 110:8302-8307.

Melzer S, Michael M, Caputi A, Eliava M, Fuchs EC, Whittington MA, Monyer H (2012) Long-range-projecting GABAergic neurons modulate inhibition in hippocampus and entorhinal cortex. Science 335:1506-1510.

Mendels J, Frazer A, Fitzgerald RG, Ramsey TA, Stokes JW (1972) Biogenic amine metabolites in cerebrospinal fluid of depressed and manic patients. Science 175:1380-1382.

Menzaghi F, Heinrichs SC, Pich EM, Tilders FJ, Koob GF (1993a) Functional impairment of hypothalamic corticotropin-releasing factor neurons with immunotargeted toxins enhances food intake induced by neuropeptide Y. Brain Res 618:76-82.

Menzaghi F, Heinrichs SC, Pich EM, Weiss F, Koob GF (1993b) The role of limbic and hypothalamic corticotropin-releasing factor in behavioral responses to stress. Ann N Y Acad Sci 697:142-154.

Merali Z, Du L, Hrdina P, Palkovits M, Faludi G, Poulter MO, Anisman H (2004) Dysregulation in the suicide brain: mRNA expression of corticotropin-releasing hormone receptors and GABA(A) receptor subunits in frontal cortical brain region. J Neurosci 24:1478-1485.

Meyendorff E, Lerer B, Moore NC, Bow J, Gershon S (1985) Methylphenidate infusion in euthymic bipolars: effect of carbamazepine pretreatment. Psychiatry Res 16:303-308.

Minassian A, Henry BL, Young JW, Masten V, Geyer MA, Perry W (2011) Repeated assessment of exploration and novelty seeking in the human behavioral pattern monitor in bipolar disorder patients and healthy individuals. PLoS One 6:e24185.

Mineur YS, Prasol DJ, Belzung C, Crusio WE (2003) Agonistic behavior and unpredictable chronic mild stress in mice. Behav Genet 33:513-519.

Mingozzi F, High KA (2013) Immune responses to AAV vectors: overcoming barriers to successful gene therapy. Blood 122:23-36.

Minichiello L, Korte M, Wolfer D, Kuhn R, Unsicker K, Cestari V, Rossi-Arnaud C, Lipp HP, Bonhoeffer T, Klein R (1999) Essential role for TrkB receptors in hippocampus-mediated learning. Neuron 24:401-414.

Moffett MC, Goeders NE (2007) CP-154,526, a CRF type-1 receptor antagonist, attenuates the cue-and methamphetamine-induced reinstatement of extinguished methamphetamine-seeking behavior in rats. Psychopharmacology (Berl) 190:171-180.

Mogilnicka E, Czyrak A, Maj J (1987) Dihydropyridine calcium channel antagonists reduce immobility in the mouse behavioral despair test; antidepressants facilitate nifedipine action. Eur J Pharmacol 138:413-416.

Monory K, et al. (2006) The endocannabinoid system controls key epileptogenic circuits in the hippocampus. Neuron 51:455-466.

Moore RY, Bloom FE (1978) Central catecholamine neuron systems: anatomy and physiology of the dopamine systems. Annu Rev Neurosci 1:129-169.

Moosmang S, Haider N, Klugbauer N, Adelsberger H, Langwieser N, Muller J, Stiess M, Marais E, Schulla V, Lacinova L, Goebbels S, Nave KA, Storm DR, Hofmann F, Kleppisch T (2005) Role of hippocampal Cav1.2 Ca2+ channels in NMDA receptor-independent synaptic plasticity and spatial memory. J Neurosci 25:9883-9892.

Moreau JL, Kilpatrick G, Jenck F (1997) Urocortin, a novel neuropeptide with anxiogenic-like properties. Neuroreport 8:1697-1701.

Morin SM, Ling N, Liu XJ, Kahl SD, Gehlert DR (1999) Differential distribution of urocortin- and corticotropin-releasing factor-like immunoreactivities in the rat brain. Neuroscience 92:281-291.

Morris JF, Pow DV (1991) Widespread release of peptides in the central nervous system: quantitation of tannic acid-captured exocytoses. Anat Rec 231:437-445.

Morris R (1984) Developments of a water-maze procedure for studying spatial learning in the rat. J Neurosci Methods 11:47-60.

Moy SS, Nadler JJ, Perez A, Barbaro RP, Johns JM, Magnuson TR, Piven J, Crawley JN (2004) Sociability and preference for social novelty in five inbred strains: an approach to assess autistic-like behavior in mice. Genes Brain Behav 3:287-302.

Muglia L, Jacobson L, Dikkes P, Majzoub JA (1995) Corticotropin-releasing hormone deficiency reveals major fetal but not adult glucocorticoid need. Nature 373:427-432.

Muglia LJ, Jacobson L, Weninger SC, Karalis KP, Jeong K, Majzoub JA (2001) The physiology of corticotropin-releasing hormone deficiency in mice. Peptides 22:725-731.

Mulders WH, Meek J, Hafmans TG, Cools AR (1997) Plasticity in the stress-regulating circuit: decreased input from the bed nucleus of the stria terminalis to the hypothalamic paraventricular nucleus in Wistar rats following adrenalectomy. Eur J Neurosci 9:2462-2471.

Muller MB, Holsboer F (2006) Mice with mutations in the HPA-system as models for symptoms of depression. Biol Psychiatry 59:1104-1115.

Muller MB, Zimmermann S, Sillaber I, Hagemeyer TP, Deussing JM, Timpl P, Kormann MS, Droste SK, Kuhn R, Reul JM, Holsboer F, Wurst W (2003) Limbic corticotropin-releasing hormone receptor 1 mediates anxiety-related behavior and hormonal adaptation to stress. Nat Neurosci 6:1100-1107.

Munck A, Guyre PM, Holbrook NJ (1984) Physiological functions of glucocorticoids in stress and their relation to pharmacological actions. Endocr Rev 5:25-44.

Muramatsu T, Inoue K, Iwasaki S, Yamauchi T, Hayashi T, Kiriike N (2006) Corticotropin-releasing factor receptor type 1, but not type 2, in the ventromedial hypothalamus modulates dopamine release in female rats. Pharmacol Biochem Behav 85:435-440.

Murgatroyd C, Patchev AV, Wu Y, Micale V, Bockmuhl Y, Fischer D, Holsboer F, Wotjak CT, Almeida OF, Spengler D (2009) Dynamic DNA methylation programs persistent adverse effects of early-life stress. Nat Neurosci 12:1559-1566.

Murray F, Smith DW, Hutson PH (2008) Chronic low dose corticosterone exposure decreased hippocampal cell proliferation, volume and induced anxiety and depression like behaviours in mice. Eur J Pharmacol 583:115-127.

Myers-Schulz B, Koenigs M (2012) Functional anatomy of ventromedial prefrontal cortex: implications for mood and anxiety disorders. Mol Psychiatry 17:132-141.

Nadler JJ, Moy SS, Dold G, Trang D, Simmons N, Perez A, Young NB, Barbaro RP, Piven J, Magnuson TR, Crawley JN (2004) Automated apparatus for quantitation of social approach behaviors in mice. Genes Brain Behav 3:303-314.

Nagelhus EA, Ottersen OP (2013) Physiological roles of aquaporin-4 in brain. Physiol Rev 93:1543-1562.

Nemeroff CB, Owens MJ, Bissette G, Andorn AC, Stanley M (1988) Reduced corticotropin releasing factor binding sites in the frontal cortex of suicide victims. Arch Gen Psychiatry 45:577-579.

Nemeroff CB, Widerlov E, Bissette G, Walleus H, Karlsson I, Eklund K, Kilts CD, Loosen PT, Vale W (1984) Elevated concentrations of CSF corticotropin-releasing factor-like immunoreactivity in depressed patients. Science 226:1342-1344.

Nestler EJ, Hyman SE, Malenka RC (2009) Molecular Neuropharmacology: A Foundation for Clinical Neuroscience. New York: McGraw-Hill.

Nestler EJ, Barrot M, Dileone RJ, Eisch AJ, Gold SJ, Monteggia LM (2002) Neurobiology of depression. Neuron 34:13-25.

Nestler EJ, Carlezon WA, Jr. (2006) The mesolimbic dopamine reward circuit in depression. Biol Psychiatry 59:1151-1159.

Nestler EJ, Hyman SE (2010) Animal models of neuropsychiatric disorders. Nat Neurosci 13:1161-1169.

Neufeld-Cohen A, Evans AK, Getselter D, Spyroglou A, Hill A, Gil S, Tsoory M, Beuschlein F, Lowry CA, Vale W, Chen A (2010a) Urocortin-1 and -2 double-deficient mice show robust anxiolytic phenotype and modified serotonergic activity in anxiety circuits. Mol Psychiatry 15:426-41, 339.

Neufeld-Cohen A, Tsoory MM, Evans AK, Getselter D, Gil S, Lowry CA, Vale WW, Chen A (2010b) A triple urocortin knockout mouse model reveals an essential role for urocortins in stress recovery. Proc Natl Acad Sci U S A 107:19020-19025.

Nieuwenhuizen AG, Rutters F (2008) The hypothalamic-pituitary-adrenal-axis in the regulation of energy balance. Physiol Behav 94:169-177.

Norris CM, Halpain S, Foster TC (1998) Reversal of age-related alterations in synaptic plasticity by blockade of L-type Ca2+ channels. J Neurosci 18:3171-3179.

Nuechterlein KH, Dawson ME (1984) A heuristic vulnerability/stress model of schizophrenic episodes. Schizophr Bull 10:300-312.

Olney JW, Farber NB (1995) Glutamate receptor dysfunction and schizophrenia. Arch Gen Psychiatry 52:998-1007.

Olschowka JA, O'Donohue TL, Mueller GP, Jacobowitz DM (1982a) Hypothalamic and extrahypothalamic distribution of CRF-like immunoreactive neurons in the rat brain. Neuroendocrinology 35:305-308.

Olschowka JA, O'Donohue TL, Mueller GP, Jacobowitz DM (1982b) The distribution of corticotropin releasing factor-like immunoreactive neurons in rat brain. Peptides 3:995-1015.

Olton DS, Samuelson RJ (1976) Remembrance of Places Passed - Spatial Memory in Rats. Journal of Experimental Psychology-Animal Behavior Processes 2:97-116.

Ong JC, Brody SA, Large CH, Geyer MA (2005) An investigation of the efficacy of mood stabilizers in rodent models of prepulse inhibition. J Pharmacol Exp Ther 315:1163-1171.

Orozco-Cabal L, Pollandt S, Liu J, Shinnick-Gallagher P, Gallagher JP (2006) Regulation of synaptic transmission by CRF receptors. Rev Neurosci 17:279-307.

Osakada F, Mori T, Cetin AH, Marshel JH, Virgen B, Callaway EM (2011) New rabies virus variants for monitoring and manipulating activity and gene expression in defined neural circuits. Neuron 71:617-631.

Oshio K, Watanabe H, Yan D, Verkman AS, Manley GT (2006) Impaired pain sensation in mice lacking Aquaporin-1 water channels. Biochem Biophys Res Commun 341:1022-1028.

Owens MJ (2004) Selectivity of antidepressants: from the monoamine hypothesis of depression to the SSRI revolution and beyond. J Clin Psychiatry 65 Suppl 4:5-10.

Ozbolt LB, Nemeroff CB (2013) HPA Axis Modulation in the Treatment of Mood Disorders. In: Psychiatric Disorders - New Frontiers in Affective Disorders (Dieter Schoepf, ed), InTech.

Paez-Pereda M, Hausch F, Holsboer F (2011) Corticotropin releasing factor receptor antagonists for major depressive disorder. Expert Opin Investig Drugs 20:519-535.

Pammer C, Gorcs T, Palkovits M (1990) Peptidergic innervation of the locus coeruleus cells in the human brain. Brain Res 515:247-255.

Papadopoulos MC, Saadoun S, Verkman AS (2008) Aquaporins and cell migration. Pflugers Arch 456:693-700.

Papadopoulos MC, Verkman AS (2013) Aquaporin water channels in the nervous system. Nat Rev Neurosci 14:265-277.

Parker KJ, Maestripieri D (2011) Identifying key features of early stressful experiences that produce stress vulnerability and resilience in primates. Neurosci Biobehav Rev 35:1466-1483.

Paxinos G, Franklin KBJ (2001) A stereotaxic atlas of the mouse brain. San Diego, CA: Academic Press.

Pearlson GD, Wong DF, Tune LE, Ross CA, Chase GA, Links JM, Dannals RF, Wilson AA, Ravert HT, Wagner HN, Jr., . (1995) In vivo D2 dopamine receptor density in psychotic and nonpsychotic patients with bipolar disorder. Arch Gen Psychiatry 52:471-477.

Peet M, Peters S (1995) Drug-induced mania. Drug Saf 12:146-153.

Peeters F, Nicolson NA, Berkhof J (2004) Levels and variability of daily life cortisol secretion in major depression. Psychiatry Res 126:1-13.

Pelizza L, Ferrari A (2009) Anhedonia in schizophrenia and major depression: state or trait? Ann Gen Psychiatry 8:22.

Pentkowski NS, Litvin Y, Blanchard DC, Vasconcellos A, King LB, Blanchard RJ (2009) Effects of acidic-astressin and ovine-CRF microinfusions into the ventral hippocampus on defensive behaviors in rats. Horm Behav 56:35-43.

Perona MT, Waters S, Hall FS, Sora I, Lesch KP, Murphy DL, Caron M, Uhl GR (2008) Animal models of depression in dopamine, serotonin, and norepinephrine transporter knockout mice: prominent effects of dopamine transporter deletions. Behav Pharmacol 19:566-574.

Perrin M, Donaldson C, Chen R, Blount A, Berggren T, Bilezikjian L, Sawchenko P, Vale W (1995) Identification of a second corticotropin-releasing factor receptor gene and characterization of a cDNA expressed in heart. Proc Natl Acad Sci U S A 92:2969-2973.

Perrin MH, Donaldson CJ, Chen R, Lewis KA, Vale WW (1993) Cloning and functional expression of a rat brain corticotropin releasing factor (CRF) receptor. Endocrinology 133:3058-3061.

Perry W, Minassian A, Feifel D, Braff DL (2001) Sensorimotor gating deficits in bipolar disorder patients with acute psychotic mania. Biol Psychiatry 50:418-424.

Peters A, Regidor J (1981) A reassessment of the forms of nonpyramidal neurons in area 17 of cat visual cortex. J Comp Neurol 203:685-716.

Picard M, Juster RP, McEwen BS (2014) Mitochondrial allostatic load puts the 'gluc' back in glucocorticoids. Nat Rev Endocrinol 10:303-310.

Picardo MA, Guigue P, Bonifazi P, Batista-Brito R, Allene C, Ribas A, Fishell G, Baude A, Cossart R (2011) Pioneer GABA cells comprise a subpopulation of hub neurons in the developing hippocampus. Neuron 71:695-709.

Picconi B, Gardoni F, Centonze D, Mauceri D, Cenci MA, Bernardi G, Calabresi P, Di LM (2004) Abnormal Ca2+-calmodulin-dependent protein kinase II function mediates synaptic and motor deficits in experimental parkinsonism. J Neurosci 24:5283-5291.

Pitts MW, Todorovic C, Blank T, Takahashi LK (2009) The central nucleus of the amygdala and corticotropin-releasing factor: insights into contextual fear memory. J Neurosci 29:7379-7388.

Popoli M, Yan Z, McEwen BS, Sanacora G (2012) The stressed synapse: the impact of stress and glucocorticoids on glutamate transmission. Nat Rev Neurosci 13:22-37.

Porsolt RD, Anton G, Blavet N, Jalfre M (1978) Behavioural despair in rats: a new model sensitive to antidepressant treatments. Eur J Pharmacol 47:379-391.

Porsolt RD, Bertin A, Jalfre M (1977) Behavioral despair in mice: a primary screening test for antidepressants. Arch Int Pharmacodyn Ther 229:327-336.

Poulin JF, Arbour D, Laforest S, Drolet G (2009) Neuroanatomical characterization of endogenous opioids in the bed nucleus of the stria terminalis. Prog Neuropsychopharmacol Biol Psychiatry 33:1356-1365.

Poulin JF, Castonguay-Lebel Z, Laforest S, Drolet G (2008) Enkephalin co-expression with classic neurotransmitters in the amygdaloid complex of the rat. J Comp Neurol 506:943-959.

Powell SB, Young JW, Ong JC, Caron MG, Geyer MA (2008) Atypical antipsychotics clozapine and quetiapine attenuate prepulse inhibition deficits in dopamine transporter knockout mice. Behav Pharmacol 19:562-565.

Preil J, Muller MB, Gesing A, Reul JM, Sillaber I, van Gaalen MM, Landgrebe J, Holsboer F, Stenzel-Poore M, Wurst W (2001) Regulation of the hypothalamic-pituitary-adrenocortical system in mice deficient for CRH receptors 1 and 2. Endocrinology 142:4946-4955.

Prickaerts J, Moechars D, Cryns K, Lenaerts I, van CH, Goris I, Daneels G, Bouwknecht JA, Steckler T (2006) Transgenic mice overexpressing glycogen synthase kinase 3beta: a putative model of hyperactivity and mania. J Neurosci 26:9022-9029.

Provencal N, Suderman MJ, Guillemin C, Massart R, Ruggiero A, Wang D, Bennett AJ, Pierre PJ, Friedman DP, Cote SM, Hallett M, Tremblay RE, Suomi SJ, Szyf M (2012) The signature of maternal rearing in the methylome in rhesus macaque prefrontal cortex and T cells. J Neurosci 32:15626-15642.

Pulvirenti L, Koob GF (1993) Lisuride reduces psychomotor retardation during withdrawal from chronic intravenous amphetamine self-administration in rats. Neuropsychopharmacology 8:213-218.

Quax RA, Manenschijn L, Koper JW, Hazes JM, Lamberts SW, van Rossum EF, Feelders RA (2013) Glucocorticoid sensitivity in health and disease. Nat Rev Endocrinol 9:670-686.

Radulovic J, Blank T, Eckart K, Radulovic M, Stiedl O, Spiess J (1999a) CRF and CRF receptors. Results Probl Cell Differ 26:67-90.

Radulovic J, Ruhmann A, Liepold T, Spiess J (1999b) Modulation of learning and anxiety by corticotropin-releasing factor (CRF) and stress: differential roles of CRF receptors 1 and 2. J Neurosci 19:5016-5025.

Rainnie DG, Bergeron R, Sajdyk TJ, Patil M, Gehlert DR, Shekhar A (2004) Corticotrophin releasing factor-induced synaptic plasticity in the amygdala translates stress into emotional disorders. J Neurosci 24:3471-3479.

Rajkowska G, Miguel-Hidalgo JJ (2007) Gliogenesis and glial pathology in depression. CNS Neurol Disord Drug Targets 6:219-233.

Redgate ES, Fahringer EE (1973) A comparison of the pituitary adrenal activity elicited by electrical stimulation of preoptic, amygdaloid and hypothalamic sites in the rat brain. Neuroendocrinology 12:334-343.

Refojo D, Schweizer M, Kuehne C, Ehrenberg S, Thoeringer C, Vogl AM, Dedic N, Schumacher M, von WG, Avrabos C, Touma C, Engblom D, Schutz G, Nave KA, Eder M, Wotjak CT, Sillaber I, Holsboer F, Wurst W, Deussing JM (2011) Glutamatergic and dopaminergic neurons mediate anxiogenic and anxiolytic effects of CRHR1. Science 333:1903-1907.

Regev L, Ezrielev E, Gershon E, Gil S, Chen A (2010) Genetic approach for intracerebroventricular delivery. Proc Natl Acad Sci U S A 107:4424-4429.

Rein ML, Deussing JM (2012) The optogenetic (r)evolution. Mol Genet Genomics 287:95-109.

Reith J, Benkelfat C, Sherwin A, Yasuhara Y, Kuwabara H, Andermann F, Bachneff S, Cumming P, Diksic M, Dyve SE, Etienne P, Evans AC, Lal S, Shevell M, Savard G, Wong DF, Chouinard G, Gjedde A (1994) Elevated dopa decarboxylase activity in living brain of patients with psychosis. Proc Natl Acad Sci U S A 91:11651-11654.

Ren ZG, Porzgen PP, Youn YH, Sieber-Blum M (2003) Ubiquitous embryonic expression of the norepinephrine transporter. Dev Neurosci 25:1-13.

Reul JM, de Kloet ER (1985) Two receptor systems for corticosterone in rat brain: microdistribution and differential occupation. Endocrinology 117:2505-2511.

Reuter M (2002) Impact of cortisol on emotions under stress and nonstress conditions: a pharmacopsychological approach. Neuropsychobiology 46:41-48.

Reyes BA, Fox K, Valentino RJ, Van Bockstaele EJ (2006) Agonist-induced internalization of corticotropin-releasing factor receptors in noradrenergic neurons of the rat locus coeruleus. Eur J Neurosci 23:2991-2998.

Reyes BA, Glaser JD, Van Bockstaele EJ (2007) Ultrastructural evidence for co-localization of corticotropin-releasing factor receptor and mu-opioid receptor in the rat nucleus locus coeruleus. Neurosci Lett 413:216-221.

Reyes BA, Valentino RJ, Xu G, Van Bockstaele EJ (2005) Hypothalamic projections to locus coeruleus neurons in rat brain. Eur J Neurosci 22:93-106.

Reyes TM, Lewis K, Perrin MH, Kunitake KS, Vaughan J, Arias CA, Hogenesch JB, Gulyas J, Rivier J, Vale WW, Sawchenko PE (2001) Urocortin II: a member of the corticotropin-releasing factor (CRF) neuropeptide family that is selectively bound by type 2 CRF receptors. Proc Natl Acad Sci U S A 98:2843-2848.

Rhees RW, Al-Saleh HN, Kinghorn EW, Fleming DE, Lephart ED (1999) Relationship between sexual behavior and sexually dimorphic structures in the anterior hypothalamus in control and prenatally stressed male rats. Brain Res Bull 50:193-199.

Rice CJ, Sandman CA, Lenjavi MR, Baram TZ (2008) A novel mouse model for acute and long-lasting consequences of early life stress. Endocrinology 149:4892-4900.

Riediger M, Wrzus C, Klipker K, Muller V, Schmiedek F, Wagner GG (2014) Outside of the laboratory: Associations of working-memory performance with psychological and physiological arousal vary with age. Psychol Aging 29:103-114.

Riekkinen M, Schmidt B, Kuitunen J, Riekkinen P, Jr. (1997) Effects of combined chronic nimodipine and acute metrifonate treatment on spatial and avoidance behavior. Eur J Pharmacol 322:1-9.

Ripke S, et al. (2011) Genome-wide association study identifies five new schizophrenia loci. Nature Genetics 43:969-U77.

Robbins TW (2000) Chemical neuromodulation of frontal-executive functions in humans and other animals. Exp Brain Res 133:130-138.

Robison CL, Meyerhoff JL, Saviolakis GA, Chen WK, Rice KC, Lumley LA (2004) A CRH1 antagonist into the amygdala of mice prevents defeat-induced defensive behavior. Ann N Y Acad Sci 1032:324-327.

Rodaros D, Caruana DA, Amir S, Stewart J (2007) Corticotropin-releasing factor projections from limbic forebrain and paraventricular nucleus of the hypothalamus to the region of the ventral tegmental area. Neuroscience 150:8-13.

Rodriguez CI, Buchholz F, Galloway J, Sequerra R, Kasper J, Ayala R, Stewart AF, Dymecki SM (2000) High-efficiency deleter mice show that FLPe is an alternative to Cre-loxP. Nat Genet 25:139-140.

Roozendaal B, McGaugh JL (2011) Memory modulation. Behav Neurosci 125:797-824.

Roozendaal B, Okuda S, de Quervain DJ, McGaugh JL (2006) Glucocorticoids interact with emotion-induced noradrenergic activation in influencing different memory functions. Neuroscience 138:901-910.

Roozendaal B, Schelling G, McGaugh JL (2008) Corticotropin-releasing factor in the basolateral amygdala enhances memory consolidation via an interaction with the beta-adrenoceptor-cAMP pathway: dependence on glucocorticoid receptor activation. J Neurosci 28:6642-6651.

Rostkowski AB, Leitermann RJ, Urban JH (2013) Differential activation of neuronal cell types in the basolateral amygdala by corticotropin releasing factor. Neuropeptides 47:273-280.

Roybal K, Theobold D, Graham A, DiNieri JA, Russo SJ, Krishnan V, Chakravarty S, Peevey J, Oehrlein N, Birnbaum S, Vitaterna MH, Orsulak P, Takahashi JS, Nestler EJ, Carlezon WA, Jr., McClung CA (2007) Mania-like behavior induced by disruption of CLOCK. Proc Natl Acad Sci U S A 104:6406-6411.

Russo SJ, Murrough JW, Han MH, Charney DS, Nestler EJ (2012) Neurobiology of resilience. Nat Neurosci 15:1475-1484.

Russo SJ, Nestler EJ (2013) The brain reward circuitry in mood disorders. Nat Rev Neurosci 14:609-625.

Ryabinin AE, Tsoory MM, Kozicz T, Thiele TE, Neufeld-Cohen A, Chen A, Lowery-Gionta EG, Giardino WJ, Kaur S (2012) Urocortins: CRF's siblings and their potential role in anxiety, depression and alcohol drinking behavior. Alcohol 46:349-357.

Sahuque LL, Kullberg EF, Mcgeehan AJ, Kinder JR, Hicks MP, Blanton MG, Janak PH, Olive MF (2006) Anxiogenic and aversive effects of corticotropin-releasing factor (CRF) in the bed nucleus of the stria terminalis in the rat: role of CRF receptor subtypes. Psychopharmacology (Berl) 186:122-132.

Sajdyk TJ, Schober DA, Gehlert DR, Shekhar A (1999) Role of corticotropin-releasing factor and urocortin within the basolateral amygdala of rats in anxiety and panic responses. Behav Brain Res 100:207-215.

Sakanaka M, Shibasaki T, Lederis K (1987) Corticotropin releasing factor-like immunoreactivity in the rat brain as revealed by a modified cobalt-glucose oxidase-diaminobenzidine method. J Comp Neurol 260:256-298.

Sandi C, Pinelo-Nava MT (2007) Stress and memory: behavioral effects and neurobiological mechanisms. Neural Plast 2007:78970.

Sandin M, Jasmin S, Levere TE (1990) Aging and cognition: facilitation of recent memory in aged nonhuman primates by nimodipine. Neurobiol Aging 11:573-575.

Sapolsky RM, Romero LM, Munck AU (2000) How do glucocorticoids influence stress responses? Integrating permissive, suppressive, stimulatory, and preparative actions. Endocr Rev 21:55-89.

Sartor GC, Aston-Jones G (2012) Regulation of the ventral tegmental area by the bed nucleus of the stria terminalis is required for expression of cocaine preference. Eur J Neurosci 36:3549-3558.

Sartori SB, Hauschild M, Bunck M, Gaburro S, Landgraf R, Singewald N (2011) Enhanced fear expression in a psychopathological mouse model of trait anxiety: pharmacological interventions. PLoS One 6:e16849.

Savitz J, Solms M, Ramesar R (2005) Neuropsychological dysfunction in bipolar affective disorder: a critical opinion. Bipolar Disord 7:216-235.

Sawchenko PE, Swanson LW, Vale WW (1984a) Co-expression of corticotropin-releasing factor and vasopressin immunoreactivity in parvocellular neurosecretory neurons of the adrenalectomized rat. Proc Natl Acad Sci U S A 81:1883-1887.

Sawchenko PE, Swanson LW, Vale WW (1984b) Corticotropin-releasing factor: co-expression within distinct subsets of oxytocin-, vasopressin-, and neurotensin-immunoreactive neurons in the hypothalamus of the male rat. J Neurosci 4:1118-1129.

Sax KW, Strakowski SM, Zimmerman ME, DelBello MP, Keck PE, Jr., Hawkins JM (1999) Frontosubcortical neuroanatomy and the continuous performance test in mania. Am J Psychiatry 156:139-141.

Schaaf CP, Sabo A, Sakai Y, Crosby J, Muzny D, Hawes A, Lewis L, Akbar H, Varghese R, Boerwinkle E, Gibbs RA, Zoghbi HY (2011) Oligogenic heterozygosity in individuals with high-functioning autism spectrum disorders. Hum Mol Genet 20:3366-3375.

Schmidt MV, Schulke JP, Liebl C, Stiess M, Avrabos C, Bock J, Wochnik GM, Davies HA, Zimmermann N, Scharf SH, Trumbach D, Wurst W, Zieglgansberger W, Turck C, Holsboer F, Stewart MG, Bradke F, Eder M, Muller MB, Rein T (2011) Tumor suppressor down-regulated in renal cell carcinoma 1 (DRR1) is a stress-induced actin bundling factor that modulates synaptic efficacy and cognition. Proc Natl Acad Sci U S A 108:17213-17218.

Schonig K, Schwenk F, Rajewsky K, Bujard H (2002) Stringent doxycycline dependent control of CRE recombinase in vivo. Nucleic Acids Res 30:e134.

Schwartz MW, Woods SC, Porte D, Jr., Seeley RJ, Baskin DG (2000) Central nervous system control of food intake. Nature 404:661-671.

Seale JV, Wood SA, Atkinson HC, Bate E, Lightman SL, Ingram CD, Jessop DS, Harbuz MS (2004) Gonadectomy reverses the sexually diergic patterns of circadian and stress-induced hypothalamic-pituitary-adrenal axis activity in male and female rats. J Neuroendocrinol 16:516-524.

Seasholtz AF, Burrows HL, Karolyi IJ, Camper SA (2001) Mouse models of altered CRH-binding protein expression. Peptides 22:743-751.

Seasholtz AF, Valverde RA, Denver RJ (2002) Corticotropin-releasing hormone-binding protein: biochemistry and function from fishes to mammals. J Endocrinol 175:89-97.

Seifert G, Schilling K, Steinhauser C (2006) Astrocyte dysfunction in neurological disorders: a molecular perspective. Nat Rev Neurosci 7:194-206.

Seifert R, Wenzel-Seifert K (2002) Constitutive activity of G-protein-coupled receptors: cause of disease and common property of wild-type receptors. Naunyn Schmiedebergs Arch Pharmacol 366:381-416.

Seisenberger C, Specht V, Welling A, Platzer J, Pfeifer A, Kuhbandner S, Striessnig J, Klugbauer N, Feil R, Hofmann F (2000) Functional embryonic cardiomyocytes after disruption of the L-type alpha1C (Cav1.2) calcium channel gene in the mouse. J Biol Chem 275:39193-39199.

Selye H (1936) A syndrome produced by diverse nocuous agents. Nature 138.

Selye H (1955) Stress and Disease. Science 122:625-631.

Shaham Y, Erb S, Leung S, Buczek Y, Stewart J (1998) CP-154,526, a selective, non-peptide antagonist of the corticotropin-releasing factor1 receptor attenuates stress-induced relapse to drug seeking in cocaine- and heroin-trained rats. Psychopharmacology (Berl) 137:184-190.

Shaltiel G, Maeng S, Malkesman O, Pearson B, Schloesser RJ, Tragon T, Rogawski M, Gasior M, Luckenbaugh D, Chen G, Manji HK (2008) Evidence for the involvement of the kainate receptor subunit GluR6 (GRIK2) in mediating behavioral displays related to behavioral symptoms of mania. Mol Psychiatry 13:858-872.

Shastry BS (1997) On the functions of lithium: the mood stabilizer. Bioessays 19:199-200.

Shepherd JK, Grewal SS, Fletcher A, Bill DJ, Dourish CT (1994) Behavioural and pharmacological characterisation of the elevated "zero-maze" as an animal model of anxiety. Psychopharmacology (Berl) 116:56-64.

Shin LM, Liberzon I (2010) The neurocircuitry of fear, stress, and anxiety disorders. Neuropsychopharmacology 35:169-191.

Shinnick-Gallagher P, McKernan MG, Xie J, Zinebi F (2003) L-type voltage-gated calcium channels are involved in the in vivo and in vitro expression of fear conditioning. Ann N Y Acad Sci 985:135-149.

Sik A, Hajos N, Gulacsi A, Mody I, Freund TF (1998) The absence of a major Ca2+ signaling pathway in GABAergic neurons of the hippocampus. Proc Natl Acad Sci U S A 95:3245-3250.

Silberman Y, Matthews RT, Winder DG (2013) A corticotropin releasing factor pathway for ethanol regulation of the ventral tegmental area in the bed nucleus of the stria terminalis. J Neurosci 33:950-960.

Silberman Y, Winder DG (2013) Emerging role for corticotropin releasing factor signaling in the bed nucleus of the stria terminalis at the intersection of stress and reward. Front Psychiatry 4:42.

Singru PS, Wittmann G, Farkas E, Zseli G, Fekete C, Lechan RM (2012) Refeeding-activated glutamatergic neurons in the hypothalamic paraventricular nucleus (PVN) mediate effects of melanocortin signaling in the nucleus tractus solitarius (NTS). Endocrinology 153:3804-3814.

Sinnegger-Brauns MJ, Hetzenauer A, Huber IG, Renstrom E, Wietzorrek G, Berjukov S, Cavalli M, Walter D, Koschak A, Waldschutz R, Hering S, Bova S, Rorsman P, Pongs O, Singewald N, Striessnig J (2004) Isoform-specific regulation of mood behavior and pancreatic beta cell and cardiovascular function by L-type Ca2+ channels. Journal of Clinical Investigation 113:1430-1439.

Sinnegger-Brauns MJ, Huber IG, Koschak A, Wild C, Obermair GJ, Einzinger U, Hoda JC, Sartori SB, Striessnig J (2009) Expression and 1,4-dihydropyridine-binding properties of brain L-type calcium channel isoforms. Mol Pharmacol 75:407-414.

Sirinathsinghji DJ, Rees LH, Rivier J, Vale W (1983) Corticotropin-releasing factor is a potent inhibitor of sexual receptivity in the female rat. Nature 305:232-235.

Sklar P, et al. (2011) Large-scale genome-wide association analysis of bipolar disorder identifies a new susceptibility locus near ODZ4. Nat Genet 43:977-983.

Sklar P, et al. (2008) Whole-genome association study of bipolar disorder. Mol Psychiatry 13:558-569.

Skorzewska A, Bidzinski A, Hamed A, Lehner M, Turzynska D, Sobolewska A, Maciejak P, Szyndler J, Wislowska-Stanek A, Plaznik A (2008) The influence of CRF and alpha-helical CRF(9-41) on rat fear responses, c-Fos and CRF expression, and concentration of amino acids in brain structures. Horm Behav 54:602-612.

Skucas VA, Mathews IB, Yang J, Cheng Q, Treister A, Duffy AM, Verkman AS, Hempstead BL, Wood MA, Binder DK, Scharfman HE (2011) Impairment of select forms of spatial memory and neurotrophin-dependent synaptic plasticity by deletion of glial aquaporin-4. J Neurosci 31:6392-6397.

Slattery DA, Cryan JF (2012) Using the rat forced swim test to assess antidepressant-like activity in rodents. Nat Protoc 7:1009-1014.

Smeets T, Wolf OT, Giesbrecht T, Sijstermans K, Telgen S, Joels M (2009) Stress selectively and lastingly promotes learning of context-related high arousing information. Psychoneuroendocrinology 34:1152-1161.

Smith GW, Aubry JM, Dellu F, Contarino A, Bilezikjian LM, Gold LH, Chen R, Marchuk Y, Hauser C, Bentley CA, Sawchenko PE, Koob GF, Vale W, Lee KF (1998) Corticotropin releasing factor receptor 1-deficient mice display decreased anxiety, impaired stress response, and aberrant neuroendocrine development. Neuron 20:1093-1102.

Smith K (2011) Trillion-dollar brain drain. Nature 478:15.

Smith LA, Cornelius V, Warnock A, Tacchi MJ, Taylor D (2007) Pharmacological interventions for acute bipolar mania: a systematic review of randomized placebo-controlled trials. Bipolar Disord 9:551-560.

Smith MA, Makino S, Kvetnansky R, Post RM (1995) Stress and glucocorticoids affect the expression of brain-derived neurotrophic factor and neurotrophin-3 mRNAs in the hippocampus. J Neurosci 15:1768-1777.

Smithies O, Koralewski MA, Song KY, Kucherlapati RS (1984) Homologous recombination with DNA introduced into mammalian cells. Cold Spring Harb Symp Quant Biol 49:161-170.

Sommershof A, Aichinger H, Engler H, Adenauer H, Catani C, Boneberg EM, Elbert T, Groettrup M, Kolassa IT (2009) Substantial reduction of naive and regulatory T cells following traumatic stress. Brain Behav Immun 23:1117-1124.

Somogyi P, Tamas G, Lujan R, Buhl EH (1998) Salient features of synaptic organisation in the cerebral cortex. Brain Res Brain Res Rev 26:113-135.

Spielewoy C, Roubert C, Hamon M, Nosten-Bertrand M, Betancur C, Giros B (2000) Behavioural disturbances associated with hyperdopaminergia in dopamine-transporter knockout mice. Behav Pharmacol 11:279-290.

Spiga F, Lightman SL, Shekhar A, Lowry CA (2006) Injections of urocortin 1 into the basolateral amygdala induce anxiety-like behavior and c-Fos expression in brainstem serotonergic neurons. Neuroscience 138:1265-1276.

St-Onge L, Furth PA, Gruss P (1996) Temporal control of the Cre recombinase in transgenic mice by a tetracycline responsive promoter. Nucleic Acids Res 24:3875-3877.

Stahn C, Buttgereit F (2008) Genomic and nongenomic effects of glucocorticoids. Nat Clin Pract Rheumatol 4:525-533.

Steiner J (1972) A questionnaire study of risk-taking in psychiatric patients. Br J Med Psychol 45:365-374.

Stengel A, Goebel M, Million M, Stenzel-Poore MP, Kobelt P, Monnikes H, Tache Y, Wang L (2009) Corticotropin-releasing factor-overexpressing mice exhibit reduced neuronal activation in the arcuate nucleus and food intake in response to fasting. Endocrinology 150:153-160.

Stenzel-Poore MP, Cameron VA, Vaughan J, Sawchenko PE, Vale W (1992) Development of Cushing's syndrome in corticotropin-releasing factor transgenic mice. Endocrinology 130:3378-3386.

Stenzel-Poore MP, Heinrichs SC, Rivest S, Koob GF, Vale WW (1994) Overproduction of corticotropin-releasing factor in transgenic mice: a genetic model of anxiogenic behavior. J Neurosci 14:2579-2584.

Stephens B, Mueller AJ, Shering AF, Hood SH, Taggart P, Arbuthnott GW, Bell JE, Kilford L, Kingsbury AE, Daniel SE, Ingham CA (2005) Evidence of a breakdown of corticostriatal connections in Parkinson's disease. Neuroscience 132:741-754.

Steptoe A, Kivimaki M (2012) Stress and cardiovascular disease. Nat Rev Cardiol 9:360-370.

Stevens HE, Leckman JF, Coplan JD, Suomi SJ (2009) Risk and resilience: early manipulation of macaque social experience and persistent behavioral and neurophysiological outcomes. J Am Acad Child Adolesc Psychiatry 48:114-127.

Stone EA, Lin Y (2008) An anti-immobility effect of exogenous corticosterone in mice. Eur J Pharmacol 580:135-142.

Stratakis CA, Sarlis NJ, Berrettini WH, Badner JA, Chrousos GP, Gershon ES, Detera-Wadleigh SD (1997) Lack of linkage between the corticotropin-releasing hormone (CRH) gene and bipolar affective disorder. Mol Psychiatry 2:483-485.

Stuhmer T, Puelles L, Ekker M, Rubenstein JL (2002) Expression from a Dlx gene enhancer marks adult mouse cortical GABAergic neurons. Cereb Cortex 12:75-85.

Sugawara M, Hashimoto K, Hattori T, Takao T, Suemaru S, Ota Z (1988) Effects of lithium on the hypothalamo-pituitary-adrenal axis. Endocrinol Jpn 35:655-663.

Sun N, Abil Z, Zhao H (2012) Recent advances in targeted genome engineering in mammalian systems. Biotechnol J 7:1074-1087.

Sun N, Cassell MD (1993) Intrinsic GABAergic neurons in the rat central extended amygdala. J Comp Neurol 330:381-404.

Sutton RE, Koob GF, Le MM, Rivier J, Vale W (1982) Corticotropin releasing factor produces behavioural activation in rats. Nature 297:331-333.

Swanson LW, Hartman BK (1975) The central adrenergic system. An immunofluorescence study of the location of cell bodies and their efferent connections in the rat utilizing dopamine-beta-hydroxylase as a marker. J Comp Neurol 163:467-505.

Swanson LW, Sawchenko PE, Rivier J, Vale WW (1983) Organization of ovine corticotropin-releasing factor immunoreactive cells and fibers in the rat brain: an immunohistochemical study. Neuroendocrinology 36:165-186.

Swerdlow NR, Koob GF (1987) Dopamine, Schizophrenia, Mania and Depression - Toward A Unified Hypothesis of Cortico-Striato-Pallido-Thalamic Function. Behavioral and Brain Sciences 10:197-207.

Swerdlow NR, Shoemaker JM, Stephany N, Wasserman L, Ro HJ, Geyer MA (2002) Prestimulus effects on startle magnitude: sensory or motor? Behav Neurosci 116:672-681.

Swerdlow NR, Weber M, Qu Y, Light GA, Braff DL (2008) Realistic expectations of prepulse inhibition in translational models for schizophrenia research. Psychopharmacology (Berl) 199:331-388.

Swiergiel AH, Takahashi LK, Kalin NH (1993) Attenuation of stress-induced behavior by antagonism of corticotropin-releasing factor receptors in the central amygdala in the rat. Brain Res 623:229-234.

Sztainberg Y, Chen A (2012) Neuropeptide Regulation of Stress-Induced Behavior: Insights from the CRF/Urocortin Family. In: Handbook of Neuroendocrinology (Georg Fink, Donald Pfaff, Jon Levine, eds), pp 355-375. London, Waltham, San Diego: Academic press, Elsevier.

Sztainberg Y, Kuperman Y, Justice N, Chen A (2011) An anxiolytic role for CRF receptor type 1 in the globus pallidus. J Neurosci 31:17416-17424.

Sztainberg Y, Kuperman Y, Tsoory M, Lebow M, Chen A (2010) The anxiolytic effect of environmental enrichment is mediated via amygdalar CRF receptor type 1. Mol Psychiatry 15:905-917.

Tagliaferro P, Morales M (2008) Synapses between corticotropin-releasing factor-containing axon terminals and dopaminergic neurons in the ventral tegmental area are predominantly glutamatergic. J Comp Neurol 506:616-626.

Takacs VT, Freund TF, Gulyas AI (2008) Types and synaptic connections of hippocampal inhibitory neurons reciprocally connected with the medial septum. Eur J Neurosci 28:148-164.

Taki K, Kaneko T, Mizuno N (2000) A group of cortical interneurons expressing mu-opioid receptor-like immunoreactivity: a double immunofluorescence study in the rat cerebral cortex. Neuroscience 98:221-231.

Tan LA, Xu K, Vaccarino FJ, Lovejoy DA, Rotzinger S (2009) Teneurin C-terminal associated peptide (TCAP)-1 attenuates corticotropin-releasing factor (CRF)-induced c-Fos expression in the limbic system and modulates anxiety behavior in male Wistar rats. Behav Brain Res 201:198-206.

Tandberg E, Larsen JP, Aarsland D, Cummings JL (1996) The occurrence of depression in Parkinson's disease - A community-based study. Archives of Neurology 53:175-179.

Tandon R, Gaebel W, Barch DM, Bustillo J, Gur RE, Heckers S, Malaspina D, Owen MJ, Schultz S, Tsuang M, van OJ, Carpenter W (2013) Definition and description of schizophrenia in the DSM-5. Schizophr Res 150:3-10.

Taniguchi H (2014) Genetic dissection of GABAergic neural circuits in mouse neocortex. Front Cell Neurosci 8:8.

Taniguchi H, He M, Wu P, Kim S, Paik R, Sugino K, Kvitsiani D, Fu Y, Lu J, Lin Y, Miyoshi G, Shima Y, Fishell G, Nelson SB, Huang ZJ (2011) A resource of Cre driver lines for genetic targeting of GABAergic neurons in cerebral cortex. Neuron 71:995-1013.

Tazi A, Swerdlow NR, LeMoal M, Rivier J, Vale W, Koob GF (1987) Behavioral activation by CRF: evidence for the involvement of the ventral forebrain. Life Sci 41:41-49.

Tenenbaum L, Chtarto A, Lehtonen E, Velu T, Brotchi J, Levivier M (2004) Recombinant AAV-mediated gene delivery to the central nervous system. J Gene Med 6 Suppl 1:S212-S222.

Tessner KD, Mittal V, Walker EF (2011) Longitudinal study of stressful life events and daily stressors among adolescents at high risk for psychotic disorders. Schizophr Bull 37:432-441.

Tezval H, Jahn O, Todorovic C, Sasse A, Eckart K, Spiess J (2004) Cortagine, a specific agonist of corticotropin-releasing factor receptor subtype 1, is anxiogenic and antidepressive in the mouse model. Proc Natl Acad Sci U S A 101:9468-9473.

Thenral ST, Vanisree AJ (2012) Peripheral assessment of the genes AQP4, PBP and TH in patients with Parkinson's disease. Neurochem Res 37:512-515.

Thibault O, Gant JC, Landfield PW (2007) Expansion of the calcium hypothesis of brain aging and Alzheimer's disease: minding the store. Aging Cell 6:307-317.

Thoeringer CK, Henes K, Eder M, Dahlhoff M, Wurst W, Holsboer F, Deussing JM, Moosmang S, Wotjak CT (2012) Consolidation of remote fear memories involves Corticotropin-Releasing Hormone (CRH) receptor type 1-mediated enhancement of AMPA receptor GluR1 signaling in the dentate gyrus. Neuropsychopharmacology 37:787-796.

Thomas CE, Ehrhardt A, Kay MA (2003) Progress and problems with the use of viral vectors for gene therapy. Nat Rev Genet 4:346-358.

Thomas KR, Capecchi MR (1987) Site-directed mutagenesis by gene targeting in mouse embryo-derived stem cells. Cell 51:503-512.

Timpl P, Spanagel R, Sillaber I, Kresse A, Reul JM, Stalla GK, Blanquet V, Steckler T, Holsboer F, Wurst W (1998) Impaired stress response and reduced anxiety in mice lacking a functional corticotropin-releasing hormone receptor 1. Nat Genet 19:162-166.

Tjoumakaris SI, Rudoy C, Peoples J, Valentino RJ, Van Bockstaele EJ (2003) Cellular interactions between axon terminals containing endogenous opioid peptides or corticotropin-releasing factor in the rat locus coeruleus and surrounding dorsal pontine tegmentum. J Comp Neurol 466:445-456.

Tomioka R, Okamoto K, Furuta T, Fujiyama F, Iwasato T, Yanagawa Y, Obata K, Kaneko T, Tamamaki N (2005) Demonstration of long-range GABAergic connections distributed throughout the mouse neocortex. Eur J Neurosci 21:1587-1600.

Tomioka R, Rockland KS (2007) Long-distance corticocortical GABAergic neurons in the adult monkey white and gray matter. J Comp Neurol 505:526-538.

Toth K, Borhegyi Z, Freund TF (1993) Postsynaptic targets of GABAergic hippocampal neurons in the medial septum-diagonal band of broca complex. J Neurosci 13:3712-3724.

Toth K, Freund TF (1992) Calbindin D28k-containing nonpyramidal cells in the rat hippocampus: their immunoreactivity for GABA and projection to the medial septum. Neuroscience 49:793-805.

Toth M, Gresack JE, Bangasser DA, Plona Z, Valentino RJ, Flandreau EI, Mansuy IM, Merlo-Pich E, Geyer MA, Risbrough VB (2014) Forebrain-Specific CRF Overproduction During Development is Sufficient to Induce Enduring Anxiety and Startle Abnormalities in Adult Mice. Neuropsychopharmacology 39:1409-1419.

Touma C, Gassen NC, Herrmann L, Cheung-Flynn J, Bull DR, Ionescu IA, Heinzmann JM, Knapman A, Siebertz A, Depping AM, Hartmann J, Hausch F, Schmidt MV, Holsboer F, Ising M, Cox MB, Schmidt U, Rein T (2011) FK506 binding protein 5 shapes stress responsiveness: modulation of neuroendocrine reactivity and coping behavior. Biol Psychiatry 70:928-936.

Tovote P, Meyer M, Ronnenberg A, Ogren SO, Spiess J, Stiedl O (2005) Heart rate dynamics and behavioral responses during acute emotional challenge in corticotropin-releasing factor receptor 1-deficient and corticotropin-releasing factor-overexpressing mice. Neuroscience 134:1113-1122.

Trompet S, Westendorp RG, Kamper AM, de Craen AJ (2008) Use of calcium antagonists and cognitive decline in old age. The Leiden 85-plus study. Neurobiol Aging 29:306-308.

Tronche F, Kellendonk C, Kretz O, Gass P, Anlag K, Orban PC, Bock R, Klein R, Schutz G (1999) Disruption of the glucocorticoid receptor gene in the nervous system results in reduced anxiety. Nat Genet 23:99-103.

Tsai HC, Zhang F, Adamantidis A, Stuber GD, Bonci A, de LL, Deisseroth K (2009) Phasic firing in dopaminergic neurons is sufficient for behavioral conditioning. Science 324:1080-1084.

Tye KM, Deisseroth K (2012) Optogenetic investigation of neural circuits underlying brain disease in animal models. Nat Rev Neurosci 13:251-266.

Tye KM, Mirzabekov JJ, Warden MR, Ferenczi EA, Tsai HC, Finkelstein J, Kim SY, Adhikari A, Thompson KR, Andalman AS, Gunaydin LA, Witten IB, Deisseroth K (2013) Dopamine neurons modulate neural encoding and expression of depression-related behaviour. Nature 493:537-541.

Tye KM, Prakash R, Kim SY, Fenno LE, Grosenick L, Zarabi H, Thompson KR, Gradinaru V, Ramakrishnan C, Deisseroth K (2011) Amygdala circuitry mediating reversible and bidirectional control of anxiety. Nature 471:358-362.

Ugolini G (2010) Advances in viral transneuronal tracing. J Neurosci Methods 194:2-20.

Ulrich-Lai YM, Herman JP (2009) Neural regulation of endocrine and autonomic stress responses. Nat Rev Neurosci 10:397-409.

Ungless MA, Singh V, Crowder TL, Yaka R, Ron D, Bonci A (2003) Corticotropin-releasing factor requires CRF binding protein to potentiate NMDA receptors via CRF receptor 2 in dopamine neurons. Neuron 39:401-407.

Urani A, Chourbaji S, Gass P (2005) Mutant mouse models of depression: candidate genes and current mouse lines. Neurosci Biobehav Rev 29:805-828.

Vale W, Rivier C, Brown MR, Spiess J, Koob G, Swanson L, Bilezikjian L, Bloom F, Rivier J (1983) Chemical and biological characterization of corticotropin releasing factor. Recent Prog Horm Res 39:245-270.

Vale W, Spiess J, Rivier C, Rivier J (1981) Characterization of a 41-residue ovine hypothalamic peptide that stimulates secretion of corticotropin and beta-endorphin. Science 213:1394-1397.

Valentino RJ, Chen S, Zhu Y, Aston-Jones G (1996) Evidence for divergent projections to the brain noradrenergic system and the spinal parasympathetic system from Barrington's nucleus. Brain Res 732:1-15.

Valentino RJ, Foote SL, Aston-Jones G (1983) Corticotropin-releasing factor activates noradrenergic neurons of the locus coeruleus. Brain Res 270:363-367.

Valentino RJ, Page M, Van BE, Aston-Jones G (1992) Corticotropin-releasing factor innervation of the locus coeruleus region: distribution of fibers and sources of input. Neuroscience 48:689-705.

Valentino RJ, Van Bockstaele E (2008) Convergent regulation of locus coeruleus activity as an adaptive response to stress. Eur J Pharmacol 583:194-203.

Valentino RJ, Wehby RG (1988) Corticotropin-releasing factor: evidence for a neurotransmitter role in the locus ceruleus during hemodynamic stress. Neuroendocrinology 48:674-677.

Valjent E, Bertran-Gonzalez J, Herve D, Fisone G, Girault JA (2009) Looking BAC at striatal signaling: cell-specific analysis in new transgenic mice. Trends Neurosci 32:538-547.

Van Bockstaele EJ, Colago EE, Valentino RJ (1998) Amygdaloid corticotropin-releasing factor targets locus coeruleus dendrites: substrate for the co-ordination of emotional and cognitive limbs of the stress response. J Neuroendocrinol 10:743-757.

Van Bockstaele EJ, Peoples J, Valentino RJ (1999) A.E. Bennett Research Award. Anatomic basis for differential regulation of the rostrolateral peri-locus coeruleus region by limbic afferents. Biol Psychiatry 46:1352-1363.

van den Brandt J., Luhder F, McPherson KG, de Graaf KL, Tischner D, Wiehr S, Herrmann T, Weissert R, Gold R, Reichardt HM (2007) Enhanced glucocorticoid receptor signaling in T cells impacts thymocyte apoptosis and adaptive immune responses. Am J Pathol 170:1041-1053.

van den Pol AN (2012) Neuropeptide transmission in brain circuits. Neuron 76:98-115.

van Gaalen MM, Steckler T (2000) Behavioural analysis of four mouse strains in an anxiety test battery. Behav Brain Res 115:95-106.

van Gaalen MM, Stenzel-Poore MP, Holsboer F, Steckler T (2002) Effects of transgenic overproduction of CRH on anxiety-like behaviour. Eur J Neurosci 15:2007-2015.

Van Pett K, Viau V, Bittencourt JC, Chan RK, Li HY, Arias C, Prins GS, Perrin M, Vale W, Sawchenko PE (2000) Distribution of mRNAs encoding CRF receptors in brain and pituitary of rat and mouse. J Comp Neurol 428:191-212.

van Versendaal D, Rajendran R, Saiepour MH, Klooster J, Smit-Rigter L, Sommeijer JP, De Zeeuw CI, Hofer SB, Heimel JA, Levelt CN (2012) Elimination of inhibitory synapses is a major component of adult ocular dominance plasticity. Neuron 74:374-383.

Vaughan J, Donaldson C, Bittencourt J, Perrin MH, Lewis K, Sutton S, Chan R, Turnbull AV, Lovejoy D, Rivier C (1995) Urocortin, a mammalian neuropeptide related to fish urotensin I and to corticotropin-releasing factor. Nature 378:287-292.

Vestergaard P, Sorensen T, Hoppe E, Rafaelsen OJ, Yates CM, Nicolaou N (1978) Biogenic amine metabolites in cerebrospinal fluid of patients with affective disorders. Acta Psychiatr Scand 58:88-96.

Vetter DE, Li C, Zhao L, Contarino A, Liberman MC, Smith GW, Marchuk Y, Koob GF, Heinemann SF, Vale W, Lee KF (2002) Urocortin-deficient mice show hearing impairment and increased anxiety-like behavior. Nat Genet 31:363-369.

Vicentini E, Arban R, Angelici O, Maraia G, Perico M, Mugnaini M, Ugolini A, Large C, Domenici E, Gerrard P, Bortner D, Mansuy IM, Mangiarini L, Merlo-Pich E (2009) Transient forebrain over-expression of CRF induces plasma corticosterone and mild behavioural changes in adult conditional CRF transgenic mice. Pharmacol Biochem Behav 93:17-24.

Vinkers CH, Risbrough VB, Geyer MA, Caldwell S, Low MJ, Hauger RL (2007) Role of dopamine D1 and D2 receptors in CRF-induced disruption of sensorimotor gating. Pharmacol Biochem Behav 86:550-558.

Vita N, Laurent P, Lefort S, Chalon P, Lelias JM, Kaghad M, Le FG, Caput D, Ferrara P (1993) Primary structure and functional expression of mouse pituitary and human brain corticotrophin releasing factor receptors. FEBS Lett 335:1-5.

Volkow ND, Wang GJ, Fowler JS, Logan J, Gatley SJ, Hitzemann R, Chen AD, Dewey SL, Pappas N (1997) Decreased striatal dopaminergic responsiveness in detoxified cocaine-dependent subjects. Nature 386:830-833.

von Wolff G, Avrabos C, Stepan J, Wurst W, Deussing JM, Holsboer F, Eder M (2011) Voltage-sensitive dye imaging demonstrates an enhancing effect of corticotropin-releasing hormone on neuronal activity propagation through the hippocampal formation. J Psychiatr Res 45:256-261.

Wagner KV, Wang XD, Liebl C, Scharf SH, Muller MB, Schmidt MV (2011) Pituitary glucocorticoid receptor deletion reduces vulnerability to chronic stress. Psychoneuroendocrinology 36:579-587.

Walsh JJ, Friedman AK, Sun H, Heller EA, Ku SM, Juarez B, Burnham VL, Mazei-Robison MS, Ferguson D, Golden SA, Koo JW, Chaudhury D, Christoffel DJ, Pomeranz L, Friedman JM, Russo SJ, Nestler EJ, Han MH (2014) Stress and CRF gate neural activation of BDNF in the mesolimbic reward pathway. Nat Neurosci 17:27-29.

Wanat MJ, Hopf FW, Stuber GD, Phillips PE, Bonci A (2008) Corticotropin-releasing factor increases mouse ventral tegmental area dopamine neuron firing through a protein kinase C-dependent enhancement of Ih. J Physiol 586:2157-2170.

Wang HL, Wayner MJ, Chai CY, Lee EH (1998) Corticotrophin-releasing factor produces a long-lasting enhancement of synaptic efficacy in the hippocampus. Eur J Neurosci 10:3428-3437.

Wang J, Fang Q, Liu Z, Lu L (2006) Region-specific effects of brain corticotropin-releasing factor receptor type 1 blockade on footshock-stress- or drug-priming-induced reinstatement of morphine conditioned place preference in rats. Psychopharmacology (Berl) 185:19-28.

Wang L, Rotzinger S, Al CA, Elias CF, Barsyte-Lovejoy D, Qian X, Wang NC, De CA, Belsham D, Bittencourt JC, Vaccarino F, Lovejoy DA (2005) Teneurin proteins possess a carboxy terminal sequence with neuromodulatory activity. Brain Res Mol Brain Res 133:253-265.

Wang X, Su H, Copenhagen LD, Vaishnav S, Pieri F, Shope CD, Brownell WE, De BM, Paylor R, Bradley A (2002) Urocortin-deficient mice display normal stress-induced anxiety behavior and autonomic control but an impaired acoustic startle response. Mol Cell Biol 22:6605-6610.

Wang XD, Chen Y, Wolf M, Wagner KV, Liebl C, Scharf SH, Harbich D, Mayer B, Wurst W, Holsboer F, Deussing JM, Baram TZ, Muller MB, Schmidt MV (2011a) Forebrain CRHR1 deficiency attenuates chronic stress-induced cognitive deficits and dendritic remodeling. Neurobiol Dis 42:300-310.

Wang XD, Labermaier C, Holsboer F, Wurst W, Deussing JM, Muller MB, Schmidt MV (2012) Early-life stress-induced anxiety-related behavior in adult mice partially requires forebrain corticotropin-releasing hormone receptor 1. Eur J Neurosci 36:2360-2367.

Wang XD, Rammes G, Kraev I, Wolf M, Liebl C, Scharf SH, Rice CJ, Wurst W, Holsboer F, Deussing JM, Baram TZ, Stewart MG, Muller MB, Schmidt MV (2011b) Forebrain CRF(1) modulates early-life stress-programmed cognitive deficits. J Neurosci 31:13625-13634.

Wang XD, Su YA, Wagner KV, Avrabos C, Scharf SH, Hartmann J, Wolf M, Liebl C, Kuhne C, Wurst W, Holsboer F, Eder M, Deussing JM, Muller MB, Schmidt MV (2013) Nectin-3 links CRHR1 signaling to stress-induced memory deficits and spine loss. Nat Neurosci 16:706-713.

Warwick BP, Romsos DR (1988) Energy balance in adrenalectomized ob/ob mice: effects of dietary starch and glucose. Am J Physiol 255:R141-R148.

Weiner DM, Levey AI, Sunahara RK, Niznik HB, O'Dowd BF, Seeman P, Brann MR (1991) D1 and D2 dopamine receptor mRNA in rat brain. Proc Natl Acad Sci U S A 88:1859-1863.

Weninger SC, Dunn AJ, Muglia LJ, Dikkes P, Miczek KA, Swiergiel AH, Berridge CW, Majzoub JA (1999) Stress-induced behaviors require the corticotropin-releasing hormone (CRH) receptor, but not CRH. Proc Natl Acad Sci U S A 96:8283-8288.

White JA, McKinney BC, John MC, Powers PA, Kamp TJ, Murphy GG (2008) Conditional forebrain deletion of the L-type calcium channel Ca V 1.2 disrupts remote spatial memories in mice. Learn Mem 15:1-5.

Whitnall MH (1993) Regulation of the hypothalamic corticotropin-releasing hormone neurosecretory system. Prog Neurobiol 40:573-629.

Wiersma A, Baauw AD, Bohus B, Koolhaas JM (1995) Behavioural activation produced by CRH but not alpha-helical CRH (CRH-receptor antagonist) when microinfused into the central nucleus of the amygdala under stress-free conditions. Psychoneuroendocrinology 20:423-432.

Wilcock DM, Vitek MP, Colton CA (2009) Vascular amyloid alters astrocytic water and potassium channels in mouse models and humans with Alzheimer's disease. Neuroscience 159:1055-1069.

Willner P (2005) Chronic mild stress (CMS) revisited: consistency and behavioural-neurobiological concordance in the effects of CMS. Neuropsychobiology 52:90-110.

Wirgenes KV, Tesli M, Inderhaug E, Athanasiu L, Agartz I, Melle I, Hughes T, Andreassen OA, Djurovic S (2014) ANK3 gene expression in bipolar disorder and schizophrenia. Br J Psychiatry.

Wise RA (1980) Action of drugs of abuse on brain reward systems. Pharmacol Biochem Behav 13 Suppl 1:213-223.

Wise RA, Morales M (2010) A ventral tegmental CRF-glutamate-dopamine interaction in addiction. Brain Res 1314:38-43.

Wise RA, Rompre PP (1989) Brain dopamine and reward. Annu Rev Psychol 40:191-225.

Witten IB, Lin SC, Brodsky M, Prakash R, Diester I, Anikeeva P, Gradinaru V, Ramakrishnan C, Deisseroth K (2010) Cholinergic interneurons control local circuit activity and cocaine conditioning. Science 330:1677-1681.

Wong LF, Goodhead L, Prat C, Mitrophanous KA, Kingsman SM, Mazarakis ND (2006) Lentivirus-mediated gene transfer to the central nervous system: therapeutic and research applications. Hum Gene Ther 17:1-9.

Wong ML, Kling MA, Munson PJ, Listwak S, Licinio J, Prolo P, Karp B, McCutcheon IE, Geracioti TD, Jr., DeBellis MD, Rice KC, Goldstein DS, Veldhuis JD, Chrousos GP, Oldfield EH, McCann SM, Gold PW (2000) Pronounced and sustained central hypernoradrenergic function in major depression with melancholic features: relation to hypercortisolism and corticotropin-releasing hormone. Proc Natl Acad Sci U S A 97:325-330.

World Health Organisation (2008) The Global Burden of Disease: 2004 Update.

Wunderlich FT, Wildner H, Rajewsky K, Edenhofer F (2001) New variants of inducible Cre recombinase: a novel mutant of Cre-PR fusion protein exhibits enhanced sensitivity and an expanded range of inducibility. Nucleic Acids Res 29:E47.

Xia Y, Driscoll JR, Wilbrecht L, Margolis EB, Fields HL, Hjelmstad GO (2011) Nucleus accumbens medium spiny neurons target non-dopaminergic neurons in the ventral tegmental area. J Neurosci 31:7811-7816.

Xiao M, Hu G (2014) Involvement of aquaporin 4 in astrocyte function and neuropsychiatric disorders. CNS Neurosci Ther 20:385-390.

Xu F, Gainetdinov RR, Wetsel WC, Jones SR, Bohn LM, Miller GW, Wang YM, Caron MG (2000) Mice lacking the norepinephrine transporter are supersensitive to psychostimulants. Nat Neurosci 3:465-471.

Yan XX, Toth Z, Schultz L, Ribak CE, Baram TZ (1998) Corticotropin-releasing hormone (CRH)-containing neurons in the immature rat hippocampal formation: light and electron microscopic features and colocalization with glutamate decarboxylase and parvalbumin. Hippocampus 8:231-243.

Yizhar O, Fenno LE, Davidson TJ, Mogri M, Deisseroth K (2011a) Optogenetics in neural systems. Neuron 71:9-34.

Yizhar O, Fenno LE, Prigge M, Schneider F, Davidson TJ, O'Shea DJ, Sohal VS, Goshen I, Finkelstein J, Paz JT, Stehfest K, Fudim R, Ramakrishnan C, Huguenard JR, Hegemann P, Deisseroth K (2011b) Neocortical excitation/inhibition balance in information processing and social dysfunction. Nature 477:171-178.

Young JW, Henry BL, Geyer MA (2011) Predictive animal models of mania: hits, misses and future directions. Br J Pharmacol 164:1263-1284.

Young JW, Minassian A, Paulus MP, Geyer MA, Perry W (2007) A reverse-translational approach to bipolar disorder: rodent and human studies in the Behavioral Pattern Monitor. Neurosci Biobehav Rev 31:882-896.

Zahm DS, Cheng AY, Lee TJ, Ghobadi CW, Schwartz ZM, Geisler S, Parsely KP, Gruber C, Veh RW (2011) Inputs to the midbrain dopaminergic complex in the rat, with emphasis on extended amygdala-recipient sectors. J Comp Neurol 519:3159-3188.

Zaja-Milatovic S, Milatovic D, Schantz AM, Zhang J, Montine KS, Samii A, Deutch AY, Montine TJ (2005) Dendritic degeneration in neostriatal medium spiny neurons in Parkinson disease. Neurology 64:545-547.

Zalutskaya AA, Arai M, Bounoutas GS, Abou-Samra AB (2007) Impaired adaptation to repeated restraint and decreased response to cold in urocortin 1 knockout mice. Am J Physiol Endocrinol Metab 293:E259-E263.

Zeng XN, Sun XL, Gao L, Fan Y, Ding JH, Hu G (2007) Aquaporin-4 deficiency down-regulates glutamate uptake and GLT-1 expression in astrocytes. Mol Cell Neurosci 34:34-39.

Zerucha T, Stuhmer T, Hatch G, Park BK, Long Q, Yu G, Gambarotta A, Schultz JR, Rubenstein JL, Ekker M (2000) A highly conserved enhancer in the Dlx5/Dlx6 intergenic region is the site of cross-regulatory interactions between Dlx genes in the embryonic forebrain. J Neurosci 20:709-721.

Zhang F, Vierock J, Yizhar O, Fenno LE, Tsunoda S, Kianianmomeni A, Prigge M, Berndt A, Cushman J, Polle J, Magnuson J, Hegemann P, Deisseroth K (2011) The microbial opsin family of optogenetic tools. Cell 147:1446-1457.

Zhang F, Wang LP, Boyden ES, Deisseroth K (2006) Channelrhodopsin-2 and optical control of excitable cells. Nat Methods 3:785-792.

Zhang F, Wang LP, Brauner M, Liewald JF, Kay K, Watzke N, Wood PG, Bamberg E, Nagel G, Gottschalk A, Deisseroth K (2007) Multimodal fast optical interrogation of neural circuitry. Nature 446:633-639.

Zhang M, Cai J (2005) Extract of Ginkgo biloba leaves reverses yohimbine-induced spatial working memory deficit in rats. Behav Pharmacol 16:651-656.

Zhu Y, Pintar JE (1998) Expression of opioid receptors and ligands in pregnant mouse uterus and placenta. Biol Reprod 59:925-932.

Ziegler DR, Cullinan WE, Herman JP (2002) Distribution of vesicular glutamate transporter mRNA in rat hypothalamus. J Comp Neurol 448:217-229.

Zorrilla EP, Koob GF (2010) Progress in corticotropin-releasing factor-1 antagonist development. Drug Discov Today 15:371-383.

Zorrilla EP, Tache Y, Koob GF (2003) Nibbling at CRF receptor control of feeding and gastrocolonic motility. Trends Pharmacol Sci 24:421-427.

Zorrilla EP, Valdez GR, Nozulak J, Koob GF, Markou A (2002) Effects of antalarmin, a CRF type 1 receptor antagonist, on anxiety-like behavior and motor activation in the rat. Brain Res 952:188-199.

LIST OF PUBLICATIONS

Vogl AM, Brockmann MM, Giusti SA, Maccarrone G, Vercelli CA, Bauder CA, Richter JS, Roselli F, Hafner A, **Dedic N**, Wotjak CT, Vogt-Weisenhorn DM, Choquet D, Turck CW, Stein V, Deussing JM, Refojo D (2014). *Suppression of Nedd8 conjugation impairs spine development, destabilizes synapses and leads to adult cognitive deterioration*. Nat Neuroscience, Epub ahead of print.

Gassen NC, Hartmann J, Zschocke J, Stepan J, Hafner K, Zellner A, Kirmeier T, Kollmannsberger L, Wagner KV, **Dedic N**, Balsevich G, *Deussing JM, Kloiber S, Lucae S, Holsboer F, Eder M, Uhr M, Ising M, Schmidt MV, Rein T (2014). Association of FKBP51 with Priming of Autophagy Pathways and Mediation of Antidepressant Treatment Response: Evidence in Cells, Mice, and Humans.* PLoS Med. 11(11):e1001755.

Kratzer S, Mattusch C, Metzger MW, **Dedic N**, Noll-Hussong M, Kafitz KW, Eder M, Deussing JM, Holsboer F, Kochs E, Rammes G (2013). *Activation of CRH receptor type 1 expressed on glutamatergic neurons increases excitability of CA1 pyramidal neurons by the modulation of voltage-gated ion channels.* Front Cell Neuroscience, 7:91.

Hartmann J, Wagner KV, **Dedic N**, Marinescu D, Scharf SH, Wang XD, Deussing JM, Hausch F, Rein T, Schmidt U, Holsboer F, Müller MB, Schmidt MV (2012). *Fkbp52 heterozygosity alters behavioral, endocrine and neurogenetic parameters under basal and chronic stress conditions in mice*. Psychoneuroendocrinology. 37(12):2009-21.

Dedic N, Touma C, Romanowski CP, Schieven M, Kühne C, Ableitner M, Lu A, Holsboer F, Wurst W, Kimura M, Deussing JM (2011). *Assessing Behavioural Effects of Chronic HPA Axis Activation Using Conditional CRH-Overexpressing Mice.* Cell Mol Neurobiol, 32(5):815-28.

Dedic N, Walser SM and Deussing JM (2011). *Mouse Models of Depression, Psychiatric Disorders - Trends and Developments*, Toru Uehara (Ed.), ISBN: 978-953-307-745-1, InTech, Available from: http://www.intechopen.com/articles/show/title/mouse-models-of-depression.

Refojo D, Schweizer M, Kuehne C, Ehrenberg S, Thoeringer C, Vogl AM, **Dedic N**, Schumacher M, von Wolff G, Avrabos C, Touma C, Engblom D, Schütz G, Nave KA, Eder M, Wotjak CT, Sillaber I, Holsboer F, Wurst W, Deussing JM (2011). *Glutamatergic and dopaminergic neurons mediate anxiogenic and anxiolytic effects of CRHR1*. Science, 333(6051):1903-7.

ACKNOWLEDGMENTS

My deepest gratitude goes to Dr. Jan Deussing for his constant support, guidance, training and encouragement throughout the last years, and for simply being a great mentor. Thank you for enabling me to develop and pursue my own ideas.

I would also like to thank Prof. Dr. Wolfgang Wurst for supervising my thesis, and his support and advice on many of the projects. I would like to acknowledge and thank the examination board, Prof. Dr. Angelika E. Schnieke, PD. Dr. Mathias V. Schmidt, Prof. Dr. Wolfgang Wurst and Prof. Dr. Alfons Gierl for their time and effort to evaluate my thesis.

I am deeply indebted to PD. Dr. Mathias Schmidt for his permanent support and for all his advice and expertise regarding behavioral experiments.
A heartfelt gratitude also goes to Dr. Damian Refojo for teaching me a lot about scientific thinking and reasoning. Thank you for all your ideas and fruitful discussions, but also for the many enjoyable football-moments.
My gratitude also goes to Prof. Dr. Alon Chen for his support, optimism and enthusiasm about the projects.

Many of the projects would not have been possible without the help, input, ideas and moral support of Claudia Kühne and Marcel Schieven. Claudia, thank you for making the CCK-project possible and for your constant encouragement. Marcel, thank you for all your help in the past four years, especially during the tiresome behavioral experiments. It has been a lot of fun to work with you.

I would especially like to thank all the colleagues that I have had the pleasure to work with in the past four years: Dr. Annette Vogl for all her scientific input, advice and help with many of the experiments, and for all the nice and memorable moments in and outside the lab; Michael Metzger for the electrophysiological measurements, his positive spirit and always delivering our sequencing probes on time; Adam Kolarz for conducting the startle and PPI experiments and numerous scientific and non-scientific discussions; Julia Richter for many laughs and for being an outstanding tennis-partner; Dr. Sebastian Giusti for all his help and advice and the best Flan ever; Karina Gomes for help and performance of many of the virus-studies and surgeries. My thanks also go to Sandra Walser, Marisa Brockmann, Katja Stangl, Mira

Jakovcevski, Julia Bender, Stefanie Unkmeir, Anna Möbus and Sabrina Bauer for their continuous help and for creating a great working atmosphere.

My gratitude also goes to all our collaborators for their support and willingness to help us with many of the projects: Prof. Dr. Elisabeth Binder and Dr. Divya Mehta for the human genetic analyses; Dr. Carsten Wotjak, Benedikt Bedenk and Dr. Elmira Anderzhanova for help and support with microdialysis and WCM experiments; Dr. Mathias Eder, Dr. Gerhard Rammes and Charilaos Avrabos for electrophysiological assessments; Dr. Valery Grinevich and his lab for the adenovirus preparations; Dr. Chadi Touma for assistance with many behavioral experiments; Dr. Daniela Vogt-Weisenhorn for her scientific input during the thesis committee meetings.

Jakob, thank you for all your enduring encouragement and support throughout the good and the bad times.

Finally I would like to thank my parents and my brother for their ongoing support, constant faith and love.

EIDESSTATTLICHE ERKLÄRUNG

Hiermit versichere ich an Eides statt, dass ich die vorliegende Dissertation

'*Genetic dissection of CRH-controlled neurocircuitries of stress*'

selbstständig und ohne unerlaubte Hilfe angefertigt habe. Ich habe mich dabei keiner anderen als der von mir ausdrücklich bezeichneten Hilfsmittel und Quellen bedient. Ferner versichere ich, dass ich mich zu keiner Zeit anderweitig um die Erlangung des Doktorgrades beworben habe.

Teile der Einleitung sowie Abschnitte 4.1.1. und 4.2. des Ergebnisteils wurde im Verlauf der Dissertation veröffentlicht:

Dedic N, Touma C, Romanowski CP, Schieven M, Kühne C, Ableitner M, Lu A, Holsboer F, Wurst W, Kimura M, Deussing JM (2011*). Assessing Behavioural Effects of Chronic HPA Axis Activation Using Conditional CRH-Overexpressing Mice*. Cell Mol Neurobiol, 32(5):815-28.

Dedic N, Walser SM and Deussing JM (2011). *Mouse Models of Depression, Psychiatric Disorders - Trends and Developments*, Toru Uehara (Ed.), ISBN: 978-953-307-745-1, InTech, Available from: http://www.intechopen.com/articles/show/title/mouse-models-of-depression.

Refojo D, Schweizer M, Kuehne C, Ehrenberg S, Thoeringer C, Vogl AM, **Dedic N**, Schumacher M, von Wolff G, Avrabos C, Touma C, Engblom D, Schütz G, Nave KA, Eder M, Wotjak CT, Sillaber I, Holsboer F, Wurst W, Deussing JM (2011). *Glutamatergic and dopaminergic neurons mediate anxiogenic and anxiolytic effects of CRHR1*. Science, 333(6051):1903-7.

I hereby confirm that the dissertation

'Genetic dissection of CRH-controlled neurocircuitries of stress'

is the result of my own work and that I have only used sources or materials listed and specified in the dissertation.

München, Juli 2014

Nina Dedic